World Journal of Gastroenterology®

Volume 13 Number 2
January 14, 2007

National Journal Award
2005

The WJG Press

The WJG Press, Apartment 1066 Yishou Garden, 58 North Langxinzhuang Road, PO Box 2345, Beijing 100023, China
Telephone: +86-10-85381892
Fax: +86-10-85381893
E-mail: wjg@wjgnet.com
http: //www.wjgnet.com

ISSN 1007-9327 CN 14-1219/R Local Post Offices Code No. 82-261

World Journal of Gastroenterology www.wjgnet.com Volume 13 Number 2 Jan 14 2007

ISSN 1007-9327
CN 14-1219/R

World Journal of Gastroenterology®

Indexed and Abstracted in:

Current Contents®/Clinical Medicine, Science Citation Index Expanded (also known as SciSearch®) and Journal Citation Reports/Science Edition, *Index Medicus*, MEDLINE and PubMed, Chemical Abstracts, EMBASE/Excerpta Medica, Abstracts Journals, *Nature Clinical Practice Gastroenterology and Hepatology*, CAB Abstracts and Global Health.
ISI JCR 2003-2000 IF: 3.318, 2.532, 1.445 and 0.993.

Volume 13 Number 2
January 14, 2007

World J Gastroenterol
2007 January 14; 13(2): 165-328
Online Submissions
www.wjgnet.com/wjg/index.jsp
www.wjgnet.com
Printed on Acid-free Paper

A Weekly Journal of Gastroenterology and Hepatology

National Journal Award
2005

World Journal of Gastroenterology®

Volume 13 Number 2
January 14, 2007

The WJG Press

Contents

World Journal of Gastroenterology
Volume 13 **Number** 2 **January** 14, 2007

Contents

World Journal of Gastroenterology
Volume 13 **Number** 2 **January** 14, 2007

Contents

Responsible E-Editor for this issue: Shao-Hua Bai

C-Editor for this issue: Gianfranco D Alpini, PhD, Professor

Responsible S-Editor for this issue: Xing-Xia Yang

World Journal of Gastroenterology (*World J Gastroenterol , WJG*), a leading international journal in gastroenterology and hepatology, has an established reputation for publishing first class research on esophageal cancer, gastric cancer, liver cancer, viral hepatitis, colorectal cancer, and *H pylori* infection, providing a forum for both clinicians and scientists, and has been indexed and abstracted in Current Contents®/Clinical Medicine, Science Citation Index Expanded (also known as SciSearch®) and Journal Citation Reports/Science Edition, *Index Medicus*, MEDLINE and PubMed, Chemical Abstracts, EMBASE/Excerpta Medica, Abstracts Journals, *Nature Clinical Practice Gastroenterology and Hepatology*, CAB Abstracts and Global Health. ISI JCR 2003-2000 IF: 3.318, 2.532, 1.445 and 0.993. *WJG* is a weekly journal published by The WJG Press. The publication date is on 7th, 14th, 21st, and 28th every month. The *WJG* is supported by The National Natural Science Foundation of China, No. 30224801 and No.30424812, which was founded with a name of *China National Journal of New Gastroenterology* on October 1,1995, and renamed as *WJG* on January 25, 1998.

HONORARY EDITORS-IN-CHIEF
Ke-Ji Chen, *Beijing*
Li-Fang Chou, *Taipei*
Zhi-Qiang Huang, *Beijing*
Shinn-Jang Hwang, *Taipei*
Min-Liang Kuo, *Taipei*
Nicholas F LaRusso, *Rochester*
Jie-Shou Li, *Nanjing*
Geng-Tao Liu, *Beijing*
Lein-Ray Mo, *Tainan*
Fa-Zu Qiu, *Wuhan*
Eamonn M Quigley, *Cork*
David S Rampton, *London*
Rudi Schmid, *kentfield*
Nicholas J Talley, *Rochester*
Guido NJ Tytgat, *Amsterdam*
H-P Wang, *Taipei*
Jaw-Ching Wu, *Taipei*
Meng-Chao Wu, *Shanghai*
Ming-Shiang Wu, *Taipei*
Jia-Yu Xu, *Shanghai*
Ta-Sen Yeh, *Taoyuan*

PRESIDENT AND EDITOR-IN-CHIEF
Lian-Sheng Ma, *Beijing*

EDITOR-IN-CHIEF
Bo-Rong Pan, *Xi'an*

ASSOCIATE EDITORS-IN-CHIEF
Gianfranco D Alpini, *Temple*
Bruno Annibale, *Roma*
Roger William Chapman, *Oxford*
Chi-Hin Cho, *Hong Kong*
Alexander L Gerbes, *Munich*
Shou-Dong Lee, *Taipei*
Walter Edwin Longo, *New Haven*
You-Yong Lu, *Beijing*
Masao Omata, *Tokyo*
Harry HX Xia, *Hanover*

SCIENCE EDITORS
Director: Jing Wang, *Beijing*
Deputy Director: Jian-Zhong Zhang, *Beijing*

MEMBERS
Ye Liu, *Beijing*
Xing-Xia Yang, *Beijing*

LANGUAGE EDITORS
Director: Jing-Yun Ma, *Beijing*
Deputy Director: Xian-Lin Wang, *Beijing*

MEMBERS
Gianfranco D Alpini, *Temple*
BS Anand, *Houston*
Richard B Banati, *Lidcombe*
Giuseppe Chiarioni, *Valeggio*
John Frank Di Mari, *Texas*
Shannon S Glaser, *Temple*
Mario Guslandi, *Milano*
Martin Hennenberg, *Bonn*
Atif Iqbal, *Omaha*
Manoj Kumar, *Nepal*
Patricia F Lalor, *Birmingham*
Ming Li, *New Orleans*
Margaret Lutze, *Chicago*
Jing-Yun Ma, *Beijing*
Daniel Markovich, *Brisbane*
Sabine Mihm, *Göttingen*
Francesco Negro, *Genève*
Bernardino Rampone, *Siena*
Richard A Rippe, *Chapel Hill*
Stephen E Roberts, *Swansea*
Ross C Smith, *Sydney*
Seng-Lai Tan, *Seattle*
Xian-Lin Wang, *Beijing*
Eddie Wisse, *Keerbergen*
Daniel Lindsay Worthley, *Bedford*
Li-Hong Zhu, *Beijing*

COPY EDITORS
Gianfranco D Alpini, *Temple*
Sujit Kumar Bhattacharya, *Kolkata*
Filip Braet, *Sydney*
Kirsteen N Browning, *Baton Rouge*
Radha K Dhiman, *Chandigarh*
John Frank Di Mari, *Texas*
Shannon S Glaser, *Temple*
Martin Hennenberg, *Bonn*
Eberhard Hildt, *Berlin*
Patricia F Lalor, *Birmingham*
Ming Li, *New Orleans*
Margaret Lutze, *Chicago*
MI Torrs, *Jaén*
Sri Prakash Misra, *Allahabad*
Giovanni Monteleone, *Rome*
Giovanni Musso, *Torino*
Valerio Nobili, *Rome*
Osman Cavit Ozdogan, *Istanbul*
Francesco Perri, *San Giovanni Rotondo*
Thierry Piche, *Nice*
Bernardino Rampone, *Siena*
Richard A Rippe, *Chapel Hill*
Ross C Smith, *Sydney*
Daniel Lindsay Worthley, *Bedford*
George Y Wu, *Farmington*
Jian Wu, *Sacramento*

EDITORIAL ASSISTANT
Yan Jiang, *Beijing*

PUBLISHED BY
The WJG Press

PRINTED BY
Printed in Beijing on acid-free paper by Beijing Kexin Printing House

COPYRIGHT
© 2007 Published by The WJG Press. All rights reserved; no part of this publication may be reproduced, stored in a retrieval system, or transmitted in any form or by any means, electronic, mechanical, photocopying, recording, or otherwise without the prior permission of The WJG Press. Authors are required to grant *WJG* an exclusive licence to publish. Print ISSN 1007-9327
CN 14-1219/R.

SPECIAL STATEMENT
All articles published in this journal represent the viewpoints of the authors except where indicated otherwise.

EDITORIAL OFFICE
World Journal of Gastroenterology,
The WJG Press, Apartment 1066 Yishou Garden, 58 North Langxinzhuang Road, PO Box 2345, Beijing 100023, China
Telephone: +86-10-85381892
Fax: +86-10-85381893
E-mail: wjg@wjgnet.com
http://www.wjgnet.com

SUBSCRIPTION AND AUTHOR REPRINTS
Jing Wang
The WJG Press, Apartment 1066 Yishou Garden, 58 North Langxinzhuang Road, PO Box 2345, Beijing 100023, China
Telephone: +86-10-85381892
Fax: +86-10-85381893
E-mail: j.wang@wjgnet.com
http://www.wjgnet.com

SUBSCRIPTION INFORMATION
Institutional Price 2007: USD 1500.00
Personal Price 2007: USD 700.00

INSTRUCTIONS TO AUTHORS
Full instructions are available online at http://www.wjgnet.com/wjg/help/instructions.jsp. If you do not have web access please contact the editorial office.

PO Box 2345, Beijing 100023, China
www.wjgnet.com
wjg@wjgnet.com

World J Gastroenterol 2007 January 14; 13(2): 165-169
World Journal of Gastroenterology ISSN 1007-9327
© 2007 The WJG Press. All rights reserved.

EDITORIAL

Role of endosonography in non-malignant pancreatic diseases

Kyung W Noh, Surakit Pungpapong, Massimo Raimondo

Kyung W Noh, Surakit Pungpapong, Massimo Raimondo, Division of Gastroenterology and Hepatology, Mayo Clinic College of Medicine, Jacksonville, FL, United States
Correspondence to: Massimo Raimondo, MD, FACG, Associate Professor of Medicine, Mayo Clinic College of Medicine, 4500 San Pablo Road, Jacksonville, FL 32224, United States. raimondo.massimo@mayo.edu
Telephone: +1-904-9536982 Fax: +1-904-9537260
Received: 2006-07-25 Accepted: 2006-10-05

Abstract

Endoscopic ultrasound (EUS) has emerged as a valuable tool in the evaluation of benign and malignant pancreatic diseases. The ability to obtain high quality images and perform fine-needle aspiration (FNA) has led EUS to become the diagnostic test of choice when evaluating the pancreas. This article will review the role of EUS in benign pancreatic diseases.

© 2007 The WJG Press. All rights reserved.

Key words: Endosonography; Chronic pancreatitis; Pancreatic cyst

Noh KW, Pungpapong S, Raimondo M. Role of endosonography in non-malignant pancreatic diseases. *World J Gastroenterol* 2007; 13(2): 165-169

http://www.wjgnet.com/1007-9327/13/165.asp

INTRODUCTION

Endoscopic ultrasound (EUS) was developed in part to better evaluate the pancreas. As the ultrasound probe lies in close proximity of the pancreas, high quality images can be obtained and FNA can be performed under ultrasound guidance. EUS is considered safer and less invasive than endoscopic retrograde pancreatography (ERP). Thus, EUS is an important diagnostic test when evaluating the pancreas, especially in the setting of benign pancreatic diseases.

CHRONIC PANCREATITIS

EUS appearance

The diagnosis of chronic pancreatitis *via* EUS is based on parenchymal and ductal criteria on examination of the pancreas. The presence of 5 or more criteria is generally considered highly suggestive or diagnostic of chronic pancreatitis and the presence of 2 or less criteria generally rules out the diagnosis of chronic pancreatitis.

To make the EUS diagnosis of chronic pancreatitis, one must understand the "normal" sonographic features of the pancreas. Several features were initially established by standard transabdominal ultrasound examinations of the pancreas. A "normal pancreas" was determined through studies such as that of Ikeda *et al*[1] who reported features of the pancreas in a large screening program in Japan. The pancreatic parenchyma in the absence of disease should appear homogeneous and have a "salt and pepper" appearance (Figure 1). The pancreatic duct should be seen as a smooth tubular structure coursing through the center of the pancreas. Side branches should not be visible.

The features of chronic pancreatitis can be divided into those that pertain to the parenchyma and the duct. These have been previously described by Lees[2,3] and Wiersema[4]. The parenchymal features include: hyperechogenic foci, hyperechogenic strands, lobulation, cysts, and calcifications; the ductal features include: main duct dilation, main duct irregularity, hyperechogenic main duct margins, and visible side branch ducts (Table 1).

Hyperechogenic foci and strands are bright echoes or string-like structures that may correlate histologically with thickened fibrous deposits[5]. These findings can be seen in patients with a normal pancreas, especially in older individuals. When hyperechogenic strands form a distinct "lobule", this is called lobulation (Figure 2). The pancreas thus appears inhomogeneous. This feature is more strongly associated with chronic pancreatitis as compared to hyperechogenic foci and strands alone. Calcifications of the pancreas are seen as hyperechoic or bright areas with acoustic shadowing. This feature is almost pathognomonic of chronic pancreatitis. Cysts are anechoic round or oval structures. Pancreatic cysts will be discussed further in the later sections of this article.

The size of a normal pancreatic duct is considered to be less than 3 mm in the head, 2 mm in the body and 1 mm in the tail of the pancreas. A larger duct is considered to be abnormal except in older patients when found as an isolated finding. An irregular duct correlates with focal dilation and narrowing of the main pancreatic duct. If a side branch is visible, this is considered a feature of chronic pancreatitis.

The threshold for EUS diagnosis of chronic pancreatitis can be varied. A lower threshold such as greater than 3 criteria will produce a high sensitivity, but a low specificity. By contrast, using a higher threshold such as greater than 5 criteria will produce a low sensitivity and a high specificity. Thus, if the purpose of the examination

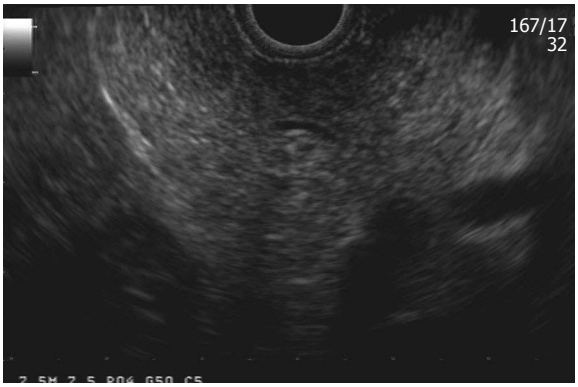

Figure 1 Normal pancreas.

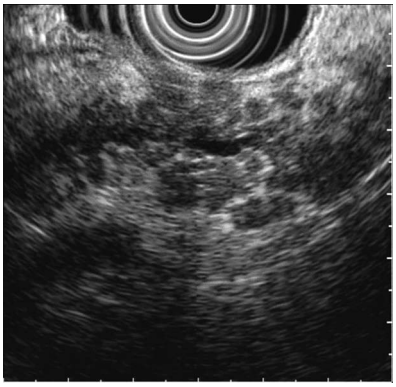

Figure 2 Lobular pancreas.

Table 1 Features of chronic pancreatitis

EUS criteria	Appearance	Histological correlate
Hyperechoic foci	Small distinct focus of bright echo	Focal fibrosis
Hyperechoic strands	Small string like bright echo	Bridging fibrosis
Lobularity	Rounded homogenous areas separated by hyperechoic strands	Fibrosis, glandular atrophy
Cyst	Abnormal anechoic round or oval structure	Cysts, pseudocyst
Calcification	Hyperechoic lesion with acoustic shadowing	Parenchymal calcification
Ductal dilation	> 3 mm in head, > 2 mm in body, > 1 mm in tail	Duct dilation
Side branch dilation	Small anechoic structure outside the main pancreatic duct	Side branch dilation
Duct irregularity	Coarse uneven outline of the duct	Focal dilation, narrowing
Hyperechoic duct margins	Hyperechoic margins of the main pancreatic duct	Periductal fibrosis

is to exclude disease, a low threshold should be used. However, if the purpose is to establish the diagnosis chronic pancreatitis, a higher threshold should be used.

Another important fact is that not all factors are equal when diagnosing chronic pancreatitis. The features of lobulation and calcification are suggestive of chronic pancreatitis even in the absence of other criteria. As mentioned earlier, some features such as a dilated duct can be a "normal" finding in older individuals[1]. Currently, there is no accepted scoring system to take these factors into consideration.

Recent experimental evidence suggests the complementary role of increased levels of an inflammatory mediator such as the interleukin 8 (IL-8) in pancreatic juice and EUS to diagnose chronic pancreatitis[6]. In this study, the specificity of the combination of tests (both increased pancreatic juice levels of IL-8 and abnormal EUS) reached 100%. Until these data are confirmed in larger studies, clinical judgment must be used to make a diagnosis of chronic pancreatitis.

The lack of a gold standard for diagnosis other than histology has pressed some investigators to explore the role of EUS-FNA in chronic pancreatitis. Hollerbach *et al*[7] performed EUS-FNA in 27 patients with different degrees of severity (as measured by ERP criteria). EUS was 97% sensitive but only 60% specific for the diagnosis of chronic pancreatitis. The only advantage of EUS-FNA in this study was represented by an increased negative predictive value. Few patients developed self-limited abdominal pain after the procedure, but no major complications were observed.

More recently, DeWitt *et al*[8] published their experience with EUS-FNA using the trucut needle which provides a core biopsy of the pancreas for histology. The results were compared with EUS and ERP. The authors observed poor agreement between EUS and EUS with trucut biopsy and only fair agreement between ERP and EUS with trucut biopsy. Therefore, the results of these studies induce caution when considering EUS-FNA (including the trucut needle) to diagnose chronic pancreatitis.

Conversely, EUS with trucut biopsy may have a significant role when considering the diagnosis of autoimmune chronic pancreatitis. Though the most characteristic endosonographic finding of this condition is diffuse pancreatic parenchyma enlargement (so-called sausage shape), there may be overlap with the non-autoimmune form of the disease or with cases of a pseudotumorous pancreatitis. Levy *et al*[9] reported their experience on 19 patients with autoimmune pancreatitis. In 10 patients who had EUS-FNA, the material retrieved was not adequate for the cytopathologist to make the diagnosis. However, the combination of the trucut needle and the immunohistochemistry staining for IgG 4 allowed the Authors to reach the correct final diagnosis of chronic autoimmune pancreatitis in virtually all patients. The authors concluded that though the EUS with trucut helps to make the diagnosis of autoimmune pancreatitis, this condition has still a low prevalence and a high suspicion of the disease with appropriate clinical presentation is necessary.

PANCREATIC CYSTS

EUS appearance

Improved imaging techniques and more frequent imaging of the abdomen has led to increased discovery of pancreatic cysts. These cysts pose a diagnostic and therapeutic challenge as the pathology ranges from benign pseudocysts to malignant cystic neoplasms. EUS plays an important role in the diagnosis and management of pancreatic cysts as allows for high quality images and the ability to perform fine needle aspiration.

Pseudocysts account for approximately 90% of pancreatic cystic lesions. Serous cystadenomas (SCA), mucinous cystadenomas (MCA) and intraductal papillary mucinous neoplasms (IPMN) account for the majority of the remaining 10% of cysts. Pseudocysts and SCA have little or no malignant potential as opposed to MCA and IPMN which are potentially malignant or malignant. Thus, it is important to identify mucinous cystic lesions.

Pseudocysts are inflammatory fluid collections that arise in the setting of acute or chronic pancreatitis. These cysts are anechoic, thick walled structures. Septations are rare and regional inflammatory lymph nodes may be seen. Aspiration of cyst fluid will reveal dark, thin fluid containing inflammatory cells and high levels of amylase.

SCA are benign cystic lesions of the pancreas[10] with the exception of a few case reports[11-13]. They have a female predilection and are most commonly discovered in the 7th decade of life[10,14,15]. These cysts are generally microcystic, but solid and macrocystic variants have been described[16-19]. This leads to a honeycomb appearance in cross-section. Central or "sunburst" calcification is considered pathognomonic, but is found in less than 20% of cases[15,20]. Cytology obtained from EUS guided FNA of these cysts is often non-diagnostic[21]. However, when an adequate sample is obtained, this will reveal cuboidal cells without the presence of mucin.

MCA are generally macrocystic, composed of a small number of discrete compartments greater than 2 cm in size[15]. The septations are thick, irregular and occasionally a peripheral area of calcification is present[22]. It has a female predilection, mostly present in the body-tail region of the pancreas and occur most commonly in the 5th to 7th decade of life[15,20,23]. The presence of mural nodules is suggestive of invasive carcinoma. The cyst fluid of MCA is viscous and clear. Cytology will reveal mucin rich fluid with columnar mucinous cells[15].

The EUS appearance of IPMN includes segmental or diffuse dilation of the main pancreatic duct or multiple pancreatic cysts that arise from the branch ducts of the main pancreatic duct. There is an equal or slightly higher incidence of IPMNs among males than in females. The peak incidence is in the 6th and 7th decade of life[15,24]. Like MCA, the cyst fluid is viscous, clear and will contain mucinous epithelial cells[15].

Cyst fluid analysis

Cyst fluid analysis of tumor markers has been studied to differentiate among benign and pre-malignant pancreatic cysts. In the Cooperative Pancreatic Cyst Study, the authors compared the findings of pancreatic cyst fluid of one hundred twelve patients obtained *via* EUS-FNA to surgical histology. EUS morphology, fluid cytology and cystic fluid tumor markers were evaluated. The results demonstrated that cyst fluid CEA levels (optimal cut-off 192 ng/mL) provided the greatest accuracy in differentiating mucinous versus non-mucinous pancreatic cysts. In addition, the accuracy of cyst fluid CEA was higher than that of EUS morphology, cyst fluid cytology or any combination of tests[25]. However, cyst fluid tumor marker values alone cannot definitively discriminate between mucinous and non-mucinous pancreatic cysts as there is overlap of CEA levels in these cysts[25,26].

New techniques

Trucut biopsy of the pancreatic cyst wall has been investigated as a possible method of diagnosing pancreatic cysts. Levy *et al*[27] performed EUS guided trucut biopsies (EUS-TCB) in ten patients. In seven patients, a diagnosis was established and no complications were reported. Although promising, EUS-TCB can be difficult to perform in the head of the pancreas given the risk of puncturing surrounding vasculature. In addition, the curvature of the scope may not allow for effective firing of the biopsy needle.

The role of pancreatic cyst fluid molecular analysis in predicting the pathology of the pancreatic cysts has been investigated. Khalid *et al*[28] analyzed pancreatic cystic fluid obtained *via* EUS-FNA in thirty-six patients with confirmed surgical histology. The authors hypothesized that polymerase chain reaction (PCR) amplification of DNA from whole or lysed cells shed into the cyst fluid may be predictive of cyst pathology. A high level of mutational damage would predict an underlying malignancy. In addition, as malignant cysts would have high cell turnover, cyst fluid DNA content may be higher in malignant cysts. Ten of the eleven malignant cysts carried multiple mutations as compared to no mutations in all ten benign cysts. The total amount of DNA in the malignant cysts was significantly higher than in the benign cysts.

INTERVENTIONAL EUS

Celiac plexus block

Pain associated with chronic pancreatitis can be difficult to control[29]. Often narcotic pain medications are required, but these are associated with significant adverse effects including constipation, nausea, vomiting and dependence. As pancreatic pain is mainly transmitted through the celiac plexus, celiac plexus neurolysis or block has been employed to manage pain related to pancreatic cancer or chronic pancreatitis. Initially, this was performed surgically or percutaneously. EUS-guided celiac plexus neurolysis was introduced by Wiersema *et al*[30] which was found to be as effective as the surgical or percutaneous approaches for the management of pancreatic cancer related pain. This technique was applied to manage pain from chronic pancreatitis[31,32]. Gress *et al*[31] reported a series of ninety patients with chronic pancreatitis who underwent EUS-guided celiac plexus block using Bupivacaine and Triamcinolone. Fifty-five percent of patients reported

a decrease in pain symptoms at 4 and 8 wk. A smaller percentage of patients experienced pain relief at 12 and 24 wk. The study was limited by a lack of a placebo arm which allows for potential bias. The use of celiac plexus block for the management of chronic pancreatitis pain remains uncertain and further studies are necessary.

Drainage of pseudocyst

Pancreatic pseudocysts may develop as sequela of acute or chronic pancreatitis. They can be asymptomatic and often resolve with time. However, when they become symptomatic or enlarge to greater than 6 cm in size, drainage is indicated. Traditionally, drainage of pseudocysts was performed surgically. However, percutaneous and endoscopic techniques have gained favor given the mortality and morbidity of surgery. The location of puncture for transgastric and transduodenal drainage of pseudocysts was determined by the bulge caused by the pseudocyst into the lumen. In the absence of a bulge, puncture of the cyst was a "blind" process increasing the risk of perforation and hemorrhage[33,34]. EUS allows for transgastric or transduodenal drainage of the pseudocyst under real time ultrasound guidance and thus minimizes the risk of complications. Various techniques have been described in the literature[34-42].

CONCLUSIONS

EUS is an essential tool in evaluating benign pancreatic diseases. Chronic pancreatitis and cystic lesions of the pancreas pose a diagnostic challenge. EUS carries an advantage over CT scans and endoscopic retrograde pancreatography in the diagnosis of chronic pancreatitis as it has the ability to detect parenchymal changes evident in early chronic pancreatitis. In the cases of pancreatic cysts, EUS allows for direct sampling of cyst fluid under ultrasound guidance to differentiate between cystic lesions of the pancreas. Overall, the ability to obtain important information regarding the pancreas through high quality images and FNA in a relatively safe manner is the main advantage of EUS.

REFERENCES

1 **Ikeda M**, Sato T, Morozumi A, Fujino MA, Yoda Y, Ochiai M, Kobayashi K. Morphologic changes in the pancreas detected by screening ultrasonography in a mass survey, with special reference to main duct dilatation, cyst formation, and calcification. *Pancreas* 1994; **9**: 508-512

2 **Lees WR**. Endoscopic ultrasonography of chronic pancreatitis and pancreatic pseudocysts. *Scand J Gastroenterol Suppl* 1986; **123**: 123-129

3 **Lees WR**, Vallon AG, Denyer ME, Vahl SP, Cotton PB. Prospective study of ultrasonography in chronic pancreatic disease. *Br Med J* 1979; **1**: 162-164

4 **Wiersema MJ**, Hawes RH, Lehman GA, Kochman ML, Sherman S, Kopecky KK. Prospective evaluation of endoscopic ultrasonography and endoscopic retrograde cholangiopancreatography in patients with chronic abdominal pain of suspected pancreatic origin. *Endoscopy* 1993; **25**: 555-564

5 **Sahai AV**. EUS and chronic pancreatitis. *Gastrointest Endosc* 2002; **56**: S76-S81

6 **Pungpapong S**, Noh KW, Al-Haddad M, Wallace MB, Woodward TA, Raimondo M. Combined pancreatic juice IL-8 concentration and EUS are highly predictive to diagnosis chronic pancreatitis. *Gastroenterology* 2006; **130**: A-13

7 **Hollerbach S**, Klamann A, Topalidis T, Schmiegel WH. Endoscopic ultrasonography (EUS) and fine-needle aspiration (FNA) cytology for diagnosis of chronic pancreatitis. *Endoscopy* 2001; **33**: 824-831

8 **DeWitt J**, McGreevy K, LeBlanc J, McHenry L, Cummings O, Sherman S. EUS-guided Trucut biopsy of suspected nonfocal chronic pancreatitis. *Gastrointest Endosc* 2005; **62**: 76-84

9 **Levy MJ**, Reddy RP, Wiersema MJ, Smyrk TC, Clain JE, Harewood GC, Pearson RK, Rajan E, Topazian MD, Yusuf TE, Chari ST, Petersen BT. EUS-guided trucut biopsy in establishing autoimmune pancreatitis as the cause of obstructive jaundice. *Gastrointest Endosc* 2005; **61**: 467-472

10 **Pyke CM**, van Heerden JA, Colby TV, Sarr MG, Weaver AL. The spectrum of serous cystadenoma of the pancreas. Clinical, pathologic, and surgical aspects. *Ann Surg* 1992; **215**: 132-139

11 **Abe H**, Kubota K, Mori M, Miki K, Minagawa M, Noie T, Kimura W, Makuuchi M. Serous cystadenoma of the pancreas with invasive growth: benign or malignant? *Am J Gastroenterol* 1998; **93**: 1963-1966

12 **Fujii H**, Kubo S, Hirohashi K, Kinoshita H, Yamamoto T, Wakasa K. Serous cystadenoma of the pancreas with atypical cells. Case report. *Int J Pancreatol* 1998; **23**: 165-169

13 **Ohta T**, Nagakawa T, Itoh H, Fonseca L, Miyazaki I, Terada T. A case of serous cystadenoma of the pancreas with focal malignant changes. *Int J Pancreatol* 1993; **14**: 283-289

14 **Fernández-del** Castillo C, Warshaw AL. Cystic tumors of the pancreas. *Surg Clin North Am* 1995; **75**: 1001-1016

15 **Brugge WR**, Lauwers GY, Sahani D, Fernandez-del Castillo C, Warshaw AL. Cystic neoplasms of the pancreas. *N Engl J Med* 2004; **351**: 1218-1226

16 **Hashimoto M**, Watanabe G, Miura Y, Matsuda M, Takeuchi K, Mori M. Macrocystic type of serous cystadenoma with a communication between the cyst and pancreatic duct. *J Gastroenterol Hepatol* 2001; **16**: 836-838

17 **Lewandrowski K**, Warshaw A, Compton C. Macrocystic serous cystadenoma of the pancreas: a morphologic variant differing from microcystic adenoma. *Hum Pathol* 1992; **23**: 871-875

18 **Sperti C**, Pasquali C, Perasole A, Liessi G, Pedrazzoli S. Macrocystic serous cystadenoma of the pancreas: clinicopathologic features in seven cases. *Int J Pancreatol* 2000; **28**: 1-7

19 **Brugge WR**. Evaluation of pancreatic cystic lesions with EUS. *Gastrointest Endosc* 2004; **59**: 698-707

20 **Warshaw AL**, Compton CC, Lewandrowski K, Cardenosa G, Mueller PR. Cystic tumors of the pancreas. New clinical, radiologic, and pathologic observations in 67 patients. *Ann Surg* 1990; **212**: 432-443; discussion 444-445

21 **Brugge WR**. The role of EUS in the diagnosis of cystic lesions of the pancreas. *Gastrointest Endosc* 2000; **52**: S18-S22

22 **Balci NC**, Semelka RC. Radiologic features of cystic, endocrine and other pancreatic neoplasms. *Eur J Radiol* 2001; **38**: 113-119

23 **Sarr MG**, Carpenter HA, Prabhakar LP, Orchard TF, Hughes S, van Heerden JA, DiMagno EP. Clinical and pathologic correlation of 84 mucinous cystic neoplasms of the pancreas: can one reliably differentiate benign from malignant (or premalignant) neoplasms? *Ann Surg* 2000; **231**: 205-212

24 **Kimura W**, Sasahira N, Yoshikawa T, Muto T, Makuuchi M. Duct-ectatic type of mucin producing tumor of the pancreas-new concept of pancreatic neoplasia. *Hepatogastroenterology* 1996; **43**: 692-709

25 **Brugge WR**, Lewandrowski K, Lee-Lewandrowski E, Centeno BA, Szydlo T, Regan S, del Castillo CF, Warshaw AL. Diagnosis of pancreatic cystic neoplasms: a report of the cooperative pancreatic cyst study. *Gastroenterology* 2004; **126**: 1330-1336

26 **Frossard JL**, Amouyal P, Amouyal G, Palazzo L, Amaris J, Soldan M, Giostra E, Spahr L, Hadengue A, Fabre M. Performance of endosonography-guided fine needle aspiration and biopsy in the diagnosis of pancreatic cystic lesions. *Am J Gastroenterol* 2003; **98**: 1516-1524

27 **Levy MJ**, Smyrk TC, Reddy RP, Clain JE, Harewood GC, Kendrick ML, Pearson RK, Petersen BT, Rajan E, Topazian MD, Wang KK, Wiersema MJ, Yusuf TE, Chari ST. Endoscopic ultrasound-guided trucut biopsy of the cyst wall for diagnosing cystic pancreatic tumors. *Clin Gastroenterol Hepatol* 2005; **3**: 974-979
28 **Khalid A**, McGrath KM, Zahid M, Wilson M, Brody D, Swalsky P, Moser AJ, Lee KK, Slivka A, Whitcomb DC, Finkelstein S. The role of pancreatic cyst fluid molecular analysis in predicting cyst pathology. *Clin Gastroenterol Hepatol* 2005; **3**: 967-973
29 **Lankisch PG**. Natural course of chronic pancreatitis. *Pancreatology* 2001; **1**: 3-14
30 **Wiersema MJ**, Wiersema LM. Endosonography-guided celiac plexus neurolysis. *Gastrointest Endosc* 1996; **44**: 656-662
31 **Gress F**, Schmitt C, Sherman S, Ciaccia D, Ikenberry S, Lehman G. Endoscopic ultrasound-guided celiac plexus block for managing abdominal pain associated with chronic pancreatitis: a prospective single center experience. *Am J Gastroenterol* 2001; **96**: 409-416
32 **Gress F**, Schmitt C, Sherman S, Ikenberry S, Lehman G. A prospective randomized comparison of endoscopic ultrasound- and computed tomography-guided celiac plexus block for managing chronic pancreatitis pain. *Am J Gastroenterol* 1999; **94**: 900-905
33 **Cremer M**, Deviere J, Engelholm L. Endoscopic management of cysts and pseudocysts in chronic pancreatitis: long-term follow-up after 7 years of experience. *Gastrointest Endosc* 1989; **35**: 1-9
34 **Sahel J**, Bastid C, Pellat B, Schurgers P, Sarles H. Endoscopic cystoduodenostomy of cysts of chronic calcifying pancreatitis: a report of 20 cases. *Pancreas* 1987; **2**: 447-453
35 **Binmoeller KF**, Seifert H, Soehendra N. Endoscopic pseudocyst drainage: a new instrument for simplified cystoenterostomy. *Gastrointest Endosc* 1994; **40**: 112
36 **Gerolami R**, Giovannini M, Laugier R. Endoscopic drainage of pancreatic pseudocysts guided by endosonography. *Endoscopy* 1997; **29**: 106-108
37 **Giovannini M**, Bernardini D, Seitz JF. Cystogastrotomy entirely performed under endosonography guidance for pancreatic pseudocyst: results in six patients. *Gastrointest Endosc* 1998; **48**: 200-203
38 **Giovannini M**, Pesenti C, Rolland AL, Moutardier V, Delpero JR. Endoscopic ultrasound-guided drainage of pancreatic pseudocysts or pancreatic abscesses using a therapeutic echo endoscope. *Endoscopy* 2001; **33**: 473-477
39 **Grimm H**, Binmoeller KF, Soehendra N. Endosonography-guided drainage of a pancreatic pseudocyst. *Gastrointest Endosc* 1992; **38**: 170-171
40 **Seifert H**, Dietrich C, Schmitt T, Caspary W, Wehrmann T. Endoscopic ultrasound-guided one-step transmural drainage of cystic abdominal lesions with a large-channel echo endoscope. *Endoscopy* 2000; **32**: 255-259
41 **Seifert H**, Faust D, Schmitt T, Dietrich C, Caspary W, Wehrmann T. Transmural drainage of cystic peripancreatic lesions with a new large-channel echo endoscope. *Endoscopy* 2001; **33**: 1022-1026
42 **Wiersema MJ**. Endosonography-guided cystoduodenostomy with a therapeutic ultrasound endoscope. *Gastrointest Endosc* 1996; **44**: 614-617

S- Editor Liu Y **L- Editor** Alpini GD **E- Editor** Lu W

PO Box 2345, Beijing 100023, China
www.wjgnet.com
wjg@wjgnet.com

World J Gastroenterol 2007 January 14; 13(2): 170-174
World Journal of Gastroenterology ISSN 1007-9327
© 2007 The WJG Press. All rights reserved.

EDITORIAL

Pancreatitis-associated protein: From a lectin to an anti-inflammatory cytokine

Daniel Closa, Yoshiharu Motoo, Juan L Iovanna

Daniel Closa, Department of Experimental Pathology, IIBB-CSIC, IDIBAPS, Barcelona, Spain
Yoshiharu Motoo, Department of Medical Oncology, Kanazawa Medical University, Ishikawa, Japan
Juan L Iovanna, INSERM U.624, Stress Cellulaire, Marseille, France
Correspondence to: Dr. Daniel Closa, Experimental Pathology Dept., IIBB-CSIC, c/ Rosselló 161, 7º, Barcelona 08036, Spain. dcabam@iibb.csic.es
Telephone: +34-93-3638307 Fax: +34-93-3638301
Received: 2006-07-07 Accepted: 2006-10-12

Abstract

Pancreatitis-associated protein (PAP) was discovered in the pancreatic juice of rats with acute pancreatitis. PAP is a 16 kDa secretory protein structurally related to the C-type lectins although classical lectin-related function has not been reported yet. Then, it was demonstrated that PAP expression may be activated in some tissues in a constitutive or injury- and inflammation-induced manner. More recently, it has been found that PAP acts as an anti-inflammatory factor *in vitro* and *in vivo*. PAP expression can be induced by several pro- and anti-inflammatory cytokines and by itself through a JAK/STAT3-dependent pathway. PAP is able to activate the expression of the anti-inflammatory factor SOCS3 through the JAK/STAT3-dependent pathway. The JAK/STAT3/SOCS3 pathway seems to be a common point between PAP and several cytokines. Therefore, it is reasonable to propose that PAP is a new anti-inflammatory cytokine.

© 2007 The WJG Press. All rights reserved.

Key words: Pancreatitis-associated protein; Pancreatitis; Janus kinases; STAT3; SOCS3; Anti-inflammatory; Lectin

Closa D, Motoo Y, Iovanna JL. Pancreatitis-associated protein: From a lectin to an anti-inflammatory cytokine. *World J Gastroenterol* 2007; 13(2): 170-174

http://www.wjgnet.com/1007-9327/13/170.asp

INTRODUCTION

In 1984, Keim and co-workers reported the presence of a new protein in pancreatic juice of rats after induction of acute pancreatitis[1]. This secretory protein was absent in control rats but appeared early after induction of pancreatitis and remained over-expressed for the following 3-4 d. The protein was detected also in pancreas homogenate and in zymogen granules. Due to the relationship with the induction of pancreatitis, the protein was denominated "pancreatitis associated protein" or PAP. Four years later, Tachibana and colleagues described the peptide 23 as a protein from the rat pituitary gland, which synthesis was stimulated by the growth hormone-releasing hormone and inhibited by somatostatin[2] but its primary structure remained unresolved at the time. The sequence of PAP was deduced after cloning the corresponding mRNA from rat[3] and human pancreas[4]. Only four years later Katsumata and co-workers reported that in fact, peptide 23, identified in 1988, was identical to PAP[5]. Finally, Lasserre and colleagues found that the PAP mRNA was overexpressed in 7 of 29 hepatocellular carcinomas[6] and named the encoded protein HIP. Therefore, peptide 23, HIP and PAP are three names for the same protein. In this review we will call it PAP because it is the first name adopted for this protein.

In healthy pancreas, PAP is constitutively expressed in the α-cells of Langerhans islets[7]. By contrast, in the exocrine pancreas, PAP is only expressed when the acinar cells are harmed[4]. In fact, PAP expression is activated in pancreatic acinar cells in response to many injuries such as acute and chronic pancreatitis[4], hypoxia[8], toxins[9], diabetes[10], lipopolysaccharides[11], hypotransferrinaemia[12], and in the transplanted tissue[13]. However, its expression is not restricted to pancreatic tissue, and could be observed in several organs. This includes the intestine during chronic inflammatory diseases such as Crohn's disease and ulcerative colitis[14,15] and in animal models of inflammatory bowel disease (IBD)[16]. PAP is also expressed in the brain tissue of Alzheimer patients[17,18], in the luminal epithelial cells of the uterus[19] and in a sub-population of developing motoneurons and, after peripheral injury, in sensory neurons and motoneurons[20,21]. Moreover, PAP mRNA expression was found activated in about 80% of the pancreatic adenocarcinomas of ductal origin and in 30% of mucinous cystadenomas[22]. The levels of PAP mRNA expression correlated with nodal invasion, presence of distant metastases and short survival. Also, in some cases peritumoral regions overexpressed PAP[23], indicating that both tumor and peritumoral cells contribute to the high PAP serum level observed in patients with pancreatic cancer. In the liver, PAP was found strongly activated in about 30% of the primary hepatocarcinomas,

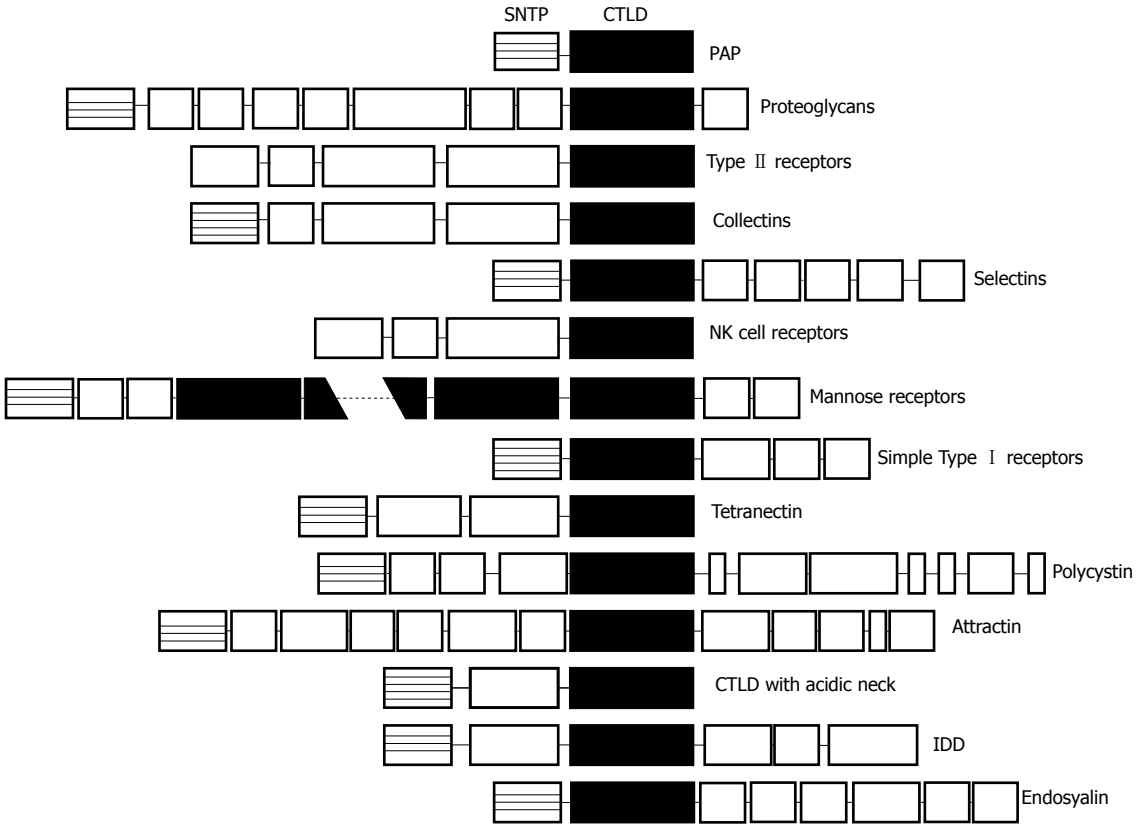

Figure 1 Schematic protein domains in the different C-type lectins. Sequences are aligned on the C-type lectin-like domain (CTLD). Note that PAP is the smallest protein member, containing only the CTLD linked to a short N-terminal peptide (SNTP).

but the forced expression of PAP in this organ does not induce tumor development[24].

PAP IS A LECTIN-RELATED PROTEIN

Computer analysis of the PAP sequence suggests a structural relationship with lectins[3]. Identities between PAP and the other animal and human lectins range from 16% to 26%. Homologous domain includes the conserved amino acids of the consensus carbohydrate binding domain of the Ca^{2+}-dependent lectins (C-type lectins) (Figure 1). However, initial attempts to characterize a carbohydrate binding activity, including erythrocyte agglutination or adsorption to affinity columns specific for different carbohydrates, failed[3]. The structural organization of the PAP gene reveals new clues to the evolutionary development of the lectin genes. The PAP coding sequence spans over six exons and the putative carbohydrate-recognition domain is encoded by exons Ⅳ, Ⅴ and Ⅵ. This gene organization suggests that PAP belongs to a new group of lectins which have evolved from the same carbohydrate-recognition domain ancestral precursor through a different process[25]. It is interesting to note that PAP is the smallest protein reported among the C-type lectins. In fact, it comprises a single carbohydrate-recognition domain linked to a signal peptide[26] whereas other C-type lectins contain the sugar-binding consensus combined with a variety of other protein domains which confer specific functions of lectins. In contrast, PAP does not have additional functional domains.

PAP IN PANCREATIC DISEASES

Early after its discovery it becomes clear that acinar cells of the pancreas are the main source of PAP in pathological situations. Using an experimental model of acute pancreatitis in rat, Morisset and co-workers found the induction of PAP and its localization in zymogen granules[27]. Bodeker and co-workers described the pattern of PAP up-regulation in exocrine pancreas during the progression of the disease[28]. The profiles obtained by Northern blot analysis with pancreatic RNAs, Western blot in pancreatic protein extracts and immunodetection are equivalent to that observed in human disease and in animal models. The absence of PAP in healthy pancreas and its strong induction observed during the early phase of the disease suggest that PAP could be a stress protein or an acute phase protein induced upon cell insult. This is of interest since pancreatic acute phase response, characterized by sudden changes in protein expression is a clear indicator of injury or infections in the pancreatic gland. Since PAP is overexpressed by pancreatic cells in response to cellular stress, it has been evaluated whether serum PAP could be an indicator of different pancreatic diseases. In an initial retrospective study[29], it has been suggested that PAP might be a useful serum marker in the following of acute pancreatitis. In particular, a continuous elevation of serum PAP concentrations indicates that pancreatitis is still in progress. Nevertheless, other studies revealed that despite severity of pancreatitis correlated with serum levels of PAP, the sensitivity of PAP did not allow distinguishing severe from mild acute pancreatitis, better than C reactive protein[30]. In the case of pancreatic cancer, PAP was also overexpressed and could be observed in malignant ductular structures in pancreatic carcinomas[22]. Other reports revealed that PAP was strongly expressed in acini adjacent to the invasive adenocarcinoma, suggesting that the main source of PAP release in the pancreatic

juice is acini[23]. Since overexpression of PAP significantly correlated with nodal involvement, distant metastasis, and short survival, it has been suggested that its expression in human pancreatic ductal adenocarcinoma could be an indicator of tumor aggressiveness[22].

PHYSIOLOGICAL FUNCTIONS OF PAP

The fact that PAP is secreted by pancreatic acinar cells into the pancreatic juice initially suggested a role for this protein in pancreatic juice homeostasis. Several data are in line with this. Pancreatic juice is supersaturated in $CaCO_3$ and, in the absence of physiological inhibitors, this salt will precipitate in crystal formation. Interestingly, lithostathine, another member of the PAP protein family, inhibits $CaCO_3$ crystal growth *in vitro*[31]. On the other hand, it has been shown that PAP can bind and aggregate several bacterial strains from the intestinal flora including Gram positive and Gram negative, aerobic and anaerobic bacteria, although without inhibiting their growth[3]. This fact suggests that PAP could act as an endogenous anti-bacterial agent that could play a protective role preventing infectious complications in acute pancreatitis. Another suggested function for PAP is related to the fact that PAP conferred significant resistance to apoptosis induced by TNFα[32] or by low doses of H_2O_2[33], indicating that during acute pancreatitis PAP generation could be part of a mechanism of pancreatic cell protection against apoptosis. This anti-apoptotic effect of PAP was also observed in liver in which PAP protects hepatocytes against TNFα-induced apoptosis[24]. An interesting role for PAP has also been observed in motoneurons. It has been reported that PAP expression is activated in developing and regenerating motoneurons[20]. This effect is related to ciliary neurotrophic factor (CNTF), which is an important survival factor for motoneurons. In cultured motoneurons, CNTF induces PAP expression which acts as an autocrine/paracrine neurotrophic factor in a subpopulation of motoneurons, by stimulating a survival pathway involving PI3 kinase, Akt kinase and NFκB[34]. Despite the obvious interest of these observations, it is difficult to link these effects with the enormous amount of PAP released by pancreas during acute pancreatitis or cellular stress. Consequently, other physiological functions, more closely related with pancreatic diseases, have been investigated.

PAP AS AN ANTI-INFLAMMATORY MEDIATOR

The initial indication that PAP could act as a modulat or of the inflammatory response has been provided by Heller and co-workers[35]. Using an *ex-vivo* model of lung perfusion, these authors observed that PAP reduces the severity of some features associated with N-formyl-methionyl-leucyl-phenyl-alanine (FMLP)-induced activation of leukocytes. This includes the generation of thromboxane B_2 and the tissue edema formation in the lung. Since PAP generation has been observed in diseases related with inflammatory processes (pancreatitis, Crohn's disease, etc.), it was speculated that PAP could act as a cell response to the inflammatory stress. This is in line with the fact that induction in the pancreas of an acute-phase response, in which PAP expression was activated, prior to triggering necrotizing pancreatitis, significantly improved the survival of the animals[36]. Studies demonstrated that the administration of anti-PAP antibodies in an experimental model of taurocholate-induced acute pancreatitis in rats was associated with increased inflammation in the pancreas, evidenced by more abundant necrosis, increased pancreatic myeloperoxidase (MPO) levels and more prominent neutrophil infiltration[37]. Similar results were observed in another study using PAP antisense oligodeoxyribonucle otides to block the expression of PAP prior to induction of pancreatitis. With this approach, pancreatitis-induced PAP expression was reduced by 55% and markers of inflammatory cell damage were increased. These include serum amylase activity, pancreas edema, serum C-reactive protein, leukocyte infiltration and fat necrosis. In addition, the expression of *IL-1α, IL-1β* and *IL-4* was increased in peripheral blood mononuclear cells[38]. Pre-treatment with PAP of the *in vitro* TNFα-stimulated macrophages results in a dose-dependent inhibition of *IL-6* and *TNFα* mRNA expression[37]. The inhibitory effect of PAP has been observed in different cell lines, including rat pancreatic acinar AR42J cells and human HT29 colon derived cells[39]. In these models, PAP prevented NFκB translocation/activation in response to TNFα, indicating that inhibition by PAP occurs, at least in part, upstream of NFκB pathway. It is of clinical interest that the anti-inflammatory effect of PAP could be observed in other organs than pancreas. For example, increased serum levels of PAP expression has been observed in IBD-affected patients and these levels correlated with clinical and endoscopic parameters. In addition, *ex vivo* experiments showed that intestinal PAP synthesis and secretion was increased in active IBD and correlated with endoscopic and histological severity of inflammatory lesions. Remarkably, PAP reduced the proinflammatory cytokines secretion of the incubation of intestinal mucosa from active Crohn's disease in a dose dependent manner[39]. Consequently, it could be suggested that the anti-inflammatory role of PAP is not restricted to the pancreas and could be a more general response of the epithelial cells against the inflammatory processes.

ANTI-INFLAMMATORY ACTIVITY OF PAP IS MEDIATED BY STAT3 ACTIVATION

The inhibitory effect of PAP on the pro-inflammatory NFκB pathway seems to be dependent on protein synthesis. This has been demonstrated in AR42J cells by using cycloheximide into the culture medium to prevent *de novo* protein synthesis[40]. As indicated above, TNFα induces overexpression of the *TNFα* gene itself and this autocrine loop could be blocked by PAP. However, PAP lost its ability when protein synthesis was inhibited by cycloheximide. This protein synthesis dependence to act as an anti-inflammatory factor shows similarities to IL-10 and IL-6, which depend in part on the synthesis of suppressor of cytokine signalling (SOCS) proteins[41,42]. Both IL-10 and IL-6 receptors are related to the JAK/STAT signal

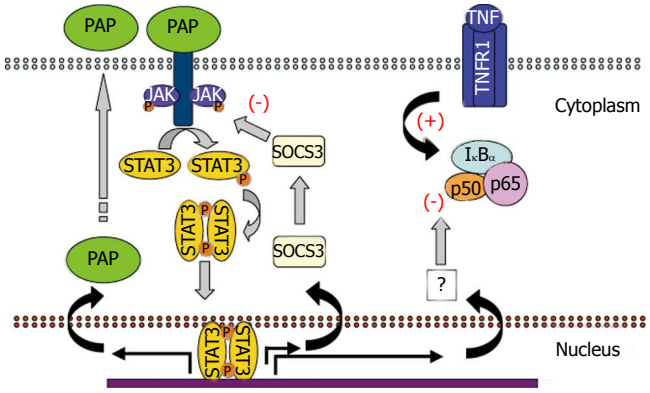

Figure 2 Anti-inflammatory pathway activated by PAP.

transduction pathways. Therefore, the relationship between PAP and JAK/STAT has also been evaluated. In a recent paper, it has been reported that PAP treatment of the AR42J cells results in a rapid and transient phosphorylation and nuclear translocation of STAT3 protein[40]. In addition, pre-treatment with JAK-specific inhibitors results in the blockage of the inhibitory effects induced by PAP. Finally, the PAP-dependent activation of STAT3 results in a strong activation of its gene target SOCS3 that in turn could be the mediator of the PAP anti-inflammatory effect. Altogether, these results indicate that PAP exerts their effects through the synthesis of a protein induced by the activation of the JAK/STAT signalling pathway. SOCS3 will be the best candidate.

PAP can be strongly induced by IL-6 and IL-10 and IL-10-related cytokines through a STAT3-mediated pathway. Interestingly, expression of PAP itself appears to be induced in pancreatic acinar cells by the presence of PAP in the medium. This is also related to the activation of STAT3 pathway since at least two functional STAT-responsible elements have been reported in the promoter of the PAP gene[43]. This self-induction suggests the existence of a positive feedback mechanism in pancreatic acinar cells *via* a PAP receptor and a cross-talk with other cytokines (Figure 2).

CONCLUDING REMARKS

PAP has been found as a 16 kDa secretory protein specifically induced in pancreas with acute pancreatitis. It has been demonstrated that PAP is activated in some tissues in a constitutive or injury- and inflammation-induced manner. PAP is structurally related to the C-type lectins although not classical lectin-related function has been reported. More recently, it has been found that PAP acts as an anti-inflammatory factor *in vitro* and *in vivo*. PAP expression can be induced by several pro- and anti-inflammatory cytokines and by itself through a JAK/STAT3-dependent pathway. PAP is able to activate the expression of the anti-inflammatory factor SOCS3 through the JAK/STAT3-dependent pathway. JAK/STAT3/SOCS3 pathway seems to be a common point between PAP and several cytokines. Therefore, it is reasonable to believe that PAP is a new anti-inflammatory cytokine.

REFERENCES

1 **Keim V**, Rohr G, Stöckert HG, Haberich FJ. An additional secretory protein in the rat pancreas. *Digestion* 1984; **29**: 242-249
2 **Tachibana K**, Marquardt H, Yokoya S, Friesen HG. Growth hormone-releasing hormone stimulates and somatostatin inhibits the release of a novel protein by cultured rat pituitary cells. *Mol Endocrinol* 1988; **2**: 973-978
3 **Iovanna J**, Orelle B, Keim V, Dagorn JC. Messenger RNA sequence and expression of rat pancreatitis-associated protein, a lectin-related protein overexpressed during acute experimental pancreatitis. *J Biol Chem* 1991; **266**: 24664-24669
4 **Orelle B**, Keim V, Masciotra L, Dagorn JC, Iovanna JL. Human pancreatitis-associated protein. Messenger RNA cloning and expression in pancreatic diseases. *J Clin Invest* 1992; **90**: 2284-2291
5 **Katsumata N**, Chakraborty C, Myal Y, Schroedter IC, Murphy LJ, Shiu RP, Friesen HG. Molecular cloning and expression of peptide 23, a growth hormone-releasing hormone-inducible pituitary protein. *Endocrinology* 1995; **136**: 1332-1339
6 **Lasserre C**, Christa L, Simon MT, Vernier P, Bréchot C. A novel gene (HIP) activated in human primary liver cancer. *Cancer Res* 1992; **52**: 5089-5095
7 **Christa L**, Carnot F, Simon MT, Levavasseur F, Stinnakre MG, Lasserre C, Thepot D, Clement B, Devinoy E, Brechot C. HIP/PAP is an adhesive protein expressed in hepatocarcinoma, normal Paneth, and pancreatic cells. *Am J Physiol* 1996; **271**: G993-G1002
8 **McKie AT**, Simpson RJ, Ghosh S, Peters TJ, Farzaneh F. Regulation of pancreatitis-associated protein (HIP/PAP) mRNA levels in mouse pancreas and small intestine. *Clin Sci (Lond)* 1996; **91**: 213-218
9 **Chen P**, Arias AE, Morisset J, Calvo E, Dagorn JC, Iovanna J, Bendayan M. Presence of pancreatitis-associated protein in pancreatic acinar cells of rats treated with chlorophenylalanine methyl ester. *Pancreas* 1996; **13**: 147-153
10 **Baeza N**, Sanchez D, Christa L, Guy-Crotte O, Vialettes B, Figarella C. Pancreatitis-associated protein (HIP/PAP) gene expression is upregulated in NOD mice pancreas and localized in exocrine tissue during diabetes. *Digestion* 2001; **64**: 233-239
11 **Vaccaro MI**, Calvo EL, Suburo AM, Sordelli DO, Lanosa G, Iovanna JL. Lipopolysaccharide directly affects pancreatic acinar cells: implications on acute pancreatitis pathophysiology. *Dig Dis Sci* 2000; **45**: 915-926
12 **Simpson RJ**, Deenmamode J, McKie AT, Raja KB, Salisbury JR, Iancu TC, Peters TJ. Time-course of iron overload and biochemical, histopathological and ultrastructural evidence of pancreatic damage in hypotransferrinaemic mice. *Clin Sci (Lond)* 1997; **93**: 453-462
13 **van der Pijl JW**, Boonstra JG, Barthellemy S, Smets YF, Hermans J, Bruijn JA, de Fijter JW, Daha MR, Dagorn JC. Pancreatitis-associated protein: a putative marker for pancreas graft rejection. *Transplantation* 1997; **63**: 995-1003
14 **Masciotra L**, Lechêne de la Porte P, Frigerio JM, Dusetti NJ, Dagorn JC, Iovanna JL. Immunocytochemical localization of pancreatitis-associated protein in human small intestine. *Dig Dis Sci* 1995; **40**: 519-524
15 **Dieckgraefe BK**, Stenson WF, Korzenik JR, Swanson PE, Harrington CA. Analysis of mucosal gene expression in inflammatory bowel disease by parallel oligonucleotide arrays. *Physiol Genomics* 2000; **4**: 1-11
16 **Lawrance IC**, Fiocchi C, Chakravarti S. Ulcerative colitis and Crohn's disease: distinctive gene expression profiles and novel susceptibility candidate genes. *Hum Mol Genet* 2001; **10**: 445-456
17 **Ozturk M**, de la Monte SM, Gross J, Wands JR. Elevated levels of an exocrine pancreatic secretory protein in Alzheimer disease brain. *Proc Natl Acad Sci USA* 1989; **86**: 419-423
18 **Duplan L**, Michel B, Boucraut J, Barthellémy S, Desplat-Jego S, Marin V, Gambarelli D, Bernard D, Berthézène P, Alescio-Lautier B, Verdier JM. Lithostathine and pancreatitis-

associated protein are involved in the very early stages of Alzheimer's disease. *Neurobiol Aging* 2001; **22**: 79-88

19 **Chakraborty C**, Vrontakis M, Molnar P, Schroedter IC, Katsumata N, Murphy LJ, Shiu RP, Friesen HG. Expression of pituitary peptide 23 in the rat uterus: regulation by estradiol. *Mol Cell Endocrinol* 1995; **108**: 149-154

20 **Livesey FJ**, O'Brien JA, Li M, Smith AG, Murphy LJ, Hunt SP. A Schwann cell mitogen accompanying regeneration of motor neurons. *Nature* 1997; **390**: 614-618

21 **Averill S**, Davis DR, Shortland PJ, Priestley JV, Hunt SP. Dynamic pattern of reg-2 expression in rat sensory neurons after peripheral nerve injury. *J Neurosci* 2002; **22**: 7493-7501

22 **Xie MJ**, Motoo Y, Iovanna JL, Su SB, Ohtsubo K, Matsubara F, Sawabu N. Overexpression of pancreatitis-associated protein (PAP) in human pancreatic ductal adenocarcinoma. *Dig Dis Sci* 2003; **48**: 459-464

23 **Rosty C**, Christa L, Kuzdzal S, Baldwin WM, Zahurak ML, Carnot F, Chan DW, Canto M, Lillemoe KD, Cameron JL, Yeo CJ, Hruban RH, Goggins M. Identification of hepatocarcinoma-intestine-pancreas/pancreatitis-associated protein I as a biomarker for pancreatic ductal adenocarcinoma by protein biochip technology. *Cancer Res* 2002; **62**: 1868-1875

24 **Simon MT**, Pauloin A, Normand G, Lieu HT, Mouly H, Pivert G, Carnot F, Tralhao JG, Brechot C, Christa L. HIP/PAP stimulates liver regeneration after partial hepatectomy and combines mitogenic and anti-apoptotic functions through the PKA signaling pathway. *FASEB J* 2003; **17**: 1441-1450

25 **Dusetti NJ**, Frigerio JM, Keim V, Dagorn JC, Iovanna JL. Structural organization of the gene encoding the rat pancreatitis-associated protein. Analysis of its evolutionary history reveals an ancient divergence from the other carbohydrate-recognition domain-containing genes. *J Biol Chem* 1993; **268**: 14470-14475

26 **Christa L**, Felin M, Morali O, Simon MT, Lasserre C, Brechot C, Sève AP. The human HIP gene, overexpressed in primary liver cancer encodes for a C-type carbohydrate binding protein with lactose binding activity. *FEBS Lett* 1994; **337**: 114-118

27 **Morisset J**, Iovanna J, Grondin G. Localization of rat pancreatitis-associated protein during bile salt-induced pancreatitis. *Gastroenterology* 1997; **112**: 543-550

28 **Bödeker H**, Fiedler F, Keim V, Dagorn JC, Iovanna JL. Pancreatitis-associated protein is upregulated in mouse pancreas during acute pancreatitis. *Digestion* 1998; **59**: 186-191

29 **Iovanna JL**, Keim V, Nordback I, Montalto G, Camarena J, Letoublon C, Lévy P, Berthézène P, Dagorn JC. Serum levels of pancreatitis-associated protein as indicators of the course of acute pancreatitis. Multicentric Study Group on Acute Pancreatitis. *Gastroenterology* 1994; **106**: 728-734

30 **Kemppainen E**, Sand J, Puolakkainen P, Laine S, Hedström J, Sainio V, Haapiainen R, Nordback I. Pancreatitis associated protein as an early marker of acute pancreatitis. *Gut* 1996; **39**: 675-678

31 **Multigner L**, Sarles H, Lombardo D, De Caro A. Pancreatic stone protein. II. Implication in stone formation during the course of chronic calcifying pancreatitis. *Gastroenterology* 1985; **89**: 387-391

32 **Malka D**, Vasseur S, Bödeker H, Ortiz EM, Dusetti NJ, Verrando P, Dagorn JC, Iovanna JL. Tumor necrosis factor alpha triggers antiapoptotic mechanisms in rat pancreatic cells through pancreatitis-associated protein I activation. *Gastroenterology* 2000; **119**: 816-828

33 **Ortiz EM**, Dusetti NJ, Vasseur S, Malka D, Bödeker H, Dagorn JC, Iovanna JL. The pancreatitis-associated protein is induced by free radicals in AR4-2J cells and confers cell resistance to apoptosis. *Gastroenterology* 1998; **114**: 808-816

34 **Nishimune H**, Vasseur S, Wiese S, Birling MC, Holtmann B, Sendtner M, Iovanna JL, Henderson CE. Reg-2 is a motoneuron neurotrophic factor and a signalling intermediate in the CNTF survival pathway. *Nat Cell Biol* 2000; **2**: 906-914

35 **Heller A**, Fiedler F, Schmeck J, Lück V, Iovanna JL, Koch T. Pancreatitis-associated protein protects the lung from leukocyte-induced injury. *Anesthesiology* 1999; **91**: 1408-1414

36 **Fiedler F**, Croissant N, Rehbein C, Iovanna JL, Dagorn JC, van Ackern K, Keim V. Acute-phase response of the rat pancreas protects against further aggression with severe necrotizing pancreatitis. *Crit Care Med* 1998; **26**: 887-894

37 **Vasseur S**, Folch-Puy E, Hlouschek V, Garcia S, Fiedler F, Lerch MM, Dagorn JC, Closa D, Iovanna JL. p8 improves pancreatic response to acute pancreatitis by enhancing the expression of the anti-inflammatory protein pancreatitis-associated protein I. *J Biol Chem* 2004; **279**: 7199-7207

38 **Zhang H**, Kandil E, Lin YY, Levi G, Zenilman ME. Targeted inhibition of gene expression of pancreatitis-associated proteins exacerbates the severity of acute pancreatitis in rats. *Scand J Gastroenterol* 2004; **39**: 870-881

39 **Gironella M**, Iovanna JL, Sans M, Gil F, Peñalva M, Closa D, Miquel R, Piqué JM, Panés J. Anti-inflammatory effects of pancreatitis associated protein in inflammatory bowel disease. *Gut* 2005; **54**: 1244-1253

40 **Folch-Puy E**, Granell S, Dagorn JC, Iovanna JL, Closa D. Pancreatitis-associated protein I suppresses NF-kappa B activation through a JAK/STAT-mediated mechanism in epithelial cells. *J Immunol* 2006; **176**: 3774-3779

41 **Berlato C**, Cassatella MA, Kinjyo I, Gatto L, Yoshimura A, Bazzoni F. Involvement of suppressor of cytokine signaling-3 as a mediator of the inhibitory effects of IL-10 on lipopolysaccharide-induced macrophage activation. *J Immunol* 2002; **168**: 6404-6411

42 **Croker BA**, Krebs DL, Zhang JG, Wormald S, Willson TA, Stanley EG, Robb L, Greenhalgh CJ, Förster I, Clausen BE, Nicola NA, Metcalf D, Hilton DJ, Roberts AW, Alexander WS. SOCS3 negatively regulates IL-6 signaling *in vivo*. *Nat Immunol* 2003; **4**: 540-545

43 **Dusetti NJ**, Ortiz EM, Mallo GV, Dagorn JC, Iovanna JL. Pancreatitis-associated protein I (PAP I), an acute phase protein induced by cytokines. Identification of two functional interleukin-6 response elements in the rat PAP I promoter region. *J Biol Chem* 1995; **270**: 22417-22421

S- Editor Liu Y **L- Editor** Zhu LH **E- Editor** Lu W

PO Box 2345, Beijing 100023, China
www.wjgnet.com
wjg@wjgnet.com

World J Gastroenterol 2007 January 14; 13(2): 175-191
World Journal of Gastroenterology ISSN 1007-9327
© 2007 The WJG Press. All rights reserved.

TOPIC HIGHLIGHT

Parimal Chowdhury, Professor, *Series Editors*

Early diabetic neuropathy: Triggers and mechanisms

Maxim Dobretsov, Dmitry Romanovsky, Joseph R Stimers

Maxim Dobretsov, Departments of Anesthesiology, Neurobiology and Developmental Sciences, University of Arkansas for Medical Sciences, 4301 West Markham Street, Little Rock, AR 72205, United States
Dmitry Romanovsky, Department of Anesthesiology, University of Arkansas for Medical Sciences, 4301 West Markham Street, Little Rock, AR 72205, United States
Joseph R Stimers, Department of Pharmacology and Toxicology, University of Arkansas for Medical Sciences, 4301 West Markham Street, Little Rock, AR 72205, United States
Supported by NIH National Institute of Diabetes and Digestive and Kidney Diseases, No. DK067248
Correspondence to: Maxim Dobretsov, Department of Anesthesiology, Slot 515, University of Arkansas for Medical Sciences, 4301 West Markham Street, Little Rock, AR 72205, United States. dobretsovmaxim@uams.edu
Telephone: +1-501-6031936 Fax: +1-501-6031951
Received: 2006-08-17 Accepted: 2006-09-26

Abstract

Peripheral neuropathy, and specifically distal peripheral neuropathy (DPN), is one of the most frequent and troublesome complications of diabetes mellitus. It is the major reason for morbidity and mortality among diabetic patients. It is also frequently associated with debilitating pain. Unfortunately, our knowledge of the natural history and pathogenesis of this disease remains limited. For a long time hyperglycemia was viewed as a major, if not the sole factor, responsible for all symptomatic presentations of DPN. Multiple clinical observations and animal studies supported this view. The control of blood glucose as an obligatory step of therapy to delay or reverse DPN is no longer an arguable issue. However, while supporting evidence for the glycemic hypothesis has accumulated, multiple controversies accumulated as well. It is obvious now that DPN cannot be fully understood without considering factors besides hyperglycemia. Some symptoms of DPN may develop with little, if any, correlation with the glycemic status of a patient. It is also clear that identification of these putative non-glycemic mechanisms of DPN is of utmost importance for our understanding of failures with existing treatments and for the development of new approaches for diagnosis and therapy of DPN. In this work we will review the strengths and weaknesses of the glycemic hypothesis, focusing on clinical and animal data and on the pathogenesis of early stages and triggers of DPN other than hyperglycemia.

© 2007 The WJG Press. All rights reserved.

Key words: Diabetes; Pre-diabetes; Neuropathy; Impaired glucose tolerance; Hyperglycemia; Insulinopenia; Insulin-resistance

Dobretsov M, Romanovsky D, Stimers JR. Early diabetic neuropathy: Triggers and mechanisms. *World J Gastroenterol* 2007; 13(2): 175-191

http://www.wjgnet.com/1007-9327/13/175.asp

INTRODUCTION

Diabetes mellitus is a complex of metabolic disorders associated with insufficiency of insulin secretion, insulin action or both, and is manifested by hyperglycemia[1-3]. Diabetes is diagnosed when fasting blood glucose exceeds 6.9 mmol/L, or casual or 2-h glucose in a glucose tolerance test exceeds 11 mmol/L[4]. Control of blood glucose in vertebrate organisms is accomplished essentially by the action of two pancreatic hormones, i.e., insulin and glucagon, with the participation of epinephrine, ACTH, growth hormone and glucocorticoids occurring under special circumstances, such as stress. Insulin is released by islet beta cells in response to an increase of blood glucose (usually after a meal). It suppresses glucose production and stimulates the uptake and storage of glucose in skeletal muscle and liver (Figure 1). It also suppresses lipogenesis in the fat tissue and stimulates amino-acid synthesis in skeletal muscle. During a fasting state, when blood glucose is low or during stress requiring mobilization of energy, insulin secretion is suppressed and glucagon is released into the circulation by pancreatic α cells, opposing the action of insulin to increase the release of stored energy resources for use by the organism (Figure 1)[5,6].

The metabolic effects of insulin are mediated by activation of its cognate receptors that are expressed in target tissues (skeletal muscle, liver, fat) in large excess compared to the amount needed for normal regulation of glucose metabolism (spare receptors[7-10]). This lays a background for and signifies the paramount importance of the glucose control mechanisms. Indeed, in type 1 diabetes, which is usually associated with idiopathic autoimmune attack and destruction of islet beta cells, more than 90% of islet cells need to be destroyed or less than 10% of insulin production should remain for overt hyperglycemia to manifest[11]. Similarly, in type 2 diabetes, associated in its early stages with decreased sensitivity of insulin-responsive

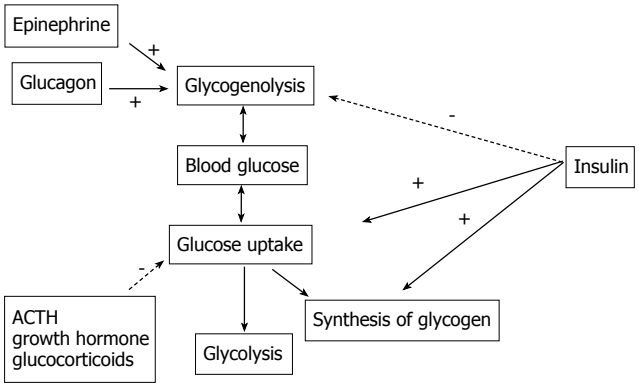

Figure 1 Hormonal regulation of systemic blood glucose.

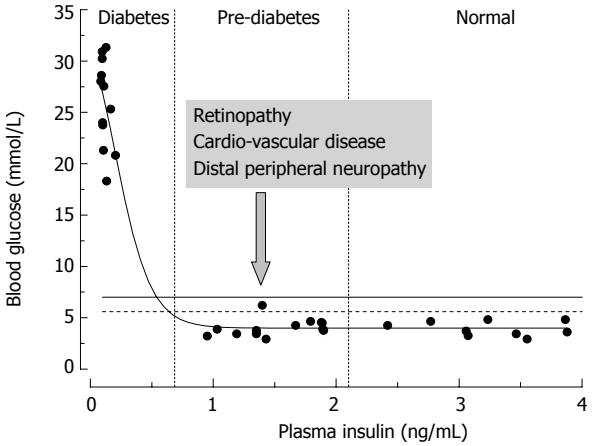

Figure 2 Relationships between rat plasma insulin and fasting blood glucose concentrations. Data are from normal and streptozotocin-injected adult Sprague-Dawley rats (the authors' unpublished observations). STZ-rats having moderate pancreatic impairment and moderately decreased plasma insulin (vertical dashed lines) do not develop overt hyperglycemia.

tissues to the action of the hormone (insulin resistance) and compensatory hyperinsulinemia, no clinical diabetes develops before muscle and fat tissue sensitivity to insulin is decreased below 50%-35% of normal[9]. In rats, and similarly in humans, plasma insulin may vary over the range of 1 to 4 ng/mL with fasting blood glucose exceeding the diabetic threshold of 6.9 mmol/L (solid line in Figure 2)[12-17] only in rare cases. In most cases, insulin must decrease to less than 0.5 ng/mL level (15% of control, 3.5 ng/mL level) in order to manifest overt hyperglycemia and diabetes.

Such a large safety factor for glucose control is of critical biological importance; however, clinically the impairment of insulin signaling in this disease process starts long before it manifests in overt hyperglycemia. With the discovery of insulin and improvement in techniques for blood glucose measurement, diabetes is not a life threatening disease by itself[18]. Therefore the long pre-clinical progression of diabetes could be a relatively minor issue; however, diabetes is associated with a variety of life threatening complications, among which distal peripheral neuropathy (DPN), cardio-vascular disease (CVD), retinopathy and renal disease are most frequent[2]. The problem is signs of these complications are frequently present prior to overt hyperglycemia and diabetes (Figure 2). Realization of this fact led to the definition of pre-diabetes as a state with moderate impairment of blood glucose control and high risk of development of overt diabetes, retinopathy and CVD[3,19]. Pre-diabetes is diagnosed when fasting blood glucose exceeds 5.6 mmol/L and/or 2-h glucose in a glucose tolerance test (GTT) exceeds 6.9 mM (impaired fasting glucose (IFG) and impaired glucose tolerance (IGT) dashed and solid horizontal lines in Figure 2, respectively)[4].

Establishing the correct lower limit for diagnosis of pre-diabetes is important because it determines whether clinical tests for complications should be performed and recommendations in life style and diet modifications should be presented to patients. In a recent study of young adult men, it was shown that fasting glucose exceeding 4.82 mmol/L constitutes an independent risk factor for developing type 2 diabetes in otherwise healthy subjects[20]. In another study of adult healthy men without diabetes or pre-diabetes, progressive loss of β-cell function and decrease in the first-phase of insulin secretion were detected at fasting glucose between 5.0 and 5.4 mmol/L[21]. Another clinically important issue is to understand the pathogenesis of diabetic complications, starting with pre-diabetic patients. This knowledge is required for early detection, prognosis and treatment of diabetic complications. Here we will discuss data and hypotheses for the triggers and progression of one such complication, which is distal peripheral neuropathy.

DISTAL PERIPHERAL NEUROPATHY

The prevalence of peripheral neuropathy in diabetic subjects approaches 70% and about 50% of these are cases of DPN[22-24]. The disease usually progresses to involve cardiac autonomic nerves, and as a result it is a major factor in mortality of diabetic subjects. DPN is also the major reason for loss of protective limb mechanical sensations, traumatic ulceration injures and therefore amputations[23,24]. Finally, about 11% of DPN cases are associated with chronic pain symptoms that severely diminish the quality of life and are frequently associated with depression[22,23]. The etiology of DPN is unknown and prediction of progression and treatments of the symptoms of DPN are limited[22,25-27].

Perhaps the largest problem associated with DPN, complicating its classification and treatment, is the variety of clinical presentations of this disease (Figure 3)[28-30]. Aside from a generally bilateral manifestation, distal to proximal advance and prevalence of sensory over motor impairment signs and symptoms, any two randomly selected cases of DPN may have nothing in common at the time of diagnosis and, to the extent it is known, their history and the pattern of their future progression may be very different. There are two broad categories of sensory symptoms of DPN, positive and negative[26,29]. Positive symptoms include pain, paresthesias and aberrant, exaggerated sensitivity to normally painless or moderately painful stimuli (allodynia and hyperalgesia). Negative

Positive sensory symptoms:
Chronic or Acute/Remitting:
Spontaneous:
Painless paresthesias:
numbness, tingling, pricking, burning, or creeping
Pain/dysesthesia: burning, electric, sharp, or dull/aching
Evoked pain/dysesthesia: allodynia or hyperalgesia, mechanical/tactile or thermal

Negative sensory signs/symptoms:
Decrease in sensory nerve amplitude/conduction velocity
Decrease or loss of perception:
Vibratory stimuli
Thermal stimuli (warming or cooling)
Tactile perception (light touch)
Nociception (hypoalgesia):
Thermal (heat or cold)
Mechanical (pin-prick)
Loss of tendon reflexes

Motor signs/symptoms
Decrease in motor nerve amplitude/conduction velocity
Muscle wasting

Figure 3 Signs and symptoms of distal peripheral neuropathy. Categories of symptoms most frequently manifested in humans with diabetes are given in bold.

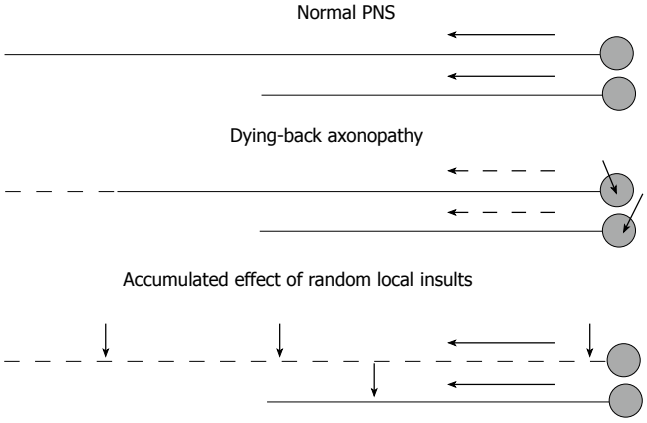

Figure 4 Hypotheses on distal-to-proximal progression of DPN. In normal PNS (top), neurons synthesize proteins in the cell body and transport them down the axon at the rate determined by axonal structural and functional needs. Impairment of synthesis or axonal transport of proteins will result in dying-back neuropathy, in which neurons with longest processes are affected first (middle). Alternatively, the neuropathy may result from effect of random local insults to the axon, with probability of accumulation of a critical number of such insults being higher for neurons having longer axons (bottom). Short arrows indicate non-specified axonal or neuronal injuries. Long solid or dashed arrows indicate normal or compromised axonal transport (respectively).

symptoms consist of loss of sensory perception in one or several modalities. Motor symptoms, if present, manifest as muscle weakness, and thus they are also negative. Finally, a classical electrophysiological, and also negative, sign of DPN is a decrease in nerve conduction velocity (NCV) and amplitude of compound action potentials (APs) in peripheral sensory and motor nerves[23,24,26,27,31]. Furthermore, three categories of DPN, acute painful remitting neuropathy, chronic painful neuropathy and painless neuropathy with ulcer can be outlined as separate clinical entities[24,32,33]. The relationships among these entities, however, if any exist, are not known. Within each of these groups, signs of demyelination of large peripheral fibers (decrease in NCV) may or may not co-exist with signs and symptoms of large fiber axonopathy (decrease in amplitude of compound APs, loss of vibration sensation and/or loss of stretch reflexes). Loss of warm and cold perception, impairment of unmyelinated and small myelinated fibers, may or may not co-exist with signs of large fiber abnormalities[24,31,32,34-36]. Furthermore, the pain normally conducted by small unmyelinated peripheral axons may or may not be present at the same time with any of the above mentioned symptoms[22-24,26,36,37]. Finally, the modalities of pain and the degree of involvement of autonomic nervous system impairment constitute another large set of variables[22,24,33,38-40].

From experiments in animals, and by analogy with other neuropathies, it can be suggested that the pathogenesis of negative symptoms and signs of DPN is likely to be associated with demyelination and axonal atrophy and degeneration[41,42]. Failure of re-innervation will make these symptoms essentially irreversible[42-44]. Mechanisms of neuropathic pain, paresthesias and hyperalgesia are less understood[27,40]. However, it is generally accepted that abnormally intense spontaneous input from primary afferent fibers to the spinal cord is a primary trigger of these symptoms[24,27,45,46]. At least three usually overlapping conditions, resulting in such abnormal activity of peripheral axons, are well established. First is impairment of endoneurial circulation and following it ischemia[47,48]. Second is impairment of axon-glia relationships and segmental or paranodal demyelination[49,50]. The third condition is an axonal injury and following it Wallerian degeneration and neuroma[51,52]. In addition, increased excitability of regenerating, and therefore not yet properly myelinated, nerve fibers may add to the generation of aberrant peripheral discharge and pain[53,54]. At least at advanced stages, evidence for axonal, glial and vascular injuries are detectable in most cases of DPN[41,55].

Further insight into the pathogenesis of DPN is provided by its diffuse, bilateral presentation and distal to proximal progression. The former suggests that systemic rather then local conditions underlie the clinical pathology, while the latter could indicate two possibilities (Figure 4). First, DPN may be a manifestation of dying back degeneration, with the primary insult consisting of the impairment of synthesis or efferent axonal transport of proteins, therefore affecting the function of the longest axons in the body that are most dependent on these mechanisms[42]. Failure of protein synthesis, including synthesis of some important neurotrophic molecules, in diabetes could result in impaired nerve regeneration and dying back axonopathy[43,44,55,56]. Alternatively, accumulation of the effects of multiple injuries randomly located along the axon, for example demyelinating injures, may result in a clinical picture that is practically indistinguishable from dying back neuropathy[41,42,57]. The longest axons in the body will most likely be hit by a critical number of such local insults and their function will fail first.

Micro-vascular disease followed by local impairment of blood supply to the nerve fascicules may be a basis for random demyelinating insults progressing later to axonal degeneration[58-60]. It is also conceivable that both mechanisms are operating at the same time. Both demyelination and axonal degeneration were detected in human DPN by electrophysiological tests and biopsy studies[24,41,61]. Peripheral axons are the longest in the human body, and this might be an important factor explaining PNS involvement superseding the CNS complications. Another potentially important reason for the high vulnerability of PNS to diabetic injury is the relatively weak anti-oxidative defenses of peripheral neurons (see Section 3).

While the discussion above appears to encompass all the major features of DPN, multiple questions related to the pathogenesis of DPN remain unresolved. Thus whether or not dying back axonopathy or multiple local injuries or both mechanisms lead to the disease, it is not clear why, in most cases of neuropathy, sensory symptoms prevail over signs of impairment to motor axons innervating the same distal areas of the human body. Furthermore, neither of these mechanisms explains a variety of clinical presentations of DPN nor answers the question of why some diabetic patients live without any symptoms of DPN for years[62]. Finally, major questions that remain to be answered include identifying pathogenic triggers of DPN, pathogenesis of individual symptoms, and relationships among different symptoms and signs of the disease[22,24].

To illustrate the importance of the latter question, two hypothetical scenarios of DPN are shown in Figure 5. In the first scenario (Figure 5, top), there is a single pathogenic process triggering and maintaining the disease. The course of the disease and its clinical manifestations at the time of diagnosis and neurological evaluation (ovals in the Figure 5) will be determined by the duration of DPN and individual differences in the genetic backgrounds of patients. From the point of view of the symptoms revealed by a neurological exam, the second scenario (Figure 5, bottom) is identical to the first one; the critically important difference, however, is that different sets of symptoms in this scenario are triggered and driven by entirely independent pathogenic mechanisms (symptoms "a", "c", and "d" *vs* symptom "b"). Some of the branches of the pathogenic process ("b" in the first scenario) may enter an irreversible stage. Therefore, the early detection of DPN is an obligatory condition for the successful treatment of this disease. The cartoons demonstrate also that identification of all participating triggering mechanisms and symptoms associated with them is another critical step for the efficient treatment of DPN.

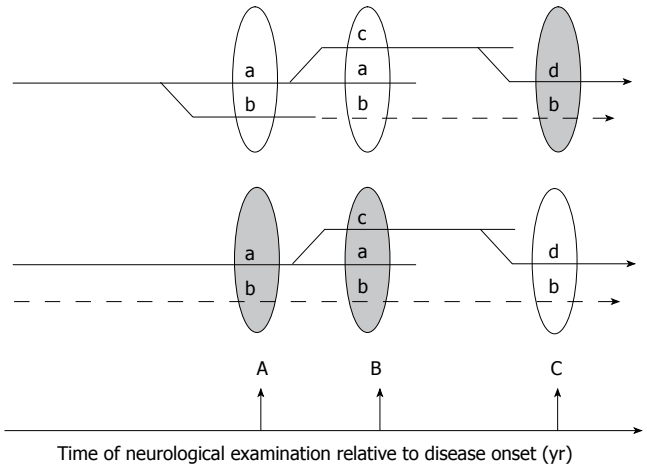

Figure 5 Hypothetical branching (top) and multi-trigger (bottom) pathogenesis of DPN. In the first scenario (top) all manifestations of the disease result from the unique branching pathogenic process, and symptom "b" discovered at the time of neurological exam B is not corrected by treatment because it has already progressed to an irreversible stage (dashed lines). Earlier diagnosis and institution of treatment (at time A) may critically change the outcome of therapy in this scenario. Alternatively (lower scenario), several independent factors may trigger and maintain the progression of DPN. In this case the therapy may fail to treat symptoms not because they are irreversible, but because the correct cause of the pathology is not identified and is not treated (dashed lines).

CHRONIC HYPERGLYCEMIA AND PATHOGENESIS OF DPN

DPN follows both type 1 and type 2 diabetes, and systemic hyperglycemia is the most obvious symptom that these types of the disease have in common[24,63,64], suggesting hyperglycemia as a universal trigger for DPN. Indeed, insulin treatment or treatment with insulin-sensitizing drugs to control hyperglycemia reverses some symptoms of DPN and delays its progression in general[65,66]. The Diabetes Control and Complications Trial (DCCT) data show that strict control of hyperglycemia in type 1 diabetes patients without clinical neuropathy decreased development of DPN in 60% of cases over 5 years of follow up study[67,68]. Well within the framework of the glycemic hypothesis, the failure to prevent all cases of DPN could be explained by the fact that glucose control can never be perfect. Type 1 and 2 patients are, on average, euglycemic for only about 62% of the day, while during the remaining 30% and 8% of the day they have various degrees of hyperglycemia and hypoglycemia, respectively[69]. Therefore, to avoid hypoglycemic crisis, the acceptable target value for blood glucose in controlled subjects is usually set to values above normal (6.7 to 10 mmol/L in DCCT and 6 mmol/L in U.K. Prospective Diabetes Study; of type 2 diabetic patients[65,68]). Another explanation for incomplete efficacy of glucose control is that, after long-standing diabetes, some neuropathic mechanisms may enter either an irreversible stage or a stage of progression that is already independent of the original trigger. With the limitations imposed by generally late diagnosis of diabetes and DPN[24,70,71], slowing of NCV, paraesthesia and painful symptoms appear to be the earliest (closest to the initiating pathogenic insult) manifestations of DPN. Therefore, it appears to be in good agreement with the glycemic hypothesis that in patients with newly diagnosed diabetes, NCV slowing and paresthesias (hyperglycemic neuropathy) can be frequently completely recovered with the establishment of euglycemia[31,42].

Further support for the glycemic hypothesis comes from research in animals, specifically rat models of type

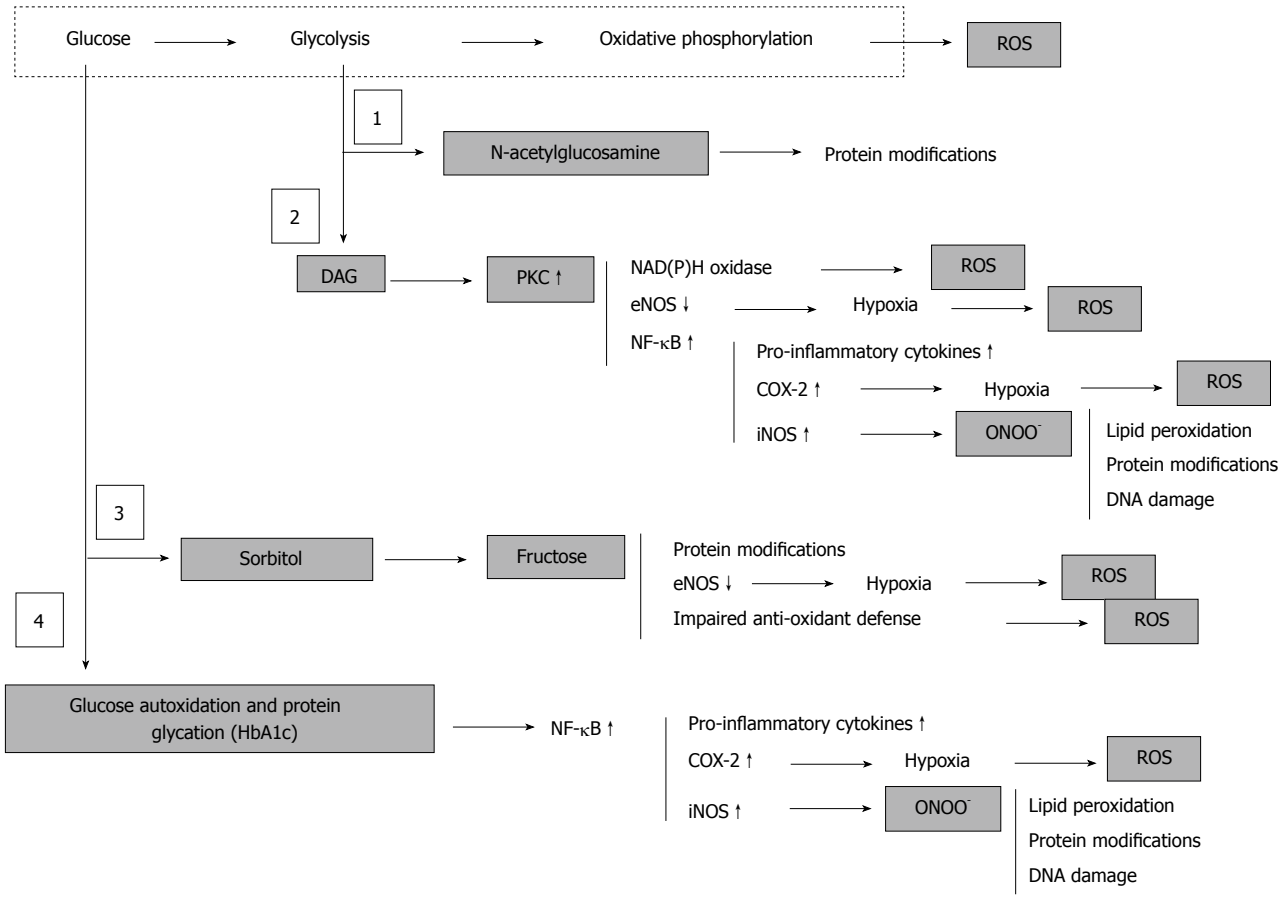

Figure 6 Hyperglycemia, derangement of cell metabolism and oxidative/nitrosative stress. Hyperglycemia associates with accumulation of fructose-6-phosphate and hexosamine pathway (1) to N-acetylglucosamine, accumulation of dihydroxyacetone phosphate and associated activation of PKC (2), activation of polyol sugar pathway (3), and glucose autoxidation and non-enzymatic protein glycation (4). These metabolic events are either regular physiologically important components cell metabolism (1, 2 and 3) or are normally under strict control of intrinsic intracellular defense mechanisms (4). However, under conditions of chronic hyperglycemia activation of these pathways leads to a global derangement of the cell and tissue homeostasis, which culminates in an uncontrolled cascade of abnormal protein modifications, oxidative/nitrosative stress and pro-inflammatory conditions.

1 diabetes (STZ-induced or spontaneous in BB-rats) and spontaneous type 2 diabetes in Zucker fatty rats[66,72] that appear to be the best studied animal models with regard to neuropathy. The short life span of rodents severely limits evaluation of chronic human diseases in these animals. Another limitation is that in behavioral tests, evoked pain manifested by limb withdrawal can be tested, but neither spontaneous pain nor changes in non-nociceptive sensory thresholds can be reliably measured in animals. Nonetheless, in general agreement with both clinical data on the earliest signs and symptoms of human DPN and the glycemic hypothesis, slowing of sensory[73-76] and motor[74,75,77-83] NCV and manifestations of evoked pain (hyperalgesia[75,84-87] and allodynia[85]) were shown to develop within the first month of onset of hyperglycemia in diabetic rats. With a longer time allowed (six to twelve months of diabetes) signs of axonopathy, demyelination and nerve degeneration can also be detected in diabetic animals[56,74,80,82,88-90]. Finally, early in the course of diabetes in rat models impairment of endoneurial blood flow and micro- and macrovascular reactivity are reported by many investigators[75,91-94]. Skin and arterial blood flow is abnormal early in diabetic patients[95-98], but no reduction in sural nerve blood flow was detected in humans with diabetes and mild DPN[99]. Thus, it is not clear whether impaired endoneurial blood flow represents a rat-specific component of DPN or if it is missed in humans because of its transient character and usually late detection of DPN in diabetic patients. In agreement with the glycemic hypothesis, all abnormalities found in rat models are reversible with normalization of blood glucose in insulin replacement experiments, and some of them (decreased pain pressure threshold) can be induced in normal rats by chronic *in vivo* perfusion of a DRG, or a segment of sciatic nerve with hyperglycemic solution[100,101].

Finally, support for the glycemic hypothesis is provided also by studies of cellular pathology associated with experimental diabetes. These studies show that practically all signs and symptoms of DPN observed in animal models may be linked to hyperglycemia-induced metabolic impairment of nerve, glial and endothelial cells in PNS. A detailed description of these studies is beyond the scope of the present work and can be found in a number of recent reviews[94,102-109]. The purpose of Figure 6 is only to provide a brief outline of cell metabolic abnormalities associated with diabetes and emphasize the findings directly relevant to the following discussion of triggers of early DPN.

Although the scheme in Figure 6 is simplified and omits many essential steps for the cascade of events [the poly (ADP-ribose) polymerase (PARP)[108]; activation and consequences of lipid peroxidation[110] are not shown], it clearly demonstrates the complexity of this cascade. Some events appear to be more specific to one type of cell than to another, and there is as yet no agreement on which events (for example activation of polyol pathway[111] or abnormally intensified oxidative phosphorylation[106]) plays a leading role in cellular impairment. Nonetheless, most of the data available indicate that all the various pathways activated by hyperglycemia converge in generation of excess reactive oxygen species (ROS). This process eventually overwhelms the intrinsic anti-oxidant mechanisms of the cell and ends in oxidative/nitrosative stress and pro-inflammatory conditions in the tissues[112-115]. The efficacy of treatment with anti-oxidants in correction of DPN in animals and humans supports this view[116-119].

In diabetic animals, oxidative stress injury develops in parallel in all major cellular elements of PNS. Injury to glial cells is responsible for the demyelination component of DPN, which may explain the decrease in NCV and painful manifestations of the disease. Oxidative stress in neurons might be responsible for axonopathy, impaired regenerative capacity of axons and negative symptoms of DPN. Glial cell injury will affect the nerve neurotrophism adding to the progression of neuronal defects. Finally, oxidative stress and impairment of nitric oxide (NO) production in the endothelium of epi- and endoneurial blood vessels results in impairment of endoneurial circulation and endoneurial hypoxia, exaggerating and speeding up the direct effect of hyperglycemic conditions on glial cells and neurons. Oxidative stress is pro-inflammatory, which affects the production of cytokines by glial cells, and provokes the recruitment of immune response cells into the affected tissue. This might be another important component of the pathogenesis and progression of DPN. Thus, combining these data and observations lays the foundation for a view of the natural history of DPN similar to that depicted in Figure 7 according to an expanded view of the glycemic hypothesis.

Perhaps the most attractive aspect of such a view of the pathogenesis of DPN is that while it suggests a unifying trigger and mechanism (hyperglycemia and oxidative stress) for all symptoms of DPN, it nevertheless remains flexible enough to leave room for individual variability in the rates of progression and spectrum of manifestations of the disease. Indeed, the actual effects of uniform pro-oxidative and pro-inflammatory conditions may differ sharply depending on differences of individual cells and tissues in their intrinsic anti-oxidant defenses and individual organisms in their immune defenses. The injuries to a single myelinating or non-myelinating Schwann cell, endothelial cell or neuron will unlikely have even subclinical significance. The death of several myelinating cells will result in a decrease of NCV in a given axon and injury to several endothelial cells may cause the closure of a given capillary. Yet there are many axons and there is regeneration of damaged axons, and there are many capillaries and regeneration of damaged and collateral capillaries. It is only after cellular defenses against the oxidative stress are overwhelmed in many cells that the sub-clinical signs of the disease may be expected to appear, and it is anticipated to take an even longer time before clinical manifestations will themselves appear. In agreement with this, *en mass* CNS cells appear to have a much higher capacity for anti-oxidative mechanisms than do PNS cells and this might be one of the reasons why diabetic neuropathy affects the CNS much later than it affects peripheral nervous functions[90,113,120].

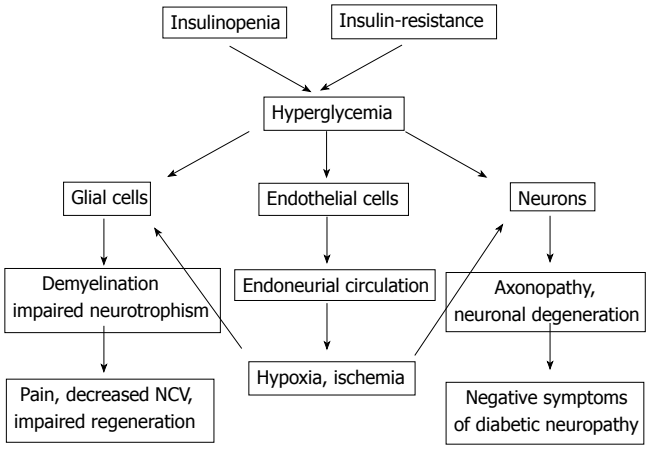

Figure 7 Pathogenesis of DPN with hyperglycemia as a major trigger of PNS injury.

DIFFICULTIES OF THE GLYCEMIC HYPOTHESIS

While apparently logical and consistent with many clinical observations and the results of animal studies, the glycemic hypothesis cannot completely explain all the data. Thus, experiments in rodents consistently demonstrate that the polyol pathway (conversion of glucose to sorbitol by aldose reductase and then to fructose by sorbitol dehydrogenase; pathway 3 in Figure 6) is an important source of reactive oxygen species, and inhibition of aldose reductase prevents or reverses many signs of DPN seen in diabetic animals[121]. The same treatment in humans, however, has shown questionable efficacy so far[27,53,122,123]. Other problems include the failure of a pre-clinical slowing of NCV[24,124] or increase in glycosylated hemoglobin[22] (HA1c, integral measure of persistent hyperglycemia; pathway 4 in Figure 6) to predict development or severity of symptoms of DPN. Also, the finding of an inverse correlation between hyperglycemia and pain severity in diabetic patients with remitting painful neuropathy at presentation[33] is inconsistent with the glycemic hypothesis. These and other similar inconsistencies certainly could be attributed to the complexity of the disease, differences in studied patient populations, or inadequate design of drug trials in terms of timing, duration or dose[121]. Similarly, the lack of absolute efficacy in glucose control in preventing DPN in humans with diabetes[68] could also be explained within the framework of the glycemic hypothesis considering the difficulty of maintaining blood glucose concentrations within the relatively narrow range of normal values, which suggests that the actual threshold for neuropathic effects of hyperglycemia is lower than was

previously thought. Therefore, recent findings of increased incidence of DPN in patients with pre-diabetes, many of whom have an impaired glucose tolerance (IGT) but not fasting hyperglycemia[22,25,70,71,125-127], appear to present the most serious challenge for the glycemic hypothesis.

The possibility that PNS injury may be triggered by exaggerated and prolonged postprandial hyperglycemic episodes, without necessarily requiring chronic hyperglycemia, should be considered to reconcile the glycemic hypothesis with observations of DPN in glucose intolerant patients[70,128-130]. Indeed, indices of large fiber function (ankle and knee reflexes and vibratory perception thresholds) were shown to decay with impairment of glucose tolerance in humans without diabetes and neuropathy[131]. Furthermore, pain is a frequent symptom of pre-diabetic DPN. An acute glucose infusion, which could be considered as an analog to a postprandial glucose surge, decreased thresholds to electrical stimulation in healthy adult volunteers[132] and decreased pain pressure thresholds in type 1 diabetic patients without clinical neuropathy[133]. In the latter study, however, no association between acute hyperglycemia and heat pain, warmth/cooling or vibration perception thresholds, was found[133]. Inconsistent with the idea that postprandial glucose changes have a neuropathic effect, no correlation was detected between short-term fluctuations in blood glucose and pain scores or heat pain thresholds in the study of type 1 and type 2 diabetic subjects with painful neuropathy[134]. Furthermore, no correlation between the number of glycemic excursions and the number of painful episodes was found in the study of type 1 patients with painless neuropathy[135].

Difficulties with the glycemic hypothesis are not unique to the human clinic. Thus in the STZ-rat model of diabetes, NCV could be corrected by a low level of insulin therapy below that required to correct hyperglycemia[89,136]. Pain pressure and von Frey filament thresholds studied in the same model demonstrate no correlation with the degree of hyperglycemia[84,101,137]. Furthermore, aldose reductase inhibitors (blockers of the polyol sugar pathway; Figure 6), given at doses sufficient to correct nerve sorbitol and fructose and heat pain thresholds, do not correct von Frey filament threshold in STZ-hyperglycemic rats[138,139]. As another example, pain pressure thresholds in type 2 diabetic Zucker rats could be corrected with insulin-like-growth factor Ⅱ (IGF-Ⅱ) that has no effect on blood glucose[86]. All these examples are taken from experiments in overtly diabetic and hyperglycemic animals. Therefore, formally the possibility remains that hyperglycemia was the triggering event for the observed abnormalities, but it is not required for the progression and maintenance of these pathologies. Whether DPN develops in pre-diabetic rats as it does in humans has not yet been studied. Since previous work has focused on diabetes, little attention has been devoted to the development of pre-diabetic animal models and studies of DPN in these models. Nonetheless, neuropathic decreases of mechanical and thermal nociceptive thresholds[140] and slowing of motor NCV[141] were observed in studies in Zucker-fatty rats. Since these are insulin-resistant but normoglycemic animals (type 2 pre-diabetes) the impaired glucose tolerance could be responsible for DPN in these animals. Recently, we described decreased pain pressure threshold in rats that were injected with STZ but remained normoglycemic[84]. These rats also had normal glucose tolerance, maintained normal levels of HbA1c, and normal concentrations of sorbitol in the nerve, suggesting that not only fasting but casual glucose also was maintained within physiological limits (Figure 8).

Thus there is solid evidence that hyperglycemia is an important factor of DPN. However, there are also both clinical and animal studies indicating that in addition to chronic and/or postprandial hyperglycemia, other pathogenic mechanisms must exist that trigger and maintain at least some of the symptoms of DPN. Identification of these factors is of critical importance for our understanding of both the natural history of pre-diabetic DPN and the pathogenesis of diabetic DPN in general[27,88].

INSULIN SIGNALING AND DPN

In the search for triggers of DPN other than hyperglycemia, it is important to note that successful reversion or postponing of DPN in clinical glucose control trials does not necessarily prove the glucose hypothesis[142]. Glucose metabolism is regulated by insulin *via* type B receptors (IR-B) abundantly expressed by liver, skeletal muscle and fat cells. Insulin receptors, however, are also expressed in central and peripheral nervous systems[143,144]. Furthermore, in PNS the highest densities of IRs are located on endothelial cells, paranodal loops of Schwann cells and medium and small size primary sensory neurons[143,144]. All these locations are strategically critical points of PNS function considering what is known about the pathogenic mechanisms of DPN. While the nervous system has mostly type A receptors (IR-A), the insulin affinities of these and IR-B receptors are similar ($K_{0.5}$ is 3 to 6 ng/mL[145]) and well within the range of circulating concentrations of insulin (1 to 6 ng/mL[12-17]). Thus, it is very possible that correction of insulin levels in treatments for Type 1 diabetes or insulin-sensitizing therapy in cases of type 2 diabetes not only corrects glucose metabolism, but also has independent effects on the function of PNS. Serious consideration of this hypothesis is warranted, first because it provides an explanation for at least some failures of glycemic controls to reverse DPN, and second because it may explain the development of DPN in pre-diabetic patients.

Insulinopenia (Type 1 diabetes and pre-diabetes)

As described in the Introduction, overt type 1 diabetes is preceded by a state of partial pancreatic damage and moderate insulinopenia in which insulin production is still satisfactory for blood glucose control[11]. The type 1 pre-diabetic state is probably short and little is known about neuropathy in these patients. The results of a recently completed follow-up to DCCT study of type 1 diabetic patients, however, has shown that regardless of the level of glycemic control, neuropathy is less prevalent in the group of patients that maintained intensive vs. conventional insulin therapy[146]. Further support for the

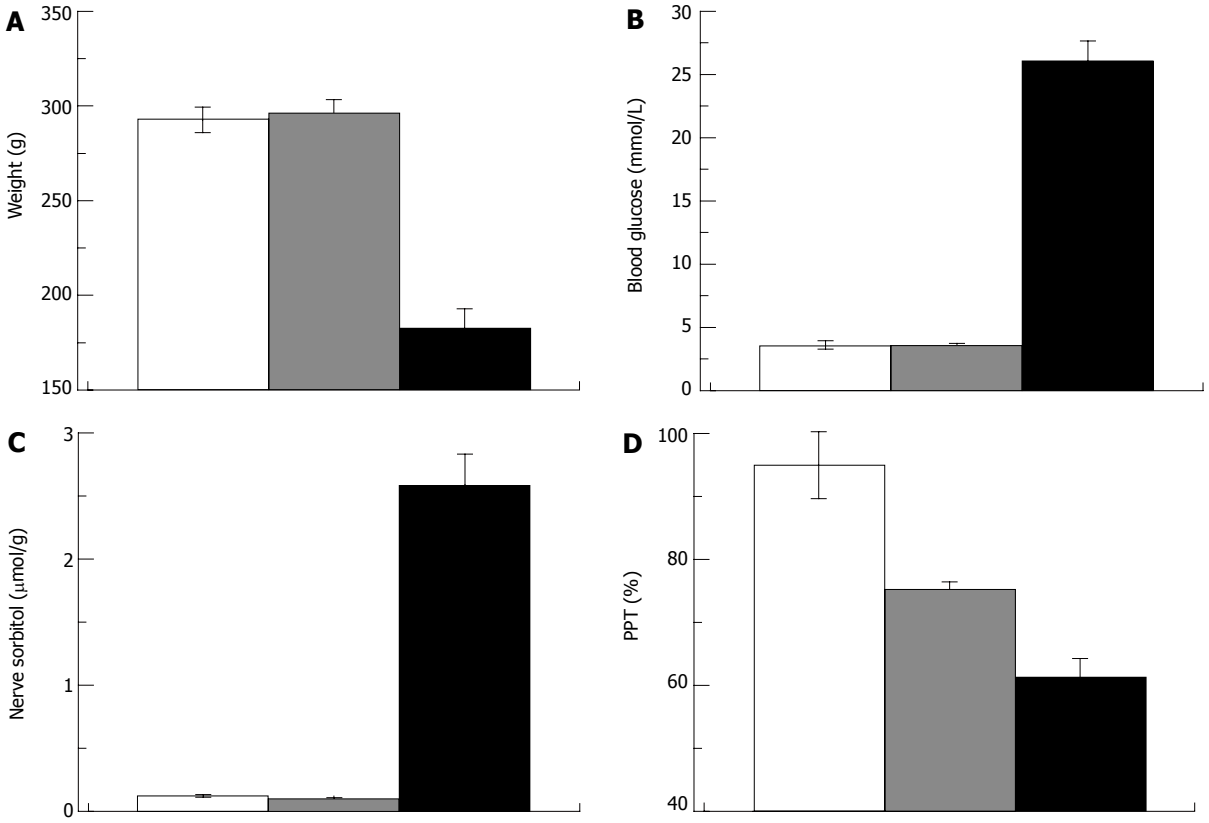

Figure 8 Pain pressure thresholds are not correlated with hyperglycemia. Weight (**A**), blood glucose (**B**), nerve sorbitol (**C**) and pain pressure thresholds (**D**) in control, STZ-normoglycemic and hyperglycemic rats (white, grey and black columns respectively; 2 wk after injection of 65 mg/kg STZ).

possibility of a direct role of insulinopenia in DPN comes from experiments in the STZ-rat model of type 1 diabetes. It was demonstrated that local insulin application to the nerve prevents motor NCV slowing in STZ-hyperglycemic rats[147]. Similarly, systemic[136] or intrathecal[89] application of insulin can correct sensory and motor NCV in STZ-treated rats without having an effect on hyperglycemia. Finally, in our experiments in rats that were injected with STZ and developed moderate insulinopenia but not fasting hyperglycemia (Figure 8), pressure pain thresholds were decreased in proportion to the degree of insulinopenia, and low dose insulin-replacement therapy corrected this defect without changes in the systemic blood glucose level (Figure 9). Taken together these data suggest that at least some signs of neuropathy (slowing of NCV, pressure-evoked pain in rats) may indeed be triggered by insulinopenia with no relevance to the blood glucose level. Another notable aspect of these experiments is that correction of nerve conduction[89,136,147] and pain pressure thresholds (Figure 9) with insulin treatment could be achieved without changes in systemic blood glucose levels, leading to an important implication that the thresholds of "metabolic" and "neuropathic" effects of insulinopenia may differ.

To date, detailed information on the relation between insulin and nerve conduction is not available. However, comparison of better studied "dose-response" relationships between insulin, blood glucose and pain pressure thresholds (Figure 10A) allows speculation that in the rat, control of glucose metabolism may tolerate at least five times lower insulin levels than does nerve function. Given that this difference was confirmed in both animals and humans, the outcome of these studies is of a great importance. This finding may explain the development of neuropathy in pre-diabetes and also suggests that neuropathy may start at stages preceding pre-diabetes, and some therapeutic interventions to correct insulin levels or insulin resistance (see next section) are warranted in pre-diabetic patients.

Differences in threshold concentrations of a ligand are usually determined by the differences in receptor properties. However, insulin affinities of IR-B and IR-A isoforms of the insulin receptor expressed in cells of organs responsible for glucose metabolism and in nerve tissue are too close to account for apparent differences in the concentrations of hormone required for maintaining normal blood glucose concentrations and normal pain pressure thresholds[145]. On the other hand, strong correlative relationships between insulin and pain pressure thresholds (Figure 9A) suggest a nearly direct link between insulin regulation and pressure pain mechanisms. The hypothesis of spare receptors[7,8,10] is the easiest way to explain this discrepancy. Thus as shown in Figure 10A, both metabolic and neuropathic effects of insulin may be described adequately within the concept of insulin binding with the same affinity ($K_{0.5}$ = 1 ng/mL) in nerve and in glucose controlling organs, if 65% of the receptor occupancy is needed to control nerve function, and only 10% of occupancy is required for glucose metabolism. Hill equations were used in this simulation; however, since the

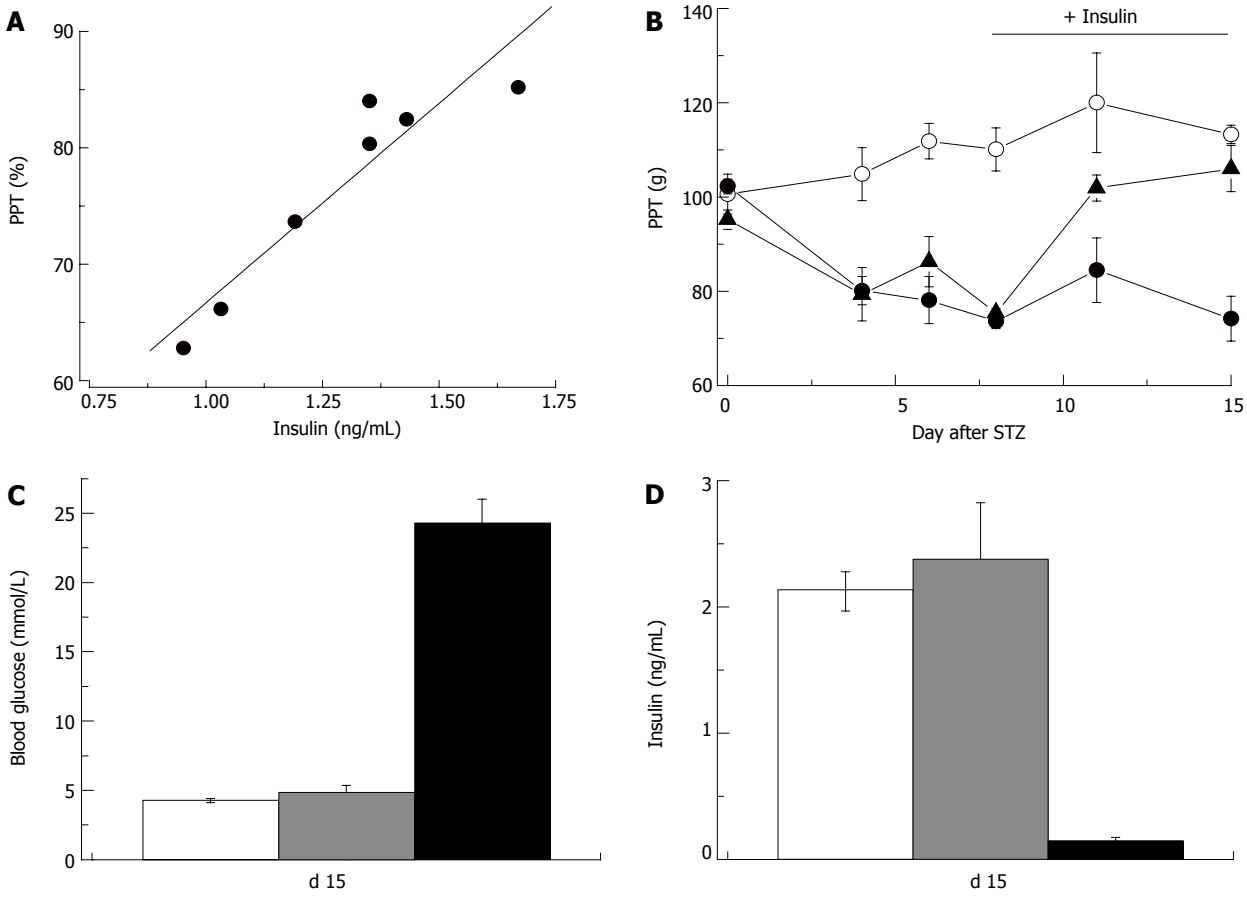

Figure 9 Insulin-dependence of pain pressure threshold in STZ-normoglycemic rats. Two weeks after injection of STZ pain pressure threshold of STZ-NG rats is decreased in proportion to the plasma insulin level (R = 0.97; **A**). Insulin replacement initiated one week after STZ injection (horizontal bar in panel **B**) does not change PPT of control or hyperglycemic rats, but corrects it in STZ-normoglycemic animals (empty and filled circles, and filled triangles, respectively). Insulin replacement, does not affect blood glucose (**C**), but normalizes plasma insulin level (**D**) in STZ-NG rats. In **C** and **D** white, grey and black columns represent control, STZ-NG and STZ-HG rats, respectively.

purpose was merely to illustrate the potential possibility of the given scenario, parameters of the equations were adjusted by a trial and error approach and no attempt was made to optimize the parameters. Some alternatives to this scenario will be discussed in section 6.1 of this review.

Insulin resistance

Prevalence of type 2 to type 1 diabetes is about 9 to 1 and most of the cases of human pre-diabetes are type 2 pre-diabetes or metabolic syndrome cases[24,125]. Over the long-term, insulin production is impaired in type 2 diabetes further increasing the incidence of DPN in this population by mechanisms described above. In a ten-year study of the natural history of type 2 diabetic patients, it was found that decreased serum insulin and increased blood glucose concentrations are independent predictors of DPN[148]. However, in early type 2 diabetes and pre-diabetes there is a compensatory hyperinsulinemia. Because of this hyperinsulinemia type 2 pre-diabetes usually spans a much longer period of time than does type 1 pre-diabetes. Thus, after 5 years only 20% to 35% of patients with impaired fasting glucose or impaired glucose tolerance develop overt hyperglycemia (see[70]). Despite this compensatory hyperinsulinemia, however, many type 2 pre-diabetic patients do develop DPN[125,126]. This latter observation suggests that in terms of neuropathic outcome, insulin resistance and insulinopenia may be equivalent states. It also suggests that increased production of insulin may fail to compensate for decreased sensitivity of PNS to regulation by insulin.

Not much experimental data exists to verify the validity of either of these suggestions. In studies in normal human volunteers, warmth detection threshold correlated with insulin but not fasting or 2-h GTT glucose, leading the authors to suggest that insulin resistance may determine some sensory functions of PNS[149]. This is also supported by observations of decreased NCV[141] and pressure pain thresholds[86] and the authors' unpublished observations in the Zucker fatty rat model of type 2 pre-diabetes. However, whether it is possible that hyperinsulinemia is effective in regulating glucose metabolism but fails to compensate for nerve insulin resistance is at this time absolutely not known. Furthermore, it is unknown if this mechanism plays a role in DPN associated with type 2 diabetes. In theory such a possibility does exist, and Figure 10B illustrates the scenario that we believe provides a useful working hypothesis for future experiments. Using "dose-response" relations as a starting point, shown in Figure 10A, the insulin resistant state that leads to type 2 diabetes may be modeled as a decrease in affinity of

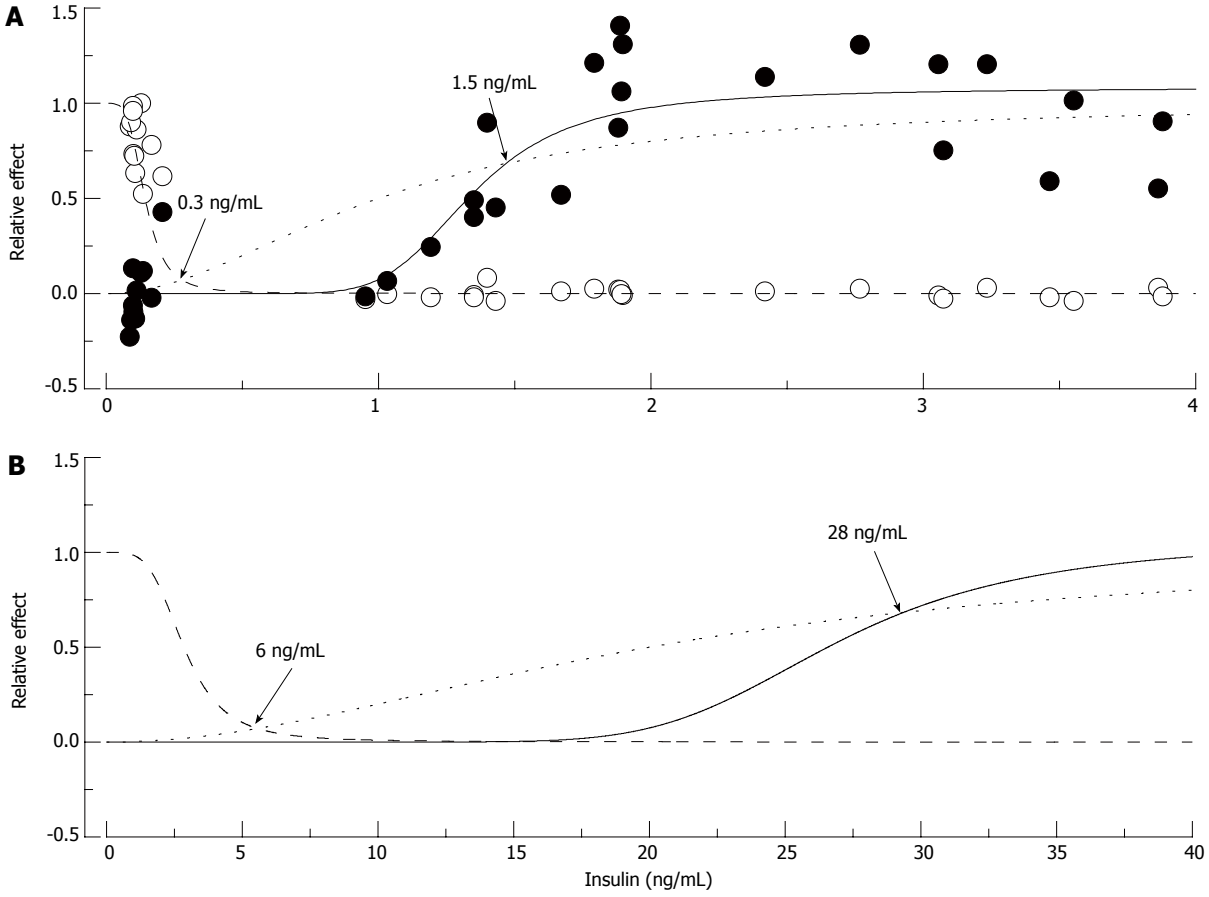

Figure 10 Putative "insulin-glucose metabolism" and "insulin-nerve function" relationships in normal and insulin-resistant rats. In **A**: Normal rats: Empty circles represent fasting glucose and filled circles pain pressure thresholds measured in control, STZ-NG and STZ-HG rats, pooled together and normalized to show relative changes of these parameter between control and diabetic animals. The data were fitted by Hill curves calculated based on the assumption that insulin binds to the receptor with an affinity of 1 ng/mL (dotted curve) and 10% and 65% occupancy of these receptors is required for maximum metabolic (intersection with dashed curve) and nerve (intersection with solid curve) effect of the hormone, respectively. In **B**: Insulin-Resistant Rats: Insulin resistant state was simulated by increasing $K_{0.5}$ of insulin binding to the receptor to 20 ng/mL. Points of intersections of the dotted curve with the dashed and solid curves recalculated with the new $K_{0.5}$ parameter show (arrows and labels) that maintaining glucose metabolism now requires about 6 ng/mL of plasma insulin, and nerve function requires at least 28 ng/mL of the hormone.

IR from 1 to 20 ng/mL, which leads to proportional rightward shifts of insulin-glucose metabolism and insulin-nerve function relationships. If the requirements of 10% and 65% occupancy of IR remain unchanged, maintenance of normal glucose metabolism under these new conditions will need about 6 ng/mL of circulating insulin and nearly 30 ng/mL insulin concentration will be the minimum needed to maintain normal PNS function. The calculated 6 ng/mL insulin concentration is in the range of insulin concentrations measured in Zucker fatty rats (5.1 to 11.7 ng/mL; model of compensated insulin resistance[150-152]). These latter numbers are, however, significantly lower than predicted by the model insulin concentration needed to maintain nerve function. Therefore, it may be speculated that the "set-point" or natural goal of compensatory hyperinsulinemia is merely to correct glucose metabolism, which is vitally important for the organism, with no concern about the less significant problem of nerve function.

Cellular mechanisms

Thus, while the connection remains speculative, the data above suggest that impairment of insulin signaling in PNS (because of decreased insulin production, insulin resistance or both) may be an important factor in the pathogenesis of DPN. Further studies are needed to confirm this hypothesis and further studies are also needed to understand the cellular mechanisms of insulin action in PNS.

Glucose is a major fuel for neurons of peripheral and central nervous systems. However, unlike that in major target tissues of insulin regulation, uptake of glucose in nervous tissue is an insulin-independent process. Therefore, the simple explanation of the neural effects of insulin to regulate the energy supply does not appear to be applicable. There should be some other role of IR in the nervous system. In the CNS, these receptors are involved in the insulin control of feeding behavior, reproductive and cognitive functions and neuromodulation[27,153]. Insulin also clearly has neurotrophic functions. It stimulates neurite outgrowth, is involved in peripheral nerve regeneration and is required for survival of sympathetic neurons (see[27]). These effects are likely very important for regeneration, which is suppressed in long-term DPN. For short term diabetes, the possibility of insulin regulation of axon-glia relationships, vascular permeability, and function of nociceptive primary afferent neurons[143,144] may be of importance. The possibility of a selective acute effect of

insulin on endoneurial blood flow (decrease) was also demonstrated by experiments in normal rats[154].

Note also that the negative cellular effects of hyperglycemia and insufficiency of insulin signaling seem to converge at some point. Pain pressure thresholds are decreased in rat models of local hyperglycemia with a time course and to a degree that is very similar to those in STZ-normoglycemic rats[101]. Since many studies support oxidative/nitrosative stress as a central event of hyperglycemic impairment, it is reasonable to suggest that oxidative/nitrosative stress can interfere with insulin regulation in some or all of the hyperglycemia-induced steps of the pathogenic cascade depicted in Figure 6. Insulin directly regulates inner mitochondrial membrane potentials and may affect oxidative phosphorylation[136]. Insulin also suppresses expression of NADPH oxidase[155] and controls expression of Nf-κB and associated inflammatory reactions[155,156]. In fact, the anti-inflammatory effects of insulin have been known since the discovery of the benefits of insulin therapy in systemic inflammatory responses to trauma or bacterial infection[157]. Insulin signaling also was shown to be linked to the regulation of Na, K-ATPase[158,159] and endothelial NO production[158,160]. These data suggest that insulinopenia does have the potential to produce the same or very similar neuropathic effects as were attributed previously solely to hyperglycemia.

OTHER FACTORS OF SIGNIFICANCE

While the above outlined insulin-signaling hypothesis of DPN appears compelling, it will certainly be corrected and modified in many of its segments to conform to the results of future studies. It can also be stated here, without reservation, that no complete picture of the pathogenesis of DPN will be created unless the roles of insulin-like growth factors and C-peptide are considered in addition to hyperglycemia and insulin signaling in PNS[142].

Insulin-like growth factors (IGFs)

IGFs are produced in the kidney, spinal cord, skeletal muscle and peripheral glia. IGFs possess multiple neurotrophic functions, including control of neuronal survival, neurite outgrowth and regeneration, and expression of genes encoding axonal cytoskeletal proteins (tubulins and neurofilaments)[142,161-166]. Interestingly, IGF-1 appears to be involved in the regulation of resistance to oxidative stress[167]. IGFs primarily act *via* specific receptors, but since IGFs are present in the circulation in a 100-fold excess compared to insulin, they may also bind to and activate IR, mimicking some but not all affects of insulin[168,145,165]. It might be important in this regard that, in peripheral nerve, IGF-I receptors are co-localized with IR in sensory neurons[169,170] and Schwann cells[171] and a large fraction of them are likely hybrids composed of protein subunits of both IR-A and IGF-I receptors[143,169]. These hybrid IR/IGF receptors have substantially higher affinity to IGF-I than to insulin[172,173]. However, even when present in physiological concentrations, insulin may still bind to and activate some portion of hybrid as well as homomeric IGF-I receptors[161,174]. In addition, IGF-I may act by suppressing growth hormone and improving insulin sensitivity and insulin production in type 1 and type 2 diabetic subjects[174-178]. Insulin on the other hand, may modify kidney production of IGFs, and *via* regulation of IGF binding proteins, it may control the activity of circulating IGFs[161,175,176]. Whether, any of these multiple mechanisms participate in the apparent dissociation of the metabolic and neuropathic effects of insulinopenia remains to be determined.

Abnormal expression and levels of circulating IGFs and/or changes in expression of receptors for IGF were measured in diabetic human subjects[174], in STZ-rats (see[179-181]), and in the type 2 diabetes Zucker diabetic fatty (ZDF) rat model[86]. Furthermore, in obese Zucker rats, both insulin- and IGF-I resistances were shown to develop and mediate impaired glucose tolerance in this model of pre-diabetes[182]. Thus potentially, *via* impairment of protein synthesis, insufficiency of IGFs may add to the pathogenesis of regenerative capacity, neurodegeneration and irreversible stages of DPN[142]. This suggestion is supported by observations of recovery of NCV and reversion of atrophy of myelinated sensory axons in the sural nerve of STZ rats treated with intrathecal IGF-I[89]. In addition, the defect in IGFs or IGF-receptor expression could also add to the pathogenesis of early symptoms of DPN either directly or through modulation of insulin production or nerve sensitivity to insulin. Indeed, down-regulation of IGF-I receptors, which is observed in nerves of STZ-diabetic rats, occurs comparatively early, within 1 week after the onset of hyperglycemia[181]. Furthermore, continuous subcutaneous infusion of IGF-Ⅱ was shown to recover pain pressure thresholds to a normal level after 6 wk of diabetes in the ZDF rat model[86]. The latter observation is interesting because, in STZ-diabetic rats, a similar magnitude and early decrease in pain pressure thresholds seems to result from insulinopenia (see previous section). Affinity of IGF-Ⅱ binding to brain type insulin receptors or to IGF-I-R is two-three times lower than that of respective natural ligands[145]. Therefore, the effect of IGF-Ⅱ on mechanical hyperalgesia may still be explained within the framework of our insulin signaling hypothesis of early neuropathy. However, the possibility of a more complex regulation of pain pressure thresholds cannot be excluded. It is important also that in all the examples above the effects of treatments with IGFs occurred with no measurable changes in the glycemic status of studied animals; once again suggesting that the pathogenesis of DPN is multifactorial.

C-peptide

C-peptide is a segment of the proinsulin molecule sliced off to form insulin. Acting through both its own receptors and modulating activity of insulin receptors, C-peptide produces multiple insulin and IGF-like effects[27,183,184]. C-peptide also enhances autophosphorylation of IR and effects of insulin, and treatment with C-peptide reverses decreased expression of IGF-I, NGF and neurotrophin-3 receptors in type 1 spontaneously diabetic rats[27,183,185]. Considering these effects and the fact that

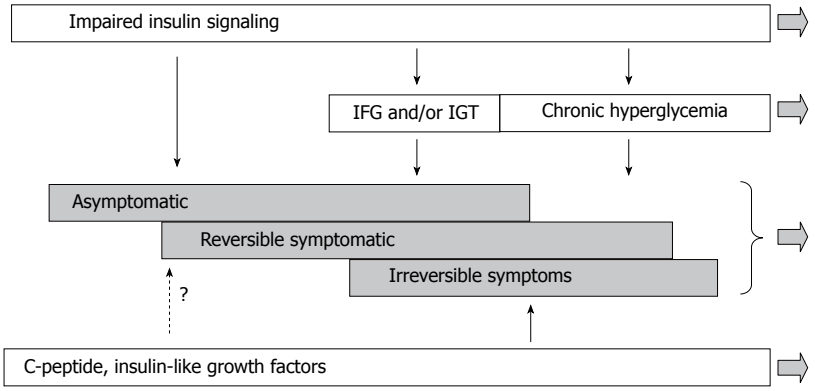

Figure 11 Modified scheme of pathogenesis of diffuse diabetic neuropathy with inclusion of insulin signaling. According to this view, the disease process starts before impairment of glucose metabolism becomes apparent. Derangement of insulin signaling in PNS triggers and maintains the neuropathy at this stage. Postprandial and chronic hyperglycemia is not the least important factor of DPN, but they become involved at relatively advanced stages of DPN. C-peptide and IGFs insufficiencies represent another important set of pathogenic mechanisms; however, the role of these mechanisms in early DPN remains undetermined.

C-peptide is secreted in equimolar concentrations with insulin, it can be concluded that C-peptide insufficiency may have an important role in the pathogenesis of type 1 diabetes[75,183,184]. In agreement with this implication, in patients with recently diagnosed type 1 diabetes, C-peptide treatment was shown to correct sensory NCV and vibration perception[186]. C-peptide treatment also corrects skin microcirculation in diabetic patients[187] and endoneurial blood flow and NCV slowing[75], thermal hyperalgesia, atrophy and degeneration of C-fibers[185] in BB/Wor type 1 diabetes rat model.

As expected, no differences in plasma C-peptide levels were found in pre-diabetic patients and patients with type 2 diabetes of short duration (less than 5 years from diagnosis), even though the number and severity of the signs and symptoms of DPN differed substantially between these groups[128]. What is less clear in the same study is a lack of detectable deficiency of C-peptide in advanced type 2 diabetes patients (more than 5 years) who could have been expected to start developing insulinopenia. In general, however, multiple questions remain to be resolved in relation to C-peptide and its role and mechanisms of action in DPN. Similar to conditions of chronic or postprandial hyperglycemia or impaired insulin- or IGF-signaling, C-peptide deficiency appears to affect activity of Na,K-ATPase, NO production and neurotrophism, but the C-peptide mediated regulation does not appear to depend on oxidative stress, which is apparently important in the pathogenesis of these conditions[75,188]. It is also not clear whether any of the symptoms may be directly attributed to C-peptide insufficiency in DPN. Endoneurial blood flow, NCV and heat nociception appear to be the foremost candidates[186,187], but antioxidant treatments and insulin replacement correct these abnormalities in STZ rats at least as efficiently as does C-peptide replacement in the BB/Wor rat model of type 1 diabetes.

CONCLUSION

DPN is a frequent and troublesome complication of diabetes mellitus. Diabetes manifests in a case-specific variety of signs and symptoms, and associates with complex biochemical, functional and structural abnormalities of the peripheral nervous system. While the obvious hyperglycemia present in diabetes can explain the development of these abnormalities, data suggest that other factors may also contribute. We have discussed the evidence for insulinopenia in type 1 diabetes or insulin resistance in type 2 diabetes as causal factors in the development of DPN. We have suggested that these two cases actually represent a single cause of impaired insulin signaling. Considering the role of insulin signaling in DPN more completely explains the changes in nerve function in pre-diabetic or early diabetic patients and animal models. This does not preclude hyperglycemia also as a factor in DPN, but allows a more complete picture of the disease process (Figure 11). In addition to insulin signaling, some evidence also exists for a role of IGF and C-peptide in mediating DPN. The pathogenesis of DPN is obviously multifactorial, and despite long-standing efforts, remains poorly understood. This work has also suggested that insulin signaling has effects that occur with different levels of receptor occupancy. Thus insulin action on nerve function requires a higher level of receptor occupancy than does insulin action on glycemic control. This could be explained by different levels of receptor coupling to second messenger signaling pathways in nerve versus liver or muscle. Future studies should elucidate these mechanisms so that a clearer picture of DPN can be obtained, especially in pre-diabetes where early detection could improve therapeutic outcomes.

REFERENCES

1 **American Diabetes Association**. Diagnosis and classification of diabetes mellitus. *Diabetes Care* 2006; **29** Suppl 1: S43-S48
2 **Diabetes in America**. Bethesda MR: National Diabetes Data Group, NIH, 1995: 1-733
3 **American Diabetes Association**. Report of the Expert Committee on the Diagnosis and Classification of Diabetes Mellitus. *Diabetes Care* 1997; **20**: 1183-1197
4 **American Diabetes Association**. Standards of medical care in diabetes--2006. *Diabetes Care* 2006; **29** Suppl 1: S4-S42
5 **Stryer L**. Biochemistry. New York: W.H. Freeman and Company, 1988: 1-1089
6 **Zierler K**. Whole body glucose metabolism. *Am J Physiol* 1999; **276**: E409-E426
7 **Kono T**, Barham FW. The relationship between the insulin-binding capacity of fat cells and the cellular response to insulin. Studies with intact and trypsin-treated fat cells. *J Biol Chem* 1971; **246**: 6210-6216
8 **Gliemann J**, Gammeltoft S, Vinten J. Time course of insulin-receptor binding and insulin-induced lipogenesis in isolated rat fat cells. *J Biol Chem* 1975; **250**: 3368-3374
9 **Kahn BB**, Rossetti L. Type 2 diabetes--who is conducting the orchestra? *Nat Genet* 1998; **20**: 223-225
10 **Olefsky JM**. Insensitivity of large rat adipocytes to the antilipolytic effects of insulin. *J Lipid Res* 1977; **18**: 459-464

11 **Eisenbarth GS**. Type I diabetes mellitus. A chronic autoimmune disease. *N Engl J Med* 1986; **314**: 1360-1368
12 **Kobayashi T**, Kamata K. Effect of insulin treatment on smooth muscle contractility and endothelium-dependent relaxation in rat aortae from established STZ-induced diabetes. *Br J Pharmacol* 1999; **127**: 835-842
13 **Burcelin R**, Eddouks M, Kande J, Assan R, Girard J. Evidence that GLUT-2 mRNA and protein concentrations are decreased by hyperinsulinaemia and increased by hyperglycaemia in liver of diabetic rats. *Biochem J* 1992; **288** (Pt 2): 675-679
14 **Rossetti L**, Giaccari A. Relative contribution of glycogen synthesis and glycolysis to insulin-mediated glucose uptake. A dose-response euglycemic clamp study in normal and diabetic rats. *J Clin Invest* 1990; **85**: 1785-1792
15 **Rossetti L**, Shulman GI, Zawalich W, DeFronzo RA. Effect of chronic hyperglycemia on in vivo insulin secretion in partially pancreatectomized rats. *J Clin Invest* 1987; **80**: 1037-1044
16 **Russell JW**, Golovoy D, Vincent AM, Mahendru P, Olzmann JA, Mentzer A, Feldman EL. High glucose-induced oxidative stress and mitochondrial dysfunction in neurons. *FASEB J* 2002; **16**: 1738-1748
17 **Lin CY**, Higginbotham DA, Judd RL, White BD. Central leptin increases insulin sensitivity in streptozotocin-induced diabetic rats. *Am J Physiol Endocrinol Metab* 2002; **282**: E1084-E1091
18 **Patlak M**. New weapons to combat an ancient disease: treating diabetes. *FASEB J* 2002; **16**: 1853
19 **Genuth S**, Alberti KG, Bennett P, Buse J, Defronzo R, Kahn R, Kitzmiller J, Knowler WC, Lebovitz H, Lernmark A, Nathan D, Palmer J, Rizza R, Saudek C, Shaw J, Steffes M, Stern M, Tuomilehto J, Zimmet P. Follow-up report on the diagnosis of diabetes mellitus. *Diabetes Care* 2003; **26**: 3160-3167
20 **Tirosh A**, Shai I, Tekes-Manova D, Israeli E, Pereg D, Shochat T, Kochba I, Rudich A. Normal fasting plasma glucose levels and type 2 diabetes in young men. *N Engl J Med* 2005; **353**: 1454-1462
21 **Godsland IF**, Jeffs JA, Johnston DG. Loss of beta cell function as fasting glucose increases in the non-diabetic range. *Diabetologia* 2004; **47**: 1157-1166
22 **Argoff CE**, Cole BE, Fishbain DA, Irving GA. Diabetic peripheral neuropathic pain: clinical and quality-of-life issues. *Mayo Clin Proc* 2006; **81**: S3-11
23 **Vinik AI**, Newlon P, Milicevic Z, McNitt P, Stansberry KB. Diabetic neuropathies: an overview of clinical aspects. In: LeRoith D, Taylor SI, Olefsky JM, editors. Diabetes Mellitus. Philadelphia, New-York: Lippincott-Raven Publishers, 1996: 737-751
24 **Vinik AI**, Mehrabyan A. Diabetic neuropathies. *Med Clin North Am* 2004; **88**: 947-999, xi
25 **Polydefkis M**, Griffin JW, McArthur J. New insights into diabetic polyneuropathy. *JAMA* 2003; **290**: 1371-1376
26 **Horowitz SH**. Diabetic neuropathy. *Clin Orthop Relat Res* 1993; **296**: 78-85
27 **Sugimoto K**, Murakawa Y, Sima AA. Diabetic neuropathy--a continuing enigma. *Diabetes Metab Res Rev* 2000; **16**: 408-433
28 **Bastyr EJ**, Price KL, Bril V. Development and validity testing of the neuropathy total symptom score-6: questionnaire for the study of sensory symptoms of diabetic peripheral neuropathy. *Clin Ther* 2005; **27**: 1278-1294
29 **Dyck PJ.** Detection, characterization, and staging of polyneuropathy: assessed in diabetics. *Muscle Nerve* 1988; **11**: 21-32
30 **Boulton AJ**, Vinik AI, Arezzo JC, Bril V, Feldman EL, Freeman R, Malik RA, Maser RE, Sosenko JM, Ziegler D. Diabetic neuropathies: a statement by the American Diabetes Association. *Diabetes Care* 2005; **28**: 956-962
31 **Thomas PK**. Classification, differential diagnosis, and staging of diabetic peripheral neuropathy. *Diabetes* 1997; **46** Suppl 2: S54-S57
32 **Young RJ**, Zhou YQ, Rodriguez E, Prescott RJ, Ewing DJ, Clarke BF. Variable relationship between peripheral somatic and autonomic neuropathy in patients with different syndromes of diabetic polyneuropathy. *Diabetes* 1986; **35**: 192-197
33 **Young RJ,** Ewing DJ, Clarke BF. Chronic and remitting painful diabetic polyneuropathy. Correlations with clinical features and subsequent changes in neurophysiology. *Diabetes Care* 1988; **11**: 34-40
34 **Maser RE**, Nielsen VK, Bass EB, Manjoo Q, Dorman JS, Kelsey SF, Becker DJ, Orchard TJ. Measuring diabetic neuropathy. Assessment and comparison of clinical examination and quantitative sensory testing. *Diabetes Care* 1989; **12**: 270-275
35 **Navarro X**, Kennedy WR, Fries TJ. Small nerve fiber dysfunction in diabetic neuropathy. *Muscle Nerve* 1989; **12**: 498-507
36 **Ellenberg M**. Diabetic neuropathy: clinical aspects. *Metabolism* 1976; **25**: 1627-1655
37 **Boulton AJ**. Management of diabetic peripheral neuropathy. *Clinical Diabetes* 2005; **23**: 9-15
38 **Belgrade MJ**, Cole BE, McCarberg BH, McLean MJ. Diabetic peripheral neuropathic pain: case studies. *Mayo Clin Proc* 2006; **81**: S26-S32
39 **Pfeifer MA**, Ross DR, Schrage JP, Gelber DA, Schumer MP, Crain GM, Markwell SJ, Jung S. A highly successful and novel model for treatment of chronic painful diabetic peripheral neuropathy. *Diabetes Care* 1993; **16**: 1103-1115
40 **Benbow SJ**, MacFarlane IA. Painful diabetic neuropathy. *Baillieres Best Pract Res Clin Endocrinol Metab* 1999; **13**: 295-308
41 **Dyck PJ**, Giannini C. Pathologic alterations in the diabetic neuropathies of humans: a review. *J Neuropathol Exp Neurol* 1996; **55**: 1181-1193
42 **Thomas PK**. Diabetic neuropathy: mechanisms and future treatment options. *J Neurol Neurosurg Psychiatry* 1999; **67**: 277-279
43 **Zochodne DW**. Neurotrophins and other growth factors in diabetic neuropathy. *Semin Neurol* 1996; **16**: 153-161
44 **Liuzzi FJ**, Bufton SM, Vinik AI. Streptozotocin-induced diabetes mellitus causes changes in primary sensory neuronal cytoskeletal mRNA levels that mimic those caused by axotomy. *Exp Neurol* 1998; **154**: 381-388
45 **Koltzenburg M**, Scadding J. Neuropathic pain. *Curr Opin Neurol* 2001; **14**: 641-647
46 **Torebjörk HE**, Lundberg LE, LaMotte RH. Central changes in processing of mechanoreceptive input in capsaicin-induced secondary hyperalgesia in humans. *J Physiol* 1992; **448**: 765-780
47 **Ochoa JL**, Torebjörk HE. Paraesthesiae from ectopic impulse generation in human sensory nerves. *Brain* 1980; **103**: 835-853
48 **Mogyoros I**, Bostock H, Burke D. Mechanisms of paresthesias arising from healthy axons. *Muscle Nerve* 2000; **23**: 310-320
49 **Wallace VC**, Cottrell DF, Brophy PJ, Fleetwood-Walker SM. Focal lysolecithin-induced demyelination of peripheral afferents results in neuropathic pain behavior that is attenuated by cannabinoids. *J Neurosci* 2003; **23**: 3221-3233
50 **Sima AA**, Nathaniel V, Bril V, McEwen TA, Greene DA. Histopathological heterogeneity of neuropathy in insulin - dependent and non-insulin-dependent diabetes, and demonstration of axo- glial dysjunction in human diabetic neuropathy. *J Clin Invest* 1988; **81**: 349-364
51 **Dyck PJ**, Lambert EH, O'Brien PC. Pain in peripheral neuropathy related to rate and kind of fiber degeneration. *Neurology* 1976; **26**: 466-471
52 **Bonica JJ**. The Managment of Pain. In: Loeser JD, Chapman CR, Fordyce WE. Philadelphia, London: Lea & Febiger, 1990: 1-958
53 **Hotta N**, Toyota T, Matsuoka K, Shigeta Y, Kikkawa R, Kaneko T, Takahashi A, Sugimura K, Koike Y, Ishii J, Sakamoto N. Clinical efficacy of fidarestat, a novel aldose reductase inhibitor, for diabetic peripheral neuropathy: a 52-week multicenter placebo- controlled double-blind parallel group study. *Diabetes Care* 2001; **24**: 1776-1782
54 **Brown MJ**, Martin JR, Asbury AK. Painful diabetic neuropathy. A morphometric study. *Arch Neurol* 1976; **33**: 164-171
55 **Britland ST**, Young RJ, Sharma AK, Clarke BF. Association of painful and painless diabetic polyneuropathy with different patterns of nerve fiber degeneration and regeneration. *Diabetes* 1990; **39**: 898-908
56 **Sima AA**. Peripheral neuropathy in the spontaneously diabetic BB-Wistar-rat. An ultrastructural study. *Acta Neuropathol* 1980; **51**: 223-227
57 **Waxman SG**. Pathophysiology of nerve conduction: relation to diabetic neuropathy. *Ann Intern Med* 1980; **92**: 297-301

58 **Johnson PC**, Doll SC, Cromey DW. Pathogenesis of diabetic neuropathy. *Ann Neurol* 1986; **19**: 450-457
59 **Dyck PJ**, Karnes JL, O'Brien P, Okazaki H, Lais A, Engelstad J. The spatial distribution of fiber loss in diabetic polyneuropathy suggests ischemia. *Ann Neurol* 1986; **19**: 440-449
60 **Dyck PJ**, Lais A, Karnes JL, O'Brien P, Rizza R. Fiber loss is primary and multifocal in sural nerves in diabetic polyneuropathy. *Ann Neurol* 1986; **19:** 425-439
61 **Dyck PJ**, Gutrecht JA, Bastron JA, Karnes WE, Dale AJ. Histologic and teased-fiber measurements of sural nerve in disorders of lower motor and primary sensory neurons. *Mayo Clin Proc* 1968; **43**: 81-123
62 **Malik RA**. The pathology of human diabetic neuropathy. *Diabetes* 1997; **46** Suppl 2: S50-S53
63 **Nathan DM**. The pathophysiology of diabetic complications: how much does the glucose hypothesis explain? *Ann Intern Med* 1996; **124**: 86-89
64 **Vinik AI**. Advances in diabetes for the millennium: new treatments for diabetic neuropathies. *MedGenMed* 2004; **6**: 13
65 **Skyler JS**. Effect of glycemic control on diabetes complications and on the prevention of diabetes. *Clinical Diabetes* 2004; **22**: 162-166
66 **Chronic Complications in Diabetes**. Ed: Sima AA. Animal Models and Chronic Complications. Amsterdam: Harwood Academic Publishers, 2000: 1-277
67 **Lasker RD**. The diabetes control and complications trial. Implications for policy and practice. *N Engl J Med* 1993; **329**: 1035-1036
68 **DCCT**. The effect of intensive treatment of diabetes on the development and progression of long-term complications in insulin-dependent diabetes mellitus. The Diabetes Control and Complications Trial Research Group. *N Engl J Med* 1993; **329**: 977-986
69 **Bode BW**, Schwartz S, Stubbs HA, Block JE. Glycemic characteristics in continuously monitored patients with type 1 and type 2 diabetes: normative values. *Diabetes Care* 2005; **28**: 2361-2366
70 **Singleton JR**, Smith AG, Bromberg MB. Increased prevalence of impaired glucose tolerance in patients with painful sensory neuropathy. *Diabetes Care* 2001; **24**: 1448-1453
71 **Novella SP**, Inzucchi SE, Goldstein JM. The frequency of undiagnosed diabetes and impaired glucose tolerance in patients with idiopathic sensory neuropathy. *Muscle Nerve* 2001; **24**: 1229-1231
72 **Animal Models of Diabetes**. Sima AA, Shafrir E, editors. A Primer. Amsterdam: Harwood Academic Publishers, 2001: 1-364
73 **Moore SA**, Peterson RG, Felten DL, O'Connor BL. A quantitative comparison of motor and sensory conduction velocities in short- and long-term streptozotocin- and alloxan-diabetic rats. *J Neurol Sci* 1980; **48**: 133-152
74 **Weis J**, Dimpfel W, Schröder JM. Nerve conduction changes and fine structural alterations of extra- and intrafusal muscle and nerve fibers in streptozotocin diabetic rats. *Muscle Nerve* 1995; **18:** 175-184
75 **Stevens MJ**, Zhang W, Li F, Sima AA. C-peptide corrects endoneurial blood flow but not oxidative stress in type 1 BB/Wor rats. *Am J Physiol Endocrinol Metab* 2004; **287**: E497-E505
76 **Zochodne DW**, Ho LT, Allison JA. Dorsal root ganglia microenvironment of female BB Wistar diabetic rats with mild neuropathy. *J Neurol Sci* 1994; **127**: 36-42
77 **Ferreira LD**, Huey PU, Pulford BE, Ishii DN, Eckel RH. Sciatic nerve lipoprotein lipase is reduced in streptozotocin-induced diabetes and corrected by insulin. *Endocrinology* 2002; **143**: 1213-1217
78 **Coppey LJ,** Davidson EP, Dunlap JA, Lund DD, Yorek MA. Slowing of motor nerve conduction velocity in streptozotocin-induced diabetic rats is preceded by impaired vasodilation in arterioles that overlie the sciatic nerve. *Int J Exp Diabetes Res* 2000; **1**: 131-143
79 **Qiang X**, Satoh J, Sagara M, Fukuzawa M, Masuda T, Sakata Y, Muto G, Muto Y, Takahashi K, Toyota T. Inhibitory effect of troglitazone on diabetic neuropathy in streptozotocin-induced diabetic rats. *Diabetologia* 1998; **41**: 1321-1326
80 **Sima AA**, Brismar T. Reversible diabetic nerve dysfunction: structural correlates to electrophysiological abnormalities. *Ann Neurol* 1985; **18**: 21-29
81 **Sima AA**, Lattimer SA, Yagihashi S, Greene DA. Axo-glial dysjunction. A novel structural lesion that accounts for poorly reversible slowing of nerve conduction in the spontaneously diabetic bio-breeding rat. *J Clin Invest* 1986; **77**: 474-484
82 **Greene DA**, Chakrabarti S, Lattimer SA, Sima AA. Role of sorbitol accumulation and myo-inositol depletion in paranodal swelling of large myelinated nerve fibers in the insulin-deficient spontaneously diabetic bio-breeding rat. Reversal by insulin replacement, an aldose reductase inhibitor, and myo-inositol. *J Clin Invest* 1987; **79**: 1479-1485
83 **Shimoshige Y**, Ikuma K, Yamamoto T, Takakura S, Kawamura I, Seki J, Mutoh S, Goto T. The effects of zenarestat, an aldose reductase inhibitor, on peripheral neuropathy in Zucker diabetic fatty rats. *Metabolism* 2000; **49**: 1395-1399
84 **Romanovsky D**, Hastings SL, Stimers JR, Dobretsov M. Relevance of hyperglycemia to early mechanical hyperalgesia in streptozotocin-induced diabetes. *J Peripher Nerv Syst* 2004; **9**: 62-69
85 **Chen SR**, Pan HL. Hypersensitivity of spinothalamic tract neurons associated with diabetic neuropathic pain in rats. *J Neurophysiol* 2002; **87:** 2726-2733
86 **Zhuang HX**, Wuarin L, Fei ZJ, Ishii DN. Insulin-like growth factor (IGF) gene expression is reduced in neural tissues and liver from rats with non-insulin-dependent diabetes mellitus, and IGF treatment ameliorates diabetic neuropathy. *J Pharmacol Exp Ther* 1997; **283**: 366-374
87 **Piercy V**, Banner SE, Bhattacharyya A, Parsons AA, Sanger GJ, Smith SA, Bingham S. Thermal, but not mechanical, nociceptive behavior is altered in the Zucker Diabetic Fatty rat and is independent of glycemic status. *J Diabetes Complications* 1999; **13**: 163-169
88 **Schmidt RE**, Dorsey DA, Beaudet LN, Parvin CA, Zhang W, Sima AA. Experimental rat models of types 1 and 2 diabetes differ in sympathetic neuroaxonal dystrophy. *J Neuropathol Exp Neurol* 2004; **63**: 450-460
89 **Brussee V,** Cunningham FA, Zochodne DW. Direct insulin signaling of neurons reverses diabetic neuropathy. *Diabetes* 2004; **53**: 1824-1830
90 **Schmeichel AM**, Schmelzer JD, Low PA. Oxidative injury and apoptosis of dorsal root ganglion neurons in chronic experimental diabetic neuropathy. *Diabetes* 2003; **52**: 165-171
91 **Cameron NE,** Cotter MA, Low PA. Nerve blood flow in early experimental diabetes in rats: relation to conduction deficits. *Am J Physiol* 1991; **261**: E1-E8
92 **Nagamatsu M**, Nickander KK, Schmelzer JD, Raya A, Wittrock DA, Tritschler H, Low PA. Lipoic acid improves nerve blood flow, reduces oxidative stress, and improves distal nerve conduction in experimental diabetic neuropathy. *Diabetes Care* 1995; **18**: 1160-1167
93 **Cameron NE**, Cotter MA, Jack AM, Basso MD, Hohman TC. Protein kinase C effects on nerve function, perfusion, Na(+), K(+)-ATPase activity and glutathione content in diabetic rats. *Diabetologia* 1999; **42**: 1120-1130
94 **Way KJ**, Katai N, King GL. Protein kinase C and the development of diabetic vascular complications. *Diabet Med* 2001; **18**: 945-959
95 **Hamdy O**, Ledbury S, Mullooly C, Jarema C, Porter S, Ovalle K, Moussa A, Caselli A, Caballero AE, Economides PA, Veves A, Horton ES. Lifestyle modification improves endothelial function in obese subjects with the insulin resistance syndrome. *Diabetes Care* 2003; **26**: 2119-2125
96 **Huvers FC**, De Leeuw PW, Houben AJ, De Haan CH, Hamulyak K, Schouten H, Wolffenbuttel BH, Schaper NC. Endothelium-dependent vasodilatation, plasma markers of endothelial function, and adrenergic vasoconstrictor responses in type 1 diabetes under near-normoglycemic conditions. *Diabetes* 1999; **48**: 1300-1307
97 **Khan F**, Elhadd TA, Greene SA, Belch JJ. Impaired skin microvascular function in children, adolescents, and young

adults with type 1 diabetes. *Diabetes Care* 2000; **23**: 215-220
98 **Caballero AE**, Arora S, Saouaf R, Lim SC, Smakowski P, Park JY, King GL, LoGerfo FW, Horton ES, Veves A. Microvascular and macrovascular reactivity is reduced in subjects at risk for type 2 diabetes. *Diabetes* 1999; **48**: 1856-1862
99 **Theriault M**, Dort J, Sutherland G, Zochodne DW. Local human sural nerve blood flow in diabetic and other polyneuropathies. *Brain* 1997; **120** (Pt 7): 1131-1138
100 **Dobretsov M**, Hastings SL, Stimers JR, Zhang JM. Mechanical hyperalgesia in rats with chronic perfusion of lumbar dorsal root ganglion with hyperglycemic solution. *J Neurosci Methods* 2001; **110**: 9-15
101 **Dobretsov M**, Hastings SL, Romanovsky D, Stimers JR, Zhang JM. Mechanical hyperalgesia in rat models of systemic and local hyperglycemia. *Brain Res* 2003; **960**: 174-183
102 **King RH**. The role of glycation in the pathogenesis of diabetic polyneuropathy. *Mol Pathol* 2001; **54**: 400-408
103 **Srivastava SK**, Ramana KV, Bhatnagar A. Role of aldose reductase and oxidative damage in diabetes and the consequent potential for therapeutic options. *Endocr Rev* 2005; **26**: 380-392
104 **Yabe-Nishimura C**. Aldose reductase in glucose toxicity: a potential target for the prevention of diabetic complications. *Pharmacol Rev* 1998; **50**: 21-33
105 **Reusch JE**. Diabetes, microvascular complications, and cardiovascular complications: what is it about glucose? *J Clin Invest* 2003; **112**: 986-988
106 **Brownlee M**. The pathobiology of diabetic complications: a unifying mechanism. *Diabetes* 2005; **54**: 1615-1625
107 **Pieper GM.** Review of alterations in endothelial nitric oxide production in diabetes: protective role of arginine on endothelial dysfunction. *Hypertension* 1998; **31**: 1047-1060
108 **Pacher P**, Szabó C. Role of poly(ADP-ribose) polymerase-1 activation in the pathogenesis of diabetic complications: endothelial dysfunction, as a common underlying theme. *Antioxid Redox Signal* 2005; **7**: 1568-1580
109 **Wang Y**, Schmeichel AM, Iida H, Schmelzer JD, Low PA. Ischemia-reperfusion injury causes oxidative stress and apoptosis of Schwann cell in acute and chronic experimental diabetic neuropathy. *Antioxid Redox Signal* 2005; **7**: 1513-1520
110 **Chait A**, Brunzell JD. Diabetes, lipids, and atherosclerosis. In: LeRoith D, Taylor SI, Olefsky JM. Diabetes Mellitus. Philadelphia, New York: Lippincott-Raven Publishers, 1996: 772-777
111 **Obrosova IG**. Increased sorbitol pathway activity generates oxidative stress in tissue sites for diabetic complications. *Antioxid Redox Signal* 2005; **7**: 1543-1552
112 **Kellogg AP**, Pop-Busui R. Peripheral nerve dysfunction in experimental diabetes is mediated by cyclooxygenase-2 and oxidative stress. *Antioxid Redox Signal* 2005; **7**: 1521-1529
113 **Greene DA**, Stevens MJ, Obrosova I, Feldman EL. Glucose-induced oxidative stress and programmed cell death in diabetic neuropathy. *Eur J Pharmacol* 1999; **375**: 217-223
114 **Feldman EL**. Oxidative stress and diabetic neuropathy: a new understanding of an old problem. *J Clin Invest* 2003; **111**: 431-433
115 **Ceriello A**, Motz E. Is oxidative stress the pathogenic mechanism underlying insulin resistance, diabetes, and cardiovascular disease? The common soil hypothesis revisited. *Arterioscler Thromb Vasc Biol* 2004; **24**: 816-823
116 **Kishi Y**, Schmelzer JD, Yao JK, Zollman PJ, Nickander KK, Tritschler HJ, Low PA. Alpha-lipoic acid: effect on glucose uptake, sorbitol pathway, and energy metabolism in experimental diabetic neuropathy. *Diabetes* 1999; **48**: 2045-2051
117 **Ametov AS**, Barinov A, Dyck PJ, Hermann R, Kozlova N, Litchy WJ, Low PA, Nehrdich D, Novosadova M, O'Brien PC, Reljanovic M, Samigullin R, Schuette K, Strokov I, Tritschler HJ, Wessel K, Yakhno N, Ziegler D. The sensory symptoms of diabetic polyneuropathy are improved with alpha-lipoic acid: the SYDNEY trial. *Diabetes Care* 2003; **26**: 770-776
118 **Maritim AC**, Sanders RA, Watkins JB. Diabetes, oxidative stress, and antioxidants: a review. *J Biochem Mol Toxicol* 2003; **17**: 24-38
119 **Johansen JS**, Harris AK, Rychly DJ, Ergul A. Oxidative stress and the use of antioxidants in diabetes: linking basic science to clinical practice. *Cardiovasc Diabetol* 2005; **4**: 5-25
120 **Petersen M**, LaMotte RH. Relationships between capsaicin sensitivity of mammalian sensory neurons, cell size and type of voltage gated Ca-currents. *Brain Res* 1991; **561**: 20-26
121 **Obrosova IG,** Van Huysen C, Fathallah L, Cao XC, Greene DA, Stevens MJ. An aldose reductase inhibitor reverses early diabetes-induced changes in peripheral nerve function, metabolism, and antioxidative defense. *FASEB J* 2002; **16**: 123-125
122 **Young RJ**, Ewing DJ, Clarke BF. A controlled trial of sorbinil, an aldose reductase inhibitor, in chronic painful diabetic neuropathy. *Diabetes* 1983; **32**: 938-942
123 **Martyn CN**, Reid W, Young RJ, Ewing DJ, Clarke BF. Six-month treatment with sorbinil in asymptomatic diabetic neuropathy. Failure to improve abnormal nerve function. *Diabetes* 1987; **36**: 987-990
124 **Boulton AJ**, Malik RA, Arezzo JC, Sosenko JM. Diabetic somatic neuropathies. *Diabetes Care* 2004; **27**: 1458-1486
125 **Singleton JR**, Smith AG, Russell J, Feldman EL. Polyneuropathy with Impaired Glucose Tolerance: Implications for Diagnosis and Therapy. *Curr Treat Options Neurol* 2005; **7**: 33-42
126 **Russell JW**, Feldman EL. Impaired glucose tolerance--does it cause neuropathy? *Muscle Nerve* 2001; **24**: 1109-1112
127 **Singleton JR**, Smith AG, Bromberg MB. Painful sensory polyneuropathy associated with impaired glucose tolerance. *Muscle Nerve* 2001; **24**: 1225-1228
128 **Pittenger GL**, Mehrabyan A, Simmons K, Amandarice C, Barlow P, Vinik AI. Small fiber neuropathy is associated with the metabolic syndrome. *Metab Syndr Relat Disord* 2005; **3**: 113-121
129 **Sumner CJ**, Sheth S, Griffin JW, Cornblath DR, Polydefkis M. The spectrum of neuropathy in diabetes and impaired glucose tolerance. *Neurology* 2003; **60**: 108-111
130 **Monnier L**, Mas E, Ginet C, Michel F, Villon L, Cristol JP, Colette C. Activation of oxidative stress by acute glucose fluctuations compared with sustained chronic hyperglycemia in patients with type 2 diabetes. *JAMA* 2006; **295**: 1681-1687
131 **de Neeling JN**, Beks PJ, Bertelsmann FW, Heine RJ, Bouter LM. Peripheral somatic nerve function in relation to glucose tolerance in an elderly Caucasian population: the Hoorn study. *Diabet Med* 1996; **13**: 960-966
132 **Morley GK**, Mooradian AD, Levine AS, Morley JE. Mechanism of pain in diabetic peripheral neuropathy. Effect of glucose on pain perception in humans. *Am J Med* 1984; **77**: 79-82
133 **Thye-Rønn P**, Sindrup SH, Arendt-Nielsen L, Brennum J, Hother-Nielsen O, Beck-Nielsen H. Effect of short-term hyperglycemia per se on nociceptive and non-nociceptive thresholds. *Pain* 1994; **56**: 43-49
134 **Chan AW**, MacFarlane IA, Bowsher D. Short term fluctuations in blood glucose concentrations do not alter pain perception in diabetic-patients with and without painful peripheral neuropathy. *Diabetes Res* 1990; **14**: 15-19
135 **Oyibo SO**, Prasad YD, Jackson NJ, Jude EB, Boulton AJ. The relationship between blood glucose excursions and painful diabetic peripheral neuropathy: a pilot study. *Diabet Med* 2002; **19**: 870-873
136 **Huang TJ**, Price SA, Chilton L, Calcutt NA, Tomlinson DR, Verkhratsky A, Fernyhough P. Insulin prevents depolarization of the mitochondrial inner membrane in sensory neurons of type 1 diabetic rats in the presence of sustained hyperglycemia. *Diabetes* 2003; **52**: 2129-2136
137 **Maneuf YP**, Blake R, Andrews NA, McKnight AT. Reduction by gabapentin of K+-evoked release of [3H]-glutamate from the caudal trigeminal nucleus of the streptozotocin-treated rat. *Br J Pharmacol* 2004; **141**: 574-579
138 **Calcutt NA**, Jorge MC, Yaksh TL, Chaplan SR. Tactile allodynia and formalin hyperalgesia in streptozotocin-diabetic rats: effects of insulin, aldose reductase inhibition and lidocaine. *Pain* 1996; **68**: 293-299

139 **Calcutt NA**, Freshwater JD, Mizisin AP. Prevention of sensory disorders in diabetic Sprague-Dawley rats by aldose reductase inhibition or treatment with ciliary neurotrophic factor. *Diabetologia* 2004; **47**: 718-724

140 **Roane DS**, Porter JR. Nociception and opioid-induced analgesia in lean (Fa/-) and obese (fa/fa) Zucker rats. *Physiol Behav* 1986; **38**: 215-218

141 **Oltman CL**, Coppey LJ, Gellett JS, Davidson EP, Lund DD, Yorek MA. Progression of vascular and neural dysfunction in sciatic nerves of Zucker diabetic fatty and Zucker rats. *Am J Physiol Endocrinol Metab* 2005; **289**: E113-E122

142 **Ishii DN**. Implication of insulin-like growth factors in the pathogenesis of diabetic neuropathy. *Brain Res Brain Res Rev* 1995; **20**: 47-67

143 **Sugimoto K**, Murakawa Y, Zhang W, Xu G, Sima AA. Insulin receptor in rat peripheral nerve: its localization and alternatively spliced isoforms. *Diabetes Metab Res Rev* 2000; **16**: 354-363

144 **Sugimoto K,** Murakawa Y, Sima AA. Expression and localization of insulin receptor in rat dorsal root ganglion and spinal cord. *J Peripher Nerv Syst* 2002; **7**: 44-53

145 **Frasca F**, Pandini G, Scalia P, Sciacca L, Mineo R, Costantino A, Goldfine ID, Belfiore A, Vigneri R. Insulin receptor isoform A, a newly recognized, high-affinity insulin-like growth factor II receptor in fetal and cancer cells. *Mol Cell Biol* 1999; **19**: 3278-3288

146 **Martin CL**, Albers J, Herman WH, Cleary P, Waberski B, Greene DA, Stevens MJ, Feldman EL. Neuropathy among the diabetes control and complications trial cohort 8 years after trial completion. *Diabetes Care* 2006; **29**: 340-344

147 **Singhal A**, Cheng C, Sun H, Zochodne DW. Near nerve local insulin prevents conduction slowing in experimental diabetes. *Brain Res* 1997; **763**: 209-214

148 **Partanen J**, Niskanen L, Lehtinen J, Mervaala E, Siitonen O, Uusitupa M. Natural history of peripheral neuropathy in patients with non-insulin-dependent diabetes mellitus. *N Engl J Med* 1995; **333**: 89-94

149 **Delaney CA**, Mouser JV, Westerman RA. Insulin sensitivity and sensory nerve function in non-diabetic human subjects. *Neurosci Lett* 1994; **180**: 277-280

150 **Jacob S**, Streeper RS, Fogt DL, Hokama JY, Tritschler HJ, Dietze GJ, Henriksen EJ. The antioxidant alpha-lipoic acid enhances insulin-stimulated glucose metabolism in insulin-resistant rat skeletal muscle. *Diabetes* 1996; **45**: 1024-1029

151 **Broca C**, Breil V, Cruciani-Guglielmacci C, Manteghetti M, Rouault C, Derouet M, Rizkalla S, Pau B, Petit P, Ribes G, Ktorza A, Gross R, Reach G, Taouis M. Insulinotropic agent ID-1101 (4-hydroxyisoleucine) activates insulin signaling in rat. *Am J Physiol Endocrinol Metab* 2004; **287**: E463-E471

152 **Wong V**, Stavar L, Szeto L, Uffelman K, Wang CH, Fantus IG, Lewis GF. Atorvastatin induces insulin sensitization in Zucker lean and fatty rats. *Atherosclerosis* 2006; **184**: 348-355

153 **Freychet P**. Insulin receptors and insulin actions in the nervous system. *Diabetes Metab Res Rev* 2000; **16**: 390-392

154 **Kihara M**, Zollman PJ, Smithson IL, Lagerlund TD, Low PA. Hypoxic effect of exogenous insulin on normal and diabetic peripheral nerve. *Am J Physiol* 1994; **266**: E980-E985

155 **Dandona P,** Mohanty P, Chaudhuri A, Garg R, Aljada A. Insulin infusion in acute illness. *J Clin Invest* 2005; **115**: 2069-2072

156 **Nedrebø T**, Karlsen TV, Salvesen GS, Reed RK. A novel function of insulin in rat dermis. *J Physiol* 2004; **559**: 583-591

157 **Jeschke MG**, Einspanier R, Klein D, Jauch KW. Insulin attenuates the systemic inflammatory response to thermal trauma. *Mol Med* 2002; **8**: 443-450

158 **Davel AP**, Rossoni LV, Vassallo DV. Effects of ouabain on the pressor response to phenylephrine and on the sodium pump activity in diabetic rats. *Eur J Pharmacol* 2000; **406**: 419-427

159 **Sweeney G**, Klip A. Regulation of the Na+/K+-ATPase by insulin: why and how? *Mol Cell Biochem* 1998; **182**: 121-133

160 **Steinberg HO,** Brechtel G, Johnson A, Fineberg N, Baron AD. Insulin-mediated skeletal muscle vasodilation is nitric oxide dependent. A novel action of insulin to increase nitric oxide release. *J Clin Invest* 1994; **94**: 1172-1179

161 **Ranke MB**. Insulin-like growth factor-I treatment of growth disorders, diabetes mellitus and insulin resistance. *Trends Endocrinol Metab* 2005; **16:** 190-197

162 **Recio-Pinto E**, Rechler MM, Ishii DN. Effects of insulin, insulin-like growth factor-II, and nerve growth factor on neurite formation and survival in cultured sympathetic and sensory neurons. *J Neurosci* 1986; **6:** 1211-1219

163 **Mill JF**, Chao MV, Ishii DN. Insulin, insulin-like growth factor II, and nerve growth factor effects on tubulin mRNA levels and neurite formation. *Proc Natl Acad Sci U S A* 1985; **82**: 7126-7130

164 **Near SL**, Whalen LR, Miller JA, Ishii DN. Insulin-like growth factor II stimulates motor nerve regeneration. *Proc Natl Acad Sci U S A* 1992; **89**: 11716-11720

165 **Dupont J,** Khan J, Qu BH, Metzler P, Helman L, LeRoith D. Insulin and IGF-1 induce different patterns of gene expression in mouse fibroblast NIH-3T3 cells: identification by cDNA microarray analysis. *Endocrinology* 2001; **142**: 4969-4975

166 **Meier C**, Parmantier E, Brennan A, Mirsky R, Jessen KR. Developing Schwann cells acquire the ability to survive without axons by establishing an autocrine circuit involving insulin-like growth factor, neurotrophin-3, and platelet-derived growth factor-BB. *J Neurosci* 1999; **19:** 3847-3859

167 **Holzenberger M**, Dupont J, Ducos B, Leneuve P, Géloën A, Even PC, Cervera P, Le Bouc Y. IGF-1 receptor regulates lifespan and resistance to oxidative stress in mice. *Nature* 2003; **421**: 182-187

168 **Rajkumar K**, Krsek M, Dheen ST, Murphy LJ. Impaired glucose homeostasis in insulin-like growth factor binding protein-1 transgenic mice. *J Clin Invest* 1996; **98**: 1818-1825

169 **Karagiannis SN**, King RH, Thomas PK. Colocalisation of insulin and IGF-1 receptors in cultured rat sensory and sympathetic ganglion cells. *J Anat* 1997; **191** (Pt 3): 431-440

170 **Craner MJ**, Klein JP, Black JA, Waxman SG. Preferential expression of IGF-I in small DRG neurons and down-regulation following injury. *Neuroreport* 2002; **13**: 1649-1652

171 **Cheng HL**, Randolph A, Yee D, Delafontaine P, Tennekoon G, Feldman EL. Characterization of insulin-like growth factor-I and its receptor and binding proteins in transected nerves and cultured Schwann cells. *J Neurochem* 1996; **66**: 525-536

172 **Jonas HA**, Harrison LC. The human placenta contains two distinct binding and immunoreactive species of insulin-like growth factor-I receptors. *J Biol Chem* 1985; **260**: 2288-2294

173 **Moxham CP**, Duronio V, Jacobs S. Insulin-like growth factor I receptor beta-subunit heterogeneity. Evidence for hybrid tetramers composed of insulin-like growth factor I and insulin receptor heterodimers. *J Biol Chem* 1989; **264**: 13238-13244

174 **Bondy CA**, Underwood LE, Clemmons DR, Guler HP, Bach MA, Skarulis M. Clinical uses of insulin-like growth factor I. *Ann Intern Med* 1994; **120**: 593-601

175 **Saukkonen T**, Amin R, Williams RM, Fox C, Yuen KC, White MA, Umpleby AM, Acerini CL, Dunger DB. Dose-dependent effects of recombinant human insulin-like growth factor (IGF)-I/IGF binding protein-3 complex on overnight growth hormone secretion and insulin sensitivity in type 1 diabetes. *J Clin Endocrinol Metab* 2004; **89**: 4634-4641

176 **Clemmons DR**, Moses AC, McKay MJ, Sommer A, Rosen DM, Ruckle J. The combination of insulin-like growth factor I and insulin-like growth factor-binding protein-3 reduces insulin requirements in insulin-dependent type 1 diabetes: evidence for in vivo biological activity. *J Clin Endocrinol Metab* 2000; **85**: 1518-1524

177 **Thrailkill KM**, Quattrin T, Baker L, Kuntze JE, Compton PG, Martha PM. Cotherapy with recombinant human insulin-like growth factor I and insulin improves glycemic control in type 1 diabetes. RhIGF-I in IDDM Study Group. *Diabetes Care* 1999; **22**: 585-592

178 **Cusi K**, DeFronzo R. Recombinant human insulin-like growth factor I treatment for 1 week improves metabolic control in type 2 diabetes by ameliorating hepatic and muscle insulin resistance. *J Clin Endocrinol Metab* 2000; **85**: 3077-3084

179 **Schmidt RE**, Dorsey DA, Beaudet LN, Peterson RG. Analysis of the Zucker Diabetic Fatty (ZDF) type 2 diabetic rat model suggests a neurotrophic role for insulin/IGF-I in diabetic

autonomic neuropathy. *Am J Pathol* 2003; **163**: 21-28
180 **Busiguina S**, Fernandez AM, Barrios V, Clark R, Tolbert DL, Berciano J, Torres-Aleman I. Neurodegeneration is associated to changes in serum insulin-like growth factors. *Neurobiol Dis* 2000; **7**: 657-665
181 **Chen HS**, Shan YX, Yang TL, Lin HD, Chen JW, Lin SJ, Wang PH. Insulin deficiency downregulated heat shock protein 60 and IGF-1 receptor signaling in diabetic myocardium. *Diabetes* 2005; **54**: 175-181
182 **Jacob RJ**, Sherwin RS, Greenawalt K, Shulman GI. Simultaneous insulinlike growth factor I and insulin resistance in obese Zucker rats. *Diabetes* 1992; **41**: 691-697
183 **Sima AA**. Diabetic neuropathy in type 1 and type 2 diabetes and the effects of C-peptide. *J Neurol Sci* 2004; **220**: 133-136
184 **Sima AA**, Zhang W, Grunberger G. Type 1 diabetic neuropathy and C-peptide. *Exp Diabesity Res* 2004; **5:** 65-77
185 **Kamiya H**, Zhang W, Sima AA. C-peptide prevents nociceptive sensory neuropathy in type 1 diabetes. *Ann Neurol* 2004; **56**: 827-835
186 **Ekberg K**, Brismar T, Johansson BL, Jonsson B, Lindström P, Wahren J. Amelioration of sensory nerve dysfunction by C-Peptide in patients with type 1 diabetes. *Diabetes* 2003; **52**: 536-541
187 **Forst T**, Kunt T, Pohlmann T, Goitom K, Engelbach M, Beyer J, Pfützner A. Biological activity of C-peptide on the skin microcirculation in patients with insulin-dependent diabetes mellitus. *J Clin Invest* 1998; **101**: 2036-2041
188 **Rola R**, Szulczyk P. Quantitative differences between kinetic properties of Na(+) currents in postganglionic sympathetic neurones projecting to muscular and cutaneous effectors. *Brain Res* 2000; **857**: 327-336

S- Editor Liu Y **L- Editor** Lutze M **E- Editor** Bi L

PO Box 2345, Beijing 100023, China
www.wjgnet.com
wjg@wjgnet.com

World J Gastroenterol 2007 January 14; 13(2): 192-218
World Journal of Gastroenterology ISSN 1007-9327
© 2007 The WJG Press. All rights reserved.

TOPIC HIGHLIGHT

Parimal Chowdhury, Professor, *Series Editors*

Advances in small animal mesentery models for *in vivo* flow cytometry, dynamic microscopy, and drug screening

Ekaterina I Galanzha, Valery V Tuchin, Vladimir P Zharov

Ekaterina I Galanzha, Vladimir P Zharov, Philips Classic Laser Laboratories, University of Arkansas for Medical Sciences (UAMS), Little Rock, AR, United States
Ekaterina I Galanzha, Valery V Tuchin, Department of Optics and Biomedical Physics, Research-Educational Institute of Optics and Biophotonics, Saratov State University, Saratov, Russia
Supported by NIH/NIBIB; No. EB001858, EB-000873, EB005123
Correspondence to: Ekaterina I Galanzha, MD, PhD, DSc, Philips Classic Laser Laboratories, University of Arkansas for Medical Sciences (UAMS), 4301 W. Markham St., Little Rock, AR 72205-7199, United States. egalanzha@uams.edu
Telephone: +1-501-5267620 Fax: +1-501-6868029
Received: 2006-10-10 Accepted: 2006-11-30

© 2007 The WJG Press. All rights reserved.

Key words: Lymph microcirculation; Transmission digital microscopy; Rat mesentery; Flow cytometry; Photothermal technique

Galanzha EI, Tuchin VV, Zharov VP. Advances in small animal mesentery models for *in vivo* flow cytometry, dynamic microscopy, and drug screening. *World J Gastroenterol* 2007; 13(2): 192-218

http://www.wjgnet.com/1007-9327/13/192.asp

Abstract

Using animal mesentery with intravital optical microscopy is a well-established experimental model for studying blood and lymph microcirculation *in vivo*. Recent advances in cell biology and optical techniques provide the basis for extending this model for new applications, which should generate significantly improved experimental data. This review summarizes the achievements in this specific area, including *in vivo* label-free blood and lymph photothermal flow cytometry, super-sensitive fluorescence image cytometry, light scattering and speckle flow cytometry, microvessel dynamic microscopy, infrared (IR) angiography, and high-speed imaging of individual cells in fast flow. The capabilities of these techniques, using the rat mesentery model, were demonstrated in various studies; e.g., real-time quantitative detection of circulating and migrating individual blood and cancer cells, studies on vascular dynamics with a focus on lymphatics under normal conditions and under different interventions (e.g. lasers, drugs, nicotine), assessment of lymphatic disturbances from experimental lymphedema, monitoring cell traffic between blood and lymph systems, and high-speed imaging of cell transient deformability in flow. In particular, the obtained results demonstrated that individual cell transportation in living organisms depends on cell type (e.g., normal blood or leukemic cells), the cell's functional state (e.g., live, apoptotic, or necrotic), and the functional status of the organism. Possible future applications, including *in vivo* early diagnosis and prevention of disease, monitoring immune response and apoptosis, chemo- and radio-sensitivity tests, and drug screening, are also discussed.

INTRODUCTION

It is difficult to access the gastrointestinal tract with powerful intravital high-resolution optical microscopy. One unique exception is the mesentery, which has as its main functions maintaining digestive organs in their proper positions while simultaneously providing routes for nerves and for blood and lymph vessels. To date, small animal mesentery is a well-established experimental model for studying blood and lymph microcirculation *in vivo*.

Historically, the first microscopic observation of the mesenteric lymph microvessels of a guinea pig was performed by Arnold Heller in 1869[1]. During the first 30-50 years of the 20th century, extensive *in vivo* studies of mesenteric microcirculation were undertaken[2-4]. In particular, the basics of capillary circulation were first studied in rat mesentery[3]. Later, this model was successfully used to study the fundamentals of the microvascular physiology of blood (i.e., microvascular rheology, hemodynamics, vasomotion, hematocrit, permeability of the vascular wall, flow velocity) and lymph (i.e., phasic contractile activity, flow velocity, and the diameter of small lymphatics) systems[5-26]. Using rat mesentery, Sekizuka *et al*[24] performed real-time videoanalysis of contractile lymphatic motion in rat mesentery and determined quantitatively the dynamics of the frequency of these contractions. Benoit *et al*[22] and Dixon *et al*[26] obtained basic data about relationships among lymphatic contractile activity, vessel diameter, and lymph flow velocity[23]. In particular, they established the correlation between cyclic fluctuations of lymph velocity

and vessel wall motion during the phasic contraction. Most of the results related to microvessel diameter and contractile activity were obtained with conventional transmission optical microscopy alone.

The mesentery model has also been used to study the effects of various hormones, mediators, drugs, and other environmental impacts on microcirculation, including the influence of histamine, norepinephrine, dopamine, dobutamine, PO_2, substance P, L-NAME, methylene blue, leukotrienes, histamine, platelet activating factor, temperature, low-power laser radiation, X-radiation, and others[3,20,27-34]. In particular, this model was used in the first study of the effects of nitric oxide (NO) on lymph microvessels *in vivo*: Shirasawa *et al*[35] showed the influence of a NO synthase inhibitor on lymphatic diameter and contractile activity, which was reversed after applying an endogenous NO donor (L-arginine). This model has also been employed to study microcirculation disturbances in experimental models of diseases such as diabetes, ischemia, hemorrhage, shock, inflammation, tumor, edema, and others[2,4,13,21,22,36,37].

Recent discoveries in cell biology (e.g., identification of the genes, such as VEGF-C and VEGF-D, expressed by endothelium or endothelial growth factors for lymphatics), along with advances in optical techniques (e.g., lasers, high-speed digital cameras, powerful software) have increased interest in this model and its capabilities for studying the fundamentals of blood and lymph microcirculation, including its potential for the molecular imaging of individual cells *in vivo*[38-40]. Nevertheless, some methods used in most experiments have limitations. For example, the majority of the results about platelets [e.g., platelet thrombosis, or their interaction with white blood cells (WBCs) or vessel walls], red blood cells (RBCs), and tumor cells were obtained with what are currently the most powerful techniques, such as fluorescent labe ling[12,13,21,41-43]. However, despite significant progress in the development of new labels[44-46] (e.g., quantum dots, fluorescent-specific antibodies[47]), these techniques *in vivo* (as in many other experiments *in vitro*) are potentially subject to photobleaching (despite the short exposure time), or cytotoxicity. Moreover, growing evidence shows that fluorescence labeling may seriously distort genuine cell properties, even without evident toxicity, and cellular physiologic functions. For example, acridine orange and Rhodamine 6G, traditional fluorescent dyes for leukocytes, have been demonstrated to be mutagenic and carcinogenic, and possibly cause phototoxic effects[48-51]. Fluorescence imaging of lymphatics by injecting fluorescein isothiocyanate (FITC)-dextran into the interstitial space led to elevated interstitial pressure and altered lymph viscosity[52]. These findings may raise some concern about the kinetics of labeled cells in flow, particularly about the main cause and the real rate of cell elimination from circulation, the actual properties of apoptotic or cancer cells, or the strong influence of the tags due to phagocytosis, or the interaction of tags with other cells[53-55]. All these concerns gain importance in *in vivo* studies in humans, and add to interest in developing label-free imaging. The mesentery model with advanced optical technique can provide a good quality of label-free imaging of moving cells.

In mesenteric microvessels, the imaging of flowing cells *in vivo* without any staining or labeling was realized mainly with transmission microscopy for slow moving, rolling (30-70 μm/s), and adhesive WBCs[10,12,14,15,17]. The monitoring of single RBCs and their small aggregates has usually been performed in two modes: 1) in selected microvessels (small venules or capillaries) with slow flow using a frame rate of 20-30 frames per second (fps), or 2) using a short time-exposure mode (~0.1-1 ms) by which only single images of fast-moving cells can be captured[56-58]. Only a few studies demonstrated relatively high-speed imaging for measuring flow velocity in the range of 750-2500 fps in blood flow, and approximately 500 fps in lymph flow[19,26,59]. Due to motion distortion, these speeds are not quite fast enough to image shape and subcellular structures of individual fast-moving cells. For example, imaging in blood microvessels, with typical flow velocities of 5-10 mm/s, requires imaging speed ranges of 5000-10 000 fps[58]. Additionally, simultaneous high-speed imaging with high optical resolution of individual moving cells has not yet been developed *in vivo*. This is crucial for *in vivo* flow cytometry (FC).

In this review, which is based on our 15 years of experience in this area, we summarize both our previous data, which are scattered or presented in difficult-to-access publications, as well as our latest achievements in *in vivo* label-free FC, high-speed imaging, and vessel dynamics, focusing on real-time monitoring of circulating and migrating blood and cancer cells in blood and lymph systems, and especially on our studies of microlymphatic function in normal and pathological states and under the impact of different therapeutic interventions.

FEATURES OF THE LYMPHATIC SYSTEM

Unlike the circular blood network, the lymphatic vasculature is an open-ended system that transports lymph from tissue to the blood system[60,61]. The initial lymphatics collect fluid and cells from the interstitial space of tissue and form the afferent (prenodal) lymph, which is transported through valvular prenodal lymphatics to the lymph nodes. In the lymph nodes, some fluid, debris, and pathogens are removed from lymph, while cells (mainly lymphocytes) are added to lymph. Lymph leaves the lymph node by efferent collecting lymphatics, and passes through the thoracic duct and enters into the inferior vena cava. During this process, some cells and proteins can re-circulate in the blood system-tissue-lymph system-blood system pathway. In contrast to blood, which is moved by one motor, the heart, the motion of lymph is primarily maintained by rhythmic contractions of vessel walls, called phasic contractions. Such contractions are initiated by pacemakers along vessels. Additionally, lymph vessels have well-developed bicuspid funnel-shaped valves (collagen sheets with filaments covered on both sides by endothelium), which are dispersed at regular intervals along the vessel and divide it into functional units-lymphangions (the fragment of the lymph vessel between input and output valves). The valves can block lymphatic lumen to prevent (at least partially) backflow and contribute to a

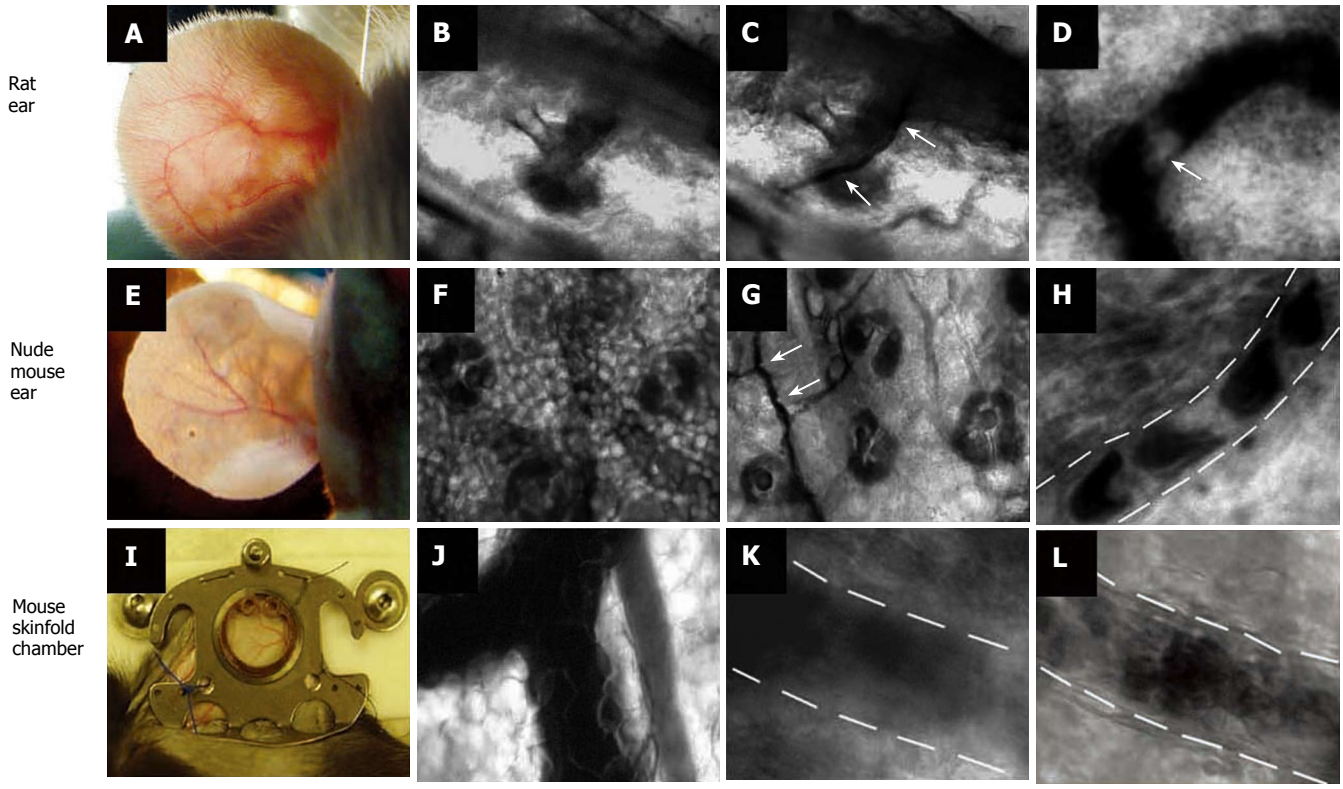

Figure 1 Label-free imaging of blood vessels in different animal models. Rat ear (with hair): **A**: External view of large vessel; **B**, **C**: transmission images of microvessel at low magnification (4 ×) before (**B**) and after (**C**) topical administration of an optical clearing agent such as glycerol (arrows show microvessel); **D**: high-resolution image of rolling WBC (arrow) in a venula (magnification 40 ×). Ear of nude mouse: **E**: external view of large vessels; **F**, **G**: transmission images of microvessels at low magnification (10 ×) before (**F**) and after (**G**) topical administration of glycerol (arrows show microvessel); **H**: high-resolution image of individual RBCs in a capillary (magnification 100 ×); **I**: large vessels in skinfold chamber of a mouse; **J**: transmission image of blood microvessel at low magnification (10 ×); **K**, **I**: high-resolution image of a venula before (**K**) and after (**I**) topical administration of glycerol (40 ×).

unidirectional flow. Some external forces, such as muscle contractions, respiratory movements, and intestinal peristalsis, can also maintain lymph motion. In general, lymph flow is turbulent, has an oscillating character, and is slower than blood motion. The lymphatics in an entire living organism have multi-level regulation, including the central nervous system, hormones, and local substances such as mediators, pH, and Ca ions[1,24,26,29,60-69].

Compared to the well-studied blood system, our understanding of lymph function is limited; however, rat mesentery, with its unique structure that we describe here, may help to fill knowledge gaps in this under-explored system. Below, we present a brief comparison of different animal models emphasizing the advantage of rat mesentery for monitoring single-cell transport under normal and pathologic conditions.

ANIMAL MODELS

Microcirculation has been successfully studied using optical microscopy in various animal models (e.g., rabbit or mouse ear, hamster or mouse dorsal skin-flap window or skin-fold chamber, or open cremaster muscle)[52-55,59,63,70-73]. The use of these models for high-resolution imaging of individual flowing or static cells may be somewhat limited because of significant light scattering from surrounding tissue (e.g., skin or muscles) and/or the relatively deep location of vessels below the skin. Image quality in these particular models can be improved in two ways: (1) by using thin hairless skin (e.g. ear of nude mouse ~270 μm thick), or (2) by decreasing light scattering using a recently developed optical clearing method combined with spectral selection (e.g. use a "green" filter to increase blood vessel contrast)[74-77].

Figure 1 illustrates our few attempts using these models and transmission microscopy to obtain high-resolution images of individual cells in blood flow without staining. In particular, we compared images of blood microvessels of ordinary (i.e. with hair, Figure 1A-D) and nude (i.e., hairless, Figure 1E-H) ear skin of rats and mice, and with mouse dorsal skin-fold chamber (Figure 1I-L). The best results were obtained with the nude mouse ear model in combination with optical clearing and a spectral filter in the range of the maximum absorption of hemoglobin, around 570-580 nm (Figure 1F-H). The dorsal skin-fold model provided a poorer quality image of an individual cell as compared with the RBC images of the skin-fold chamber (Figure 1L) and with RBC images of nude mouse ear (Figure 1H), and required an invasive procedure. In general, even after many improvements, all of these models provide monitoring of individual cells only in selected capillaries with single-file flow (RBCs travel in one line with the same velocity). In addition, the images of colorless lymphatics in skin can be obtained mainly with additional labeling with fluorescent or absorbing contrast agents (e.g. FITC-dextran and dyes such as isosulfan blue,

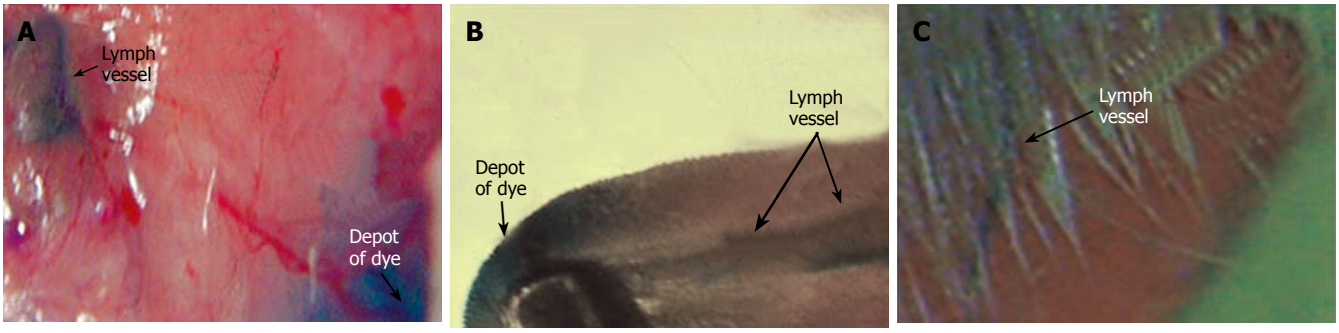

Figure 2 Imaging of lymph vessels using contrast agents in different rat models. Lymphatics labeled by a 1% solution of lymphazurin in muscles of (**A**) abdomen wall, (**B**) tongue, and (**C**) pad.

lymphazurin, and others; Figure 2)[52,78-80]. However, these procedures do not provide information on cell dynamics in flow or valve functioning.

In general, the best targets for conventional transmission microscopy are relatively transparent animal structures such as zebrafish, and vascular nets of the hamster cheek pouch[63,81-84]; however, these models are not ideal for studying lymph or blood vessels. The zebrafish (tropical fish) model is very different from human anatomy and physiology, and while the hamster cheek pouch model is good for visualizing blood microvessels, the lymphatics in the hamster cheek pouch are not well developed, preventing us from simultaneously studying blood and lymph systems, if desired.

To date, the best optical images of both lymph and blood microvessels have been obtained in the mesentery of small cold-blooded (frog) and mammalian (mouse, cat, rabbit, guinea pig, and rat) animals. However, the capillaries of frog mesenteric microvessels are relatively larger in diameter and their sensitivity to environmental impacts is markedly less than that of mammals[3]. Of the mammalian models, the rat is an excellent model in terms of size, physiology, and pharmacokinetics for broadening medical applications, including single-cell diagnostics[85-88]. Additionally, some rat models are able to mimic select human diseases. This is particularly important for understanding common mechanisms of microvessel physiology and pathology (edema, inflammation, tumor), as well as for studying specific features of mesenteric microvasculature under normal conditions (to maintain homeostasis in the abdominal space) and in mesentery-related diseases (e.g. mesothelioma, sclerosing mesenteritis, panniculitis, acute mesenteric vein thrombosis, tumor metastasis).

Mesentery consists of thin (8-15 μm), relatively transparent, duplex connective tissue, which is divided into triangular, relatively transparent windows by arteries (400-500 μm in diameter) and veins (600-700 μm in diameter) obscured by adipose tissue (Figure 3D)[3,89-91]. The smaller branches of these vessels leave the adipose regions and pass into the microvascular net (Figure 3E), which spreads out into transparent areas. On the venous side of the capillaries, there is an accumulation of initial lymphatics (Figure 3E-G). These initial lymphatics then pass into larger valvular lymphatics, which are located parallel with and very close to the venules (Figure 3E, H).

Thus, rat mesentery triangulars contains all the typical components of a microvascular net: a blood microvessel network including arterioles (diameter, 7-60 μm; velocity, 5-10 mm/s), venules (10-70 μm; 0.5-3 mm/s), and capillaries (5-9 μm; 0.1-1.4 mm/s), as well as well-developed microlymphatic vessels (diameter, 50-250 μm; velocity 0-7 mm/s) and clearly distinguishable initial lymphatics with migrating cells[3,24,26,58,66,92-94]. Figure 3 shows typical images obtained with the optical schematics portrayed in Figure 4.

The specific functional features of mesenteric vasculature involve a considerable gradient of venular permeability, a preponderance of fluid filtration, and a relatively low proportion (~15%) of re-absorption of interstitial fluid by capillaries[95,96]. Additionally, rat mesenteric blood microvascular is characterized by many communications between the capillary loops arising from neighboring arterioles with well-developed arterio-venous anastomoses, which shunt blood from arteriola to venula[3]. This structure can facilitate adaptation and maintenance of blood flow under different conditions.

For medical imaging, the main advantage of mesenteric microcirculation is that a single layer of blood and well-developed lymph microvessels lies in one plane (Figure 4B), which facilitates continuous observation of all components of the microvascular network (from arteriola to venula, together with lymph microvessels, Figure 3H), as well as label-free, high-resolution imaging of individual cells with almost ideal optical conditions (Figure 3I-N). Light is slightly attenuated, mainly in the relatively thin vessel wall, without any influence from other tissues, as it is in other models. The refractive indexes in the typical spectral range of 400-700 nm used for studies are lower for rat mesenteric tissue (n = 1.38) than for rat skin (n = 1.40-1.42) and, especially, for the epidermis (n = 1.55) for humans; thus, it is close to that of water (n = 1.33)[97]. As a result, these optical and geometric features significantly reduce unwanted scattered light, allowing the use of a microscopic objective with a high numerical aperture (up to 1.4) and high magnification (60× - 100×). Optical reflectance spectra from lymph vessels obtained *in vivo* with a fiber optic spectrometer (Model 1000, Ocean Optics, Inc., USA) demonstrated slight spectral features and time-dependence within 1-2 s (Figure 5), which can

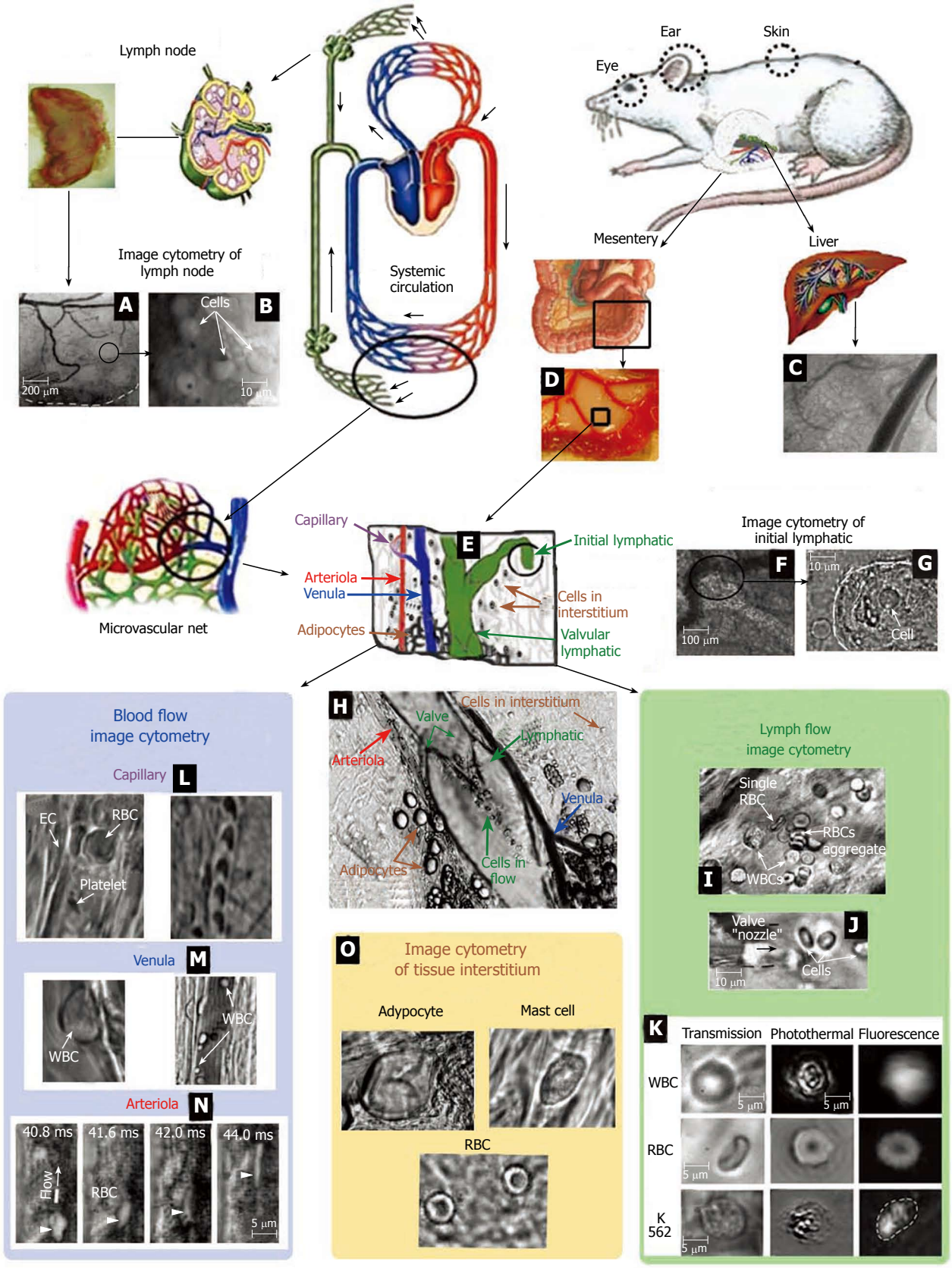

Figure 3 *In vivo* monitoring of microcirculation using rat mesentery. **A**, **B**: Sections of a single lymph node at different magnifications (4 × and 100 ×, respectively); **C**: liver section (10 ×); **D**: section of intestine with mesentery; **E**: schematic of typical tissue microvascular unit; **F**, **G**: initial lymphatic (4 × and 100 ×); **H**: section of mesenteric tissue with valvular lymph vessel and surrounding blood vessels (10 ×); **I**: high-resolution imaging of single WBCs and RBCs, as well as their aggregates in lymph flow (100 ×); **J**: valve tip with fast-flowing cells (100 ×); **K**: transmission, photothermal, and fluorescence images of individual WBC, RBC, and K562 leukemic cell in lymph flow; **L**: capillary at different magnifications, (left) high-resolution images of RBCs, platelets, and endothelial cells (EC) in capillary wall (100 ×) and (right) parachute-like RBCs at low magnification (10 ×); **M**: rolling WBC in venula (100 ×, 10 ×); **N**: four sequential high-resolution images of RBC shapes in fast arteriolar flow (velocity of 5 mm/s; 40 ×); **O**: high-resolution images of adipocyte, mast cell, and RBCs in the interstitial space (100 ×).

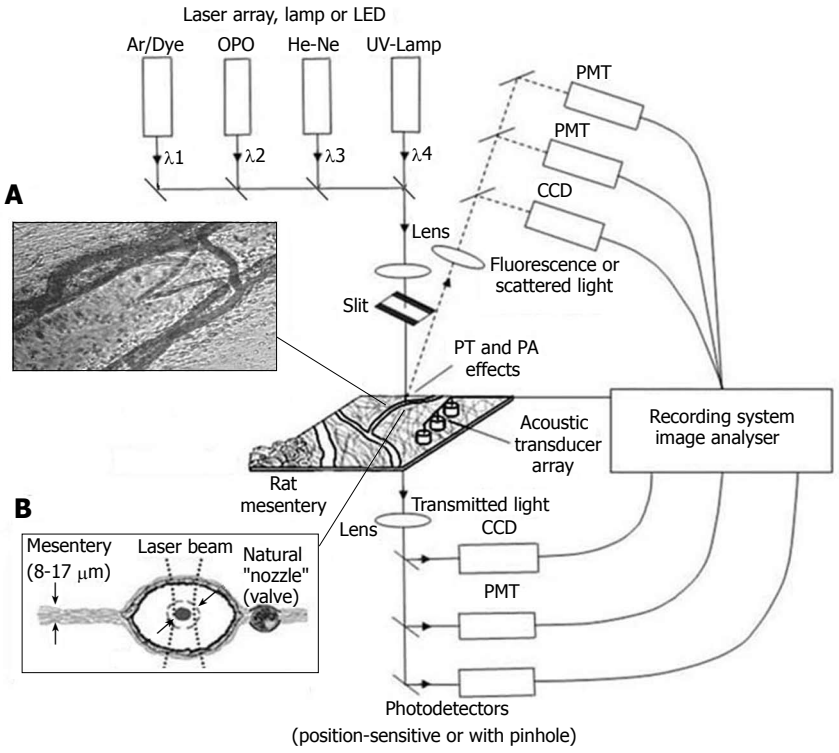

Figure 4 Integrated, multispectral FC *in vivo*. **A**: Typical transmission image of rat mesentery segment with lymph and blood microvessels; **B**: Schematic of the mesentery cross-section.

be explained by specific lymph flow oscillations[98]. An additional advantage of the mesenteric model is the good penetration of the reagents into the mesenteric lining. Thus, the responses of the microvascular network to different environmental impacts can be studied relatively easily using a simple topical application.

The well-developed procedure for preparing rat mesentery for studying microcirculation include anesthetizing the rat (ketamine/xylazine, 50/10 mg/kg, i.m.), followed by a laparotomy by mid-abdominal incision (~1 cm), gently exteriorizing the intestinal loop with mesentery from the abdomen and positioning it on a customized thermostabilizing microscope stage, which maintains the body temperature at approximately 37.7℃ [2,3,22-28,35,58,66,94]. The mesentery is bathed with a constant diffusion of warm Ringer's solution with a phosphate buffer and 1% bovine serum albumin (37℃, pH 7.4). In principle, these procedures may introduce some limitations and artifacts related to the anesthesia, the minimal but invasive surgical intervention, and periodic small vibrations of the mesentery due to intestinal motion[19,99]. However, according to experimental data gathered during at least 2-3 h of acute observation after microsurgery, these procedures do not produce marked changes in microvessel function (diameter, phasic activity, valve function, lymph flow) or in metabolic or respiratory parameters. Furthermore, the short timeframe during which the rapidly circulating cells are in the microvessels of the exposed mesenteric area significantly reduces the influence of this exposure on the properties of the flowing cells. Additionally, to decrease the effects of the surgical manipulations and to stabilize the microvascular parameters, the monitoring of cells in blood and lymph flow begins approximately 15 min after the laparotomy[93]. Coating the intestinal loop with oxygen-impermeable plastic foil helps maintain stable physiological

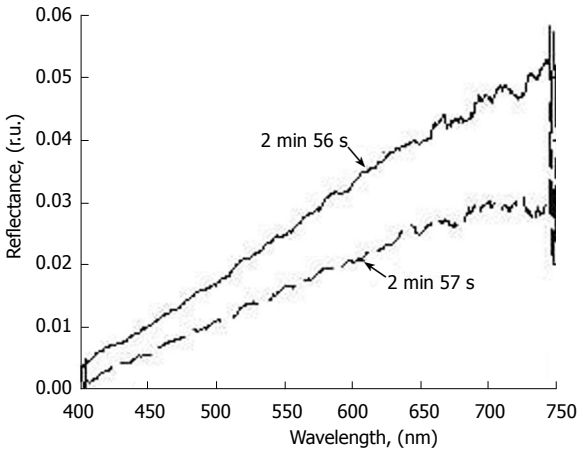

Figure 5 Time-resolved reflection spectra from the same point on the lymphatic vessel (D = 128 μm) at different times.

parameters for up to 5 h[100]. Our data also demonstrate that it is possible to repeat the surgical procedure to periodically monitor the same microcirculation area during the development of chronic pathology, even over a 2-mo timeframe[101]. To exclude the influence of microsurgery itself on the microcirculation, the data from experimental groups were usually compared with those from the corresponding control group, which undergo a mid-abdominal microincision without any other interventions.

In general, based upon our experience and the experiences of other groups, this easy-to-access mesentery microvessel model, which has significant features and advantages (see above) with only a few minor limitations, is a very promising vehicle for real-time monitoring, with the highest optical resolution, of individual static, migrating, and circulating cells (e.g. WBCs, RBCs, cancer cells, and

many others). Such a model is essential for studying immune function and the transport of proteins, cells, and liquid between the blood and lymph systems under normal and pathologic (lymphedema, metastasis, and many other lymph-related diseases) states.

INTEGRATED IMAGING SYSTEM

Recent progress in optical techniques enabled the development of a multi-module, multi-functional experimental system that integrates transmission digital microscopy (TDM), a photothermal (PT) method, a highly sensitive fluorescent and speckle technique with advanced charge-coupled device (CCD) or complementary metal oxide semiconductor (CMOS) cameras (Figure 4). The primary application of this system was for *in vivo* FC. Indeed, although *in vitro* FC is a powerful, established diagnostic method[102], only an *in vivo* study can assess physiologic and pathologic processes involving cell metabolism and cell-cell interactions (e.g., adhesion, aggregation, rolling effects, migration through vessel walls) in the real, complex environment of living organisms[53-55,84,99,103]. Further, invasive isolation of cells from their native environment and their processing may not only introduce artifacts, but also make it impossible to examine the same cell population over long time periods. Adaptation of FC for *in vivo* studies required overcoming problems related to light scattering by vessel walls and surrounding tissues, fluctuation of cell velocity, cell position in a vessel, and precautions with labeling procedures[53,54].

TDM module

TDM was built on the technical platform of an upright Olympus BX-51 microscope and provides the following functions: (1) imaging of relatively large structures such as lymph and blood microvessels with relatively low magnification (4 × -10 ×, Figure 3H); (2) quantitative dynamic evaluation of blood and lymph microvessel diameter, parameters of lymphatic phasic contractions and valve activity, and cell concentration in flow; (3) determination of cell velocity in lymph flow by video-recording cell movement [so-called particle image velocimetry (PIV)];[18,19] (4) navigation of the pulse laser beams on the desired area of the mesentery in other optical methods; and (5) single-cell identification at high magnification (40 ×, 60 ×, and 100 ×, water immersion)[58,94,104]. In particular, the mesentery model provides a unique opportunity to simultaneously image *in vivo*, with the highest optical resolution (~300 nm), individual cells in blood microvessels (Figure 3L and M) and small lymphatics (Figure 3F, G, I-K), tissue interstitium (Figure 3O), and lymph nodes (Figure 3A and B) located in the root of the mesentery and even in the liver.

The images were recorded with several digital cameras: a black-and-white Cohu 2122 and a color Nicon DXM1200, with speeds up to 25 fps and a minimal exposure time of 0.04 s. These speeds were sufficient to image relatively slow-moving individual cells, such as rolling leukocytes (30-70 μm/s), in blood flow (Figure 3M). We also used a highly sensitive CCD camera (Cascade 650, Photometrics) with speed of up to 500 fps and with a minimal exposure time of 0.1 ms. A high-speed CMOS camera (model MV-D1024-160-CL8; Photonfocus, Switzerland), with speeds of 10 000 fps for an area of 128 × 128 pixels and 39 000 fps for an area of 128 × 16 pixels, provided high-resolution imaging of fast-moving RBCs in blood flow (2-10 mm/s in arterioles and large venules, Figure 3N) and WBCs in valvular lymphatics (ranging from 0 to 7 mm/s). Scion Image (Scion Corp.), Nicon software (ACT-1), and WinX/32 V2.5.18.1 (Roper Scientific) were used for processing, capturing, measuring, and editing images of the moving cells.

Using TDM in the bright-field mode, the combination of light absorption and scattering effects on cells made it possible to visualize and identify most blood cells without conventional labeling and vital staining. In particular, due to relatively strong light absorption by RBCs, these single cells in flow appeared mostly as dark objects in the trans-illumination mode, while weakly absorbing WBCs and platelets appeared either as light objects (e.g., in the presence of many more strongly absorbing RBCs in blood flow or with dominant scattering effects) or, in contrast, as slightly dark objects (e.g., in the transparent plasma without RBCs). In the "packed" flow, RBCs sometimes exhibited bright margins or were seen as light objects due to multiple scattering effects. This is because the light, during propagation through many other RBCs and before reaching the plane of focus, was significantly scattered and attenuated through absorption, resulting in dominant scattering light around imaged cells.

The integration of high-resolution and high-speed monitoring improves PIV in the dynamic range and enhances spatial resolution and measurement accuracy. In particular, our technique enables us to measure the velocity of individual cells up to 10 mm/s without marked optical distortion of cell images in packed multi-file blood flow[104]. However, the low absorption sensitivity of TDM makes it impossible to differentiate individual cells with slight differences in absorption in fast flow *in vivo* (e.g. different WBCs or cancer cells).

PT module

To detect low-absorbing cells, PT methods were used with no cell labeling and inherence to scattered light. With these methods, absorption by non-fluorescent cellular components (most of which are naturally weakly fluorescent) is measured by monitoring thermal (due to picosecond-scale non-radiative relaxation of the absorbed energy) and accompanying effects directly in cells[105-109]. For non-fluorescent samples, PT methods currently offer the highest sensitivity for the absorption coefficient, on the order of 10^{-5}-10^{-6} cm^{-1}, which makes it possible to non-invasively (a short-term temperature elevation ⩽ 1-5℃) detect a single, unlabeled biomolecule with a sensitivity comparable to that of laser-fluorescence methods (i.e. with labeling)[109-111]. This absorption sensitivity threshold of the PT technique is at least four to five orders of magnitude better (e.g., 10^{-2}-10^{-3} cm^{-1} for single cells) than that of TDM, with the capability to measure absorption spectra at the subcellular level in weakly absorbing cells (e.g. WBCs

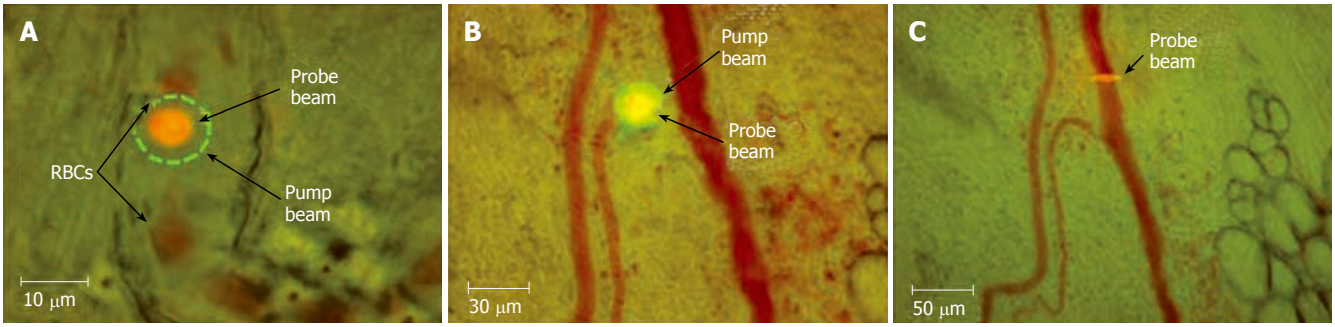

Figure 6 Typical positions of probe (red) and pump (green) laser beams during PT imaging. **A**: Circular beams in a blood capillary (cell velocity, ~0.5 mm/s; magnification, 100 ×); **B**: Overlapping pump and probe pulses in an artery (cell velocity, ~2 mm/s; magnification, 10 ×); **C**: an ellipsoidal beam geometry in a blood vessel (cell velocity, ~5 mm/s; magnification, 10 ×).

or cancer cells).

Briefly, in the first PT imaging (PTI) mode, individual cells were irradiated with a short, focused pump laser pulse of a tunable optical parametric oscillator (OPO) laser (wavelength, 420-2300 nm; pulse width, 8 ns; pulse energy, 0.1-10^3 μJ; Lotis Ltd., Minsk, Belarus; Figure 6)[109,112,113]. Time-resolved monitoring of temperature-dependent variations of the refractive index around the absorbing cellular structures or whole cells was accomplished with thermal-lens (thermolens) or phase-contrast imaging (Olympus BX51 microscope with a CCD camera; AE-260E, Apogee Inc.) using a second, collinear laser pulse of a Raman shifter (wavelength, 639 nm; pulse width, 13 ns; pulse energy, 10 nJ). In particular, in the phase contrast mode, a customized phase-contrast microobjective (20 ×) with a Zernike coaxial quarter-wave filter was used to image the probe laser beam. The diameters of the pump- and probe-beam spots were varied 20-40 μm and 15-25 μm, respectively.

A second thermolens mode made it possible to record a whole cell's time-resolved integral PT response *via* the defocusing effects of a collinear, intensity-stabilized He-Ne laser probe beam (wavelength, 633 nm; diameter, 15 μm; energy, 2 mW) as detected with a photodiode through a pinhole (0.5 mm). The PT response was recorded with a Tektronix TDS 3032B oscilloscope. In the presence of gaps between neighboring cells in lymph and blood flow (typical for small lymphatics and blood capillaries), we used a circular laser-beam geometry (Figure 6A). At short distances, selected experiments were performed with an elliptical beam shape (Figure 6C).

In contrast to TDM, the PT technique was able to identify low-absorbing cells (e.g. normal and apoptotic WBCs or cancer cells) in blood and lymph flow *in vivo* on the basis of their differences in integral and local absorption associated with specific heme proteins[58,77,94,114-118].

Laser speckle microscopy (LSM) module

Because of the varying velocities and trajectories of cell motion in cross-sections of vessels, time-consuming TDM is not well suited for rapidly estimating mean cell velocity in the presense of many cells in flow. The limitations of TDM were partially solved using the LSM technique (Figure 7)[66,68,98,119-122]. Laser radiation from a focused He-Ne laser beam (633 nm) scattered by a diffusely scattering object has a specific, speckle structure (Figure 7A and B), resulting from the interference of independent contributions from a large number of randomly distributed scattering centers. Detection of the speckle fluctuation' s intensity (Figure 7C) with a photodetector provides information of flow velocity estimated through the width of the power spectrum of these fluctuations or from the width of their autocorrelation function (Figure 7D and E). Figure 7D illustrates the spectrum recorded for the central part of a vessel (axial lymph flow), while Figure 7E demonstrates spectra obtained at points placed near the vessel wall. Such changes indicate that velocity decreases from a vessel's center to its periphery, which enables monitoring of the profile patterns of lymph-flow velocity for microlymphatics.

To increase its ability to measure the absolute value and direction of flow, we also used the speckle-correlation mode, which uses two photodetectors to record the intensity in fluctuations of the speckle field at two points[123,124]. The described algorithm was verified *in vivo* by measuring lymph flow in a lymphatic vessel with LSM (Figure 7F curve 1) and TDM (Figure 7F curve 2). There was relatively good correlation (coefficient of linear regression = 0.72) between the two methods; however, the LSM mode had advantages, such as rapid calculation of lymph-flow velocity (compared to TDM). On the other hand, combining LSM with TDM allowed us to: (1) monitor the quantitative dynamics of cell velocity in lymph or blood flow; (2) verify data from the speckle method; (3) obtain a profile of lymph velocity through the changing shapes of the speckle signal from the center region to the near-wall region; and (4) determine the dynamic relationships among changes in lymph flow velocity and other functional activities of lymphatics. This integrated schematic also has the potential for speckle-imaging of mesenteric structures at cellular and subcellular levels, including detection of individual cell rotation and functional state (e.g., live, apoptotic, and necrotic) in flow[118].

Fluorescent module

A fluorescence module was added to the integrated system to verify PT data and for independent applications using specific fluorescent tags to identify different cells with similar shapes and sizes (e.g. lymphocytes and leukemia

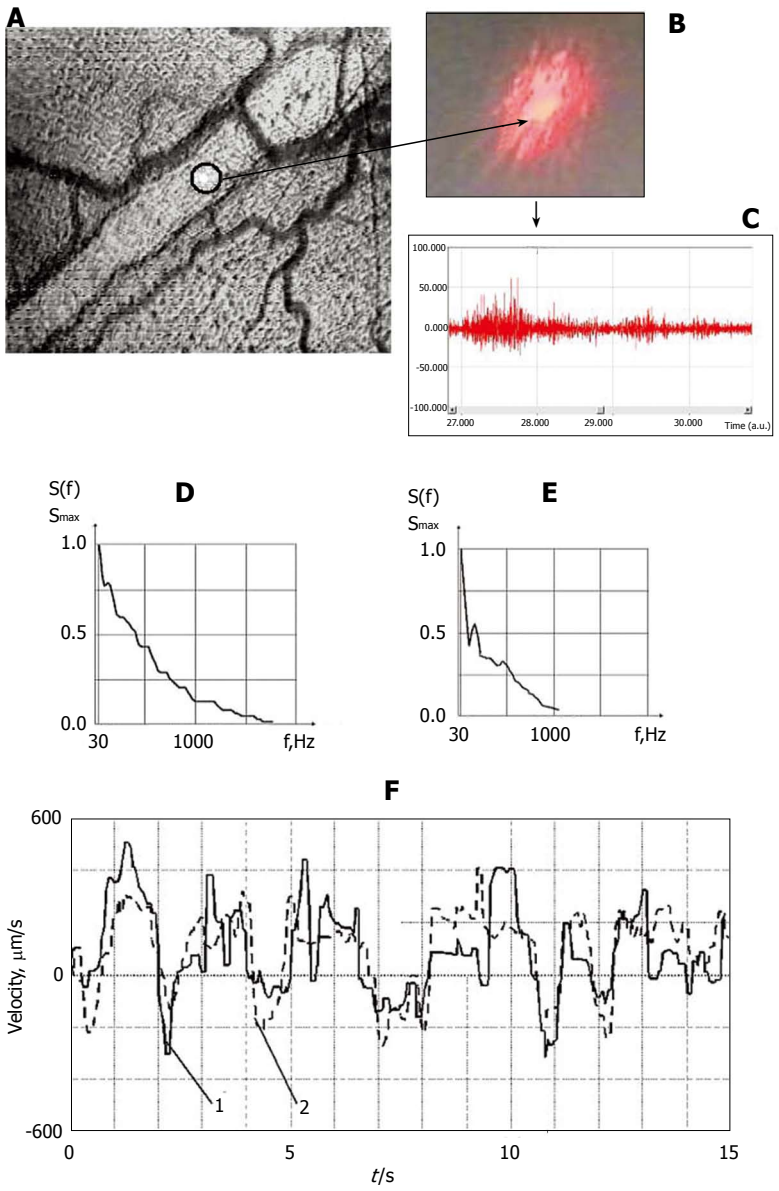

Figure 7 Integration of laser speckle and transmission microscopies for studying lymph flow dynamics. **A**: A laser beam was focused into a small-diameter spot (~5 μm) on axial lymph flow (microvessel diameter 55 μm); **B**: Lymph flow randomly modulated the focused Gaussian beam to provide scattered dynamic speckles images; **C**: Scattered intensity fluctuations were detected by a photodetector and transformed into an electrical output signal. **D** and **E**: Spectral shapes from scanning the lymphatic cross-section: (**D**) the spectrum when the laser beam was focused in axial flow and (**E**) when the laser beam was focused in flow near the lymphatic wall; **F**: Real-time dynamics of lymph-flow velocity in a lymph microvessel, recorded with a laser speckle technique (curve 1) and by processing the video recording (curve 2).

cells)[116,94]. Fluorescent imaging was performed with CCD cameras (Cascade 650, Photometrics, color Nicon DXM1200) and a super-sensitive PentaMAX camera with an intensifier (Princeton Instruments, Inc.).

STUDY OF MICROLYMPHATIC DYNAMICS

Label-free time-resolved lymphography

An essential ingredient in studying the functional activity of lymph microvessels is to know when the observed functions approximate normal conditions. The previously described imaging system allowed us to obtain such basic information on intact lymph microcirculation, including quantitative measurements such as indices of phasic contraction and valve function, the numbers of microvessels with lymph flow, the numbers of cells in lymph, and lymph flow velocity[58,66,101,125].

TDM images of rat mesentery at two relatively small magnifications (4 ×, field of view 250 × 350 μm and 10 ×, field of view 125 × 175 μm) allowed us to visualize the initial (Figure 3F) and valvular lymphatics (Figure 3H), the vessel wall, lymphatic valves, and cells in lymph flow, as well as neighboring blood microvessels. In particular, we studied small valvular lymphatics with mean diameters of 147 ± 3 μm. Half of these lymphatics in a normal state had spontaneous phasic contractions[101].

The rate (frequency) of contractions and contraction amplitude (the percentage difference between maximum and minimum diameters during contraction) vary significantly[66]. Benoit *et al*[22] found that the lymphangions with phasic contractions have mean end diastolic diameters of 69.2 ± 6.5 μm and systolic diameters of 39.4 ± 5.6 μm (i.e. an amplitude of 43%). In another paper, the same authors showed that lymphatics with mean end diastolic diameters of 106.9 ± 13.7 μm have a systolic diameter of 69.8 ± 8.8 μm (i.e. amplitude of 35%)[30]. From our data, lymphangions had mean diastolic diameters of 147 ± 3 μm and amplitudes of 29% ± 9%[58]. Thus summarized, these data indicate that the larger lymphatics have smaller amplitudes of phasic contractions. Our detailed analysis of relationships between diameter and amplitude revealed that the lymphangion with larger diameters have less amplitude

(Figure 8, unpublished), which is in line with the results presented above. In addition, we believe that the amplitude of phasic contractions should be analyzed in relation to valve activity; indeed, the amplitude of phasic contractions in lymphangions with active valves was 31% ± 4%, while in lymphangions with non-active valves it was only 6% ± 2%[66].

The majority of lymphatics with phasic contractions (78%) have active valves, which periodically open and close. An average activity rate (frequency of closing-opening cycles per minute) was 9-12/min[58,66,101,125].

Cells are moved in 85% of lymphangions and they are not found in 15% of lymphangions[66,125]. It is well known that some parts of blood capillaries do not work normally[61]. We speculate that the same situation may occur in lymphatics, in which activity can start under some specific circumstances, for example during disease development (e.g., lymphedema).

Lymph flow velocity is usually estimated by measuring cell velocity. Our measurements with a conventional video camera (25-30 fps) revealed that mean cell velocity in an axial flow in the non-valvular central part of mesenteric lymphangions (i.e. approximately equal distance between input and output valves) is 211-262 μm/s on average, with a maximum of 1-2 mm/s)[58,66,101,125]. When lymph flow goes through the valve, the phase contraction leads to acceleration of flow because of the narrow valve nozzle. In turn, this leads to significantly increased cell velocity.

Lymph usually moves in the forward direction for a short period of time; then, the motion is interrupted and the lymph stops for up to 1-1.5 s. After that, the lymph flow starts in the reverse direction. Usually, cells oscillate at a rate of 50-70 oscillations per minute[126]. Figure 9 shows oscillations during 15 s in a non-valvular part of an individual lymphangion (mean diameter in the investigated site = 170 ± 5 μm; mean cell velocity during the investigated time = 168 ± 6 μm/s)[126]. In some rare microvessels, the time-averaged velocity of lymph flow equaled zero. In this case, lymphocytes only oscillated relative to a position without the leak-back of lymph. Using a high-speed videotape recorder (2000 fps), Sekizuka *et al*[24] demonstrated that maximum cell velocity in rat mesenteric lymphatics was 2-3 mm/s. Later, using a relatively high-speed camera (500 fps), Zaviewa *et al* determined that maximum cell velocity in some mesenteric lymphatics may reach 7 mm/s and their oscillations correlate with phasic contractions[26]. Probably, such variability of cell velocity may result from different experimental conditions.

It is important that the analysis of lymph flow requires that we estimate both cellular and plasma velocities (analogous to blood flow). In fact, Starr *et al*[8] found that the blood flow in cat mesenteric microvessels *in vivo* is characterized by a discrepancy between RBC and plasma velocities. This discrepancy is dependent on the elastic properties of RBCs and flow dynamics, including plasma shear and pressure field. We expect a similar phenomenon in lymph flow, especially due to its oscillating character; however, these effects require further quantitative verification.

Depending on lymph flow velocity and vessel structure, cell distribution in the cross-section of the lymphangion varies[58,66,125]. Most often, at relatively low velocities and/or in the non-active valves (80% of cases), cell distribution was relatively uniform. However, at high velocities and/or in functioning valves (20% of cases), most cells were concentrated near the vessel axis.

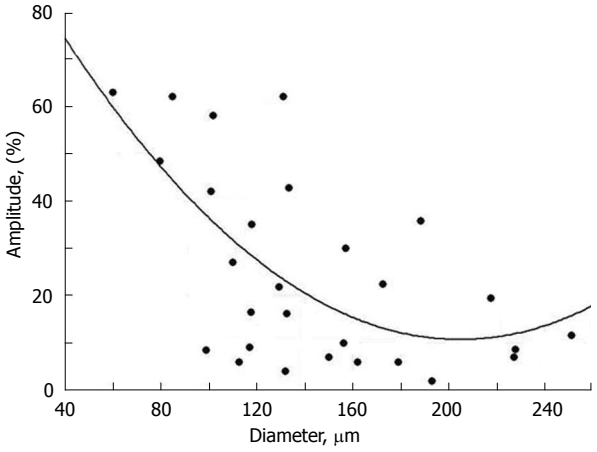

Figure 8 Diameter-amplitude relationship in rat mesenteric lymphangion. Cycles-experimental data, solid curve-approximation (A = 109.3-0.96 × D + 0.0024 × D^2, where A: amplitude and D: diameter).

It is well known that lymph has markedly lower concentrations of cells than blood. However, there is relatively little data about cell concentration in prenodal lymph. In particular, cell concentrations range from 200 to 1000 cells/μL in prenodal sheep's lymph and 100 cells/μL in prenodal rabbit's lymph[127,128]. It was found that approximately 1 × 10^6 cells/h (1.7 × 10^4 cells/min) go through a single prenodal (afferent) sheep's lymphatic[129,130].

According to our data, the cell concentration in rat mesenteric prenodal lymphatics is larger. Specifically, we measured the number of cells in a 50 μm × 50 μm square in the central part of a lymphangion from a rat mesenteric microvessel using 2D-imaging[66]. Because the depth of field was approximately 28 μm, the number of cells was determined in a 50 μm × 50 μm × 28 μm volume (i.e., 7 × 10^{-5} μL of lymph). Data is summarized in Table 1 (taking into account distribution of cells in a cross-section of a lymphangion, see above). Finally, the mean concentration of cells in the lymph flow of intact mesenteric microvessels was estimated as approximately 0.5-1 × 10^5 cells/μL. From these data, the average percent of cell fraction in lymphatics was 5.5%. This parameter is analogous to hematocrit in the blood system, and may be called lymphocrit. It is interesting that a 5%-6% level of hematocrit can be found only in blood capillaries, as compared to that in arterioles with diameters from 60-70 μm, in which the hematocrit achieved 20%-30%. Cell flux in the prenodal lymph was estimated to be 10-50 cells/s. The cell concentration in flow is usually higher in vessels with higher lymph flow velocities, and is somewhat correlated with the amplitude of phase contractions and rate of valve activity[66]. Recent data obtained by Dixon *et al*[131] with a high-speed video system and by capturing multiple contraction cycles in rat mesenteric lymphatic preparations with smaller diameters (91 ± 9 μm) revealed that lymphocyte densities were 12 000 ± 5200 cells/μL

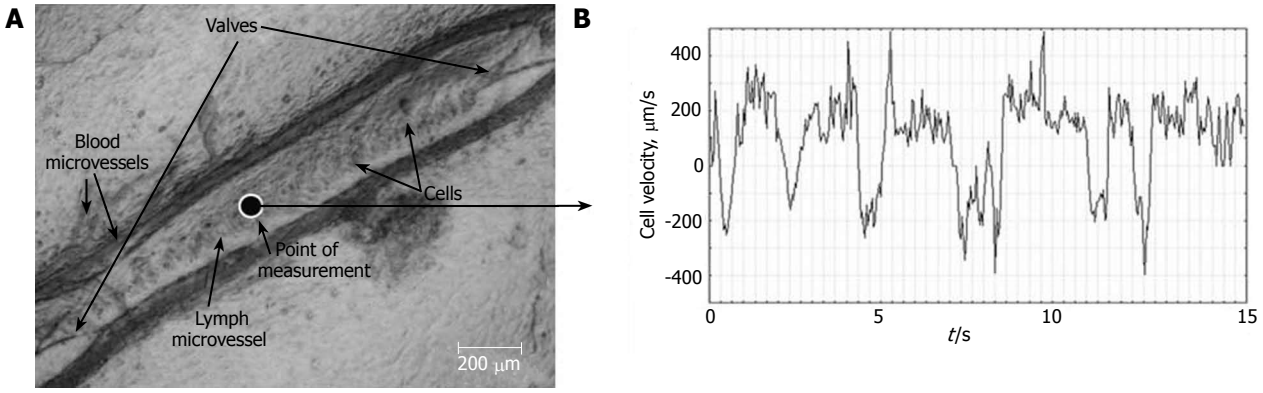

Figure 9 Real-time dynamics of cell velocity in axial lymph flow within the non-valvular segment of a lymphangion (mean diameter of 170 ± 5 μm) without phasic contractions and valve activities, measured by processing the video recording (μm/s) for 15 s.

Table 1 Relationship between lymphocrit and other parameters of microlymphatic function

	Cell concentration, cells/μL	Lymphocrit %	Proportion of Lymphangions %	Diameter μm	Parameters of phasic contractions		Valve activity per minute	Cell velocity (μm/s)
					Amplitude (%)	Count of contractions per minute		
Group 1	$< 3.75 \times 10^4$	< 2	22	$106 \pm 9^{a,b}$	$50 \pm 15^{a,b}$	12 ± 2	8 ± 0.5^{b}	161 ± 191
Group 2	3.75×10^4-12.2×10^4	2-6	45	141 ± 8^{a}	$28 \pm 7^{a,c}$	12 ± 1	11 ± 1	254 ± 151
Group 3	$> 12.2 \times 10^4$	> 6	33	165 ± 9^{b}	$14 \pm 5^{b,c}$	15 ± 1	16 ± 2.5^{b}	214 ± 19

$^{a}P < 0.05$, *vs* Group 2; $^{b}P < 0.05$, *vs* Group 3; $^{c}P < 0.05$, *vs* Group 3.

and cell flux was 990 ± 260 cells/min.

The relationship between lymphocrit and pathologies is still unknown. There are indications that the leg massage of healthy rabbits stimulates lymph flow and increases cell concentration, while leg edema due to venous pressure rising is not accompanied by an elevation in cell concentration[128].

Data about cell composition in afferent lymph are very limited and have been obtained in *in vitro* tests. In particular, 80%-90% of cells in normal prenodal lymph are related to mature lymphocytes, 5%-20% to macrophages and dendritic cells, and 0%-10% to other cells (e.g. basophilic blast cells, RBCs)[127]. The composition of WBC types changes based upon the pathology. For example, it is estimated that there is a significanct appearance of neutrophils in experimental peritonitis in sheep. Other important problems are the mechanisms by which different cells (e.g. metastatic tumor cells) enter into peripheral lymphatics. Recently, Azzali studied tumor-associated absorbing lymphatics in the peritumor area of fixed tissue specimens (adenocarcinoma, melanoma, colorectal cancer) using light microscopy, transmission electron microscopy, and histochemistry with 3-D image reconstruction[132]. He found that cancer cells can enter into lymphatics through intraendothelial channels (1.8-2.1 μm in diameter and 6.8-7.2 μm in length). These results are very promising, but such a mechanism remains to be proven in living cells *in vivo*.

Lymph and blood flow cytometry in vivo

We demonstrated the first application of the PT techniques for lymph and blood PT flow cytometry (PTFC) *in vivo* integrated with TDM[94,115,116,133]. To minimize cell image distortion due to spatial cell-radial fluctuations in lymph flow (up to 50 μm in 150-μm-diameter lymph vessels), cells were imaged immediately after passing through a lymphatic valve, which played the role of a natural nozzle, focusing the cells near the vessel axis (Figure 3J). Thus, lymphatic valves provided a natural type of "hydrodynamic focusing" (a term used in *in vitro* FC involving an artificial nozzle) to limit lateral fluctuation of cells up to a few micrometers.

High-resolution and high-speed TDM imaging provides a real-time monitoring of individual cells in blood (Figure 3L-N) and lymph flow (Figure 3I-K), as well as static and migrating cells in the interstitium (Figure 3O), lymph nodes (Figure 3A and B), and even in liver (Figure 3C)[58,94]. The high spatial resolution offered by TDM (300-500 nm at 40× - 100× magnification with water immersion) makes it possible to identify some types of moving cells based upon their sizes and shapes (e.g. WBCs and RBCs; Figure 3K). We can even monitor the rotation of a single RBC (Figure 10A-C) and visualize intralymphatic cell aggregates of different sizes in intact microlymphatics (Figure 10D-F).

PT module in integrated FC allows us to obtain PT images of flowing cells (e.g., lymphocytes, RBCs, and leukemic cells) with an absorption sensitivity approximately four orders of magnitude greater than the sensitivity of transmittance microscopy (Figure 3K, left and middle columns)[94]. In particular, PT images revealed the subcellular structures of these cells (Figure 3K, middle column) associated with the spatial distribution of cytochromes in lymphocytes and cancer cells and of hemoglobin in RBCs, which were not clearly visible with

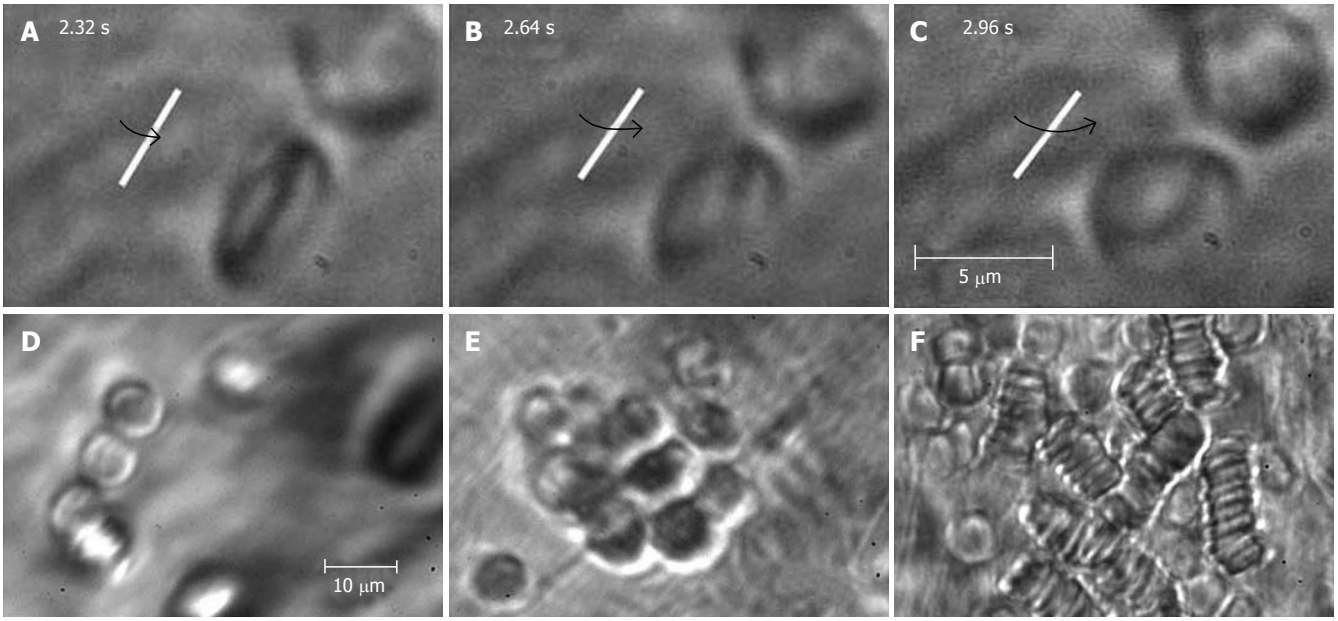

Figure 10 High-resolution monitoring of cell behavior in lymph flow. Top row (**A**-**C**): three sequential images of an individual RBC's rotation in lymph flow (lymphatic diameter 185 μm, mean cell velocity 220 μm/s, magnification 100 ×). Bottom row: moving aggregates of different sizes in lymph flow; **D**: Unstable aggregate of a few cells in intact lymphatic; **E**: large aggregate of RBCs in lymph flow resulting from venous insufficiency; **F**: rouleaux formation when numerous RBCs appeared in lymph flow due to laser-induced hemorrhage (magnification 100 ×).

TDM (Figure 3K, left column). Fluorescence images, obtained with a high-sensitivity CCD camera with an intensifier (PentaMAX, Princeton Instruments, Inc.), showed high image contrast (Figure 3K, right column) similar to that of PT images, although inconvenient staining procedures were required. Specifically, leukocytes were labeled with Rhodamine 6G. RBCs and K562 cells were labeled with FITC and MitoTracker Red, respectively. Because of differences in the optical properties of normal and cancerous cells, especially mitochondrial distribution[134,135], which can be visualized with the PT technique, we can assume that PTFC has the potential to distinguish these cells after further improvements.

PT-signal tracings from flowing cells in blood (Figure 11A) and lymph (Figure 11B-E) microvessels were obtained as a function of time[116,94] . Due to their different absorption properties, the significant (40-60-fold) differences in the integral PT amplitudes from RBCs and WBCs (lymphocytes) allowed us to distinguish cells using only the thermolens mode (i.e. even without imaging). Cells were also identified through differences in cooling times (6-10 μs for RBCs, and 20-25 μs for lymphocytes). PT signals from RBCs in blood flow showing a purely positive component indicate a linear positive PT response from the cells at a low laser energy level with no cell damage (temperature increase is usually 5-10℃, Figure 11A). The amplitude differences indicate differences in average absorption and reflect the natural heterogeneity of RBCs. The negative signal component from cells in lymph flow presented in Figure 11D is related to laser-induced photodamage through bubble formation around strongly absorbing cellular zones that have been overheated. The presence of both positive and negative components in the PT-signal amplitude tracing (Figure 11E) indicated a noninvasive condition for lymphocytes (which have a high photodamage threshold) and an invasive condition for RBCs (which have a low photodamage threshold) at the same energy level. Decreasing the laser energy level

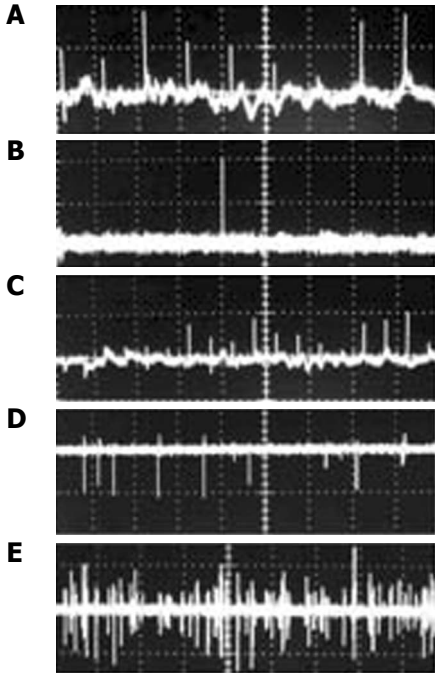

Figure 11 Typical PT-signal tracings from blood cells in blood and lymph flow: **A**: RBCs in blood flow; **B**: rare RBC in lymph flow; **C**: growing number of RBCs in lymph flow during laser-induced hemorrhage; **D**: laser-induced damage of RBCs in lymph flow and lymphocytes in lymph flow in linear and nonlinear PT modes; and **E**: lymphocytes and RBCs in lymph flow. Laser parameters: wavelength, 525 nm; energy/amplitude/time scale/division: (**A**), 0.3 μJ/50 mV/100 ms; (**B**), 0.5 μJ/20 mV/1 s/div; (**C**) 0.6 μJ/100 mV/200 ms/div, (**D**) 5 μJ/500 mV/4 s/div; and (**E**) 145 μJ/100 mV/10 s, respectively.

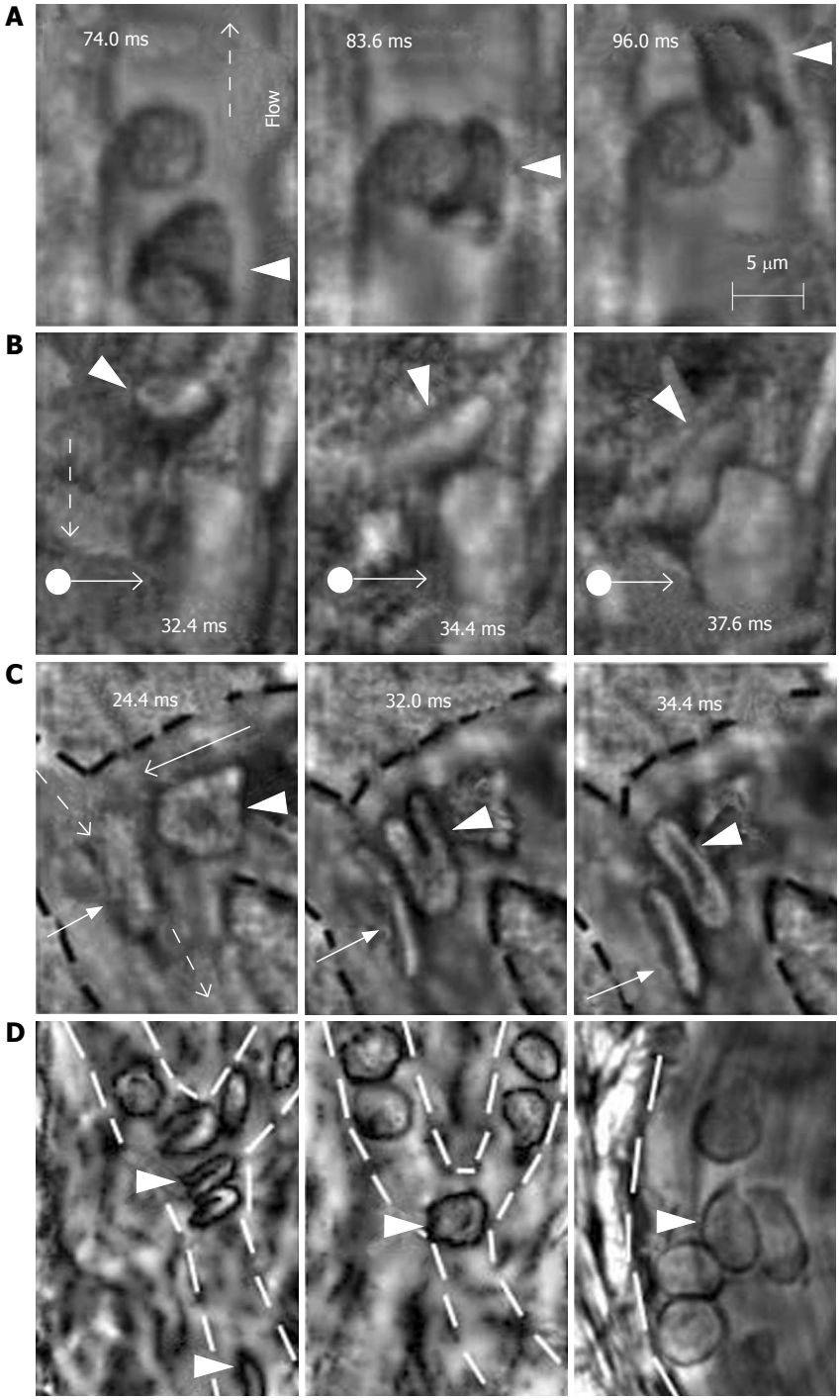

Figure 12 High-resolution, high-speed monitoring of cells in blood flow. RBCs are indicated by conventional arrows and triangle; rolling WBCs by arrows originating from filled circles; and direction of flow by dashed lines. **A**-**C**: behavior of normal RBCs and WBCs in flow (1250-2500 fps; 40 ×); **D**: The shapes of normal (left) and diamide-treated (middle) RBCs in single-file flow of small venula (diameter ~10 μm), and (right) adhesion of diamide-treated RBCs to wall of the relatively large venula (diameter -40 μm).

allows us to selectively identify rare RBCs in lymph flow. For example, Figure 11B shows the detection of single RBCs at a low laser energy level. This level did not produce notable PT signals from the many lymphocytes in lymph flow because of their low absorption. Laser-induced vessel injury led to a fast-growing number of RBCs in lymph flow (Figure 11C). The next tracing shows that the PT signals from RBCs at a relatively high laser energy level led to cell damage (Figure 11D).

HIGH-SPEED IMAGING OF INDIVIDUAL CELLS IN FAST BLOOD FLOW

This technique, using an advanced high-speed CMOS camera, reveals the high deformability of parachute-like RBCs as they are squeezed at 0.6 mm/s through a narrow gap between the vessel wall and rigid adherent cells on the opposite wall (Figure 12A)[104]. It also shows how quickly the relatively fast-flowing RBCs (~1 mm/s) change shape as they interact with the much more slowly moving (so-called rolling) leukocytes (~0.1 mm/s; Figure 12B). We also observed significant dynamic deformation of two RBCs in merging flow streams in a bifurcation zone (Figure 12C), and extremely fast stretching (0.4 ms at 2500 fps) of initially discoid RBCs to ~0.7-0.9 μm (Figure 3N). Our technique has provided relatively good contrast images of both slow- (20 μm/s, Figure 3L, left) and fast-flowing (2.5 mm/s) single platelets in blood microvessels. The best-quality images of platelets were obtained in the RBC-free

space of the microvessel lumen.

We also performed time-resolved monitoring of cell deformability. In particular, diamide (20 mg/kg) was injected in a rat's tail vein to increase the rigidity of RBCs *in vivo*. We observed a drug-induced decrease in the deformability of RBCs in fast blood flow (up to 5 mm/s) compared to RBCs in normal conditions, with maximum centrifugal forces acting on cells in curved capillaries (Figure 12D, left and middle). In addition, diamide led to adhesion of abnormal RBCs to vessel walls (Figure 12D, right). To our knowledge, this was the first time that these phenomena have been observed with high-speed, high-resolution imaging *in vivo*. After additional study, potential applications of this technique may include fundamental studies of dynamic cell-cell interactions in native flow or the identification of abnormal cells (e.g., cancerous cells or sickle RBCs) using their different dynamic deformability as new biological markers that are sensitive to disease development or to different interventions.

IMAGE CYTOMETRY OF STATIC CELLS AND TISSUE STRUCTURES

Interstitium

Figure 3O shows typical high-resolution TDM images of mast cells, adipocytes, and slow-moving RBCs in mesenteric interstitium[58,101]. This technique also provides distinct images of fibrils, as well as other static and migrating cells. In some cases, the phase-contrast images demonstrated better contrast of margins and sub-cellular structures for selected single cells in interstitium than does non phase-contrast at high magnification (100 ×, with water immersion), which prevents overlapping refractive heterogeneities of connective tissue (see images of mast cell and adipocytes in Figure 3O).

Lymph and blood microvessel walls

With TDM, we obtained high-resolution images of (1) distinct individual blood endotheliocytes (EC) of the capillary wall (Figure 3L, left); (2) the initial lymphatic wall with cells (e.g. leukocytes) migrated from interstitium (Figure 3G); and (3) lymphatic wall and valvular cusp structures of larger vessels[58].

Lymph node

Using a minimally invasive procedure, we demonstrated real-time, *in vivo* monitoring of individual cells in different domains of mesenteric lymph nodes (e.g., medullary sinus, light and marginal zones of marginal sinus) in their native state (unpublished data, Figure 3B)[94].

STUDY OF ENVIRONMENTAL IMPACTS ON LYMPHATICS

To date, the effects of environmental and therapeutic interventions on blood microcirculation have been studied in appropriate detail in humans and in different animal models, including the rat mesentery; however, the lymphatic system has received much less attention in spite of the many biological and medical problems associated with microlymphatic functioning and its disturbance in different diseases, including cancer metastasis, venous insufficiency, infections, inflammation, lymphatic malformations, and especially lymphedema[29,40,62]. To partially fill this knowledge gap, we used a rat model with an integrated optical technique to quantitatively study lymph and blood dynamics under different impacts, including chemical, drug, and physical interventions. In our study, we chose interventions that have effects on lymphatics that are unknown (dimethyl sulfoxide); incompletely known (β-adrenoceptor agonist and β_1- and β_2-adrenoceptor antagonists, donors of NO, low-power laser radiation); or controversial (inhibitors of NO-synthase). These effects were studied by real-time monitoring of the diameters and parameters of phasic contractions, and changes in lymph flow velocity, valve activity, and cell behavior in microvasculature.

Effects of adrenergic agonists and antagonists

One of the most important regulators of the vasculature is adrenergic regulation through α- and β-adrenoreceptors[61]. The effects of adrenergic agonists and antagonists on diameter and phasic contractions of microlymphatics have been described in *in vitro* or *in vivo* tests[22,29,30]. It is known that norepinephrine applied topically or injected intravenously instantly reduces the diameter and increases the contraction frequency of rat mesenteric lymphatics, while isoproterinol has opposite effects[29]. Moreover, the attempts to study the effects of α-adrenoagonists and antagonists on lymph flow in microvessels were made using calculated parameters of lymph outflow (as calculated with the following assumptions: strongly cylindrical, unchanging geometry of lymph vessel with unidirectional lymph flow)[22,30]. It was shown that α-adrenergic regulation of lymph outflow in mesenteric lymphatics is through α_1-receptors[30].

In our tests, we clarified the effects of a β-adrenoceptor agonist and antagonist (and their subtypes) on cell flow velocity *via* the direct monitoring of lymph flow, and determined the relationships between cell velocity and other parameters of microlymphatic function (diameter, amplitude and rate of phasic contractions, rate of valve activity) (Table 2). Isoprenaline, a β-adrenoceptor agonist, (10^{-5} mol/L, 15 min of topical application) caused dose- and time-dependent responses: 5 min following topical application, the percentage of contracting lymphangions was decreased from 60% to 33% and lymph flow velocity was inhibited from 134 ± 13 μm/s to 82 ± 19 μm/s ($P < 0.05$). Then, at 15 min, 40% of lymphangions exhibited lymphostasis accompanied by vessel constriction and depression of phasic activity. The adrenoceptor antagonists metoprolol (β_1) and butoxamin (β_2) were also applied topically at the same parameters (10^{-5} mol/L, 15 min). Both antagonists stimulated phasic contractions in non-active lymphangions. However, the effect of metoprolol was more marked, increasing the proportion of microlymphatics with contractile activity to 66%, while butoxamin stimulated phasic activity in only 32% of non-active lymphangions. As a result, metoprolol's action significantly increased lymph flow velocity (from 136 ± 14 μm/s to 198 ± 24 μm/s, $P < 0.02$), while it did not change with butoxamin. Based upon this data, we assume

Table 2 Effects of 15-min topical application of different vasoactive drugs on lymph microvessel functions

Drug	Diameter	Phasic activity	Lymph flow velocity
Sodium Nitroprusside (10^{-5} mol/L)	Dilation	Slight short-time inhibition	Unchanged
N-Nitro-L-Arginine (10^{-4} mol/L)	Unchanged	Stimulation	Stimulation
Isoprenaline (10^{-5} mol/L)	Constriction	Inhibition	Inhibition up to stasis
Metoprolol (10^{-5} mol/L)	Unchanged	Stimulation	Stimulation
Butoxamin (10^{-5} mol/L)	Unchanged	Slight stimulation	Unchanged
Dymethyl Sulfoxide, (30%)	Constriction	Stimulation	Stimulation in 50% of lymphangions
			Inhibition in 39% of lymphangions (without phasic contractions)

Table 3 Effects of 30% DMSO at the topical application on blood microvessel diameter

	Arterioles			Venules	
Before application	16.5 ± 0.49	25.3 ± 0.69	16.1 ± 0.79	24.9 ± 0.74	34.8 ± 0.66
After DMSO application					
1 min	17.4 ± 0.67	25.8 ± 1.09	18.6 ± 0.98[a]	29.6 ± 1.29[a]	39.0 ± 2.25
2 min	16.9 ± 0.83	28.1 ± 0.80[a]	19.2 ± 1.11[a]	28.9 ± 1.33[a]	38.8 ± 1.53[a]

Significant differences from state before application, [a]$P < 0.05$.

that lymph microvessels (and probably similar large lymph vessels), have β_1- and β_2- adrenoceptors.

No effects

Another essential regulative substance of lymph mesenteric microvessel function *in vivo* is nitric oxide (NO)[35,66,136,137]. According to our data, intravenous injection of an NO donor (sodium nitroprusside, 100 μg/kg, i.e. drug concentration in blood is 5×10^{-5} mol/L) caused slight dilation of lymphatics within 30 min[136]. However, sodium nitroprusside does not affect lymph flow. The response of lymphatics to direct topical application of sodium nitroprusside (10^{-5} mol/L, 30 min) was similar but more intense: dilation of lymphangions for 25 ± 2.5 μm was accompanied by slight transient inhibition of the proportion of lymphatics with phasic contractions and active valves[137].

While the hyper-production of NO does not change lymph flow, the inhibition of NO synthesis stimulated lymph motion (Table 2). Topical application of N-nitro-L-arginine, a known inhibitor of NO (10^{-4} mol/L, 30 min), first caused (fifth minute of application) a short-term decrease in the amplitude of phasic contractions (from 23% ± 3% to 11% ± 1%, $P < 0.001$) and stimulation of valve activity (rate of valve activity increased from 6 ± 1 to 11 ± 2 per min, $P < 0.05$)[66,137]. Then, from the tenth minute, we observed permanent stimulation of phasic activity and lymph flow. Shirasawa and coauthors concluded that a 15-min application of an NO donor and an inhibitor of NO synthase portray the direct effects of NO on microvessel walls[35]. Therefore, we speculate that NO can regulate lymph flow in microvessels due to (at least, partly) the direct action of NO on the endothelium and the smooth muscles of lymph microvessel walls.

Pharmacological effects of dimethyl sulfoxide (DMSO)

DMSO has a wide spectrum of biological activities, including high penetrating activity and significant vasoactive effects on blood vessels[138,139]. It is used for local treatment of trauma, arthrosis, and rheumatoid arthritis[140,141]. The effects of DMSO on the microlymphatic system are unknown. Experimental studies have revealed that a 30-min topical application of 30% DMSO caused specific, dynamic microvascular changes in blood and lymph[66,142]. Immediately after application (within the first minute), there was stasis within 100% of venules and 85%-95% of arterioles, with significant dilation (dilation began earlier and the diameter increased more in venules than in arterioles) and hemorrhaging around venules (Table 3). The marked responses of lymphatics started later (15 min of DMSO application), and appeared as a significant increase in lymph-flow velocity from 190 ± 12 μm/s (before DMSO application) to 233 ± 20 μm/s ($P < 0.05$) accompanied by stimulation of phasic contractions in 21% of lymphangion and decreasing of diameter. In parallel, the 39% of lymphatics is characterized by lymphostasis development (Table 2). Obtained on DMSO' s impacts on lymph and blood microvascular function can be used for assessment the possible side effects of this drug.

Effect of low-power laser irradiation

Publication of the positive clinical effects of low-power laser therapy, including lymphedema treatment, stimulated our interest in studying lymphatic response to this radiation[143-145]. The effects of low-power laser radiation (He-Ne laser) on intact lymph microvessels were studied at three radiation intensities-450 mW/cm^2, 45 mW/cm^2, and 14 mW/cm^2-each with an exposure time of 15 min[66,136,146]. Laser power of 14 mW/cm^2 did not have a significant effect on lymph microvessel function. After 5 min of irradiation at 45 mW/cm^2, 70% of lymphatics were dilated an average of 8 ± 1 μm ($P < 0.01$). After 15 min, the proportion of microvessels

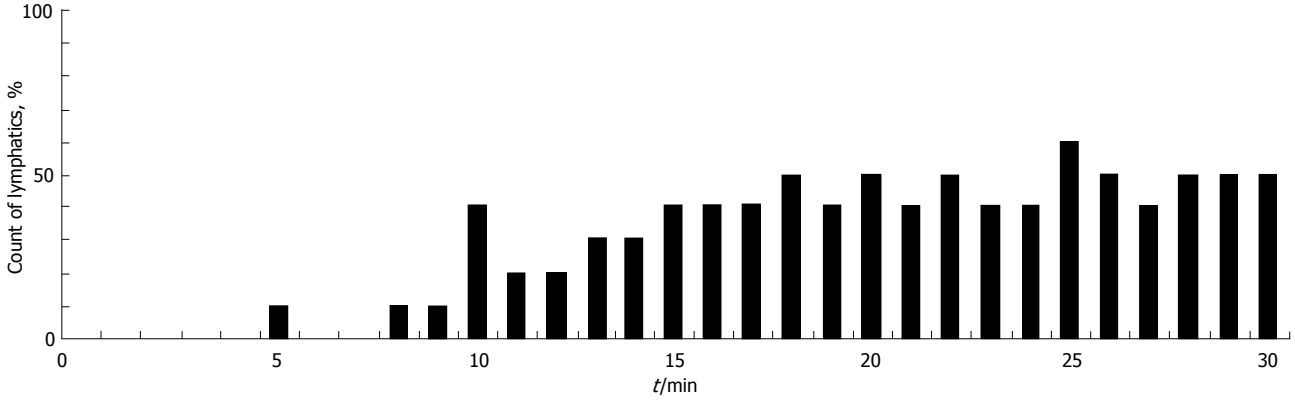

Figure 13 The percentage of lymphangions exhibiting phasic contractions during 30 min of irradiation with a He-Ne laser (450 mW/cm^2).

that were dilated (60%-70%) did not change, and phasic contractions appeared in 21% of lymphatics. When the lymphatics were irradiated at the highest laser power (450 mW/cm^2), similar dilation of the majority of microvessels was observed. Simultaneously, 15 min of laser radiation at 450 mW/cm^2 significantly stimulated contractions within a larger number of vessels (45%) than did irradiation at 45 mW/cm^2. The mean contractile amplitude of irradiated vessels was 1.5-fold greater than that of intact lymphatics (44% ± 5% compared to the amplitude of spontaneous contractions of 29% ± 9%). Increasing the irradiating time up to 30 min at 450 mW/cm^2 did not change the degree of lymphatic dilation and just slightly increased the proportion of lymphatics with phasic contractions (Figure 13). These laser effects were maintained up to 30 min after irradiation. None of the doses of laser radiation affected how the valve functioned. Thus, our data is in line with the results of Carati *et al*[32] in that low-power laser radiation may improve lymph drainage by stimulating phasic contractions and by dilation of microvessels.

High-power laser treatment of vascular abnormalities

Rat mesentery microvasculature is very useful as a model for laser treatment of port-wine stains and other vascular abnormalities. In particular, in one study, rat mesenteric blood vessels were irradiated with a laser pulse (585 nm, 0.2-0.6 ms pulse duration, 0.5-30 J/cm^2 radiant exposure)[147]. Video microscopy was used to assess vessel dilation, formation of intravascular thrombi, bubble formation, and vessel rupture. Changes in reflection during a laser pulse were measured by simultaneously recording the temporal behavior of the incident and reflected light. A threshold radiant exposure of approximately 3 J/cm^2 was found to produce changes in the optical properties of blood *in vivo*, confirming previous *in vitro* results. Often, laser exposure induced a significant increase in vessel diameter, up to three-four times the initial diameter within 200 ms after laser exposure. Sometimes, immediately after the pulse, round structures, interpreted as being gas bubbles, were seen within the vessel lumen.

We obtained similar results in our study with a 10 ms laser pulse (585 nm, 0.5-30 J/cm^2 radiant exposure). In addition, local hemorrhaging around venules with rupture of venular walls occurred at lower radiant exposures than in arterioles with smaller diameters (due to the more effective cooling effects in smaller vessels; Figure 14A and B). For the first time, significant constriction of neighboring lymphatics was observed, up to obliteration of lumina and lymph stasis (Figure 14C and D). Additionally, hemorrhage in the interstitium led to the entry of many RBCs (visualized as distinct red points by TDM) into the lymph flow. The PT mode of integrated PTFC proved this fact. In particular, PT-signal tracing specific for RBC laser energy levels showed a growing number of RBCs in lymph flow during laser-induced hemorrhage (Figure 11C).

Preliminary data from intravenous injection of 100-nm gold nanoparticles followed by laser irradiation of the mesentery demonstrate a decrease in the blood vessel damage threshold (approximately 3-5 times) compared to the damage induced without nanoparticles, despite the sub-optimal parameters of the laser used [wavelength was outside the maximum absorption of the nanoparticles (~525 nm), and of relatively long pulse duration]. Nevertheless, to our knowledge, this was the first demonstration of the application of nanotechnology to treat blood vessels with laser-activaded gold nanoparticles and their nanoclusters[148-154].

Combined action of laser and drugs

Sodium nitroprusside increased the sensitivity of lymph microvessels to low-power He-Ne laser radiation[136]. After intravenous injection of sodium nitroprusside (100 μg/kg), application of He-Ne laser radiation at the lowest power (14 mW/cm^2 for 15 min) stimulated phasic contractions in 44% of lymph microvessels against a background of stable dilation caused by the drug. Contractions occurred at a rate of 6-25/min and had amplitudes of 8-22 μm. In comparison, this dose of laser radiation alone had no notable effect on the phasic contractions of intact microvessels. Such an approach could have great potential for developing innovative therapies for some diseases (e.g., lymphedema).

Nicotine intoxication

Nicotine, an important component of cigarette smoke, was shown to be indirectly responsible for inducing

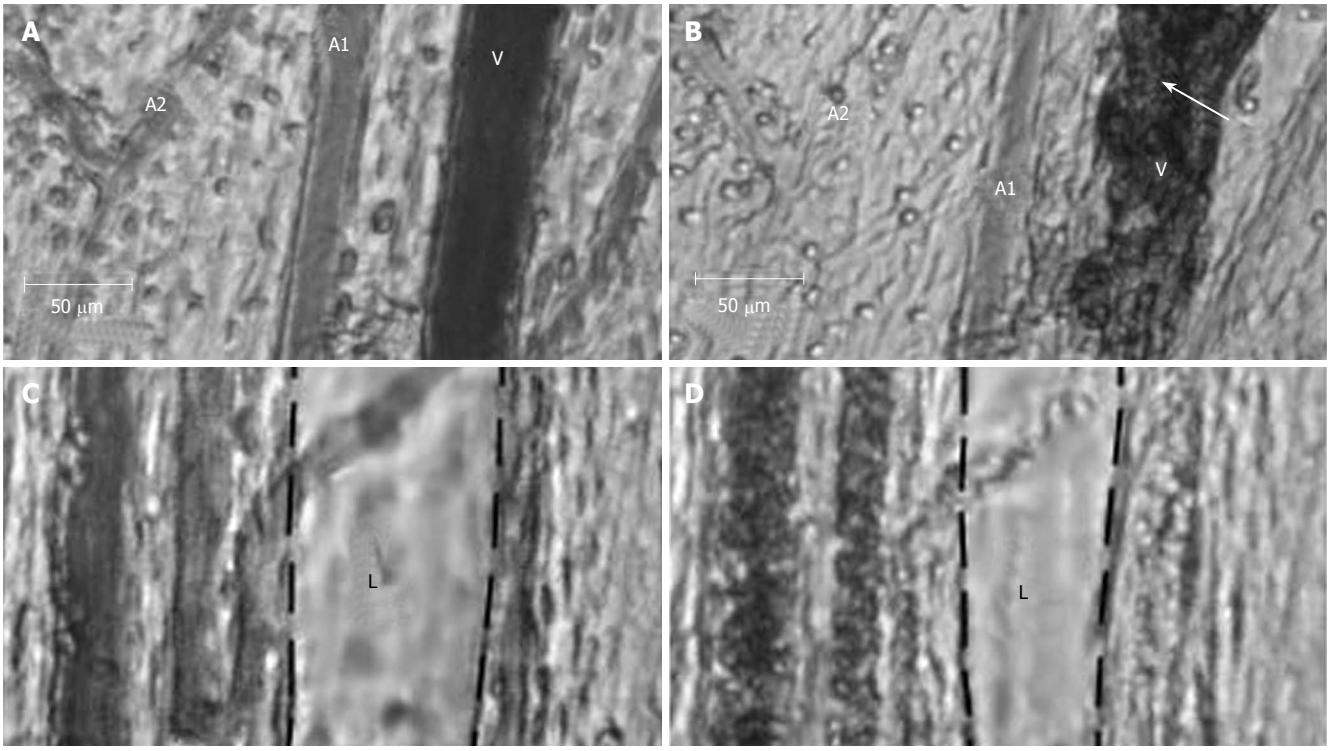

Figure 14 Effect of a laser pulse (585 nm, 10-ms pulse duration, 0.5-30 J/cm^2 radiant exposure) on blood and lymph microvessels *in vivo*. **A**: Intact venule (V) and arterioles (A1 and A2) with good blood flow; **B**: Damage to these microvessels immediately after laser pulse: local hemorrhage (arrow) around the venule (V) and stasis in a small arteriole (A2); **C**: Intact lymphatic (L) before laser pulse (black dash line shows internal margin of lymphatic wall); **D**: Laser-induced constriction of the lymphatic, which coincided with stasis in neighboring venules.

pathology in many tissues, both human and animal[155-157]. Exposure to cigarette smoke increases the nicotine level in the blood to a maximum in less than 10 s. Therefore, the immediate responses of the vascular network to the action of nicotine appear to be important in the development of acute pathology. The pathological effects of nicotine on blood microcirculation have been reported in sufficient detail, but its impact on the lymphatic system remains obscure.

We uncovered the first experimental evidence of potential active participation of lymph microvessels in the mechanisms of nicotine's effects *in vivo*[158]. The influence of nicotine on microlymphatics was determined using three routes of nicotine administration: (1) direct topical application in various concentrations (0.001 mmol/L, 10 mmol/L, and 100 mmol/L solutions) for 15 min; (2) acute injection of nicotine solution (10 mmol/L) through a cannulated vein; and (3) chronic administration for 14 d *via* subcutaneous injection from a mini-osmotic pump (10 mmol/L solution; 0.5 μL/h delivery rate).

The topical application showed that the most significant responses of microlymphatics to nicotine's impact were at 10 mmol/L and 100 mmol/L doses. In particular, the concentration of 10 mmol/L caused a significant, immediate short-term (12-40 s) constriction of 100% of the lymphangions. The effect started within 3-5 s of application (67% of cases) or after ~3 min of nicotine exposure (33% of cases). The lymphatic diameter was decreased by 34% ± 7% (more than ~2 times the amplitude of spontaneous phasic contractions before nicotine application). In all cases with the highest concentration of nicotine (100 mmol/L), the same immediate constrictions were associated with the slowing of lymph flow, local stable constriction of lymph microvessels, asynchronous motion of the lymphatic wall, stasis in blood microvessels, and disturbances of respiration. Thus, under the direct impact of nicotine, there were significant changes in small lymphatic function *in vivo*, which were dose and time dependent. We hypothesize that the obtained effects were the result of the direct action of nicotine on lymph microvessels and probably reflect specific endothelial dysfunction and/or injury of the contractile ability of the lymphatic wall.

Acute nicotine intoxication delivered intravenously slightly relaxed the lymphatics and was sometimes accompanied by slowing of lymph flow and short-term stasis in blood microvessels. Chronic intoxication using a 10 mmol/L concentration (effective at the topical application) did not markedly change the function of lymphatic and blood microvessels and did not differ markedly from that in the intact state. The absence of effects may be the result of adaptation of the microcirculation to the action of nicotine.

Thus, nicotine induces marked changes in small lymphatic function *via* its acute, direct impact *in vivo*. The observed microlymphatic disturbances due to the action of nicotine may be an important mechanism in the complex, immediate reaction of a healthy organism to cigarette smoke. The acute lymphatic damage caused by nicotine could be more crucial in some pathologies or treatments, and suggests that nicotine may contribute to vascular abnormalities and tissue edema.

EXPERIMENTAL MODELING OF DIFFERENT PATHOLOGIES

Damage to lymph microcirculation is an important mechanism underlying the development of many diseases (e.g., tumor, inflammation, infections, intoxications, lymphedema, lymphatic malformation) and often determines their severity[29,40,62,159]. Because rat mesentery is a highly informative *in vivo* model for functional analysis of lymph microdynamics, this animal model was used by us to study the mechanisms of microlymphatic disturbances resulting from different pathologies, such as models of staphylococcal intoxication, pathological stress, lymphedema, and venous insufficiency.

Staphylococcal intoxication

It is well known that α-toxin (α-hemolysin) is the protein produced by *Staphylococcus aureus* and causes serious blood circulatory disturbances with its appearance in blood during staphylococcal diseases; however, its effect on lymph microcirculation is still poorly understood[160-162]. In our study, we used an exotoxic complex (ETC) produced by culture *Staphylococcus aureus* O-15[66,142,163-166]. The main component of this complex is α-toxin (titer ~ 1:640); additionally, it contains a small amount of δ-toxin (titer ~ 1:64). Endotoxins, enterotoxins, and protein A are completely absent.

The staphylococcal intoxication was introduced by intravenous injection of ETC (0.2 mg/100 g) into the tail vein, after which we monitored microcirculation for 30 min. This dose caused serious intoxication. Animals with acute exotoxic shock (those dying within 30 min of ETC introduction) were excluded from the analysis. Disturbances of lymph microcirculation began immediately; after 1 min, the diameters of 75% of the lymphatics were slightly decreased (by 7 ± 2 μm). Between the fifth and tenth minutes of observation, in parallel with vasoconstriction, ETC induced pathologic phasic contractions, characterized by asynchronous wall motion, in half of the lymphatics. After 30 min, lymphatic disturbances were expanded by the development of lymphostasis in 53% of cases.

The resulting effects were due primarily to the direct action of the toxic complex on the lymphatics, as the topical application of ETC in the investigated microlymphatics caused similar microvascular disturbances during a 60-min period. In particular, after a short latent period (58 ± 9 s), ETC induced marked decreasing of lymphangion diameters (36 ± 11 μm from the initial diameter) and stimulated pathologic phasic contractions in 60% of cases. Pathologic phasic activity is characterized by irregular motion of lymphatic walls and defective relaxation (after contraction, the diastolic diameter is sometimes less than it was before). We observed simultaneous abnormalities in blood microvasculature (slowing down of blood flow in venules; increasing migration of leukocytes through venular walls into tissue; and local accumulation of leukocytes around blood microvessels and, as a result, compression of venules into irregular shapes). From the thirtieth to the sixtieth minute of observation, the pathologic constriction of lymph microvessels progressed to complete obliteration of the lymphatic lumen, inhibition of phasic contractions, and gradual development of lymphostasis in 90%-98% of lymphatics. In parallel, we observed blood flow slowing up to stasis and small hemorrhages around venules.

The underlying mechanisms of microlymphatic disturbances include the well-known ability of α-toxin to form the specific Ca^{2+} channels in cell membranes and, correspondingly, to disturb the transport Ca^{2+} in the smooth muscles of the vascular wall and, probably, in the pacemaker cells[167,168]. Thus, these data revealed that an important mechanism of staphylococcal vascular disturbances is damage to the lymph microcirculation. Therefore, therapies for staphylococcal pathology require the correction of microlymphatic dysfunction.

Pathologic effects on lymph microvessels are partially reversible by He-Ne laser radiation and some vasoactive drugs (Euphyllin, Verapamil, DMSO)[66,142,165,166]. In particular, irradiation of the mesentery (450 mW/cm^2 during the first 15 min following ETC application) attenuates typical toxin constriction. In contrast, preliminarily irradiating *in vitro* ETC (20 mW/cm^2, 60 min) attenuates development of lymphostasis: a 60-min application of non-irradiated ETC causes lymphostasis in 88% of lymphangia, while irradiated ETC led to lymphostasis in 57% of lymph microvessels. Thus, low-power laser radiation can attenuate lymphotoxic action *via* its effect on microlymphatic walls, as well as on the properties of ETC itself[166].

However, the most effective corrections of microlymphatic disturbances can be achieved by DMSO. It has been noted above that the effects of DMSO after ETC application (dilation of lymphatics, inhibition of pathologic phasic activity, restoration of lymph flow) are different from the effects on intact lymphatics. Moreover, these local, positive effects are associated with an increase in the duration of animal life, which has been demonstrated in experiments on mice injected with lethal doses of ETC[66,142,165].

Study of experimental lymphedema

Lymphedema is a complication of lymphatic drainage decompensation that may happen during congenital lymphatic dysplasia, hepatic cirrhosis, venous insufficiency, obstruction or surgical extirpation of lymph nodes[159,169,170]. In particular, post-mastectomy lymphedema (PML) develops in 25%-50% of cases after breast cancer treatment[171]. Generally, lymphedema damages the local lymphovascular network (e.g. in affected extremities) causing insufficient and abnormal lymph transport and, correspondingly, accumulation of protein-rich fluid in the interstitial space (tissue edema)[159,169,172]. Because the microvascular network is the principal site for fluid exchange between blood, lymph, and interstitial space, detailed studies of lymph microvessel disturbances during lymphedema have great importance. The efficacy of existing therapeutic treatments for PML is controversial, and clear scientific data have not emerged on the mechanisms of lymphedema development[143,170,171].

Obtaining data from human subjects involves many difficulties (e.g., unpredictability of the time of clinical

onset of PML, limitations of diagnostic methods, *etc.*)[170,173]. In experimental studies in rat, dog, and rabbit extremities, the multi-layers of lymph vascular networks, the rapid development of a good collateral network, and sufficient angiogenesis permit quick restoration of lymph pathways and drainage function, leading to prompt resolution of even acute edema without the appearance of long-term or chronic edema[174-177]. This precludes an informed study of chronic or long-term edema.

In light of these facts, the development of lymphedema in rat mesentery may make the detailed study of lymph and blood microvessel function in acute and chronic edema, because the single layer of vessels in this animal model reduces the opportunity for rapid development of collateral lymph flow. In our study, experimental lymphedema was created by microsurgical removal of regional lymph nodes (lymphadenectomy) or ligation of the collecting vein[101,126,178,179]. Then, the direct quantitative measurement of tissue water was performed in parallel to monitoring blood and lymph vessel activity, including mapping individual cell transport in microvessels and tissue.

After lymphadenectomy, dynamic observation of amounts of water revealed increasing edema from 30 min to 1 wk; the greatest degree of edema occurred at 1 wk with a gradual decrease in edema from 1 to 11 wk[101]. At the thirtieth minute post lymphadenectomy, these effects were accompanied by acute constriction of lymph vessels and slowing of lymph flow velocity from 302 ± 41 μm/s before extirpation to 155 ± 30 μm/s after extirpation ($P < 0.01$). After 1 wk of lymphedema, the lymphatics were overloaded (diameter increased from 133 ± 6 μm in their intact state to 147 ± 4 μm after lymphadenectomy, $P < 0.05$) with slowing lymph flow. Four weeks after lymphadenectomy, the amount of water in tissue included a range from significant compensation to progressive development of edema. In spite of this, lymph microvessels of all experimental animals (with compensation or with decompensation of edema) revealed significant dysfunction and structure damage (dilation, slowing of lymph flow, degenerative changes in the microlymphatic wall). Eleven weeks after lymphedema, we observed various microvascular disturbances, including lymphatic fibrosis at edema decompensation and significant dilation of lymph microvessels or lymphangiogenesis at edema compensation.

We obtained experimental evidence of the significant role of blood microvessels during lymphedema development after lymphadenectomy, which before was either not clear or was controversial. Marked changes in blood microvessels started at the stage of well-developed tissue edema and marked lymphatic disturbances. We observed dilation of blood microvessels, venules, and expansion of the microvascular network without significant hemorrhage in the interstitium[101].

Acute venous insufficiency (30 min after vein ligation) led to significant edema[101,126,178,179]. The comparison of acute lymphedema after lymphadenectomy and venous insufficiency revealed several similar changes, including inhibition of lymph flow and phasic activity. The specific disturbances after vein ligation included marked dilation of the blood vascular network; slowing (up to stasis) of blood flow in venules; and multiple hemorrhages adjacent to the venules and, as a result, the presence of many RBCs in the lymph.

Thus, unknown mechanisms of microvascular damage as well as the correlation between the functions of lymph microvessels, blood microvessels, and tissue edema in dynamic lymphedema development *in vivo* was established, which is important both for understanding mechanisms of lymphedema and for developing new treatment strategies.

Experimental model of sound-related stress

Experimental pathologic stress (2 h of immobilization and interrupted sound, 120 dB, 150-500 Hz) on rats led to significant (20%) increase in microlymphatic diameters ($P < 0.01$); intensification of lymph flow (mean cell velocity increased from 227 ± 8 μm/s in intact rats to 295 ± 12 μm/s in the stressed animals, $P < 0.001$), and stimulation of phasic contractions in 75% of lymphatics[179-181]. The resulting changes in lymph microvessel function probably stimulate lymph drainage and, therefore, play an adaptive role in this pathology.

REAL-TIME QUANTITATIVE MONITORING OF INDIVIDUAL CELL TRANSPORT *IN VIVO*

Normal rat lymphocytes, rat basophilic leukemia (RBL-1) cells, K562 human leukemia cells, and rat RBCs (for each cell type, 10^7-10^8 cells/mL) were labeled with FITC and introduced separately by bolus injection (100 μL) into the tail vein of rats with normal blood circulation or with acute venous insufficiency (ligation of collecting mesenteric vein). Over the next 30-60 min, we monitored in real-time the fluorescently labeled circulating, rolling, and adhesive cells in mesenteric blood vessels (diameter, 30-50 μm) and lymph microvessels (diameter, 120-180 μm), as well as visualized the distribution of the cells in mesenteric interstitial space. Simultaneous fluorescence and transmission imaging allowed us to distinguish the position of a single labeled cell. Accumulation of cells in mesenteric lymph nodes and the right lobe of the liver was monitored *in vivo* 60-90 min after the injections; each organ had been carefully exposed through a mid-abdominal incision and placed on a thermostabilizing microscope stage. To minimize light scattering by tissue and obtain deep, clear images of lymph nodes, we applied optical immersion technology (optical clearing method) using glycerol, which is an osmotic chemical[182,183]. In addition, the concentration of labeled cells in the systemic blood circulation was estimated by sampling blood through a catheter.

Normal and leukemic cell transport: a comparative analysis

We observed a significant number of rat RBCs, WBCs (lymphocytes), and leukemic cells in blood microvessels immediately after injection; 85%-95% of the cells were cleared from the microcirculation within the first 30 min (Figure 15A and B). In comparison, only a few human leukemia cells were found in the blood circulation within

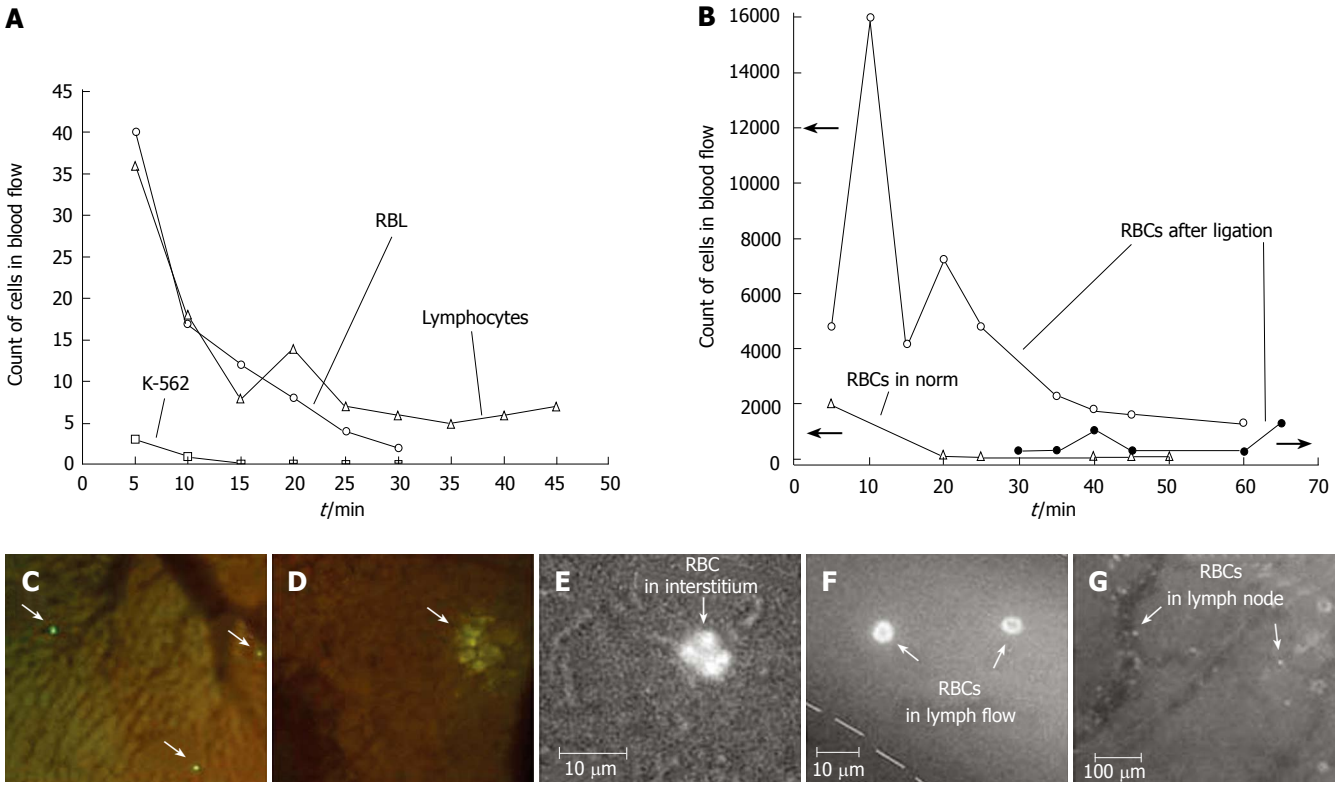

Figure 15 **A**: Monitoring of labeled rat lymphocytes, and rat (RBL) and human (K562) leukemia cells in blood vessels of rat mesentery; **B**: Simultaneous monitoring of RBCs in blood and lymph systems under normal conditions and with venous insufficiency; **C**, **D**: *In vivo* imaging of liver with (**C**) lymphocytes and (**D**) RBL leukemia cells. Monitoring RBC migration from blood vessel (**E**) through interstitium to (**F**) lymph vessel and (**G**) lymph node.

the first 5-10 min (Figure 15A), probably because 95% of the cells were cleared by a strong immune response immediately after injection. These cells then migrated into the interstitial space and were quickly destroyed. No cells appeared in lymphatic vessels during the first 60 min of observation.

In the first 5 min after bolus injections of WBCs or RBCs labeled with FITC (10^6 cells of each type in bolus), 50 times more RBCs were present in the circulation than were normal WBCs. Normal WBCs were detected in blood flow more often than rat leukemia cells (RBL-1 cells). RBL-1 cells, being ~1.5-2 times larger than normal WBCs, probably plugged small microvessels, thus decreasing the number of cells detected. In particular, Figure 15A shows that the number of WBCs was slightly higher than that of RBL-1 cells, although fewer WBCs (10^6 cells in bolus) than RBL-1 cells (10^7 cells in bolus) were injected. At 60-90 min of observation, both types of cells had accumulated mainly in the liver (Figure 15C and D). WBCs were visualized in liver as clearly distinguishable individual cells (Figure 15C), whereas RBL-1 cells appeared as a fluorescent spot (Figure 15D), probably because cells were destroyed in the liver, and only the rest of the dye was visible. However, both types of cells were identified after 3 h of observation in blood samples from large vessels; there were more WBCs than RBL-1 cells (10^3 *vs* 10^2). Thus, although the migrations of leukemic cells and normal cells in the same living organism represent some shared properties, they also display significantly distinct features. In the future, these distinct features may be used as diagnostic criteria for leukemia. Since the presented approach is able to analyze the transport of lymphocyte (important participants of immune response) it offers the potential to study *in vivo* immune responses at cellular and molecular levels.

Cell transport dynamic from blood to lymph during edema

The modeling of acute venous insufficiency and tissue edema caused marked changes in normal cell migration[101]. In particular, after injection of labeled RBCs, we observed a 5-min increase in the absolute number of labeled cells in the slowing blood flow of edematous tissue compared with normal blood flow (Figure 15B). Then, the slow-down of blood flow at the edema led to the output of many RBCs (10-15 min of observation) from blood vessels in mesenteric interstitium, where the trajectory of their motion is represented as episodic zigzag lines with mean velocities of 10-20 μm/s. As a result, RBCs moved through the interstitium to the lymphatics. After 30 min of monitoring, RBCs were identified in lymph flow (Figure 15F), and then in mesenteric lymph nodes (40-60 min of observation; Figure 15G). Thus, our integrated optical technique demonstrates unique capabilities for real-time monitoring of labeled cells in blood and lymph flow, as well as the migration of these cells into tissue interstitium and regional lymph nodes.

In vivo detection of flowing apoptotic cells

Apoptosis is referred to as programmed physiological cell death. *In vivo* study of apoptosis is crucial for understanding the fundamentals of cell biology; optimization of

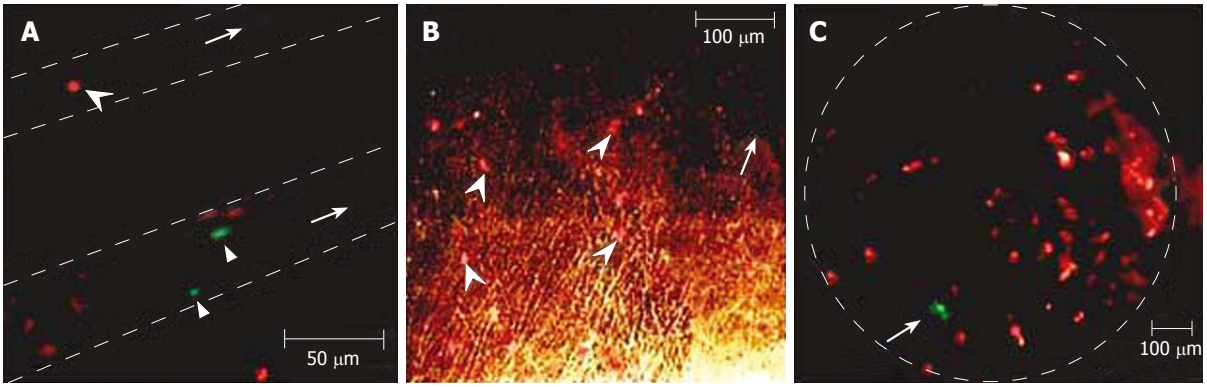

Figure 16 **A**: Apoptotic (arrowhead, red) and normal (two arrow triangles, green) cells in two blood vessels (dashed lines); **B**: Apoptotic cells (arrowhead, red) in interstitium (arrow shows one vessel); **C**: Normal (arrow, green) and apoptotic (red) cells in a lymph node (dashed line).

radiation therapy and chemotherapy; diagnosis of many diseases (e.g., metastasis development, cardiovascular diseases, hematological diseases, autoimmune diseases, neurodegenerative diseases, Alzheimer's disease); and assessment of acute organ transplant rejection or the effect of immunosuppressive drugs[134,184-195]. Despite significant progress in studying apoptosis *in vitro* with many powerful assays, adapting these assays to *in vivo* study of apoptosis is extremely difficult[184,185].

In our experiments, WBCs extracted from a rat underwent apoptosis after exposure to dexamethasone. They were then labeled with rhodamine 6G (red fluorescent emission). In addition, normal WBCs were labeled with FITC (green emission). A 50/50 mixture of labeled apoptotic and normal WBCs was injected into a rat's tail vein, and the appearance of the WBCs was monitored in rat mesentery venules with integrated PTFC. The fluorescence measurements (obtained by counting the number of cells in images) demonstrated the appearance of both normal and apoptotic cells in blood microvessel flow during the first minute (Figure 16A), and rapid clearing of apoptotic cells from circulation, with a half-life of ~8 min. We also observed: (1) rolling apoptotic cells in small venules within 10 min after the injections, (2) the appearance of apoptotic cells in the interstitium after 15 min (Figure 16B), and (3) significant accumulation of apoptotic cells in mesenteric lymph nodes (Figure 16C) after 30 min (see details of node location in Figure 3A and B).

Thus, the obtained results demonstrate that individual cell migration in living organisms depends on: (1) the morphological type of normal and abnormal cells (e.g. WBCs versus RBCs, WBCs versus leukemic cells), (2) the functional state of the cell (e.g. living versus apoptotic cells), and (3) the functional status of the entire organism (e.g. in norm versus in acute venous insufficiency at tissue edema). The high sensitivity of the PT technique to nanoscale morphologic events during apoptosis demonstrated *in vitro*[112-113], in combination with conventional fluorescent assays, makes it possible to apply this technique for detection of apoptotic cells *in vivo*.

IR ANGIOGRAPHY AND LYMPHGRAPHY

Indocianine green (ICG) is a well-known, relatively harmless dye for IR blood angiography and IR imaging of lymph nodes in human and animals[196-201]. Within the first seconds after intravenous injection, there is a shift in the absorption spectrum of ICG from 780 nm to 805 nm (spectral stabilization) due to two processes: polymerization of ICG molecules and their binding to plasma proteins and lipoproteins[196]. Plasma clearance of ICG is biphasic, showing a rapid first phase with a half-life of 4-6 min and a secondary phase with a half-life of more than 1 h[197]. ICG is eliminated from an organism by the enterohepatic route[197].

The imaging of blood vasculature by ICG is a well-known conventional approach; however, identification of the lymph microvascular network with ICG has not been previously studied. Recently, we performed first experiments with microlymphatics. Using TDM and fluorescent microscopy, we monitored typical microvascular units (venula, arteriola, and lymph microvessel of rat mesentery; Figure 17) after intravenous ICG injection (0.2 mL/100 g in rat's tail vein). Excitation at a wavelength of 805 nm, 0.25 mW/cm^2, was provided by continuous diode laser, and the re-emitted fluorescence was filtered at 830 nm and then detected using an intensified highly sensitive camera (PentoMAX, Roper Scientific). Our preliminary studies demonstrated that the first IR image of the venula appears 70-80 s after injection; then, in a short period of time (first 2 min after injection), dye appeared in the arteriola (Figure 17B). Forty to fifty minutes after injection, ICG accumulated (at least partly) in lymph microvessels (Figure 17C). Thus, ICG may potentially be used for study of blood and lymph microcirculation (IR angiography and lymphography), including a monitoring traffic dye in blood and lymph vascular nets.

CONCLUSIONS

As demonstrated in this paper, rat mesentery, in combination with advanced optical techniques, is an attractive animal model for *in vivo* lymph- and blood flow cytometry, high-resolution high speed cell imaging, IR time-resolved angiography and lymphography, real-time monitoring of cells traffic through tissue in norm, during diseases or in response to therapy.

Specifically, the capabilities of this model may include:

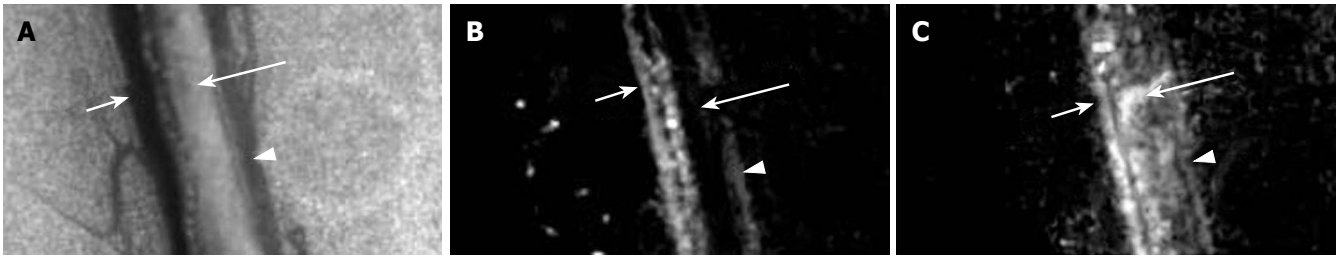

Figure 17 ICG IR blood and lymph microangiography. Transmission image before ICG injection (venula: short arrow, arteriola: triangle, lymph microvessel: long arrow) (**A**). Fluorescence images (excitation 805 nm; emission 830 nm) at the (**B**) 15th and (**C**) 45th min after ICG injection.

(1) analysis of cell pathways in tissue (blood microvessel, interstitium, afferent lymphatics) with migration through microvessel walls and accumulation in lymph nodes and liver; (2) quantitative monitoring of changes in the number of normal or abnormal cells in blood and lymph flow (blood and lymph FC); (3) identification of moving and static cells, including rare abnormal cells and apoptotic cells, through their size, shape, and specific sub-cellular structures; (4) high-resolution, high-speed monitoring of lymph and blood microrheology (e.g. transient deformability, cell aggregation), and interactions between different moving cells and between moving cells and endothelial cells of the vessel wall; (5) quantitative assessment of the clearance rate of circulating cells in lymph and blood flow; (6) analysis of *in vivo* immune responses at cellular and molecular levels; (7) *in vivo* monitoring of the circulation and migration of chylomicrons, bacteria, and viruses; (8) monitoring of dynamic thrombus and blood clot formation (with and without platelet participation); (9) label-free IR microvessel angiography and lymphography.

These advantages are crucial, both for understanding basic cell biology (e.g. metabolism and apoptosis), cell flow dynamics, and for conducting clinical studies of early disease diagnoses (e.g., cancer, sickle diseases, leukemia, edema, inflammation, infections) or assessment of innovative therapeutic interventions (pharmaceuticals, nicotine, lasers, or γ-radiation). Other potential applications may include radio and drug screening *in vivo* based on the previously described, promising *in vitro* techniques.

It is hoped that this review will serve not only as a helpful progress report and to provide certain leads for further research, but will also help attract the scientific interest and support that are required to solve these problems.

ACKNOWLEDGMENTS

The authors thank Grigory E Brill, PhD, DSc (Saratov Medical State University, Russia); Sergey S Ulianov, PhD, DSc (Saratov State University, Russia); Qingming Luo, PhD (Institute for Biomedical Photonics, Huazhong University of Science and Technology, China); Ivan V Fedosov, PhD (Saratov State University, Russia); Anastasia V Solovieva, PhD (Saratov Medical State University, Russia). We thank Tatiana V Stepanova for assisting with animal experiments, Dmitri O Lapotko, PhD for his significant contribution in the development of the PT setup, and Scott Ferguson, for assisting with laser measurements. We also thank the Office of Grants and Scientific Publications at the University of Arkansas for Medical Sciences for editorial assistance during the preparation of this manuscript.

REFERENCES

1 **Aukland K**. Arnold Heller and the lymph pump. *Acta Physiol Scand* 2005; **185**: 171-180
2 **Zweifach BW**, Lowenstein B, Chambers R. Response of blood capillaries to acute hemorrhage in the rat. *Am J Physiol* 1944; **142**: 80-93
3 **Chambers R**, Zweifach BW. Topography and function of the mesenteric capillary circulation. *Am J Anat* 1944; **75**: 173-205
4 **Wiggers CJ**. Peripheral circulation. *Annu Rev Physiol* 1947; **9**: 255-300
5 **Gaehtgens P**, Meiselman HJ, Wayland H. Erythrocyte flow velocities in mesenteric microvessels of the cat. *Microvasc Res* 1970; **2**: 151-162
6 **Johnson PC**. Red cell separation in the mesenteric capillary network. *Am J Physiol* 1971; **221**: 99-104
7 **Zweifach BW**, Prather JW. Micromanipulation of pressure in terminal lymphatics in the mesentery. *Am J Physiol* 1975; **228**: 1326-1335
8 **Starr MC**, Frasher WG. In vivo cellular and plasma velocities in microvessels of the cat mesentery. *Microvasc Res* 1975; **10**: 102-106
9 **Lipowsky HH**, Usami S, Chien S. In vivo measurements of "apparent viscosity" and microvessel hematocrit in the mesentery of the cat. *Microvasc Res* 1980; **19**: 297-319
10 **Firrell JC**, Lipowsky HH. Leukocyte margination and deformation in mesenteric venules of rat. *Am J Physiol* 1989; **256**: H1667-H1674
11 **Seki J**. Flow pulsation and network structure in mesenteric microvasculature of rats. *Am J Physiol* 1994; **266**: H811-H821
12 **Yamaki K**, Lindbom L, Thorlacius H, Hedqvist P, Raud J. An approach for studies of mediator-induced leukocyte rolling in the undisturbed microcirculation of the rat mesentery. *Br J Pharmacol* 1998; **123**: 381-389
13 **Frenette PS**, Moyna C, Hartwell DW, Lowe JB, Hynes RO, Wagner DD. Platelet-endothelial interactions in inflamed mesenteric venules. *Blood* 1998; **91**: 1318-1324
14 **Jiang Y**, Liu AH, Zhao KS. Studies on the flow and distribution of leukocytes in mesentery microcirculation of rats. *World J Gastroenterol* 1999; **5**: 231-234
15 **Pearson MJ**, Lipowsky HH. Influence of erythrocyte aggregation on leukocyte margination in postcapillary venules of rat mesentery. *Am J Physiol Heart Circ Physiol* 2000; **279**: H1460-H1471
16 **Osterloh K**, Gaehtgens P, Pries AR. Determination of microvascular flow pattern formation in vivo. *Am J Physiol Heart Circ Physiol* 2000; **278**: H1142-H1152
17 **He P**, Wang J, Zeng M. Leukocyte adhesion and microves-

sel permeability. *Am J Physiol Heart Circ Physiol* 2000; **278**: H1686-H1694
18 **Sugii Y**, Nishio S, Okamoto K. In vivo PIV measurement of red blood cell velocity field in microvessels considering mesentery motion. *Physiol Meas* 2002; **23**: 403-416
19 **Sugii Y**, Nishio S, Okamoto K. Measurement of a velocity field in microvessels using a high resolution PIV technique. *Ann N Y Acad Sci* 2002; **972**: 331-336
20 **Golub AS**, Pittman RN. Erythrocyte-associated transients in PO2 revealed in capillaries of rat mesentery. *Am J Physiol Heart Circ Physiol* 2005; **288**: H2735-H2743
21 **Ohshima N**. Engineering approaches to the microcirculation studies. *Clin Hemorheol Microcirc* 2006; **34**: 27-34
22 **Benoit JN**, Zawieja DC, Goodman AH, Granger HJ. Characterization of intact mesenteric lymphatic pump and its responsiveness to acute edemagenic stress. *Am J Physiol* 1989; **257**: H2059-H2069
23 **Benoit JN**. Relationships between lymphatic pump flow and total lymph flow in the small intestine. *Am J Physiol* 1991; **261**: H1970-H1978
24 **Sekizuka E**, Ohshio C, Minamitani H. Automatic analysis of moving images for the lymphocyte velocity measurement. *Microcirculation annual* 1995; **11**: 107-108
25 **Takahashi T**, Shibata M, Kamiya A. Mechanism of macromolecule concentration in collecting lymphatics in rat mesentery. *Microvasc Res* 1997; **54**: 193-205
26 **Dixon JB**, Zawieja DC, Gashev AA, Coté GL. Measuring microlymphatic flow using fast video microscopy. *J Biomed Opt* 2005; **10**: 064016
27 **Zweifach BW**, Kivy-Rosenberg E. Microcirculatory effects of whole-body X-irradiation and radiomimetic procedures. *Am J Physiol* 1965; **208**: 492-498
28 **Ferguson MK**, Shahinian HK, Michelassi F. Lymphatic smooth muscle responses to leukotrienes, histamine and platelet activating factor. *J Surg Res* 1988; **44**: 172-177
29 **Aukland K**, Reed RK. Interstitial-lymphatic mechanisms in the control of extracellular fluid volume. *Physiol Rev* 1993; **73**: 1-78
30 **Benoit JN**. Effects of alpha-adrenergic stimuli on mesenteric collecting lymphatics in the rat. *Am J Physiol* 1997; **273**: R331-R336
31 **Kimura M**, Mitani H, Bandoh T, Totsuka T, Hayashi S. Mast cell degranulation in rat mesenteric venule: effects of L-NAME, methylene blue and ketotifen. *Pharmacol Res* 1999; **39**: 397-402
32 **Carati CJ**, **Jobling J**, Fouyaxis J and **Gannon BJ.** Effect of low level laser on mesenteric lymphatics and blood vessels in-vivo. *Progress in Microcirculation Research* 1999; **10**: 77-80
33 **Torres LN**, Torres Filho IP. Determination of macromolecular exchange and PO2 in the microcirculation: a simple system for in vivo fluorescence and phosphorescence videomicroscopy. *Braz J Med Biol Res* 2001; **34**: 129-135
34 **Amerini S**, Ziche M, Greiner ST, Zawieja DC. Effects of substance P on mesenteric lymphatic contractility in the rat. *Lymphat Res Biol* 2004; **2**: 2-10
35 **Shirasawa Y**, Ikomi F, Ohhashi T. Physiological roles of endogenous nitric oxide in lymphatic pump activity of rat mesentery in vivo. *Am J Physiol Gastrointest Liver Physiol* 2000; **278**: G551-G556
36 **Arshi K**, Bendayan M, Ghitescu LD. Alterations of the rat mesentery vasculature in experimental diabetes. *Lab Invest* 2000; **80**: 1171-1184
37 **Yanagi K**, Ohshima N. Angiogenic vascular growth in the rat peritoneal disseminated tumor model. *Microvasc Res* 1996; **51**: 15-28
38 **Hayes H**, Kossmann E, Wilson E, Meininger C, Zawieja D. Development and characterization of endothelial cells from rat microlymphatics. *Lymphat Res Biol* 2003; **1**: 101-119
39 **Ji RC**. Characteristics of lymphatic endothelial cells in physiological and pathological conditions. *Histol Histopathol* 2005; **20**: 155-175
40 **Witte MH**, Jones K, Wilting J, Dictor M, Selg M, McHale N, Gershenwald JE, Jackson DG. Structure function relationships in the lymphatic system and implications for cancer biology. *Cancer Metastasis Rev* 2006; **25**: 159-184
41 **Morisaki H**, Katayama T, Kotake Y, Ito M, Handa M, Ikeda Y, Takeda J, Suematsu M. Carbon monoxide modulates endotoxin-induced microvascular leukocyte adhesion through platelet-dependent mechanisms. *Anesthesiology* 2002; **97**: 701-709
42 **Mouthon MA**, Vereycken-Holler V, Van der Meeren A, Gaugler MH. Irradiation increases the interactions of platelets with the endothelium in vivo: analysis by intravital microscopy. *Radiat Res* 2003; **160**: 593-599
43 **Yamagata K**, Kumagai K. Experimental study of lymphogenous peritoneal cancer dissemination: migration of fluorescent-labelled tumor cells in a rat model of mesenteric lymph vessel obstruction. *J Exp Clin Cancer Res* 2000; **19**: 211-217
44 **Bornhop DJ**, Contag CH, Licha K, Murphy CJ. Advance in contrast agents, reporters, and detection. *J Biomed Opt* 2001; **6**: 106-110
45 **Contag PR**, Olomu IN, Stevenson DK, Contag CH. Bioluminescent indicators in living mammals. *Nat Med* 1998; **4**: 245-247
46 **Ebert B**, Sukowski U, Grosenick D, Wabnitz H, Moesta KT, Licha K, Becker A, Semmler W, Schlag PM, Rinneberg H. Near-infrared fluorescent dyes for enhanced contrast in optical mammography: phantom experiments. *J Biomed Opt* 2001; **6**: 134-140
47 **Becker MD**, Planck SR, Crespo S, Garman K, Fleischman RJ, Dullforce P, Seitz GW, Martin TM, Parker DC, Rosenbaum JT. Immunohistology of antigen-presenting cells in vivo: a novel method for serial observation of fluorescently labeled cells. *Invest Ophthalmol Vis Sci* 2003; **44**: 2004-2009
48 **Nestmann ER**, Douglas GR, Matula TI, Grant CE, Kowbel DJ. Mutagenic activity of rhodamine dyes and their impurities as detected by mutation induction in Salmonella and DNA damage in Chinese hamster ovary cells. *Cancer Res* 1979; **39**: 4412-4417
49 **Saetzler RK**, Jallo J, Lehr HA, Philips CM, Vasthare U, Arfors KE, Tuma RF. Intravital fluorescence microscopy: impact of light-induced phototoxicity on adhesion of fluorescently labeled leukocytes. *J Histochem Cytochem* 1997; **45**: 505-513
50 **Zdolsek JM**. Acridine orange-mediated photodamage to cultured cells. *APMIS* 1993; **101**: 127-132
51 **Abbitt KB**, Rainger GE, Nash GB. Effects of fluorescent dyes on selectin and integrin-mediated stages of adhesion and migration of flowing leukocytes. *J Immunol Methods* 2000; **239**: 109-119
52 **Berk DA**, Swartz MA, Leu AJ, Jain RK. Transport in lymphatic capillaries. II. Microscopic velocity measurement with fluorescence photobleaching. *Am J Physiol* 1996; **270**: H330-H337
53 **Novak J**, Georgakoudi I, Wei X, Prossin A, Lin CP. In vivo flow cytometer for real-time detection and quantification of circulating cells. *Opt Lett* 2004; **29**: 77-79
54 **Georgakoudi I**, Solban N, Novak J, Rice WL, Wei X, Hasan T, Lin CP. In vivo flow cytometry: a new method for enumerating circulating cancer cells. *Cancer Res* 2004; **64**: 5044-5047
55 **Wei X**, Sipkins DA, Pitsillides CM, Novak J, Georgakoudi I, Lin CP. Real-time detection of circulating apoptotic cells by in vivo flow cytometry. *Mol Imaging* 2005; **4**: 415-416
56 **Pries AR**, Eriksson SE, Jepsen H. Real-time oriented image analysis in microcirculatory research. *Proc SPIE* 1989; **1357**: 257-263
57 **Skalak R**, Branemark PI. Deformation of red blood cells in capillaries. *Science* 1969; **164**: 717-719
58 **Galanzha EI**, Tuchin VV, Zharov VP. In vivo integrated flow image cytometry and lymph/blood vessels dynamic microscopy. *J Biomed Opt* 2005; **10**: 054018
59 **Kim S**, Popel AS, Intaglietta M, Johnson PC. Aggregate formation of erythrocytes in postcapillary venules. *Am J Physiol Heart Circ Physiol* 2005; **288**: H584-H590
60 **Rusznyak I**, Foldi M, Szabo G. Lymphatics and Lymph Circulation. 2nd ed. London: Pergamon, 1967
61 **Human Physiology**, Schmidt RF, Thews G, editors. Berlin

Heidelberg: Springer-Verlag, 1989
62 **Brown P**. Lymphatic system: unlocking the drains. *Nature* 2005; **436**: 456-458
63 **Schmid-Schönbein GW**. Microlymphatics and lymph flow. *Physiol Rev* 1990; **70**: 987-1028
64 **McHale NG**. Role of the lymph pump and its control. *NIPS* 1995; **10**: 112-117
65 **Vajda J**, Tomcsik M. The structure of the valves of the lymphatic vessels. *Acta Anat* (Basel) 1971; **78**: 521-531
66 **Galanzha EI**, Brill GE, Aizu Y, Ulyanov SS, Tuchin VV. Speckle and Doppler Methods of Blood and Lymph Flow Monitoring. In: Handbook of Optical Biomedical Diagnostics, Bellingham: SPIE Press, 2002: 875-937
67 **Galanzha EI**, Tuchin VV, Zharov VP, Solovieva AV, Stepanova TV, Brill GE. The diagnosis of lymph microcirculation on rat mesentery in vivo. *Proc SPIE* 2003; **4965**: 325- 333
68 **Galanzha EI**, Ulyanov SS, Tuchin VV, Brill GE, Solov`eva AV, Sedykh AV. Comparison of lymph and blood flow in microvessels: coherent optical measurements. *Proc SPIE* 2000; **4163**: 94-98
69 **Johnston MG**. The intrinsic lymph pump: progress and problems. *Lymphology* 1989; **22**: 116-122
70 **Mordon S**, Begu S, Buys B, Tourne-Peteilh C, Devoisselle JM. Study of platelet behavior in vivo after endothelial stimulation with laser irradiation using fluorescence intravital videomicroscopy and PEGylated liposome staining. *Microvasc Res* 2002; **64**: 316-325
71 **Baez S**. An open cremaster muscle preparation for the study of blood vessels by in vivo microscopy. *Microvasc Res* 1973; **5**: 384-394
72 **Haier J**, Korb T, Hotz B, Spiegel HU, Senninger N. An intravital model to monitor steps of metastatic tumor cell adhesion within the hepatic microcirculation. *J Gastrointest Surg* 2003; **7**: 507-514; discussion 514-515
73 **Schacht V**, Berens von Rautenfeld D, Abels C. The lymphatic system in the dorsal skinfold chamber of the Syrian golden hamster in vivo. *Arch Dermatol Res* 2004; **295**: 542-548
74 **Vargas G**, Readinger A, Dozier SS, Welch AJ. Morphological changes in blood vessels produced by hyperosmotic agents and measured by optical coherence tomography. *Photochem Photobiol* 2003; **77**: 541-549
75 **Galanzha EI**, Tuchin VV, Solov`eva AV, Stepanova TV, Luo Q, Cheng H. Skin backreflectance and microvascular system functioning at the action of osmotic agents. *J Phys D: Appl Phys* 2003; **36**: 1-8
76 **Zharov V**, Galanzha E, Shashkov E, Khlebtsov N, Tuchin V. *In vivo* photoacoustic flow cytometry for real-time monitoring of circulating cells and nanoparticles. *SPIE News room* 2006
77 **Zharov V**, Galanzha E, Shashkov E, Khlebtsov N, Tuchin V. *In vivo* integrated photoacoustic flow cytometry: Application for monitoring circulating cancer cells labeled with gold nanorods. Fifth Workshop on Optical Imaging from Bench to Bedside at the national Institutes of Health 2006: 126
78 **Kalchenko V**, Plaks V. Intravital Video Microscopy – From Simple Solutions to a Multiuser Core Facility. *Proc RMS* 2005; **40**: 221-226
79 **Kersey TW**, Van Eyk J, Lannin DR, Chua AN, Tafra L. Comparison of intradermal and subcutaneous injections in lymphatic mapping. *J Surg Res* 2001; **96**: 255-259
80 **Hirsch JI**, Tisnado J, Cho SR, Beachley MC. Use of isosulfan blue for identification of lymphatic vessels: experimental and clinical evaluation. *AJR Am J Roentgenol* 1982; **139**: 1061-1064
81 **Bowen CH**, Albertine KH. Initial lymphatics are present in the loose areolar connective tissue of the golden hamster's cheek pouch. *Microvasc Res* 1988; **35**: 236-241
82 **Schwerte T**, Pelster B. Digital motion analysis as a tool for analysing the shape and performance of the circulatory system in transparent animals. *J Exp Biol* 2000; **203**: 1659-1669
83 **Yaniv K**, Isogai S, Castranova D, Dye L, Hitomi J, Weinstein BM. Live imaging of lymphatic development in the zebrafish. *Nat Med* 2006; **12**: 711-716
84 **Weinstein B**. Vascular cell biology in vivo: a new piscine paradigm? *Trends Cell Biol* 2002; **12**: 439-445
85 **Baker HJ**, Lindsey JR, Weisbroth SH. The Laboratory Rat. New York: Academic, 1979
86 **Gill TJ**. The rat in biomedical research. *Physiologist* 1985; **28**: 9-17
87 **Gill TJ**, Smith GJ, Wissler RW, Kunz HW. The rat as an experimental animal. *Science* 1989; **245**: 269-276
88 **Murakami T**, Kobayashi E. Color-engineered rats and luminescent LacZ imaging: a new platform to visualize biological processes. *J Biomed Opt* 2005; **10**: 41204
89 **Gahm T**, Witte S. Measurement of the optical thickness of transparent tissue layers. *J Microsc* 1986; **141**: 101-110
90 **Barber BJ**, Oppenheimer J, Zawieja DC, Zimmermann HA. Variations in rat mesenteric tissue thickness due to microvasculature. *Am J Physiol* 1987; **253**: G549-G556
91 **Ghassemifar R**, Franzén L. A double-embedding technique for thin tissue membranes. *Biotech Histochem* 1992; **67**: 363-366
92 **Physiology of Blood Circulation: Physiology of vascular system**. Tkachenko BI, editor. Leningrad: Nauka, 1984 (in Russian)
93 **Chernuh AM**, Alexandrov PN, Alexeev OV. Microcirculation. Moscow: Medicine, 1984 (in Russian)
94 **Zharov VP**, Galanzha EI, Tuchin VV. In vivo photothermal flow cytometry: imaging and detection of individual cells in blood and lymph flow. *J Cell Biochem* 2006; **97**: 916-932
95 **Hauck G**. Functional aspects of the topical relationship between blood capillaries and lymphatics of the mesentery. *Pflugers Arch* 1973; **339**: 251-256
96 **Hauck G**. Origin of the mesenteric lymphatics and their topical relationship to the blood capillaries. *Bibl Anat* 1973; **12**: 356-360
97 **Tuchin VV**. The lasers and fiber optic in biomedical research. Saratov: Saratov State University Press, 1998 (In Russian)
98 **Galanzha EI**, Tuchin VV, Ulyanov SS, Solov'eva AV, Luo Q, Cheng H. Optical properties of lymph flow in single microvessels: biomicroscopic, speckle-interferometric, and spectroscopic measurements. *Proc SPIE* 2001; **4434**: 197-203
99 **Scheinecker C**. Application of in vivo microscopy: evaluating the immune response in living animals. *Arthritis Res Ther* 2005; **7**: 246-252
100 **Horstick G**, Kempf T, Lauterbach M, Ossendorf M, Kopacz L, Heimann A, Lehr HA, Bhakdi S, Meyer J, Kempski O. Plastic foil technique attenuates inflammation in mesenteric intravital microscopy. *J Surg Res* 2000; **94**: 28-34
101 **Galanzha EI**, Tuchin VV, Zharov VP. Optical monitoring of microlympatic disturbances during experimental lymphedema, *Lymphat Res Biol*, 2007: In press
102 **Givan AL**. Principles of flow cytometry: an overview. *Methods Cell Biol* 2001; **63**: 19-50
103 **Chung A**, Karlan S, Lindsley E, Wachsmann-Hogiu S, Farkas DL. In vivo cytometry: a spectrum of possibilities. *Cytometry A* 2006; **69**: 142-146
104 **Zharov VP**, Galanzha EI, Menyaev Y, Tuchin VV. In vivo high-speed imaging of individual cells in fast blood flow. *J Biomed Opt* 2006; **11**: 054034
105 **Zharov VP**, Letokhov VS. Laser Optoacoustic Spectroscopy. Berlin Heidelberg, New York: Springer-Verlag, 1986
106 **Zharov VP**. Laser optoacoustic spectroscopy in chromatography. In: Laser Analytical Spectrochemistry. Letokhov VS, editor. Boston, Mass: Bristol, 1986: 229-271
107 **Lapotko D**, Kuchinsky G, Potapnev M, Pechkovsky D. Photothermal image cytometry of human neutrophils. *Cytometry* 1996; **24**: 198-203
108 **Lapotko D**, Romanovskaya T, Kutchinsky G, Zharov V. Photothermal studies of modulating effect of photoactivated chlorin on interaction of blood cells with bacteria. *Cytometry* 1999; **37**: 320-326
109 **Zharov VP** and Lapotko DO. Photothermal imaging of nanoparticles and cells (review). *IEEE J Sel Topics Quant Electron* 2005; **11**: 733-751
110 **Tokeshi M**, Uchida M, Hibara A, Sawada T, Kitamori T. Determination of subyoctomole amounts of nonfluorescent

molecules using a thermal lens microscope: subsingle-molecule determination. *Anal Chem* 2001; **73**: 2112-2116
111 **Tamaki E**, Sato K, Tokeshi M, Sato K, Aihara M, Kitamori T. Single-cell analysis by a scanning thermal lens microscope with a microchip: direct monitoring of cytochrome c distribution during apoptosis process. *Anal Chem* 2002; **74**: 1560-1564
112 **Zharov VP**, Galitovsky V, Chowdhury P. Nanocluster model of photothermal assay: application for high-sensitive monitoring of nicotine-induced changes in metabolism, apoptosis, and necrosis at a cellular level. *J Biomed Opt* 2005; **10**: 44011
113 **Zharov VP**, Galitovskiy V, Lyle CS, Chambers TC. Superhigh-sensitivity photothermal monitoring of individual cell response to antitumor drug. *J Biomed Opt* 2006; 11: 064034
114 **Zharov VP**, Galanzha EI, Shashkov EV, Khlebtsov NG, Tuchin VV. In vivo photoacoustic flow cytometry for monitoring of circulating single cancer cells and contrast agents. *Opt Lett* 2006; **31:** 3623-3625
115 **Zharov VP**, Galanzha EI, Tuchin VV. Photothermal image flow cytometry in vivo. *Opt Lett* 2005; **30**: 628-630
116 **Zharov VP**, Galanzha EI, Tuchin VV. Integrated photothermal flow cytometry in vivo. *J Biomed Opt* 2005; **10**: 051502
117 **Zharov VP**, Galanzha EI, Tuchin VV. Confocal photothermal flow cytometry in vivo. *Proc SPIE* 2005; **5697**: 167-176
118 **Zharov V**, Menyaev Y, Shashkov E, Galanzha E, Khlebtsov B, Scheludko A, Zimnyakov D, and Tuchin V. Fluctuation of probe beam in thermolens schematics as potential indicator of cell metabolism, apoptosis, necrosis and laser impact. *Proc SPIE* 2006; **6085**: 10-21
119 **Bednov AA**, Ul'yanov SS, Tuchin VV, Brill GE, Zakharova (Galanzha) EI. Investigation of lymph dynamics by speckle-interferometry method. *Applied Nonlinear Dynamics* 1996; **4**: 45-54
120 **Bednov AA**, Brill GE, Tuchin VV, Ul`yanov SS, Zakharova (Galanzha) EI. Blood flow measurements in microvessels using focused laser beam diffraction phenomenon. *Proc SPIE* 1994; **2370**: 379-383
121 **Starukhin P**, Ulyanov S, Galanzha E, Tuchin V. Blood-flow measurements with a small number of scattering events. *Appl Opt* 2000; **39**: 2823-2830
122 **Ul`yanov SS**, Tuchin VV, Bednov AA, Zakharova (Galanzha) EI, Brill GE. The application of Speckle Interferometry for the Monitoring of Blood and Lymph Flow in Microvessels. *Lasers in Med Sci* 1997; **12**: 31-41
123 **Fedosov IV**, Ulianov SS, Galanzha EI, Galanzha VA, Tuchin VV. Laser Doppler and Speckle techniques for bioflow measurements. In: Handbook of Coherent Domain Optical Methods. *Springer*, 2004; XLII, **1**: 397-437
124 **Fedosov IV**, Tuchin VV, Galanzha EI, Solov'eva AV, Stepanova TV. Recording of lymph flow dynamics in microvessels using correlation properties of scattered coherent radiation. *Quantum Electronics* 2002; **32**: 970-974
125 **Brill' GE**, Galanzha EI, Ul'ianov SS, Tuchin VV, Stepanova TV, Solov'eva AV. [Functional organization of lymphatic microvessels of the rat mesentery]. *Ross Fiziol Zh Im I M Sechenova* 2001; **87**: 600-607
126 **Galanzha EI**, Tuchin VV, Solovieva AV, Zharov VP. Experimental evaluation on the transmission optical microscopy for the diagnosis of lymphedema. J Xray Sci Technol 2002; **10**: 215-223
127 **Smith JB**, McIntosh GH, Morris B. The traffic of cells through tissues: a study of peripheral lymph in sheep. *J Anat* 1970; **107**: 87-100
128 **Ikomi F**, Hunt J, Hanna G, Schmid-Schönbein GW. Interstitial fluid, plasma protein, colloid, and leukocyte uptake into initial lymphatics. *J Appl Physiol(1985)* 1996; **81**: 2060-2067
129 **Young AJ**. The physiology of lymphocyte migration through the single lymph node in vivo. *Semin Immunol* 1999; **11**: 73-83
130 **Hall JG**, Morris B. The origin of the cells in the efferent lymph from a single lymph node. *J Exp Med* 1965; **121**: 901-910
131 **Dixon JB**, Greiner ST, Gashev AA, Cote GL, Moore JE, Zawieja DC. Lymph flow, shear stress, and lymphocyte velocity in rat mesenteric prenodal lymphatics. *Microcirculation* 2006; **13**: 597-610
132 **Azzali G**. On the transendothelial passage of tumor cell from extravasal matrix into the lumen of absorbing lymphatic vessel. *Microvasc Res* 2006; **72**: 74-85
133 **Zharov V**, Galanzha E and Tuchin V. Photothermal imaging of moving cells in lymph and blood flow in vivo. *Proc SPIE* 2004; **5320**: 256-263
134 **Gourley PL**, Hendricks JK, McDonald AE, Copeland RG, Barrett KE, Gourley CR, Singh KK, Naviaux RK. Mitochondrial correlation microscopy and nanolaser spectroscopy - new tools for biophotonic detection of cancer in single cells. *Technol Cancer Res Treat* 2005; **4**: 585-592
135 **Gourley PL**, Hendricks JK, McDonald AE, Copeland RG, Barrett KE, Gourley CR, Naviaux RK. Ultrafast nanolaser flow device for detecting cancer in single cells. *Biomed Microdevices* 2005; **7**: 331-339
136 **Brill GE**, Tuchin VV, Zakharova (Galanzha) EI, Ul`yanov SS. Influence of low power laser irradiation on lymph microcirculation at the increasing of NO production. *Proc SPIE* 1999; **3726**: 157-162
137 **Galanzha EI**, Brill' GE, Solov'eva AV, Stepanova TV. [Nitric oxide in the lymphatic microvessel regulation]. *Ross Fiziol Zh Im I M Sechenova* 2002; **88**: 983-989
138 **Pitts LH**, Young AR, McCulloch J, MacKenzie E. Vasomotor effects of dimethyl sulfoxide on cat cerebral arteries in vitro and in vivo. *Stroke* 1986; **17**: 483-487
139 **Jacob SW**, Herschler R. Pharmacology of DMSO. *Cryobiology* 1986; **23**: 14-27
140 **Lockie LM**, Norcross BM. A clinical study on the effects of dimethyl sulfoxide in 103 patients with acute and chronic musculoskeletal injuries and inflammations. *Ann N Y Acad Sci* 1967; **141**: 599-602
141 **Spruance SL**, McKeough MB, Cardinal JR. Dimethyl sulfoxide as a vehicle for topical antiviral chemotherapy. *Ann N Y Acad Sci* 1983; **411**: 28-33
142 **Brill' GE**, Zakharova EI. [The effect of dimethyl sulfoxide on the changes in the lymph microcirculation induced by staphylococcal toxin]. *Eksp Klin Farmakol* 1998; **61**: 54-56
143 **Piller NB**, Thelander A. Treatment of chronic postmastectomy lymphedema with low level laser therapy: a 2.5 year follow-up. *Lymphology* 1998; **31**: 74-86
144 **Carati CJ**, Anderson SN, Gannon BJ, Piller NB. Treatment of postmastectomy lymphedema with low-level laser therapy: a double blind, placebo-controlled trial. *Cancer* 2003; **98**: 1114-1122
145 **Kaviani A**, Yousefi R, Mortaz HS and Ghodsi M. Postmastectomy lymphedema; application of low-level laser therapy. *Laser Sur Med* 2003; **S15**: 66-68
146 **Brill GE**, Zakharova (Galanzha) EI. Influence of low power laser radiation on lymphatic microvessels. Abstract book of the 5th Congress of the Asian-Pacific Association for Laser Medicine and Surgery; 1994 Nov. 20-25; Tel Aviv, Israel. Israel, 1994: 17
147 **Verkruysse W**, Beek JF, VanBavel E, van Gemert MJ, Spaan JA. Laser pulse impact on rat mesenteric blood vessels in relation to laser treatment of port wine stain. *Lasers Surg Med* 2001; **28**: 461-468
148 **Zharov VP**, Galitovsky V and Viegas M. Photothermal detection of local thermal effects during selective nanophotothermolysis. *Appl Phys Lett* 2003; **83**: 4897-4899
149 **Zharov VP**, Galitovskaya EN, Johnson C, Kelly T. Synergistic enhancement of selective nanophotothermolysis with gold nanoclusters: potential for cancer therapy. *Lasers Surg Med* 2005; **37**: 219-226
150 **Zharov VP**, Letfullin RR, and Galitovskaya EN. Microbubbles-overlapping mode for laser killing of cancer cells with absorbing nanoparticle clusters. *J Physics D: Appl Phys* 2005; **38**: 2571-2581
151 **Zharov VP**, Kim JW,Curiel DT, Everts M. Self-assembling nanoclusters in living systems: application for integrated

photothermal nanodiagnostics and nanotherapy. *J Nanomedicine* 2005; **1**: 326-345
152 **Zharov VP**, Mercer KE, Galitovskaya EN, Smeltzer MS. Photothermal nanotherapeutics and nanodiagnostics for selective killing of bacteria targeted with gold nanoparticles. *Biophys J* 2006; **90**: 619-627
153 **Everts M**, Saini V, Leddon JL, Kok RJ, Stoff-Khalili M, Preuss MA, Millican CL, Perkins G, Brown JM, Bagaria H, Nikles DE, Johnson DT, Zharov VP, Curiel DT. Covalently linked Au nanoparticles to a viral vector: potential for combined photothermal and gene cancer therapy. *Nano Lett* 2006; **6**: 587-591
154 **Saini V**, Zharov VP, Brazel CS, Nikles DE, Johnson DT, Everts M. Combination of viral biology and nanotechnology: new applications in nanomedicine. *Nanomedicine* 2006; **2**: 200-206
155 **Chowdhury P**, MacLeod S, Udupa KB, Rayford PL. Pathophysiological effects of nicotine on the pancreas: an update. *Exp Biol Med* (Maywood) 2002; **227**: 445-454
156 **A report of Surgeon General: The Health Consequences of Smoking**. Department of Health & Human Services, Public Health Services, Centers for Disease Control & Prevention, National Center for chronic disease prevention and health promotion, office of smoking & health, Washington, D.C. 2004
157 **Armitage AK**, Dollery CT, George CF, Houseman TH, Lewis PJ, Turner DM. Absorption and metabolism of nicotine from cigarettes. *Br Med J* 1975; **4**: 313-316
158 **Galanzha EL**, Chowhury P, Tuchim VV, Zharov VP. Monitoring of nicotine impact in microlymphatics of rat mesentery with time-resolved microscopy. *Lymphology* 2005; **38**: 181-192
159 **Jeltsch M**, Tammela T, Alitalo K, Wilting J. Genesis and pathogenesis of lymphatic vessels. *Cell Tissue Res* 2003; **314**: 69-84
160 **Arbuthnott JP**. Staphylococcal α-toxin. In: Microbiological toxins. New York, 1970: 189-236
161 **Brown DA**. Some effects of staphylococcal alpha-toxin on the cardiovascular system. *Br J Pharmacol Chemother* 1966; **26**: 580-590
162 **Thelestam M**, Blomqvist L. Staphylococcal alpha toxin--recent advances. *Toxicon* 1988; **26**: 55-65
163 **Brill GE**, Sergeev IP, Glazkova EI, Morokhovets NV. [Effect of staphylococcal toxin on the microcirculatory system]. *Patol Fiziol Eksp Ter* 1992; (**1**): 21-23
164 **Brill GE**, Zakharova (Galanzha) EI. The lymphatic microvessels disfunction under the influence of staphylococcal toxin. Proceedings of the 6th World Congress for Microcirculation; 1996 Aug 25-30; Munich, Germany. Messmer K, Kubler WM, editors. International Proceedings Division: Monduzzi Editore, 1996: 179-182
165 **Brill GE**, Zakharova (Galanzha) EI. Pharmacological correction of lymph microcirculation disorders induced by staphylococcal toxin. Proceedings of the 6th World Congress for Microcirculation; 1996 Aug 25-30; Munich, Germany. Messmer K, Kubler WM, editors. International Proceedings Division: Monduzzi Editore, 1996: 175-177
166 **Brill GE**, Zakharova (Galanzha) EI. Modification of lymphoconstriction action of staphylococcal toxin by laser radiation. *Laser Tech Optoelectronics* 1992; **1-2**: 36-39
167 **Harshman S**, Boquet P, Duflot E, Alouf JE, Montecucco C, Papini E. Staphylococcal alpha-toxin: a study of membrane penetration and pore formation. *J Biol Chem* 1989; **264**: 14978-14984
168 **Ward RJ**, Leonard K. The Staphylococcus aureus alpha-toxin channel complex and the effect of Ca^{2+} ions on its interaction with lipid layers. *J Struct Biol* 1992; **109**: 129-141
169 **Browse NL**, Stewart G. Lymphoedema: pathophysiology and classification. *J Cardiovasc Surg* (Torino) 1985; **26**: 91-106
170 **The diagnosis and treatment of peripheral lymphedema**. Consensus document of the International Society of Lymphology. *Lymphology* 2003; **36**: 84-91
171 **Bruns F**, Schueller P. Novel Treatment Options in Secondary Lymphedema. *AAHPM Bulletin* 2005; 5-7
172 **Szuba A**, Rockson SG. Lymphedema: anatomy, physiology and pathogenesis. *Vasc Med* 1997; **2**: 321-326
173 **Witte CL**, Witte MH, Unger EC, Williams WH, Bernas MJ, McNeill GC, Stazzone AM. Advances in imaging of lymph flow disorders. *Radiographics* 2000; **20**: 1697-1719
174 **Földi E**, Földi M, Clodius L. The lymphedema chaos: a lancet. *Ann Plast Surg* 1989; **22**: 505-515
175 **Gregl A**. [Secondary leg edema--experimental study]. *Z Lymphol* 1988; **12**: 48-53
176 **Pflug JJ**, Calnan JS. The experimental production of chronic lymphoedema. *Br J Plast Surg* 1971; **24**: 1-9
177 **Kinjo O**, Kusaba A. Lymphatic vessel-to-isolated-vein anastomosis for secondary lymphedema in a canine model. *Surg Today* 1995; **25**: 633-639
178 **Galanzha EI**, Tuchin VV, Solov'eva AV, Stepanova TV, Brill GE and Zharov VP. Development imaging and experimental model for studying pathogenesis and treatment efficacy of postmastectomy lymphedema. *Proc SPIE* 2002; **4624**: 123-129
179 **Galanzha EI**, Solov'eva AV, Stepanova TV, Tuchin VV, Brill GE and Zharov VP. Analysis of lymph microcirculation in norm, at the experimental lymphedema and pathological stress on animal model. Abstracts of the 22nd Meeting of the European Society for Microcirculation. Exeter, Devon, United Kingdom. August 28-30, 2002. *J Vasc Res* 2002; **39** Suppl 1**:** 9-99
180 **Solov'eva AV**, Brill GE, Galanzha EI, Stepanova TV. Stress-induced changes in lymph microcirculation. *Proc SPIE* 2004; **4241**: 309-311
181 **Solov'eva AV**, Galanzha EI, Stepanova TV, Brill' GE. Changes in lymph microcirculation during pathological stress. *Bull Exp Biol Med* 2002; **134**: 241-243
182 **Tuchin VV**. Optical clearing of tissue and blood using the immersion method. *J Phys D: Appl Phys* 2005; **38**: 2497-2518
183 **Tuchin VV**. Optical immersion as a new tool for controlling the optical properties of tissues and blood. *Laser Physics* 2005; **15**: 1109-1136
184 **Columbano A**. Cell death: current difficulties in discriminating apoptosis from necrosis in the context of pathological processes in vivo. *J Cell Biochem* 1995; **58**: 181-190
185 **Brauer M**. In vivo monitoring of apoptosis. *Prog Neuropsychopharmacol Biol Psychiatry* 2003; **27**: 323-331
186 **Darzynkiewicz Z**, Bedner E, Traganos F. Difficulties and pitfalls in analysis of apoptosis. *Methods Cell Biol* 2001; **63**: 527-546
187 **Alenzi FQ**, Wyse RK, Altamimi WG. Apoptosis as a tool for therapeutic agents in haematological diseases. *Expert Opin Biol Ther* 2004; **4**: 407-420
188 **Haas RL**, de Jong D, Valdés Olmos RA, Hoefnagel CA, van den Heuvel I, Zerp SF, Bartelink H, Verheij M. In vivo imaging of radiation-induced apoptosis in follicular lymphoma patients. *Int J Radiat Oncol Biol Phys* 2004; **59**: 782-787
189 **Yan SD**, Stern DM. Mitochondrial dysfunction and Alzheimer's disease: role of amyloid-beta peptide alcohol dehydrogenase (ABAD). *Int J Exp Pathol* 2005; **86**: 161-171
190 **Gradl G**, Gaida S, Gierer P, Mittlmeier T, Vollmar B. In vivo evidence for apoptosis, but not inflammation in the hindlimb muscle of neuropathic rats. *Pain* 2004; **112**: 121-130
191 **Al-Gubory KH**. Fibered confocal fluorescence microscopy for imaging apoptotic DNA fragmentation at the single-cell level in vivo. *Exp Cell Res* 2005; **310**: 474-481
192 **Chan K**, Truong D, Shangari N, O'Brien PJ. Drug-induced mitochondrial toxicity. *Expert Opin Drug Metab Toxicol* 2005; **1**: 655-669
193 **Alenzi FQ**. Apoptosis and diseases: regulation and clinical relevance. *Saudi Med J* 2005; **26**: 1679-1690
194 **Hunter AL**, Choy JC, Granville DJ. Detection of apoptosis in cardiovascular diseases. *Methods Mol Med* 2005; **112**: 277-289
195 **Nagata S**. Apoptosis and autoimmune diseases. *IUBMB Life* 2006; **58**: 358-362
196 **Desmettre T**, Devoisselle JM, Mordon S. Fluorescence properties and metabolic features of indocyanine green (ICG) as related to angiography. *Surv Ophthalmol* 2000; **45**: 15-27
197 **Bollinger A**, Saesseli B, Hoffmann U, Franzeck UK. Intravital detection of skin capillary aneurysms by videomicroscopy with indocyanine green in patients with progressive systemic sclerosis and related disorders. *Circulation* 1991; **83**: 546-551

198 **Borotto E**, Englender J, Pourny JC, Naveau S, Chaput JC, Lecarpentier Y. Detection of the fluorescence of GI vessels in rats using a CCD camera or a near-infrared video endoscope. *Gastrointest Endosc* 1999; **50**: 684-688

199 **Wei X**, Runnels JM, Lin CP. Selective uptake of indocyanine green by reticulocytes in circulation. *Invest Ophthalmol Vis Sci* 2003; **44**: 4489-4496

200 **Kitai T**, Inomoto T, Miwa M, Shikayama T. Fluorescence navigation with indocyanine green for detecting sentinel lymph nodes in breast cancer. *Breast Cancer* 2005; **12**: 211-215

201 **Moneta G**, Brülisauer M, Jäger K, Bollinger A. Infrared fluorescence videomicroscopy of skin capillaries with indocyanine green. *Int J Microcirc Clin Exp* 1987; **6**: 25-34

S- Editor Liu Y **L- Editor** Lutze M **E- Editor** Bai SH

PO Box 2345, Beijing 100023, China
www.wjgnet.com
wjg@wjgnet.com

World J Gastroenterol 2007 January 14; 13(2): 219-223
World Journal of Gastroenterology ISSN 1007-9327
© 2007 The WJG Press. All rights reserved.

REVIEW

Differential diagnosis between functional and organic intestinal disorders: Is there a role for non-invasive tests?

Francesco Costa, Maria Gloria Mumolo, Santino Marchi, Massimo Bellini

Francesco Costa, Maria Gloria Mumolo, Santino Marchi, Massimo Bellini, Section of Gastroenterology, Department of Internal Medicine,University of Pisa, Pisa, Italy
Correspondence to: Francesco Costa, MD, PhD, Dipartimento di Medicina Interna - S.O. di Gastroenterologia, Universita' di Pisa, Ospedale S. Chiara, Via Roma, PISA 67-56122, Italy. fcosta@med.unipi.it
Telephone: +39-50-993485-918720 Fax: +39-50-993050
Received: 2006-08-11 Accepted: 2006-11-11

Abstract

Abdominal pain and bowel habits alterations are common symptoms in the general population. The investigation to differentiate organic from functional bowel disorders represents a considerable burden both for patients and public health service. The selection of patients who should undergo endoscopic and/or radiological procedures is one of the key points of the diagnostic process, which should avoid the abuse of invasive and expensive tests as well as the underestimation of potentially harmful diseases. Over the coming years, clinicians and researchers will be challenged to develop strategies to increase the patient's compliance and to reduce the economic and social costs of the intestinal diseases.

© 2007 The WJG Press. All rights reserved.

Key words: Intestinal diseases; Intestinal inflammation; Functional bowel disorders; Faecal markers

Costa F, Mumolo MG, Marchi S, Bellini M. Differential diagnosis between functional and organic intestinal disorders: Is there a role for non-invasive tests? *World J Gastroenterol* 2007; 13(2): 219-223

http://www.wjgnet.com/1007-9327/13/219.asp

INTRODUCTION

For the sake of simplicity, bowel diseases have been divided into organic (OBD) and functional (FBD) disorders. In the past, FBD was merely considered an "umbrella" for many clinical pictures where the term functional reflected an unknown etiology and/or pathogenesis and their existence was even denied by some physicians[1,2]. In the last years, the fast-growing insight into the pathogenesis of intestinal diseases has been narrowing the field of disturbances "not explained by structural or biochemical abnormalities", in parallel with the progress of diagnostic tools and the development of novel technologies. Recent evidences, such as the role of serotonin in visceral functions[3-5], the post-infective onset of irritable bowel syndrome (IBS)[6] or data about potential neuroendocrine dysfunctions[7] shed light on the phenomena underlying FBD. The "biopsychosocial model" focused on the complex interplay among genetics, environment, psychosocial and physiological factors, significantly contributed to clarify the true genesis of "functional" symptoms and to modify both treatment and clinical outcome[8]. However, while the new scenario of pathogenesis suggests an overlapping between morphologic and functional abnormalities, in clinical practice the distinction is maintained in prognostic terms, as "functional" identifies scarcely evolutive and virtually harmless conditions.

As the intestine reacts to different stimuli with a limited array of symptoms, the investigation to differentiate OBD and FBD represents a considerable burden for both the patients and public health service.

The selection of patients who should undergo endoscopic and/or radiological procedures is one of the key points of the diagnostic process, which should avoid the abuse of invasive and expensive tests as well as the underestimation of potentially dangerous diseases. In particular, we should take into account the high prevalence and increasing incidence of colo-rectal cancer which, at an early stage, can be successfully treated by endoscopic resection. Nevertheless, colonoscopy is not advisable in all patients with abdominal complaints in the absence of "red flag" features (age > 45 years, anaemia, bleeding, fever, weight loss, etc.) (Figure 1). Chronic or recurrent abdominal pain and bowel habit alterations are common symptoms in the general population. Because a wide range of etiologies may underlie these symptoms, they do not allow a differential diagnosis between OBD (neoplasm, infectious enteritis, Crohn's disease, celiac disease, etc.) and FBD. Moreover, patients may present overlapping syndromes as OBD and FBD , are not mutually exclusive and can be present in the same patient. FBD, mainly IBS, which affect 5%-20% of general population, are the most common intestinal disorders in both primary and secondary care[9-11]. Most patients are diagnosed and treated by general practitioners (GPs) and only those unresponsive to conventional treatment[10,12] are eventually referred to a gastroenterologist[9,13].

In order to improve the positive identification of

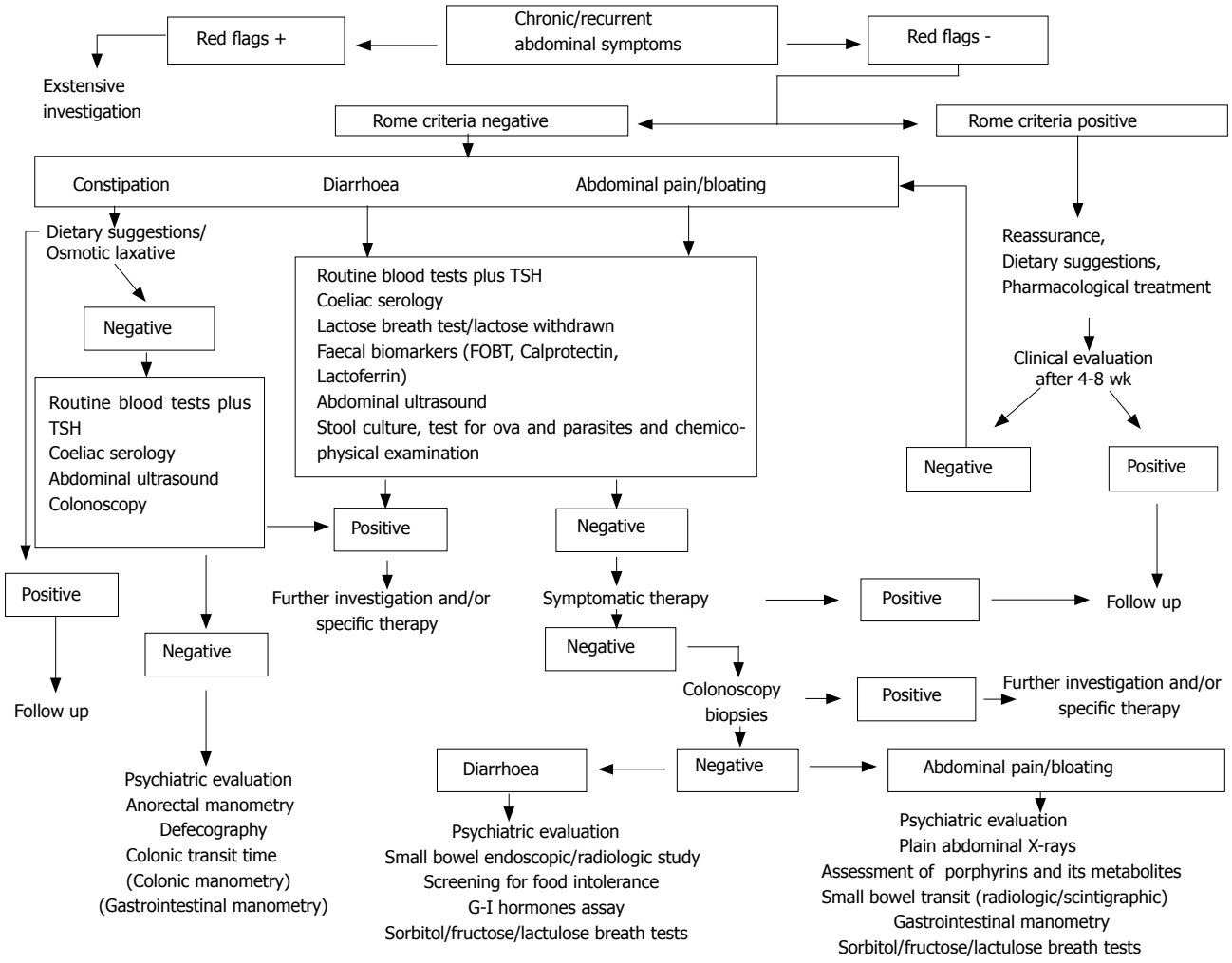

Figure 1 Suggested approach to the diagnosis of chronic abdominal symptoms.

patients affected with FBD, the Rome classification system has been developed. Although these guidelines have raised controversies about duration, frequency, severity and terminology itself of symptoms, they have created a common language for FBD and are now considered the gold standard. Unfortunately, Rome criteria have been developed by and for specialists working in the secondary care setting; they are ignored by many GPs and considered by others, as well as by many specialists, too complex and time-consuming and/or restrictive, suitable only for the tertiary care setting and for research purposes[14]. Therefore, many GPs and gastroenterologists are confident of making a correct diagnosis based on their personal criteria[14,15] and, in the absence of any biological or instrumental marker, FBD is still an exclusive diagnosis which often require extensive investigation. The recent Rome Ⅲ criteria appear to be simpler and less restrictive and hopefully will help the diagnosis of FBD on clinical basis[16].

When FBD is suspected, the clinical criteria can be combined with a number of non-invasive diagnostic tools. Unfortunately serological biomarkers of inflammation such as erythrocyte sedimentation rate, C-reactive protein, white cell count, platelet count, are not sufficiently sensitive or sufficiently specific because they do not directly reflect the level of local inflammation[17-19]. The faecal occult blood test is of little use in detecting inflammatory bowel diseases (IBD) and has a low sensitivity for the diagnosis of colon cancer, especially at an early stage[20,21]. Therefore, in recent years considerable effort has been devoted to find alternative solutions. The latest knowledge about the pathogenesis of FBD (infection, food allergy or intolerance)[22-24], have focused attention on the role of microscopic inflammation, bacterial overgrowth, altered immunity and even more subtle alterations, whose effects are detectable in non-invasive manner, by analysing stools, breath samples and blood.

FAECAL MARKERS

Neutrophil-derived proteins

Faecal neutrophil-derived proteins (mainly calprotectin and lactoferrin) assessment is receiving increasing attention as promising tools to differentiate OBD and FBD; although their clinical use needs definitive confirmation especially in the work-up of FBD, they could be the putative ideal test for non-invasive assessment of intestinal inflammation[25-27].

Calprotectin is a 36-kDa calcium and zinc binding protein that accounts for about 60% of total proteins in the cytosol fraction of neutrophil granulocytes[28,29]. An

increase in faecal calprotectin levels in IBD, colorectal cancer and non-steroidal anti-inflammatory drugs enteropathy has been reported[30-33]. In a study of Dolwani, faecal calprotectin was superior to small bowel barium follow-up in identifying patients with organic diseases[34]. In Crohn's disease (CD) and ulcerative colitis (UC), its levels closely correlated with the faecal excretion of ^{111}In-labelled leukocytes, which is considered to be the gold standard for measuring intestinal inflammation[35] and recently it has been reported that a high faecal calprotectin concentration may identify those IBD patients in remission who are at risk of early relapse[36,37]. Calprotectin has a high negative predictive value for intestinal inflammation. It has low specificity for intestinal pathology but, at a cut-off of 30 mg/L (150 μg/g of faeces by the new method), it showed a sensitivity of 100% in discriminating between active Crohn's disease and IBS[27]. The combined use of presence/absence of alarm features, Rome criteria and calprotectin test proved to be a non-invasive, effective mean of screening patients for organic intestinal disease[38].

Lactoferrin is an iron-binding protein contained in organic fluid, intestinal mucus and in neutrophils. Similarly to calprotectin, faecal lactoferrin proved to be a simple, sensitive marker of intestinal inflammation[25,39,40].

DNA

The molecular genetics of colorectal cancer provided the basis for the analysis of faecal DNA[41]. Colonoscopy is the best tool for the diagnosis of colorectal cancer but it cannot be proposed for a systematic screening of the entire population > 50 years of age. The recent availability of faecal-based, multi-target DNA panel has allowed a better sensitivity than faecal occult blood test for the detection of colorectal cancer[21]. This panel consists of different mutations (*K-ras* gene, *APC* gene, *p53* gene), markers of microsatellite-instability and markers of disordered apoptosis, clearly involved in the progression of colorectal cancer. Although the performance of faecal DNA testing is not comparable to colonoscopy, it is simple and non-invasive, therefore its use at frequent intervals might compensate for the lower diagnostic accuracy[21].

Pancreatic elastase

Chronic pancreatitis is a frequent cause of abdominal pain and diarrhoea whose diagnosis often requires complex and expensive procedures. The assessment of pancreatic elastase on stools seems to offer a better performance than previous non-invasive tests (i.e. serology, Pancreolauryl test, faecal tests for pancreatic enzyme) with a high sensitivity for moderate and severe pancreatic insufficiency[42,43]; this faecal test, like faecal neutrophil-derived protein assessment, is easy to perform, requires a single stool sample and offers a great advantage in terms of patient's compliance. Although most authors reported poor sensitivity for mild disease, its use has been recommended as a first choice test in patients with chronic diarrhoea of putative pancreatic origin[44].

If these experimental data are confirmed in large controlled studies, the routine use of faecal tests might contribute to the selection of patients with abdominal complaints both in the first diagnosis and in the follow-up avoiding invasive and expensive procedures.

BREATH TESTS

Breath analysis is a simple and safe alternative to invasive tests to investigate digestive functions. Exhaled hydrogen (H_2) and carbon (C) can be employed to assess malabsorption, gastrointestinal motility and *H pylori* infection. H_2 in humans is produced only by bacterial fermentation of carbohydrates[45]. This process has been related to the onset of symptoms such as diarrhoea, bloating and abdominal pain[46,47]. Different hydrogen breath tests are currently used to detect carbohydrate malabsorption. Lactose, fructose, sorbitol are the most commonly tested carbohydrates, although their role in symptoms of FBD is controversial, and the prevalence of lactose, fructose and sorbitol malabsorption in IBS patients is not different from healthy subjects[48].

Small intestinal bacterial overgrowth (SIBO) is a malabsorption syndrome characterized by more than 105 colonic type bacterial/mL of jejunal juice described in case of structural bowel alterations (surgical blind loop, stenosis, etc), motility disturbances (pseudo-obstruction, diabetic autonomic neuropathy, sclerodermia) and also present in chronic diseases (liver cirrhosis, chronic pancreatitis, chronic renal failure)[49]. Recent data also indicate that an altered gut flora may play a pathogenic role both in IBS and IBD[50,51]. It has been shown that eradication of SIBO eliminates IBS symptoms in 48% of patients[52]. Although jejunal culture is considered the gold standard for the diagnosis of SIBO, some drawbacks limit its widespread use; thus, glucose and lactulose breath tests are commonly employed. Breath tests based on the excretion of CO_2 subsequently measured by a mass spectrometer have been developed; they employ a variety of ^{13}C substrates to investigate the exocrine pancreatic function (^{13}C triolein, ^{13}C mixed chain triglyceride)[53], gastric emptying (^{13}C octanoate)[54], as well as in the diagnosis of *H pylori* infection (^{13}C urea)[55].

The simplicity and the safety of breath tests encouraged a widespread use, but the data on their low diagnostic accuracy should be taken into account and their use on regular basis cannot be recommended in clinical practice[56].

SERUM

Recent literature highlighted that approximately 4% of patients diagnosed as IBS are affected with celiac disease[57]. Altered bowel habits and abdominal pain, the clinical hallmark of IBS, are common in celiac patients, and serological assessment for anti-endomysial and anti-transglutaminase antibodies should be performed as a first level test when IBS is suspected. Many patients suffering from abdominal pain and/or bowel habit changes perceive their symptoms as related to some form of dietary intolerance and show a good response to an exclusive diet. Nevertheless, any attempt to correlate food-specific IgE production and chronic abdominal symptoms has been disappointing[24,58]. Although it has been reported

that sometimes IgE-mediated reactivity can present with chronic abdominal complaints, the measurement of food-specific IgE antibody concentrations to ascertain food intolerance in FBD is not justified and should be discouraged[59]. Preliminary data showed that high titres of food-specific IgG4 antibodies are present in IBS patients suggesting a diagnostic role in those cases of IBS who could benefit mostly by an exclusive diet[60]. Their clinical follow-up and further research are needed to clarify the importance of these findings and their role in clinical practice.

CONCLUSION

Likely the near future will lead to a deep revision of the concept of "functional disorder". The striking progress in our knowledge of the molecular basis of diseases is identifying new models for FBD pathogenesis, which tend to be less "functional" and more "organic".

These new evidences will have a relevant effect on the clinical management of intestinal diseases. We are not far from the time when the development of minimally or non-invasive techniques will allow an accurate diagnosis, a serial monitoring and a "real time" adjustment of therapy.

REFERENCES

1 **Drossman DA**. Functional GI disorders: what's in a name? *Gastroenterology* 2005; **128**: 1771-1772
2 **Christensen J**. Heraclides or the physician. *Gastroenterol Int* 1990; **3**: 45-48
3 **Gershon MD**. Review article: roles played by 5-hydroxytryptamine in the physiology of the bowel. *Aliment Pharmacol Ther* 1999; **13** Suppl 2: 15-30
4 **Camilleri M**. Pharmacogenomics and functional gastrointestinal disorders. *Pharmacogenomics* 2005; **6**: 491-501
5 **Bellini M**, Rappelli L, Blandizzi C, Costa F, Stasi C, Colucci R, Giannaccini G, Marazziti D, Betti L, Baroni S, Mumolo MG, Marchi S, Del Tacca M. Platelet serotonin transporter in patients with diarrhea-predominant irritable bowel syndrome both before and after treatment with alosetron. *Am J Gastroenterol* 2003; **98**: 2705-2711
6 **Drossman DA**. Mind over matter in the postinfective irritable bowel. *Gut* 1999; **44**: 306-307
7 **Dinan TG**, Quigley EM, Ahmed SM, Scully P, O'Brien S, O'Mahony L, O'Mahony S, Shanahan F, Keeling PW. Hypothalamic-pituitary-gut axis dysregulation in irritable bowel syndrome: plasma cytokines as a potential biomarker? *Gastroenterology* 2006; **130**: 304-311
8 **Drossman DA**. The functional gastrointestinal disorders and the Rome II process. *Gut* 1999; **45** Suppl 2: II1-II5
9 **Jones R**, Lydeard S. Irritable bowel syndrome in the general population. *BMJ* 1992; **304**: 87-90
10 **Thompson WG**, Heaton KW, Smyth GT, Smyth C. Irritable bowel syndrome in general practice: prevalence, characteristics, and referral. *Gut* 2000; **46**: 78-82
11 **Drossman DA**, Camilleri M, Mayer EA, Whitehead WE. AGA technical review on irritable bowel syndrome. *Gastroenterology* 2002; **123**: 2108-2131
12 **Gladman LM**, Gorard DA. General practitioner and hospital specialist attitudes to functional gastrointestinal disorders. *Aliment Pharmacol Ther* 2003; **17**: 651-654
13 **Heaton KW**, O'Donnell LJ, Braddon FE, Mountford RA, Hughes AO, Cripps PJ. Symptoms of irritable bowel syndrome in a British urban community: consulters and nonconsulters. *Gastroenterology* 1992; **102**: 1962-1967
14 **Bellini M**, Tosetti C, Costa F, Biagi S, Stasi C, Del Punta A, Monicelli P, Mumolo MG, Ricchiuti A, Bruzzi P, Marchi S. The general practitioner's approach to irritable bowel syndrome: from intention to practice. *Dig Liver Dis* 2005; **37**: 934-939
15 **Vandvik PO**, Aabakken L, Farup PG. Diagnosing irritable bowel syndrome: poor agreement between general practitioners and the Rome II criteria. *Scand J Gastroenterol* 2004; **39**: 448-453
16 **Longstreth GF**, Thompson WG, Chey WD, Houghton LA, Mearin F, Spiller RC. Functional bowel disorders. *Gastroenterology* 2006; **130**: 1480-1491
17 **Cronin CC**, Shanahan F. Immunological tests to monitor inflammatory bowel disease--have they delivered yet? *Am J Gastroenterol* 1998; **93**: 295-297
18 **Gabay C**, Kushner I. Acute-phase proteins and other systemic responses to inflammation. *N Engl J Med* 1999; **340**: 448-454
19 **Suffredini AF**, Fantuzzi G, Badolato R, Oppenheim JJ, O'Grady NP. New insights into the biology of the acute phase response. *J Clin Immunol* 1999; **19**: 203-214
20 **Tibble J**, Sigthorsson G, Foster R, Sherwood R, Fagerhol M, Bjarnason I. Faecal calprotectin and faecal occult blood tests in the diagnosis of colorectal carcinoma and adenoma. *Gut* 2001; **49**: 402-408
21 **Imperiale TF**, Ransohoff DF, Itzkowitz SH, Turnbull BA, Ross ME. Fecal DNA versus fecal occult blood for colorectal-cancer screening in an average-risk population. *N Engl J Med* 2004; **351**: 2704-2714
22 **Barbara G**, Stanghellini V, De Giorgio R, Cremon C, Cottrell GS, Santini D, Pasquinelli G, Morselli-Labate AM, Grady EF, Bunnett NW, Collins SM, Corinaldesi R. Activated mast cells in proximity to colonic nerves correlate with abdominal pain in irritable bowel syndrome. *Gastroenterology* 2004; **126**: 693-702
23 **Gonsalkorale WM**, Perrey C, Pravica V, Whorwell PJ, Hutchinson IV. Interleukin 10 genotypes in irritable bowel syndrome: evidence for an inflammatory component? *Gut* 2003; **52**: 91-93
24 **Atkinson W**, Sheldon TA, Shaath N, Whorwell PJ. Food elimination based on IgG antibodies in irritable bowel syndrome: a randomised controlled trial. *Gut* 2004; **53**: 1459-1464
25 **Kane SV**, Sandborn WJ, Rufo PA, Zholudev A, Boone J, Lyerly D, Camilleri M, Hanauer SB. Fecal lactoferrin is a sensitive and specific marker in identifying intestinal inflammation. *Am J Gastroenterol* 2003; **98**: 1309-1314
26 **Limburg PJ**, Ahlquist DA, Sandborn WJ, Mahoney DW, Devens ME, Harrington JJ, Zinsmeister AR. Fecal calprotectin levels predict colorectal inflammation among patients with chronic diarrhea referred for colonoscopy. *Am J Gastroenterol* 2000; **95**: 2831-2837
27 **Tibble J**, Teahon K, Thjodleifsson B, Roseth A, Sigthorsson G, Bridger S, Foster R, Sherwood R, Fagerhol M, Bjarnason I. A simple method for assessing intestinal inflammation in Crohn's disease. *Gut* 2000; **47**: 506-513
28 **Dale I**, Fagerhol MK, Naesgaard I. Purification and partial characterization of a highly immunogenic human leukocyte protein, the L1 antigen. *Eur J Biochem* 1983; **134**: 1-6
29 **Fagerhol MK**, Andersson KB, Naess-Andresen CF, Brandtzaeg P, Dale I. Calprotectin (the LI leukocyte protein). In: Smith V, Dedman JR, editors. Stimulus Response Coupling: the role of intracellular calcium-binding proteins. Boca Raton FL: CRC Press Inc, 1990: 187-210
30 **Røseth AG**, Aadland E, Jahnsen J, Raknerud N. Assessment of disease activity in ulcerative colitis by faecal calprotectin, a novel granulocyte marker protein. *Digestion* 1997; **58**: 176-180
31 **Costa F**, Mumolo MG, Bellini M, Romano MR, Ceccarelli L, Arpe P, Sterpi C, Marchi S, Maltinti G. Role of faecal calprotectin as non-invasive marker of intestinal inflammation. *Dig Liver Dis* 2003; **35**: 642-647
32 **Kronborg O**, Ugstad M, Fuglerud P, Johne B, Hardcastle J, Scholefield JH, Vellacott K, Moshakis V, Reynolds JR. Faecal calprotectin levels in a high risk population for colorectal neoplasia. *Gut* 2000; **46**: 795-800
33 **Tibble JA**, Sigthorsson G, Foster R, Scott D, Fagerhol MK,

Roseth A, Bjarnason I. High prevalence of NSAID enteropathy as shown by a simple faecal test. *Gut* 1999; **45**: 362-366
34 **Dolwani S**, Metzner M, Wassell JJ, Yong A, Hawthorne AB. Diagnostic accuracy of faecal calprotectin estimation in prediction of abnormal small bowel radiology. *Aliment Pharmacol Ther* 2004; **20**: 615-621
35 **Røseth AG**, Schmidt PN, Fagerhol MK. Correlation between faecal excretion of indium-111-labelled granulocytes and calprotectin, a granulocyte marker protein, in patients with inflammatory bowel disease. *Scand J Gastroenterol* 1999; **34**: 50-54
36 **Tibble JA**, Sigthorsson G, Bridger S, Fagerhol MK, Bjarnason I. Surrogate markers of intestinal inflammation are predictive of relapse in patients with inflammatory bowel disease. *Gastroenterology* 2000; **119**: 15-22
37 **Costa F**, Mumolo MG, Ceccarelli L, Bellini M, Romano MR, Sterpi C, Ricchiuti A, Marchi S, Bottai M. Calprotectin is a stronger predictive marker of relapse in ulcerative colitis than in Crohn's disease. *Gut* 2005; **54**: 364-368
38 **Tibble JA**, Sigthorsson G, Foster R, Forgacs I, Bjarnason I. Use of surrogate markers of inflammation and Rome criteria to distinguish organic from nonorganic intestinal disease. *Gastroenterology* 2002; **123**: 450-460
39 **Sugi K**, Saitoh O, Hirata I, Katsu K. Fecal lactoferrin as a marker for disease activity in inflammatory bowel disease: comparison with other neutrophil-derived proteins. *Am J Gastroenterol* 1996; **91**: 927-934
40 **Parsi MA**, Shen B, Achkar JP, Remzi FF, Goldblum JR, Boone J, Lin D, Connor JT, Fazio VW, Lashner BA. Fecal lactoferrin for diagnosis of symptomatic patients with ileal pouch-anal anastomosis. *Gastroenterology* 2004; **126**: 1280-1286
41 **Sidransky D**, Tokino T, Hamilton SR, Kinzler KW, Levin B, Frost P, Vogelstein B. Identification of ras oncogene mutations in the stool of patients with curable colorectal tumors. *Science* 1992; **256**: 102-105
42 **Löser C**, Möllgaard A, Fölsch UR. Faecal elastase 1: a novel, highly sensitive, and specific tubeless pancreatic function test. *Gut* 1996; **39**: 580-586
43 **Glasbrenner B**, Schön A, Klatt S, Beckh K, Adler G. Clinical evaluation of the faecal elastase test in the diagnosis and staging of chronic pancreatitis. *Eur J Gastroenterol Hepatol* 1996; **8**: 1117-1120
44 **Thomas PD**, Forbes A, Green J, Howdle P, Long R, Playford R, Sheridan M, Stevens R, Valori R, Walters J, Addison GM, Hill P, Brydon G. Guidelines for the investigation of chronic diarrhoea, 2nd edition. *Gut* 2003; **52** Suppl 5: v1-v15
45 **Levitt MD**. Production and excretion of hydrogen gas in man. *N Engl J Med* 1969; **281**: 122-127
46 **Böhmer CJ**, Tuynman HA. The effect of a lactose-restricted diet in patients with a positive lactose tolerance test, earlier diagnosed as irritable bowel syndrome: a 5-year follow-up study. *Eur J Gastroenterol Hepatol* 2001; **13**: 941-944
47 **Farup PG**, Monsbakken KW, Vandvik PO. Lactose malabsorption in a population with irritable bowel syndrome: prevalence and symptoms. A case-control study. *Scand J Gastroenterol* 2004; **39**: 645-649
48 **Nelis GF**, Vermeeren MA, Jansen W. Role of fructose-sorbitol malabsorption in the irritable bowel syndrome. *Gastroenterology* 1990; **99**: 1016-1020
49 **Teo M**, Chung S, Chitti L, Tran C, Kritas S, Butler R, Cummins A. Small bowel bacterial overgrowth is a common cause of chronic diarrhea. *J Gastroenterol Hepatol* 2004; **19**: 904-909
50 **Franchimont D**, Vermeire S, El Housni H, Pierik M, Van Steen K, Gustot T, Quertinmont E, Abramowicz M, Van Gossum A, Devière J, Rutgeerts P. Deficient host-bacteria interactions in inflammatory bowel disease? The toll-like receptor (TLR)-4 Asp299gly polymorphism is associated with Crohn's disease and ulcerative colitis. *Gut* 2004; **53**: 987-992
51 **Quigley EM**. Irritable bowel syndrome and inflammatory bowel disease: interrelated diseases? *Chin J Dig Dis* 2005; **6**: 122-132
52 **Pimentel M**, Chow EJ, Lin HC. Eradication of small intestinal bacterial overgrowth reduces symptoms of irritable bowel syndrome. *Am J Gastroenterol* 2000; **95**: 3503-3506
53 **Vantrappen GR**, Rutgeerts PJ, Ghoos YF, Hiele MI. Mixed triglyceride breath test: a noninvasive test of pancreatic lipase activity in the duodenum. *Gastroenterology* 1989; **96**: 1126-1134
54 **Ghoos YF**, Maes BD, Geypens BJ, Mys G, Hiele MI, Rutgeerts PJ, Vantrappen G. Measurement of gastric emptying rate of solids by means of a carbon-labeled octanoic acid breath test. *Gastroenterology* 1993; **104**: 1640-1647
55 **Soll AH**. Consensus conference. Medical treatment of peptic ulcer disease. Practice guidelines. Practice Parameters Committee of the American College of Gastroenterology. *JAMA* 1996; **275**: 622-629
56 **Simrén M**, Stotzer PO. Use and abuse of hydrogen breath tests. *Gut* 2006; **55**: 297-303
57 **Spiegel BM**, DeRosa VP, Gralnek IM, Wang V, Dulai GS. Testing for celiac sprue in irritable bowel syndrome with predominant diarrhea: a cost-effectiveness analysis. *Gastroenterology* 2004; **126**: 1721-1732
58 **Monsbakken KW**, Vandvik PO, Farup PG. Perceived food intolerance in subjects with irritable bowel syndrome--etiology, prevalence and consequences. *Eur J Clin Nutr* 2006; **60**: 667-672
59 **Sampson HA**, Sicherer SH, Birnbaum AH. AGA technical review on the evaluation of food allergy in gastrointestinal disorders. American Gastroenterological Association. *Gastroenterology* 2001; **120**: 1026-1040
60 **Zar S**, Benson MJ, Kumar D. Food-specific serum IgG4 and IgE titers to common food antigens in irritable bowel syndrome. *Am J Gastroenterol* 2005; **100**: 1550-1557

S- Editor Wang GP **L- Editor** Ma JY **E- Editor** Lu W

PO Box 2345, Beijing 100023, China
www.wjgnet.com
wjg@wjgnet.com

World J Gastroenterol 2007 January 14; 13(2): 224-227
World Journal of Gastroenterology ISSN 1007-9327
© 2007 The WJG Press. All rights reserved.

REVIEW

Importance of performance status for treatment outcome in advanced pancreatic cancer

Stefan Boeck, Axel Hinke, Ralf Wilkowski, Volker Heinemann

Stefan Boeck, Volker Heinemann, Department of Internal Medicine Ⅲ, Klinikum Grosshadern, Ludwig-Maximilians-University of Munich, Marchioninistrasse 15, 81377 Munich, Germany
Axel Hinke, WISP Research Institute, Karl-Benz-Str. 1, 40764 Langenfeld, Germany
Ralf Wilkowski, Department of Radiooncology, Klinikum Grosshadern, Ludwig-Maximilians-University of Munich, Marchioninistrasse 15, Munich 81377, Germany
Correspondence to: Professor Volker Heinemann, Department of Internal Medicine Ⅲ, Klinikum Grosshadern, Ludwig-Maximilians-University of Munich, Marchioninistrasse 15, Munich 81377,
Germany. volker.heinemann@med.uni-muenchen.de
Telephone: +49-89-70950 Fax: +49-89-70955256
Received: 2006-10-31 Accepted: 2006-12-11

Abstract

Despite progress in the treatment of advanced and metastatic pancreatic cancer (PC), the outcome of this disease remains dismal for the majority of patients. Given the moderate efficacy of treatment, prognostic factors may help to guide treatment decisions. Several trials identified baseline performance status as an important prognostic factor for survival. Unfit patients with a Karnofsky performance status (KPS) below 70% only have a marginal benefit from chemotherapy with gemcitabine (Gem) and may often benefit more from optimal supportive care. Once, however, the decision is taken to apply chemotherapy, KPS may be used to select either mono- or combination chemotherapy. Patients with a good performance status (KPS = 90%-100%) may have a significant and clinically relevant survival benefit from combination chemotherapy. By contrast, patients with a poor performance status (KPS $\leqslant$ 80%) have no advantage from intensified therapy and should rather receive single-agent treatment.

© 2007 The WJG Press. All rights reserved.

Key words: Chemotherapy; Gemcitabine; Pancreatic cancer; Performance status; Prognostic factor

Boeck S, Hinke A, Wilkowski R, Heinemann V. Importance of performance status for treatment outcome in advanced pancreatic cancer. *World J Gastroenterol* 2007; 13(2): 224-227

http://www.wjgnet.com/1007-9327/13/224.asp

INTRODUCTION

Advanced pancreatic cancer (PC) is an incurable disease and without appropriate treatment survival is limited to 3-4 mo. Since Burris *et al*[1] demonstrated the superiority of gemcitabine (Gem) over bolus 5-fluorouracil (5-FU), single-agent Gem has evolved as a standard of care. Numerous trials consistently support the notion that Gem alone may induce a median overall survival (OS) of 5-7 mo and a 1-year-survival of 11%-25%[2]. A great effort has been undertaken to improve these results by use of combination chemotherapy. Up to now, only two combinations, Gem plus erlotinib[3] and Gem plus capecitabine[4] have provided a significant prolongation of survival when compared to Gem alone.

Due to the moderate progress derived from chemotherapy, the question arises if subgroups of patients can be identified who benefit most from specific treatment strategies. Previous studies already tried to identify prognostic factors such as pre-treatment CA 19-9 levels[5,6], inflammatory response markers like C-reactive protein (CRP) or cytokines[7,8], serum-albumin levels[9] or pre-treatment performance status[10-12]. In this overview we analysed Karnofsky performance status (KPS) as a prognostic factor to define a patient group which may benefit from more intensive therapy as opposed to those patients who should rather receive single-agent treatment.

CLINICAL TRIALS

Single-agent therapy

The clinical importance of the KPS for the outcome of PC patients treated with Gem was first elucidated by Storniolo and co-workers[13]. Within an investigational new drug treatment program 3023 patients were evaluated. The analysis of baseline efficacy factors indicated that patients with a KPS $\geqslant$ 70% had a median survival of 5.5 mo as compared to only 2.4 mo observed in patients with a KPS < 70%. Also median time to disease progression (TTP) was greater in the good performance group (2.9 *vs* 1.7 mo, respectively). Interestingly, best tumor response was comparable between the two groups (12% *vs* 10%) supporting the notion that in PC response to therapy is only a poor surrogate endpoint for survival. In view of this analysis, it appears unlikely that patients with a KPS < 70% actually benefit from therapy and the conclusion may be drawn that chemotherapy with Gem should rather be withheld in patients with a very poor performance status.

Table 1 Influence of performance status on median survival in randomized phase Ⅲ trials

	Overall Survival (mo)		
	KPS 60-80	KPS 90-100	Reference
Gemcitabine + Cisplatin	4.9[1]	10.7	Heinemann *et al*
Gemcitabine	4.8[1]	6.9	
Statistical significance	$P = 0.64$	$P = 0.051$	
Gemcitabine + 5-FU/FA	3.4	8.5	Riess *et al*
Gemcitabine	4.9	6.2	
Statistical significance	$P = 0.62$	$P = 0.172$	
Gemcitabine + Capecitabine	5.3	10.1	Herrmann *et al*
Gemcitabine	7.0	7.5	
Statistical significance	$P = 0.22$	$P = 0.024$	

KPS = Karnofsky performance status, [1]subgroup with poor performance status defined as KPS 70%-80%.

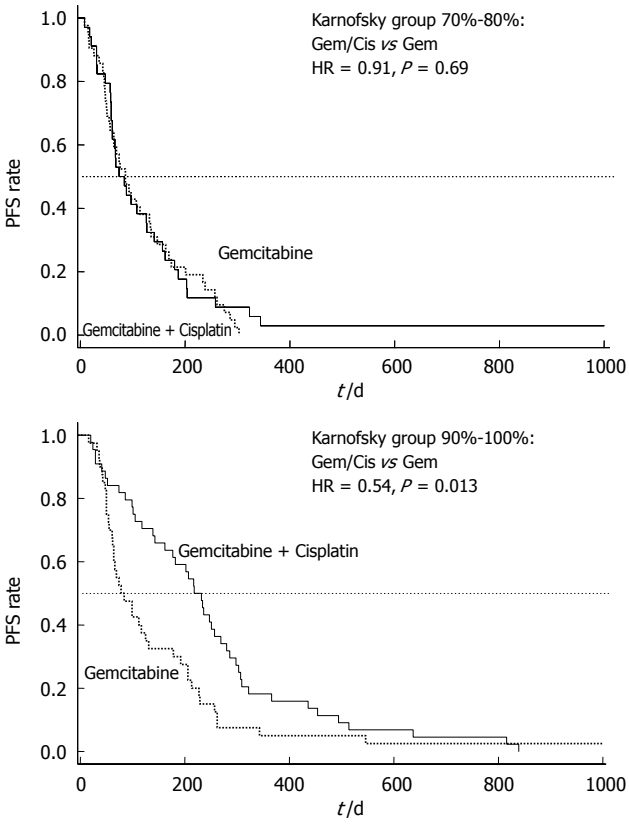

Figure 1 Randomized phase Ⅲ trial comparing gemcitabine (Gem) *vs* gemcitabine plus cisplatin (Cis): Subgroups KPS 70%-80% and KPS 90%-100%; Progression-free survival (PFS) by treatment arm (HR = hazard ratio).

Gemcitabine plus Cisplatin

The combination of Gem and cisplatin is based on a synergistic cytotoxic interaction of the two agents, namely the propensity of Gem to inhibit repair of cisplatin-induced DNA damage. In a randomized phase Ⅲ trial Gem plus cisplatin was compared to single-agent Gem[14]. In the combination arm, Gem (1000 mg/m^2) and cisplatin (50 mg/m^2) were both applied in a biweekly fashion, while in the single-agent arm Gem was given at a dose of 1000 mg/m^2 weekly times three in a 4-wk regimen. One hundred ninety-five patients with histologically confirmed advanced PC (KPS > 70%) were randomized and survival was evaluated as the primary end-point.

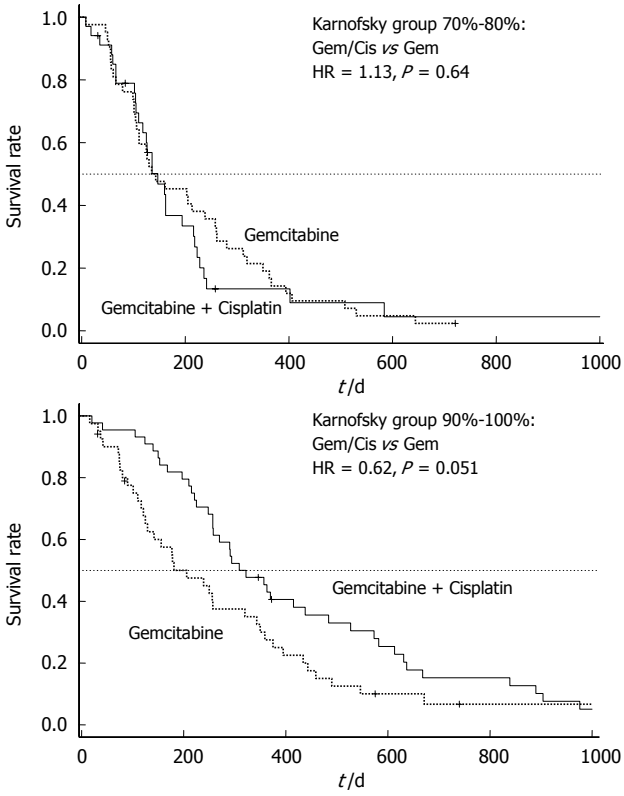

Figure 2 Randomized phase Ⅲ trial comparing gemcitabine (Gem) *vs* gemcitabine plus cisplatin (Cis): Subgroups KPS 70%-80% and KPS 90%-100%; Overall survival (OS) by treatment arm (HR = hazard ratio).

In a post-hoc analysis of this trial, patients were divided into groups with good (KPS = 90%-100%) and poor performance status (KPS = 70%-80%). Patients with a poor performance status at base-line (KPS 70%-80%) had no benefit from combination therapy as compared to Gem alone and comparably disappointing results were obtained for progression free survival (PFS: 2.8 *vs* 2.9 mo, $P = 0.69$) and OS (4.9 *vs* 4.8 mo, $P = 0.64$) (Table 1). By contrast, patients with a good KPS (90%-100%) who underwent treatment with Gem/cisplatin had a significantly longer PFS compared to patients treated with single-agent Gem (7.7 *vs* 2.8 mo, $P = 0.013$) (Figure 1). This prolongation of PFS also translated into a prolonged median OS (10.7 *vs* 6.9 mo), that reached a borderline level of statistical significance ($P = 0.051$) (Figure 2).

In the univariate analysis for prognostic factors, KPS (HR = 0.52, $P = 0.006$) and stage of disease (HR = 1.55, $P = 0.0048$) had a significant impact on survival, while age, gender, tumor grading and treatment arm did not. These data were confirmed in a multivariate analysis which identified KPS (HR = 0.59, $P = 0.0051$) and stage of disease (HR = 1.65, $P = 0.022$) as independent determinants of overall survival[14].

Gemcitabine plus 5-FU

The CONKO-002 trial compared the combination of Gem plus folinic acid (FA) and 5-FU to single-agent Gem[15]. In this randomized phase Ⅲ trial Gem was given at a dose of 1000 mg/m^2 together with FA 200 mg/m^2 and 5-FU 750 mg/m^2 weekly times four every six weeks. In the comparator arm, single-agent Gem was applied ac-

cording to the Burris regimen (1000 mg/m^2 weekly × 7 followed by two weeks rest and a subsequent application on d 1, 8, and 15 every four weeks[11]). Both treatment arms induced nearly identical results for tumor response rates (Gem/FA/5-FU *vs* Gem: RR = 4.8% *vs* 7.2%), median time to tumor progression (TTP = 3.5 *vs* 3.5 mo), and median survival time (OS = 5.9 *vs* 6.2 mo). Also in this trial, the subgroup analysis indicated that patients with a poor performance status (KPS = 60%-80%) responded in a different way compared to the good performance group (KPS = 90%-100%). In patients with a poor performance status, combination treatment induced a worse survival than gemcitabine alone (3.4 *vs* 4.9 mo). By contrast, a strong trend towards an improved survival was observed in the good performance group treated within the combination arm (8.5 *vs* 6.2 mo, $P = 0.172$) (Table 1).

Gemcitabine plus Capecitabine

Herrmann and co-workers performed a randomized trial comparing Gem (1000 mg/m^2, d 1 + 8, q 3 wk) plus capecitabine (650 mg/m^2 po bid d 1-14 q 3 wk) to Gem given according to the Burris-regimen[16]. While the combination induced a higher median PFS than Gem alone (4.8 *vs* 4.0 mo) and a longer median OS (8.4 mo *vs* 7.3 mo), these results failed to reach the level of statistical significance. In the unfavorable KPS group (60%-80%), survival with Gem/capecitabine was inferior to Gem alone (5.3 *vs* 7.0 mo), while in the good performance group the combination induced a significantly superior survival time (10.1 *vs* 7.5 mo, $P = 0.024$) (Table 1).

CONCLUSION

Despite recent advances in systemic treatment of patients with advanced PC, the prognosis still remains poor. Thus, pre-treatment patient selection, based on prognostic factors, for different therapeutic options (e.g. supportive care only, single-agent chemotherapy, combination chemotherapy) may turn out to gain clinical importance. Additionally, these prognostic factors may also be a useful for the design of future trials in advanced PC.

In the present review, we summarized the clinical importance of performance status as a prognostic factor for OS. In a randomized trial comparing Gem plus cisplatin to Gem alone potential prognostic factors such as stage of disease, KPS, treatment arm, age, sex, and pathological tumor grade were evaluated in a univariate analysis. Only pre-treatment KPS and distant metastasis could be identified as significant prognostic factors for OS. In a multivariate analysis, both could be confirmed as independent prognostic factors for PFS and OS[14]. The importance of performance status has already been observed by Louvet and co-workers who compared the Gem plus oxaliplatin combination to single-agent Gem[12]. He reported that distant metastasis and a poor PS (ECOG 2) at baseline were independent negative prognostic factors. These data were further supported by van Cutsem *et al*[9] who investigated the efficacy of Gem plus tipifarnib in a large randomized phase Ⅲ trial. ECOG performance status and stage of disease (locally advanced *vs* metastatic) were, besides tumor differentiation and albumin levels, highly significant prognostic factors for survival in a univariate analysis.

Once performance status is defined as a clinically relevant prognosticator for patient outcome, the question needs to be asked if performance status can also be used to guide adequate treatment selection. Storniolo *et al*[13] clearly demonstrated that the benefit from single-agent Gem is very low if patients with a KPS < 70% are treated. More often than not these patients will rather benefit from optimal supportive care.

Once, however, the decision is taken that a patient should receive chemotherapy it needs to be clarified if combination or single-agent chemotherapy is likely to provide an optimal therapeutic result. The relevance of KPS in this particular question was investigated based on a randomized trial comparing the Gem/cisplatin combination to Gem alone. In a retrospective subgroup analysis, patients with a good KPS (90%-100%) had a clear benefit from the Gem/cisplatin combination with regard to PFS (7.7 *vs* 2.8 mo, $P = 0.013$) and OS (10.7 *vs* 6.9 mo, $P = 0.051$). Outcome of patients with a poor KPS (70%-80%) was, however, not affected by the choice of treatment. Similar observations were also reported in two further phase Ⅲ trials[15,16]. While none of them demonstrated a significant superiority of combination chemotherapy for the whole study population, both trials could show a clinical relevant benefit for patients with a good performance status.

In conclusion, Gem-based combination regimens have the potential to prolong survival in patients with a good KPS, whereas patients with a poor KPS have no advantage and may as well receive single-agent Gem. Consideration of the performance status may, therefore, help to select adequate treatment strategies and thus may provide a reasonable step towards individualized therapy. Individualization of treatment becomes necessary since the benefit from more intensive combination chemotherapy can only be expected in defined subgroups of PC patients.

REFERENCES

1 **Burris HA**, Moore MJ, Andersen J, Green MR, Rothenberg ML, Modiano MR, Cripps MC, Portenoy RK, Storniolo AM, Tarassoff P, Nelson R, Dorr FA, Stephens CD, Von Hoff DD. Improvements in survival and clinical benefit with gemcitabine as first-line therapy for patients with advanced pancreas cancer: a randomized trial. *J Clin Oncol* 1997; **15**: 2403-2413

2 **Heinemann V**. Gemcitabine in the treatment of advanced pancreatic cancer: a comparative analysis of randomized trials. *Semin Oncol* 2002; **29**: 9-16

3 **Moore MJ**, Goldstein D, Hamm J, Finger A, Hecht J, Gallinger S, Au H, Ding K, Christy-Bittel J, Parulekar W. Erlotinib plus gemcitabine compared to gemcitabine alone in patients with advanced pancreatic cancer. A phase III trial of the National Cancer Institute of Canada Clinicals trials group [NCIC-CTG]. *Proc Am Soc Clin Oncol* 2005; **23**: 1

4 **Cunningham D**, Chau I, Stocken D, Davies C, Dunn J, Valle J, Smith D, Steward W, Harper P, Neoptolemos J. Phase III randomised comparison of gemcitabine (GEM) versus gemcitabine plus capecitabine (GEM-CAP) in patients with advanced pancreatic cancer. *Eur J Cancer Suppl* 2005; **3**: 11

5 **Saad ED**, Machado MC, Wajsbrot D, Abramoff R, Hoff PM, Tabacof J, Katz A, Simon SD, Gansl RC. Pretreatment CA 19-9 level as a prognostic factor in patients with advanced pancreatic cancer treated with gemcitabine. *Int J Gastrointest*

Cancer 2002; **32**: 35-41
6 **Maisey NR**, Norman AR, Hill A, Massey A, Oates J, Cunningham D. CA19-9 as a prognostic factor in inoperable pancreatic cancer: the implication for clinical trials. *Br J Cancer* 2005; **93**: 740-743
7 **Sawaki A**, Kanemitsu Y, Mizuno N, Takahashi K, Nakamura T, Ioka T, Tanaka S, Nakaizumi A, Salem AA, Ueda R, Yamao K. Practical prognostic index for patients with metastatic pancreatic cancer treated with gemcitabine. *J Gastroenterol Hepatol* 2008; **23**: 1292-1297
8 **Ebrahimi B**, Tucker SL, Li D, Abbruzzese JL, Kurzrock R. Cytokines in pancreatic carcinoma: correlation with phenotypic characteristics and prognosis. *Cancer* 2004; **101**: 2727-2736
9 **Van Cutsem E**, van de Velde H, Karasek P, Oettle H, Vervenne WL, Szawlowski A, Schoffski P, Post S, Verslype C, Neumann H, Safran H, Humblet Y, Perez Ruixo J, Ma Y, Von Hoff D. Phase III trial of gemcitabine plus tipifarnib compared with gemcitabine plus placebo in advanced pancreatic cancer. *J Clin Oncol* 2004; **22**: 1430-1438
10 **Ishii H**, Okada S, Nose H, Yoshimori M, Aoki K, Okusaka T. Prognostic factors in patients with advanced pancreatic cancer treated with systemic chemotherapy. *Pancreas* 1996; **12**: 267-271
11 **Ueno H**, Okada S, Okusaka T, Ikeda M. Prognostic factors in patients with metastatic pancreatic adenocarcinoma receiving systemic chemotherapy. *Oncology* 2000; **59**: 296-301
12 **Louvet C**, Labianca R, Hammel P, Lledo G, Zampino MG, André T, Zaniboni A, Ducreux M, Aitini E, Taïeb J, Faroux R, Lepere C, de Gramont A. Gemcitabine in combination with oxaliplatin compared with gemcitabine alone in locally advanced or metastatic pancreatic cancer: results of a GERCOR and GISCAD phase III trial. *J Clin Oncol* 2005; **23**: 3509-3516
13 **Storniolo AM**, Enas NH, Brown CA, Voi M, Rothenberg ML, Schilsky R. An investigational new drug treatment program for patients with gemcitabine: results for over 3000 patients with pancreatic carcinoma. *Cancer* 1999; **85**: 1261-1268
14 **Heinemann V**, Quietzsch D, Gieseler F, Gonnermann M, Schönekäs H, Rost A, Neuhaus H, Haag C, Clemens M, Heinrich B, Vehling-Kaiser U, Fuchs M, Fleckenstein D, Gesierich W, Uthgenannt D, Einsele H, Holstege A, Hinke A, Schalhorn A, Wilkowski R. Randomized phase III trial of gemcitabine plus cisplatin compared with gemcitabine alone in advanced pancreatic cancer. *J Clin Oncol* 2006; **24**: 3946-3952
15 **Riess H**, Helm A, Niedergethmann M, Schmidt-Wolf I, Moik M, Hammer C, Zippel K, Weigang-Köhler K, Stauch M, Oettle H. A randomised, prospective, multicenter phase III trial of gemcitabine, 5-fluorouracil (5-FU), folinic acid vs gemcitabine alone in patients with advanced pancreatic cancer. *Proc Am Soc Clin Oncol* 2005; **23**: 4009
16 **Herrmann R**, Bodoky G, Ruhstaller T, Glimelius B, Saletti P, Bajetta E, Schueller J, Bernhard J, Dietrich D, Scheithauer W. Gemcitabine (G) plus Capecitabine (C) versus G alone in locally advanced or metastatic pancreatic cancer: A randomized phase III study of the Swiss Group for Clinical Cancer Research (SAKK) and the Central European Cooperative Oncology Group (CECOG). *Proc Am Soc Clin Oncol* 2005; **23**: 4010

S- Editor Liu Y **L- Editor** Rippe RA **E- Editor** Liu WF

PO Box 2345, Beijing 100023, China
www.wjgnet.com
wjg@wjgnet.com

World J Gastroenterol 2007 January 14; 13(2): 228-235
World Journal of Gastroenterology ISSN 1007-9327
© 2007 The WJG Press. All rights reserved.

LIVER CANCER

Interferon-α response in chronic hepatitis B-transfected HepG2.2.15 cells is partially restored by lamivudine treatment

Shi-He Guan, Mengji Lu, Petra Grünewald, Michael Roggendorf, Guido Gerken, Jörg F Schlaak

Shi-He Guan, Petra Grünewald, Guido Gerken, Jörg F Schlaak, Department of Gastroenterology and Hepatology, University Hospital of Essen, Essen, Germany
Shi-He Guan, Mengji Lu, Michael Roggendorf, Institute of Virology, University Hospital of Essen, Essen, Germany
Shi-He Guan, Department of Laboratory Medicine, the first Affiliated Hospital of Anhui Medical University, China
Supported by grants from the Deutsche Forschungsgemeinschaft (DFG SCHL 377/2-2, LU 669/2-1 and GRK 1045/1)
Correspondence to: Jörg F Schlaak, MD, Professor of Medicine, Department of Gastroenterology and Hepatology, University Hospital of Essen, Hufelandstr. 55, Essen 45122, Germany. joerg.schlaak@uni-essen.de
Telephone: +49-201-7232518 Fax: +49-201-7235749
Received: 2006-08-08 Accepted: 2006-09-20

Abstract

AIM: To characterize the IFN-response and its modulation by the antiviral compound lamivudine in HBV-transfected HepG2.2.15 cells.

METHODS: HepG2.2.15 and HepG2 cells were stimulated with various concentrations of IFN-α2a in the presence or absence of lamivudine. Then, total RNA was extracted and analysed by customised cDNA arrays and northern blot for interferon-inducible genes (ISGs). In addition, cellular proteins were extracted for EMSA and western blot. HBV replication was assessed by southern blot or ELISAs for HBsAg and HBeAg.

RESULTS: Two genes (MxA, Cig5) with completely abolished and 4 genes (IFITM1, -2, -3, and 6-16) with partially reduced IFN-responses were identified in HepG2.2.15 cells. In 2 genes (IFITM1, 6-16), the response to IFN-α could be restored by treatment with lamivudine. This effect could not be explained by a direct modulation of the Jak/Stat signalling pathway since EMSA and western blot experiments revealed no suppression of Stat1 activation and ISGF3 formation after stimulation with IFN-α in HepG2.2.15 compared to HepG2 cells.

CONCLUSION: These results are consistent with the assumption that chronic hepatitis B may specifically modulate the cellular response to IFN by a selective blockage of some ISGs. Antiviral treatment with lamivudine may partially restore ISG expression by reducing HBV gene expression and replication.

© 2006 The WJG Press. All rights reserved.

Key words: Hepatitis B; IFN-α; Gene expression; Lamivudine

Guan SH, Lu M, Grünewald P, Roggendorf M, Gerken G, Schlaak JF. Interferon-α response in chronic hepatitis B-transfected HepG2.2.15 cells is partially restored by lamivudine treatment. *World J Gastroenterol* 2007; 13(2): 228-235

http://www.wjgnet.com/1007-9327/13/228.asp

INTRODUCTION

Hepatitis B (HBV) is a hepatotropic DNA virus capable of causing both acute and chronic hepatitis in humans. It is estimated that over 350 million people are chronically infected with HBV worldwide. Currently approved therapeutic strategies for treatment of HBV include interferon-alpha (IFN-α), the nucleoside analogue lamivudine and the nucleotide analogue adefovir[1,2]. However, only a minority of patients treated with IFN-α has a long-term sustained response with 'eradication' of the virus. Patients with a high viral load, in particular, rarely respond to IFN therapy. Treatment with lamivudine, on the other hand, is complicated by a high rate of viral resistance and a high relapse rate after cessation of therapy, respectively[3]. Both the emergence of viral resistance and relapse after therapy are often associated with a hepatitis flare, which can sometimes be fatal. Thus, novel strategies are needed to improve treatment for this disease.

To develop new regimens it is necessary to gain further insights into the interactions between HBV and the main antiviral system of the host, the IFN-system. It has been shown that type I and type II interferons are able to suppress HBV-replication in livers from HBV-transgenic mice[4-6]. This could also be demonstrated *in vitro* by using immortalized hepatocyte cell lines from these animals[7] and involves elimination of pregenomic RNA-containing capsids, inhibition of DNA replication and reduction of steady-state levels of HBV transcripts. The effector mechanisms that have been associated with IFN-induced suppression of HBV-replication include MxA[8] and proteasome mediated activities[9,10]. Additional data suggest a role for GTP-binding proteins, signalling and various other molecules in the control of HBV replication[11]. HBV can

counteract these antiviral effector mechanisms by inhibiting proteasome activities in an HBX-dependent manner[12] and by suppressing MxA expression at the promoter level[13]. Furthermore, it has been shown that HBV replicated at higher levels in HBV-transgenic mice crossed with IRF-1 or PKR deficient mice while replication was unchanged in transgenic mice crossed with RNase L deficient mice[14].

Assuming that HBV may interfere with the expression of ISGs, one would predict that the ISG expression in cell lines with and without HBV may be different and this would be modulated by inhibition of HBV gene expression and replication. The present study was performed to test this hypothesis. Using customized cDNA arrays for ISGs, we could identify 2 ISGs (MxA and Cig5) that are completely abolished in HBV-transfected HepG2.2.15 cells and 4 genes (IFITM1, -2, -3 and 6-16) with partially reduced responses. This suppression could partially be restored in 2 genes (IFITM1, 6-16) by treatment with the nucleoside analogue lamivudine suggesting an additional therapeutic mechanism for this drug.

MATERIALS AND METHODS

Cell culture

HepG2.2.15 cells were kindly provided by G. Acs (Mount Sinai Medical Cancer, New York, NY) and maintained in Dulbecco's Modified Eagle's Medium, supplemented with 2 mmol/L L-glutamine 50 IU/mL of penicillin, 50 mg/L of streptomycin, 500 mg/L of G418, 5% (vol/vol) fetal bovine serum, at 37℃ in humidified incubators at 5% CO_2. The cells were seeded at a density of 8×10^5 cells and maintained in a confluent state for 2 to 3 d before being treated with antiviral compounds. At first, various concentrations from 0.04 μmol/L to 100 μmol/L of lamivudine were used to reach the suitable drug concentration, which profoundly suppressed HBV replication without cytotoxicity. At the same time, a time course of drug action also was evaluated. Over a period of 10 d lamivudine was added to the medium daily, then the cells were stimulated by addition of IFN-α for 6 h. Thereafter, the media were collected and DNA or RNA was extracted for further analysis.

Analysis of secreted HBV particles

Detection of HBsAg and HBeAg was carried out by using a commercially available kit (Dade Behring) according to the manufacturer's instructions. Medium samples collected from HepG2.2.15 cells were centrifuged at 1200 rpm for 10 min to remove cellular debris, transferred to clean tubes and stored at -20℃ until analysed. HBsAg and HBeAg amounts were evaluated from absorbance reading values (450 nm) compared to the constructed controls.

HBV DNA analysis

Extracellular virion HBV-DNA analysis: Medium of HepG2.2.15 cells was collected and centrifuged (10 min, 2000 × g), and polyethylene glycol (M_r, 8000) was added to the supernatant at a concentration of 10% (wt/vol) followed by overnight precipitation at 4℃. The virions were pelletted (30 min, 10 000 × g), and the pellet was resuspended in lysis buffer (10 mmol/L Tris-Cl, 5 mmol/L EDTA, 150 mmol/L NaCl, 1% SDS) at room temperature for 15 min. Proteinase K was added at a concentration of 500 μg/mL and the suspension incubated for 2 h at 56℃. The digest was extracted with phenol/chloroform, 1:1 (vol/vol) or chloroform, respectively, and the DNA was precipitated with 2.5 vol. of ethanol. The DNA pellet was dissolved in TE solution and then spotted onto Hybond-N+ membranes. Alternatively, the DNA was electrophoresed in 1.2% agarose gel followed by blotting onto Hybond-N+ membranes. The bolt was hybridized with a ^{32}P-labeled HBV DNA probe (digested by Nsi I from plasmids that contained the full length HBV genome sequence dimer and labelled with a RediprimeTM Ⅱ Random prime labelling system), washed with 2 × SSC/0.1% SDS at room temperature for 20 min, twice, and 0.1 × SSC/0.1% SDS at 60℃ for 45 min, and then autoradiographed. The intensity of the autoradiographic dots or bands was quantitated using the Cyclone Storage Phosphor System (Packard Instrument Company, Median, Conn.). All drug concentrations were tested in duplicate or triplicate, with antiviral effects being scored as the amount of HBV DNA present in the media relative to that in untreated controls.

Intracellular HBV replicative intermediates (RI) analysis: HepG2.2.15 cells were consecutively treated with various concentrations of lamivudine for 10 d. The cytoplasmic preparations containing HBV core particles were isolated from the treated cells. Cells were lysed with lysis buffer (50 mmol/L Tris-Cl, PH 7.4, 150 mmol/L NaCl, 5 mmol/L $MgCl_2$, 0.5% NP-40) at room temperature for 5-10 min. The cytoplasmic fraction was separated from the nuclear fraction by centrifugation. Unprotected DNA was removed by adjusting cytoplasmic preparations so that they contained 10 mmol/L $MgCl_2$ and 500 μg/mL of DNase I (Roche, Germany) followed by a 1 h incubation at 37℃. To extract replicative intermediates (RI), EDTA, sodium dodecyl sulfate (SDS), NaCl and proteinase K (QIAGEN) were added separately and sequentially to final concentrations of 10 mmol/L EDTA, 1% SDS, 100 mmol/L NaCl and 500 mg/L of proteinase K. The sample was incubated for 1.5 h at 56℃ and then subjected to sequential phenol and chloroform extraction and isopropanol precipitation. Precipitated nucleic acids were resuspended in a small volume of TE solution and digested with 100 mg/L of RNase (Roche, Germany) for 1 h at 37℃. Twenty micrograms of cytoplasmic preparations containing HBV replicative intermediates DNA (RI) were then analysed by electrophoresis in 1.2% agarose gels, followed by blotting onto Hybond-N+ membranes. The bolt was hybridized with a 32P-labeled HBV DNA probe (digested by Nsi I from plasmids which contain full length HBV genome sequence dimer, and labelled with a RediprimeTM Ⅱ Random prime labelling system), washed with 2 × SSC/0.1% SDS at room temperature for 20 min, twice, and 0.1 × SSC/0.1% SDS at 60℃ for 45 min, and then autoradiographed as described above.

RNA extraction

Total RNA was isolated from cells using Trizol according

to the manufacturer's instructions. RNA quantity and quality was assessed by determination of the optical density at 260 and 280 nm using spectrophotometry and additional visualisation by agarose gel electrophoresis.

Gene expression profiling by customized cDNA macroarrays

Radiolabelled cDNA was generated from 20 μg total RNA by reverse transcription with Superscript Ⅱ (Gibco, MD) in the presence of ^{32}P-dCTP. Residual RNA was hydrolysed by alkaline treatment at 70℃ for 20 min and the cDNA was purified using G-50 columns (Amersham Pharmacia, UK). Before hybridisation to the macroarrays the labelled cDNA was mixed with 50 μg COT-DNA (Gibco) and 10 μg Poly-A DNA (Sigma), denatured at 95℃ for 5 min and hybridised for 1h to minimise non-specific binding. Preparation of the macroarrays (representing 150 known ISGs), hybridisation of the radioactive cDNAs and scanning and analysis of the macroarrays were carried out as described previously[15].

Northern blot analysis

5 μg of total RNA was electrophoresed through a 1.2% agarose gel containing formaldehyde and then transferred to Hybond-N+ membranes. The immobilized RNA was hybridized with a ^{32}P-labeled DNA probe (IMAGE clones PCR products, purified with Gel Extract kit, QIAGEN).

Electrophoretic Mobility Shift Assay

At 80% to 90% confluence, cells were stimulated with IFN-α for 6 h. Preparations of nuclear extracts were performed according to the instruction of the manufacturer (PIERCE, NE-PERTM Nuclear Extraction Reagent). Nuclear extracts/DNA binding reactions were performed in 20 μL containing 15 μg nuclear extract protein and 4 μL Gel Shift Binding 5 × Buffer (20% glycerol, 5 mmol/L $MgCl_2$, 2.5 mmol/L EDTA, 2.5 mmol/L DTT, 250 mmol/L Tris-Cl, PH 7.5, 0.25 mg/mL Poly (dI-dC) ·Poly (dI-dC)). ISRE/GAS consensus oligonucleotides (5'-AAG TAC TTT CAG TTT CAT ATT ACT CTA-3') from the promoter region of the IFN-α responsive genes were used. Mutant oligonucleotides (5'-AAG TAC TTT CAG TGG TCT ATT ACT CTA-3') were used as control. The probes were end-labeled with γ-^{32}P-ATP (U K, 3000 Ci/mol) at room temperature for 20 min. Complexes were separated from the probe in 4% naive poly-acrylamide gel in 0.5 × TBE buffer. The gels were subsequently dried and autoradiographed.

Western blot analysis

After interferon treatment, cells were washed once with ice-cold phosphate-buffered saline. Cells were lysed on ice for 30 min in 0.5 mL lysis buffer containing 50 mmol/L Tris, pH 8.0, 10% Glycerol, 0.5% NP40, 150 mmol/L NaCl, 1 mmol/L DTT, 1 mmol/L EDTA, 1 mmol/L Sodiumorthovanadate, 170 mg/L phenylmethylsulfonyl fluoride, 2 mg/L Aprotinin, 1 mg/L Leupeptin. Lysates were cleared by centrifugation in a microcentrifuge at high speed for 30 min at 4℃. Protein concentration of the supernatant was measured with Bradford reagent. Equal amounts (100 μg) of proteins were suspended in sodium-dodecyl sulphate (SDS)-sample buffer, boiled for 5 min and separated by electrophoresis (NuPAGE 4%-12% Bis-Tris Gel, Invitogen). The separated proteins were transferred to a polyvinylidene difluoride membrane (Hybond-P^{TM}, Amersham Biosciences). After blocking for 1 h at room temperature in 10% non-fat dry milk in Tris-buffered saline with 0.1% Tween-20 (TBST) or 1% BSA for antibodies specific for phosphorylated epitopes, membranes were incubated with anti-p38, anti-pp38 (Santa Cruz), anti-Stat1, anti-Stat1(pY701) and anti-ERK1, anti-ERK1/2(pT202/pY204) (BD Biosciences) overnight at 4℃, and thereafter with horseradish peroxidase-conjugated anti-rabbit or anti-Mouse IgG (1:5000) (Amersham Biosciences) for 1 h at room temperature. The proteins were detected with enhanced chemiluminescence reagent (ECL, Amersham).

Southern blot analysis

Twenty micrograms of cytoplasmic preparations containing HBV replicative intermediates (RI) DNA were analysed by Southern blotting as above.

RESULTS

Differential expression of ISGs in HepG2.2.15 and HepG2 upon stimulation with IFN-α

Type 1 IFNs are known to induce an intracellular antiviral state against many viruses. Therefore, we developed a customized cDNA array methodology to study the expression of IFN stimulated genes (ISGs). At present, this system permits the analysis of several hundred genes of interest. A substantial spectrum of known ISGs is analysed with this macroarray (Table 1). The sensitivity of this method has also been assessed previously[15]. Conventionally, in most micro- and macroarray systems a 2-fold change in the expression level is regarded as being significant.

In the established hepatoma cell line, hepG2.2.15 with stably transfected HBV genomes[16], ISG expression was examined using the cDNA macroarrays (Table 2). While many ISGs, e.g., 2-5 OAS, IFI 17, and RING4, were normally stimulated by IFN-α, several other ISGs were expressed at a lower level compared with the ISG expression in HepG2 cells. The induction of 2 ISGs, MxA and Cig5, was completely inhibited in HepG2.2.15 cells, while a partial inhibition was observed for 4 ISGs, IFITM1, IFITM2, IFITM3, and 6-16 (Table 1, Figure 1). Thus, only a subgroup of ISGs was down regulated in HepG2.2.15.

Analysis of the IFN response in HepG2.2.15 and HepG2 cells

The results above suggested that the IFN-signalling pathway is only partially inhibited in HepG2.2.15. Western blotting and EMSA and were carried out to analyse Stat1 activation and ISGF3 formation in HepG2 and HepG2.2.15 cells. The phosphorylated form of Stat1 was detected by western blot in IFN-α treated cells (Figure 2). The phosphorylation of Stat1 was enhanced in HepG2.2.15, compared with HepG2. Furthermore, Figure 3 showed that the formation of ISGF3 in HepG2.2.15 cells occurred after IFN-α stimulation, as occured in HepG2 cells.

Table 1 Complete list of genes investigated in this study

Gene Name	Acc. No.	Gene Name	Acc. No.	Gene Name	Acc. No.
101F6	AA544950	IFI 16	M63838	Mdm2	Z12020
2-5 OAS	X02875	IFI 41	L22342	MEN1	U93237
2-5 OAS	D00068	IFI 44	D28915	Met	AA410591
5' nucleotidase	X55740	IFI 6-16	BC015603	Mig	X72755
60S Ribosomal protein L11	U43522	IFI27	X67325	MIP-1b/CCL4	NM_002984
72 kDa type IV collagenase	J03210	IFI4	X79448	MLK 2	X90846
9-27	J04164	IFIT 1	M24594	MMP-1	M13509
ADAM-10	AF009615	IFIT4	U72882	MxA	M33882
ADAM-17	U69611	IFIT4	AF083470	MxA	M33882
akt-1	NM_005163	IFITM2	X57351	MxB	M30818
akt-2	M77198	IFITM3	X57352	MxB	M30818
Alpha-1-antiproteinase	K01396	IFN omega 1	X58822	NCAM	M74387
Alpha-crystallin	U05569	IFN-AR1	J03171	NF-IL-6	X52560
ATF-2	X15875	IFN-AR2	L42243	NFkB	M58603
Auto Ag SS-A/Ro	NM_003141	IFN-g	M29383	NKC-4	M59807
bad	U66879	IFN-GR1	J03143	n-myc	Y00664
BAK1	X84213	IFN-GR2	U05875	p19	U40343
BAX	U19599	IFI 17	J04164	p48/ISGF3g	M87503
Bax	L22474	IFP 35	U72882	p53	M14694
bcl-2	M14745	IFP-53	X62570	p57Kip2	U22398
BRCA1	U14680	IFRG28	AJ251832	p70 S6 kinase	M60724
BST2	D28137	ikBa	M69043	PAI-1	M16006
BTG1	X61123	IL-1 α	M28983	PCBP	M80563
Calcyclin	J02763	IL-10	M57627	PDGF-alpha	X06374
Calretiulin	M84739	IL-10 R α	U00672	PDK1	Y15056
CASP	AJ006470	IL-10 R β	Z17227	PDK2	NM_002611
Caspase 7	U67319	IL-12R β	U64198	Phosph. Scram. 1	AF098642
Caspase 8	X98172	IL13RA	U81379	Phosph.glycerate kin.	V00572
Caspase-1	M87507	IL13RA 2	U70981	Pi3-kinase	NM_006219
Caspase-9	U60521	IL-15	U14407	PIAS x-beta	AF077954
Cat. o-methyltransferase	M58525	IL-15RA	U31628	pig7	AF010312
CBFA	NM_004349	IL-18	D49950	pim-1	M16750
CBP	U85962	IL-18 bprot	AB019504	PK R	AF072860
CCR1	L09230	IL2	U25676	PKR	U50648
CCR5	U54994	IL-2R α	K03122	plectin (PLEC1)	U53204
CD5	X04391	IL2RG	D11086	PLOD2	U84573
cdk inhibitor p27KIP1	U10909	IL6	X04602	PML-1	M79462
C-fox	NM_005252	IL-8	M28130	PPP3CA	L14778
CG12-1	AF070675	IL8RB	L19593	Pro. 4-hydroxyl.	M24486
C-jun	J04111	iNOS	L09210	Prot.-ATPase-like pr.	D89052
C-myc	L00058	Int-6	U62962	PTEN	U96180
C-myc	V00568	Integrin β 7	M62880	pyridoxal kinase	U89606
Collagen α1 (I)	Z74615	integrin-β-6	NM_000888	raf (c-raf-1)	X03484
Collagen α2 (I)	J03464	IP-10	X02530	RAP46/Bag-1	Z35491
Collagen, type XVI, alpha 1	M92642	IP-30	J03909	RbAp48	X74262
Complement compound C1r	J04080	IRF 1	X14454	Reticulocalbin	D42073
COX17	L77701	IRF 4	U52682	RGS2	NM_002923
Cpp32	NM_004346	IRF 5	U51127	RHO	NM_000539
CREB	NM_004379	IRF-1	L05072	RHO GDP-dis.inh. 2	L20688
CTRL-1	X71877	IRF-2	X15949	RING 10	NM_004159
CXCR4	AF005058	Irf-7	U73036	RING4	X57522
Cyclin D1	M64349	ISG15	AA406020	Smad1	U59423
Cyp19 (aromata)	M28420	ISG15	M13755	Smad2	AF027964
Cys-X-Cys,member 11	AF030514	ISG-56K	M24594	Smad4	U44378
DEAD box binding protein 1	AF077951	KIAA0129	D50919	Smad5	U73825
DEAD-box protein p72	U59321	KIAA0235	D87078	Smad7	AF015261
Destrin	S65738	KIAA0284	AB006622	SnoN	X15219
DP (β1)	M83664	LIPA	U04285	SOCS 3/ssi-3	AB004904
DR-α	J00194	LMP-2	X66401	SOCS 4/CIS 4	AB006968
E2F-1	U47677	L-selectin	M25280	SOCS1	N91935

Gene Name	Acc. No.	Gene Name	Acc. No.	Gene Name	Acc. No.
egr-1	X52541	Mad 4	X03541	SOCS-1	NM_003745
Elastase 2	M34379	MAP2K1	NM_002755	SOCS2	AF020590
ERM	X76184	MAP2K1IP1	NM_021970	SOCS-3	NM_003955
F-actin capping protein	U56637	MAP2K2	L11285	Stannin	NM_003498
Farn. pyro. syn.	J05262	MAP2K3	NM_002756	STAT 6	U16031
FAS/Apo-1	M67454	MAP2K4	L36870	STAT1 (91kDa)	M97935
fas-ligand	U08137	MAP2K5	NM_002757	STAT1 (91kDa)	M97935
Fibronectin-1	X02761	MAP2K6	U39657	STAT2	M97934
FK506 binding protein 6	AF038847	MAP2K7	AF022805	STAT4	L78440
FKHRL1	AF041336	MAP3K1	AF042838	STAT5A	L41142
Folate receptor	X62753	MAP3K11	NM_002419	STAT5B	U47686
gadd45	M60974	MAP3K14	NM_003954	Succinyl CoA Ligase	AF058953
Galectin-1	J04456	MAP3K2	NM_006609	TAP1 (Ring4)	L21204
Gamma actin	X04098	MAP3K3	U78876	TFE3	X96717
Gamma2-adaptin (G2AD)	AF068706	MAP3K4	NM_005922	TGF-bR1	L11695
GAPDH	X01677	MAP3K5	NM_005923	TGF-bR2	D50683
GATA 3	X58072	MAP3K7	NM_003188	TGF-bR3	L07594
GBP-1	M55542	MAP4K1	NM_007181	TGIF	X89750
GBP-2	M55543	MAP4K3	NM_003618	TIMP-1	M59906
Granzyme B	M17016	MAPK10	NM_002753	TIMP-2	J05593
GSK3	NM_002093	MAPK11	NM_002751	TIMP-3	U14394
HCV-ass. p44	D28915	MAPK12	NM_002969	TIMP-4	U76456
HLA-A (MHCI Ag B27)	NM_002116	MAPK13	AF004709	TNF-alpha	X01394
HLA-E	X56841	MAPK14	NM_001315	TRAF6	U78798
Homo sapins STAT	M97936	MAPK3	X60188	Transferrin	M12530
Hou	U32849	MAPK6	NM_002748	Transthyretin	D00096
HPAST protein	AF001434	MAPK7	NM_002749	TRIP14	L40387
hsf1 (tcf5)	M64673	MAPK8	NM_002750	trk oncogene	X03541
hsp90 (CDw52)	X15183	MAPK8IP2	NM_012324	TTF-2	AF073771
Hypoxia-ind. Factor-1	U22431	MAPK9	U35003	UBE2L6	AA292074
ICAM-1	M24283	MAPKAPK2	NM_004759	VCAM -1	M30257
ICSB 1	M91196	MAPKAPK3	NM_004635	VEGF-C	U43142
IDO	M34455	MCP-1/CCL2	X14768	Virpirin (Cig5)	AF026941

Genes of interest were selected from the UniGene database. These genes comprise known ISGs and genes of intrinsic interest which might or might not be induced by IFNs in different cell systems. They include genes involved in cell proliferation, immune responses and the responses to a variety of cytokines. 5′ IMAGE clones with 0.5-0.8 kb length were chosen and obtained from RZPD, Berlin, Germany.

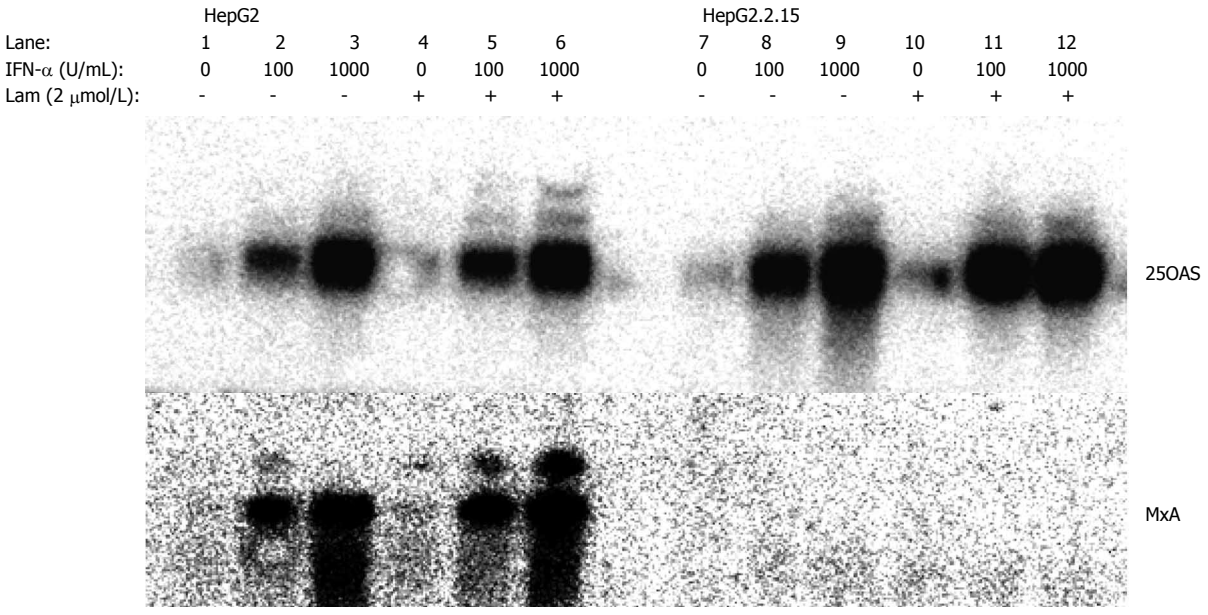

Figure 1 Northern blot analysis of ISG expression and its modulation by lamivudine in HepG2 and HepG2.2.15 cells. HepG2 and HepG2.2.15 cells were cultured in the absence or presence of 2 μmol/L of lamivudine for 10 d. Then, the cells were stimulated with 100 or 1000 IU/mL of IFN-α for 6 h. Total cellular RNAs were isolated for Northern blotting hybridization. Lam: lamivudine.

Table 2 Suppression of ISG induction in HepG2.2.15 cells, effect of lamivudine treatment

Gene	Acc. No.	HepG2	2.2.15	HepG2 /lam	2.2.15 /lam
Ⅰ complete inhibition					
MxA	M33882	5.9	0.6	4.0	0.8
cig5	AF026941	2.2	0.9	2.1	1.2
Ⅱ partial inhibition					
IFITM3	X57352	3.4	1.6	3.4	1.8
IFITM2	X57351	2.7	1.6	2.2	1.8
Ⅲ reversible inhibition					
IFI 6-16	BC015603	7.9	4.4	7.2	6.5
IFITM1	M24594	4.9	2.5	4.8	4.6
Ⅳ no inhibition					
2-5OAS	D00068	3.8	4.0	4.4	5.8
MxB	M30818	1.4	2.0	1.4	1.9
Caspase 7	U67319	2.3	2.4	2.2	2.1
IFI 17	J04164	3.3	2.9	2.8	2.7
IFI 27	X67325	1.9	2.1	1.8	2.2
IFI T4	U72882	2.7	1.9	2.6	1.8
RING4	X57522	2.4	2.3	2.5	3.5

Cells were stimulated with 100 U/mL IFN-α for 6 h with or without pretreatment with 2 μmol/L lamivudine for 10 d. Then, RNA was isolated and assayed by cDNA macroarray. Data are shown as fold induction compared to the untreated control. Lam: Lamivudine.

These data clearly show that the IFN-signalling pathway is generally not blocked in HepG2.2.15 cells. The results consistently show that both steps were evenly enhanced in HepG2.2.15. In addition, activation of ERK and p38 MAPKinase was not altered in HepG2.2.15 cells (data not shown).

Reduction of the production of HBV proteins and the HBV replication by lamivudine treatment

The difference in ISG expression in HepG2 and HepG2.2.15 cell lines may be partly due to the presence of HBV replication in the later one. Consequently, the ISG expression in HepG2.2.15 would change if the HBV gene expression or replication is suppressed. To test this hypothesis, we determined the optimal condition to reduce HBV gene expression and replication using the nucleoside analogue lamivudine. HepG2.2.15 cells were treated with lamivudine at various concentrations from 0.04 μmol/L to 100 μmol/L. The antiviral activity was determined by quantitation of secreted HBsAg and HBeAg particles, extracellular virions and intracellular HBV replicative intermediates (RI). Figure 4A shows that treatment with lamivudine led to a significant reduction of secreted HBsAg and HBeAg in the supernatant of HepG2.2.15 cells. Parallel to the reduction of HBsAg and HBeAg production, the extracellular virion DNA in the culture supernatant of HepG2.2.15 cells and intracellular HBV replicative intermediates (RI) decreased after treatment with 2 μmol/L or 20 μmol/L of lamivudine for 10 d (Figure 4B and C). Maximal levels of suppression of HBV were observed after 10 d of lamivudine treatment. At that time, levels of RI were not more than 1.5% of controls in cultures of the 2 μmol/L treatment group. Based on these results, we chose

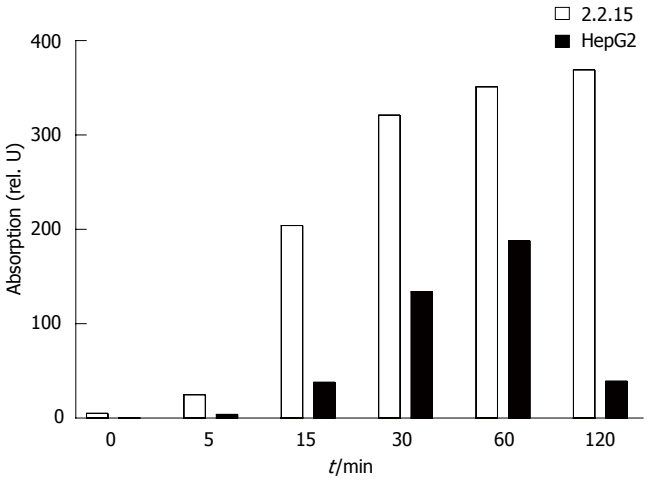

Figure 2 Analysis of Stat1 phosphorylation after IFN-α stimulation in HepG2 and HepG2.2.15 cells. Cells were stimulated with 100 U/mL of IFN-α for the indicated time points. Then, nuclear proteins were extracted and analysed by western blot. Data were quantified using Imagequant and are shown as relative units.

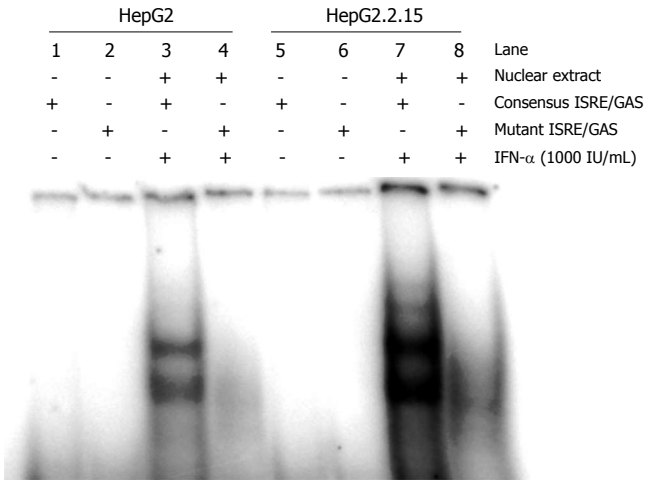

Figure 3 Analysis of ISGF3 formation after IFN-α stimulation in HepG2 and HepG2.2.15 cells. HepG2 and HepG2.2.15 cells were stimulated with 1000 IU/mL of IFN-α for 6 h followed by isolation of nuclear extracts (NE-PER™ reagent kits) for EMSA analysis.

a concentration of 2 μmol/L and duration of 10 d to suppress HBV replication in our system to study the modulatory effects of lamivudine on the IFN-response.

The IFN response in HepG2.2.15 and HepG2 cells after lamivudine treatment

The effect of lamivudine on ISG expression in HepG2.2.15 and HepG2 was investigated by using gene macroarrays. No effect was observed for the stimulation of MxA and Cig5 expression by lamivudine treatment (Table 2). Both genes did not respond with an increased expression upon IFN-α stimulation. An increase of the IFN-α concentration to 1000 units per mL or a prolonged incubation with IFN-α did not change the expression of MxA and cig5. The reduced induction of IFITM 2 and IFITM 3 expression could not be enhanced by lamivudine treatment. In contrast, IFITM1 and 6-16 expression could

be restored by lamivudine treatment of HepG2.2.15 cells (Table 1, Figure 1). This indicates that lamivudine can only partially normalize the IFN-response in HBV-transfected HepG2.2.15 cells at concentrations that profoundly inhibit viral replication and secretion of viral particles. Lamivudine had no effect on ISG expression in HepG2 cells and did not enhance the induction of many other ISGs, such as 2.5 OAS and MxB.

DISCUSSION

In the present work, we found that HepG2.2.15 and HepG2 respond differently to IFN-α. Several ISGs were not induced in HepG2.2.15 while they were expressed in HepG2 cells after IFN-α. There may be multiple reasons for the different ISG expression profiles in these cell lines, though HepG2.2.15 was derived from HepG2[16]. Previous data indicated that the expression of the IFN-inducible gene MxA was specifically inhibited by HBV proteins in HBV-transfected HepG2 or HuH7 cells[13], and this was accompanied by diminished antiviral activity of IFN[17]. In our study, we confirmed this finding with MxA expression being completely diminished in HBV-transfected HepG2.2.15 cells. In addition, we showed that additional ISG (Cig5, IFITM1, -2, -3 and 6-16) expression was completely abolished or partially reduced by HBV. The majority of ISGs, however, are expressed and inducible in both HepG2 and HepG2.2.15 cells, indicating that the HBV gene expression and replication had no effect on these ISGs. Consistently, Rosmorduc *et al*[17] demonstrated that 2´5OAS expression is not affected by HBV. Our results support the view that the HBV-mediated inhibition of the IFN-response, if any, represents a specific rather than global effect. The Stat1 activation or ISGF3 formation in HepG2.2.15 cells appeared to be normal, indicating that the Jak/Stat signalling pathway is intact and functional. These findings are corroborated by the data from Fernandez *et al*[13] who demonstrated that the inhibition of MxA induction in HepG2 cells occurs at the promoter level.

We then asked the question whether the HBV-mediated suppressive effect on the IFN-response could be reverted by treatment with the nucleoside analogue lamivudine, which is an effective inhibitor of HBV replication *in vitro*[18] and *in vivo*[19,20]. Lamivudine is phosphorylated within the cell and then incorporated into nascent viral DNA by the HBV polymerase during replication[21] resulting in the termination of HBV DNA elongation. Lamivudine also inhibits reverse transcriptase activity directly through competitive inhibition. Although some reports indicate that lamivudine exerts synergistic effects with IFN, the underlying mechanisms are not clear[22,23]. To answer this question we first established the optimal conditions for *in vitro* treatment of HepG2.2.15 cells with lamivudine. The results indicated that lamivudine exerted potent antiviral activities in our system as it strongly suppressed the formation of HBV replicative intermediates and extracellular HBV DNA at concentrations that correspond well to plasma levels found in patients that are treated with this drug. However, HBsAg and HBeAg secretion was only down regulated and not completely blocked. After treatment with lamivudine for 10 d, the induction of IFITM1 and 6-16 expression could be enhanced while MxA, Cig5, IFITM2 and IFITM3 induction remained unchanged. This indicates that lamivudine can at least partially improve the impaired IFN response in HBV-transfected cells. IFITM 1 to 3 and 6-16 belong to a family called small ISGs[24]. IFITM 1 to 3 are classified as members of the 1-8 group while 6-16 is a member of the ISG12 group. These genes were under the control of multiple elements responding to IFN-α stimulation including ISGF3 and interferon. It is likely that the lamivudine treatment partially reduces HBV gene expression and therefore contributes to the improved

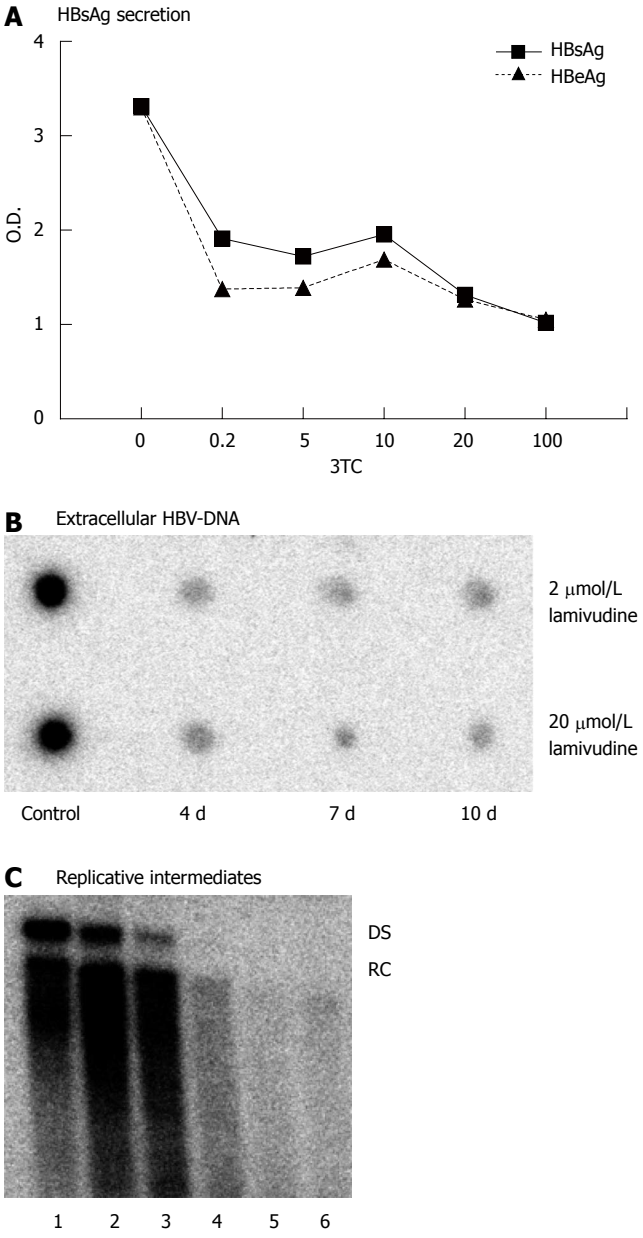

Figure 4 Antiviral effects of lamivudine in HepG2.2.15 cells. **A**: HepG2.2.15 cells were cultivated with various concentrations (0 to 100 μmol/L) of 3 TC for 10 d. Then, supernatants were harvested and assayed for the presence of HBsAg and HBeAg by ELISA; **B**: HepG2.2.15 cells were treated with 2 or 20 μmol/L of lamivudine for 4, 7 and 10 d, respectively. Then, supernatants were collected and extracellular HBV-DNA was analyzed by dot blot hybridization; **C**: HepG2.2.15 cells were treated with various concentrations of lamivudine for 10 d. Then, intracellular HBV replicative intermediates were isolated for southern blotting. Lane 1: control, lane 2: 0.04 μmol/L, lane 3: 0.2 μmol/L, lane 4: 5 μmol/L, lane 5: 25 μmol/L, lane 6: 125 μmol/L, RC, relaxed circular HBV-DNA; DS, double stranded linear HBV-DNA.

ISG expression. On the other hand, the continuing HBV protein production may still dominantly interfere with the expression of many ISGs, such as cig5 and IFITM3.

These findings are corroborated by our study that shows an improved IFN response of PBMC from HBV patients after treatment with adefovir. Some reports have also suggested a restoration of weak T helper cell and CTL responses after initiation of lamivudine therapy[25,26]. Although it is certainly a possibility, it still remains to be determined whether this effect can be explained by an enhanced responsiveness to IFNs.

In conclusion, our results suggest that HBV specifically modulates the IFN response in HepG2 cells by a selective suppression of certain ISGs. This suppression is at least partially reversible by antiviral treatment with the nucleoside analogue lamivudine.

REFERENCES

1 **Hadziyannis SJ**, Papatheodoridis GV, Vassilopoulos D. Treatment of HBeAg-negative chronic hepatitis B. *Semin Liver Dis* 2003; **23**: 81-88
2 **Heathcote J**. Treatment of HBe antigen-positive chronic hepatitis B. *Semin Liver Dis* 2003; **23**: 69-80
3 **Lok AS**, Lai CL, Leung N, Yao GB, Cui ZY, Schiff ER, Dienstag JL, Heathcote EJ, Little NR, Griffiths DA, Gardner SD, Castiglia M. Long-term safety of lamivudine treatment in patients with chronic hepatitis B. *Gastroenterology* 2003; **125**: 1714-1722
4 **Guidotti LG**, Ando K, Hobbs MV, Ishikawa T, Runkel L, Schreiber RD, Chisari FV. Cytotoxic T lymphocytes inhibit hepatitis B virus gene expression by a noncytolytic mechanism in transgenic mice. *Proc Natl Acad Sci USA* 1994; **91**: 3764-3768
5 **Guidotti LG**, Guilhot S, Chisari FV. Interleukin-2 and alpha/beta interferon down-regulate hepatitis B virus gene expression in vivo by tumor necrosis factor-dependent and -independent pathways. *J Virol* 1994; **68**: 1265-1270
6 **Wieland SF**, Guidotti LG, Chisari FV. Intrahepatic induction of alpha/beta interferon eliminates viral RNA-containing capsids in hepatitis B virus transgenic mice. *J Virol* 2000; **74**: 4165-4173
7 **Pasquetto V**, Wieland SF, Uprichard SL, Tripodi M, Chisari FV. Cytokine-sensitive replication of hepatitis B virus in immortalized mouse hepatocyte cultures. *J Virol* 2002; **76**: 5646-5653
8 **Gordien E**, Rosmorduc O, Peltekian C, Garreau F, Bréchot C, Kremsdorf D. Inhibition of hepatitis B virus replication by the interferon-inducible MxA protein. *J Virol* 2001; **75**: 2684-2691
9 **Robek MD**, Boyd BS, Wieland SF, Chisari FV. Signal transduction pathways that inhibit hepatitis B virus replication. *Proc Natl Acad Sci USA* 2004; **101**: 1743-1747
10 **Robek MD**, Wieland SF, Chisari FV. Inhibition of hepatitis B virus replication by interferon requires proteasome activity. *J Virol* 2002; **76**: 3570-3574
11 **Wieland SF**, Vega RG, Müller R, Evans CF, Hilbush B, Guidotti LG, Sutcliffe JG, Schultz PG, Chisari FV. Searching for interferon-induced genes that inhibit hepatitis B virus replication in transgenic mouse hepatocytes. *J Virol* 2003; **77**: 1227-1236
12 **Zhang Z**, Protzer U, Hu Z, Jacob J, Liang TJ. Inhibition of cellular proteasome activities enhances hepadnavirus replication in an HBX-dependent manner. *J Virol* 2004; **78**: 4566-4572
13 **Fernández M**, Quiroga JA, Carreño V. Hepatitis B virus downregulates the human interferon-inducible MxA promoter through direct interaction of precore/core proteins. *J Gen Virol* 2003; **84**: 2073-2082
14 **Guidotti LG**, Morris A, Mendez H, Koch R, Silverman RH, Williams BR, Chisari FV. Interferon-regulated pathways that control hepatitis B virus replication in transgenic mice. *J Virol* 2002; **76**: 2617-2621
15 **Schlaak JF**, Hilkens CM, Costa-Pereira AP, Strobl B, Aberger F, Frischauf AM, Kerr IM. Cell-type and donor-specific transcriptional responses to interferon-alpha. Use of customized gene arrays. *J Biol Chem* 2002; **277**: 49428-49437
16 **Sells MA**, Chen ML, Acs G. Production of hepatitis B virus particles in Hep G2 cells transfected with cloned hepatitis B virus DNA. *Proc Natl Acad Sci USA* 1987; **84**: 1005-1009
17 **Rosmorduc O**, Sirma H, Soussan P, Gordien E, Lebon P, Horisberger M, Bréchot C, Kremsdorf D. Inhibition of interferon-inducible MxA protein expression by hepatitis B virus capsid protein. *J Gen Virol* 1999; **80** (Pt 5): 1253-1262
18 **Doong SL**, Tsai CH, Schinazi RF, Liotta DC, Cheng YC. Inhibition of the replication of hepatitis B virus in vitro by 2',3'-dideoxy-3'-thiacytidine and related analogues. *Proc Natl Acad Sci USA* 1991; **88**: 8495-8499
19 **Nevens F**, Main J, Honkoop P, Tyrrell DL, Barber J, Sullivan MT, Fevery J, De Man RA, Thomas HC. Lamivudine therapy for chronic hepatitis B: a six-month randomized dose-ranging study. *Gastroenterology* 1997; **113**: 1258-1263
20 **Honkoop P**, de Man RA, Zondervan PE, Schalm SW. Histological improvement in patients with chronic hepatitis B virus infection treated with lamivudine. *Liver* 1997; **17**: 103-106
21 **Cammack N**, Rouse P, Marr CL, Reid PJ, Boehme RE, Coates JA, Penn CR, Cameron JM. Cellular metabolism of (-) enantiomeric 2'-deoxy-3'-thiacytidine. *Biochem Pharmacol* 1992; **43**: 2059-2064
22 **Korba BE**, Cote P, Hornbuckle W, Schinazi R, Gangemi JD, Tennant BC, Gerin JL. Enhanced antiviral benefit of combination therapy with lamivudine and alpha interferon against WHV replication in chronic carrier woodchucks. *Antivir Ther* 2000; **5**: 95-104
23 **Janssen HL**, van Zonneveld M, Senturk H, Zeuzem S, Akarca US, Cakaloglu Y, Simon C, So TM, Gerken G, de Man RA, Niesters HG, Zondervan P, Hansen B, Schalm SW. Pegylated interferon alfa-2b alone or in combination with lamivudine for HBeAg-positive chronic hepatitis B: a randomised trial. *Lancet* 2005; **365**: 123-129
24 **Martensen PM**, Justesen J. Small ISGs coming forward. *J Interferon Cytokine Res* 2004; **24**: 1-19
25 **Boni C**, Bertoletti A, Penna A, Cavalli A, Pilli M, Urbani S, Scognamiglio P, Boehme R, Panebianco R, Fiaccadori F, Ferrari C. Lamivudine treatment can restore T cell responsiveness in chronic hepatitis B. *J Clin Invest* 1998; **102**: 968-975
26 **Boni C**, Penna A, Ogg GS, Bertoletti A, Pilli M, Cavallo C, Cavalli A, Urbani S, Boehme R, Panebianco R, Fiaccadori F, Ferrari C. Lamivudine treatment can overcome cytotoxic T-cell hyporesponsiveness in chronic hepatitis B: new perspectives for immune therapy. *Hepatology* 2001; **33**: 963-971

S- Editor Wang J **L- Editor** Lutze M **E- Editor** Bai SH

PO Box 2345, Beijing 100023, China
www.wjgnet.com
wjg@wjgnet.com

World J Gastroenterol 2007 January 14; 13(2): 236-243
World Journal of Gastroenterology ISSN 1007-9327
© 2007 The WJG Press. All rights reserved.

BASIC RESEARCH

Correlation between *in vitro* and *in vivo* immunomodulatory properties of lactic acid bacteria

Benoit Foligne, Sophie Nutten, Corinne Grangette, Véronique Dennin, Denise Goudercourt, Sabine Poiret, Joelle Dewulf, Dominique Brassart, Annick Mercenier, Bruno Pot

Benoit Foligne, Sophie Nutten, Corinne Grangette, Véronique Dennin, Denise Goudercourt, Sabine Poiret, Joelle Dewulf, Annick Mercenier, Bruno Pot, Bactéries Lactiques et Immunité des Muqueuses, Institut Pasteur de Lille, France
Dominique Brassart, Danisco France, Culture Division, France; present address: Nestlé Nutrition, Vevey, Switzerland
Sophie Nutten, Annick Mercenier, Nestlé Research Center, Nutrition and Health Department, Lausanne, Switzerland
Supported by the EU granted QLK1-2000-00146 DEPROHEALTH research program, Institut Pasteur de Lille funding and funds from DANISCO France
Correspondence to: Dr. Bruno Pot, Bactéries Lactiques et Immunité des Muqueuses, Institut Pasteur de Lille, 1 Rue du Professeur Calmette, BP 245, Lille cedex F-59019, France. bruno.pot@ibl.fr
Telephone: +33-3-20871191 Fax: +33-3-20871192
Received: 2006-09-09 Accepted: 2006-12-07

Abstract

AIM: To investigate the correlation between the *in vitro* immune profile of probiotic strains and their ability to prevent experimental colitis in mice.

METHODS: *In vitro* immunomodulation was assessed by measuring interleukin (IL)-12p70, IL-10, tumor necrosis factor alpha (TNFα) and interferon γ (IFNγ) release by human peripheral blood mononuclear cells (PBMCs) after 24 h stimulation with 13 live bacterial strains. A murine model of acute TNBS-colitis was next used to evaluate the prophylactic protective capacity of the same set of strains.

RESULTS: A strain-specific *in vivo* protection was observed. The strains displaying an *in vitro* capacity to induce higher levels of the anti-inflammatory cytokine IL-10 and lower levels of the inflammatory cytokine IL-12, offered the best protection in the *in vivo* colitis model. In contrast, strains leading to a low IL-10/IL-12 cytokine ratio could not significantly attenuate colitis symptoms.

CONCLUSION: These results show that we could predict the *in vivo* protective capacity of the studied lactic acid bacteria (LAB) based on the cytokine profile we established *in vitro*. The PBMC-based assay we used may thus serve as a useful primary indicator to narrow down the number of candidate strains to be tested in murine models for their anti-inflammatory potential.

© 2007 The WJG Press. All rights reserved.

Key words: Inflammatory bowel disease; Probiotics; Cytokines; Peripheral blood mononuclear cells; Trinitrobenzene sulfonate-induced colitis

Foligne B, Nutten S, Grangette C, Dennin V, Goudercourt D, Poiret S, Dewulf J, Brassart D, Mercenier A, Pot B. Correlation between *in vitro* and *in vivo* immunomodulatory properties of lactic acid bacteria. *World J Gastroenterol* 2007; 13(2): 236-243

http://www.wjgnet.com/1007-9327/13/236.asp

INTRODUCTION

Probiotic lactobacilli and bifidobacteria are increasingly recognized as a way to prevent and/or treat intestinal disorders[1]. Probiotic treatment has been successful in a limited number of clinical inflammatory bowel disease (IBD) trials[2,3], as well as in various experimental rodent models for acute and chronic intestinal inflammation[4]. Cytokines are key regulators of inflammation in IBD, and several pro-inflammatory and immune regulatory cytokines are dysregulated in the mucosa of IBD patients. Probiotic–mediated immunomodulation represents an interesting option in the management of IBD[5] and it was shown that both the systemic and mucosal immune systems can be modulated by orally delivered bacteria[6-8]. However, not all candidate probiotics have been proven equally efficient due to the differences in survival and persistence of the strain in the gastro-intestinal tract, and/or to strain-specific interactions of the probiotic with the host immune system[9-11]. The selection of a successful protective strain may therefore rely on the proper screening of a large number of candidate strains for their technological and immunomodulatory performance.

However, it remains challenging to set up *in vitro* tests with a fair predictive value that would allow us to narrow down the number of candidate strains to be tested in animal models. Until now, results of *in vitro* studies have rarely been linked to *in vivo* effects[12,13]. This could possibly be explained by the variety of parameters that may interfere in the systematic comparison of strains such as the bacterial preparations used (viability, growth phase, dose and timing of administration), possible time effects (early *versus* late

immune responses), or physiological status and type of eukaryotic cells used. When testing human peripheral blood mononuclear cells (PBMCs), the *in vitro* experiment may also be influenced by the method of PBMC preparation as well as the variable responsiveness of the donors[10,14,15]. Once identified, however, these parameters/factors can be controlled by using standardized methodologies[16], allowing, on the one hand, to classify strains according to the *in vitro* differences in their interaction with human immunocompetent cells and, on the other hand, to confirm *in vivo* the "protective capacity" of the best candidate strains (showing between 30% and 70% reduction of the inflammatory score)[16,17]. In this paper we addressed the question whether prophylaxis by oral consumption of live non-pathogenic lactic acid bacteria (LAB) in experimental colitis actually matches their *in vitro* stimulation profile on human PBMCs. Cytokine profiles released *in vitro* by human PBMC stimulated with 13 bacterial strains were compared with the protection they offered in a murine trinitrobenzene sulfonate (TNBS) model of acute colitis. The results of this study demonstrate that the *in vitro* immune profiling of the strains is indeed predictive of their *in vivo* protective effect in a mouse colitis model. These findings support the idea that promising LAB strains for IBD alleviation may be discriminated from non-protective ones using *in vitro* and *in vivo* assays.

MATERIALS AND METHODS

Bacterial strains and growth conditions

Bacterial strains and their origin are shown in Table 1. *Lactobacillus* strains were grown under limited aeration at 37℃ in MRS medium (Difco) and *Bifidobacterium* strains were grown anaerobically in MRS supplemented with 0.05% L-cysteine-hydrochloride (Sigma). *Lactococcus lactis* MG1363 was grown at 30℃ in M17 medium supplemented with 0.5% glucose. *E. coli* and *S. gordonii* were grown at 37℃ in LB and BHI medium (Difco), respectively. The number of live bacteria (CFU) was deduced from the absorbance at 600 nm (A_{600}), using a calibration curve for each strain. For immune cell stimulation, bacterial cells were grown till stationary phase, washed and resuspended at 1×10^9 CFU/mL in phosphate buffered saline (PBS) containing 20% glycerol and stored at -80℃ until used for assays. For *in vivo* experiments, bacteria were grown for 18 h, washed twice in sterile PBS (pH 7.2) and resuspended at 1×10^9 CFU/mL in 0.2 mol/L $NaHCO_3$ buffer (pH 8.8) containing 2% glucose.

PBMC isolation

PBMCs were isolated from peripheral blood of healthy donors as previously described[18]. Briefly, after a Ficoll gradient centrifugation (Pharmacia, Uppsala, Sweden), mononuclear cells were collected, washed in RPMI 1640 medium (Live technologies, Paisley, Scotland) and adjusted to 2×10^6 cells/mL in RPMI 1640 supplemented with gentamicin (150 μg/mL), L-glutamine (2 mmol/L), and 10% foetal calf serum (FCS) (Gibco-BRL).

Induction of cytokine release

PBMCs (2×10^6 cells/mL) were seeded in 24-well tissue culture plates (Corning, NY). Twenty microliters of a thawed bacterial suspension at 10^9 CFU/mL were added (bacteria:cell ratio of 10:1). PBS containing 20% glycerol was used as a negative (non-stimulated) control. On the basis of preliminary time-course studies, 24 h stimulation corresponded to the best time point for cytokine responses of bacteria stimulated-PBMCs. After 24 h stimulation at 37℃ in an atmosphere of air with 5% CO_2, culture supernatants were collected, clarified by centrifugation and stored at -20℃ until cytokine analysis. Neither medium acidification nor bacterial proliferation was observed. Cytokines were measured by ELISA using BD pharmingen antibody pairs (BD Biosciences, San Jose, Ca, USA) for tumor necrosis factor alpha (TNFα), interleukin (IL)-10, interferon γ (IFNγ) and IL-12p70, according to the manufacturer's recommendations.

Table 1 Strains used with their origin

Bacterial species /subspecies	Strain designation	Type of isolate, source and/or reference
Lactobacillus salivarius subsp salivarius	Ls33	Commercial strain
Lactobacillus rhamnosus	Lr32	Commercial strain
Lactobacillus casei	Bl23	ATCC[1] 393, plasmid-cured
Lactobacillus acidophilus	NCFM	Human, commercial strain
Lactobacillus acidophilus	IPL[3] 908	Commercial isolate
Lactobacillus plantarum	NCIMB 8826	Human, NCIMB[2] collection
Lactobacillus plantarum	Lp115	Commercial strain
Bifidobacterium animalis subsp *lactis*	BL04	Commercial strain
Bifidobacterium animalis subsp *lactis*	BI07	Commercial strain
Bifidobacterium bifidum	BB02	Commercial strain
Lactococcus lactis	MG1363	Cheese starter derivative[42]
Streptococcus gordonii	V288 (Challis)	ATCC[1] 35105
Escherichia coli (non-pathogenic)	TG1	Cloning strain[43]

[1]ATCC: American type culture collection, Manassas, (VA), USA; [2]NCIMB: National collection of industrial and marine bacteria, Terry Research Station, Aberdeen, Scotland; [3]Institut Pasteur Lille, Lille, France.

Induction of colitis and inflammation scoring

Animal experiments were performed in an accredited establishment (number 59-35009; Institut Pasteur de Lille, France) and approved guidelines, according to French Ethical Committee and European Union Normatives (number 86/609/CEE). BALB/c and C57/Bl6 mice (female, 8 wk) were obtained from Charles River (St Germain sur l'Arbresle, France). A standardized murine TNBS colitis model was used in which sublethal levels of inflammation were induced[16]. Briefly, a 50 μL solution of 100 mg/kg (BALB/c mice) or 180 mg/kg (C57Bl6 mice) TNBS (Sigma) in 50% ethanol was slowly administered in the colon *via* a 3.5 F catheter. Bacterial suspensions (100 μL), containing 1×10^9 CFU/mL in $NaHCO_3$ buffer (or buffer alone for controls) were administered intragastrically to mice each day, starting 5 d before until d 1 after TNBS administration. The mice were weighed and killed 48 h after TNBS administration. Colons were removed, washed and opened. Inflammation grading was performed by two

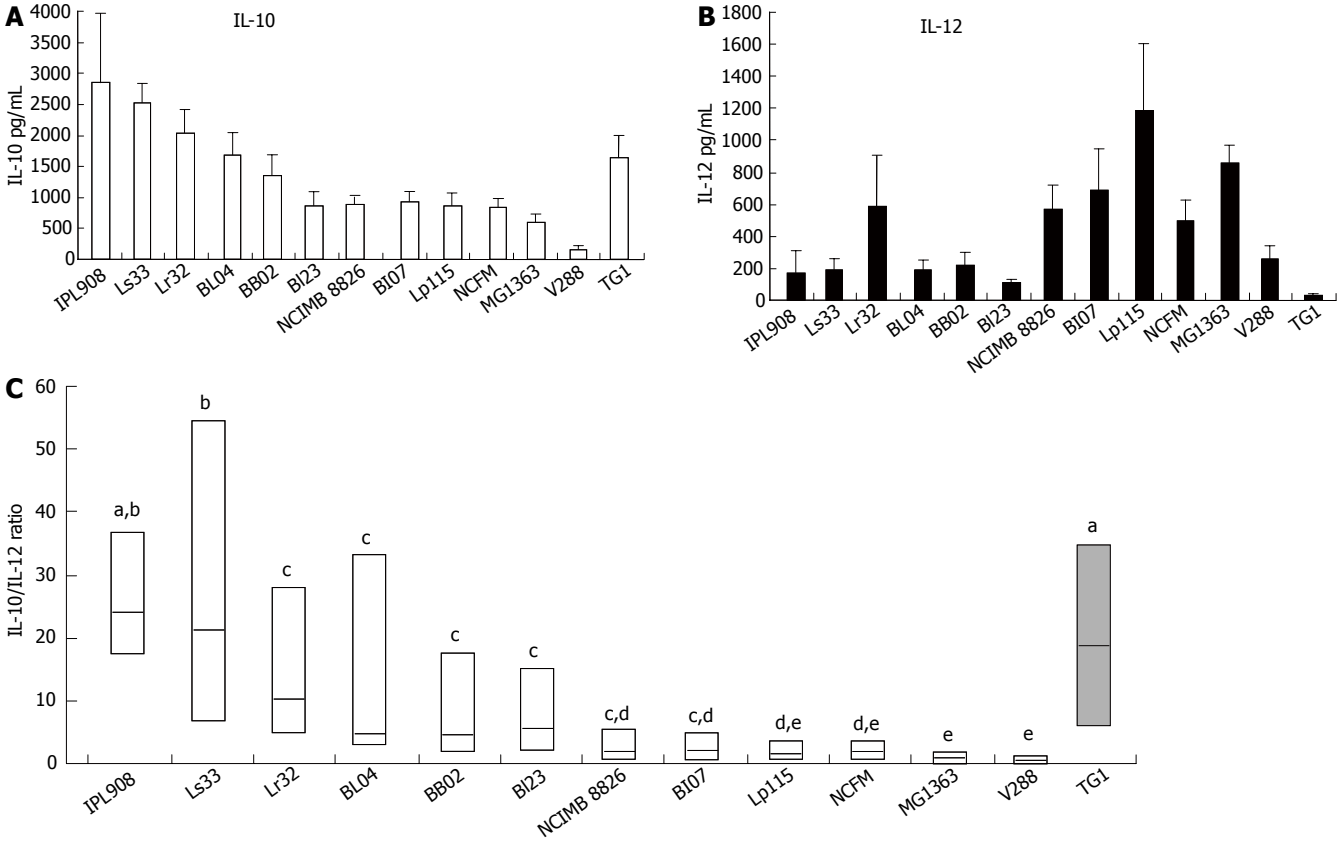

Figure 1 Strain-specific patterns of IL-10 (**A**) and IL-12p70 (**B**) release for various bacterial strains and IL-10/IL-12 ratios (**C**) for 6 to 12 independent healthy donors. Bars represent the mean ± SE values in pg/mL for 6 to 12 independent healthy donors. Ranked box and whisker plots show the median values and first to third quartiles in boxes. Different letters indicate significant differences according to Mann-Whitney *U* test ($P < 0.05$).

blinded observers, using the Wallace scoring method[19]. Results are expressed as % protection, corresponding to the reduction of the mean macroscopic inflammation score of bacteria-treated mice ($n = 10$) in comparison to the mean score of TNBS-treated control mice ($NaHCO_3$ buffer-treated mice, $n = 10$)[16]. Histological analysis was performed on hematoxylin/eosin-stained 5 μm tissue sections from colon samples fixed in 10% formalin and embedded in paraffin.

Statistical analysis

Results were analyzed by the non-parametric one-way analysis of variance and Mann-Whitney *U* test. Differences were judged to be statistically significant when the *P* value was < 0.05. For *in vivo* experiments, only protection levels exceeding 30% (positive and negative) were considered to be relevant, as previously described[16]. For the calculation of the IL-10/IL-12 ratio, all undetectable IL-12 values (below 50 pg/mL) were arbitrarily set at 50 pg/mL level to normalize aberrant quotients. Association of variables was analyzed by the *P* value-assigned Spearman rank correlation coefficient.

RESULTS

Cytokine release by PBMCs is strain specific

The *in vitro* immunostimulation by 13 live bacterial strains (Table 1) of PBMCs collected from 6 to 12 independent donors, revealed distinct and typical patterns of cytokine release. TNFα release was quite uniform for the different LAB investigated, while IFNγ showed variations tending to parallel IL-12 profiles (data not shown). IL-10 and IL-12 levels displayed a strain-specific pattern (Figure 1A and B). Variations in IL-10 concentrations were substantial with values ranging between 200 and 3000 pg/mL depending on the bacterial strain. For IL-12, we also observed significant variations between strains, covering a range of cytokine levels of 50 to 1200 pg/mL. As IL-10 and IL-12 appeared to be the most discriminative cytokines, we used the IL-10/IL-12 ratio (Figure 1C) to distinguish between strains exhibiting a "pro-" *versus* "anti-inflammatory" profile (low *versus* high IL-10/IL-12 ratio, respectively). This approach was found to be useful to identify strains with marked opposite profiles, but did not allow discrimination of strains with median cytokine ratios.

The variation in absolute cytokine concentrations released by PBMCs derived from different donors was examined by conducting successive experiments with a limited set of 6 strains (*E. coli* TG1, *L. salivarius* Ls33, *L. casei* Bl23, *L. plantarum* NCIMB 8826, *Lc. lactis* MG1363 and *L. acidophilus* NCFM). In general, for a variety of individual donors, the ranking of strains was quite reproducible: the most potent "anti-inflammatory" strains induced the highest IL-10 responses in all donors, while other strains were stronger IL-12 inducers in most donors. As an example, Figure 2A and B shows the IL-10 and IL-12 expression profiles for four donors in response to the six "reference" strains used. Relative differences

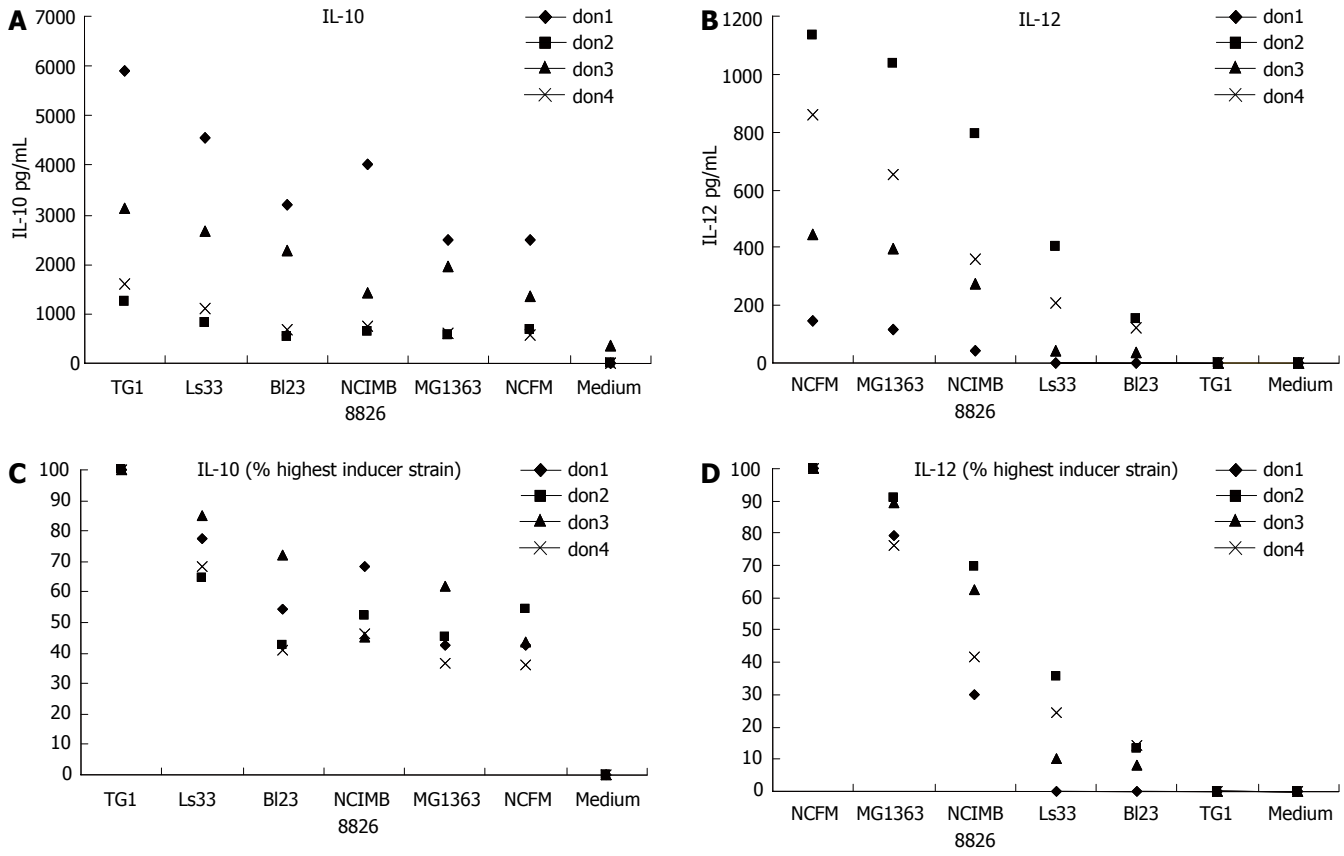

Figure 2 IL-10 (**A**) and IL-12p70 (**B**) release in 4 distinct individual human PBMC donors and the expression level of IL-10 (**C**) and IL-12p70 (**D**). Individual values are represented in pg/mL while IL-10 and IL-12p70 levels are expressed as % of the highest inducer strain. [a]$P < 0.05$.

between two strains, expressed as a percentage of the highest inducer, taken as internal control, were quite constant for all donors (Figures 2C and D). For example, we consistently found 35% and 82% difference ($P < 0.05$) between the strains *L. salivarius* Ls33 and *L. acidophilus* NCFM, for IL-10 and IL-12 induction, respectively. Based on these observations, both strains could be compared in a semi-quantitative way, using their average IL-10 and IL-12 release patterns upon stimulation of PBMCs from four different donors. To that extent we calculated a full matrix of *P*-values for the IL-10/IL-12 ratios obtained from several overlapping studies with reference strains as well as new isolates, for at least 4 PBMC donors, which allowed us to rank strains from an "anti-inflammatory" to a "pro-inflammatory" profile.

When applied to the 13 strains used in this study, this methodology established a semi-quantitative ranking, which could classify strains *L. salivarius* Ls33*, L. casei* Bl23*, L. rhamnosus* Lr32*, L. acidophilus* IPL908 as more anti-inflammatory than the three bifidobacteria and the two *L. plantarum* strains. *Lc. lactis* MG1363*, S. gordonii* V288 and *L. acidophilus* NCFM® strains showed a slightly pro-inflammatory profile with a very low IL-10/IL-12 ratio.

Protection of TNBS-induced colitis was strain-specific

We investigated the protective effect of the 13 strains studied *in vitro* against TNBS-induced colitis in mice (Figure 3). Ls33, Lr32, Bl23, IPL908 and BL04 strains consistently led to a considerable attenuation of colitis (data represent the result of usually 2 to 4 distinct experiments), with reduced weight loss, improved clinical parameters (rectal bleeding, stool consistency, *i.e.* liquid pasty stool and diarrhoea, lethargy; data not shown) and reduced macroscopic inflammation scores. Considering the % protection as the reduction of the mean macroscopic inflammation score of bacteria-treated mice ($n = 10$) in comparison to the mean score of TNBS-treated control mice, the *Lactobacillus plantarum* strains and the BB02 and Bl07 bifiidobacterial strains induced moderate but significant levels of protection. In contrast, no improvement in colitis was observed for the strains *L. acidophilus* NCFM*, Lc. lactis* MG1363 or *S. gordonii* V288 and for the non-pathogenic *E. coli* TG1. None of these strains, however, aggravated the symptoms of colitis. Histological analysis corroborated these findings, showing dramatic improvement in epithelial lesions of the animals receiving protective strains, with a significant decrease in goblet cells and crypt loss (data not shown), and reduced inflammatory infiltrates (mainly neutrophils) accompanied with a reduction of the colon wall thickness to almost normal levels (Figure 4).

Additional experiments confirmed this strain-specific protection in mice with a different genetic background (C57/Bl6 mice). The protection observed in BALB/c mice with *L. salivarius* Ls33 (56.5% ± 7.2%, $P < 0.01$) was confirmed in C57/Bl6 mice (47%, $P < 0.01$), whereas the *L. acidophilus* NCFM® and *E. coli* strains alleviated colitis neither in BALB/c mice (-12.5% ± 2.7%, NS; and +19.4% ± 3.7%, NS, respectively) nor in C57/Bl6 (+26%, NS; and -6.4%, NS, respectively).

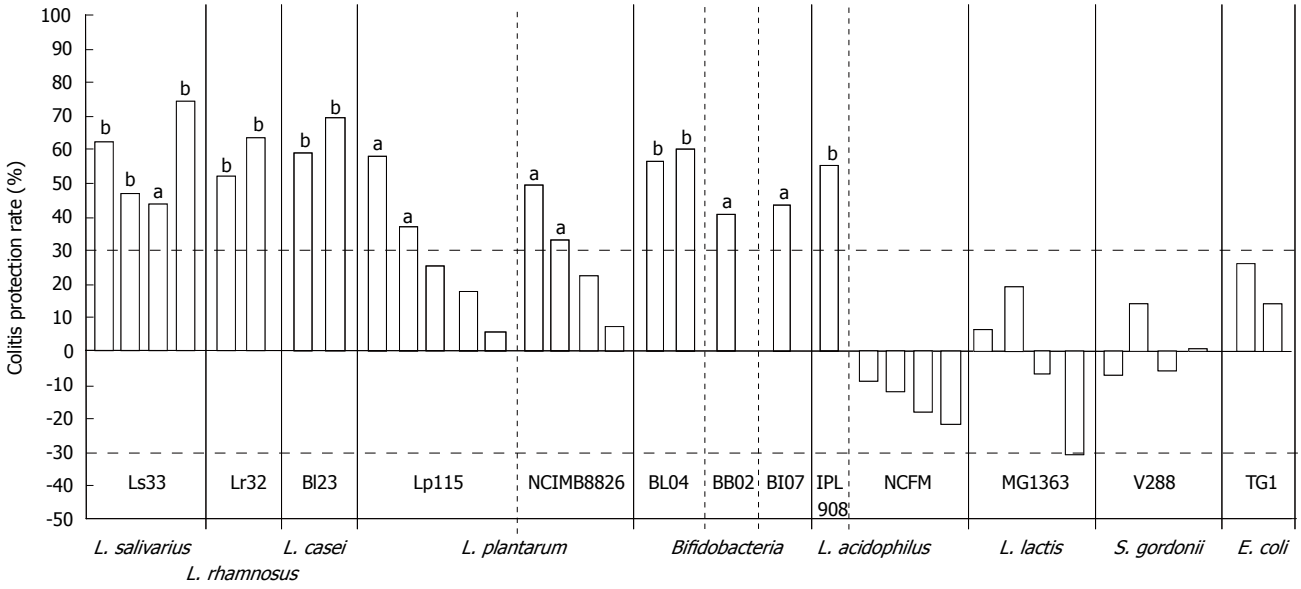

Figure 3 Protective effect of LAB strains against TNBS-induced colitis in BALB/c mice. Results are expressed as a % reduction of the mean macroscopic inflammation of mice treated with LAB as compared to the mean score of non-treated mice. Colitis index was assessed 48 h after TNBS administration. Each bar represents an independent experiment and corresponds to the ratio of control and LAB-treated mice groups (n = 10). $^{a}P < 0.05$, $^{b}P < 0.01$ *vs* TNBS-control group. The horizontal dashed lines indicate the 30% threshold of the uncertain statistical significance.

In vivo / In vitro correlation

Considering both *in vitro* and *in vivo* results, it was evident that strains displaying the highest *in vitro* anti-inflammatory profile (a high IL-10/IL-12 ratio) were the most protective in the *in vivo* colitis model, while those leading to intermediary *in vitro* IL-10/IL-12 ratios showed limited protection. In contrast, bacteria characterized by a low anti-inflammatory potential (low IL-10/IL-12 ratio) did not improve inflammation at all. As a result, with the exception of the Gram-negative *E. coli*, the ranking of all Gram-positive bacteria investigated, based on the *in vitro* cytokine profiling, closely matched the ranking based on the improvement of colitis symptoms. Although this link could not be expressed as an "exact linear" association between % protection and IL-10/IL-12 ratio, it was found to be highly significant using the Spearman rank correlation coefficient (r_s = 0.825, P <0.001) (Figure 5).

DISCUSSION

Immunomodulation through probiotics represents one of the current treatment options for IBD[5,20] and specific strains may stimulate immunomodulatory mediators, inhibit pro-inflammatory cytokines and influence the phenotypes of immunocompetent cells with subsequent events such as migration of dendritic cells and induction of regulatory T cells[15,21]. The mechanisms of action of probiotics are most probably multi-factorial, involving a variety of effector signals, cell types and receptors[22], and strains may differ in their respective ability to trigger these signals considering both immunocompetent and intestinal epithelial cells[23]. It has been proposed that some probiotics are able to prevent or restore intestinal homeostasis after an immune dysregulation, improving mucosal barrier functions as well as down-regulating inflammatory responses[24,25].

In this study, we aimed at developing a simple and standardized *in vitro* test allowing preliminary classification of candidate probiotic strains according to their immune modulation capacity that would be predictive of their *in vivo* effect. To this end, we ranked 13 LAB strains with reference to the IL10/IL12 cytokine ratio induced on human PBMCs and further assessed their protective effect against TNBS-induced colitis in mice.

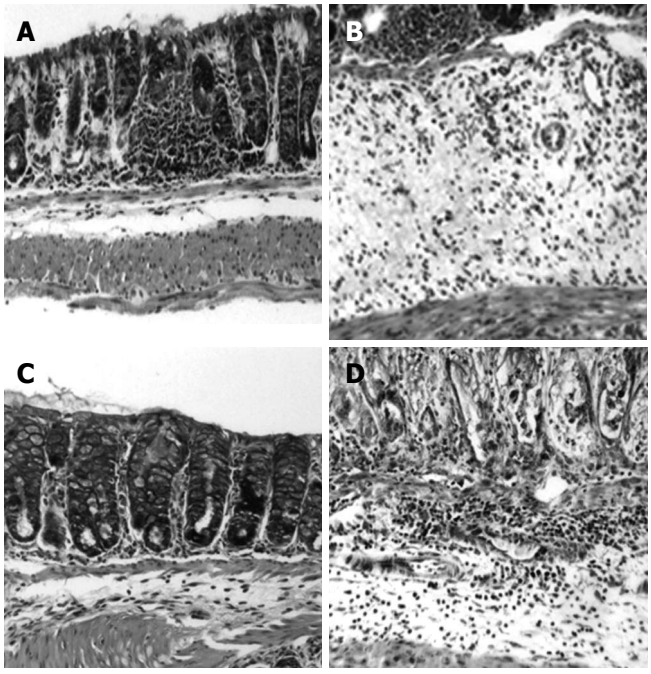

Figure 4 Hematoxylin/eosin staining of representative cross-sections of murine (BALB/c) distal colon (HE, x 20). **A**: Normal appearance of the colon from a negative control mice; **B**: Thickening of the colon wall accompanied with massive inflammatory infiltrate and muscular necrosis 2 d after TNBS-induction of colitis; **C**: Reduction of histological damage in *L. salivarius* Ls33-treated mice after TNBS administration; **D**: Lack of histological improvement of colitis in *L. acidophilus* NCFM-treated mice after TNBS administration.

We observed strong strain-specific variations of the *in vitro* cytokine induction profiles after stimulation of immunocompetent cells, which confirms the results reported in previous studies[9-11,15,26]. We also noted that differences between blood donors did not prevent us ranking the strains based on their cytokine responses as the relative responses of PBMCs to various LAB were consistent from one donor to another. PBMCs from healthy donors can thus be used to screen the immunomodulatory activity of candidate probiotic strains and this test/assay appears to be a good indicator of *in vivo* anti-inflammatory strains. Despite the fact that this assay does not clarify the physiological mechanism(s) involved, it seems to mimic how the immune system may sense the bacterial strains and consequently polarise the immune response. Strains leading to a high IL-10/IL-12 ratio would more easily slow down an early Th1 response.

In accordance with this hypothesis, we found differences in the *in vivo* protective capacity of the 13 studied strains against TNBS-induced inflammation[27]. This strain-specificity has already been described in other experimental models of colitis[28-31]. The variations we observed between different LAB strains in this respect cannot simply be explained by differences in persistence, especially when daily administrations maintain the level of bacteria in the gastro-intestinal tract. Of note, we have previously verified whether the anti-inflammatory profiles could in any way be linked to *in vitro* properties such as gastric juice (pepsin/pancreatin) and bile salt resistance, epithelial cell adhesion and *in vivo* intestinal persistence (unpublished data). However, no link was found between them.

Above all, we have demonstrated in this study that the ranking of strains obtained on the basis of an *in vitro* IL-10/IL-12 cytokine induction ratio closely matches the ranking of the *in vivo* ability of the strains to attenuate experimental colitis. The concordance between the *in vitro* and *in vivo* assays has been illustrated in the case of a cell-wall mutant of *L. plantarum*[18]. The importance of the IL-10/IL-12 ratio has also recently been highlighted by Peran *et al*[32] who showed that administration of a specific strain of *Lactobacillus salivarius* subsp. *salivarius* could improve the recovery of inflamed tissue in a TNBS model of rat colitis. This strain was selected among 30 LAB strains for eliciting the best IL-10/IL-12 and IL-10/TNFα ratios. Unfortunately, no strains exhibiting a moderate or low IL-10/IL-12 profile were included in the *in vivo* study, which could have validated the proposed screening strategy. Similarly, *in vitro* tests on immunocompetent cells have been used successfully to study the effect of distinct bacterial fractions (intact cell walls, protoplast and polysaccharide-peptidoglycans) of the strain *Lactobacillus casei* Shirota[33]. Using the ability of this strain to inhibit the LPS-induced IL-6 in mice bone marrow derived-DCs and PBMCs isolated from ulcerative colitis patients, the authors could establish that the polysaccharide-peptidoglycan complex was the most efficient compound to improve chronic colitis and ileitis in their mice model. Another example attesting similar links between *in vitro* macrophage stimulation and related protection in a murine TNBS model of colitis was reported for the anti-inflammatory drug "catapolside"[34], leading to clinical trials in IBD patients in Korea.

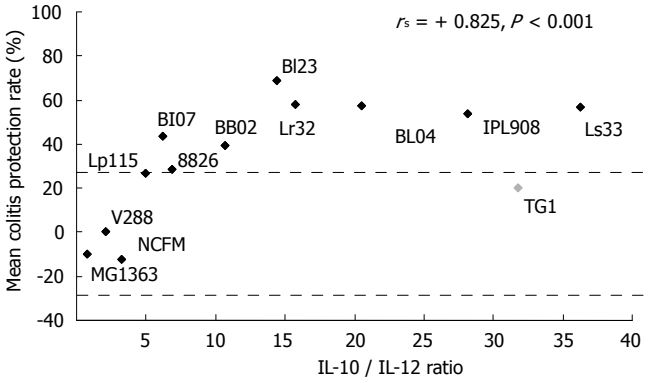

Figure 5 Correlation between the average protection against experimental colitis and the mean IL-10/IL-12 ratios obtained *in vitro*, for all investigated strains. Spearman coefficient (r_s = 0.825, P < 0.001). The horizontal dashed lines indicate the 30% threshold of unprotectiveness.

Recently, the PBMC IL-10/IL-12 ratio has also been used to follow the immunomodulatory properties of probiotics in a clinical study on irritable bowel syndrome (IBS)[31]. Despite different aetiology and characteristics, IBD and IBS share some aspects of immune dysregulation, and IBS has been documented to be associated with low-grade inflammation. Concomitantly to alleviation of the main IBS symptoms, the authors showed normalization of the PBMC IL-10/IL-12 ratio in patients receiving probiotics *versus* placebo, showing that *in vivo* probiotic efficiency can be correlated to specific *in vitro* assays.

Despite the positive correlation observed between *in vivo* protection and *in vitro* cytokine ratio, some restrictions are clear. First of all, the link is not valid for Gram-negative bacteria. Gram-negative bacteria, including both non-pathogenic and pathogenic strains, are well known to be potent inducers of monocytic IL-10, while Gram-positive species preferentially stimulate IL-12 [10]. These observations do not exclude Gram-negative strains from being anti-inflammatory. For example, bacteria such as the *E. coli* strain Nissle[35] or virulence-attenuated *Yersinia pseudotuberculosis* mutants[36] have been shown to be able to reduce colonic lesions and inflammatory mediators in murine models of experimental colitis. Secondly, it is not excluded that *Lactobacillus* strains may moderate colitis by non immune-related modes of action, as for example by acting on barrier integrity or influencing the oxidative pathway[37]. Alternatively, LAB strains with a rather pro-inflammatory profile may have other health benefits which substantiate their probiotic status[38,39].

The methods described in this paper can be used to screen a larger set of potential probiotic strains for their immunomodulatory properties, since they are relatively simple and quite reproducible. We are currently building a reference database including both *in vitro* cytokine profiles, as well as protection levels measured in the TNBS mice model for selected reference strains. This database encompasses strains and blends used in former clinical trials in IBD (i.e. *L. rhamnosus* GG, VSL#3 and *E. coli* strain Nissle[2,3,40,41]), which could further support

and validate the predictive value of the screening strategy presented in this paper.

In conclusion, our results linked *in vitro* and *in vivo* anti-inflammatory properties of a series of LAB and confirm that potential probiotic strains can be pre-screened *in vitro* for their immunomodulating potential, before animal and clinical investigations. This allows pre-selection of probiotics able to modulate the host immune system in a specific way while reducing considerably the use of animals for screening purposes. Besides these ethical considerations, the comparative study of strains carefully selected for either pro- or anti-inflammatory properties will assist further investigation of the mechanism(s) by which specific probiotics signal to the host.

COMMENTS

Background

Evidence exists for the protective role of selected probiotic strains in inflammatory bowel disease. Probiotic strains have clearly been shown to differ in their *in vitro* interaction with immunocompetent cells, especially in terms of cytokine responses. No clear link has been established so far between the *in vitro* immunomodulation potential (e.g. on PBMC's) of the probiotic strain and its ability to prevent experimental colitis in mice (e.g. in TNBS- induced colitis). The use of simple *in vitro* methods to select the most efficient strains for possible clinical trials will improve the quality and reduce the costs of this type of research.

Research frontiers

Improving gastrointestinal function is important for IBD patients and fundamental research is needed to develop new treatments for such pathogenesis. Probiotics are generally accepted to be one of these alternative methods. Few original research papers, however, have evaluated the potential of this approach by focusing on the level of the bacterial strain or strains used.

Probiotic-mediated immunomodulation represents an interesting option in the management of IBD and there is evidence that the immune system can be modulated by orally delivered bacteria. However, in some animal and clinical studies, probiotics did not show the expected beneficial effect. The selection of a successful protective strain may rely on a proper screening of a large number of candidate strains for their technological and immunomodulatory performance, as recently published in *WJG*. Together with proper *in vitro* analytical methods, the use of a reliable animal model is therefore indispensable. Using a well-standardized animal model, we have demonstrated that consistent differences in anti-inflammatory potential of several orally administered lactic acid bacteria could be observed in TNBS-induced colitis.

In the present study we linked for the first time the results of *in vitro* and *in vivo* anti-inflammatory readouts for 13 selected LAB, and confirmed herewith the strain-specific nature of the potential of probiotics to modulate the host's immune system and in assisting in the alleviation of intestinal disorders, IBD in particular.

Innovations and breakthroughs

Linking *in vitro* and *in vivo* anti-inflammatory properties of a series of LAB can confirm the interest of screening potential probiotic strains using *in vitro* assays, before launching animal and clinical investigations. This allows not only the pre-selection of probiotics able to modulate the host's immune system in a specific way while reducing considerably the use of animals for screening purposes, but also results in a classification of microorganisms that could be useful for the study or comparison of other probiotic properties. So, besides ethical considerations, the comparative study of strains carefully selected for either pro- or anti-inflammatory properties will assist further investigation of the mechanism(s) by which specific probiotics signal to the host.

Applications

The use of probiotic strains in IBD treatment has been controversial, because of some major drawbacks. The first is the type of inflammatory disease targeted (Crohn's disease on the one hand, with low success levels, *versus* ulcerative colitis and pouchitis where treatment was more successful). The second is that a comparison between a therapeutic preventive application in combination with or without traditional medication, is not always clear. The third is that the choice of strains or the mixture thereof is often made rather artificially and driven by available commercial preparations which are not necessarily developed or suitable for this type of medical application. Using the described selection procedure, the influence of well-selected strains (e.g. with expected positive and negative performance as anti-inflammatory agent) in different conditions (with or without traditional medication) of a selected animal model (prophylactic or therapeutic) can be evaluated unequivocally. The results should not only allow to select the best possible conditions for the follow-up clinical study but will also help to understand the underlying mechanisms and factors that influence the efficiency of the application.

Terminology

The TNBS mouse model of colitis is a hapten-induced experimental model (TNBS = 2, 4, 6-trinitrobenzene sulfonic acid), which has proven to be a very useful model for studying certain forms of human inflammatory bowel disease. This model has e.g. been used to show that an IL-12-driven, Th1 T cell-mediated inflammation of the colon is not only prevented by systemic administration of anti-IL-12 antibody, but can also be treated this way. Consequently anti-IL-12 is currently used in the treatment of Crohn's disease. Other studies with this model have established that mucosal inflammation and/or its prevention depend partially on a balance between pro-inflammatory Th1 T cell responses and anti-inflammatory TGF-β and IL-10 responses.

Peer review

This is an interesting study showing that *in vitro* assays using human PBMCs can partially translate to murine models of colitis giving an indication of the level of expected protection of this particular model of colitis using IL-10/IL-12 ratios. It would be interesting to discover whether this held out if colitis was induced before administration of the probiotic (perhaps a more physiological approach for therapy). However, this does offer some insight into prophylactic approaches for managing patients in remission.

REFERENCES

1 **Bergonzelli GE**, Blum S, Brussow H, Corthésy-Theulaz I. Probiotics as a treatment strategy for gastrointestinal diseases? *Digestion* 2005; **72**: 57-68

2 **Kruis W**, Fric P, Pokrotnieks J, Lukás M, Fixa B, Kascák M, Kamm MA, Weismueller J, Beglinger C, Stolte M, Wolff C, Schulze J. Maintaining remission of ulcerative colitis with the probiotic *Escherichia coli* Nissle 1917 is as effective as with standard mesalazine. *Gut* 2004; **53**: 1617-1623

3 **Gionchetti P**, Rizzello F, Helwig U, Venturi A, Lammers KM, Brigidi P, Vitali B, Poggioli G, Miglioli M, Campieri M. Prophylaxis of pouchitis onset with probiotic therapy: a double-blind, placebo-controlled trial. *Gastroenterology* 2003; **124**: 1202-1209

4 **Mahida YR**, Rolfe VE. Host-bacterial interactions in inflammatory bowel disease. *Clin Sci* (Lond) 2004; **107**: 331-341

5 **Hart AL**, Stagg AJ, Kamm MA. Use of probiotics in the treatment of inflammatory bowel disease. *J Clin Gastroenterol* 2003; **36**: 111-119

6 **Chapat L**, Chemin K, Dubois B, Bourdet-Sicard R, Kaiserlian D. *Lactobacillus casei* reduces CD8+ T cell-mediated skin inflammation. *Eur J Immunol* 2004; **34**: 2520-2528

7 **Maassen CB**, van Holten-Neelen C, Balk F, den Bak-Glashouwer MJ, Leer RJ, Laman JD, Boersma WJ, Claassen E. Strain-dependent induction of cytokine profiles in the gut by orally administered Lactobacillus strains. *Vaccine* 2000; **18**: 2613-2623

8 **McCarthy J**, O'Mahony L, O'Callaghan L, Sheil B, Vaughan EE, Fitzsimons N, Fitzgibbon J, O'Sullivan GC, Kiely B, Collins JK, Shanahan F. Double blind, placebo controlled trial of two probiotic strains in interleukin 10 knockout mice and mechanistic link with cytokine balance. *Gut* 2003; **52**: 975-980

9 **Fujiwara D**, Inoue S, Wakabayashi H, Fujii T. The anti-allergic effects of lactic acid bacteria are strain dependent and mediated by effects on both Th1/Th2 cytokine expression and balance. *Int Arch Allergy Immunol* 2004; **135**: 205-215

10 **Hessle C**, Andersson B, Wold AE. Gram-positive bacteria are potent inducers of monocytic interleukin-12 (IL-12) while gram-negative bacteria preferentially stimulate IL-10 produc-

tion. *Infect Immun* 2000; **68**: 3581-3586
11 **Kimoto H**, Mizumachi K, Okamoto T, Kurisaki J. New *Lactococcus* strain with immunomodulatory activity: enhancement of Th1-type immune response. *Microbiol Immunol* 2004; **48**: 75-82
12 **O'Mahony L**, O'Callaghan L, McCarthy J, Shilling D, Scully P, Sibartie S, Kavanagh E, Kirwan WO, Redmond HP, Collins JK, Shanahan F. Differential cytokine response from dendritic cells to commensal and pathogenic bacteria in different lymphoid compartments in humans. *Am J Physiol Gastrointest Liver Physiol* 2006; **290**: G839-G845
13 **Peña JA**, Rogers AB, Ge Z, Ng V, Li SY, Fox JG, Versalovic J. Probiotic *Lactobacillus* spp. diminish *Helicobacter hepaticus*-induced inflammatory bowel disease in interleukin-10-deficient mice. *Infect Immun* 2005; **73**: 912-920
14 **Christensen HR**, Frøkiaer H, Pestka JJ. Lactobacilli differentially modulate expression of cytokines and maturation surface markers in murine dendritic cells. *J Immunol* 2002; **168**: 171-178
15 **Hart AL**, Lammers K, Brigidi P, Vitali B, Rizzello F, Gionchetti P, Campieri M, Kamm MA, Knight SC, Stagg AJ. Modulation of human dendritic cell phenotype and function by probiotic bacteria. *Gut* 2004; **53**: 1602-1609
16 **Foligné B**, Nutten S, Steidler L, Dennin V, Goudercourt D, Mercenier A, Pot B. Recommendations for improved use of the murine TNBS-induced colitis model in evaluating anti-inflammatory properties of lactic acid bacteria: technical and microbiological aspects. *Dig Dis Sci* 2006; **51**: 390-400
17 **Foligné B**, Grangette C, Pot B. Probiotics in IBD: mucosal and systemic routes of administration may promote similar effects. *Gut* 2005; **54**: 727-728
18 **Grangette C**, Nutten S, Palumbo E, Morath S, Hermann C, Dewulf J, Pot B, Hartung T, Hols P, Mercenier A. Enhanced antiinflammatory capacity of a *Lactobacillus plantarum* mutant synthesizing modified teichoic acids. *Proc Natl Acad Sci USA* 2005; **102**: 10321-10326
19 **Wallace JL**, MacNaughton WK, Morris GP, Beck PL. Inhibition of leukotriene synthesis markedly accelerates healing in a rat model of inflammatory bowel disease. *Gastroenterology* 1989; **96**: 29-36
20 **Fedorak RN**, Madsen KL. Probiotics and the management of inflammatory bowel disease. *Inflamm Bowel Dis* 2004; **10**: 286-299
21 **Braat H**, van den Brande J, van Tol E, Hommes D, Peppelenbosch M, van Deventer S. *Lactobacillus rhamnosus* induces peripheral hyporesponsiveness in stimulated CD4+ T cells via modulation of dendritic cell function. *Am J Clin Nutr* 2004; **80**: 1618-1625
22 **Servin AL**. Antagonistic activities of lactobacilli and bifidobacteria against microbial pathogens. *FEMS Microbiol Rev* 2004; **28**: 405-440
23 **Riedel CU**, Foata F, Philippe D, Adolfsson O, Eikmanns BJ, Blum S. Anti-inflammatory effects of bifidobacteria by inhibition of LPS-induced NF-kappaB activation. *World J Gastroenterol* 2006; **12**: 3729-3735
24 **Llopis M**, Antolín M, Guarner F, Salas A, Malagelada JR. Mucosal colonisation with *Lactobacillus casei* mitigates barrier injury induced by exposure to trinitronbenzene sulphonic acid. *Gut* 2005; **54**: 955-959
25 **Oshima T**, Laroux FS, Coe LL, Morise Z, Kawachi S, Bauer P, Grisham MB, Specian RD, Carter P, Jennings S, Granger DN, Joh T, Alexander JS. Interferon-gamma and interleukin-10 reciprocally regulate endothelial junction integrity and barrier function. *Microvasc Res* 2001; **61**: 130-143
26 **He F**, Morita H, Ouwehand AC, Hosoda M, Hiramatsu M, Kurisaki J, Isolauri E, Benno Y, Salminen S. Stimulation of the secretion of pro-inflammatory cytokines by *Bifidobacterium* strains. *Microbiol Immunol* 2002; **46**: 781-785
27 **Sheil B**, McCarthy J, O'Mahony L, Bennett MW, Ryan P, Fitzgibbon JJ, Kiely B, Collins JK, Shanahan F. Is the mucosal route of administration essential for probiotic function? Subcutaneous administration is associated with attenuation of murine colitis and arthritis. *Gut* 2004; **53**: 694-700
28 **Cross ML**, Gill HS. Can immunoregulatory lactic acid bacteria be used as dietary supplements to limit allergies? *Int Arch Allergy Immunol* 2001; **125**: 112-119
29 **Osman N**, Adawi D, Ahrne S, Jeppsson B, Molin G. Modulation of the effect of dextran sulfate sodium-induced acute colitis by the administration of different probiotic strains of *Lactobacillus* and *Bifidobacterium*. *Dig Dis Sci* 2004; **49**: 320-327
30 **Shibolet O**, Karmeli F, Eliakim R, Swennen E, Brigidi P, Gionchetti P, Campieri M, Morgenstern S, Rachmilewitz D. Variable response to probiotics in two models of experimental colitis in rats. *Inflamm Bowel Dis* 2002; **8**: 399-406
31 **O'Mahony L**, McCarthy J, Kelly P, Hurley G, Luo F, Chen K, O'Sullivan GC, Kiely B, Collins JK, Shanahan F, Quigley EM. Lactobacillus and bifidobacterium in irritable bowel syndrome: symptom responses and relationship to cytokine profiles. *Gastroenterology* 2005; **128**: 541-551
32 **Peran L**, Camuesco D, Comalada M, Nieto A, Concha A, Diaz-Ropero MP, Olivares M, Xaus J, Zarzuelo A, Galvez J. Preventative effects of a probiotic, *Lactobacillus salivarius* ssp. *salivarius*, in the TNBS model of rat colitis. *World J Gastroenterol* 2005; **11**: 5185-5192
33 **Matsumoto S**, Hara T, Hori T, Mitsuyama K, Nagaoka M, Tomiyasu N, Suzuki A, Sata M. Probiotic *Lactobacillus*-induced improvement in murine chronic inflammatory bowel disease is associated with the down-regulation of pro-inflammatory cytokines in lamina propria mononuclear cells. *Clin Exp Immunol* 2005; **140**: 417-426
34 **Kim SW**, Choi SC, Choi EY, Kim KS, Oh JM, Lee HJ, Oh HM, Kim S, Oh BS, Kimm KC, Lee MH, Seo GS, Kim TH, Oh HC, Woo WH, Kim YS, Pae HO, Park DS, Chung HT, Jun CD. Catalposide, a compound isolated from catalpa ovata, attenuates induction of intestinal epithelial proinflammatory gene expression and reduces the severity of trinitrobenzene sulfonic Acid-induced colitis in mice. *Inflamm Bowel Dis* 2004; **10**: 564-572
35 **Schultz M**, Strauch UG, Linde HJ, Watzl S, Obermeier F, Göttl C, Dunger N, Grunwald N, Schölmerich J, Rath HC. Preventive effects of Escherichia coli strain Nissle 1917 on acute and chronic intestinal inflammation in two different murine models of colitis. *Clin Diagn Lab Immunol* 2004; **11**: 372-378
36 **Marceau M**, Dubuquoy L, Caucheteux-Rousseaux C, Foligne B, Desreumaux P, Simonet M. Yersinia pseudotuberculosis anti-inflammatory components reduce trinitrobenzene sulfonic acid-induced colitis in the mouse. *Infect Immun* 2004; **72**: 2438-2441
37 **Lamine F**, Eutamène H, Fioramonti J, Buéno L, Théodorou V. Colonic responses to *Lactobacillus farciminis* treatment in trinitrobenzene sulphonic acid-induced colitis in rats. *Scand J Gastroenterol* 2004; **39**: 1250-1258
38 **Varcoe JJ**, Krejcarek G, Busta F, Brady L. Prophylactic feeding of *Lactobacillus acidophilus* NCFM to mice attenuates overt colonic hyperplasia. *J Food Prot* 2003; **66**: 457-465
39 **Sanders ME**, Klaenhammer TR. Invited review: the scientific basis of *Lactobacillus acidophilus* NCFM functionality as a probiotic. *J Dairy Sci* 2001; **84**: 319-331
40 **Mimura T**, Rizzello F, Helwig U, Poggioli G, Schreiber S, Talbot IC, Nicholls RJ, Gionchetti P, Campieri M, Kamm MA. Once daily high dose probiotic therapy (VSL#3) for maintaining remission in recurrent or refractory pouchitis. *Gut* 2004; **53**: 108-114
41 **Prantera C**, Scribano ML, Falasco G, Andreoli A, Luzi C. Ineffectiveness of probiotics in preventing recurrence after curative resection for Crohn's disease: a randomised controlled trial with *Lactobacillus* GG. *Gut* 2002; **51**: 405-409
42 **Gasson MJ**. Plasmid complements of *Streptococcus lactis* NCDO 712 and other lactic streptococci after protoplast-induced curing. *J Bacteriol* 1983; **154**: 1-9
43 **Sambrook J**, Fritsch EF, Maniatis T. Molecular cloning: a laboratory manual, 2nd ed. New York: Cold Spring Harbor Laboratory, 1989

S- Editor Liu Y **L- Editor** Wang XL **E- Editor** Bai SH

PO Box 2345, Beijing 100023, China
www.wjgnet.com
wjg@wjgnet.com

World J Gastroenterol 2007 January 14; 13(2): 244-249
World Journal of Gastroenterology ISSN 1007-9327
© 2007 The WJG Press. All rights reserved.

BASIC RESEARCH

Rescue of the albino phenotype by introducing a functional tyrosinase minigene into Kunming albino mice

Dong Xiao, Ying Yue, Xin-Yan Deng, Bing Huang, Zhong-Min Guo, Yun Ma, Yi-Li Lin, Xun Hong, Huan Tang, Kang Xu, Xi-Gu Chen

Dong Xiao, Ying Yue, Xin-Yan Deng, Bing Huang, Zhong-Min Guo, Yun Ma, Yi-Li Lin, Xun Hong, Kang Xu, Xi-Gu Chen, Center of Experimental Animals, Sun Yat-sen University, Guangzhou 510080, Guangdong Province, China
Dong Xiao, Institute of Comparative Medicine and Center of Experimental Animals, Southern Medical University, Guangzhou 510515, Guangdong Province, China
Huan Tang, Department of Animal Science, College of Basic Medicine, the Third Military Medical University, Chongqing 400038, China
Supported by the National Natural Science Foundation of China, No. 30271177 and No. 39870676; National 9th Five-year Program, No. 101033; Major Science and Technology Projects of Guangdong Province, No. B602; Natural Science Foundation of Guangdong Province, No. 021903; Postdoctoral Fellowship Foundation of China (Series 29); Special Fund of Scientific Instrument Collaborative Share-net in Guangzhou. No. 2006176
Correspondence to: Xi-Gu Chen, Professor, Center of Experimental Animals, Sun Yat-Sen University, Guangzhou 510080, Guangdong Province, China. xiguchen@163.com
Telephone: +86-20-33151566 Fax: +86-20-87331230
Received: 2006-09-20 Accepted: 2006-11-24

Abstract

AIM: To use the tyrosinase minigene as a visual marker to perform microinjection training and improve the techniques related with transgene to greatly elevate the efficiency of gene transfer.

METHODS: A mouse tyrosinase minigene, i.e., TyBS, in which the 2.25-kb authentic genomic 5′ non-coding flanking sequence of mouse tyrosinase was fused to a mouse tyrosinase cDNA, was introduced into the fertilized eggs of outbred Kunming albino mice.

RESULTS: Of the 11 animals that developed from the injected eggs, two mice (P1 and #8) exhibited pigmented hair (P1) and eyes (P1 and #8), as confirmed by PCR analysis for the tyrosinase minigene integrated into the genome. When founder P1 was bred to Kunming male mouse, six progeny out of 11 offspring inherited the transgene and the pigmented-eye phenotype.

CONCLUSION: Taken together, these results suggest that this minigene encodes the active tyrosinase protein and that its 5′ flanking region contains the sequences regulating the expression of mouse tyrosinase gene as expected. We have rescued the albino phenotype by introduction and expression of a functional tyrosinase minigene in the Kunming albino mouse and the transgene can be passed to subsequent generation. These findings also indicate that TyBS can be a useful visual marker gene in the co-transgenic experiments.

© 2007 The WJG Press. All rights reserved.

Key words: Kunming mouse; Albino; Tyrosinase minigene; Transgenic mice; Melanization; Phenotypic rescue

Xiao D, Yue Y, Deng XY, Huang B, Guo ZM, Ma Y, Lin YL, Hong X, Tang H, Xu K, Chen XG. Rescue of the albino phenotype by introducing a functional tyrosinase minigene into Kunming albino mice. *World J Gastroenterol* 2007; 13(2): 244-249

http://www.wjgnet.com/1007-9327/13/244.asp

INTRODUCTION

Visible pigmentation in the mammals results from the synthesis and distribution of melanin in skin, hair bulbs and eyes[1-3]. Tyrosinase is the first and rate-limiting enzyme in the pathway for melanin production in melanocytes of the skin and eyes[1-3]. Mutation of the tyrosinase gene is a common cause of a similar phenotype in all vertebrates, known as albinism, due to a lack of melanin pigment[1,3]. In mouse, the albino phenotype is characterized by a total absence of pigmentation due to a mutation in the tyrosinase gene; several point mutations within the tyrosinase gene have been found, which can inactivate its function to result in oculocutaneous albinism (OCA)[1,3]. In mouse, the classical albino (*c*) mutation corresponds to a single-point mutation in the first exon of the tyrosinase gene, which brings about an amino acid mutation Cys103Ser, leading to the accumulation of a non-functional protein[4,5]. When mice are homozygous (*c*/*c*) for mutations that inactivate the tyrosinase gene, mice are albino regardless of the genotype at the other loci[1,3]. The entire common albino inbred strains of laboratory mice, such as FVB/N, BALB/c, *etc*, belonging to OCA, have the same point mutation in the tyrosinase gene, indicating that these strains are derived from a common ancestor[5]. The albino phenotype has been successfully corrected through the tyrosinase transgene, which can express the active tyrosinase in transgenic mice[5-18], rabbits[19], fish[20-22] and other vertebrates

expressing tyrosinase functional transgenes[23].

The Human and Model Organism Genome Projects have revealed the sequence information of many genes. A significant challenge for scientists over the next few decades is to annotate the human and model organism genomes with functional information. Genetically engineered mice will play a vital role in the study of the functional genome.

The production of transgenic mice, involving an intensive sequence of procedures in genetics, molecular biology, embryology and animal science, is usually time-consuming and labor-consuming. One problem with learning to do microinjections is that it can be a long wait between the time the microinjections are done and the time that the results are known, particularly if one waits until the microinjected embryos have developed into weaning age mice before screening. How to easily and rapidly assay for a successful pronuclear? There are a number of constructs that are particularly useful when learning to do microinjections. Among them, tyrosinase can be used to allow the visual identification of transgenic mice at birth in the first and all subsequent generations. Microinjection of a tyrosinase minigene into embryos from an albino mouse strain can result in gene cure of the albino defect and the pigment synthesis[5,6,18]. Pigmented mice with dark eyes can be easily identified by simply visible inspection at birth. In fact, the pigment epithelial cells of the retina begin to synthesize melanin by P10.5 of embryonic development[8,26] so that transgenic mice can be typically identified by visual inspection of the fetuses 2 wk after microinjection. The microinjection can be done using albino inbred strains (such as FVB/N and BALB/c) and inexpensive outbred albino strains (such as ICR and Kunming mice). Another advantage of the tyrosinase minigene is the fact that it is not detrimental to the health of the transgenic animals.

Therefore, we decided to use the tyrosinase minigene as a visual marker to perform microinjection training and improve the techniques related with transgene to greatly elevate the efficiency of gene transfer in our center.

MATERIALS AND METHODS

Production of the tyrosinase minigene transgenic mice

The tyrosinase minigene TyBS[5] used for microinjection was generously provided by Dr. P.A. Overbeek (Howard Hughes Medical Institute, Department of Cell Biology, Baylor College of Medicine, Houston, TX, USA) and Dr. F Beermann (Swiss Institute for Experimental Cancer Research, Switzerland).

Transgenic mice were generated by microinjection of single cell embryos using standard techniques[27]. The Kunming mouse strain, supplied by Center of Experimental Animals, Sun Yat-Sen University, was used as the source of embryos for the micromanipulation and for the subsequent breeding trials. For microinjection, the 4.1-kb fragment of tyrosinase minigene (Figure 1) was released free from the vector backbone of pTyBS[5] via digestion with *Eco*R I and *Kpn* I, thereafter isolated and purified using the QIA quick gel extraction kit (Qiagen, Hilden, Germany), diluted to a final concentration of 2

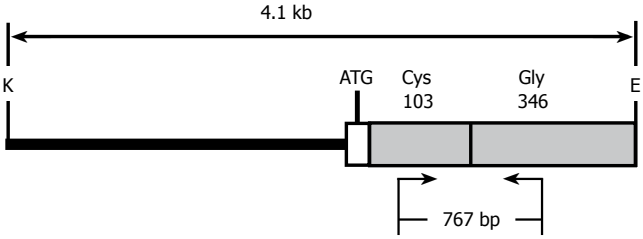

Figure 1 The structure of tyrosinase minigene construct TyBS used for microinjection. The construct contains a 2.25-kb tyrosinase promoter, i.e., 5' non-coding flanking sequence of mouse tyrosinase, as a single thick line plus 65 bp of tyrosinase exon I (to the *Xho* I site) and 1.785-kb *Xho* I-*Eco*R I fragment (shaded) (derived from Tyrs-J) containing tyrosinase cDNA and 3' non-coding flanking sequence. TyBS encodes cysteine at amino acid 103 and glycine at amino acid 346. The 4.1-kb injected fragment was obtained by pTyBS digestion with *Kpn* I and *Eco*R I. The restriction sites are: E, *Eco*R I; K, *Kpn* I. The primers specific for TyBS used in PCR reaction (small arrows) and the expected size of PCR products are indicated.

μg/mL DNA in injection buffer (10 mmol/L Tris/0.1 mmol/L EDTA, pH 7.4), and then microinjected into the pronuclear of one cell-stage fertilized embryos [Kunming mouse (♀) × Kunming mouse (♂)]. About 20-25 DNA-injected fertilized eggs that survived microinjection were implanted into the oviducts of one recipient pseudopregnant Kunming mouse 2-3 h after injection or the next day as previously described[27]. Potential transgenic founders were weaned at 3 wk of age. The offsprings were firstly screened for the presence of the transgene via pigmentation phenotypes derived from the existence of the functional tyrosinase minigene, followed by PCR analysis performed on the tail genomic DNA prepared with standard protocols[28]. All animal care and experimentation were performed according to the Study and Ethical Guidelines for Animal Care, handling and termination established by the Subcommittee of Sun Yat-Sen University on laboratory animal care. The presented work was approved by the ethical committee of Sun Yat-sen University and is covered by Chinese animal husbandary legislation.

Genotype analysis by PCR

PCR was performed on tail genomic DNA to further identify which mice have tyrosinase minigene integrated into their genome. The sequences of the forward primer (FP) within exon 1 and reverse primer (RP) within exon 4 used to amplify a 767-bp fragment of the tyrosinase minigene were: 5'-GGTTTCAACTGCGGAAACTG-3' (forward) and 5'-TGTGAGTGGACTGGCAAATC-3' (reverse) (Figure 1). PCR conditions were as follows: pre-denaturation at 94℃ for 7 min, followed by 30 amplification cycles of denaturation at 94℃ for 1 min, primer annealing at 58℃ for 1 min, and extension at 72℃ for 1 min 30 s, and finally an additional extension at 72℃ for 10 min. TyBS construct DNA was used as the positive control for each PCR reaction, and genomic DNA from normal Kunming mice was employed as a negative control for each PCR test. DNA samples were considered positive for a particular transgene if a band of the predicted size in the test samples was present with no amplification occurring in the control sample. Endogenous genomic

tyrosinase sequence was not amplified under this PCR conditions chosen here.

Mouse propagation and transmission

At 6-8 wk of age, founders shown to be transgenic for the tyrosinase minigene were mated with normal Kunming mice to generate F1. Pigmented F1 animals derived from founder, as well as albino non-transgenic littermates were further analyzed for the inheritance of the tyrosinase transgene by PCR using tyrosinase-FP/RP primers. PCR protocols for TyBS were noted above.

RESULTS

Rescue of the albino phenotype by tyrosinase transgene

Within the coding sequences of the tyrosinase gene, a G to C transversion at nucleotide 308, leading to a cysteine (Cys) to serine (Ser) mutation at amino acid 103, is sufficient to abrogate pigment production in mice[5]. This same base pair change is fully conserved in the classical albino strains of laboratory mice, such as FVB/N and BALB/c[5]. Albino Kunming mice are an outbred mouse strain that is homozygous mutant at the albino (*c*) locus. An albino mutation carried in the Kunming mouse strain should be also the result of a base substitution from G to C in exon I. It is, therefore, reasonable to expect that the albino phenotype can be rescued by introducing a functional tyrosinase minigene, such as TyBS, into albino embryos.

The tyrosinase minigene TyBS construct[5] used for microinjection is illustrated in Figure 1. As the expression of the tyrosinase minigene is easily detected by the pigmented phenotype, this gene can be used as a visual marker for the production of transgenic animals.

Of the 45 embryos transferred to the recipient females, 11 embryos developed to term. Two individuals of 11 siblings were transgenic, as demonstrated by pigmentation phenotype in the eyes (Figure 2A-D, F and G) and coat (Figure 2C, D and F), and PCR analyses (Figures 3A and B).

Furthermore, two TyBS transgenic mice, i.e. P1 (Figure 2A and B) and #8 (Figure 2G) which died 48 h after birth, had dark eyes at birth, and were immediately identifiable as transgenic mice. Although the extent of the coat pigmentation was non-standard like the wild-type phenotype, founder P1 exhibited the partially pigmented phenotype (Figure 2C, D and F). Over time, the coat of P1 with nearly black eyes (Figure 2A-D, F) became more heavily pigmented (light grey to dark grey) (Figure 2C, D and F), while the eye and fur phenotypes of non-transgenic littermate controls remained pink and albino throughout life (Figure 2C-E), respectively.

Transmissibility of the foreign transgene

To determine whether the TyBS transgene was transmitted to the next generation, at 6 wk of age female P1 was back-crossed to the parental mouse strain to give F1 generation. The progeny of P1 was analyzed for the inheritance of the transgene by eye phenotype, coat pigmentation and PCR.

From the cross between P1 and normal Kunming mouse, 11 offspring were obtained. Although all of littermates from P1 died immediately at birth, it was found that six out of the 11 siblings exhibited the pigmented eyes at birth (Figure 2H), as verified by PCR (Figure 3C).

Non-mosaic transgenic mice with one site of integration should transmit the transgenic DNA in a Mendelian fashion to about 50% of their offspring, whereas mosaic mice generally show a frequency of transmission of 25% or less. Note that founder mice that have more than one site of integration can produce litters where 75% or more of the offspring are transgenic, although the percent transmission for any one site of integration is expected to be average 50% or less[29,30]. It was concluded that founder P1, successfully transmitting the transgene in a Mendelian fashion to about 55% (6/11) of its progeny, is non-mosaic transgenic mouse.

Taken together, these data demonstrate that founder P1 can transmit the transgene to subsequent generation and its progeny show an inherited characteristic phenotype of pigmented eyes.

DISCUSSION

Coat color of the tyrosinase transgenic mice

Pigmentary genes are the first mammalian genes to be studied, mostly because of the obvious phenotypes associated with their mutations[23]. In this study, founder P1, harboring the tyrosinase minigene TyBS, exhibited light pigmentation, but non-standard wild-type coat color in the skin, although over time, P1 coat became more heavily pigmented. Similarly, the transgenic mice carrying TyBS construct showed considerable variation in the intensity of pigmentation, the coat colors were found to range from grayish to brownish, and none of the mice were black[5].

Actually, all these standard tyrosinase constructs, including TyBS, driven by the limited amount of 5' tyrosinase upstream regulatory sequences (ranging from 270- to 5500-bp promoter sequences) displayed a high degree of variability in coat pigmentation between independent lines[14,30-34], and the coat pigmentation did not reach the normal levels observed in the wild-type phenotype[6,18,30-32,35,36]. For example, in an evaluation of 39 transgenic founder animals and 44 transgenic lines, 5 phenotypic patterns of pigmentation were consistently observed, including albino, dark, light, mottled and Himalayan[32]. In fact, the tyrosinase minigene which is sufficient to produce normal levels of both eumelanin and phaeomelanin can give normal black or brown pigmentation on the appropriate non-agouti genetic backgrounds[5,32]. These abnormally expressional patterns might have been explained by position effects. In summary, these findings demonstrate that other regulatory regions within the tyrosinase gene are required to sustain the faithful expression of tyrosinase transgene, independent of integration site.

By flanking a tyrosinase minigene with tandem copies of the chicken β-globin 5' HS4 insulator, there is a significant reduction in variability among transgenic lines, with the resulting mice exhibiting the similar levels of coat pigmentation, which, in turn, improves the yield of phenotypically expected transgenic founders resulting from each microinjection session, and consequently reduces

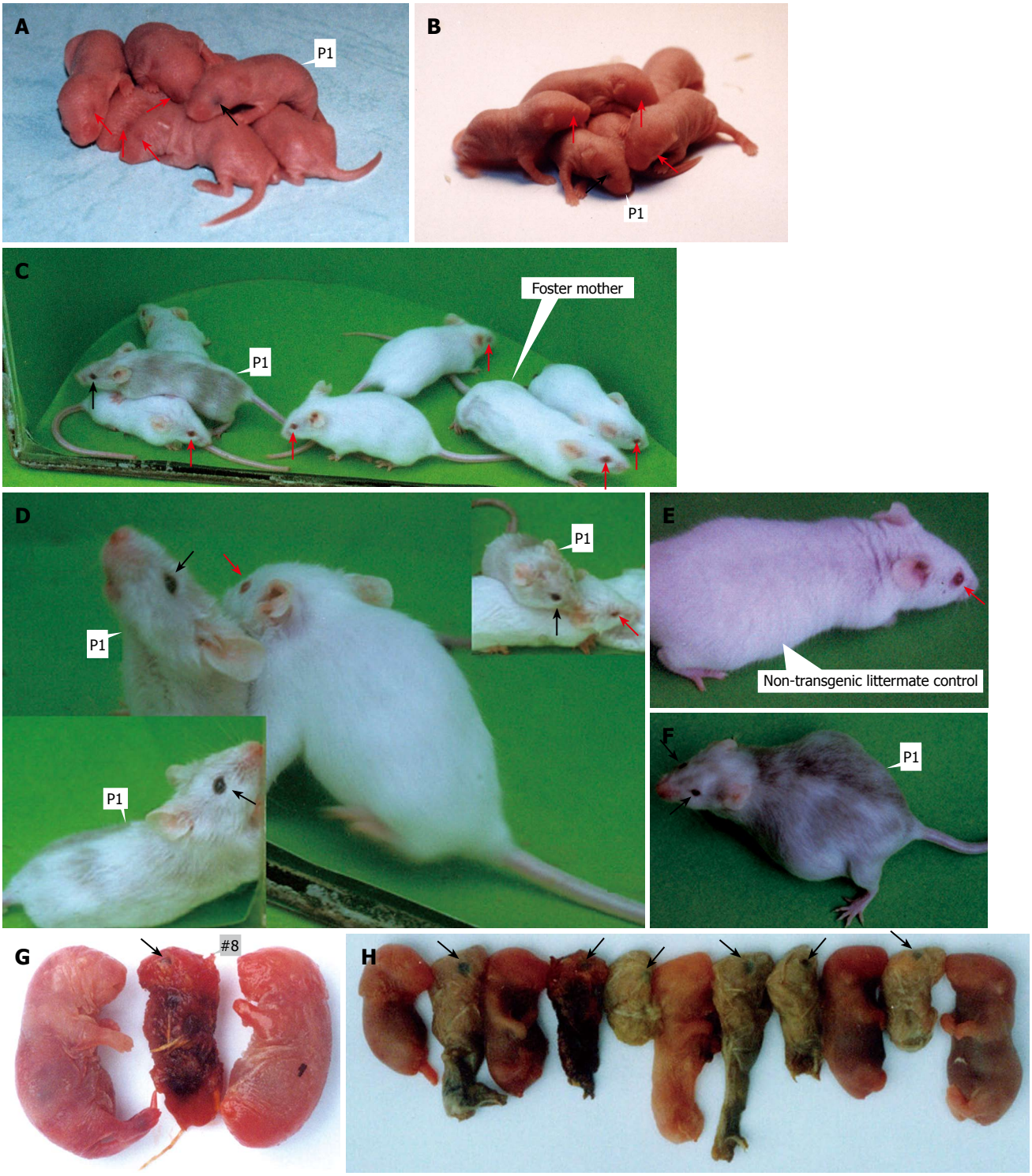

Figure 2 Eye and coat colors of tyrosinase minigene transgenic Kunming albino mice. One foster mother gave birth to six F0 pups (**A**-**F**); among the littermates, only one mouse (referred to as P1) had the pigmented eyes at birth. On July 15, another foster mother produced three F0 pups (**G**); of three siblings, only one mouse (referred to as #8) indicated the pigmented eyes at birth. P1 (♀) was crossed with normal Kunming albino mouse to give birth to 11 F1 offspring (**H**). All of the common albino strains of laboratory mice, such as FVB/N, BALB/c, and Kunming mouse (in China), have pink eyes and albino skin. (**A** and **B**) The **2**-d-old littermates. At birth, one pigmented mouse (P1) with dark eyes could be easily and immediately identified as a transgenic mouse by simple visual inspection. (**C**) The 4-wk-old littermates and Kunming albino foster mother. Founder P1 exhibited black eyes and light grey fur when compared to the non-transgenic littermate controls and Kunming albino foster mother with pink eyes and albino skin. No differences in phenotypes between transgenic mouse and the controls and foster mother except for melanization in eyes and hairs. Actually, the Kunming albino mouse was also used as a recipient strain for TyBS transgene in this project. (**D**) Eye color of the 4-wk-old P1 mouse compared with one of the non-transgenic littermates. One of the non-transgenic littermates (right of the middle map) had pink eyes, while at this age the heterozygote P1 (left of the middle map, upper and lower) had nearly black eyes. (**E** and **F**) The 8-wk-old non-transgenic littermate control and the adult P1 mouse (8-wk old), respectively. The non-transgenic littermate control (**E**, left) had pink eyes and albino coat, while at this age the heterozygote P1 mouse (**F**, right) had nearly black eyes and dark grey coat. Over time, the coat of P1 mouse became more heavily pigmented, while the eye and fur phenotypes of non-transgenic littermate control remained pink and albino throughout the life, respectively. (**G**) Eye color of the 1.5-d old #8 compared with its littermates. At birth, #8 with dark eyes could be easily and immediately identified as transgenic mice by simple visual inspection. Unfortunately, #8 as well as non-transgenic littermates without dark eyes were killed by foster mother 1.5 d after birth. **(H)** Eye color of F1 offspring (11) developed from mating of P1 and normal Kunming albino mouse. Founder P1 (♀) was back-crossed to normal Kunming albino mouse to produce eleven F1 generation. Unluckily, all of F1 offspring (11), born on September 8, died immediately at birth. P1 also deceased one month after delivery as it did not recover from giving birth to pubs. Of the 11 animals that developed from the mating aforementioned, six mice exhibited pigmented eyes. → and → indicate the pigmented eyes and non-pigmented eyes (pink), respectively.

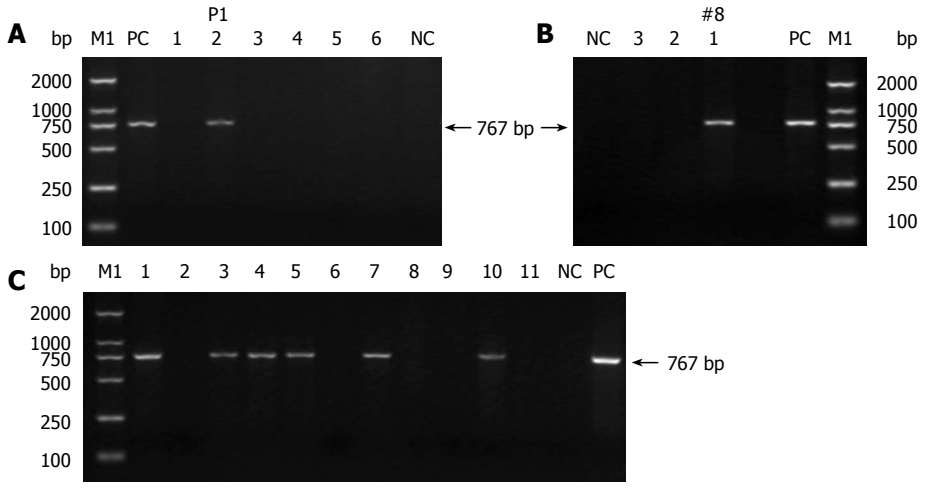

Figure 3 PCR detection of TyBS gene from genomic DNA of the potential transgenic founders (**A** and **B**) and subsequent generation(s) (**C**). Lane M1: DL 2000 DNA Marker (TaKaRa); lane PC: positive control (TyBS as template); lane NC: negative control using genomic DNA from normal Kunming mice as template. The arrows indicate the positions of PCR products amplified by the primers shown in Figure 1. (**A**) Littermates (F0, six mice) were verified for the transgene presence by PCR analysis. Lanes 1-6: genomic DNA from the potential founder(s) of 6 littermates; Lane 2: 767-bp band amplified from genomic DNA of P1 with pigmentation in the eyes. (**B**) Littermates (F0, three mice) were confirmed for the transgene presence by PCR analysis. Lanes 1-3: genomic DNA from the potential founder(s) of three siblings. Lane 1: 767-bp band amplified from genomic DNA of #8 with pigmentation in the eyes. Other details are as in Figure 2G. (**C**) Littermates (F1, 11 mice) were examined for the transgene presence by PCR analysis. The founder P1 (♀) was crossed with normal Kunming mouse to produce 11 littermates (F1) with six mice with pigmented eyes. Lanes 1-11: genomic DNA from F1 offspring derived from P1; Lanes 1, 3-5, 7, 10: 767-bp specific band amplified from genomic DNA of F1 offspring exhibiting pigmented eyes.

animal requirements for transgenic production[37].

Co-injection strategy for visually identifying the transgenic mice

Screening transgenic animals is usually time-consuming and labor-consuming. It would be very helpful if the transgenic animals could be identified by the visible inspection at birth. The functional tyrosinase gene introduced into an albino mouse strain leads to pigmentation in eyes and skin with high penetrance, and pigmented mice with dark eyes can be immediately identified by simply visible inspection at birth[23], as further confirmed by this study.

When two or several transgenic constructs are co-injected into single-cell fertilized embryos, the co-injected constructs typically co-integrate into the genome, where the transgene can independently express[38]. Theoretically, co-injection of tyrosinase transgenic construct with any other construct(s) should result in a certain percentage of transgenic mice carrying both transgenes at a single chromosomal site[23]. Additionally, co-injection experiments with the agouti transgenes and other transgenes demonstrated co-integration of the two constructs at the same chromosomal site in approximately 95% of F1 progeny, allowing transgene inheritance to be visibly detected[39]. The direct and visual detection of pigmentation in tyrosinase transgenic animals generated in the albino genetic backgrounds was repeatedly proposed by independent teams as a visual marker in co-injection strategies for the rapid detection of the successful tran sgenesis[12,30-33,35] and by our practices (data not shown). The utility of tyrosinase minigene co-injection with other construct(s) of interest is a useful adjunct to allow rapidly visual identification of transgenic mice at birth.

Moreover, another advantage of co-injection strategy is the fact that homozygous mice in most families can be identified by simply visual inspection, since the homozygous mice have darker coat colors, reflecting the increased gene dosage[32].

The co-injection strategy improves the yield of phenotypically desirable transgenic founder mice resulting from each microinjection session, and consequently reduces animal requirements for the transgenic production and routine genetic validation of transgenic lines.

In summary, we have successfully rescued the albino phenotype by introducing a functional tyrosinase gene into Kunming albino mouse. It should be pointed out here that TyBS and other tyrosinase transgenic constructs can be fused with any of the other genes and microinjected into fertilized eggs from albino murine strains in order to produce melanin pigments as an excellently visible marker for the generation and breeding of transgenic mice.

ACKNOWLEDGMENTS

We thank Dr. CY Fan (Department of Pathology and Otolaryngology, University of Arkansas for Medical Sciences, USA) for his unstinting advices and technical guidance in making transgenic mice, for his supportive and friendly attitude toward our projects. We thank Dr. F Beermann (Swiss Institute for Experimental Cancer Research, Switzerland) for kindly gifting the plasmids of ptrTyr5 and pTyBS, Dr. PA Overbeek (Howard Hughes Medical Institute, Department of Cell Biology, Baylor College of Medicine, Houston, TX, USA) for providing the vectors (e.g., pTyBS and pTy811C), and Professor G Schutz [Deutsches Krebsforschungszentrum (DKFZ), Heidelberg, Germany] for providing the plasmid ptrTyr5. We are also indebted to the expert technical assistance of JY Han, HH Zhang, GG Qiu, WG Huang, FY Chen, FR Ni, JY Xie and JH Wang, Center of Experimental Animals, Sun Yat-Sen University.

REFERENCES

1 **del Marmol V**, Beermann F. Tyrosinase and related proteins in mammalian pigmentation. *FEBS Lett* 1996; **381**: 165-168
2 **Nadeau JH**. Modifier genes in mice and humans. *Nat Rev Genet* 2001; **2**: 165-174
3 **Oetting WS**. The tyrosinase gene and oculocutaneous albinism type 1 (OCA1): A model for understanding the molecular biology of melanin formation. *Pigment Cell Res* 2000; **13**: 320-325
4 **Jackson IJ**. Molecular and developmental genetics of mouse coat color. *Annu Rev Genet* 1994; **28**: 189-217
5 **Yokoyama T**, Silversides DW, Waymire KG, Kwon BS, Takeuchi T, Overbeek PA. Conserved cysteine to serine mutation in tyrosinase is responsible for the classical albino mutation in laboratory mice. *Nucleic Acids Res* 1990; **18**: 7293-7298
6 **Beermann F**, Ruppert S, Hummler E, Bosch FX, Müller G, Rüther U, Schütz G. Rescue of the albino phenotype by introduction of a functional tyrosinase gene into mice. *EMBO J* 1990; **9**: 2819-2826
7 **Beermann F**, Schmid E, Ganss R, Schütz G, Ruppert S. Molecular characterization of the mouse tyrosinase gene: pigment cell-specific expression in transgenic mice. *Pigment Cell Res* 1992; **5**: 295-299
8 **Beermann F**, Schmid E, Schütz G. Expression of the mouse tyrosinase gene during embryonic development: recapitulation of the temporal regulation in transgenic mice. *Proc Natl Acad Sci USA* 1992; **89**: 2809-2813
9 **Ganss R**, Montoliu L, Monaghan AP, Schütz G. A cell-specific enhancer far upstream of the mouse tyrosinase gene confers high level and copy number-related expression in transgenic mice. *EMBO J* 1994; **13**: 3083-3093
10 **Jeffery G**, Brem G, Montoliu L. Correction of retinal abnormalities found in albinism by introduction of a functional tyrosinase gene in transgenic mice and rabbits. *Brain Res Dev Brain Res* 1997; **99**: 95-102
11 **Jeffery G**, Schütz G, Montoliu L. Correction of abnormal retinal pathways found with albinism by introduction of a functional tyrosinase gene in transgenic mice. *Dev Biol* 1994; **166**: 460-464
12 **Kang JK**, Kim JH, Lee SH, Kim DH, Kim HS, Lee JE, Seo JS. Development of spontaneous hyperplastic skin lesions and chemically induced skin papillomas in transgenic mice expressing human papillomavirus type 16 E6/E7 genes. *Cancer Lett* 2000; **160**: 177-183
13 Klüppel **M**, Beermann F, Ruppert S, Schmid E, Hummler E, Schütz G. The mouse tyrosinase promoter is sufficient for expression in melanocytes and in the pigmented epithelium of the retina. *Proc Natl Acad Sci USA* 1991; **88**: 3777-3781
14 **Porter SD**, Hu J, Gilks CB. Distal upstream tyrosinase S/MAR-containing sequence has regulatory properties specific to subsets of melanocytes. *Dev Genet* 1999; **25**: 40-48
15 **Schedl A**, Beermann F, Thies E, Montoliu L, Kelsey G, Schütz G. Transgenic mice generated by pronuclear injection of a yeast artificial chromosome. *Nucleic Acids Res* 1992; **20**: 3073-3077
16 **Takeuchi T**, Tanaka S, Tanaka M. Expression of tyrosinase gene in transgenic mice: programmed versus non-programmed expression. *J Invest Dermatol* 1993; **100**: 141S-145S
17 **Tanaka S**, Takeuchi T. Expression of tyrosinase gene in transgenic albino mice: the heritable patterned coat colors. *Pigment Cell Res* 1992; **5**: 300-303
18 **Tanaka S**, Yamamoto H, Takeuchi S, Takeuchi T. Melanization in albino mice transformed by introducing cloned mouse tyrosinase gene. *Development* 1990; **108**: 223-227
19 **Aigner B**, Brem G. Tyrosinase as a marker gene and model for screening transgenes in mice and rabbits. *Theriogenology* 1993; **39**: 177
20 **Hyodo-Taguchi Y**, Winkler C, Kurihara Y, Schartl A, Schartl M. Phenotypic rescue of the albino mutation in the medakafish (Oryzias latipes) by a mouse tyrosinase transgene. *Mech Dev* 1997; **68**: 27-35
21 **Fu L**, Mambrini M, Perrot E, Chourrout D. Stable and full rescue of the pigmentation in a medaka albino mutant by transfer of a 17 kb genomic clone containing the medaka tyrosinase gene. *Gene* 2000; **241**: 205-211
22 **Tseng FS**, Liao IC, Tsai HJ. Transient expression of mouse tyrosinase gene in albino walking catfish Clarias fuscus by subcutaneous microinjection. *Fish Sci* 1995; **61**: 163
23 **Giraldo P**, Montoliu L. Artificial chromosome transgenesis in pigmentary research. *Pigment Cell Res* 2002; **15**: 258-264
24 **Bockamp E**, Maringer M, Spangenberg C, Fees S, Fraser S, Eshkind L, Oesch F, Zabel B. Of mice and models: improved animal models for biomedical research. *Physiol Genomics* 2002; **11**: 115-132
25 **van der Weyden L**, Adams DJ, Bradley A. Tools for targeted manipulation of the mouse genome. *Physiol Genomics* 2002; **11**: 133-164
26 **Le Douarin N**. The Neural Crest. Cambridge: Cambridge University Press, 1997: 1-600
27 **Nagy A**, Gertsensten M, Vintersten K, Behringer R. Manipulating the Mouse Embryo: A Laboratory Manual. 3rd ed. New York: Cold Spring Harbor Press, 2003: 1-600
28 **Sambrook JE**, Fritsch F, Maniatis T. Molecular Cloning: A Laboratory Manual. 3rd ed. New York: Cold Spring Harbor Laboratory Press, 2001: 1-800
29 **Tymms MJ**, Kola I. Gene knockout protocols. Totowa: Humana Press Inc, 2001: 1-370
30 **Overbeek PA**. Factors affecting transgenic animal production. In: Pinkert CA. Transgenic Animal Technology: A Laboratory Handbook. San Diego: Academic Press Inc, 1994: 69-114
31 **Aigner B**, Brem G. Tyrosinase as a marker gene for studying transmission and expression of transgenes in mice. *Transgenics* 1994; **1**: 417-429
32 **Methot D**, Reudelhuber TL, Silversides DW. Evaluation of tyrosinase minigene co-injection as a marker for genetic manipulations in transgenic mice. *Nucleic Acids Res* 1995; **23**: 4551-4556
33 **Overbeek PA**, Aguilar-Cordova E, Hanten G, Schaffner DL, Patel P, Lebovitz RM, Lieberman MW. Coinjection strategy for visual identification of transgenic mice. *Transgenic Res* 1991; **1**: 31-37
34 **Porter SD**, Meyer CJ. A distal tyrosinase upstream element stimulates gene expression in neural-crest-derived melanocytes of transgenic mice: position-independent and mosaic expression. *Development* 1994; **120**: 2103-2111
35 **Beermann F**, Ruppert S, Hummler E, Schütz G. Tyrosinase as a marker for transgenic mice. *Nucleic Acids Res* 1991; **19**: 958
36 **Montoliu L**, Schedl A, Kelsey G, Lichter P, Larin Z, Lehrach H, Schütz G. Generation of transgenic mice with yeast artificial chromosomes. *Cold Spring Harb Symp Quant Biol* 1993; **58**: 55-62
37 **Potts W**, Tucker D, Wood H, Martin C. Chicken beta-globin 5'HS4 insulators function to reduce variability in transgenic founder mice. *Biochem Biophys Res Commun* 2000; **273**: 1015-1018
38 **Behringer RR**, Ryan TM, Palmiter RD, Brinster RL, Townes TM. Human gamma- to beta-globin gene switching in transgenic mice. *Genes Dev* 1990; **4**: 380-389
39 **Kucera GT**, Bortner DM, Rosenberg MP. Overexpression of an Agouti cDNA in the skin of transgenic mice recapitulates dominant coat color phenotypes of spontaneous mutants. *Dev Biol* 1996; **173**: 162-173

S- Editor Liu Y **L- Editor** Kumar M **E- Editor** Liu WF

PO Box 2345, Beijing 100023, China
www.wjgnet.com
wjg@wjgnet.com

World J Gastroenterol 2007 January 14; 13(2): 250-256
World Journal of Gastroenterology ISSN 1007-9327
© 2007 The WJG Press. All rights reserved.

BASIC RESEARCH

Antiproliferation and apoptosis induction of paeonol in HepG2 cells

Shu-Ping Xu , Guo-Ping Sun, Yu-Xian Shen, Wei Wei, Wan-Ren Peng, Hua Wang

Shu-Ping Xu, Yu-Xian Shen, Wei Wei, Institute of Clinical Pharmacology of Anhui Medical University, Key Laboratory of Antiinflammatory and Immunological Pharmacology in Anhui Province, Key Laboratory of Research and Development of Chinese Medicine of Anhui province, Hefei 230032, Anhui Province, China
Guo-Ping Sun, Wan-Ren Peng, Department of Oncology, The First Affiliated Hospital of Anhui Medical University, Hefei 230022, Anhui Province, China
Hua Wang, Department of Oncology, Provincial Hospital of Anhui, Hefei 230001, Anhui Province, China
Supported by the Natural Science Foundation of Anhui Province, No. 00044414, No. 050430901; the Key Project of the Natural Science Foundation of the Department of Education, Anhui Province, No. 2003Kj037zd and the Natural Science Foundation of the Department of Health, Anhui Province, No. 2002A025
Correspondence to: Dr. Guo-Ping Sun, Department of Oncology, The First Affiliated Hospital of Anhui Medical University, No. 210, Ji Xi Road, Hefei 230022, Anhui Province, China. sunguoping@ahmu.edu.cn
Telephone: +86-551-2922354
Received: 2006-09-09 Accepted: 2006-11-20

Abstract

AIM: To investigate the antiproliferative effect of paeonol (Pae) used alone or in combination with chemotherapeutic agents [cisplatin (CDDP), doxorubicin (DOX) and 5-fluorouracil (5-FU)] on human hepatoma cell line HepG2 and the possible mechanisms.

METHODS: The cytotoxic effect of drugs on HepG2 cells was measured by 3-(4, 5-dimethylthiazol-2-yl)-2, 5-diphenyltetra-zolium bromide (MTT) assay. Morphologic changes were observed by acridine orange (AO) fluorescence staining. Cell cycle and apoptosis rate were detected by flow cytometry (FCM). Drug-drug interactions were analyzed by the coefficient of drug interaction (CDI).

RESULTS: Pae (7.81-250 mg/L) had an inhibitory effect on the proliferation of HepG2 cells in a dose-dependent manner, with the IC_{50} value of (104.77 ± 7.28) mg/L. AO fluorescence staining and FCM assays showed that Pae induced apoptosis and arrested cell cycle at S phase in HepG2 cells. Further, different extent synergisms were observed when Pae (15.63, 31.25, 62.5 mg/L) was combined with CDDP (0.31-2.5 mg/L), DOX (0.16-1.25 mg/L), or 5-FU (12.5-100 mg/L) at appropriate concentrations. The IC_{50} value of the three drugs decreased dramatically when combined with Pae ($P < 0.01$). Of the three different combinations, the sensitivity of cells to drugs was considerably different.

CONCLUSION: Pae had a significant growth-inhibitory effect on the human hepatoma cell line HepG2, which may be related to apoptosis induction and cell cycle arrest. It also can enhance the cytotoxicity of chemotherapeutic agents on HepG2 cells, and the S phase arrest induced by Pae may be one of the mechanisms of these interactions.

© 2007 The WJG Press. All rights reserved.

Key words: Paeonol; Hepatocellular carcinoma; Apoptosis; Cell cycle; Cisplatin; Doxorubicin; 5-fluorouracil; Synergistic effect

Xu SP, Sun GP, Shen YX, Wei W, Peng WR, Wang H. Antiproliferation and apoptosis induction of paeonol in HepG2 cells. *World J Gastroenterol* 2007; 13(2): 250-256

http://www.wjgnet.com/1007-9327/13/250.asp

INTRODUCTION

Hepatocellular carcinoma (HCC) is the fifth most common cancer and the third leading cause of cancer-related death worldwide[1]. Eighty percent of the burden is borne by countries in Asia and Sub-Saharan Africa[2]. Although recent advances in management with a multidisciplinary approach results in improved local and regional disease control, the 5-year survival rate is still less than 10%[3]. Thus it is imperative to develop more effective and low-toxic chemotherapy agents.

Chinese herbal medicines are now attracting great attention in the world, which also show promising effects in treatment of cancers, including HCC[4]. Paeonol (Pae, 2-hydroxy-4-methoxyacetophenone, Figure 1), is a natural product extracted from the root of Paeonia Suffruticosa Andrew[5]. In our previous study, the antineoplastic activity of Pae has been demonstrated both in various cell lines[6] and in animal models[7,8]. The present study was designed to investigate the antiproliferative effect of Pae used alone or in combination with chemotherapeutic drugs [cisplatin (CDDP), doxorubicin (DOX) and 5-fluorouracil (5-FU)] on human hepatoma cell line HepG2 and the possible mechanisms.

MATERIALS AND METHODS

Cells and culture conditions

Human hepatocellular carcinoma cell line HepG2 was

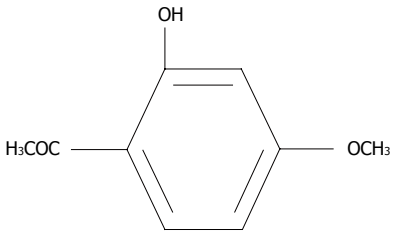

Figure 1 Structure of Pae (2-hydroxy-4-methoxyacetophenone).

purchased from Shanghai Institute of Hepatocarcinoma. HepG2 cells were cultured in Dulbecco's modified Eagle's medium (DMEM) supplemented with 10% fetal bovine serum (FBS) and incubated at 37℃ in a humidified atmosphere with 5% CO_2.

Drugs and reagents

Pae Injection was purchased from the First Pharmaceutical Factory of Shanghai, China (Cat. No. 990402, 10 mg/2 mL); CDDP Injection was purchased from Nanjing Pharmaceutical Co. Ltd, China (Cat. No. 20050602, 20 mg/20 mL); DOX was provided by Wanle Pharmaceutical Inc., Shenzhen, China (Cat. No. 0407E1, 10 mg/ampoule); 5-FU Injection was supplied by Shanghai Haipu Pharmaceutical Factory, China (Cat. No. 031109, 0.25 g/10 mL); DMEM was purchased from GIBCO BRL, Life Technologies Inc. (New York, USA); 3-[4, 5-dimethylthiazol-2-yl]-2, 5-diphenyltetra-zolium bromide (MTT) and acridine orange (AO) were from Sigma Co., USA. DNA-Prep-Reagents Kit was provided by Beckman Coulter Co. USA(Cat. No. 760279K).

In vitro cytotoxicity assay

HepG2 cells were seeded in 96-well plates at a density of 1-5 × 10^3 cells/well in 100 μL DMEM containing 10% FBS overnight. Nonadherent cells were removed by gentle washing. Then cells were treated with various concentrations of the drugs. After 44 h of drug exposure, 20 μL MTT solution (5 g/L) was added to each well for another 4 h at 37℃. The formazine was solved in 150 μL/well dimethyl sulfoxide (DMSO) and the absorbance was detected at 490 nm using ELx800 Strip reader (Bio-Tek, USA). The percentage of cytotoxicity was calculated as follows: Cytotoxicity (%) = (1-A_{490} of experimental well)/A_{490} of control well. The median inhibitory concentration (IC_{50}) (defined as the drug concentration at which cell growth was inhibited by 50%) was assessed from the dose-response curves.

Analysis of in vitro drug interaction

The coefficient of drug interaction (CDI) was used to analyze the synergistically inhibitory effect of drug combinations[9]. CDI is calculated as follows: CDI = AB/(A × B). According to the absorbance of each group, AB is the ratio of the combination groups to control group; A or B is the ratio of the single agent groups to control group. Thus CDI value less than, equal to or greater than 1 indicates that the drugs are synergistic, additive or antagonistic, respectively. CDI less than 0.7 indicates that the drugs are significantly synergistic.

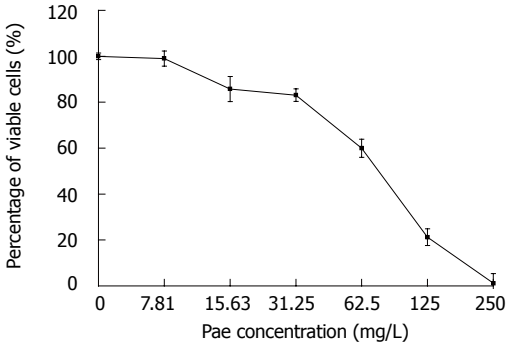

Figure 2 Dose-dependent cytotoxicity of Pae in HepG2 cells. Data are presented as mean ± SE (error bar) of triplicate experiments.

AO fluorescence staining

Cells were cultured in 6-well plates containing cover slips overnight. After incubation with Pae for 24 h, the cover slips were washed twice with PBS, fixed with 95% ethanol for 15 min, acidified with 1% acetic acid for 30 s, dyed with 0.1 g/L AO for 10 min, differentiated with 0.1 mol/L $CaCl_2$ for 2 min, and then washed with PBS 3 times. The cover slips were sealed and observed under a fluorescence microscope (OLYMPUS, Japan).

Flow cytometry assay

Cells were cultured in 6-well plates and allowed to grow to 75%-80% confluency. Nonadherent cells were removed by gentle washing, and the media were removed and replaced with fresh medium containing Pae at the desired concentrations. After exposure to drugs for 24 h, cells were collected and centrifuged at 1500 r/min in a 15 mL tube for 10 min. The cells were washed twice with PBS and resuspended in 50 μL fixing buffer at a room temperature for 20 s, then 500 μL propidium iodide (PI) staining buffer was added in the dark at room temperature for 30 min (according to the procedure program of the DNA-Prep Coulter reagents kit). A minimum of 1 × 10^5 cells for each group was analyzed using an EPICS XL-MCL model Coulter counter. Cell cycle distribution was analyzed using Mcycle software.

Statistical analysis

Biostatistical analyses were done using the SPSS 11.5 software package. All experiments were repeated at least three times. Results of multiple experiments are given as the mean ± SE. Non-parametric Kruskal-Wallis test was used to detect differences among the different experimental groups. Mann-Whitney *U* test was subsequently used for statistical evaluation in two-group comparisons. Pearson correlation coefficients were used for continuous independent and dependent variables. A level of $P < 0.05$ was accepted as statistically significant.

RESULTS

Effect of pae on the proliferation of HepG2 cells

We first examined the effect of Pae on the proliferation of HepG2 cells. As shown in Figure 2, a dramatic dose-

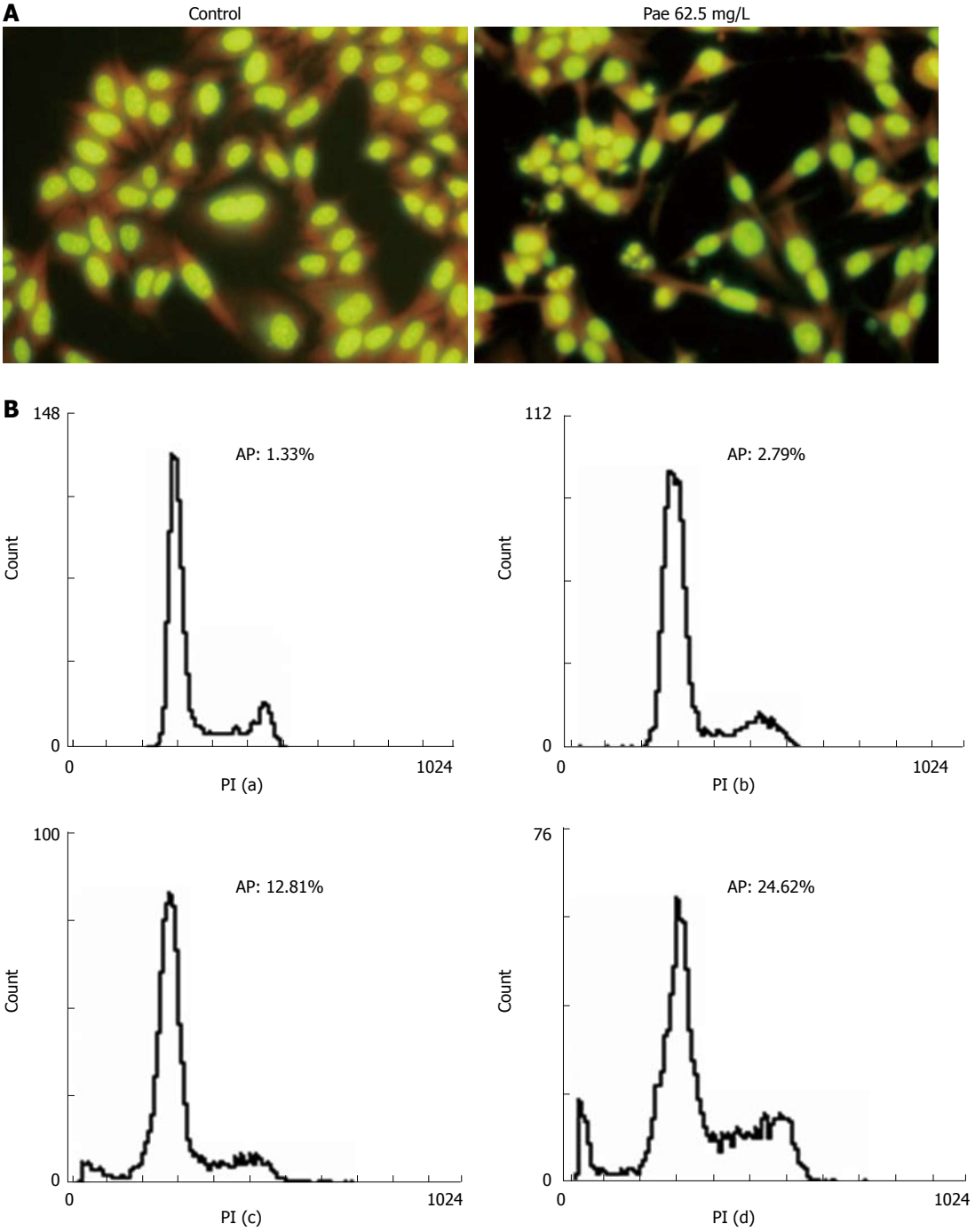

Figure 3 Effect of Pae on apoptosis in $HepG_2$ cells. **A**: Morphological changes of $HepG_2$ cells treated with Pae 62.5 mg/L (× 320); **B**: Flow cytometry analysis of $HepG_2$ cells treated with Pae for 24 h. (a). Control; (b).Pae 31.25 mg/L; (c).Pae 62.5 mg/L; (d).Pae 125 mg/L.

dependent reduction of cell viability was seen in cells incubated with Pae at concentrations of 7.81-250 mg/L for 48 h. The *r* value of dose-effect curves was 0.959 ($P < 0.01$) and the IC_{50} value of Pae was (104.77 ± 7.28) mg/L ($P < 0.01$).

Effects of Pae on apoptosis in $HepG_2$ cells

Morphological evidence of apoptosis was demonstrated by AO fluorescence staining. AO could be seen in all cells and the nuclei appeared green and chromatin was stained yellow (Figure 3A). Cells treated with Pae showed typically apoptotic changes, such as chromatin condensation, membrane blebing, deformed and fragmented nuclei.

FCM assay was performed to analyze apoptosis in $HepG_2$ cells treated with various concentrations of Pae for 24 h. It was found that the sub-G_1 peak appeared before G_1 phase, which represents apoptotic cell population (Figure 3B), in a dose- and time-dependent manner (Figure 4).

Effects of Pae on cell cycle in $HepG_2$ cells

Mcycle software was used to analyze the kinetic changes of cell cycle distribution. In untreated $HepG_2$ controls, cells were present in G_0/G_1 (71.79% ± 2.76%), S (20.31%

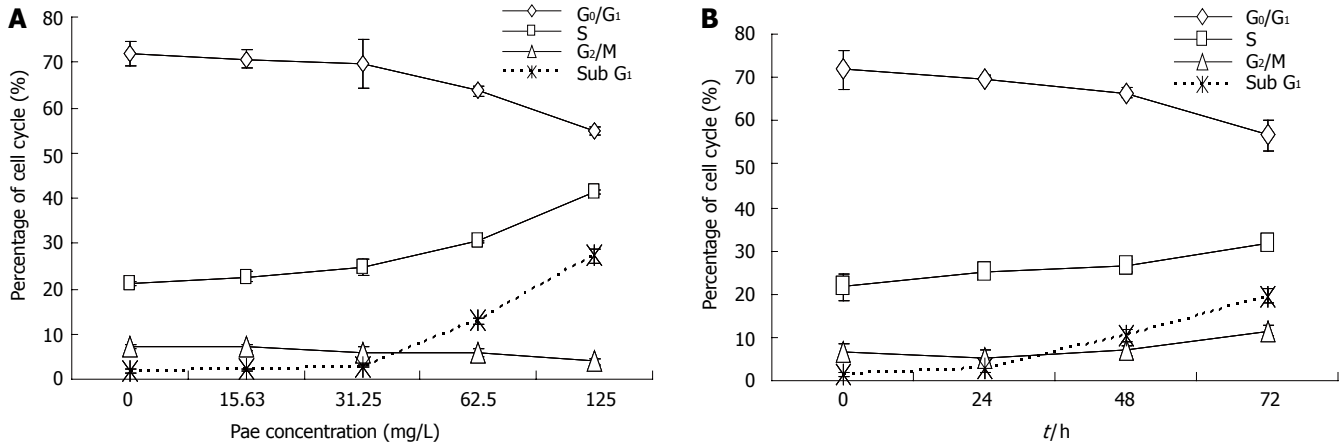

Figure 4 Effect of Pae on cell cycle in HepG2 cells. The distribution of cells in the sub-G1, G0/G1, S, and G2/M phases of the cell cycle were calculated and plotted. (**A**): Dose-dependent curve of cell cycle distribution induced by Pae. (**B**): Time-dependent curve of cell cycle distribution induced by Pae 31.25 mg/L. Each point represents triplicate experiments. Bars ± SE.

± 0.58%), and G2/M (7.16% ± 0.57%) phases. For HepG2 cells exposed to various concentrations of Pae, the S-phase fraction increased while G0/G1 fraction decreased in a dose-dependent manner (Figure 4A). And the percentages of cells in S phase increased to 24.98% ± 1.63%, 26.54% ± 1.53%, 31.72% ± 4.85% after 24, 48, and 72 h, respectively, when compared with untreated control cells, which was accompanied by a concomitant decrease of cells in the G0/G1 phase of the cell cycle (Figure 4B). It indicated that Pae might arrest the cell cycle at the S phase, and this blockage of cell cycle may prevent cells from entering M phase.

Pae enhancing the cytotoxicity of chemotherapeutic drugs on HepG2 cells

Growth-inhibition assays were performed to investigate whether Pae can enhance the antiproliferative effects of chemotherapeutic agents on HepG2 cells. Three doses of Pae (15.63, 31.25 and 62.5 mg/L) were combined with different concentrations of CDDP, DOX, and 5-FU, respectively. For each experiment, a dose-response curve of each single chemotherapeutic agent and its combination with Pae was drawn, which showed that Pae increased the cytotoxicity of CDDP, DOX, and 5-FU on HepG2 cells. The IC_{50} value of the three drugs decreased dramatically at different extents when combined with Pae. For example, in the presence of 15.63, 31.25 and 62.5 mg/L Pae, the IC_{50} of CDDP reduced from 0.591 ± 0.053 mg/L to 0.366 ± 0.011, 0.161 ± 0.018, 0.007 ± 0.002 mg/L, respectively. That of DOX reduced from 0.489 ± 0.124 mg/L to 0.175 ± 0.043, 0.037 ± 0.012, 0.032 ± 0.005 mg/L. And that of 5-FU reduced from 310.783 ± 13.094 mg/L to 161.759 ± 9.507, 8.646 ± 2.331, 5.021 ± 0.962 mg/L, respectively ($P < 0.01$, Figure 5A-C).

We analyzed the nature of the interaction between Pae and the three drugs using CDI, which quantitatively measures the interaction of two drugs. As shown in Figure 5D, Pae and CDDP yielded synergistic interactions across a wide concentration range. The synergistic effect was most prominent when 15.63 mg/L Pae was combined with 1.25 mg/L CDDP (CDI < 0.7). While a significant synergistic effect was only obtained when Pae concentration reached 31.25 and 62.5 mg/L in combination with 0.16 mg/L and 0.31 mg/L DOX, respectively. When DOX reached 1.25 mg/L, the interaction was antagonistic (Figure 5E). Pae had a relatively weak activity to enhance the antiproliferative effect of 5-FU in HepG2 cells. If the concentrations of drugs were too high or too low, the synergistic cytotoxic effects could not be achieved. The combinations of Pae at 31.25 mg/L and 5-FU at 12.5 and 25 mg/L exhibited significantly synergistic activity against HepG2 cells, while an antagonistic effect was observed at 62.5 mg/L of Pae in combination with 25-100 mg/L of 5-FU (Figure 5F).

DISCUSSION

Currently, a variety of cytotoxic and antiproliferative agents have been tested in HCC treatment, which are used alone, or in combination with other drugs or other treatment modalities[10]. Agents with partial response rates near or above 10% include DOX, CDDP and 5-FU[11-13]. However, high doses of these drugs lead to severe toxicities, which have a negative effect on patients' survival. The use of less toxic doses in combination with other anti-proliferative agents would be desirable[14-17].

Pae is isolated from the herb *Pycnostelma paniculatum* (Bunge) K.S., and the root of the plant *Paeonia Suffruticosa* Andrew[5]. It is a white needle crystal with a relatively low-melting point of 51℃-52℃. The molecular weight of Pae is 166.18 ku and the molecular formula is $C_9H_{10}O_3$[18]. Pae possesses extensive pharmacological activities such as sedation, hypnosis, antipyresis, analgesic, antioxidation, antiinflammation, and immunoregulation[19]. Additionally, Pae had minimal systemic toxicity (LD_{50} 3430 mg/kg) when it was orally administrated to mice[20]. In our previous study, the antineoplastic activity of Pae has been demonstrated both in cell lines, such as human erythromyeloid cell line K562, breast cancer gene cell line T6-17, human hepatoma cell line Bel-7404, and cervical

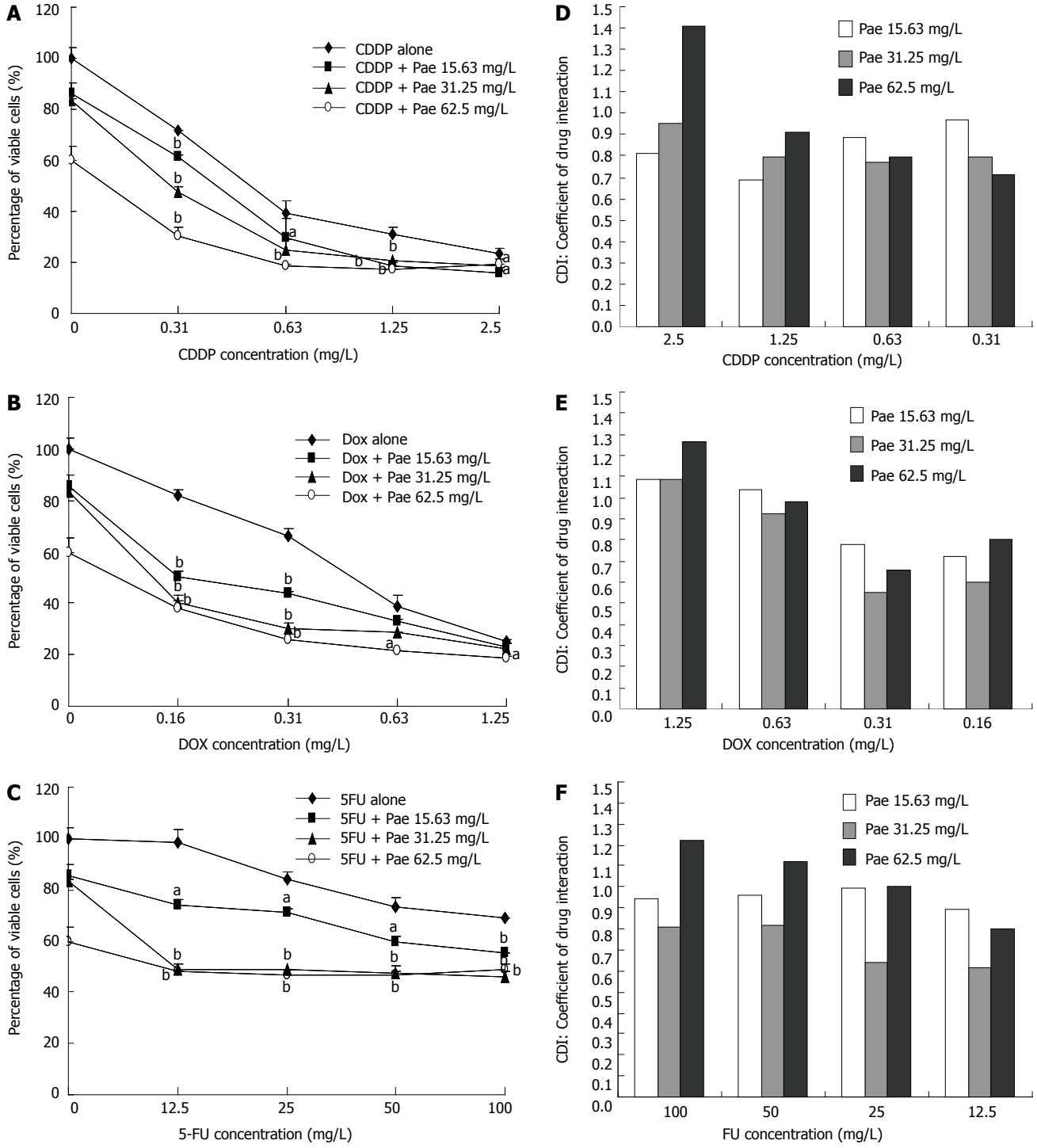

Figure 5 The synergistically antiproliferative effect of Pae combined with CDDP (**A**), DOX (**B**), or 5-FU (**C**) on HepG2 cells. The dots represent the concentrations of chemotherapeutic drugs as 0 on the dose-response curves which means treatment with Pae alone. Data are presented as mean ± SE of triplicate experiments. $^{a}P < 0.05$, $^{b}P < 0.01$, *vs* chemotherapeutic drugs alone. And CDI for the combination treatment of Pae with CDDP (**D**), DOX (**E**), or 5-FU (**F**) on HepG2 cells.

cancer cell line Hela[6], and in animal models bearing HepA hepatocarcinoma[7,8]. Ji *et al*[21] demonstrated that Pae at a low concentration had synergetic effects with 5-FU, MMC and CDDP on inhibiting the proliferation of human colorectal cancer cell line HT-29.

In the present study, Pae exhibited growth inhibition to HepG2 cells in a dose-dependent manner, with the IC_{50} value of 104.77 (± 7.28 mg/L) mg/L. Although the exact mechanism of the cytotoxicity of Pae against HepG2 cells is not entirely clear, many potential mechanisms have been proposed for the growth inhibition of Pae in cultured cells and animal models. These mechanisms include induction of apoptosis[22-23] and immunoregulation such as promoted lymphocyte proliferation, IL-2 production by splenocytes, and TNF-α production by PMφ from the model mice[7,8]. Apoptosis is a mechanism by which cells undergo death to control cell proliferation or in response to DNA damage. A tumor occurs when the balance of

cell proliferation and cell death is broken[24]. Induction of apoptosis is an effective strategy for cancer therapy[25]. In the present study, the cells treated with Pae showed typical characteristics of apoptosis. Similarly, apoptotic peak appeared before G_1 phase after treatment with Pae, which resulted from the internucleosomal degradation of DNA, in a dose- and time-dependent manner. Moreover, the $HepG_2$ cells exposed to Pae for 24 h showed depletion of the G_0/G_1 fraction and accumulation in S-phase. Accumulation in S-phase has also been reported by Liu *et al*[22], in which Pae could induce cell cycle disturbance and S phase of the HT-29 cells was increased, while G_0/G_1 and G_2/M phase of the cells were decreased. The S phase arrest and apoptosis induction of Pae on $HepG_2$ cells might be its main mechanism.

Meanwhile, $HepG_2$ cells were treated with the combinations of Pae and different chemotherapeutic agents. The results indicated that the growth inhibitory effect of CDDP, DOX, or 5-FU, respectively, was enhanced significantly by Pae at appropriate concentrations. Among the three agents examined, CDDP showed the most wide synergistic effect with Pae. The synergistic effect was most prominent (CDI < 0.7 =) when 15.63 mg/L Pae was combined with 1.25 mg/L CDDP. This indicated that the combination of Pae and CDDP at certain concentrations might help reduce nausea, vomiting and serious kidney toxicity of CDDP. Similar results that Pae in combination with anticancer drugs had synergistic effects at lower concentrations and had antagonistic effects at higher concentrations were observed in DOX and 5-FU, but with different sensitivities. The S phase arrest of Pae may be one of the mechanisms related with these interactions. 5-FU belongs to cell cycle specific agents, which acts specifically on cells in S phase[26]. The cytotoxic effects of CDDP and DOX are generally considered to be non-cell-cycle specific[27-28]. Nevertheless, DOX has the most killing effect on S phase cells[28]. CDDP is most specific to G_1 phase cells, while it also has strong effects on cells in S phase[29]. Further studies are needed to investigate the mechanisms of these synergisms, which favor the reasonable application of Pae to HCC treatment.

ACKNOWLEDGMENTS

We thank Dr. Zhimin Zhai and Qing Li for FACS analysis, the Central Laboratory of the Provincial Hospital of Anhui.

COMMENTS

Background

Hepatocellular carcinoma (HCC) is a major contributor to cancer incidence and mortality in the world. No effective treatment is available by now. Therefore, there is a critical need to develop more strategies for chemotherapy of hepatoma.

Research frontiers

Currently, a variety of cytotoxic and antiproliferative agents have been tested in HCC treatment, which are used alone, or in combination with other drugs or with different modalities of treatment. Chinese herbal medicines are now attracting great attention in the world, which also show promising effects in HCC therapy. Paeonol, a natural product extracted from the root of Paeonia Suffruticosa Andrew, has shown antineoplastic activities both in cell lines and in animal models.

Innovations and breakthroughs

This is the first report on the antiproliferation, induction of apoptosis and cell cycle arrest by Pae in $HepG_2$ cells.

Applications

Pae may be expected to be effective and useful as a new agent in hepatoma chemotherapy.

Peer review

The authors examine the cytotoxic effect of Pae only in $HepG_2$ cells. It remains unclear whether the effect of Pae in $HepG_2$ cells can be generalized to other hepatoma cells. The authors should examine the effect of Pae using a panel of hepatoma cell lines; The data in Figure 4 suggested that Pae induces S-phase arrest in $HepG_2$ cells. However, the molecular basis for S-phase arrest is not clearly shown. The authors should examine whether Pae has an effect in cells arrested at G_1/S phase using pre-treatment of cells such as hydroxyurea. It would be important to examine the expression of p21, p27 CDK1 and cyclinA after treatment with Pae.

REFERENCES

1 **Parkin DM**, Bray F, Ferlay J, Pisani P. Estimating the world cancer burden: Globocan 2000. *Int J Cancer* 2001; **94**: 153-156
2 **McGlynn KA**, London WT. Epidemiology and natural history of hepatocellular carcinoma. *Best Pract Res Clin Gastroenterol* 2005; **19**: 3-23
3 **Johnson PJ**. Hepatocellular carcinoma: is current therapy really altering outcome? *Gut* 2002; **51**: 459-462
4 **Shu X**, McCulloch M, Xiao H, Broffman M, Gao J. Chinese herbal medicine and chemotherapy in the treatment of hepatocellular carcinoma: a meta-analysis of randomized controlled trials. *Integr Cancer Ther* 2005; **4**: 219-229
5 **Riley CM**, Ren TC. Simple method for the determination of paeonol in human and rabbit plasma by high-performance liquid chromatography using solid-phase extraction and ultraviolet detection. *J Chromatogr* 1989; **489**: 432-437
6 **Sun GP**, Wang H, Shen YX, Xu SY. Inhibitory effects of paeonol on the proliferation on four tumor cell lines. *Anhui Yiyao* 2004; **8**: 85-87
7 **Sun GP**, Shen YX, Zhang LL, Zhou AW, Wei W, Xu SY. Study on immunomodulation and antitumor activity of paeonol in HepA tumor mice. *Zhongguo Yaolixie Tongbao* 2003; **19**:160-162
8 **Sun GP**, Shen YX, Zhang LL, Wang H, Wei W, Xu SY. Antitumor effect of paeonol in vitro and in vivo. *Anhui Keji Xueyuan Xuebao* 2002; **37**: 183-185
9 **Cao SS**, Zhen YS. Potentiation of antimetabolite antitumor activity in vivo by dipyridamole and amphotericin B. *Cancer Chemother Pharmacol* 1989; **24**: 181-186
10 **Zhu AX**. Systemic therapy of advanced hepatocellular carcinoma: how hopeful should we be? *Oncologist* 2006; **11**: 790-800
11 **Okada S**, Okazaki N, Nose H, Shimada Y, Yoshimori M, Aoki K. A phase 2 study of cisplatin in patients with hepatocellular carcinoma. *Oncology* 1993; **50**: 22-26
12 **Lai CL**, Wu PC, Chan GC, Lok AS, Lin HJ. Doxorubicin versus no antitumor therapy in inoperable hepatocellular carcinoma. A prospective randomized trial. *Cancer* 1988; **62**: 479-483
13 **Lin DY**, Lin SM, Liaw YF. Non-surgical treatment of hepatocellular carcinoma. *J Gastroenterol Hepatol* 1997; **12**: S319-S328
14 **Leung TW,** Patt YZ, Lau WY, Ho SK, Yu SC, Chan AT, Mok TS, Yeo W, Liew CT, Leung NW, Tang AM, Johnson PJ**.** Complete pathological remission is possible with systemic combination chemotherapy for inoperable hepatocellular carcinoma. *Clin Cancer Res* 1999; **5**: 1676-1681
15 **Yeo W**, Mok TS, Zee B, Leung TW, Lai PB, Lau WY, Koh J, Mo FK, Yu SC, Chan AT, Hui P, Ma B, Lam KC, Ho WM, Wong HT, Tang A, Johnson PJ. A randomized phase III study of doxorubicin versus cisplatin/interferon alpha-2b/doxorubicin/fluorouracil (PIAF) combination chemotherapy

for unresectable hepatocellular carcinoma. *J Natl Cancer Inst* 2005; **97**: 1532-1538

16 **Lee J,** Park JO, Kim WS, Park SH, Park KW, Choi MS, Lee JH, Koh KC, Paik SW, Yoo BC, Joh J, Kim K, Jung CW, Park YS, Im YH, Kang WK, Lee MH, Park K. Phase II study of doxorubicin and cisplatin in patients with metastatic hepatocellular carcinoma. *Cancer Chemother Pharmacol* 2004; **54**: 385-390

17 **Yin XY**, Lü MD, Liang LJ, Lai JM, Li DM, Kuang M. Systemic chemo-immunotherapy for advanced-stage hepatocellular carcinoma. *World J Gastroenterol* 2005; **11**: 2526-2529

18 **Mimura K**, Baba S. Determination of paeonol metabolites in man by the use of stable isotopes. *Chem Pharm Bull (Tokyo)* 1981; **29**: 2043-2050

19 **Sun YC**, Shen YX, Sun GP. Advances in the studies of major pharmacological activity of paeonol. *Zhongchengyao Zazhi* 2004; **26**: 579-582

20 **Jiang SP**, Chen YX. Advances in the research and its clinical application of Cynanchum paniculatum (Bge.) Kitag. Zhongguo Zhongyao Zazhi 1994; **19**: 311-314

21 **Ji CY**, Tan SY, Liu CQ. Inhibitory effect of paeonol on the proliferation of human colorectal cancer cell line HT-29 and its synergistic effect with chemotherapy agents. *Zhongguo Zhongyao Zazhi* 2005; **17**: 122-124

22 **Liu CQ**, Tan SY, Ji CY, Luo HS, Yu JP. The effects of paeonol on inhibiting the proliferation of human colorectal cancer cell line HT-29 and its molecule mechanism. *Zhongguo Yaolixie Tongbao* 2005; **21**: 1251-1254

23 **Sun GP**, Wang H, Shen YX, Zhai ZM, Wei W, Xu SY. Study on effects of paeonol in inhibiting growth of K562 and inducing its apoptosis. *Zhongguo Yaolixie Tongbao* 2004; **20**: 550-552

24 **Evan GI**, Vousden KH. Proliferation, cell cycle and apoptosis in cancer. *Nature* 2001; **411**: 342-348

25 **Kerr JF**, Winterford CM, Harmon BV. Apoptosis. Its significance in cancer and cancer therapy. *Cancer* 1994; **73**: 2013-2026

26 **Petru E,** Sevin BU, Haas J, Ramos R, Perras J. A correlation of cell cycle perturbations with chemosensitivity in human ovarian cancer cells exposed to cytotoxic drugs in vitro. *Gynecol Oncol* 1995; **58**: 48-57

27 **Bergerat JP**, Barlogie B, Göhde W, Johnston DA, Drewinko B. In vitro cytokinetic response of human colon cancer cells to cis-dichlorodiammineplatinum(II). *Cancer Res* 1979; **39**: 4356-4363

28 **Takahashi K**, Ebihara K, Honda Y, Nishikawa K, Kita M, Oomura M, Shibasaki C. Antitumor activity of cis-dichlorodiammineplatinum(II) and its effect on cell cycle progression. *Gan To Kagaku Ryoho* 1982; **9**: 624-631

29 **Potter AJ**, Rabinovitch PS. The cell cycle phases of DNA damage and repair initiated by topoisomerase II-targeting chemotherapeutic drugs. *Mutat Res* 2005; **572**: 27-44

S- Editor Liu Y **L- Editor** Zhu LH **E- Editor** Ma WH

PO Box 2345, Beijing 100023, China
www.wjgnet.com
wjg@wjgnet.com

World J Gastroenterol 2007 January 14; 13(2): 257-263
World Journal of Gastroenterology ISSN 1007-9327
© 2007 The WJG Press. All rights reserved.

CLINICAL RESEARCH

Detection of disseminated pancreatic cells by amplification of cytokeratin-19 with quantitative RT-PCR in blood, bone marrow and peritoneal lavage of pancreatic carcinoma patients

Katrin Hoffmann, Christiane Kerner, Wolfgang Wilfert, Marc Mueller, Joachim Thiery, Johann Hauss, Helmut Witzigmann

Katrin Hoffmann, Christiane Kerner, Johann Hauss, Helmut Witzigmann, Department of Visceral, Transplantation, Thoracic and Vascular Surgery, University of Leipzig, Germany
Wolfgang Wilfert, Marc Mueller, Joachim Thiery, Institute of Laboratory Medicine, Clinical Chemistry and Molecular Diagnostics, University of Leipzig, Germany
Correspondence to: Dr. Katrin Hoffmann, Department of General Surgery, Ruprecht Karls University of Heidelberg, Im Neuenheimer Feld 110, Heidelberg 69120, Germany. katrin.hoffmann@med.uni-heidelberg.de
Telephone: +49-6221-566110 Fax: +49-6221-564215
Received: 2006-09-05 Accepted: 2006-11-28

Abstract

AIM: To evaluate the diagnostic potential of cytokeratin-19 (CK-19) mRNA for the detection of disseminated tumor cells in blood, bone marrow and peritoneal lavage in patients with ductal adenocarcinoma of the pancreas.

METHODS: Sixty-eight patients with pancreatic cancer (n = 37), chronic pancreatitis (n = 16), and non-pancreatic benign surgical diseases (n = 15, control group) were included in the study. Venous blood was taken preoperatively, intraoperatively and at postoperative d 1 and 10. Preoperative bone marrow aspirates and peritoneal lavage taken before mobilization of the tumor were analyzed. All samples were evaluated for disseminated tumor cells by CK-19-specific nested-PCR and quantitative fluorogenic RT-PCR.

RESULTS: CK-19 mRNA expression was increased in 24 (64%) blood samples and 11 (30%) of the peritoneal lavage samples in the patients with pancreatic cancer. In 15 (40%) of the patients with pancreatic cancer, disseminated tumor cells were detected in venous blood and bone marrow and/or peritoneal lavage. In the peritoneal lavage, the detection rates were correlated with the tumor size and the tumor differentiation. CK-19 levels were increased in pT3/T4 and moderately/poorly differentiated tumors (G2/G3). Pancreatic cancer patients with at least one CK-19 mRNA-positive sample showed a trend towards shorter survival. Pancreatic cancer patients showed significantly increased detection rates of disseminated tumor cells in blood and peritoneal lavage compared to the controls and the patients with chronic pancreatitis.

CONCLUSION: Disseminated tumor cells can be detected in patients with pancreatic ductal adenocarcinoma by CK-19 fluorogenic RT-PCR. In peritoneal lavage, detection rate is correlated with tumor stage and differentiation. In the clinical use, CK-19 is suitable for the distinction between malignant and benign pancreatic disease in combination with other tumor-specific markers.

© 2007 The WJG Press. All rights reserved.

Key words: Tumor cell dissemination; Pancreatic cancer; Cytokeratin-19

Hoffmann K, Kerner C, Wilfert W, Mueller M, Thiery J, Hauss J, Witzigmann H. Detection of disseminated pancreatic cells by amplification of cytokeratin-19 with quantitative RT-PCR in blood, bone marrow and peritoneal lavage of pancreatic carcinoma patients. *World J Gastroenterol* 2007; 13(2): 257-263

http://www.wjgnet.com/1007-9327/13/257.asp

INTRODUCTION

Pancreatic cancer is one of the top five causes of cancer death in the Western world. The 5-year survival rates are around 4%[1,2]. Tumor resection is associated with prolonged survival and postoperative adjuvant chemotherapy may further improve long-term results[3,4]. However, curative treatment of most patients fails due to local recurrence and hepatic metastases occurring within two years after surgery[5,6]. Occult micro-metastases caused by disseminated tumor cells are the most limiting factor for the improvement of mortality rates. Their influence on prognosis and development of new therapeutic strategies has not yet been completely elucidated.

Disseminated tumor cells are not ascertainable with current staging methods. Additional to cytology, immunohistochemical analysis is the standard for identification of tumor cells. Despite improvement of detection rates by conventional cytology, conflicting result regarding the prognostic relevance have been reported[7]. Several studies focused on molecular biological approaches for the qualitative or semi-quantitative verification of tumor cell dissemination in pancreatic cancer[8-12]. Reverse transcriptase polymerase chain reaction (RT-PCR) has a high sensitivity and allows the identification of approximately 1 tumor cell in 10^7 normal peripheral mononuclear blood cells[13]. Using qualitative PCR methods, varying frequency of gene transcripts and false positive results have been reported[14-16]. Therefore, tumor cell detection in patients with ductal adenocarcinoma of the pancreas is still a matter of debate.

Nowadays CEA and CA 19-9 are established as clinical markers for pancreatic cancer. However, expressions of these antigens have also been reported in cholangitis, chronic pancreatitis and various gastrointestinal tumors[17]. Various studies used cytokeratin-19 (CK-19) for pancreatic cell detection. CK-19 has been identified as a reliable marker for epithelial cell differentiation[18]. It is specific for undifferentiated pancreatic ductal cells and homogenously expressed at high levels in primary pancreatic adenocarcinoma and pancreatic carcinoma metastases[19,20]. CK-19 is not expressed in hematopoetic cells and therefore suited for detection of disseminated pancreatic cells in the peripheral blood[19,21].

Here, we report on the expression of CK-19 mRNA in blood, bone marrow and peritoneal lavage in 68 patients. Nested-PCR and quantitative fluorogenic RT-PCR were used to detect dissemination of pancreatic cells in patients with pancreatic cancer, chronic pancreatitis and non-pancreatic benign surgical diseases. The purpose of this study was to evaluate the potential of qualitative nested-PCR and quantitative RT-PCR for the detection of disseminated pancreatic cells and the differentiation between chronic pancreatitis and pancreatic cancer.

MATERIALS AND METHODS

Patients

This prospective study was approved by the Ethical Commission of the University of Leipzig and informed written consent was obtained from each patient. Peripheral blood samples, bone marrow aspirations and peritoneal lavage of 68 patients were analyzed. Thirty-seven patients with histologically confirmed primary pancreatic cancer, 16 patients with chronic pancreatitis and 15 controls with non-pancreatic benign surgical diseases participated in the study. In all patients, diagnosis was confirmed by the resected specimen or tumor biopsy for non-resectable cancers (n = 11). Patients with pancreatic cancer were staged according to the UICC guidelines 2005[22]. According to the UICC stage, 4 (10%) patients had stage Ⅰ, 3 (8%) stage Ⅱ, 19 (51%) stage Ⅲ, and 11 (29%) stage Ⅳ pancreatic cancer. The survival time of the patients ranged between 3 and 48 mo (median survival: 12 mo). Patients with cancer of the common bile duct, the ampulla of Vater or the duodenum were excluded from the study.

Samples

Four blood samples were obtained from each patient through central venous catheter 30 min preoperatively, intraoperatively after mobilization of the pancreas and 24 h as well as 10 d after the operation. Bone marrow samples were obtained after induction of general anesthesia by aspiration from the iliac crest and heparinized. Peritoneal lavage was performed immediately after exploration of the abdominal cavity. About 500 mL of sterile isotonic sodium chloride solution was instilled, removed after irrigation and then EDTA buffer was added.

RNA extraction and cDNA synthesis

All samples were diluted and washed with 10 mL of erythrocyte lysis buffer. The mononuclear cell fraction was isolated by Ficoll-Isopaque (Amersham, Braunschweig, Germany). Total RNA was extracted using guanidinium-isothiocyanate-phenol-chloroform-based method (Trizol, Gibco BRL, Life Technologies, Gaithersburg, USA). RNA integrity was checked electrophoretically and quantified spectrophotometrically. First strand cDNA was generated from 3 μg of total RNA diluted with 10 μL of RNase-free water using 1 μL of Random Hexamer Primer (Roche Diagnostics, Basel, Switzerland) and incubated for 10 min at 68℃. After chilling on ice, 7 μL of master mixture, according to Superscript Ⅱ kit (Invitrogen, Carlsbad, USA), was added and after 60 min of incubation at 42℃, the reaction was inactivated for 10 min at 80℃.

Qualitative nested-PCR

Qualitative analysis of CK-19 expression was carried out using nested-PCR. Two different pairs of primer (n-PCR1/n-PCR2) were designed. The second set of primers amplifies inside the amplification sites of n-PCR1 primers to improve the specificity of PCR. Then 5 μL of cDNA was diluted with 45 μL of mixture containing 1 μL of each n-PCR1 primer, 10 × PCR buffer, dNTP PCR, AmpliTaq polymerase (Perkin Elmer Life and Analytical Sciences, Boston, USA) and DNase-free water for first round PCR. The conditions for PCR step one and two were one cycle at 95℃ for 3 min, followed by 40 cycles at 57℃ for 20 s, 72℃ for 50 s and a final extension at 72℃ for 10 min. For second round PCR, 1 μL of aliquot of the first round PCR product was added to 49 μL of master mixture containing 1 μL of each n-PCR2 primer. Two negative controls were included per run. Ten microliters of all PCR products were electrophoresed on 20 g/L agarose gels and visualized after ethidium bromide staining (Table 1).

Quantitative RT-PCR

CK-19 and housekeeping genes beta-actin primers and fluorogenic probes were designed using Primer Express software (Primerexpress Version 2.0, Perkin Elmer) (Table 1). PCR primers and probes have been positioned to span exon-intron boundaries. Amplification and detection of CK-19 a and b pseudogen are unlikely because probe and

Table 1 Sequences for quantitative RT-PCR and nested-PCR primers and flourescent probes

	Forward primer	Reverse primer	Length (bp)
TaqMan primer CK-19	5'-GAAGGCCTGAAGGAAGAGCTG-3'	5'-CCTCCCACTTGGCCCCT-3'	80
TaqMan primer beta-actin	5'-TCCAGAGGCGCTCTTCCA-3'	5'-CGCACTTCATGATCGAGTTGA-3'	86
Vector primer CK-19	5'-AACTCCAGGATTGTCCTGCAG-3'	5'-TCCCGGTTCAATTCTTCAGTC-3'	401
Vector primer beta-actin	5'-GCACCACTGGCATTGTCATG-3'	5'-CCACACGGAGTACTTGCGC-3'	581
Nested-PCR primer CK-19	5'-AACTCCAGGATTGTCCTGCAG-3'	5'-TCCCGGTTCAATTCTTCAGTC-3'	401
Nested-PCR primer CK-19	5'-GAAGGCCTGAAGGAAGAGCTG-3'	5'-CCTCCCACTTGGCCCCT-3'	80
Probe CK-19	5'-CCTACCTGAAGAAGAACCATGAGGAGGAAATCAGTA-3'		
Probe beta-actin	5′-CCTCCTTCCTGGGCATGGAGTCCTG-3′		

primer contain several mismatches. mRNA quantification was carried out using the one tube, one enzyme fluorogenic RT-PCR protocol[23]. Ten microliters of cDNA was diluted with 40 μL of master mixture containing TaqPolymerase, dNTP mixture and 10 × AmpliTaq buffer A, 200 nmol/L probe, 900 nmol/L primer and 25 mmol/L $MgCl_2$. After 10 min of denaturation at 95℃, PCR was carried out for 40 cycles at 95℃ for 15 s and extension at 60℃ for 60 s in the presence of the probe. RT-PCR monitoring was achieved by measuring the fluorescent signal of the probe at the end of the annealing phase of each cycle. mRNA quantification was recorded and analyzed with the ABI 7700 Prism Sequence detection system (Perkin Elmer Applied Biosystems, Foster City, CA, USA). Two no-template controls were used to monitor contamination in every run. Accurate quantification was achieved through generation of standard curves by serial dilution of CK-19 and beta-actin RNA transcribed by RNA polymerase. The sensitivity of the technique was evaluated by serial control analysis obtained in dilution experiments with CK-19-expressing cancer cell lines (CaPan2, PANC1). It was possible to detect the CK-19 mRNA expression of one cell of the cell lines in 1 mL of normal peripheral blood.

Evaluation criteria

For nested-PCR, the samples were tested twice. If a CK-19 signal was detected, the sample was judged positive. The fluorogenic RT-PCR assay was done twice for each sample. The average value of both duplicates for each sample was used as quantitative value. Samples were excluded from the investigation if the expression of the house-keeping gene beta-actin was below 10^6 copies. The ratio of copies of CK 19 mRNA per 10^6 copies of beta-actin mRNA was used for further analysis. The introduction of a cut-off was required, due to high illegitimate background transcription in the control group. The samples which exceeded the maximum value of the CK-19 mRNA expression in the control group were defined as CK-19 mRNA-positive.

Statistical analysis

Mann-Whitney rank sum test was used for quantitative analysis to asses the differences in the means. Fisher's exact test was used for qualitative analysis. Two-tailed *P* value less than 0.05 was considered statistically significant. Kaplan-Meier and log-rank test were used for analysis of survival. Statistical analysis was carried out using SigmaStat 1.0 software (Jandel Scientific Corp., Erkrath, Germany).

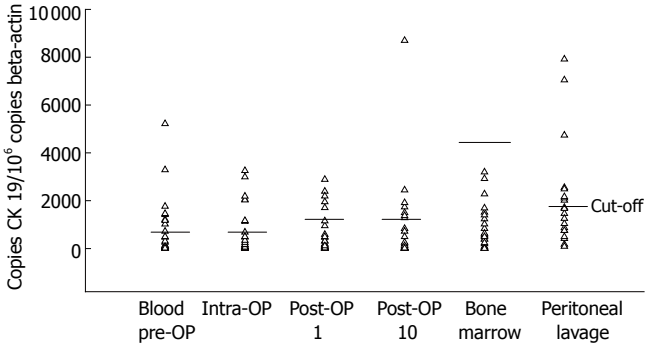

Figure 1 Quantitative values of cytokeratin-19 transcription in blood, bone marrow and peritoneal lavage of the patients with pancreatic cancer. [1]Cut-off: Maximal expression of CK-19 mRNA in healthy control patients.

RESULTS

Qualitative nested-PCR

CK-19 mRNA expression was detectable in the blood in 65% (24/37) of the patients with pancreatic cancer, 53% (8/16) of the patients with chronic pancreatitis and 18% (3/15) of the control group. The analysis of the bone marrow samples revealed detectable CK-19 mRNA in 56% (21/37) of pancreatic cancer patients, 46% (7/16) of chronic pancreatitis patients and 66% (10/15) of the control group. In 51% (19/37) of the patients with pancreatic cancer and 46% (7/16) of the patients with chronic pancreatitis and 46% (7/15) of the control group, CK-19 mRNA was detectable in the peritoneal lavage. There was no statistically significant difference between the groups.

Quantitative real-time RT-PCR

Blood, bone marrow and peritoneal lavage samples of 37 patients with pancreatic cancer were analyzed by CK-19 fluorogenic RT-PCR. CK-19 mRNA transcripts were detected in 70% (26/37) of blood samples, 67% (25/37) of bone marrow aspirates and 54% (20/37) of peritoneal lavage samples. In 40% (15/37) of the patients, PCR result was obtained from at least two compartments. We found that 64% (24/37) of the blood samples and 30% (11/37) of the peritoneal lavage samples showed CK-19 mRNA expression above the cut-off value and were defined as CK-19 mRNA-positive (Figure 1).

The CK-19 signal exceeded the cut-off value in 21% (8/37) of the pre-operatively and 19% (7/37) of the

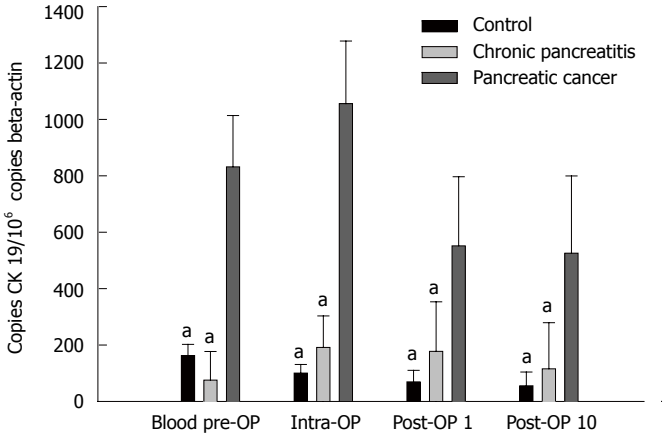

Figure 2 Quantitative analysis of CK-19 expression in blood (mean ± SD). $^{a}P < 0.05$ *vs* pancreatic cancer.

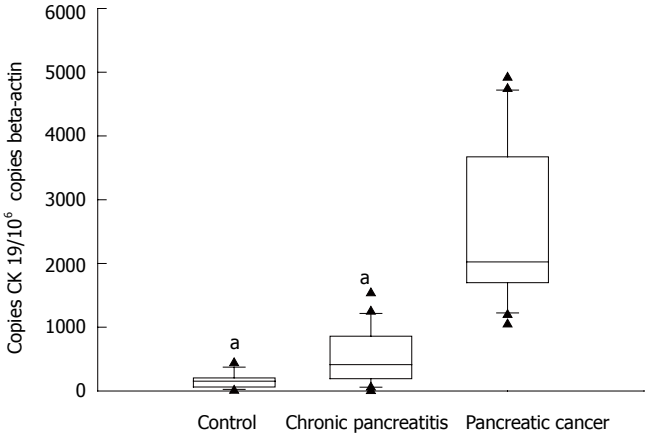

Figure 3 Quantitative CK-19 expression in peritoneal lavage of the patients with pancreatic cancer (mean ± SD, $^{a}P < 0.05$ *vs* pancreatic cancer).

intraoperatively taken blood samples. Likewise, 13% (5/37) of the samples taken at the first postoperative day and 10% (4/37) of the samples taken at the 10th postoperative day showed expression of CK-19 mRNA. The median mRNA expression was significantly increased in the patients compared to the control group at the four time points ($P < 0.05$) (Figure 2). The CK-19 levels showed a trend to increase intraoperatively and decrease at the 1st and 10th postoperative days below the pre-operative level ($P = 0.07$). We found 64% (24/37) of the bone marrow samples exhibited detectable CK-19 mRNA expression. None of the samples exceeded the CK-19 mRNA expression of the control group. The detection rate was not statistically different. In the peritoneal lavage, CK-19 signal was detected in 54% (20/37); 30% (11/37) of these samples exceeded the maximum level of the control group and were found to be CK-19 mRNA-positive. Compared to the control group, the median CK-19 mRNA expression was at least 10-fold increased (533 ± 121 copies CK-19/10^6 copies beta-actin *vs* 6262 ± 557 copies CK 19/10^6 copies beta-actin, $P < 0.01$) (Figure 3) .

The correlation analysis of marker detection and stage of disease was performed for blood, bone marrow and peritoneal lavage. In peritoneal lavage, CK-19 mRNA levels correlated with the tumor size and were increased 3 times in the patients with a pT3/pT4 tumor compared to the patients with pT1/pT2 tumors (874 ± 87 copies/10^6 copies beta-actin *vs* 2884 ± 473 copies/10^6 copies beta-actin ($P < 0.05$). Detection rates were increased for the patients with moderate or poorly differentiated tumors (pG2/pG3) compared to the patients with well differentiated tumors (pG1) (3560 ± 302 copies CK-19/10^6 copies beta-actin *vs* 1055 ± 88 copies CK-19/10^6 copies beta-actin, $P < 0.05$) (Figure 4). The detection rates were not significantly different regarding the N stage or in blood and bone marrow samples. At the endpoint of the study, 14 patients had died of metastasized disease or tumor recurrence; 57% (8/14) of these patients had at least one CK-19 positive sample. No significant difference in the median survival was observed between the patients with positive CK-19 mRNA expression and negative CK-19 mRNA expression (10 mo *vs* 15 mo, $P = 0.15$).

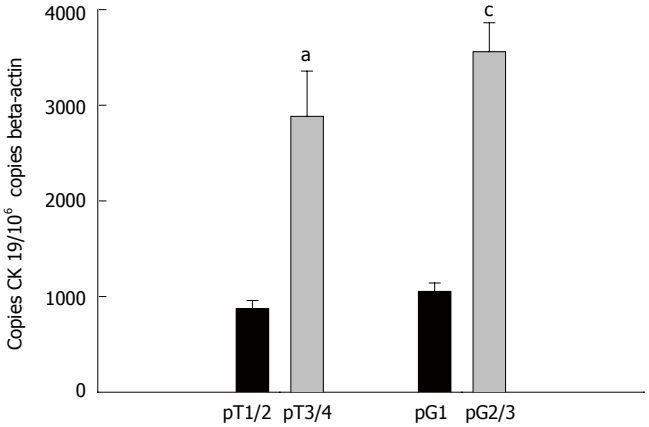

Figure 4 Quantitative CK-19 expression in peritoneal lavage of the patients with tumors (mean ± SD). $^{a}P < 0.05$ *vs* pT1/2; $^{c}P < 0.05$ *vs* pG1.

Blood, bone marrow and peritoneal lavage samples of 31 patients without malignancies (15 patients of the control group and 16 patients with chronic pancreatitis) were evaluated. CK-19 expression was detectable in 80% (12/15) of the samples taken from the control group. The highest detectable CK-19 signal was used as the base line for the cut-off values which were as follows: blood preoperatively 1064 copies CK-19 per 10^6 copies beta-actin, intraoperatively 984 copies CK-19 per 10^6 copies beta-actin, 1st and 10th postoperative days 1179 copies CK-19 per 10^6 copies beta-actin; bone marrow 4200 copies CK-19 per 10^6 copies beta-actin; and peritoneal lavage 1600 copies CK-19 per 10^6 copies beta-actin.

CK-19 mRNA could be detected in 80% (12/16) of the blood samples, 53% (8/16) of the bone marrow aspirates and 60% (9/16) of peritoneal lavage of the patients with chronic pancreatitis. No analyzed sample exceeded the maximal CK-19 mRNA expression of the control group. We observed a five-fold lower CK-19 signal in the peripheral blood compared to the patients with pancreatic cancer (142 ± 138 copies/10^6 copies beta-actin *vs* 741 ± 278 copies/10^6 copies beta-actin). The gene expression was significantly different at the four investigated time points ($P < 0.01$) (Figure 2). Analysis

of the bone marrow samples did not reveal any obvious difference in the CK-19 mRNA expression between the investigated groups. Compared to the patients with pancreatic cancer, the median CK-19 mRNA expression in the peritoneal lavage was 10-fold lower in the patients with chronic pancreatitis (261 ± 134 copies/10^6 copies beta-actin *vs* 3319 ± 484 copies/10^6 copies beta-actin, $P < 0.01$).

DISCUSSION

The long-term survival rates for patients with pancreatic cancer remain low. Without treatment, the 5-year survival rates are 0.4% to 4%[1,24]. Up to 80% of patients develop recurrent disease within 2 years after tumor resection[5]. Despite progress in adjuvant therapy and application of new chemo-radio-immunotherapy protocols, the high recurrence rate is the most limiting factor for the improvement of the patients prognosis[3,25]. Therefore, more sensitive staging methods are needed for this kind of tumor. Minimal residual disease caused by the spread of tumor cells into the circulation either before or during surgery is discussed as a main reason for early metastases and local recurrence in pancreatic cancer[26,27]. To detect tumor cells in the circulation, several studies have focused on cytokeratins and their potential role as tumor-specific markers[11,12,20,28-32]. However, conventional cytology, immunohistochemistry and molecular biological approaches reported conflicting results regarding the prevalence of CK-19 positive disseminated tumor cells and the impact on the prognosis of patients[12,33]. A reason for this is the target gene expression by non-neoplastic cells. False-positive results caused by illegitimate background transcription of CK-19 as seen in this study pose a major problem for qualitative PCR analysis. Gene transcription of CK-19 in healthy control groups and patients with benign disease has been reported in up to 80% of the analyzed samples[14,16]. In order to prevent false-positive results and increase the specificity, samples in this study were analyzed by quantitative RT-PCR. This approach facilitated the definition of cut-off values representing the maximal target gene expression in the control group. Regarding the results of nested-PCR in our study group, the qualitative PCR analysis of CK-19 expression can not be recommended for the detection of disseminated pancreatic cells.

Despite detection rates between 4%-100% using K-ras, CEA and cytokeratines as markers, up to now, tumor cell dissemination in the blood is not identified as an independent prognostic marker in pancreatic cancer[12,34-39]. In our sample series, 64% of peripheral blood samples taken from the patients with pancreatic cancer were detected to be CK-19-positive by quantitative fluorogenic RT-PCR. To reflect the dynamics of tumor cell dissemination during surgical intervention, blood samples were analyzed at four different time points showing target gene detection rates significantly higher compared to the control group. As described for K-ras and CEA mRNA, the amount of detectable CK-19 transcripts showed a trend to increase intraoperatively and decrease postoperatively below the preoperative level[26,36,37]. In consistent with Aihara *et al*[29], the CK-19 mRNA expression in the peripheral blood in our study showed higher levels.

Various studies have focused on the detection of disseminated pancreatic tumor cells in the bone marrow. Though positive detection rates have been reported between 24% and 58% for different markers, the tumor cell detection in the bone marrow does not correlate with tumor stage and is not an independent prognostic marker[11,12,34,35]. There is only one study by Soeth *et al*[36] demonstrating a benefit in survival in patients with CK-20-negative bone marrow aspirates. The data obtained in our study confirm the results of Dimmler *et al*[14], who dissuade from use of CK-19 for analysis of bone marrow due to high levels of illegitimate background expression in healthy controls. In contrast, peritoneal lavage was identified to be suitable to represent the actual state of tumor dissemination. The immunohistochemical analysis of the peritoneal lavage reported detection rates between 20% and 58% for marker-positive pancreatic cells[34,35,37-39]. Compared to the analysis by Inoue *et al*[40] who reported 10% of K-ras mRNA-positive cells, our detection rate of CK-19 positive cells was 30%. To the best of our knowledge, this sample series is the first report that shows a correlation between the CK-19 mRNA expression in the peritoneal lavage and the tumor size and tumor differentiation. A correlation between positive tumor cell detection and impaired patient survival as reported for cytological analysis by Yachida *et al*[37] and Makary *et al*[41] could not be detected.

Besides the detection of dissemination of neoplastic cells, the differentiation between malignant and benign pancreatic disease is of major interest for clinicians. Up to now, several markers such as K-ras, p53 and CEA failed as serum marker for a differential diagnosis[17,42]. CK 19-9 is the best characterized serum marker but has no absolute specificity. This is the first study that evaluates CK-19 mRNA expression in different compartments for the potential to differentiate between pancreatic cancer and chronic pancreatitis. In our study, the patients with pancreatic cancer showed an unequivocally increased CK-19 expression compared to the patients with chronic pancreatitis. Ten-fold higher expression levels in the peripheral blood as well as in the peritoneal lavage from the pancreatic cancer patients compared to the chronic pancreatitis patients indicated that quantitative fluorogenic RT-PCR is suited for the distinction between malignant and benign pancreatic disease.

In conclusion, our data suggest that CK-19-positive tumor cells can be detected in patients with pancreatic carcinoma in venous blood and peritoneal lavage by using fluorogenic RT-PCR. The prevalence of isolated tumor cells in peritoneal lavage increases significantly with the tumor stage and differentiation. The application of highly sensitive RT-PCR technique may improve the staging of patients and the monitoring of the residual tumor cell burden within the context of adjuvant systemic therapies. For the clinical use, the combination of tumor-specific markers is indispensable to increase the specificity of this test.

COMMENTS

Background

Pancreatic cancer is one of the top five causes of cancer death in the Western world. Occult micro-metastases caused by disseminated tumor cells are the most limiting factor for the improvement of mortality rates.

Research frontiers

Additional to cytology, immunohistochemical analysis is the standard for identification of disseminated tumor cells. Nevertheless, conflicting results regarding the prognostic relevance have been reported. Molecular biological approaches, such as reverse transcriptase polymerase chain reaction (RT-PCR), have a high sensitivity and specificity and might be more suitable for the analysis of disseminated tumor cells.

Innovations and breakthroughs

Various studies used cytokeratin-19 (CK-19) for pancreatic cell detection that has been identified as a reliable marker for epithelial cell differentiation and is homogenously expressed at high levels in primary pancreatic adenocarcinoma and pancreatic carcinoma metastases. Until now, CK-19 mRNA expression has not been identified as an independent prognostic indicator in pancreatic cancer.

Applications

Our data suggest that CK-19-positive tumor cells can be detected in patients with pancreatic carcinoma in venous blood and peritoneal lavage by using fluorogenic RT-PCR. The prevalence of isolated tumor cells in peritoneal lavage increases significantly with the tumor stage and differentiation. The application of highly sensitive RT-PCR technique may improve the staging of patients and the monitoring of the residual tumor cell burden within the context of adjuvant systemic therapies. For the clinical use, the combination of tumor-specific markers is indispensable to increase the specificity of this test.

Peer review

The authors demonstrate that quantification of CK-19 seems to be a reliable marker for the differential diagnosis of ductal pancreatic cancer and for staging. The Material and Methods, Results and Discussion are adequate and the paper provides new information for the investigators in this field.

REFERENCES

1 **Jemal A**, Murray T, Samuels A, Ghafoor A, Ward E, Thun MJ. Cancer statistics 2003. *CA Cancer J Clin* 2003; **53**: 5-26
2 **Parkin DM**, Bray FI, Devesa SS. Cancer burden in the year 2000. The global picture. *Eur J Cancer* 2001; **37** Suppl 8: S4-S66
3 **Neoptolemos JP**, Stocken DD, Friess H, Bassi C, Dunn JA, Hickey H, Beger H, Fernandez-Cruz L, Dervenis C, Lacaine F, Falconi M, Pederzoli P, Pap A, Spooner D, Kerr DJ, Büchler MW. A randomized trial of chemoradiotherapy and chemotherapy after resection of pancreatic cancer. *N Engl J Med* 2004; **350**: 1200-1210
4 **Wagner M**, Redaelli C, Lietz M, Seiler CA, Friess H, Büchler MW. Curative resection is the single most important factor determining outcome in patients with pancreatic adenocarcinoma. *Br J Surg* 2004; **91**: 586-594
5 **Griffin JF**, Smalley SR, Jewell W, Paradelo JC, Reymond RD, Hassanein RE, Evans RG. Patterns of failure after curative resection of pancreatic carcinoma. *Cancer* 1990; **66**: 56-61
6 **Westerdahl J**, Andrén-Sandberg A, Ihse I. Recurrence of exocrine pancreatic cancer-local or hepatic? *Hepatogastroenterology* 1993; **40**: 384-387
7 **Vogel I**, Kalthoff H, Henne-Bruns D, Kremer B. Detection and prognostic impact of disseminated tumor cells in pancreatic carcinoma. *Pancreatology* 2002; **2**: 79-88
8 **Bilchik A**, Miyashiro M, Kelley M, Kuo C, Fujiwara Y, Nakamori S, Monden M, Hoon DS. Molecular detection of metastatic pancreatic carcinoma cells using a multimarker reverse transcriptase-polymerase chain reaction assay. *Cancer* 2000; **88**: 1037-1044
9 **Leach SD**, Rose JA, Lowy AM, Lee JE, Charnsangavej C, Abbruzzese JL, Katz RL, Evans DB. Significance of peritoneal cytology in patients with potentially resectable adenocarcinoma of the pancreatic head. *Surgery* 1995; **118**: 472-478
10 **Meszoely IM**, Lee JS, Watson JC, Meyers M, Wang H, Hoffman JP. Peritoneal cytology in patients with potentially resectable adenocarcinoma of the pancreas. *Am Surg* 2004; **70**: 208-213; discussion 213-214
11 **Thorban S**, Roder JD, Siewert JR. Detection of micrometastasis in bone marrow of pancreatic cancer patients. *Ann Oncol* 1999; **10** Suppl 4: 111-113
12 **Z'graggen K**, Centeno BA, Fernandez-del Castillo C, Jimenez RE, Werner J, Warshaw AL. Biological implications of tumor cells in blood and bone marrow of pancreatic cancer patients. *Surgery* 2001; **129**: 537-546
13 **Pantel K**, von Knebel Doeberitz M. Detection and clinical relevance of micrometastatic cancer cells. *Curr Opin Oncol* 2000; **12**: 95-101
14 **Dimmler A**, Gerhards R, Betz C, Günther K, Reingruber B, Horbach T, Baumann I, Kirchner T, Hohenberger W, Papadopoulos T. Transcription of cytokeratins 8, 18, and 19 in bone marrow and limited expression of cytokeratins 7 and 20 by carcinoma cells: inherent limitations for RT-PCR in the detection of isolated tumor cells. *Lab Invest* 2001; **81**: 1351-1361
15 **Dingemans AM**, Brakenhoff RH, Postmus PE, Giaccone G. Detection of cytokeratin-19 transcripts by reverse transcriptase-polymerase chain reaction in lung cancer cell lines and blood of lung cancer patients. *Lab Invest* 1997; **77**: 213-220
16 **Van Trappen PO**, Gyselman VG, Lowe DG, Ryan A, Oram DH, Bosze P, Weekes AR, Shepherd JH, Dorudi S, Bustin SA, Jacobs IJ. Molecular quantification and mapping of lymph-node micrometastases in cervical cancer. *Lancet* 2001; **357**: 15-20
17 **Sawabu N**, Watanabe H, Yamaguchi Y, Ohtsubo K, Motoo Y. Serum tumor markers and molecular biological diagnosis in pancreatic cancer. *Pancreas* 2004; **28**: 263-267
18 **Moll R**. Cytokeratins as markers of differentiation. Expression profiles in epithelia and epithelial tumors. *Veroff Pathol* 1993; **142**: 1-197
19 **Bouwens L**. Cytokeratins and cell differentiation in the pancreas. *J Pathol* 1998; **184**: 234-239
20 **Schüssler MH**, Skoudy A, Ramaekers F, Real FX. Intermediate filaments as differentiation markers of normal pancreas and pancreas cancer. *Am J Pathol* 1992; **140**: 559-568
21 **Ruud P**, Fodstad O, Hovig E. Identification of a novel cytokeratin 19 pseudogene that may interfere with reverse transcriptase-polymerase chain reaction assays used to detect micrometastatic tumor cells. *Int J Cancer* 1999; **80**: 119-125
22 **Wittekind C**, Compton CC, Greene FL, Sobin LH. TNM residual tumor classification revisited. *Cancer* 2002; **94**: 2511-2516
23 **Bustin SA**, Gyselman VG, Williams NS, Dorudi S. Detection of cytokeratins 19/20 and guanylyl cyclase C in peripheral blood of colorectal cancer patients. *Br J Cancer* 1999; **79**: 1813-1820
24 **Bramhall SR**, Allum WH, Jones AG, Allwood A, Cummins C, Neoptolemos JP. Treatment and survival in 13,560 patients with pancreatic cancer, and incidence of the disease, in the West Midlands: an epidemiological study. *Br J Surg* 1995; **82**: 111-115
25 **Picozzi VJ**, Traverso LW. The Virginia Mason approach to localized pancreatic cancer. *Surg Oncol Clin N Am* 2004; **13**: 663-674, ix
26 **Romsdahl MM**, Valaitis J, McGrath RG, McGrew EA. Circulating tumor cells in patients with carcinoma. Method and recent studies. *JAMA* 1965; **193**: 1087-1090
27 **Pantel K**, Schlimok G, Braun S, Kutter D, Lindemann F, Schaller G, Funke I, Izbicki JR, Riethmüller G. Differential expression of proliferation-associated molecules in individual micrometastatic carcinoma cells. *J Natl Cancer Inst* 1993; **85**: 1419-1424
28 **Vogel I**, Kalthoff H. Disseminated tumour cells. Their detection and significance for prognosis of gastrointestinal and pancreatic carcinomas. *Virchows Arch* 2001; **439**: 109-117

29 **Aihara T**, Noguchi S, Ishikawa O, Furukawa H, Hiratsuka M, Ohigashi H, Nakamori S, Monden M, Imaoka S. Detection of pancreatic and gastric cancer cells in peripheral and portal blood by amplification of keratin 19 mRNA with reverse transcriptase-polymerase chain reaction. *Int J Cancer* 1997; **72**: 408-411

30 **van Heek NT**, Tascilar M, van Beekveld JL, Drillenburg P, Offerhaus GJ, Gouma DJ. Micrometastases in bone marrow of patients with suspected pancreatic and ampullary cancer. *Eur J Surg Oncol* 2001; **27**: 740-745

31 **Wildi S**, Kleeff J, Maruyama H, Maurer CA, Friess H, Büchler MW, Lander AD, Korc M. Characterization of cytokeratin 20 expression in pancreatic and colorectal cancer. *Clin Cancer Res* 1999; **5**: 2840-2847

32 **Goldstein NS**, Bassi D. Cytokeratins 7, 17, and 20 reactivity in pancreatic and ampulla of vater adenocarcinomas. Percentage of positivity and distribution is affected by the cut-point threshold. *Am J Clin Pathol* 2001; **115**: 695-702

33 **Roder JD**, Thorban S, Pantel K, Siewert JR. Micrometastases in bone marrow: prognostic indicators for pancreatic cancer. *World J Surg* 1999; **23**: 888-891

34 **Juhl H**, Stritzel M, Wroblewski A, Henne-Bruns D, Kremer B, Schmiegel W, Neumaier M, Wagener C, Schreiber HW, Kalthoff H. Immunocytological detection of micrometastatic cells: comparative evaluation of findings in the peritoneal cavity and the bone marrow of gastric, colorectal and pancreatic cancer patients. *Int J Cancer* 1994; **57**: 330-335

35 **Vogel I**, Krüger U, Marxsen J, Soeth E, Kalthoff H, Henne-Bruns D, Kremer B, Juhl H. Disseminated tumor cells in pancreatic cancer patients detected by immunocytology: a new prognostic factor. *Clin Cancer Res* 1999; **5**: 593-599

36 **Soeth E**, Grigoleit U, Moellmann B, Röder C, Schniewind B, Kremer B, Kalthoff H, Vogel I. Detection of tumor cell dissemination in pancreatic ductal carcinoma patients by CK 20 RT-PCR indicates poor survival. *J Cancer Res Clin Oncol* 2005; **131**: 669-676

37 **Makary MA**, Warshaw AL, Centeno BA, Willet CG, Rattner DW, Fernández-del Castillo C. Implications of peritoneal cytology for pancreatic cancer management. *Arch Surg* 1998; **133**: 361-365

38 **Nakao A**, Oshima K, Takeda S, Kaneko T, Kanazumi N, Inoue S, Nomoto S, Kawase Y, Kasuya H. Peritoneal washings cytology combined with immunocytochemical staining in pancreatic cancer. *Hepatogastroenterology* 1999; **46**: 2974-2977

39 **Nomoto S**, Nakao A, Kasai Y, Inoue S, Harada A, Nonami T, Takagi H. Peritoneal washing cytology combined with immunocytochemical staining and detecting mutant K-ras in pancreatic cancer: comparison of the sensitivity and availability of various methods. *Pancreas* 1997; **14**: 126-132

40 **Inoue S**, Nakao A, Kasai Y, Harada A, Nonami T, Takagi H. Detection of hepatic micrometastasis in pancreatic adenocarcinoma patients by two-stage polymerase chain reaction/restriction fragment length polymorphism analysis. *Jpn J Cancer Res* 1995; **86**: 626-630

41 **Yachida S**, Fukushima N, Sakamoto M, Matsuno Y, Kosuge T, Hirohashi S. Implications of peritoneal washing cytology in patients with potentially resectable pancreatic cancer. *Br J Surg* 2002; **89**: 573-578

42 **Kimura W**, Zhao B, Futakawa N, Muto T, Makuuchi M. Significance of K-ras codon 12 point mutation in pancreatic juice in the diagnosis of carcinoma of the pancreas. *Hepatogastroenterology* 1999; **46**: 532-539

S- Editor Wang GP **L- Editor** Kumar M **E- Editor** Ma WH

PO Box 2345, Beijing 100023, China
www.wjgnet.com
wjg@wjgnet.com

World J Gastroenterol 2007 January 14; 13(2): 264-269
World Journal of Gastroenterology ISSN 1007-9327
© 2007 The WJG Press. All rights reserved.

CLINICAL RESEARCH

Efficacy of long term cyclic administration of the poorly absorbed antibiotic Rifaximin in symptomatic, uncomplicated colonic diverticular disease

Antonio Colecchia, Amanda Vestito, Francesca Pasqui, Giuseppe Mazzella, Enrico Roda, Francesca Pistoia, Giovanni Brandimarte, Davide Festi

Antonio Colecchia, Amanda Vestito, Francesca Pasqui, Giuseppe Mazzella, Enrico Roda, Davide Festi, Department of Internal Medicine and Gastroenterology, University of Bologna, Cristo Re Hospital, Rome, Italy
Francesca Pistoia, Department of Surgery, University of L'Aquila, Cristo Re Hospital, Rome, Italy
Giovanni Brandimarte, Department of Internal Medicine, Cristo Re Hospital, Rome, Italy
Correspondence to: Davide Festi, MD, Dipartimento di Medicina Interna e Gastroenterologia Policlinico S.Orsola, Via Massarenti 9, Bologna 40138, Italy. davide.festi@unibo.it
Telephone: +39-51-6364123 Fax: +39-51-6364123
Received: 2006-08-30 Accepted: 2006-10-20

Abstract

AIM: To comparatively evaluate the long term efficacy of Rifaximin and dietary fibers in reducing symptoms and/or complication frequency in symptomatic, uncomplicated diverticular disease.

METHODS: 307 patients (118 males, 189 females, age range: 40-80 years) were enrolled in the study and randomly assigned to: Rifaximin (400 mg bid for 7 d every month) plus dietary fiber supplementation (at least 20 gr/d) or dietary fiber supplementation alone. The study duration was 24 mo; both clinical examination and symptoms' questionnaire were performed every two months.

RESULTS: Both treatments reduced symptom frequency, but Rifaximin at a greater extent, when compared to basal values. Symptomatic score declined during both treatments, but a greater reduction was evident in the Rifaximin group (6.4 ± 2.8 and 6.2 ± 2.6 at enrollment, P = NS, 1.0 ± 0.7 and 2.4 ± 1.7 after 24 mo, $P < 0.001$, respectively). Probability of symptom reduction was higher and complication frequency lower (Kaplan-Meyer method) in the Rifaximin group ($P < 0.0001$ and 0.028, respectively).

CONCLUSION: In patients with symptomatic, uncomplicated diverticular disease, cyclic administration of Rifaximin plus dietary fiber supplementation is more effective in reducing both symptom and complication frequency than simple dietary fiber supplementation. Long term administration of the poorly absorbed antibiotic Rifaximin is safe and well tolerated by the patients, confirming the usefulness of this therapeutic strategy in the overall management of diverticular disease.

© 2007 The WJG Press. All rights reserved.

Key words: Dietary fiber; Antibiotics; Abdominal symptoms; Diverticulitis

Colecchia A, Vestito A, Pasqui F, Mazzella G, Roda E, Pistoia F, Brandimarte G, Festi D. Efficacy of long term cyclic administration of the poorly absorbed antibiotic Rifaximin in symptomatic, uncomplicated colonic diverticular disease. *World J Gastroenterol* 2007; 13(2): 264-269

http://www.wjgnet.com/1007-9327/13/264.asp

INTRODUCTION

Diverticular disease of the colon represents the most common disease affecting the large bowel in the Western world[1]; the disease is more frequent in USA than in Europe and it represents a rare clinical condition in Africa[2]. Prevalence of diverticular disease is largely age-dependent and is uncommon, with a rate less than 5%, in subjects under 40 years of age, increasing up to 65% in those aged 65 years or more[3]. Diverticular disease and its clinical consequences have recently become increasingly prevalent, paralleling western patterns of living and eating, the ageing population, and economic and industrial development[4]. Although a large majority of patients with diverticular disease will remain entirely asymptomatic for their entire life, 20% of them may manifest clinical illness[4,5] and a worse quality of life[6]. Furthermore, since available data[2,3] suggest that the incidence of diverticular disease is increasing and that its prevalence increases with age, the identification of a management strategy for the disease represents an healthy priority. Several guidelines are actually available to manage diverticular disease[7,8]; there is a consensus that conservative treatment is indicated in patients with a first attack of uncomplicated diverticulitis, since about 70% of patients treated for a first episode recover and have no further problems[9]. However, a 60% risk of developing complications has been reported in patients with recurrent attacks[2]. Conservative treatment is aimed at the relief of symptoms and at preventing

major complications[8,9]. Available evidence[10] suggests that antibiotics, and namely topical antibiotics, and dietary fibers represent useful treatments for uncomplicated diverticular disease and for preventing disease complications. Different antibiotics have been tested, but the possibility of side effect development due to their long-term use have discouraged their employment[10].

Rifaximin is a rifamycin analogue with a broad spectrum of activity similar to that of rifampicin and it is poorly absorbed in the gastrointestinal tract[11], thus conferring to this drug a high safety profile. Due to these properties, Rifaximin has been tested in different gastrointestinal diseases, and in diverticular disease too[12,13]. Two randomized clinical trials[14,15] performed in patients with uncomplicated diverticular disease showed that Rifaximin plus dietary fiber supplementation was more effective in improving symptoms than dietary fibre supplementation alone after 12 mo of treatment.

Since the uncertainties regarding the natural history of the disease, and in particular the predictors for the progression from uncomplicated to complicated disease, and the lack of a definite indication for long term management of uncomplicated disease, data on long-term treatment with topical antibiotics and dietary fibers would be necessary.

Therefore, the aim of the present study was to evaluate the long-term efficacy of cyclic administration of Rifaximin plus fiber supplementation versus fiber supplementation alone on symptoms and clinical manifestations in patients with symptomatic, but uncomplicted, diverticular disease.

MATERIALS AND METHODS

Study design

This was a multicenter, open, prospective, randomized, controlled study. Patients were randomly assigned to one of the two treatment regimens: one group received Rifaximin (400 mg bid for 7 d every month) plus dietary fiber supplementation (at least 20 gr/d) (Rifaximin group) and the other group simple dietary fiber supplementation (at least 20 gr/d) (fiber group). The study duration was 24 mo.

Patients were consecutively assigned to one group or to the other by a computer-generated randomization scheme. Informed consent was obtained from each patient and the study protocol was approved by the local Ethis Committee.

Patients

Consecutive patients with symptomatic, uncomplicated diverticular disease were enrolled. Inclusion criteria for the study were: age between 40 and 80 years, endoscopic or radiological evidence of diverticular disease of the sigmoid and/or descending colon, presence of symptoms attributable to the diverticular disease of the colon such as lower abdominal pain/discomfort, bloating, tenesmus, diarrhea and abdominal tenderness. Patients who referred the continuous presence of three, or more, of these symptoms for at least 1 mo before the enrolment entered in the study.

Exclusion criteria were represented by the presence of a solitary diverticulum of the right colon, signs of complicated diverticular disease, previous colonic surgery, neoplastic or haematological diseases, immunodeficiency, pregnancy and questionable ability to cooperate. Patients who assumed antibiotics in the previous 4 wk were also excluded.

Clinical evaluation

At enrolment and every 2 mo until the 24 mo patients underwent clinical examination; a questionnaire inquiring about the presence and severity of abdominal symptoms was also performed. Five clinical variables (lower abdominal pain/discomfort, bloating, tenesmus, diarrhea and abdominal tenderness) were graded according to the following scale: 0 = no symptoms; 1 = mild symptoms, easily tolerated; 2 = moderate symptoms, sufficient to cause interference with normal daily activities; 3 = severe, incapacitating symptoms, with inability to perform normal daily activities. Consequently the global score could range from 0 (absence of symptoms) to 15 (presence of all symptoms with the higher degree of severity).

Biochemical tests were performed at enrolment, and after 12 and 24 mo of treatment .

Statistical methods

On the presumption of a 40% reduction at 24 mo in the frequency of symptoms with dietary fiber and a 65% reduction with Rifaximin plus fiber treatment, and considering the delta between the frequencies to be either equal to or at least 25%, a two-tail significance test, a significance level of $\alpha = 0.05$, a 99% power and a 3:2 allocation ratio (in order to better satisfy the secondary end-point), the number of patients to be enrolled was 177 patients for the Rifaximin group and 110 for the fibers group. Presuming a 10% of drop-out, it was necessary to enrol 307 patients (185 for the active group and 122 for the control group)[16].

χ^2 test or Fisher's exact test were used to compare the distribution of categorical or absolute variables within the studied groups. Parametric tests (Levene's test, *t* test, one- and two-way analysis of variance and repeated-measure ANOVA) were used to analyze continuous parameters. Non-parametric tests, one-way analysis of variance (Friedman's test) and Wilcoxon test were applied to analyze the same parameters in subgroups of patients in whom a distribution normality of character being studied could not be presumed[17].

Kaplan Meier curves were used to estimate the probability of a reduction in symptom score and of complication development in the two groups of patients; differences between the two branches were evaluated by means of Log-rank test. Results were expressed as mean ± SD and a *P* value less than 0.05 was considered as statistically significant. Data analysis was performed using SPSS version 13.0.

RESULTS

Patients

Three-hundred and seven (307) patients were enrolled, 118 males and 189 females.

Table 1 shows demographic and clinical characteristics

Table 1 Demographic and clinical characteristics of study patients

	Rifaximin plus fibers (n = 184)	Fibers (n = 123)	P
Gender			
Males	68 (37.0%)	50 (40.7%)	[1]NS
Females	116 (63.0%)	73 (59.3%)	
Age (yr)	63.6 ± 11.7	60.7 ± 12.5	[2]NS
Site of diverticula			
Left colon	47 (25.5%)	26 (21.1%)	
Colon-sigma	59 (32.1%)	38 (30.9%)	[3]NS
Sigma	73 (39.7%)	56 (45.5%)	
Sigma-rectum	5 (2.7%)	3 (2.4%)	
Symptoms (%)			
Lower abdominal pain	87.5%	90.2%	[1]NS
Bloating	85.9%	78.0%	[1]NS
Tenesmus	35.3%	29.3%	[1]NS
Diarrhoea	35.9%	32.5%	[1]NS
Abdominal tenderness	71.2%	69.1%	[1]NS
Symptoms score	6.4 ± 2.8	6.2 ± 2.6	[1]NS

[1]χ^2 test with continuity correction; [2]t test; [3]χ^2 test.

Table 2 Mean baseline values of biochemical parameters

	Rifaximin plus fibers	Fibers	P
ESR (mm/h)	24.9 ± 17.7	22.8 ± 17.8	NS
Leukocytes (mm^3)	8128.1 ± 2377.7	7836.9 ± 2019.6	NS
Neutrophils (mm^3)	68.3 ± 12.1	68.7 ± 9.6	NS
Ht (%)	41.9 ± 5.3	42.2 ± 4.0	NS
Creatininemia (mg/dL)	0.97 ± 0.25	0.98 ± 0.19	NS
Blood nitrogen (mg/dL)	38.3 ± 12.7	36.5 ± 11.2	NS
Blood sodium (nmol/L)	138.8 ± 4.9	139.4 ± 17.8	NS
Potassemia (nmol/L)	4.23 ± 0.46	4.15 ± 0.35	NS
AST (IU/L)	23.9 ± 17.2	21.8 ± 10.8	NS
ALT (IU/L)	25.0 ± 23.1	22.1 ± 14.1	NS
AP (IU/L)	151.7 ± 65.4	142.4 ± 65.6	NS
γGT (IU/L)	34.8 ± 33.4	33.7 ± 26.1	NS
Total proteins (g/dL)	6.85 ± 0.58	6.90 ± 0.42	NS

t-test for corrected for multiple comparison.

Table 3 Symptom frequency (%) at baseline, after 12 and 24 mo of treatment

	Rifaximin plus fibers			Fibers			P
Mo	0	12th	24th	0	12th	24th	at 24th
Lower abdominal pain	87.5	17.2	12.9	90.2	28.8	19.2	0.05[1]
Bloating	85.9	35.0	21.9	78.0	43.3	40.3	< 0.002[1]
Tenesmus	35.3	3.2	3.9	29.3	2.9	9.6	= 0.05[1]
Diarrhoea	35.9	7.0	3.9	32.5	1.0	2.9	NS[2]
Abdominal tenderness	71.2	19.0	6.5	69.1	35.6	21.2	< 0.001[1]

[1]χ^2 test; [2]Fisher's Exact test.

of the enrolled patients: no difference was found between the two groups of patients in terms of gender, age and colonic distribution of the disease as well as frequency of abdominal symptoms and global symptom score. Diagnosis of diverticular disease was performed by colonoscopy in 46.2% of patients treated with Rifaximin and in 53.7% of patients treated with fibers, and by barium enema in 60.9% and 48.8% of patients, respectively (P = NS). Again, no difference was present at baseline between the two groups of treatment as far as biochemical parameters are concerned (Table 2).

Fourty-eight (48) patients did not complete the study, 25 patients of the Rifaximin group and 23 patients of the fibers group; 28 patients (17 of the Rifaximin group and 11 of the fibers group, P = NS, Fisher's exact test) were drop-outs: in the Rifaximin group 14 patients refused to continue the study, 2 patients died for cardiovascular disease and 1 patient for causes unrelated to diverticular disease, while in the fibers group 10 patients refused to continue the study and 1 patient underwent surgery for gallstone disease. Side effects (mainly represented by nausea, headache and weakness) occurred in 4 patients of the Rifaximin group and in 3 patients of the fibers group (P = NS). Frequency of complications was significantly different (P = 0.041) between the two groups: in fact complications occurred in 4 patients of the Rifaximin group (2 cases of rectal bleeding, and 2 of diverticulitis) and in 9 of the fiber group (4 cases of intestinal infections, 1 of rectal bleeding and 4 of diverticulitis).

The effect of treatments on clinical signs and symptoms is illustrated in Table 3: both treatments induced a significant reduction in symptom frequency in all patients after 12 mo. After 24 mo of treatment, Rifaximin was able to further reduce symptoms as lower abdominal pain, bloating, tenesmus and abdominal tenderness while no difference was observed in patients treated with fibers alone between the results observed at the 12th and the 24th mo.

The effect of treatments on the symptomatic score is shown in Figure 1: although both treatments were able to significantly reduce the symptom score, this result was differently reached: at baseline the symptom score was similar, while at the end of the study period a significant difference ($P < 0.01$) was present between the Rifaximin treated group and the fiber group (1.0 ± 0.7 and 2.4 ± 1.7, respectively).

The clinical effect of the two treatments evaluated according to the Kaplan-Meier method is shown in Figure 2: the probability of symptom remission in symptomatic patients was significantly higher ($P < 0.0001$) in the Rifaximin group than in the control group. Although the overall clinical efficacy of the two regimens is different, a similar behaviour can be observed: the cumulative survival progressively declined during the first 12 mo of treatment, remaining constant during the following 12 mo. Rifaximin treatment was also able to induce a lower frequency of recurrence of symptoms: six (3.2%) Rifaximin treated patients had a further episode of abdominal symptoms, while in the fibers group the corresponding figure was three (9.6%) patients ($P < 0.03$).

No significant alterations in biochemical tests were observed in the two groups of patients (Table 4). The probability of developing complications during the study in the two groups of patients evaluated according to the

Table 4 Mean value of biochemical parameters before and at the end of treatment period

	Rifaximin plus fibers		*P*	Fibers		*P*
	Baseline	at 24 mo		Baseline	at 24 mo	
ESR (mm/h)	24.8 ± 18.2	15.2 ± 14.4	< 0.001	23.2 ± 18.6	17.8 ± 15.3	< 0.05
Leukocytes (mm^3)	8330.3 ± 2554.4	6515.8 ± 1393.9	< 0.001	7944.9 ± 2091.4	6918.5 ± 1719.8	< 0.01
Neutrophils (mm^3)	67.8 ± 12.3	62.0 ± 10.9	< 0.005	68.9 ± 9.9	65.5 ± 8.7	< 0.03
Creatininemia (mg/dL)	0.98 ± 0.25	0.96 ± 0.21	NS	0.98 ± 0.19	0.94 ± 0.17	NS
Blood nitrogen (mg/dL)	39.4 ± 13.0	37.7 ± 10.6	NS	37.1 ± 11.3	33.7 ± 9.9	< 0.05
Blood sodium (nmol/L)	138.8 ± 5.0	140.0 ± 5.1	< 0.05	139.2 ± 5.2	139.1 ± 6.5	NS
Potassemia (nmol/L)	4.22 ± 0.45	4.21 ± 0.46	NS	4.20 ± 0.37	4.18 ± 0.30	NS
AST (IU/L)	23.2 ± 15.1	21.3 ± 12.7	NS	22.5 ± 11.1	20.8 ± 10.5	NS
ALT (U/L)	23.9 ± 14.6	21.8 ± 11.6	NS	22.7 ± 14.4	19.1 ± 8.8	< 0.05
AP (U/L)	147.3 ± 63.2	164.3 ± 65.6	< 0.05	140.6 ± 69.3	149.1 ± 62.4	NS
γGT (U/L)	33.0 ± 24.1	36.6 ± 24.3	NS	35.4 ± 27.3	30.2 ± 18.4	NS
Total proteins (g/dL)	6.85 ± 0.57	6.89 ± 0.58	NS	6.90 ± 0.44	6.78 ± 0.89	NS

t test for paired data, corrected for multiple comparison.

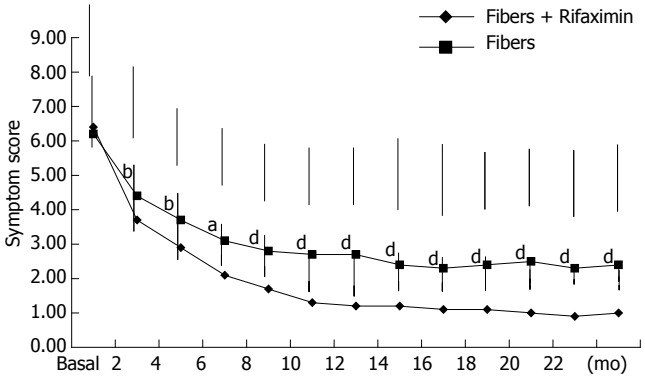

Figure 1 Changes in symptoms score after Rifaximin plus fiber supplementation and fiber supplementation alone (mean ± SD). *t* test for independent samples corrected for multiple comparison: $^{a}P < 0.05$; $^{b}P < 0.01$; $^{d}P < 0.001$.

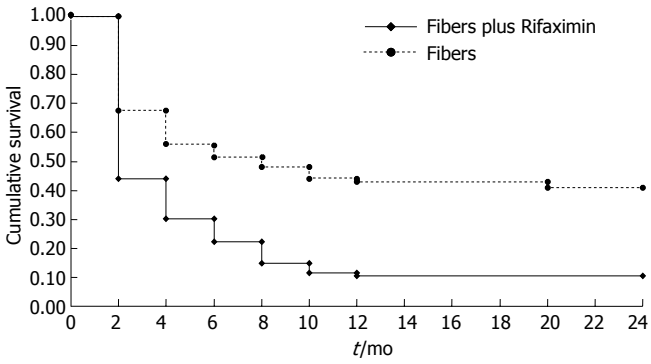

Figure 2 Probability of symptom reduction in patients treated with Rifaximin plus fibers or with fiber supplementation alone. Kaplan-Meier method: Test Log Rank: $P < 0.0001$.

Kaplan-Meier method is illustrated in Figure 3: as observed for symptoms, Rifaximin administration documented a more favourable effect, being significantly lower ($P < 0.028$) the probability of developing complications with respect to fiber supplementation. Although with a different rate of probability, both treatments induced a progressively reduced frequency of complications during the whole study period.

DISCUSSION

The present study suggest that the cyclic, long term administration of the non-absorbable antibiotic Rifaximin associated with dietary fiber supplementation is more effective than dietary fiber supplementation alone in reducing the clinical manifestations of patients with symptomatic, uncomplicated diverticular disease. Furthermore, Rifaximin treatment is more effective than fiber administration influencing the clinical course of the disease, since both probability of symptom recurrence and development of disease complications are significantly reduced.

Diverticular disease of the colon is common in developed countries and its prevalence is correlated with advancing age[1-4]. Studies on the natural history of the disease[3,5,9] have indicated that most patients with colonic diverticula remain entirely asymptomatic for their lifetime. Actually there are no definitive data to support any therapeutic recommendation, or routine follow-up regimen, for asymptomatic subjects, although it is reasonable to recommend a life-style characterized by regular physical activity and a diet high in fruit and vegetable fibers[18]. According to available guidelines[7,8] in symptomatic, but uncomplicated, diverticular disease treatment is aimed at symptom-relief and at prevention of complications (diverticulitis, hemorrage). Different agents have been proposed, such as bulking agents, antispasmodics, topical antibiotics, on the basis of different potential pathophysiological mechanism/s, i.e. abnormal colonic motility, inadequate intake of dietary fibers, intestinal bacterial overgrowth and mucosal inflammation[10,19-23].

The efficacy of fiber supplementation in the treatment of symptomatic diverticular disease remains controversial, although it is considered a mainstay for treatment[10]. The efficacy of dietary fibers in reducing symptoms and in improving intestinal function is probably related to its ability to hold water, to increase luminal intestinal mass,

to relax the intestinal wall and to lower the intraluminal pressure[24,25].

Antibiotics are routinely used in the treatment of inflammatory complications of diverticular disease. In symptomatic, but uncomplicated diverticular disease, the use of antibiotics seems without a rationale. However, recent studies have suggested the presence, at least in a sub-group of patients, of an intestinal bacterial overgrowth[21], a condition that may allow an excessive production of bowel gas with secondary development of abdominal pain, bloating and tenderness. Furthermore, intestinal bacterial overgrowth may contribute to maintain a chronic, low-grade mucosal inflammation, as suggested in irritable bowel syndrome[26], which could be responsible for symptom development[19].

Rifaximin has been tested in both uncontrolled[12,13] and controlled[14,15] clinical studies to treat symptomatic, uncomplicated diverticular disease, with encouraging results.

The mechanism by which Rifaximin improves symptoms in uncomplicated diverticular disease is unclear. It has been suggested a synergistic effect of Rifaximin and high fiber diet in reducing proliferation of gut microflora, with a consequent decrease in bacterial hydrogen and methane production and/or in expanding faecal mass, due to a decrease in bacterial degradation of fibers[15,27].

Furthermore, Rifaximin may improve symptoms and lower the frequency of disease complications reducing intestinal bacterial overgrowth[19,21]. Rifaximin may also enhance faecal bulking and faecal weight, as shown for other antibiotics[28], and decrease the intraluminal colonic pressure, one of the pathogenetic mechanisms for diverticula development[20]. Due to the therapeutic uncertainties of both Rifaximin and fiber supplementation, in the present study we decided to comparatively evaluate these two agents. The results we obtained confirm and extend to a longer period previous observations by Papi *et al*[14] and Latella *et al*[15], who found that administration for 12 mo of Rifaximin plus dietary fiber supplementation was more effective in improving symptoms than dietary fibre supplementation alone. The present study documents that the efficacy of Rifaximin plus fiber supplementation is not only maintained, but it is more evident after 24 mo of treatment than fibers alone. According to the probability curves, the beneficial clinical effect of Rifaximin treatment is more pronounced during the first 12 mo, but it may last up to 24 mo. This observation is important, since it suggests a positive effect of Rifaximin treatment on the natural history of diverticular disease. Up to now, no definitive data are available regarding the way to prevent the development/maintenance of disease symptoms and complications. As far as the last point is concerned, the present study indicates that Rifaximin treatment significantly reduces the probability of complication development and that this effect is constant during the whole study period.

In conclusion the present study documents that in patients with symptomatic, uncomplicated diverticular disease, cyclic administration of Rifaximin plus fiber supplementation is more effective in reducing symptom persistence/recurrence and complication development than dietary fiber alone. Cyclic, long term administration of this non-absorbable antibiotic is safe and well tolerated by the patients, confirming the clinical usefulness of this therapeutic strategy in the overall management of diverticular disease. Further studies are needed to better identify the mechanism/s of action of both Rifaximin and of its association with dietary fibers.

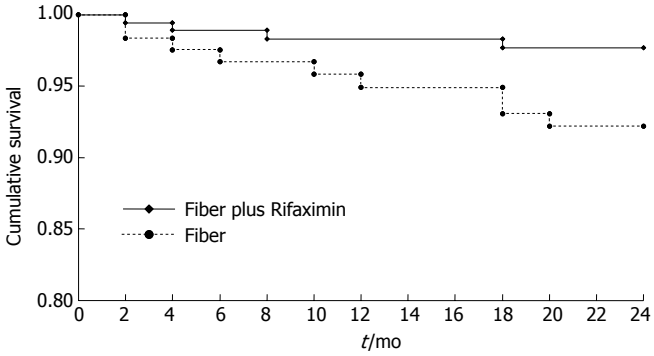

Figure 3 Probability of complication development in patients treated with Rifaximin plus fibers or with fibers supplementation alone. Kaplan-Meier method. Test Log Rank: $P = 0.028$.

REFERENCES

1 **Stollman N**, Raskin JB. Diverticular disease of the colon. *Lancet* 2004; **363**: 631-639

2 **Delvaux M**. Diverticular disease of the colon in Europe: epidemiology, impact on citizen health and prevention. *Aliment Pharmacol Ther* 2003; **18** Suppl 3: 71-74

3 **Parks TG**. Natural history of diverticular disease of the colon. *Clin Gastroenterol* 1975; **4**: 53-69

4 **Kang JY**, Melville D, Maxwell JD. Epidemiology and management of diverticular disease of the colon. *Drugs Aging* 2004; **21**: 211-228

5 **Farmakis N**, Tudor RG, Keighley MR. The 5-year natural history of complicated diverticular disease. *Br J Surg* 1994; **81**: 733-735

6 **Bolster LT**, Papagrigoriadis S. Diverticular disease has an impact on quality of life -- results of a preliminary study. *Colorectal Dis* 2003; **5**: 320-323

7 **Köhler L**, Sauerland S, Neugebauer E. Diagnosis and treatment of diverticular disease: results of a consensus development conference. The Scientific Committee of the European Association for Endoscopic Surgery. *Surg Endosc* 1999; **13**: 430-436

8 **Stollman NH**, Raskin JB. Diagnosis and management of diverticular disease of the colon in adults. Ad Hoc Practice Parameters Committee of the American College of Gastroenterology. *Am J Gastroenterol* 1999; **94**: 3110-3121

9 **Mizuki A**, Nagata H, Tatemichi M, Kaneda S, Tsukada N, Ishii H, Hibi T. The out-patient management of patients with acute mild-to-moderate colonic diverticulitis. *Aliment Pharmacol Ther* 2005; **21**: 889-897

10 **Simpson J**, Spiller R. Colonic diverticular disease. *Clin Evid* 2004; (**12**): 599-609

11 **Gillis JC**, Brogden RN. Rifaximin. A review of its antibacterial activity, pharmacokinetic properties and therapeutic potential in conditions mediated by gastrointestinal bacteria. *Drugs* 1995; **49**: 467-484

12 **Papi C**, Ciaco A, Koch M, Capurso L. Efficacy of rifaximin on symptoms of uncomplicated diverticular disease of the colon. A pilot multicentre open trial. Diverticular Disease Study Group. *Ital J Gastroenterol* 1992; **24**: 452-456

13 **Ventrucci M**, Ferrieri A, Bergami R, Roda E. Evaluation of the effect of rifaximin in colon diverticular disease by means

of lactulose hydrogen breath test. *Curr Med Res Opin* 1994; **13**: 202-206
14 **Papi C**, Ciaco A, Koch M, Capurso L. Efficacy of rifaximin in the treatment of symptomatic diverticular disease of the colon. A multicentre double-blind placebo-controlled trial. *Aliment Pharmacol Ther* 1995; **9**: 33-39
15 **Latella G**, Pimpo MT, Sottili S, Zippi M, Viscido A, Chiaramonte M, Frieri G. Rifaximin improves symptoms of acquired uncomplicated diverticular disease of the colon. *Int J Colorectal Dis* 2003; **18**: 55-62
16 **Casagrande JT**, Pike MC. An improved approximate formula for calculating sample sizes for comparing two binomial distributions. *Biometrics* 1978; **34**: 483-486
17 **Armitage P**, Berry G. Statistical methods in medical research. UK: Black-Well Scientific Publication Limited, Oxford, 1994
18 **Aldoori WH**, Giovannucci EL, Rimm EB, Wing AL, Trichopoulos DV, Willett WC. A prospective study of diet and the risk of symptomatic diverticular disease in men. Am J Clin Nutr 1994; **60**: 757-764
19 **Colecchia A**, Sandri L, Capodicasa S, Vestito A, Mazzella G, Staniscia T, Roda E, Festi D. Diverticular disease of the colon: new perspectives in symptom development and treatment. *World J Gastroenterol* 2003; **9**: 1385-1389
20 **Bassotti G**, Battaglia E, De Roberto G, Morelli A, Tonini M, Villanacci V. Alterations in colonic motility and relationship to pain in colonic diverticulosis. *Clin Gastroenterol Hepatol* 2005; **3**: 248-253
21 **Tursi A**, Brandimarte G, Giorgetti GM, Elisei W. Assessment of small intestinal bacterial overgrowth in uncomplicated acute diverticulitis of the colon. *World J Gastroenterol* 2005; **11**: 2773-2776
22 **Simpson JK**, Metcalfe DD. Mastocytosis and disorders of mast cell proliferation. *Clin Rev Allergy Immunol* 2002; **22**: 175-188
23 **Petruzziello L**, Iacopini F, Bulajic M, Shah S, Costamagna G. Review article: uncomplicated diverticular disease of the colon. *Aliment Pharmacol Ther* 2006; **23**: 1379-1391
24 **Lupton JR**, Turner ND. Potential protective mechanisms of wheat bran fiber. *Am J Med* 1999; **106**: 24S-27S
25 **Brodribb AJ**. Treatment of symptomatic diverticular disease with a high-fibre diet. *Lancet* 1977; **1**: 664-666
26 **Barbara G**, De Giorgio R, Stanghellini V, Cremon C, Corinaldesi R. A role for inflammation in irritable bowel syndrome? *Gut* 2002; **51** Suppl 1: i41-i44
27 **Papi C**, Koch M, Capurso L. Management of diverticular disease: is there room for rifaximin? *Chemotherapy* 2005; **51** Suppl 1: 110-114
28 **Kurpad AV**, Shetty PS. Effects of antimicrobial therapy on faecal bulking. *Gut* 1986; **27**: 55-58

S- Editor Liu Y **L- Editor** Alpini GD **E- Editor** Bi L

PO Box 2345, Beijing 100023, China
www.wjgnet.com
wjg@wjgnet.com

World J Gastroenterol 2007 January 14; 13(2): 270-275
World Journal of Gastroenterology ISSN 1007-9327
© 2007 The WJG Press. All rights reserved.

CLINICAL RESEARCH

Proximal gastric motility in critically ill patients with type 2 diabetes mellitus

Nam Q Nguyen, Robert J Fraser, Laura K Bryant, Marianne Chapman, Richard H Holloway

Nam Q Nguyen, Richard H Holloway, Department of Gastroenterology, Hepatology and General Medicine, Royal Adelaide Hospital, South Australia
Robert J Fraser, Laura K Bryant, Investigation and Procedures Unit, Repatriation General Hospital; South Australia
Marianne Chapman, Anaesthesia and Intensive Care, Royal Adelaide Hospital, South Australia
Supported by a project grant from the National Health and Medical Research Council of Australia.
Correspondence to: Dr Nam Q Nguyen, Department of Gastroenterology, Royal Adelaide Hospital, North Terrace, Adelaide, SA 5000, Australia. qnguyen@mail.rah.sa.gov.au
Telephone: + 61-8-82225207 Fax: + 61-8-82225885
Received: 2006-10-25 Accepted: 2006-12-12

Abstract

AIM: To investigate the proximal gastric motor response to duodenal nutrients in critically ill patients with long-standing type 2 diabetes mellitus.

METHODS: Proximal gastric motility was assessed (using a barostat) in 10 critically ill patients with type 2 diabetes mellitus (59 ± 3 years) during two 60-min duodenal infusions of Ensure® (1 and 2 kcal/min), in random order, separated by 2 h fasting. Data were compared with 15 non-diabetic critically ill patients (48 ± 5 years) and 10 healthy volunteers (28 ± 3 years).

RESULTS: Baseline proximal gastric volumes were similar between the three groups. In diabetic patients, proximal gastric relaxation during 1 kcal/min nutrient infusion was similar to non-diabetic patients and healthy controls. In contrast, relaxation during 2 kcal/min infusion was initially reduced in diabetic patients ($P < 0.05$) but increased to a level similar to healthy humans, unlike non-diabetic patients where relaxation was impaired throughout the infusion. Duodenal nutrient stimulation reduced the fundic wave frequency in a dose-dependent fashion in both the critically ill diabetic patients and healthy subjects, but not in critically ill patients without diabetes. Fundic wave frequency in diabetic patients and healthy subjects was greater than in non-diabetic patients.

CONCLUSION: In patients with diabetes mellitus, proximal gastric motility is less disturbed than non-diabetic patients during critical illness, suggesting that these patients may not be at greater risk of delayed gastric emptying.

© 2007 The WJG Press. All rights reserved.

Key words: Proximal gastric function; Diabetes mellitus type 2; Critical illness; Enteral nutrition

Nguyen NQ, Fraser RJ, Bryant LK, Chapman M, Holloway RH. Proximal gastric motility in critically ill patients with type 2 diabetes mellitus. *World J Gastroenterol* 2007; 13(2): 270-275

http://www.wjgnet.com/1007-9327/13/270.asp

INTRODUCTION

In the community, approximately 50% of patients with type 1 or 2 diabetes mellitus (DM) have gastroparesis[1]. Although gastric emptying of either a solid or semi-solid meal is consistently slow in these patients, gastric emptying of liquid meals is variable[1-4]. The aetiology of slow gastric emptying and the variable rate of liquid emptying are unclear, but may be related to hyperglycemia or autonomic neuropathy[1,5-7], factors that result in motor dysfunction of both the proximal and distal stomach[1,7,8].

Delayed gastric emptying is also common in critically ill patients[9-11] and is associated with disturbed motility of both the proximal and distal stomach[10,12,13]. In health, the proximal stomach is a major determinant of liquid gastric emptying and is regulated by feedback from the small intestine. In health, the fundus relaxes in response to the presence of nutrient in the duodenum[14]. Critically ill patients without DM have been reported to have impaired proximal gastric relaxation, reduced fundic wave activity and a failed recovery of proximal gastric volume to pre-stimulation level[12]. Currently, there are no data on the impact of DM on gastric motor function or emptying during critical illness, despite the fact that one-third of patients admitted to critical care units have DM[15]. Given that both DM and critical illness are risk factors for disturbed gastric motility, we hypothesized that critically ill patients with DM would have abnormal proximal gastric motor activity during fasting and in response to duodenal nutrient infusion, compared to non-diabetic critically ill patients and healthy humans.

MATERIALS AND METHODS

Subjects

Studies were performed in 25 sedated and mechanically ventilated critically ill patients, who were admitted to a level-3 mixed intensive care unit between January and September 2004. All patients required enteral nutrition. Ten

patients had documented type 2 DM with a mean duration of 7.9 ± 1.8 years. Seven of the diabetic patients had required insulin therapy prior to ICU admission. Formal testing for the presence of autonomic neuropathy was not performed. Fifteen critically ill patients without diabetes mellitus served as patient controls. Exclusion criteria for all patients were (1) recent major abdominal surgery, (2) any contra-indication to passage of an enteral tube, (3) administration of opioid analgesia, benzodiazepines or prokinetic therapy within the previous 24 h, and (4) previous gastric, oesophageal or intestinal surgery. All patients received an insulin infusion for blood glucose control according to a standardized protocol that started on admission and aimed to maintain blood glucose concentrations between 5.0 and 7.9 mmol/L. Data from both patient groups were compared to 10 healthy volunteers, who had no history of systemic or gastrointestinal disease and were not taking any medication. Healthy volunteers were instructed to refrain from smoking for 24 h prior to the study.

Written informed consent was obtained from healthy subjects and the next of kin of patients prior to enrolment into the study. The protocol was approved by the Human Research Ethics Committee of the Royal Adelaide Hospital.

Measurement of proximal gastric motility

Proximal gastric motility was measured using an electronic gastric barostat[16] (Distender Series Ⅱ; G&J Electronics, Ontario, Canada). A thin flaccid-walled bag with a maximum capacity of 1000 mL was attached to the distal end of the assembly, which was connected to the system *via* pressure and volume ports. Changes in proximal gastric volume were measured indirectly by changes in the volume of the polyethylene bag.

Data were stored onto a Powermac 7100 computer (Apple Computer, Cupertino, CA), using custom-written data-acquisition software (Labview: National Instruments, Austin, TX). This software was also used to program the barostat to perform distensions in stepwise increments. Recorded data were imported into a display and analysis program (Acqknowledge, Biopac System, Goleta, CA) for manual analysis.

Blood glucose concentrations

Marked hyperglycaemia may alter small intestinal feedback and adversely affect gastric motility[5-7]. Blood glucose concentrations were measured using a portable glucometer (Precision Plus, Abbott Laboratories, Bedford, USA) immediately before and every 20 min during nutrient infusion.

Protocol

All subjects were studied after at least 6 h fasting and in a 30 degree recumbent position. To standardise the sedative regimen in patients, propofol alone was used, and opioids, benzodiazepines or prokinetic agents were not administered for 24 h prior to and during the study. In patients, placement of both the barostat catheter and post-pyloric feeding tube were performed at the bedside with endoscopic assistance, without additional sedation to that required for ventilation. A 12 French × 114 cm naso-duodenal feeding tube (Flexiflo, Abbott, Ireland) was inserted into the duodenum over a guidewire (THSF-35-260, Cook, Australia). The barostat catheter was then guided through the mouth into the stomach by the endoscope. The barostat bag was inflated with 400 mL of air and gently retracted into the fundus under direct vision. Gastric contents (air and fluid) were aspirated completely prior to withdrawal of the endoscope. Correct placement of the feeding tube was confirmed by measurement of the duodenal trans-mucosal potential difference (TMPD)[16] and subsequently by radiography[13].

In healthy subjects, the barostat assembly and feeding tube were swallowed and allowed to pass into the correct position spontaneously, without the assistance of endoscopy. Duodenal nutrient infusion was achieved by inserting a silicon-rubber catheter (Dentsleeve, Adelaide, Australia) with a central feeding lumen and lead-weighted tip into the stomach. The tube passed spontaneously into the duodenum using phase 2 and 3 of the migrating motor complex. Movement of the catheter into the correct position was monitored continuously by measurement of the antro-duodenal TMPD gradient[16]. Radiological confirmation was not performed in healthy subjects. The barostat catheter was then inserted to a depth of 55 cm, the bag inflated with 400 mL of air and the assembly pulled back until resistance was felt[17].

Following confirmation that both assemblies were positioned correctly, air in the barostat bag was aspirated manually and the catheter was connected to the barostat pump. The minimum distending pressure (MDP), defined as the first pressure level that provided an intragastric bag volume of more than 30 mL, was determined[17]. The intra-bag pressure for the study was set at MDP + 2 mmHg[17]. All studies began with a 15-min baseline recording, during which normal saline (0.9% NaCl) was infused into the duodenum at a rate of 240 mL/h (baseline 1). Each subject then received two 60 minute duodenal infusions of Ensure® (Abbott Laboratories, Ohio, USA; nutrient content: 13% protein, 64% carbohydrate, 21% fat; energy density: 1 kcal/mL) at 1 and 2 kcal/min, in a randomised order. Ensure® was diluted with normal saline to 1:4 for the 1 kcal/min infusion and to 1:2 for 2 kcal/min infusion, and infused at a rate of 240 mL/h. The nutrient infusions were separated by a 2 h 'washout period', consisting of 90 min of no infusion, followed by 30 min of intraduodenal saline infusion (baseline 2). Blood samples for the measurement of blood glucose concentration were collected at baseline and every 20 min during nutrient infusion. Barostat recordings were performed continuously over 4 h. The study protocol is outlined in Figure 1.

Data analysis

Intra-bag volumes were determined at 2-min intervals and the mean baseline volume was measured over 10 min before each infusion. Changes in intra-bag volume during nutrient infusion were calculated as the difference between the actual volume and the mean baseline volume. The serial changes in bag volume during the infusions were plotted and compared. Proximal gastric relaxation was indirectly inferred by an increase in bag volume[17]. The time course for the proximal stomach to return to baseline volume af-

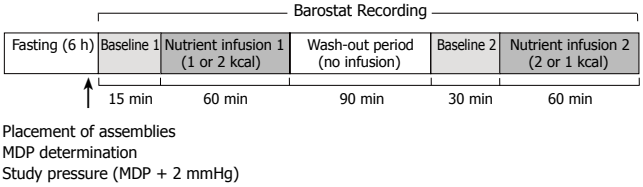

Figure 1 Schematic outline of study protocol.

ter nutrient stimulation was assessed by analysis of the 2 h "no-infusion" period; and was defined as the time taken for the relaxed fundus to return to pre-stimulation level for > 5 min. Assessment of fundic slow volume waves (FW) was also performed. These were defined as changes in proximal gastric volume of greater than 30 mL that reverted in less than 2 min to a volume within 50% of the previous level[17]. The number and amplitude of FWs (per 10 min) was determined during fasting and in response to duodenal nutrient infusion.

Statistical analysis

Data are expressed as mean ± SE. Differences in demographic characteristics, baseline volumes, MDP, FW frequency, peak volume response and the time required for the proximal stomach to return to baseline volume, were compared between the three groups using Student's unpaired *t*-test. ANOVA was used to compare the proximal gastric volume, fundic wave and blood glucose responses to nutrient infusion between the groups, with time and treatment as the factors. A P value < 0.05 was considered statistically significant.

RESULTS

Oral intubation of the assembly was tolerated well by all subjects and no complications occurred in any group. Demographic characteristics of the study groups are summarized in Table 1. The MDP was higher in both patient groups compared to healthy subjects ($P < 0.05$), but was similar between diabetic and non-diabetic patients (Table 2). Baseline proximal gastric volumes were similar between the three groups.

Proximal gastric volume response to duodenal nutrients

In response to duodenal nutrients, healthy volunteers demonstrated a "biphasic" proximal gastric volume response. Following an initial rapid relaxation, the fundus partially contracted and then exhibited a sustained relaxation throughout the remainder of the infusion (Figure 2). In non-diabetic critically ill patients, there was an overall impairment of both the initial and later phase of the response. In diabetic patients, however, there was an absence of the initial response in the first 20 min during both 1 and 2 kcal/min infusions. Thereafter, the proximal gastric volume increased to the level observed in healthy volunteers.

During the 1 kcal/min infusion there was no difference in the proximal gastric volume response between diabetic critically ill patients and the other two groups. However, during the first 20 min of the 2 kcal/min infusion, the proximal gastric volume was significantly smaller in diabetic critically ill patients than in non-diabetic critically ill patients and healthy subjects. Thereafter, the proximal gastric volume of diabetic patients was greater than that of non-diabetic patients and similar to healthy subjects (Figure 2).

Table 1 Demographic characteristics of the critically ill patients and healthy subjects

	Diabetic ICU patients (n = 10)	Non-diabetic ICU patients (n = 15)	Healthy subjects (n = 10)
Age (yr)	59 ± 3[a]	48 ± 5[a]	28 ± 3
Gender (M:F)	5:5	12:3	7:3
BMI (kg/m^2)	35 ± 3[c]	27 ± 1	25 ± 1
APACHE II score			
On admission	28.6 ± 1.5	23.2 ± 0.8	N/A
On study day	24.7 ± 1.5	21.1 ± 1.3	
Diagnoses	Sepsis (3)	Sepsis (3)	N/A
	Pneumonia (3)	Pancreatitis (2)	
	Severe asthma (1)	Head trauma (2)	
	MVA (1)	MVA (3)	
	Angioedema (1)	Cardiac failure (2)	
	Sub-arachnoid haemorrhage (1)	Burn (1)	
		Lung abscess (1)	
		Meningitis (1)	

MVA: Motor Vehicle Accident. [a]$P < 0.05$ *vs* healthy subjects; [c]$P < 0.05$ *vs* healthy subjects and non-diabetic critically ill patients.

Table 2 Comparison of proximal gastric motor activity between critically ill patients and healthy subjects

	Diabetic ICU patients (n = 10)	Non-diabetic ICU patients (n = 15)	Healthy subjects (n = 10)
MDP (mmHg)	11.9 ± 1.0[a]	11.3 ± 1.2[a]	7.1 ± 0.6
Baseline intra-gastric volume (mL)	187 ± 43	197 ± 22	182 ± 19
Time to recovery of baseline volume following infusion (min)	41 ± 15[a]	83 ± 11[c]	15 ± 4

[a]$P < 0.05$ *vs* healthy subjects; [c]$P < 0.05$ *vs* diabetic patients and healthy subjects.

Recovery of proximal gastric volume after nutrient stimulation

The proximal gastric volume returned to baseline level within 60 min following cessation of nutrient stimulation in all diabetic patients and healthy subjects, but in only 2 of the 15 non-diabetic patients. In diabetic patients, the time taken for the proximal gastric volume to return to baseline level was significantly shorter than in non-diabetic patients and longer than healthy subjects (Table 2).

Fundic volume wave frequency

At baseline, the mean frequency of FWs in diabetic patients (10.2 ± 1.7 waves/10 min) was similar to that of healthy subjects (11.8 ± 0.9 waves/10 min; $P = 0.38$), but was higher than non-diabetic patients (7.0 ± 0.8 waves/10 min; $P < 0.05$; Figure 3).

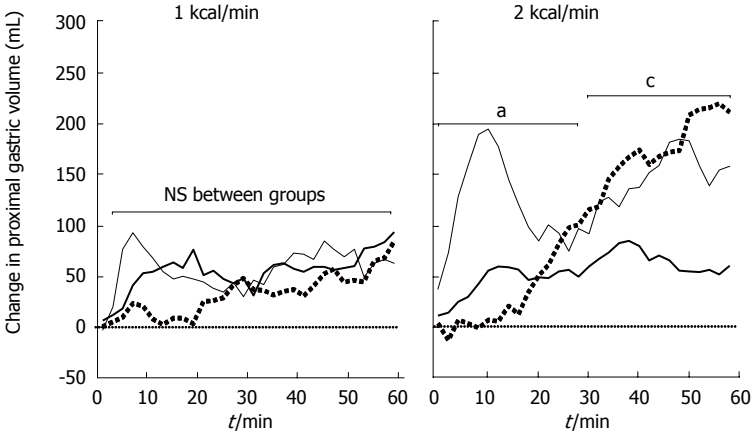

Figure 2 Changes in proximal gastric volume during duodenal nutrient stimulation (1 and 2 kcal/min) in critically ill patients and healthy subjects. $^{a}P < 0.05$, ICU patients *vs* healthy subjects during 0-30 min; $^{c}P < 0.05$, non-DM patients *vs* diabetic patients and healthy subjects during 30- 60 min.

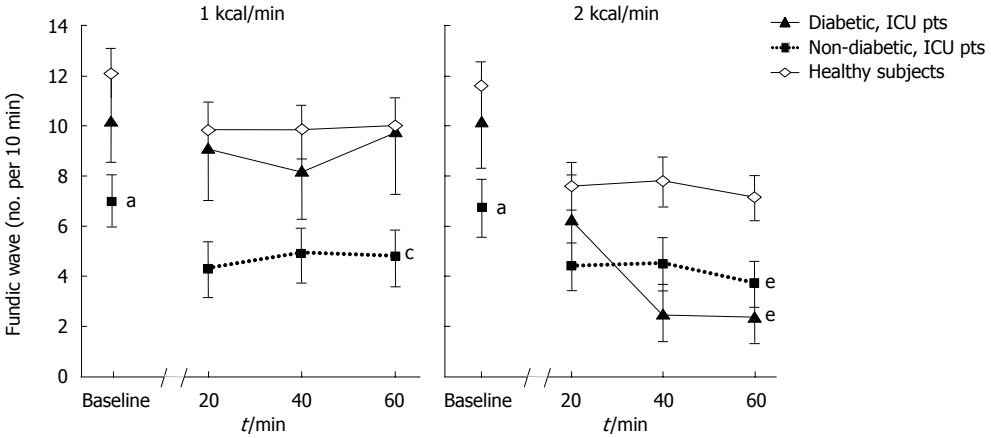

Figure 3 Frequency of fundic slow wave contractions at baseline and during duodenal nutrient infusion (1 and 2 kcal/min) in critically ill patients and healthy subjects. $^{a}P < 0.05$ *vs* healthy subjects and diabetic patients at baseline; $^{c}P < 0.05$ *vs* healthy subjects and diabetic patients during 1 kcal infusion; $^{e}P < 0.05$ *vs* healthy subjects during 2 kcal infusion.

The impact of duodenal nutrient stimulation on the frequency of FWs in diabetic patients was similar to that of healthy subjects but differed from non-diabetic patients (Figure 3). Nutrient stimulation with 1 kcal/min infusion did not reduce the mean frequency of FWs in either diabetic patients (9.0 ± 2.0 waves/10 min) or healthy subjects (9.9 ± 1.0 waves/10 min), in contrast to non-diabetic patients (4.4 ± 0.9 waves/10 min; $P < 0.05$). However, in all 3 groups the 2 kcal/min nutrient infusion significantly reduced the mean frequency of FWs compared to baseline (diabetic: 3.9 ± 1.1 waves/10 min, $P < 0.05$; healthy: 7.6 ± 0.8 waves/10 min, $P < 0.001$; non-diabetic: 4.2 ± 0.9 waves/10 min, $P < 0.05$). The magnitude of reduction in FW frequency during 2 kcal/min was greatest in diabetic patients (-6.6 ± 1.7 waves/10 min), compared to healthy subjects (-4.0 ± 0.7 waves/10 min, $P < 0.05$) and non-diabetic patients (-1.9 ± 0.6, $P < 0.001$; Figure 3).

Overall, the frequency of FWs in diabetic patients during 1 kcal/min infusion was similar to that of healthy subjects, but was higher than non-diabetic patients. In contrast, due to the greater magnitude of reduction in FW frequency by a higher nutrient load, fundic wave activity during 2 kcal/min infusion in diabetic patients was similar to that of non-diabetic patients, but less than that of healthy subjects (Figure 3).

Blood glucose concentrations

Overall, both fasting and nutrient-stimulated blood glucose concentrations were higher in critically ill patients than in healthy subjects (Figure 4). There were no significant differences in blood glucose concentrations between diabetic and non-diabetic patients, reflecting the use of an insulin infusion protocol in all patients.

DISCUSSION

This is the first study to examine proximal gastric motor activity in critically ill patients with type 2 diabetes mellitus. The results show that the response to intestinal nutrient feedback is characterized by an initial absence of proximal gastric relaxation, after which the volume increased to a level similar to that seen in healthy volunteers. Furthermore, the delayed volume response was associated with a nutrient load-dependent reduction in fundic wave activity and a slightly impaired recovery of the proximal gastric volume to baseline level. This is in contrast to non-diabetic critically ill patients, who demonstrated a sustained impairment of proximal gastric relaxation, a reduction in fundic wave activity even during 1 kcal/min infusion and a failure of the fundus to recover to baseline volume. These findings support a recent retrospective study, which suggested that type 2 diabetes mellitus may not be a risk factor for delayed gastric emptying in critical illness[18].

A notable feature of the proximal gastric response to nutrient stimulation in diabetic patients was the complete absence of proximal gastric relaxation during the first 20 min of nutrient infusion, however the reason for this re-

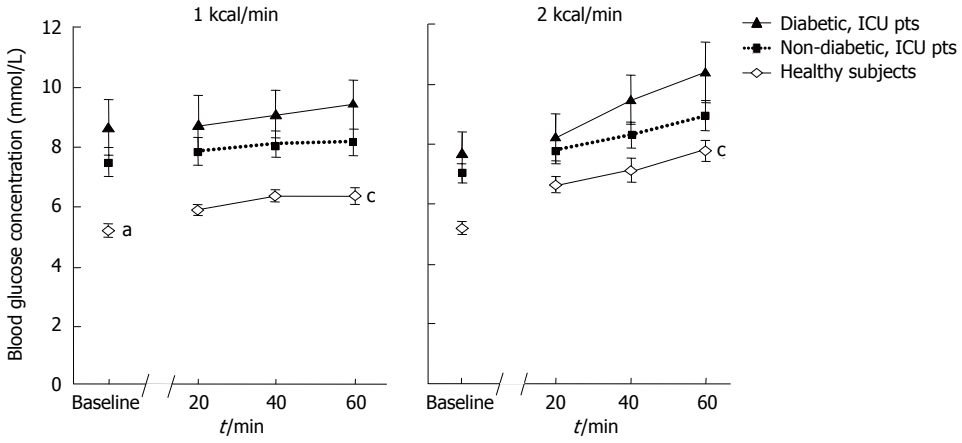

Figure 4 Blood glucose concentration at baseline and during nutrient infusion in critically ill patients and healthy subjects. $^{a}P < 0.05$ *vs* critically ill patients at baseline; $^{c}P < 0.05$ *vs* critically ill patients during nutrient infusion.

sponse remains unclear. In health, gastro-enteric feedback is regulated by neuro-hormonal pathways[14,16-19], and proximal gastric tone is modulated by a balance between the excitatory cholinergic nerves and the inhibitory nitrergic neural inputs from the vagus[20]. As autonomic dysfunction is common in patients with diabetic autonomic neuropathy[8] and during critical illness[21] the greater degree of impaired relaxation in our diabetic patients may relate to an adverse 'additive-effect' of both factors on the autonomic nervous system[20-22]. Formal testing for autonomic neuropathy was not performed in the current study as this was not feasible in the acute critical care setting. A prevalence of autonomic neuropathy of more than 50% would be expected, based on a previous study in diabetic patients with a similar mean duration of disease[23]. Furthermore, disturbances in the metabolism of nitric oxide, a key transmitter in the regulation of gastrointestinal motor function, may also be important[22]. Impaired proximal gastric relaxation is associated with altered levels of nitric oxide[1,8], and has been reported in both patients with diabetes mellitus[1] and critical illness[24]. Whilst increased cytokine production[25] and drug usage[26] can also contribute to impaired relaxation, the impact of these factors are likely to be similar between diabetic and non-DM critically ill patients and probably do not account for the differences in gastric motility seen between the groups.

Following the initial impairment of relaxation, the proximal gastric volume in diabetic critically ill patients increased to a level comparable to that of healthy subjects. This finding has not been previously reported in either patients with critical illness or diabetes mellitus alone. In the later, proximal gastric motor responses to gastric but not duodenal nutrients have been evaluated and further studies to assess this may provide useful information. The mechanisms underlying this normalization of proximal gastric motility are unknown. Despite the use of a standardized insulin protocol in all patients during the study, a small degree of hyperglycaemia occurred in diabetic patients during the latter half of the 2 kcal/min infusion (Figure 4). Although hyperglycaemia has been shown to induce proximal gastric relaxation[7], the absolute increase in blood glucose level was small and therefore unlikely to have contributed significantly to the subsequent response. The diabetic patients had a higher BMI than the healthy volunteers, however no differences in either proximal gastric volume or compliance have been reported between obese and lean subjects[27,28]. Thus, a higher BMI in diabetic patients seems unlikely to have contributed to the differences in proximal gastric motility. Opiate drugs such as morphine were excluded 24 h prior to the study, hence are unlikely to explain our findings[29].

To standardize the nutrient stimulation and enable a reliable assessment of the entero-gastric feedback response, feeds were delivered directly into the duodenum at a rate consistent with normal gastric emptying. Intra-gastric delivery of nutrients was not used in the current study because gastric emptying is frequently impaired in the critically ill. Furthermore, both gastric motility and emptying of a liquid meal may be altered by the presence of a barostat balloon[30]. In addition, intra-duodenal nutrient stimulation with 1 and 2 kcal/min nutrient loads enabled examination of the dose-dependency of the proximal gastric motor response[16,17,19].

Previous studies in critically ill patients have suggested enhanced entero-gastric feedback in response to duodenal nutrient stimulation[12]. In contrast to the non-diabetic patients, diabetic critically ill patients had a dose-dependent reduction in fundic wave activity, similar to the healthy subjects. The different responses in fundic wave activity during the 1 and 2 kcal/min nutrient loads between the diabetic and non-diabetic patients suggest that entero-gastric feedback is not increased in diabetic patients. Furthermore, apart from an initial delay in relaxation, the overall proximal gastric motor responses to nutrients in diabetic critically ill patients were similar to those of healthy subjects. As the proximal stomach is a major determinant of liquid gastric emptying[16,17,19], these findings may explain the relatively normal gastric emptying observed in this group of patients[14].

Whether differences in the 'accommodative' response to nutrients between the two patient groups affect their ability to tolerate bolus or continuous gastric feeds remains to be determined and requires further study. It is conceivable that slow continuous feeds may be better tolerated in non-diabetic critically ill patients as proximal gastric relaxation is small and slow during nutrient stimulation[9,11]. In contrast, the relatively normal 'biphasic' proximal gastric response in the diabetic critically ill patients may allow better tolerance to bolus gastric feeds.

In conclusion, proximal gastric motor responses to

duodenal nutrient are relatively normal in type 2 diabetic patients during critical illness. These motor findings support data which suggests these patients may have normal gastric emptying[18] and may be less prone to developing naso-gastric feed intolerance than non-diabetic, critically ill patients.

REFERENCES

1 **Horowitz M**, Wishart JM, Jones KL, Hebbard GS. Gastric emptying in diabetes: an overview. *Diabet Med* 1996; **13**: S16-S22

2 **Weytjens C**, Keymeulen B, Van Haleweyn C, Somers G, Bossuyt A. Rapid gastric emptying of a liquid meal in long-term Type 2 diabetes mellitus. *Diabet Med* 1998; **15**: 1022-1027

3 **Bertin E**, Schneider N, Abdelli N, Wampach H, Cadiot G, Loboguerrero A, Leutenegger M, Liehn JC, Thiefin G. Gastric emptying is accelerated in obese type 2 diabetic patients without autonomic neuropathy. *Diabetes Metab* 2001; **27**: 357-364

4 **Phillips WT**, Schwartz JG, McMahan CA. Rapid gastric emptying in patients with early non-insulin-dependent diabetes mellitus. *N Engl J Med* 1991; **324**: 130-131

5 **Rayner CK**, Samsom M, Jones KL, Horowitz M. Relationships of upper gastrointestinal motor and sensory function with glycemic control. *Diabetes Care* 2001; **24**: 371-381

6 **Fraser RJ**, Horowitz M, Maddox AF, Harding PE, Chatterton BE, Dent J. Hyperglycaemia slows gastric emptying in type 1 (insulin-dependent) diabetes mellitus. *Diabetologia* 1990; **33**: 675-680

7 **Hebbard GS**, Sun WM, Dent J, Horowitz M. Hyperglycaemia affects proximal gastric motor and sensory function in normal subjects. *Eur J Gastroenterol Hepatol* 1996; **8**: 211-217

8 **Samsom M**, Roelofs JM, Akkermans LM, van Berge Henegouwen GP, Smout AJ. Proximal gastric motor activity in response to a liquid meal in type I diabetes mellitus with autonomic neuropathy. *Dig Dis Sci* 1998; **43**: 491-496

9 **Heyland DK**, Tougas G, King D, Cook DJ. Impaired gastric emptying in mechanically ventilated, critically ill patients. *Intensive Care Med* 1996; **22**: 1339-1344

10 **Dive A**, Moulart M, Jonard P, Jamart J, Mahieu P. Gastroduodenal motility in mechanically ventilated critically ill patients: a manometric study. *Crit Care Med* 1994; **22**: 441-447

11 **Mutlu GM**, Mutlu EA, Factor P. GI complications in patients receiving mechanical ventilation. *Chest* 2001; **119**: 1222-1241

12 **Nguyen NQ**, Fraser RJ, Chapman M, Bryant LK, Holloway RH, Vozzo R, Feinle-Bisset C. Proximal gastric response to small intestinal nutrients is abnormal in mechanically ventilated critically ill patients. *World J Gastroenterol* 2006; **12**: 4383-4388

13 **Chapman M**, Fraser R, Vozzo R, Bryant L, Tam W, Nguyen N, Zacharakis B, Butler R, Davidson G, Horowitz M. Antro-pyloro-duodenal motor responses to gastric and duodenal nutrient in critically ill patients. *Gut* 2005; **54**: 1384-1390

14 **Lin HC**, Doty JE, Reedy TJ, Meyer JH. Inhibition of gastric emptying by glucose depends on length of intestine exposed to nutrient. *Am J Physiol* 1989; **256**: G404-G411

15 **Umpierrez GE**, Isaacs SD, Bazargan N, You X, Thaler LM, Kitabchi AE. Hyperglycemia: an independent marker of in-hospital mortality in patients with undiagnosed diabetes. *J Clin Endocrinol Metab* 2002; **87**: 978-982

16 **Heddle R**, Collins PJ, Dent J, Horowitz M, Read NW, Chatterton B, Houghton LA. Motor mechanisms associated with slowing of the gastric emptying of a solid meal by an intraduodenal lipid infusion. *J Gastroenterol Hepatol* 1989; **4**: 437-447

17 **Azpiroz F**, Malagelada JR. Intestinal control of gastric tone. *Am J Physiol* 1985; **249**: G501-G509

18 **Nguyen NQ**, Chapman M, Fraser RJ, Ritz M, Bryant LK, Butler R, Davidson G, Zacharakis B, Holloway RH. Long-standing type II diabetes mellitus is not a risk factor for slow gastric emptying in critically ill patients. *Intensive Care Med* 2006; **32**: 1365-1370

19 **Kelly KA**. Gastric emptying of liquids and solids: roles of proximal and distal stomach. *Am J Physiol* 1980; **239**: G71-G76

20 **Paterson CA**, Anvari M, Tougas G, Huizinga JD. Nitrergic and cholinergic vagal pathways involved in the regulation of canine proximal gastric tone: an in vivo study. *Neurogastroenterol Motil* 2000; **12**: 301-306

21 **Schmidt HB**, Werdan K, Müller-Werdan U. Autonomic dysfunction in the ICU patient. *Curr Opin Crit Care* 2001; **7**: 314-322

22 **Kellow JE**, Delvaux M, Azpiroz F, Camilleri M, Quigley EM, Thompson DG. Principles of applied neurogastroenterology: physiology/motility-sensation. *Gut* 1999; **45** Suppl 2: II17-II24

23 **Valensi P,** Pariès J, Attali JR. Cardiac autonomic neuropathy in diabetic patients: influence of diabetes duration, obesity, and microangiopathic complications--the French multicenter study. *Metabolism* 2003; **52**: 815-820

24 **Argaman Z**, Young VR, Noviski N, Castillo-Rosas L, Lu XM, Zurakowski D, Cooper M, Davison C, Tharakan JF, Ajami A, Castillo L. Arginine and nitric oxide metabolism in critically ill septic pediatric patients. *Crit Care Med* 2003; **31**: 591-597

25 **Emch GS**, Hermann GE, Rogers RC. TNF-alpha activates solitary nucleus neurons responsive to gastric distension. *Am J Physiol Gastrointest Liver Physiol* 2000; **279**: G582-G586

26 **Lee TL**, Ang SB, Dambisya YM, Adaikan GP, Lau LC. The effect of propofol on human gastric and colonic muscle contractions. *Anesth Analg* 1999; **89**: 1246-1249

27 **Park MI**, Camilleri M. Gastric motor and sensory functions in obesity. *Obes Res* 2005; **13**: 491-500

28 **Kim DY**, Camilleri M, Murray JA, Stephens DA, Levine JA, Burton DD. Is there a role for gastric accommodation and satiety in asymptomatic obese people? *Obes Res* 2001; **9**: 655-661

29 **Lefebvre RA**, Willems JL, Bogaert MG. Gastric relaxation and vomiting by apomorphine, morphine and fentanyl in the conscious dog. *Eur J Pharmacol* 1981; **69**: 139-145

30 **Ropert A**, des Varannes SB, Bizais Y, Rozé C, Galmiche JP. Simultaneous assessment of liquid emptying and proximal gastric tone in humans. *Gastroenterology* 1993; **105**: 667-674

S- Editor Liu Y **L- Editor** Iqbal A **E- Editor** Liu WF

PO Box 2345, Beijing 100023, China
www.wjgnet.com
wjg@wjgnet.com

World J Gastroenterol 2007 January 14; 13(2): 276-279
World Journal of Gastroenterology ISSN 1007-9327
© 2007 The WJG Press. All rights reserved.

CLINICAL RESEARCH

Role of ciprofloxacin in patients with cholestasis after endoscopic retrograde cholangiopancreatography

Thawee Ratanachu-ek, Pitchaya Prajanphanit, Kawin Leelawat, Suchart Chantawibul, Sukij Panpimanmas, Somboon Subwongcharoen, Jerasak Wannaprasert

Thawee Ratanachu-ek, Pitchaya Prajanphanit, Kawin Leelawat, Suchart Chantawibul, Sukij Panpimanmas, Somboon Subwongcharoen, Jerasak Wannaprasert, Department of Surgery, Rajavithi Hospital, Bangkok 10400, Thailand
Correspondence to: Thawee Ratanachu-ek, Department of Surgery, Rajavithi Hospital, Rajavithi Rd, Rajathevi, Bangkok 10400, Thailand. Thawee1958@hotmail.com
Telephone: +66-2-3548080 Fax: +66-2-3548080
Received: 2006-09-13 Accepted: 2006-11-14

Key words: Antibiotic; Cholestasis; Cholangitis; Endoscopic retrograde cholangiopancreatography; Biliary drainage

Ratanachu-ek T, Prajanphanit P, Leelawat K, Chantawibul S, Panpimanmas S, Subwongcharoen S, Wannaprasert J. Role of ciprofloxacin in patients with cholestasis after endoscopic retrograde cholangiopancreatography. *World J Gastroenterol* 2007; 13(2): 276-279

http://www.wjgnet.com/1007-9327/13/276.asp

Abstract

AIM: To determine the role of ciprofloxacin in reducing cholangitis in cholestatic patients with adequate biliary drainage after endoscopic retrograde cholangiopancreatography (ERCP).

METHODS: A randomized, controlled trial was performed in 48 cholestatic patients at Rajavithi Hospital (Tertiary Referral Center for ERCP: 600 cases per year). All the 48 patients received 200 mg ciprofloxacin intravenous injection for 30 min before starting any procedures, and then were randomly divided in two groups. Twenty-two patients in study group continually received ciprofloxacin until 48 h after ERCP. Causes of biliary obstruction, bacteriology of bile and blood (in cholangitis) and clinical cholangitis were recorded.

RESULTS: Forty-eight patients were enrolled and divided into continuous ciprofloxacin treatment group (n = 22) and discontinuous ciprofloxacin treatment group (n = 26). During ERCP, stones were found in 22 patients, malignant diseases in 24 patients and other pathologic lesions in 5 patients. One (4.5%) of the 22 patients who received ciprofloxacin and 2 (6.3%) of the 26 patients who discontinued ciprofloxacin after ERCP developed cholangitis (relative risk = 0.71; 95% CI = 0.14-3.65; P = 0.88). Bacterobilia was found in 27 (56.3%) out of 48 patients. *E. coli* and *Streptococcus viridans* were the most common organisms.

CONCLUSION: Continual use of ciprofloxacin in patients with cholestasis after adequate biliary drainage procedures plays no role in reducing cholangitis.

© 2007 The WJG Press. All rights reserved.

INTRODUCTION

Endoscopic retrograde cholangiopancreatography (ERCP) is widely used in diagnosis and treatment of biliary and pancreatic diseases[1,2]. Acute cholangitis and septicemia remain serious complications related to this technique[3]. The incidence of cholangitis is 0.8%-19%, and its mortality rate is 10%[4].

The role of prophylactic antibiotics after ERCP has been recently assessed in several placebo-controlled randomized trials[5-9]. This procedure plays an essential part in high risk patients with prosthetic valve and history of endocarditis, obstructed bile duct, pancreatic cystic lesion and inadequate common bile duct drainage[3,10]. To date, no antibiotic regimen has emerged. Most of the bacterial florae in bile of patients with cholangitis and asymptomatic bacterobilia are Gram-negative organisms such as *E. coli, Klebsella spp.* and Gram-positive organisms such as *Enterococcus fecalis*[5-6,11-13]. The choice of an antibiotic regimen should be able to cover the Gram-negative bacteria and effectively penetrates the obstructed biliary tree. Ciprofloxacin attains a concentration in bile of approximately 20% of the mean peak level in serum, even in an obstructed biliary system. This drug level is still 10 times higher than MIC of the Gram-negative bacteria and is the most effective antibiotic against the Gram-negative bacteria, as indicated in the standard guidelines[3,5,7,10,12-13].

Ciprofloxacin is highly effective against cholestasis. However, no previous clinical study has reported the role of continuous use of ciprofloxacin in cholestatic patients after ERCP. Although many professional gastrointestinal societies recommend prophylactic use of antibiotics in the treatment of obstructive jaundice patients after ERCP, no guideline has been established after adequate biliary drainage.

The aim of this study was to evaluate the effect of

ciprofloxacin in reducing the incidence of cholangitis after adequate endoscopic biliary drainage.

MATERIALS AND METHODS

Subjects

This study was a randomized, controlled trial approved by the Ethics Committee of Rajavithi Hospital. Cholestatic patients in Rajavithi Hospital (Tertiary Referral Center for ERCP), Bangkok, Thailand, admitted between June 2005 and May 2006 were included in this study. Inclusion criteria included age of 18 years or older, cholestasis (at least two from 4 criteria of total bilirubin > 2 mg/dL, serum alkaline phosphatase more than twice of normal value, alanine transaminase > 40 mmol/L and ultrasound or CT-scan showing dilated bile duct). All the patients underwent ERCP and gave their written informed consent to participate in the study. Patients were excluded from the study if they refused to participate in the study, or had endocarditis or vulvular heart disease, history of allergy to fluoroquinolone group, cholangitis or sepsis, use of antibiotics within 7 d before ERCP.

Methods

All cholestatic patients received 200 mg ciprofloxacin intravenous injection about 30 min before ERCP. Bile was aspirated before contrast medium was injected and sent to cultivation. Those who did not have biliary drainage after ERCP were excluded from this study, and ciprofloxacin was given until infection subsided. All patients who had adequate biliary drainage (defined as total relief of bile duct obstruction by stone extraction, sphincterotomy or stent replacement), were randomly divided into two groups: continuous ciprofloxacin treatment group and discontinuous ciprofloxacin treatment group. Ciprofloxacin (200 mg) intravenous injection every 12 h was given to the continuous ciprofloxacin treatment group for 48 h after ERCP, and discontinued if no infection signs and symptoms were found. The discontinuous ciprofloxacin treatment group was not given any ciprofloxacin after an adequate biliary drainage. If cholangitis occurred in any group, 200 mg ciprofloxacin intravenous injection every 12 h or other proper antibiotics (following blood or bile culture and sensitivity) were given until the infection subsided (no fever and WBC < $10 \times 10^9/m^3$) (Figure 1).

Vital signs were monitored every 8 h, liver function test and CBC count were performed once a day. Hemoculture was done if body temperature was above 38℃. Monitoring was continued until the doctor decided to discontinue it based on the following criteria, including stable vital signs, body temperature below 38℃, improvement in cholestasis and jaundice, and absence of abdominal pain.

ERCP was performed in all patients by the same endoscopist (Dr. Thawee Ratanachu-ek) under TJF-160 endoscope. After successful cannulation of the common bile duct, bile samples were obtained for bacteriological culture, and the definitive treatment for obstruction was performed. After each endoscopic procedure, endoscopes were manually washed by trained nurses according to the manufacturer's instructions.

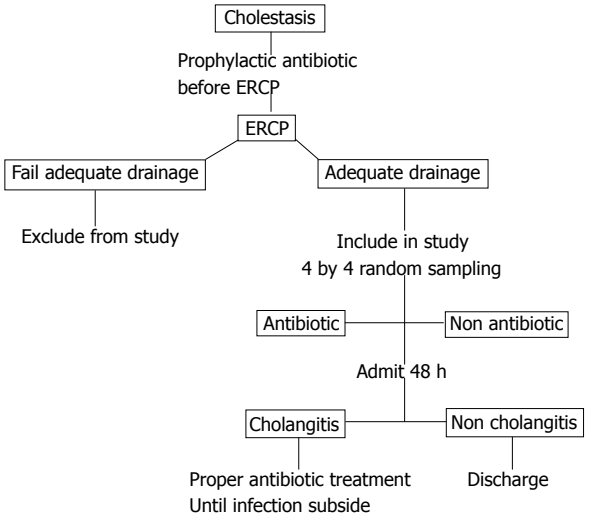

Figure 1 Flow chart of cholestasis management.

Statistical analysis

All statiscal analyses were performed using the Yates' modified chi-square test and Student's *t* test, and expressed as mean ± SD.

RESULTS

During June 2005 and May 2006, 48 patients after ERCP were enrolled in the study. All the patients received prophylactic ciprofloxacin, and divided into two groups: continuous ciprofloxacin treatment group (n = 22) and discontinuous ciprofloxacin treatment group (n = 26). The clinical characteristics and demographics in both groups were similar (Table 1). Stones were the most common cause of cholestasis in both groups. Diagnosis and intervention during ERCP are presented in Table 1.

Cholangitis was found in one (4.5%) out of 22 patients in the continuous ciprofloxacin treatment group and 2 (7.7%) out of 26 patients in the discontinuous ciprofloxacin treatment group. No sepsis and death occurred in this study.

The incidence of cholangitis was also similar in ciprofloxacin-treated patients after ERCP and controls (the relative risk = 0.71, 95% CI = 0.14 to 3.65). The total incidence of bacterobilia was 56.3% (27/48). The incidence of bacterobilia was 59.1% (13/22) in the continuous ciprofloxacin treatment group and 53.8% (14/26) in the control group (relative risk = 1.12, 95% CI = 0.60 to 2.11) (Table 2).

Gram-negative organisms were the most commonly found in the bile cultures. The bacteriology of bile cultures from both groups is illustrated in Table 3.

Three (11.1%) out of 27 patients with bacterobilia who developed cholangitis were found to have Gram-negative organisms in their blood culture. One female patient in the continuous ciprofloxacin treatment group had hepatocellular cancer, and a stent was inserted to the right anterior segment of the liver. She was febrile on the second day after ERCP, indicating that she had

Table 1 Clinical characteristics of 48 patients undergoing ERCP

Characteristic	Ciprofloxacin (*n* = 22)		None-ciprofloxacin (*n* = 26)	
	n	%	*n*	%
Sex (M:F)	13:9	59.1:40.9	11:15	42.3:57.7
Age (mean ± SD yr)	58.68 ± 13.7		61.08 ± 11.9	
Causes				
Bile duct stone	7	31.8	15	57.7
Cancer	13	59.1	11	42.3
Cholangiocarcinoma	6	27.3	6	23.1
Periampullary cancer	6	27.3	5	19.2
Hepatocellular cancer	1	4.5	0	0
Others	2	9.1	3	11.54
Bile duct stricture	1	4.5	1	3.8
Pseudocyst	1	4.5	0	0
Choledochal cyst	0	0	1	3.8
Chronicpancreatitis	0	0	1	3.8
Interventions				
Stone extraction	5	22.7	13	50
Sphincterotomy	13	59.1	14	53.8
Stent placement	16	72.7	14	53.8

Table 2 Incidence of cholangitis and bacteremia in two study groups

Complication	Ciprofloxacin post-ERCP		Relative risk	95% CI
	Yes (*n* = 22)	No (*n* = 26)		
Cholangitis	1 (4.5%)	2 (7.7%)	0.71	0.14-3.65
Bacteremia	13 (59.1%)	14 (53.8%)	1.12	0.60-2.11

Table 3 Bacterial species in cultures of bile from 48 patients

Bacterial culture	Antibiotic (22) *n* (%)	No antibiotic (26) *n* (%)	*P*
Negative	9 (40.9)	12 (46.2)	0.72
Positive	13 (59.1)	14 (53.8)	0.72
Gram negative			
E. coli	4 (30.8)	3 (21.4)	0.81
Klebsella spp.	2 (15.4)	2 (14.3)	0.73
Pseudomonas spp.	2 (15.4)	1 (7.1)	0.88
Gram positive	3 (13.6)	9 (34.6)	0.09
Streptococcus viridans	3	4 (28.6)	
Streptococcus bovis	0	1 (7.1)	
Enterococcus fecalis	0	3 (21.4)	
Staphylococcus spp.	0	1 (7.1)	
Non *C. albican*	1 (7.7)	0	

Table 4 Bile and hemoculture in three cholangitis patients

Group	Bacteriology	
	Bile culture	Hemoculture
Antibiotic group	*Streptococcus-viridans*	Negative
No antibiotic group		
First patient	*E. coli*	Negative
Second patient	*Pseudomonas spp.*	Negative

leukocytosis (WBC count was $10.8 \times 10^9/m^3$). She received 2 g ceftriazone intravenous injection daily for 11 d until infection subsided.

Two patients developed cholangitis in the discontinuous ciprofloxacin treatment group. Both received proper antibiotics until infection subsided. The results of bile cultures and hemocultures are shown in Table 4.

DISCUSSION

Bacteremia and cholangitis are the important complications of ERCP, and their incidence varies from 0.8%-19%[4]. It is known that prophylactic antibiotic treatment before ERCP plays a crucial role in the treatment of high risk patients with bile duct obstruction, pancreatic pseudocyst and inadequate cholestatic drainage[3,10-11]. However, the efficacy of such extensive use of antibiotics after ERCP has not been previously demonstrated, thus leading to the design of our study.

All the patients had mild or moderate cholangitis. This might be due to a benefit of the routine use of prophylactic ciprofloxacin in cholestatic patients before ERCP. Loperfido *et al*[14] found that small center, jaundice and male sex were risk factors for developing cholangitis after ERCP. We had only one male patient out of 3 cholangitis patients who had obstructive jaundice in our hospital (Tertiary Referral Center for ERCP: 600 cases per year).

In our study, cholangitis incidence after ERCP was lower than that in previous studies[8,9,15]. This might be attributed to the low natural incidence of the disease[4], standard sterile technique used in our hospital, and all procedures done by the same endoscopist, and our technique in collecting the bile before injecting contrast media. All these suggest that bacteriologic study and release of biliary tract pressure can reduce the incidence of pressure-induced sepsis.

E. coli, Streptococcus viridans and *Klebsiella spp.* are the most frequently isolated organisms from bile. Rung R *et al*[13] have found a similar incidence of bacterobilia (56.3%). Ciprofloxacin was chosen in our study because of its efficacy against most Gram-negative organisms (*E. coli* and *Klebsiella spp.*) which are the pathogens most frequently found in biliary tract infection[5-6,12-13,16-17] and its penetration into the obstructive biliary tree[6].

We found 12 Gram-positive bacteria in bile cultures (*Streptococcus viridans* and *Enterococcus spp.*) of the 27 bacterobilia specimens (56.3%), which is consistent with previous studies on bacteriology of bile in patients with obstructive jaundice, showing that *Streptococcus viridans* and *Enterococcus spp.* are the most common Gram-positive bacteria in bile cultures[18-23]. Clark *et al*[24] have found the same results and recommended ampicillin/sulbactam for all biliary obstructions with positive bile *Enterococci*. We conclude that once Gram positive bacteria are detected, perioperative use of appropriate antibiotics is mandatory to reduce postoperative septic complications.

The results of our trial showed no difference in the incidences of cholangitis between the two groups (4.5% in the continuous ciprofloxacin treatment group and 7.7% in discontinuous ciprofloxacin treatment group, relative risk = 0.71, 95% CI = 0.14 to 3.65, $P = 0.88$).

Alveyn CG *et al*[25] used 750 mg of ciprofloxacin taken

orally in 47 jaundice patients about 90 min before ERCP to prevent sepsis and we used the same sample size (48 patients). Our suggestion is that if a larger sample size is employed, this outcome may be strongly enforced.

In conclusion, extensive use of antibiotics after adequate drainage by ERCP in cholestatic patients does not substantially reduce the incidence of cholangitis. Continuous use of antibiotics is unnecessary in these patients. The results of this study may contribute to decreasing the drawbacks of the widespread use of antibiotics including cost, adverse effects, and emergency of resistant strains of bacteria.

REFERENCES

1 **Carr-Locke DL**. Overview of the role of ERCP in the management of diseases of the biliary tract and the pancreas**.** *Gastrointest Endosc* 2002; **56**: :S157-S160

2 **ASGE guidelines for clinical application**. The role of ERCP in diseases of the biliary tract and pancreas. American Society for Gastrointestinal Endoscopy. *Gastrointest Endosc* 1999; **50**: 915-920

3 **Rey JR**, Axon A, Budzynska A, Kruse A, Nowak A. Guidelines of the European Society of Gastrointestinal Endoscopy (E.S.G.E.) antibiotic prophylaxis for gastrointestinal endoscopy. European Society of Gastrointestinal Endoscopy. *Endoscopy* 1998; **30**: 318-324

4 **Bilbao MK**, Dotter CT, Lee TG, Katon RM. Complications of endoscopic retrograde cholangiopancreatography (ERCP). A study of 10,000 cases. *Gastroenterology* 1976; **70**: 314-320

5 **Sung JJ**, Lyon DJ, Suen R, Chung SC, Co AL, Cheng AF, Leung JW, Li AK. Intravenous ciprofloxacin as treatment for patients with acute suppurative cholangitis: a randomized, controlled clinical trial. *J Antimicrob Chemother* 1995; **35**: 855-864

6 **van den Hazel SJ**, Speelman P, Tytgat GN, Dankert J, van Leeuwen DJ. Role of antibiotics in the treatment and prevention of acute and recurrent cholangitis. *Clin Infect Dis* 1994; **19**: 279-286

7 **Mehal WZ**, Culshaw KD, Tillotson GS, Chapman RW. Antibiotic prophylaxis for ERCP: a randomized clinical trial comparing ciprofloxacin and cefuroxime in 200 patients at high risk of cholangitis. *Eur J Gastroenterol Hepatol* 1995; **7**: 841-845

8 **Niederau C**, Pohlmann U, Lübke H, Thomas L. Prophylactic antibiotic treatment in therapeutic or complicated diagnostic ERCP: results of a randomized controlled clinical study. *Gastrointest Endosc* 1994; **40**: 533-537

9 **Byl B**, Devière J, Struelens MJ, Roucloux I, De Coninck A, Thys JP, Cremer M. Antibiotic prophylaxis for infectious complications after therapeutic endoscopic retrograde cholangiopancreatography: a randomized, double-blind, placebo-controlled study. *Clin Infect Dis* 1995; **20**: 1236-1240

10 **Hirota WK**, Petersen K, Baron TH, Goldstein JL, Jacobson BC, Leighton JA, Mallery JS, Waring JP, Fanelli RD, Wheeler-Harbough J, Faigel DO. Guidelines for antibiotic prophylaxis for GI endoscopy. *Gastrointest Endosc* 2003; **58**: 475-482

11 **American Society for Gastrointestinal Endoscopy**. Antibiotic prophylaxis for gastrointestinal endoscopy. *Gastrointest Endosc* 1995; **42**: 630-635

12 **McGrath K**, Baillie J. Cholangitis. Current treatment options in gastroenterology. *Gastroenterology* 1999; **2**: 323-336

13 **Rerknimitr R**, Fogel EL, Kalayci C, Esber E, Lehman GA, Sherman S. Microbiology of bile in patients with cholangitis or cholestasis with and without plastic biliary endoprosthesis. *Gastrointest Endosc* 2002; **56**: 885-889

14 **Loperfido S**, Angelini G, Benedetti G, Chilovi F, Costan F, De Berardinis F, De Bernardin M, Ederle A, Fina P, Fratton A. Major early complications from diagnostic and therapeutic ERCP: a prospective multicenter study. *Gastrointest Endosc* 1998; **48**: 1-10

15 **Leung JW**, Venezuela RR. Cholangiosepsis: endoscopic drainage and antibiotic therapy. *Endoscopy* 1991; **23**: 220-223

16 **Brandes JW**, Scheffer B, Lorenz-Meyer H, Körst HA, Littmann KP. ERCP: Complications and prophylaxis a controlled study. *Endoscopy* 1981; **13**: 27-30

17 **Finkelstein R**, Yassin K, Suissa A, Lavy A, Eidelman S. Failure of cefonicid prophylaxis for infectious complications related to endoscopic retrograde cholangiopancreatography. *Clin Infect Dis* 1996; **23**: 378-379

18 **Siegman-Igra Y**, Schwartz D, Konforti N. Polymicrobial bacteremia. *Med Microbiol Immunol* 1988; **177**: 169-179

19 **Hochwald SN**, Burke EC, Jarnagin WR, Fong Y, Blumgart LH. Association of preoperative biliary stenting with increased postoperative infectious complications in proximal cholangiocarcinoma. *Arch Surg* 1999; **134**: 261-266

20 **Nomura T**, Shirai Y, Hatakeyama K. Enterococcal bactibilia in patients with malignant biliary obstruction. *Dig Dis Sci* 2000; **45**: 2183-2186

21 **Sheen-Chen S**, Chen W, Eng H, Sheen C, Chou F, Cheng Y, Lee T. Bacteriology and antimicrobial choice in hepatolithiasis. *Am J Infect Control* 2000; **28**: 298-301

22 **Flores C**, Maguilnik I, Hadlich E, Goldani LZ. Microbiology of choledochal bile in patients with choledocholithiasis admitted to a tertiary hospital. *J Gastroenterol Hepatol* 2003; **18**: 333-336

23 **Ryan JM**, Ryan BM, Smith TP. Antibiotic prophylaxis in interventional radiology. *J Vasc Interv Radiol* 2004; **15**: 547-556

24 **Clark CD**, Picus D, Dunagan WC. Bloodstream infections after interventional procedures in the biliary tract. *Radiology* 1994; **191**: 495-499

25 **Alveyn CG**, Robertson DA, Wright R, Lowes JA, Tillotson G. Prevention of sepsis following endoscopic retrograde cholangi opancreatography. *J Hosp Infect* 1991; **19** Suppl C: 65-70

S- Editor Wang GP **L- Editor** Wang XL **E- Editor** Bai SH

PO Box 2345, Beijing 100023, China
www.wjgnet.com
wjg@wjgnet.com

World J Gastroenterol 2007 January 14; 13(2): 280-284
World Journal of Gastroenterology ISSN 1007-9327
© 2007 The WJG Press. All rights reserved.

RAPID COMMUNICATION

Twenty-four hour intra-arterial infusion of 5-fluorouracil, cisplatin, and leucovorin is more effective than 6-hour infusion for advanced hepatocellular carcinoma

Hidenari Nagai, Masahiro Kanayama, Katsuya Higami, Kouichi Momiyama, Akiko Ikoma, Naoki Okano, Katsuhiko Matsumaru, Manabu Watanabe, Koji Ishii, Yasukiyo Sumino, Kazumasa Miki

Hidenari Nagai, Masahiro Kanayama, Katsuya Higami, Kouichi Momiyama, Akiko Ikoma, Naoki Okano, Katsuhiko Matsumaru, Manabu Watanabe, Koji Ishii, Yasukiyo Sumino, Kazumasa Miki, Division of Gastroenterology and Hepatology, Toho University Medical Center, Omori Hospital, 6-11-1, Omorinishi, Ota-ku, Tokyo 143-8541, Japan
Correspondence to: Hidenari Nagai, Division of Gastroenterology and Hepatology, Toho University Medical Center, Omori Hospital, 6-11-1, Omorinishi, Ota-ku, Tokyo 143-8541, Japan. hidenari@aol.com
Telephone: +81-3-37624151 Fax: +81-3-37638542
Received: 2006-06-19 Accepted: 2006-08-22

Key words: 5-fluorouracil; Cisplatin; Advanced hepatocellular carcinoma; Liver cirrhosis; Intra-arterial chemotherapy

Nagai H, Kanayama M, Higami K, Momiyama K, Ikoma A, Okano N, Matsumaru K, Watanabe M, Ishii K, Sumino Y, Miki K. Twenty-four hour intra-arterial infusion of 5-fluorouracil, cisplatin, and leucovorin is more effective than 6-hour infusion for advanced hepatocellular carcinoma. *World J Gastroenterol* 2007; 13(2): 280-284

http://www.wjgnet.com/1007-9327/13/280.asp

Abstract

AIM: To evaluate the time dependence of intra-arterial 5-fluorouracil (5-FU) therapy for advanced hepatocellular carcinoma (aHCC).

METHODS: Thirty-seven adult Japanese patients who had aHCC and liver cirrhosis were treated with combined intra-arterial 5-FU, cisplatin (CDDP), and leucovorin (LV). The Japan Integrated Staging score (JIS score) of each patient was 3 or more. The patients were divided into two groups, after which the 15 patients in group S were treated with 6-h infusion chemotherapy (LV at 12 mg/h, CDDP at 10 mg/h, and 5-FU at 250 mg/m^2 per 4 h) and the 22 patients in group L were treated with 24-h infusion chemotherapy (LV at 12 mg/h, CDDP at 10 mg/h, and 5-FU at 250 mg/m^2 per 22 h). Continuous infusion chemotherapy was performed *via* the proper hepatic artery every 5 d for 4 wk using an implanted drug reservoir.

RESULTS: The percentages of patients with a partial response after 4 wk of chemotherapy were 6.7% in group S and 31.8% in group L. The survival of group L was significantly better than that of group S, with the median survival time being 496 d in group L and 226 d in group S ($P < 0.05$).

CONCLUSION: Continuous 24-h intra-arterial infusion is more effective for aHCC and can markedly prolong survival time as compared to 6-h infusion.

© 2007 The WJG Press. All rights reserved.

INTRODUCTION

The majority of patients with advanced hepatocellular carcinoma (aHCC) survive no longer than 6 mo from the day of initial diagnosis[1]. It was reported that improvement of implanted drug delivery systems has made it possible to administer repeated hepatic arterial infusion of anticancer agents to patients with aHCC and that hepatic arterial infusion therapy not only improved survival but also the quality of life (QOL)[2]. Continuous local arterial infusion of 5-fluorouracil (5-FU) and cisplatin (CDDP) using an infuser pump and an implanted reservoir has been shown to prolong the survival of patients with severe advanced HCC[2-4]. Leucovorin is a biochemical modulator of 5-FU[5-7]. A randomized study showed that the regimen using CDDP, 5-FU, and leucovorin (LV) was significantly better than that of the low-dose CDDP and 5-FU alone[8]. However, there were differences of the response rate and the regimen used in these studies, such as 250 mg of 5-FU for 5 or 24 h. For staging of HCC, Cancer of the Liver Italian Program (CLIP) score[9] has been reported to be very useful[10-12]. However, it was also reported that the stratification ability and prognostic power of the Japan Integrated Staging (JIS) score[13] were superior to those of the CLIP score for staging of HCC[14]. Accordingly, this study was performed to evaluate the time dependence of intra-arterial 5-FU therapy for aHCC by using the JIS score.

MATERIALS AND METHODS

Patients

Thirty-seven adult Japanese patients who had aHCC and

Table 1 Clinical characteristic of the 37 patients with advanced HCC and HCV cirrhosis

Mean age	Group S: 68.3 yr
	Group L: 66.6 yr
Gender	Group S: 10 males, 15 females
	Group L: 15 males, 7 females
Child-Pugh classification	Group S A: 6, B: 7, C: 2
	Group L A: 11, B: 9, C: 2
Stage	Group S Ⅲ: 2, IVA: 12, IVB: 1 (Vp3: 4, Vp4: 1, vv2: 0)
	Group L Ⅲ: 1, IVA: 14, IVB: 7 (Vp3: 3, Vp4: 0, vv2: 1)
JIS score	Group S 3: 7, 4: 7, 5: 1
	Group L 3: 12, 4: 8, 5: 2

liver cirrhosis due to HCV infection (C-LC) were treated with combined intra-arterial 5-FU, CDDP, and LV at Omori Hospital, Japan between 2000 and 2005. According to the computed tomography (CT) findings, the tumors were inoperable, with a JIS score of 3 or more in all patients.

Chemotherapy regimen

The patients were divided into two groups. Group S comprised 15 patients (10 men and 5 women) who were treated with 6-h infusion chemotherapy (LV at 12 mg/h, CDDP at 10 mg/h, and 5-FU at 250 mg/m^2 per 4 h), while group L included 22 patients (15 men and 7 women) who were treated with 24-h infusion chemotherapy (LV at 12 mg/h, CDDP at 10 mg/h, and 5-FU at 250 mg/m^2 per 22 h). Doses of the chemotherapy were according to a previous report[8]. Continuous infusion chemotherapy was performed *via* the proper hepatic artery every 5 d for 4 wk using a catheter connected to a subcutaneously implanted drug delivery system. Subsequently, the same chemotherapy was continued for as long as possible.

System placement technique

In all patients, an intra-arterial catheter was inserted *via* the femoral artery and was attached to a subcutaneously implanted reservoir[15]. In principle, the gastroduodenal artery and the right gastric artery were occluded with steel coils to prevent gastroduodenal injury from anticancer agents. Written informed consent was obtained from each patient or family members after the possible complications of reservoir implantation and arterial infusion chemotherapy had been fully explained.

Evaluation of therapeutic effect

On CT scans obtained after 4 wk of treatment, the size of the intrahepatic tumors was measured as the product of the two longest perpendicular diameters of the largest tumor. CT images were acquired according to the same method as performed for pretreatment workup. The response criteria defined by the Liver Cancer Study Group of Japan were used. A complete response (CR) was defined as disappearance of the tumor and no evidence of new lesions for at least 4 wk, while a partial response (PR) was defined as reduction of the product of the two longest diameters by more than 50%. An increase of the product by more than 25% was defined as progressive disease (PD), and the changes in between PD and PR were defined as stable disease (SD). The response was also evaluated by measuring serum alpha-fetoprotein (AFP), AFP-L3, and PIVKA-Ⅱ levels in the patients with elevated levels of these markers. The survival period was defined as the interval between the start of treatment and death.

Table 2 Objective response and survival in the both group (%)

		JIS score		
	Group	3	4	5
1-yr	Group S	14.3	0.0	0.0
	Group L	50.0	16.7	16.7
2-yr	Group S	0.0	0.0	0.0
	Group L	16.7	0.0	0.0
3-yr	Group S	0.0	0.0	0.0
	Group L	16.7	0.0	0.0

Objective response rate: Group S 6.7% (1/15 cases) CR: PR: SD: PD = 0: 1: 3: 11; Group L 31.8% (7/22 cases) CR: PR: SD: PD = 0: 7: 9: 6.

Statistical analysis

The Mann-Whitney test was used to compare the patient characteristics between the two groups. Survival was evaluated by the Kaplan-Meier method, and the significance of differences in survival was determined by the log rank test. *P* value less than 0.05 was considered statistically significant.

RESULTS

The group S comprised a total of 10 men and 5 women aged 54 to 79 years (mean ± SD, 68.3 ± 7.4 years), while the group L comprised 15 men and 7 women aged 52 to 76 years old (mean ± SD, 66.6 ± 7.8 years). There was no significant difference between the both groups. The Child-Pugh class was A for 6 patients in group S and 11 patients in group L, while it was B for 7 and 9 patients, respectively, and C for 2 patients in each group. Two patients had stage Ⅲ, 12 stage ⅣA, and one patient stage ⅣB disease in group S, while the respective numbers were 1, 14, and 7 in group L. Seven patients had a JIS score of 3, seven patients had a JIS score of 4, and one patient had a JIS score of 5 in group S, while the respective numbers were 12, 8, and 2 in group L. In group S, one patient had tumor thrombi in major branches of the portal vein and four patients had tumor thrombi in the first portal branch. In group L, there was also one patient with tumor invasion into the right hepatic vein and four patients with tumor thrombi in the first portal branch (Table 1).

Response

Table 2 summarizes the response to treatment and the survival of the aHCC patients, all of whom had a JIS score ⩾ 3. In group S, one of the 15 (6.7%) patients achieved PR, but no patient achieved CR. Also, 11 of the 15 (73.3%)

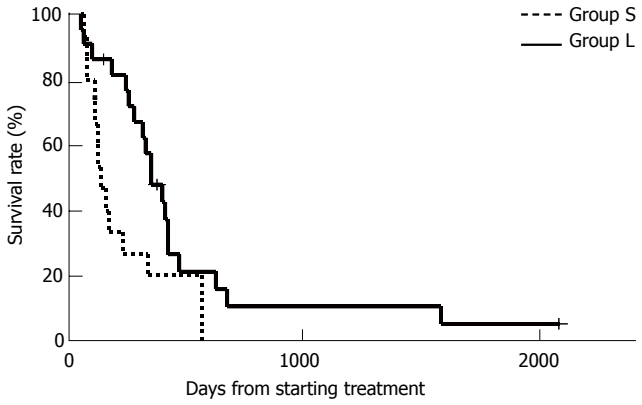

Figure 1 Survival curves plotted by the Kaplan-Meier method. The survival of group L was significantly better than that of group S. The median survival time was 496 d in group L *versus* 226 d in group S ($^aP < 0.05$, Kaplan-Meier method and log-rank test).

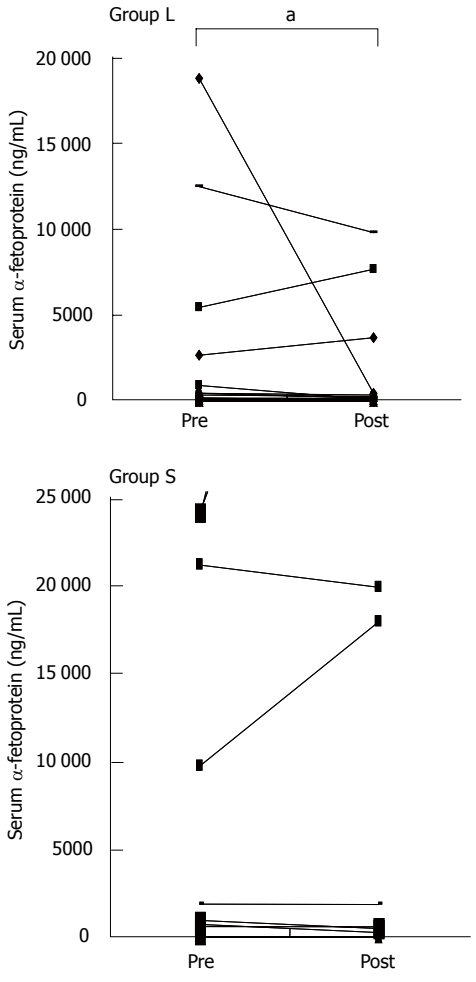

Figure 2 Changes of serum AFP following treatment in the both groups. In group L, the serum AFP level decreased significantly after treatment compared with before treatment ($^aP < 0.05$, Mann-Whitney test).

patients showed PD and 3 (20.0%) patients had SD. In group L, seven of the 22 (31.8%) patients achieved PR, although none of the patients achieved CR. Six of the 22 (27.3%) patients showed PD, but 9 (40.9%) patients had SD. The response rate in group L was significantly better than that in group S ($P < 0.05$, Mann-Whitney test).

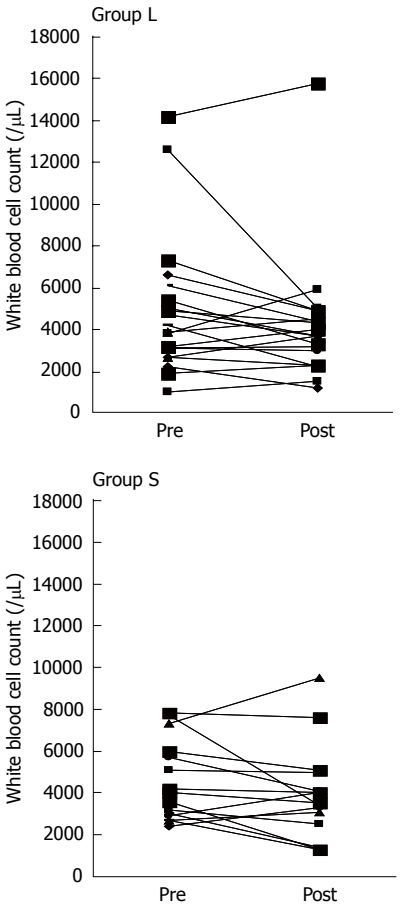

Figure 3 Changes of the white blood cell count following treatment in the both groups. There were no significant differences in either group.

Survival

In group S, the 1-year survival rates for the patients with a JIS score of 3, 4, and 5 were 14.3%, 0.0%, and 0.0%, respectively. There were no survivors for 2 years or more. In group L, the 1-year survival rates for the patients with a JIS score of 3, 4, and 5 were 50.0%, 16.7%, and 16.7%, respectively, while the 2-year survival rates for those patients were 16.7%, 0%, and 0%, respectively. None of the patients in either group survived for 3 years (Table 2). The survival of group L was significantly better than that of group S, with the median survival time being 496 d in group L and 226 d in group S ($P < 0.05$) (Figure 1).

Tumor markers

Figure 2 summarizes the changes of serum AFP following treatments in both groups. In group L, the serum AFP level decreased significantly after treatment compared with that before treatment. However, there was no significant change of the serum AFP level in group S. Moreover, there were no significant changes of the serum AFP-L3 and PIVKA-Ⅱ levels in both groups (data not shown).

Hematologic toxicity

Figure 3 summarizes the changes of the white blood cell count following treatment in both groups, showing that there were no significant differences in either of the groups. Similarly, there were no significant changes of

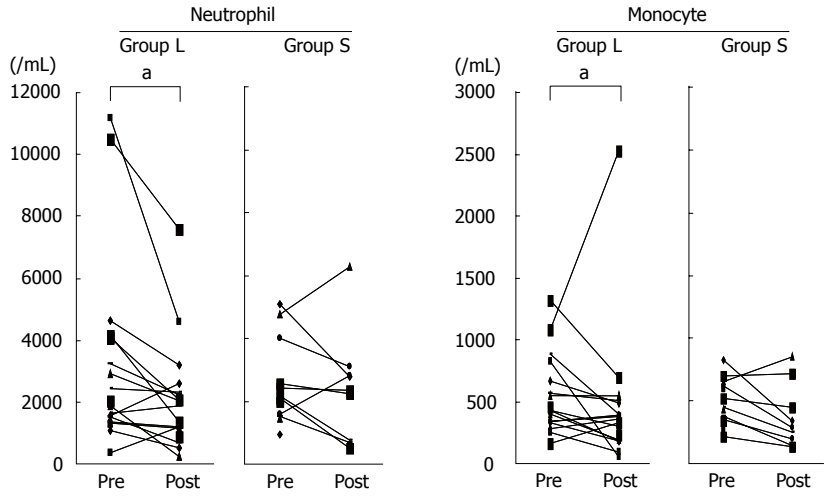

Figure 4 Changes of neutrophil and monocyte counts following treatment in the both groups. In group L, the neutrophil and monocyte counts were significantly decreased after treatment as compared with before treatment ($^aP < 0.05$, Mann-Whitney test).

lymphocyte or platelet count before and after treatment in either group (data not shown). However, the neutrophil and monocyte counts were significantly decreased after treatments in group L compared to group S (Figure 4).

DISCUSSION

The majority of patients with advanced hepatocellular carcinoma (aHCC) live no longer than 6 mo from the day of diagnosis[1]. It was also reported that the average survival of patients with aHCC was 4 mo from the onset of symptoms and 2 mo from the time of admission[16]. In the present study, one of 15 (6.7%) patients in group S achieved PR, while seven of 22 (31.8%) patients in group L reached a state of PR. The survival of group L was significantly better than that of group S, with the median survival time being 496 d in group L *versus* 226 d in group S. Moreover, the serum AFP level decreased significantly after treatment in group L, although this change was not observed in group S. Regarding hematologic toxicity, the neutrophil and monocyte counts were significantly decreased after treatment in group L, while these changes were not observed in group S. In the present study, the severity of disease was assessed by the JIS score, making it possible to observe effect of continuous intra-arterial infusion for 6 and 24 h in C-LC patients with aHCC of similar severity. It was demonstrated that the method of continuous intra-arterial infusion for 24 h was more effective and could prolong survival compared to 6-h infusion. Both treatments were effective for aHCC in the patients with C-LC, when we excluded the patients with a JIS score $\leqslant 2$ in this study. However, 24-h infusion caused a greater decrease of the neutrophil and monocyte counts compared to 6-h infusion.

5-FU and CDDP have been the most commonly used drugs in combination regimens because CDDP amplifies the effect of 5-FU by biochemical modulation in addition to its own action[6,17,18]. Moreover, LV has a synergistic effect in promoting the biochemical modulation of 5-FU. It has been reported that chemotherapy using 5-FU, CDDP, and LV is superior to other treatments (5-FU alone, CDDP alone, and 5-FU plus LV) with respect to controlling tumor growth, even if the concentrations of 5-FU and LV are reduced by half[8]. Therefore, we selected the combination of 5-FU, CDDP, and LV for intra-arterial infusion to treat aHCC, based on the employment of CDDP and LV as modulators of 5-FU. 5-FU has been reported to exhibit its anticancer effects *via* the following mechanisms: (1) Inhibition of deoxyribonucleic acid (DNA) synthesis through inactivation of thymidylate synthase (TS) by formation of a complex between methyle netetrahydrofolate (CH_2FH_4) and 5-fluoro-2'-deoxyuridine 5'-monophosphate (FdUMP), which is synthesized from 5-FU. (2) Interference with ribonucleic acid (RNA) metabolism by the uptake of phosphated 5-fluorouridine 5'-triphosphate into RNA[19]. It was also reported that a single dose of 5-FU is more effective for causing RNA dysfunction, while continuous infusion causes more DNA damage[20]. Another study showed that 5-FU was almost undetectable in the peripheral blood when 5-FU and low-dose CDDP were continuously infused *via* a central vein or *via* the hepatic artery in patients with adavanced or metastatic HCC[21]. These reports indicate that the method of continuous intra-arterial infusion for 24 h would cause more damage to tumor DNA in our C-LC patients with aHCC compared with 6-h infusion, although 24-h infusion had stronger hematologic toxicity than 6-h infusion. Our results might also be supported by the report that 5-FU has a time-dependent anticancer effect and shows stronger cell-killing activity *in vitro* when exposure is continued for a longer period[22].

In conclusion, continuous 24-h intra-arterial infusion is more effective and can prolong survival as compared with 6-h infusion in C-LC patients with aHCC, although 24-h infusion is associated with stronger hematologic toxicity.

REFERENCES

1 **Okuda K**, Ohtsuki T, Obata H, Tomimatsu M, Okazaki N, Hasegawa H, Nakajima Y, Ohnishi K. Natural history of hepatocellular carcinoma and prognosis in relation to treatment. Study of 850 patients. *Cancer* 1985; **56**: 918-928

2 **Toyoda H**, Nakano S, Kumada T, Takeda I, Sugiyama K, Osada T, Kiriyama S, Suga T, Takahashi M. The efficacy of continuous local arterial infusion of 5-fluorouracil and cisplatin through an implanted reservoir for severe advanced hepatocellular carcinoma. *Oncology* 1995; **52**: 295-299

3 **Murata K**, Shiraki K, Kawakita T, Yamamoto N, Okano H, Nakamura M, Sakai T, Deguchi M, Ohmori S, Nakano T. Low-

dose chemotherapy of cisplatin and 5-fluorouracil or doxorubicin via implanted fusion port for unresectable hepatocellular carcinoma. *Anticancer Res* 2003; **23**: 1719-1722

4 **Okuda K**, Tanaka M, Shibata J, Ando E, Ogata T, Kinoshita H, Eriguchi N, Aoyagi S, Tanikawa K. Hepatic arterial infusion chemotherapy with continuous low dose administration of cisplatin and 5-fluorouracil for multiple recurrence of hepatocellular carcinoma after surgical treatment. *Oncol Rep* 1999; **6**: 587-591

5 **O'Connell MJ**. A phase III trial of 5-fluorouracil and leucovorin in the treatment of advanced colorectal cancer. A Mayo Clinic/North Central Cancer Treatment Group study. *Cancer* 1989; **63**: 1026-1030

6 **Poon MA**, O'Connell MJ, Moertel CG, Wieand HS, Cullinan SA, Everson LK, Krook JE, Mailliard JA, Laurie JA, Tschetter LK. Biochemical modulation of fluorouracil: evidence of significant improvement of survival and quality of life in patients with advanced colorectal carcinoma. *J Clin Oncol* 1989; **7**: 1407-1418

7 **Buroker TR**, O'Connell MJ, Wieand HS, Krook JE, Gerstner JB, Mailliard JA, Schaefer PL, Levitt R, Kardinal CG, Gesme DH. Randomized comparison of two schedules of fluorouracil and leucovorin in the treatment of advanced colorectal cancer. *J Clin Oncol* 1994; **12**: 14-20

8 **Yamasaki T**, Kurokawa F, Shirahashi H, Kusano N, Hironaka K, Masuhara M, Okita K. Novel arterial infusion chemotherapy using cisplatin, 5-fluorouracil, and leucovorin for patients with advanced hepatocellular carcinoma. *Hepatol Res* 2002; **23**: 7-17

9 A new prognostic system for hepatocellular carcinoma: a retrospective study of 435 patients: the Cancer of the Liver Italian Program (CLIP) investigators. *Hepatology* 1998; **28**: 751-755

10 **Farinati F**, Rinaldi M, Gianni S, Naccarato R. How should patients with hepatocellular carcinoma be staged? Validation of a new prognostic system. *Cancer* 2000; **89**: 2266-2273

11 **Levy I**, Sherman M. Staging of hepatocellular carcinoma: assessment of the CLIP, Okuda, and Child-Pugh staging systems in a cohort of 257 patients in Toronto. *Gut* 2002; **50**: 881-885

12 **Ueno S**, Tanabe G, Sako K, Hiwaki T, Hokotate H, Fukukura Y, Baba Y, Imamura Y, Aikou T. Discrimination value of the new western prognostic system (CLIP score) for hepatocellular carcinoma in 662 Japanese patients. Cancer of the Liver Italian Program. *Hepatology* 2001; **34**: 529-534

13 **Kudo M**, Chung H, Osaki Y. Prognostic staging system for hepatocellular carcinoma (CLIP score): its value and limitations, and a proposal for a new staging system, the Japan Integrated Staging Score (JIS score). *J Gastroenterol* 2003; **38**: 207-215

14 **Kudo M**, Chung H, Haji S, Osaki Y, Oka H, Seki T, Kasugai H, Sasaki Y, Matsunaga T. Validation of a new prognostic staging system for hepatocellular carcinoma: the JIS score compared with the CLIP score. *Hepatology* 2004; **40**: 1396-1405

15 **Iwamiya T**, Sawada S, Ohta Y. Repeated arterial infusion chemotherapy for inoperable hepatocellular carcinoma using an implantable drug delivery system. *Cancer Chemother Pharmacol* 1994; **33** Suppl: S134-S138

16 **Nagasue N**, Yukaya H, Hamada T, Hirose S, Kanashima R, Inokuchi K. The natural history of hepatocellular carcinoma. A study of 100 untreated cases. *Cancer* 1984; **54**: 1461-1465

17 **LoRusso P**, Pazdur R, Redman BG, Kinzie J, Vaitkevicius V. Low-dose continuous infusion 5-fluorouracil and cisplatin: phase II evaluation in advanced colorectal carcinoma. *Am J Clin Oncol* 1989; **12**: 486-490

18 **Scanlon KJ**, Newman EM, Lu Y, Priest DG. Biochemical basis for cisplatin and 5-fluorouracil synergism in human ovarian carcinoma cells. *Proc Natl Acad Sci USA* 1986; **83**: 8923-8925

19 **Harbers E,** Chaudhuri NK, Heidelberger C. Studies on fluorinated pyrimidines. VIII. Further biochemical and metabolic investigations. *J Biol Chem* 1959; **234**: 1255-1262

20 **Iba T**, Kidokoro A, Fukunaga M, Sugiyama K, Fukunaga T, Aihara N. Effect and mechanism of orally administered leucovorin/5-fluorouracil on colon cancer. *Gan To Kagaku Ryoho* 2003; **30**: 2077-2081

21 **Tanioka H**, Tsuji A, Morita S, Horimi T, Takamatsu M, Shirasaka T, Mizushima T, Ochi K, Kiura K, Tanimoto M. Combination chemotherapy with continuous 5-fluorouracil and low-dose cisplatin infusion for advanced hepatocellular carcinoma. *Anticancer Res* 2003; **23**: 1891-1897

22 **Drewinko B**, Yang LY. Cellular basis for the inefficacy of 5-FU in human colon carcinoma. *Cancer Treat Rep* 1985; **69**: 1391-1398

S- Editor Wang J **L- Editor** Kumar M **E- Editor** Bai SH

PO Box 2345, Beijing 100023, China
www.wjgnet.com
wjg@wjgnet.com

World J Gastroenterol 2007 January 14; 13(2): 285-288
World Journal of Gastroenterology ISSN 1007-9327
© 2007 The WJG Press. All rights reserved.

RAPID COMMUNICATION

Totally laparoscopic trans-hiatal gastroesophagectomy for benign diseases of the esophago-gastric junction

Jean-Louis Dulucq, Pascal Wintringer, Ahmad Mahajna

Jean-Louis Dulucq, Pascal Wintringer, Ahmad Mahajna, Department of Abdominal Surgery, Institute of Laparoscopic Surgery, Maison de Santé Protestante, Bagatelle Hospital, Route de Toulouse 203, Talence-Bordeaux 33401, France
Correspondence to: Jean-Louis Dulucq, Department of Abdominal Surgery, Institute of Laparoscopic Surgery, Maison de Santé Protestante, Bagatelle Hospital, Route de Toulouse 203, Talence-Bordeaux 33401, France. info@ils-chirurgie.com
Telephone: +33-557-123521 Fax: +33-557-123420
Received: 2006-09-24 Accepted: 2006-12-09

13(2): 285-288

http://www.wjgnet.com/1007-9327/13/285.asp

Abstract

AIM: To prospectively present our initial experience with totally laparoscopic transhiatal esophagogastrectomies for benign diseases of the cardia and distal esophagus.

METHODS: Laparoscopic gastric mobilization and tubularization combined with transhiatal esophageal dissection and intrathoracic esophagogastric anastomosis accomplished by a circular stapler was done in 3 patients. There were 2 females and 1 male patient with a mean age of 73 ± 5 years.

RESULTS: Two patients were operated on due to benign stromal tumor of the cardia and one patient had severe oesophageal peptic stenosis. Mean blood loss was 47 ± 15 mL and mean operating time was 130 ± 10 min. There were no cases that required conversion to laparotomy. All patients were extubated immediately after surgery. Soft diet intake and ambulation times were 5.1 ± 0.4 d and 2.6 ± 0.6 d, respectively. There were no intraoperative and postoperative complications and there were no perioperative deaths. The average length of hospital stay was 9.3 ± 3 d. All procedures were curative and all resected margins were tumor free. The mean number of retrieved lymph nodes was 18 ± 8.

CONCLUSION: Laparoscopic transhiatal esophagogastrectomy for benign lesions has good effects and proves feasible and safe.

© 2007 The WJG Press. All rights reserved.

Key words: Esophagogastrectomy; Transhiatal resection; Cardial tumor; Laparoscopy; Stromal tumor

Dulucq JL, Wintringer P, Mahajna A. Totally laparoscopic trans-hiatal gastroesophagectomy for benign diseases of the esophago-gastric junction. *World J Gastroenterol* 2007;

INTRODUCTION

In recent years, the incidence of adenocarcinoma of the lower esophagus and cardia has increased[1]. Surgery remains the treatment of choice for these cancers, since it provides definitive treatment and long-term survival for some patients and offers splendid palliation for many others. The most common surgeries for resectable lesions are total gastrectomy with distal esophagectomy, Ivor Lewis esophagectomy and the blunt transhiatal procedure[2,3]. These traditional approaches are frequently associated with significant morbidity and mortality rates ranging from 5% to 10%[4-6]. With the development of minimally invasive surgery during the last decade, attempts were made to use alternative minimally invasive methods for esophageal dissection, which avoid an open thoracotomy incision and therefore reduce the associated morbidity[7-11]. However, combined methods using thoracoscopic dissection with conventional abdominal approaches have not achieved a significant reduction in respiratory morbidity, mostly due to the upper midline abdominal incision[12,13]. Better outcomes were achieved by the use of laparoscopic gastric mobilization combined with transhiatal or thoracoscopic esophageal mobilization and cervical or thoracic anastomoses[14,15].

The present study reports on our initial experience with laparoscopic gastric mobilization and transhiatal oesophageal dissection with intrathoracic esophagogastric anastomosis without abdominal, cervical or thoracic incisions for benign diseases of the cardia and distal esophagus prospectively.

MATERIALS AND METHODS

Patients

The clinical records of patients who underwent laparoscopic gastroesophagectomy in the Department of Abdominal Surgery of the Institute of Laparoscopic Surgery (ILS, Bordeaux) were collected prospectively. All patients underwent preoperative workup including upper gastrointestinal barium swallow, endoscopy with biopsies, endoscopic ultrasonography and dynamic CT scanning

of the chest, abdomen and pelvis, in order to establish the diagnosis and determine the extent and staging of the disease. Twenty-eight patients with a malignancy underwent combined laparoscopic and thoracoscopic Ivor Lewis esophagectomy and were excluded from this study. For precise laparoscopic resection in one case of a small intraluminal lesion, we used preoperative endoscopic location and applied metal clips identified by intraoperative X-ray control. Prior to the operations, all cases were reviewed at a meeting attended by staff surgeons, oncologists, gastroenterologists and pathologists. Patients were informed which procedure was expected and the possibility of conversion was discussed. All patients were put on antithrombotic prophylaxis by low-weight heparin and given elastic stockings. Postoperatively, all patients were given total parenteral nutrition for the first 5 d. A hydrosoluble contrast swallow was performed on the 5th postoperative day and if normal, enteral feeding was started.

Studied data

The patients' demographic data, surgeries, postoperative courses and outpatient follow-up were studied. The following data were collected prospectively: age, sex, preoperative work-up, types and locations of the tumor, duration of surgery, blood loss, intraoperative complications, pathological findings and nodal status, postoperative complications, hospital stay, recurrence and distant events. Variables are presented as mean and standard deviation.

Surgical techniques

The patient was placed in a 25° reverse-Trendelenburg position with split legs; the operating surgeon stood between the legs, the assistant surgeon stood on the left side of the patient and the camera holding assistant was on the right side. A total of five operating trocars were used: a 0° videoscope was introduced through a 10 mm supraumbilical trocar, two 12 mm working ports were placed to the right and left of the midline, and two 5 mm exposure trocars were in sub-xiphoid and left lateral position (Figure 1). Laparoscopic explorations were done by creating a pneumoperitoneum with CO_2 to a maximum pressure of 12 mmHg. After exploration of the peritoneal cavity the greater curvature was mobilized by dissection of the greater omentum from the transverse colon using scissors and Ligasure® (Valleylab, Tyco Healthcare Group Lp, Boulder, CO 80 301-3299, UK) or harmonic scalpel (Ethicon Endo-surgery, Cincinnati, OH. USA). The left gastric vessels were exposed and clipped and divided at their roots while the lymph nodes were dissected. The greater curvature mobilization was continued in a distal to proximal direction while the right gastric and gastroepiploic arteries were preserved. A Kocher maneuver was performed followed by gastric tubularization: After definition of the distal margin of the specimen, an endoscopic linear stapler (Ethicon Endo-surgery, Cincinnati, OH. USA) was used to divide the small curvature and create a tube of the greater curvature that would later allow anastomosis with the esophagus. The right diaphragmatic crus was dissected to expose the lower mediastinum. The fundus and abdominal esophagus were mobilized by division of the gastrophrenic peritoneal reflection and separation of the gastroesophageal junction from the left and right crus. The hiatus was entered and the mediastinal esophagus was dissected. The dissection limits were between the left and right parietal pleuras, the pericardium and left pulmonary vein anteriorly and the aorta posteriorly. The anterior and posterior vagal nerves were identified and divided and finally the esophagus was transected 2 to 3 cm above the lesion with free margins.

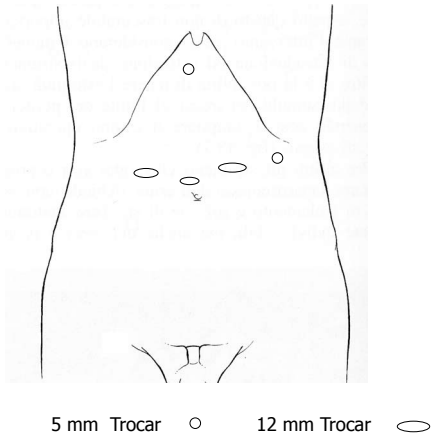

Figure 1 Trocar placement for transhiatal esophagogastrectomy.

For reconstruction a 25 mm circular stapler (Ethicon Endo-surgery, Cincinnati, OH, USA) was used to perform intracorporeal esophagogastric anastomosis. The anvil was prepared by tying a thread with a needle to the tip and then inserted into the peritoneal cavity through a port-site. The anvil was introduced through the lateral esophageal wall 1.5 cm proximal to the transection line, the needle exited through the esophageal wall and then the esophageal stump was closed by a linear endo GIA stapler. The circular stapler was introduced by enlarging one of the left sided trocar sites, entered into the still attached lesser curvature, then passed into the gastric tube. After the stapler was connected to the anvil, the esogastric anastomosis was created, and the stapler removed. The tissue doughnuts were carefully checked. The gastric tube was transected with a linear stapler proximal to the anastomosis, making sure to leave at least 1 cm of tissue so as not to create ischemia. The resected specimen was placed inside a bag (Endo Catch II, Auto Suture European Services Center, S.A., 78990 Elancourt, France) and was removed through enlargement of one of the port wounds.

RESULTS

Patients' characteristics

Between April 2002 and January 2005, we performed laparoscopic gastroesophagectomy in 3 patients. There were 2 female and 1 male patients with a mean age of 73 ± 5 years. The presenting syndromes were abdominal pain and dyspepsia in the first patient, upper gastrointestinal bleeding in the second patient, and dysphagia and weight loss in the last patient. Patients' preoperative risk was evaluated

Table 1 Patient demographics and presenting symptoms

No.	Age (yr)	Gender	ASA	Symptoms	Pathologic site	Pathology
1	67	M	1	Abdominal pain and dyspepsia	Gastroesophageal junction	Gastrointestinal stromal tumor
2	79	F	2	Upper gastrointestinal bleeding	Gastroesophageal junction	Gastrointestinal stromal tumor
3	73	F	2	Dysphagia and weight loss	Distal esophagus	Severe fibrosis

ASA: American Society of Anesthesiologists physical status score.

according to the American Society of Anesthesiologists physical status score (ASA) (Table 1).

Perioperative data

The perioperative data were as follows: Mean blood loss was 47 ± 15 mL and mean operating time was 130 ± 10 min. There were no cases that required conversion to laparotomy. All patients had their tracheal tube removed immediately after surgery. Mean stay time in Intensive Care Unit was 2.3 ± 0.5 d. Resumation of soft diet intake and ambulation times were 5.1 ± 0.4 d and 2.6 ± 0.6 d, respectively. There were no intraoperative or postoperative complications and there were no perioperative deaths. The average length of hospital stay was 9.3 ± 3 d.

Pathologic findings

Two patients were operated on for benign lesions, which were gastrointestinal stromal tumors of the gastroesophageal junction. One patient had severe fibrosis causing severe stenosis of the distal esophagus due to prolonged gastroesophageal reflux.

All procedures were curative and all resected margins were disease or tumor free. The mean tumor size of the surgical specimens was 3.1 ± 1 cm and the mean number of retrieved lymph nodes was 18 ± 8. The patients were cured of lesions and symptoms during a follow-up of 25 ± 12 mo.

DISCUSSION

In spite of modern surgical techniques and improved perioperative care, conventional surgical approaches for benign and malignant lesions of the esophagus and cardia have not significantly lowered the postoperative morbidity and mortality rates. The mortality rates from esophagectomy ranged from 8% in high volume-centers to as high as 23% in low-volume centers[16]. Respiratory complications associated with thoracotomy and prolonged deflation of the right lung during the operation, as well as infections due to anastomotic leaks are the major causes of perioperative morbidity in these surgeries. The high morbidity rates lead to increased cost, prolonged hospital stay, and occasionally, to mortality. Therefore, patients with esophageal cancer, in particular, older patients and those with co-morbid conditions may not be referred for operation at all.

During the 1970s Orringer introduced the technique of transhiatal esophagectomy, which avoids thoracotomy[3]. However, the use of an open approach has not clearly demonstrated reduction of the risk of postoperative respiratory complications or postoperative mortality. In addition, part of the dissection is "blind" with the consequent risk of bleeding, particularly from the azygus vein, and damage to the trachea and bronchi.

With the advent of minimally invasive surgical techniques, various minimally invasive surgical approaches to esophagectomy were introduced. The initial one was thoracoscopic esophagectomy combined with a laparotomy[13,17-19]. In contrast to expectations, no clear benefits were shown and in some of the early series it was clear that postoperative pulmonary complications were common following this approach[13]. Many other groups who performed thoracoscopic esophagectomy noted respiratory complications. Cuschieri noted pulmonary consolidation in 12% of 26 patients[7]. Gossot and colleagues had a 17% incidence of atelectasis requiring prolonged ventilation[20], Collard and co-workers described a 17% incidence of pneumonitis[21], and Dexter and associates reported that 3 of 13 respiratory complications were fatal[9]. A study from Hong Kong comparing thoracoscopy and open thoracotomy found no significant difference in cardiopulmonary complications[17].

Considering that postoperative pulmonary complications are mainly caused by the prolonged deflation of the right lung during the operation and that midline abdominal and thoracic incisions compromise respiratory ability, we tried to avoid laparotomy and thoracotomy using the laparoscopic transhiatal approach. This approach could reduce postoperative morbidities and speed recovery. We performed laparoscopic gastric mobilization and transhiatal esophageal dissection with intrathoracic esophagogastric anastomosis to treat benign cardial and distal esophageal tumors. Laparoscopic transhiatal esophagogastrectomy was described recently by Costi and colleagues[22], who found that this approach minimizes postoperative complications and gives good results. The technique described by Costi *et al* is quite similar to ours while the main difference is the esophago-gastric anastomosis: Costi *et al* tied the stapler's anvil to the end of an oro-gastric tube which was inserted orally down to the esophageal stump.

Our preliminary results showed that laparoscopic transhiatal esophagogastrectomy without abdominal or thoracic incisions were feasible and safe. There was no need to convert to open surgery, the estimated blood loss was minimal and there were no intraoperative complications. The operative time was shorter than in the other approaches, which necessitated patient's position change and two working fields. There were no intraoperative ventilation difficulties, all patients were extubated immediately after surgery and there were no postoperative pulmonary complications. The patients were ambulated early and the postoperative course

was uneventful in all cases. The mean hospital stay was 11 d (Hospital stay in France, unlike US or other countries, is influenced not only by medical, but also cultural and patient related factors.). We used a narrow gastric tube without pyloroplasty, to avoid the potential problems associated with dumping as supported by previous studies[23]. One concern usually raised regarding the treatment of malignant diseases by minimally invasive approaches is whether these approaches provide an adequate cancer resection, allowing free tumor margins and extensive lymph node dissection, while being minimally invasive. Previous studies concluded that the use of laparoscopic assisted transhiatal dissection for distal esophageal cancer allows enhanced tumor and nodal clearance compared with the standard transhiatal approach[24]. A randomized study comparing an extended thoracic approach and transhiatal approach in 220 patients with adenocarcinoma of the esophagus found no significant difference in survival between the 2 groups[25]. There are no randomized studies comparing the laparoscopic and open transhiatal approach for malignant lesions. Despite that all resected margins in our study were tumor free and the mean number of retrieved lymph nodes was 18 ± 8, which is comparable with the thoracoscopic and open surgery series, our strategy for malignant lesions of the cardia and distal esophagus is to perform combined laparoscopic and thoracoscopic Ivor Lewis esophagectomy with en bloc mediastinal lymhadenectomy.

In conclusion, our preliminary results demonstrate that laparoscopic transhiatal esophagogastrectomy for benign lesions of the cardia and distal esophagus has good effects and is feasible and safe. Further studies with a larger number of patients and longer follow up are needed to establish this approach.

ACKNOWLEDGMENTS

We thank Dr. Mitkal Sharon for valuable help in proofreading this paper.

REFERENCES

1 **Pera M**, Cameron AJ, Trastek VF, Carpenter HA, Zinsmeister AR. Increasing incidence of adenocarcinoma of the esophagus and esophagogastric junction. *Gastroenterology* 1993; **104**: 510-513
2 **Lewis I**. The surgical treatment of carcinoma of the oesophagus; with special reference to a new operation for growths of the middle third. *Br J Surg* 1946; **34**: 18-31
3 **Orringer MB**. Transhiatal esophagectomy without thoracotomy for carcinoma of the thoracic esophagus. *Ann Surg* 1984; **200**: 282-288
4 **Bosset JF**, Gignoux M, Triboulet JP, Tiret E, Mantion G, Elias D, Lozach P, Ollier JC, Pavy JJ, Mercier M, Sahmoud T. Chemoradiotherapy followed by surgery compared with surgery alone in squamous-cell cancer of the esophagus. *N Engl J Med* 1997; **337**: 161-167
5 **Earlam R**, Cunha-Melo JR. Oesophageal squamous cell carcinoma: I. A critical review of surgery. *Br J Surg* 1980; **67**: 381-390
6 **Watson A**. Operable esophageal cancer: current results from the West. *World J Surg* 1994; **18**: 361-366
7 **Cuschieri A**. Thoracoscopic subtotal oesophagectomy. *Endosc Surg Allied Technol* 1994; **2**: 21-25
8 **Cuschieri A**, Shimi S, Banting S. Endoscopic oesophagectomy through a right thoracoscopic approach. *J R Coll Surg Edinb* 1992; **37**: 7-11
9 **Dexter SP**, Martin IG, McMahon MJ. Radical thoracoscopic esophagectomy for cancer. *Surg Endosc* 1996; **10**: 147-151
10 **Lloyd DM**, Vipond M, Robertson GS, Hanning C, Veitch PS. Thoracoscopic oesophago-gastrectomy--a new technique for intra-thoracic stapling. *Endosc Surg Allied Technol* 1994; **2**: 26-31
11 **Watson DI**, Davies N, Jamieson GG. Totally endoscopic Ivor Lewis esophagectomy. *Surg Endosc* 1999; **13**: 293-297
12 **Gossot D**, Cattan P, Fritsch S, Halimi B, Sarfati E, Celerier M. Can the morbidity of esophagectomy be reduced by the thoracoscopic approach? *Surg Endosc* 1995; **9**: 1113-1115
13 **McAnena OJ**, Rogers J, Williams NS. Right thoracoscopically assisted oesophagectomy for cancer. *Br J Surg* 1994; **81**: 236-238
14 **DePaula AL**, Hashiba K, Ferreira EA, de Paula RA, Grecco E. Laparoscopic transhiatal esophagectomy with esophagogastroplasty. *Surg Laparosc Endosc* 1995; **5**: 1-5
15 **Jagot P**, Sauvanet A, Berthoux L, Belghiti J. Laparoscopic mobilization of the stomach for oesophageal replacement. *Br J Surg* 1996; **83**: 540-542
16 **Birkmeyer JD**, Siewers AE, Finlayson EV, Stukel TA, Lucas FL, Batista I, Welch HG, Wennberg DE. Hospital volume and surgical mortality in the United States. *N Engl J Med* 2002; **346**: 1128-1137
17 **Law S**, Fok M, Chu KM, Wong J. Thoracoscopic esophagectomy for esophageal cancer. *Surgery* 1997; **122**: 8-14
18 **Peracchia A**, Rosati R, Fumagalli U, Bona S, Chella B. Thoracoscopic esophagectomy: are there benefits? *Semin Surg Oncol* 1997; **13**: 259-262
19 **Kawahara K**, Maekawa T, Okabayashi K, Hideshima T, Shiraishi T, Yoshinaga Y, Shirakusa T. Video-assisted thoracoscopic esophagectomy for esophageal cancer. *Surg Endosc* 1999; **13**: 218-223
20 **Gossot D**, Fourquier P, Celerier M. Thoracoscopic esophagectomy: technique and initial results. *Ann Thorac Surg* 1993; **56**: 667-670
21 **Collard JM**, Lengele B, Otte JB, Kestens PJ. En bloc and standard esophagectomies by thoracoscopy. *Ann Thorac Surg* 1993; **56**: 675-679
22 **Costi R**, Himpens J, Bruyns J, Cadière GB. Totally laparoscopic transhiatal esophago-gastrectomy without thoracic or cervical access. The least invasive surgery for adenocarcinoma of the cardia? *Surg Endosc* 2004; **18**: 629-632
23 **Bemelman WA**, Taat CW, Slors JF, van Lanschot JJ, Obertop H. Delayed postoperative emptying after esophageal resection is dependent on the size of the gastric substitute. *J Am Coll Surg* 1995; **180**: 461- 464
24 **Sadanaga N**, Kuwano H, Watanabe M, Ikebe M, Mori M, Maekawa S, Hashizume M, Kitano S, Sugimachi K. Laparoscopy-assisted surgery: a new technique for transhiatal esophageal dissection. *Am J Surg* 1994; **168**: 355-357
25 **Hulscher JB**, van Sandick JW, de Boer AG, Wijnhoven BP, Tijssen JG, Fockens P, Stalmeier PF, ten Kate FJ, van Dekken H, Obertop H, Tilanus HW, van Lanschot JJ. Extended transthoracic resection compared with limited transhiatal resection for adenocarcinoma of the esophagus. *N Engl J Med* 2002; **347**: 1662-1669

S- Editor Wang GP **L- Editor** Zhu LH **E- Editor** Bai SH

PO Box 2345, Beijing 100023, China
www.wjgnet.com
wjg@wjgnet.com

World J Gastroenterol 2007 January 14; 13(2): 289-293
World Journal of Gastroenterology ISSN 1007-9327
© 2007 The WJG Press. All rights reserved.

RAPID COMMUNICATION

Impact of endoscopic ultrasound-guided fine needle biopsy for diagnosis of pancreatic masses

Julio Iglesias-Garcia, Enrique Dominguez-Munoz, Antonio Lozano-Leon, Ihab Abdulkader, Jose Larino-Noia, Jose Antunez, Jeronimo Forteza

Julio Iglesias-Garcia, Enrique Dominguez-Munoz, Jose Larino-Noia, Gastroenterology Department, University Hospital, Santiago de Compostela, Spain
Julio Iglesias-Garcia, Enrique Dominguez-Munoz, Antonio Lozano-Leon, Jose Larino-Noia, Foundation for Research in Digestive Diseases, Santiago de Compostela, Spain
Ihab Abdulkader, Jose Antunez, Jeronimo Forteza, Pathology Department, University Hospital, Santiago de Compostela, Spain
Correspondence to: Julio Iglesias-García, Gastroenterology Department, University Hospital, c/Choupana s/n 15706 Santiago de Compostela, Spain. jiglesiasg@fienad.com
Telephone: +34-981-951364 Fax: +34-981-951365
Received: 2006-09-20 Accepted: 2006-12-06

Abstract

AIM: To evaluate the diagnostic accuracy of histological evaluation of pancreatic tissue samples obtained by a modified method for recovering and processing the endoscopic ultrasound (EUS)-guided fine needle aspiration (FNA) material in the differential diagnosis of pancreatic solid masses.

METHODS: Sixty-two consecutive patients with pancreatic masses were prospectively studied. EUS was performed by the linear scanning Pentax FG-38UX echoendoscope. Three FNAs (22G needle) were carried out during each procedure. The materials obtained with first and second punctures were processed for cytological study. Materials of the third puncture were recovered into 10% formol solution by careful injection of saline solution through the needle, and processed for histological study.

RESULTS: Length of the core specimen obtained for histological analysis was 6.5 ± 5.3 mm (range 1-22 mm). Cytological and histological samples were considered as adequate in 51 (82.3%) and 52 cases (83.9%), respectively. Overall sensitivity of both pancreatic cytology and histology for diagnosis of malignancy was 68.4%. Contrary to cytology, histology was able to diagnose tumours other than adenocarcinomas, and all cases of inflammatory masses. Combination of cytology and histology allowed obtaining an adequate sample in 56 cases (90.3%), with a global sensitivity of 84.21%, specificity of 100% and an overall accuracy of 90.32%. The complication rate was 1.6%.

CONCLUSION: Adequate pancreatic core specimens for histological examination can be obtained by EUS-guided FNA. This technique is mainly useful for the diagnosis of different types of pancreatic tumours and evaluation of benign diseases.

© 2007 The WJG Press. All rights reserved.

Key words: Endoscopic ultrasound; Fine needle aspiration; Cytology; Biopsy; Pancreatic cancer

Iglesias-Garcia J, Dominguez-Munoz E, Lozano-Leon A, Abdulkader I, Larino-Noia J, Antunez J, Forteza J. Impact of endoscopic ultrasound-guided fine needle biopsy for diagnosis of pancreatic masses. *World J Gastroenterol* 2007; 13(2): 289-293

http://www.wjgnet.com/1007-9327/13/289.asp

INTRODUCTION

Differential diagnosis of pancreatic masses is a frequent clinical challenge. Therapeutic decision in this context is mainly based on the ability to establish or exclude malignancy[1]. Although ductal adenocarcinoma is the most frequent cause of pancreatic masses, other neoplasms (e.g. lymphoma, cystic tumours) and benign conditions (e.g. chronic pancreatitis) with different prognoses and treatment options can arise within the pancreas. A histological diagnosis becomes therefore highly relevant for an optimal therapeutic decision[2].

Endoscopic ultrasound (EUS)-guided fine needle aspiration (FNA) has been proved to be a safe and useful method for tissue sampling of intramural and extramural gastrointestinal lesions including the pancreas[3,4]. Cytological study of the materials obtained by FNA allows the evaluation of cellular findings suggestive of malignancy, such as anisonucleosis, nuclear membrane irregularity and nuclear enlargement. Unfortunately, inflammation causes a reactive and regenerative process leading to cellular changes that can be difficult to distinguish from well-differentiated neoplasias. Histological study of tissue samples allows the assessment of tissue architecture and cell morphology, as well as the performance of immunohistochemical analysis[5,6], thus usually providing with a higher diagnostic accuracy than cytology.

Retrieving pancreatic tissue fragments with different EUS-guided techniques has been explored. In this context,

needles of different diameters and trucut needles have been used with variable success and complication rates[7-11].

The aim of the present study was to evaluate the diagnostic accuracy of the histological evaluation of pancreatic tissue samples obtained by a modified method for recovering and processing the EUS-guided FNA material in the differential diagnosis of pancreatic solid masses.

MATERIALS AND METHODS

Subjects

Sixty-two consecutive patients (mean age 57 years, range 20 to 83 years, 35 males and 27 females), who underwent an EUS-guided FNA for the evaluation of solid pancreatic masses were prospectively included in the study over a two-years period.

Methods

In addition to abdominal ultrasound, all patients had a previous evaluation of the pancreatic mass by CT scan. Lesions were located in the head of the pancreas in 45 cases, in the body in 15 cases, and in the tail in two cases. Once the corresponding signed informed consent was obtained, EUS was performed under conscious sedation by a single operator (JIG). A standard blood coagulation analysis was performed before EUS-guided FNA, and an uncorrectable coagulation profile (prothrombin time < 60%) was considered as a contraindication for the procedure.

EUS was performed using a convex array echoendoscope (Pentax FG-38UX®), connected to an ultrasound equipment Hitachi-E6000®. FNA was performed with a standard 22-gauge needle (Sonotip Ⅱ®, Mediglobe, Germany). This needle is equipped with a round nitinol stylet covered by a 118 cm protective metal spiral coil sheath. The needle can be advanced up to 8.5 cm from the spiral sheath. The target lesion was endosonographically visualized and the region was scanned for vessels using colour and pulsed Doppler. FNA was performed from the duodenum or the stomach according to the location of the lesion in the head or the body/tail of the pancreas, respectively. Before puncture, the stylet was withdrawn several millimeters, thereby exposing the sharp needle tip. The needle was then advanced into the target tissue under endosonographic guidance (Figure 1). Once the lesion was penetrated, the stylet was advanced to the original position to "unplug" the needle, and to push out any potentially needle-clogging tissue or body fluids. The stylet was then removed and suction was applied using a 5 mL syringe while moving the needle to and fro within the lesion. Suction was released before removing the needle. This procedure was repeated three times and the material obtained was recovered as follows: (1) The samples obtained after the first and second punctures were expelled on microscope slides by pushing the needle stylet and injecting air through the needle. The material was then spread on the slides, fixed in 96% ethanol and processed for cytological study by Papanicolau staining (Figure 2). Cytology samples were evaluated for cellular preservation, background substance, cellularity, architectural integrity, and cytoplasmic and nuclear details. Cytology diagnoses were categorized into non-diagnostic,

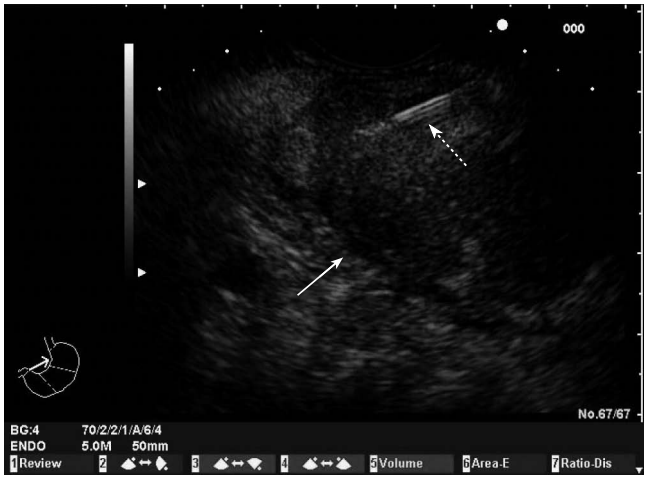

Figure 1 Endoscopic ultrasound image of a mass in the body of the pancreas. Fine needle aspiration of the mass (White arrow: pancreatic mass; Dotted arrow: FNA needle).

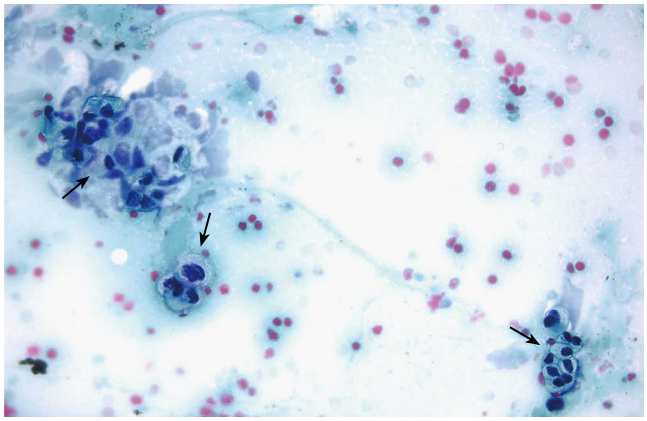

Figure 2 Cytological evaluation of a pancreatic sample obtained by EUS-guided FNA. The presence of marked cellular atypia (arrows) supports the diagnosis of adenocarcinoma of the pancreas (Papanicolau staining × 40).

negative for malignancy, and positive for malignancy, based on published criteria[12]. (2) Samples obtained after the third puncture were recovered into a tube containing a 10% formol solution by injecting 2 ml of saline solution through the needle (Figure 3). Samples were then embedded in paraffin. Tissue sections of 3 to 4 μm were stained by the classical haematoxylin-eosin technique for morphological evaluation. The sample was considered adequate if a coherent core tissue specimen from the target lesion was obtained (Figure 4).

No pathologist was present in the endoscopy room during the procedure. Samples were initially processed by the endoscopist, who was specifically trained with this aim by pathologists. Thus, no microscopic evaluation of sample adequacy was performed at that time. Two experienced pathologists examined both cytological smears and histological specimens. Cytological and histological findings were compared with the surgical specimen as gold standards in patients who were further operated upon. In non-operated patients, a clinical, morphological (EUS and CT scan) and biochemical evaluation (including serum levels of Ca 19.9) over a minimum follow-up

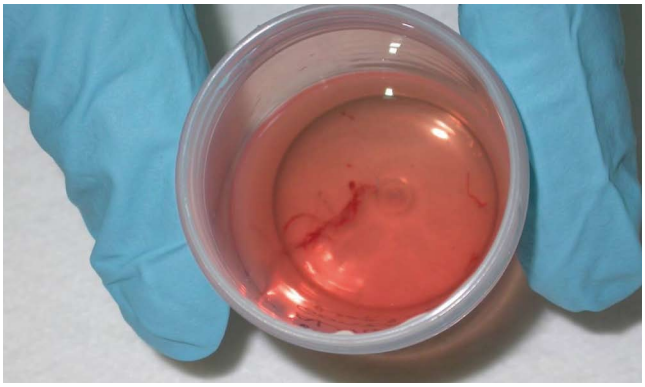

Figure 3 Core of pancreatic tissue obtained by expelling the content of the needle into a tube with 10% formol solution by careful injection of saline solution after EUS-guided FNA.

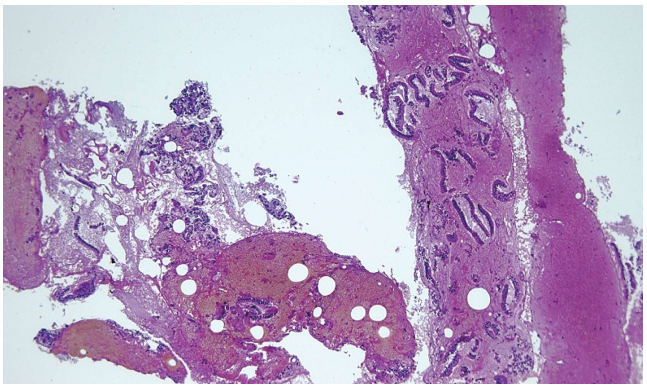

Figure 4 Adenocarcinoma of the pancreas. Histological study of the tissue sample obtained by EUS-guided FNA (HE × 5).

of at least 6 mo was considered as gold standards. The criteria for establishing a benign course of disease were thus a subjective well-being, absence of weight loss, no progression of the disease on imaging studies and no elevation of serum tumour markers.

Statistical analysis

Sensitivity, specificity, overall accuracy and positive and negative predictive values for malignancy were calculated. Data from histology and cytology are shown as percentages and 95% confidence intervals and compared by the Fisher's exact test. $P < 0.05$ was considered as significant.

RESULTS

Pancreatic masses were secondary to a malignant condition in 38 cases (61.3%), and to benign diseases in 24 cases (38.7%). Distribution of patients according to the final diagnosis based on the gold standards is shown in Table 1. A total of 27 patients underwent surgery, including 20 pancreatic adenocarcinomas, one patient with an endocrine tumour, and 6 patients with an inflammatory mass related to a chronic pancreatitis. The remaining 35 patients were followed up for a median of 10 mo (range 6-20 mo).

The length of the core specimen obtained for histological analysis was 6.5 ± 5.3 mm (range 1-22 mm). Cytological and histological samples were considered as adequate in 51 (82.3%, 95% CI, 71.0%-89.8%) and 52 cases (83.9%, 95% CI, 72.8%-91.0%), respectively (not significant). Global sensitivity of both pancreatic cytology and histology for diagnosis of malignancy was 68.4% (52.5%-80.9%).

Table 1 Distribution of patients according to the final diagnosis and number of patients correctly diagnosed by cytological and histological evaluation of samples obtained by EUS-guided FNA

Final diagnosis	*n*	Correct diagnosis by cytology	Correct diagnosis by histology	Correct diagnosis by both cytology and histology
Adenocarcinoma	33	24	21	27
Anaplastic carcinoma	1	1	1	1
Small cell lung cancer	1	0	1	1
Squamous cell carcinoma	1	1	1	1
B cell lymphoma	1	0	1	1
Endocrine carcinoma	1	0	1	1
Inflammatory process	24	17	24	24
Total	62	42	55	56

Table 2 Accuracy of EUS-guided FNA for detection of malignancy in pancreatic solid masses in cases of adequate FNA sampling (95% CI)

	Cytology	Histology	*P*
Sensitivity	76.5% (60.0-87.6)	92.85% (77.3-98.0)	0.097
Specificity	100% (81.6-100)	100% (86.2-100)	NS
Negative predictive value	68.0% (48.4-82.8)	92.3% (75.9-97.9)[a]	< 0.05
Positive predictive value	100% (87.1-100)	100% (87.1-100)	NS
Overall accuracy	84.3% (72.0-91.8)	96.1% (87.0-98.9)	0.05

NS: not significant. [a]$P < 0.05$ *vs* cytology.

Diagnostic accuracy of both techniques in cases of adequate sample is shown in Table 2. In this context, histology tended to be more sensitive and accurate, and showed a significantly higher negative predictive value for malignancy than cytology.

Histological evaluation provided a correct diagnosis in all 24 cases of inflammatory masses, compared with 17 cases correctly classified by cytology (Table 1). Although both techniques were similarly sensitive for the diagnosis of pancreatic adenocarcinomas, histology was the only one able to diagnose other tumours like lymphomas, endocrine tumours and small cell lung cancer metastasis (Table 1). The combination of cytology and histology allowed obtaining an adequate sample in 56 cases (90.3%, 95% CI, 80.4%-95.5%), and a correct diagnosis in all 24 cases of inflammatory masses and 32 cases of pancreatic malignancy (Table 1). Thus, the global sensitivity of EUS-guided FNA was 84.21% (95% CI, 69.6%-92.6%), specificity of 100% (95% CI, 86.2%-100%), and overall accuracy of 90.32% (95% CI, 80.4%-95.5%).

The complication rate of the procedure was 1.6%, and only one case of mild acute pancreatitis that resolved within three days of conservative treatment was observed. No patient died because of the procedure.

DISCUSSION

Recovery of pancreatic EUS-guided FNA specimen into a 10% formol solution by careful injection of saline through the needle allows obtaining an adequate tissue sample for histological diagnosis of pancreatic masses in most cases. Compared to cytology, histology provides a significantly higher negative predictive value for malignancy, and tends to be more accurate. In addition, tumours other than adenocarcinomas are more easily diagnosed by histology.

Several studies have evaluated the accuracy of cytology after EUS-guided FNA for the diagnostic assessment of pancreatic masses. According to those reports, an adequate cytological specimen can be obtained in 82% to 91% of cases, with a sensitivity for malignancy ranging from 64% to 96%[13-25]. In our series, the sensitivity of cytology for the diagnosis of malignancy was 68.4%, which improved up to 76.5% when only adequate samples were considered, similar to the previous report.

In previous studies showing high diagnostic yields of cytology, 3 to 6 needle passes through the lesion[16-23,26] and on-site evaluation of the FNA sample adequacy by a cytopathologist[10,27-29] was considered essential. We were able to obtain an adequate sample in 90% of cases by performing three passes, two for cytological evaluation and one for histological evaluation.

Compared to cytology, histological evaluation of a tissue sample seems to have several advantages, such as a better distinction between well-differentiated adenocarcinoma and chronic pancreatitis, an appropriate cellular subtyping and architectural analysis for the diagnosis of tumours (i.e. lymphoma), as well as the possibility of using special stains[5,6]. In our series, obtaining a core specimen for histological evaluation allowed us to categorize malignant lesions that, although rare, were impossible to be diagnosed by cytology (i.e., pancreatic lymphomas, small cell lung cancer metastasis and endocrine carcinomas). Histological analyses were also able to properly diagnose benign pancreatic lesions in all patients. However, we had difficulties in acquisition of adequate samples from pancreatic adenocarcinomas, which might be explained by the tissue features of this solid tumour, characterized by infiltrating duct-like and tubular structures embedded in a highly desmoplastic stroma[30].

Different needles and different needle diameters have been evaluated to obtain core tissue specimens for histopathological analysis[7-11]. Binmoeller *et al*[7] were able to obtain adequate tissue core specimens in 40 out of 45 patients with pancreatic masses using an 18-gauge needle. Despite that, the sensitivity for detection of a malignancy was only 53%[7]. In a more recent retrospective study, Levy *et al*[9] reported an accuracy of 85% for the diagnosis of different pancreatic and non-pancreatic lesions using a 19-gauge trucut needle, compared to a 60% accuracy achieved by the standard fine needle aspiration technique. Varadarajulu *et al*[10] compared a 19-gauge trucut needle with the standard 22-gauge needle with fine needle aspiration, and no difference in the diagnostic accuracy between both techniques was found (78% *vs* 89%). The diagnostic yield of the trucut needle biopsy is strongly limited to lesions located in the head of the pancreas[11]. This is due to the impossibility to reach within the duodenum the degree of deflection of the echoendoscope tip required to bring the target lesion to an adequate position for puncture. Larghi *et al*[11], despite performing trucut needle biopsy only in lesions accessible for the transgastric approach, were able to obtain materials in only 74% of cases, with an overall diagnostic accuracy of 61%. Contrary to these, the method described in the present study allowed us to achieve a high diagnostic accuracy for pancreatic masses located both in the head and in the body and tail of the pancreas.

Despite the advantages of obtaining tissue core specimens for histological analysis, two cases in our series of malignant pancreatic masses were only detected by cytology. This strongly argues in favour of obtaining specimens for both cytological and histological evaluation. Similar data were reported by other authors[7,9]. In fact, this approach allowed obtaining an adequate sample (either for histology and/or cytology) in 90.3% of cases, with an overall diagnostic accuracy for a malignancy as high as of 90.3%.

EUS-guided biopsy of the pancreas is a safe technique[31,32], with a slightly higher complication rate related to the use of trucut needles[10]. In fact, the risk of pancreatitis and bleeding has been reported to be higher with trucut needles than with the standard FNA needles[10], even though this was not confirmed by other authors[7,11]. A case of mild acute pancreatitis was the only complication observed in the present series after EUS-guided FNA of the pancreas. This low complication rate is similar to that reported previously using a standard 22G needle[21-25].

In conclusion, pancreatic core specimens for histological examination can be obtained by EUS-guided FNA with a 22-gauge needle by careful injection of saline through the needle and by expelling the tissue samples into a tube containing 10% formol solution. The samples obtained by this procedure are highly adequate for histological analyses allowing an appropriate evaluation of pancreatic solid masses. This technique is mainly useful for the diagnosis of different types of pancreatic tumours as well as for the evaluation of benign diseases. Combination with cytology tends to increase the sensitivity of histology for the diagnosis of pancreatic adenocarcinomas.

COMMENTS

Background

Differential diagnosis of pancreatic masses is a frequent clinical challenge. Endoscopic ultrasound (EUS)-guided fine needle aspiration (FNA) has been proved to be a safe and useful method for tissue sampling of pancreatic solid masses. Histological study of tissue samples allows the assessment of tissue architecture and cell morphology, as well as the performance of immunohistochemical analysis, thus usually providing with a higher diagnostic accuracy than cytology.

Research frontiers

Further research is needed in order to improve the diagnostic yield of EUS-guided biopsy, and to provide with better material from pancreatic lesions. Availability of adequate pancreatic tissue samples may allow performing immunohistochemical studies, molecular analysis, and evaluation of genetic mutations, thus providing the basis for a better knowledge of pancreatic diseases.

Innovations and breakthroughs

Our study demonstrates that a core specimen from pancreatic solid masses can

be obtained using a standard 22 gauge needle, thus allowing the histological evaluation of pancreatic lesions. Retrieving pancreatic tissue fragments has been explored using different types of needles (e.g., trucut needles) and different ways of sample processing. In contrast to trucut needles, our technique allows access to lesions located at the head of the pancreas with a low complication rate.

Applications

Obtaining samples of pancreatic tissue allows the histological evaluation of pancreatic solid masses, which may be of help for the diagnosis of different pancreatic tumours as well as for the evaluation of benign diseases like chronic pancreatitis.

Peer review

This paper provides support for the use of this modified method when performing fine needle biopsy of solid pancreatic masses.

REFERENCES

1 **Tamm E**, Charnsangavej C. Pancreatic cancer: current concepts in imaging for diagnosis and staging. *Cancer J* 2001; **7**: 298-311
2 **Cohen SJ**, Pinover WH, Watson JC, Meropol NJ. Pancreatic cancer. *Curr Treat Options Oncol* 2000; **1**: 375-386
3 **Rösch T**. Endoscopic ultrasonography. *Br J Surg* 1997; **84**: 1329-1331
4 **Hawes RH**. Endoscopic ultrasound. *Gastrointest Endosc Clin N Am* 2000; **10**: 161-174, viii
5 **Ribeiro A**, Vazquez-Sequeiros E, Wiersema LM, Wang KK, Clain JE, Wiersema MJ. EUS-guided fine-needle aspiration combined with flow cytometry and immunocytochemistry in the diagnosis of lymphoma. *Gastrointest Endosc* 2001; **53**: 485-491
6 **Mesa H**, Stelow EB, Stanley MW, Mallery S, Lai R, Bardales RH. Diagnosis of nonprimary pancreatic neoplasms by endoscopic ultrasound-guided fine-needle aspiration. *Diagn Cytopathol* 2004; **31**: 313-318
7 **Binmoeller KF**, Thul R, Rathod V, Henke P, Brand B, Jabusch HC, Soehendra N. Endoscopic ultrasound-guided, 18-gauge, fine needle aspiration biopsy of the pancreas using a 2.8 mm channel convex array echoendoscope. *Gastrointest Endosc* 1998; **47**: 121-127
8 **Harada N**, Kouzu T, Arima M, Isono K. Endoscopic ultrasound-guided histologic needle biopsy: preliminary results using a newly developed endoscopic ultrasound transducer. *Gastrointest Endosc* 1996; **44**: 327-330
9 **Levy MJ**, Jondal ML, Clain J, Wiersema MJ. Preliminary experience with an EUS-guided trucut biopsy needle compared with EUS-guided FNA. *Gastrointest Endosc* 2003; **57**: 101-106
10 **Varadarajulu S**, Fraig M, Schmulewitz N, Roberts S, Wildi S, Hawes RH, Hoffman BJ, Wallace MB. Comparison of EUS-guided 19-gauge Trucut needle biopsy with EUS-guided fine-needle aspiration. *Endoscopy* 2004; **36**: 397-401
11 **Larghi A**, Verna EC, Stavropoulos SN, Rotterdam H, Lightdale CJ, Stevens PD. EUS-guided trucut needle biopsies in patients with solid pancreatic masses: a prospective study. *Gastrointest Endosc* 2004; **59**: 185-190
12 **Robins DB**, Katz RL, Evans DB, Atkinson EN, Green L. Fine needle aspiration of the pancreas. In quest of accuracy. *Acta Cytol* 1995; **39**: 1-10
13 **Voss M**, Hammel P, Molas G, Palazzo L, Dancour A, O'Toole D, Terris B, Degott C, Bernades P, Ruszniewski P. Value of endoscopic ultrasound guided fine needle aspiration biopsy in the diagnosis of solid pancreatic masses. *Gut* 2000; **46**: 244-249
14 **Wiersema MJ**, Kochman ML, Cramer HM, Tao LC, Wiersema LM. Endosonography-guided real-time fine-needle aspiration biopsy. *Gastrointest Endosc* 1994; **40**: 700-707
15 **Chang KJ**, Katz KD, Durbin TE, Erickson RA, Butler JA, Lin F, Wuerker RB. Endoscopic ultrasound-guided fine-needle aspiration. *Gastrointest Endosc* 1994; **40**: 694-699
16 **Erickson RA**, Sayage-Rabie L, Beissner RS. Factors predicting the number of EUS-guided fine-needle passes for diagnosis of pancreatic malignancies. *Gastrointest Endosc* 2000; **51**: 184-190
17 **Binmoeller KF**, Rathod VD. Difficult pancreatic mass FNA: tips for success. *Gastrointest Endosc* 2002; **56**: S86-S91
18 **Bhutani MS**, Hawes RH, Baron PL, Sanders-Cliette A, van Velse A, Osborne JF, Hoffman BJ. Endoscopic ultrasound guided fine needle aspiration of malignant pancreatic lesions. *Endoscopy* 1997; **29**: 854-858
19 **Harewood GC**, Wiersema MJ. Endosonography-guided fine needle aspiration biopsy in the evaluation of pancreatic masses. *Am J Gastroenterol* 2002; **97**: 1386-1391
20 **Giovannini M**, Seitz JF, Monges G, Perrier H, Rabbia I. Fine-needle aspiration cytology guided by endoscopic ultrasonography: results in 141 patients. *Endoscopy* 1995; **27**: 171-177
21 **Gress FG**, Hawes RH, Savides TJ, Ikenberry SO, Lehman GA. Endoscopic ultrasound-guided fine-needle aspiration biopsy using linear array and radial scanning endosonography. *Gastrointest Endosc* 1997; **45**: 243-250
22 **Raut CP**, Grau AM, Staerkel GA, Kaw M, Tamm EP, Wolff RA, Vauthey JN, Lee JE, Pisters PW, Evans DB. Diagnostic accuracy of endoscopic ultrasound-guided fine-needle aspiration in patients with presumed pancreatic cancer. *J Gastrointest Surg* 2003; **7**: 118-126; discussion 127-128
23 **Wiersema MJ**, Vilmann P, Giovannini M, Chang KJ, Wiersema LM. Endosonography-guided fine-needle aspiration biopsy: diagnostic accuracy and complication assessment. *Gastroenterology* 1997; **112**: 1087-1095
24 **Chhieng DC**, Jhala D, Jhala N, Eltoum I, Chen VK, Vickers S, Heslin MJ, Wilcox CM, Eloubeidi MA. Endoscopic ultrasound-guided fine-needle aspiration biopsy: a study of 103 cases. *Cancer* 2002; **96**: 232-239
25 **Williams DB**, Sahai AV, Aabakken L, Penman ID, van Velse A, Webb J, Wilson M, Hoffman BJ, Hawes RH. Endoscopic ultrasound guided fine needle aspiration biopsy: a large single centre experience. *Gut* 1999; **44**: 720-726
26 **Erickson RA**. EUS-guided FNA. *Gastrointest Endosc* 2004; **60**: 267-279
27 **Klapman JB**, Logrono R, Dye CE, Waxman I. Clinical impact of on-site cytopathology interpretation on endoscopic ultrasound-guided fine needle aspiration. *Am J Gastroenterol* 2003; **98**: 1289-1294
28 **Jhala NC**, Jhala DN, Chhieng DC, Eloubeidi MA, Eltoum IA. Endoscopic ultrasound-guided fine-needle aspiration. A cytopathologist's perspective. *Am J Clin Pathol* 2003; **120**: 351-367
29 **Chang KJ**, Nguyen P, Erickson RA, Durbin TE, Katz KD. The clinical utility of endoscopic ultrasound-guided fine-needle aspiration in the diagnosis and staging of pancreatic carcinoma. *Gastrointest Endosc* 1997; **45**: 387-393
30 **Klöppel G**, Hruban RH, Longnecker DS, Adler G, Kern SE, Partanen TJ. Ductal adenocarcinoma of the pancreas. In: Hamilton SR, Aaltonen LA, editors. Pathology and Genetics of Tumours of the Digestive System. WHO Classification of Tumours. Lyon: IARC Press, 2000: 221-230
31 **O'Toole D**, Palazzo L, Arotçarena R, Dancour A, Aubert A, Hammel P, Amaris J, Ruszniewski P. Assessment of complications of EUS-guided fine-needle aspiration. *Gastrointest Endosc* 2001; **53**: 470-474
32 **Micames C**, Jowell PS, White R, Paulson E, Nelson R, Morse M, Hurwitz H, Pappas T, Tyler D, McGrath K. Lower frequency of peritoneal carcinomatosis in patients with pancreatic cancer diagnosed by EUS-guided FNA vs. percutaneous FNA. *Gastrointest Endosc* 2003; **58**: 690-695

S- Editor Wang GP **L- Editor** Zhu LH **E- Editor** Liu WF

PO Box 2345, Beijing 100023, China
www.wjgnet.com
wjg@wjgnet.com

World J Gastroenterol 2007 January 14; 13(2): 294-298
World Journal of Gastroenterology ISSN 1007-9327
© 2007 The WJG Press. All rights reserved.

RAPID COMMUNICATION

Immunogenicity of recombinant hepatitis B virus vaccine in patients with and without chronic hepatitis C virus infection: A case-control study

Naser Ebrahimi Daryani, Mohsen Nassiri-Toosi, Armin Rashidi, Iman Khodarahmi

Naser Ebrahimi Daryani, Mohsen Nassiri-Toosi, Armin Rashidi, Iman Khodarahmi, Department of Gastroenterology, Medical School, Tehran University of Medical Sciences, Tehran, Iran
Correspondence to: Iman Khodarahmi, Department of Gastroenterology, Medical School, Tehran University of Medical Sciences, Unit 9, No. 41 Kashani St., Dabestan Ave., Seyed Khandan, Tehran, Iran. ikhodarahm@student.tums.ac.ir
Telephone: +98-21-88468178 Fax: +98-21-22646984
Received: 2006-09-06 Accepted: 2006-12-05

Abstract

AIM: To compare the response of standard hepatitis B virus (HBV) vaccination between patients with chronic hepatitis C virus (HCV) infection and healthy individuals.

METHODS: This is a prospective case-control study. A total of 38 patients with chronic HCV infection and 40 healthy controls were included. Vaccination was performed by injection of 20 μg recombinant HBsAg into the deltoid muscle at mo 0, 1 and 6. Anti-HBs concentration was determined 3 mo after the last dose and compared between the two groups. The response pattern was characterized as (1) high-response when the anti-HBs antibody titer was > 100 IU/L, (2) low-response when the titer was 10-100 IU/L and (3) no-response when the titer was < 10 IU/L.

RESULTS: In the patient group, there were 10/38 (26.3%) non-responders, 8/38 (21.1%) low-responders and 20/38 (52.6%) high-responders. The corresponding values in the control group were 2/40 (5.0%), 7/40 (17.5%) and 31/40 (77.5%), respectively. The response pattern was statistically different between the two groups. In multivariate analysis, smoking was a significant confounder, while HCV infection lost its significant correlation with lower antibody response.

CONCLUSION: Patients with chronic HCV infection tend to respond weakly to HBV vaccination compared to healthy individuals, though this correlation is not independent according to multivariate analysis.

© 2007 The WJG Press. All rights reserved.

Key words: Immunogenicity; Hepatitis B; Vaccine; Hepatitis C; Antibody response

Daryani NE, Nassiri-Toosi M, Rashidi A, Khodarahmi I. Immunogenicity of recombinant hepatitis B virus vaccine in patients with and without chronic hepatitis C virus infection: A case-control study. *World J Gastroenterol* 2007; 13(2): 294-298

http://www.wjgnet.com/1007-9327/13/294.asp

INTRODUCTION

One major transmission route for both hepatitis C virus (HCV) and hepatitis B virus (HBV) is the parenteral route, and the sources of infection include administration of blood or blood products[1,2], intravenous drug use[3,4] and needle-stick accidents[5,6]. According to the analysis of the Third National Health and Nutrition Survey, more than 25% of HCV-positive patients in the United States had hepatitis B markers, a proportion nearly six times that in the HCV-negative group[3]. However, the actual prevalence of HBV infection in patients with HCV infection is probably underestimated[7,8]. Although it has been shown that superinfection of either HBV or HCV may suppress the other's replicative levels, coinfection with both viruses has synergistic effects with regard to histological lesions, progression to cirrhosis and cancer development[9-13]. As such it has been recommended by the National Institutes of Health (NIH) that individuals with HCV be vaccinated against HBV infection to prevent such an outcome[14].

HBV vaccination at standard doses (20 μg for adults at mo 0, 1, and 6) results in an effective antibody response in 90% to 98% of healthy individuals[15,16]. However, reduced immunogenicity of the vaccine has been established in persons with chronic liver disease, patients receiving hemodialysis, patients with HIV infection and those awaiting transplantation[17-21]. To the best of our knowledge, only a few studies, with inconsistent results, have compared the immunogenicity of standard HBV vaccination in chronic hepatitis C patients with that in healthy individuals through a case-control study[22-24]. Therefore, we found it valuable to compare the response of standard HBV vaccination between patients with chronic HCV infection and healthy individuals in a prospective case-control study.

MATERIALS AND METHODS

Subjects

Between April 2005 and August 2006, 38 patients with

chronic hepatitis C infection (patients group) and 40 healthy individuals (control group) referred to our clinic were enrolled in this case-control study. Totally there were 50 males and 28 females with a mean age of 37.6 ± 12.8 years. All participants gave written informed consent and the study protocol was approved by the Ethical Committee of Tehran University of Medical Sciences. Inclusion criteria for the patient group were: age > 18 years, HCV infection diagnosed by positive HCV serological markers assessed by ELISA (Abbott Laboratories, North Chicago, IL, USA) and confirmed by the presence of serum HCV RNA detected by PCR, chronic infection diagnosed by serum alanine aminotransferase (ALT) levels of at least twice the upper normal values (> 90 IU/L) for at least two times within a period longer than 6 mo and/or a liver biopsy showing evidence of chronic hepatitis. The control group was selected from healthy adults older than 18 years. Exclusion criteria were: pregnancy, lactation, known bleeding diathesis, current intravenous drug use, alcohol consumption > 30 g/d, history of cancer or transplantation, receiving immunosuppressive medications (excluding interferon), previous hepatitis B vaccination, history of allergy to vaccine components, current or previous hepatitis B infection (positive HBs Ag, anti-HBc Ab/anti-HBs Ab by ELISA), laboratory or clinical evidence of other chronic liver diseases including cirrhosis of any etiology, presence of HIV infection, chronic renal failure (serum creatinine > 2.5) or hemodialysis.

The following variables were recorded for all participants: age (year), sex, body mass (kg), height (m), smoking, alcohol use, history of intravenous drug use. Body mass index (BMI) was calculated by dividing mass (kg) by squared height (m^2). Liver biopsy during two years before vaccination showing the stage and grade of liver involvement according to Ishak *et al*[25] and HCV genotype (determined by PCR-RFLP) was available for 31 and 34 patients, respectively. Baseline ALT (IU/L) was determined by commercial kits for all patients.

Methods

Vaccination was performed by injection of 20 μg recombinant HBsAg (Euvax B, LG Chem, Korea) into the deltoid muscle at mo 0, 1 and 6. Anti-HBs concentration was determined 3 mo after the last dose and expressed as IU/L. The response pattern was characterized as (1) high-response when anti-HBs antibody titer was > 100 IU/L, (2) low-response when the titer was 10-100 IU/L and (3) no-response when the titer was < 10 IU/L. Patients were monitored after each vaccine dose for the occurrences of local (pain, induration, flush) and general (headache, fatigue, fever) side effects.

Statistical analysis

The results are presented as mean ± SD. χ^2 test with Fisher's exact test was used to compare qualitative variables between the groups. Student's *t* test and analysis of variance (ANOVA) were used to compare the quantitative variables between two and multiple groups, respectively. The independent predictive factors of vaccine response were identified by multivariate analysis using multiple logistic regression. Statistical analysis was conducted with SPSS 11.5 software (SPSS Inc., Chicago, IL, USA). Throughout analysis, $P < 0.05$ was considered statistically significant.

Table 1 Characteristics of patients and controls (mean ± SD)

Characteristic	Patient group (n = 38)	Control group (n = 40)	P
Age (yr)	41.1 ± 10.3[a]	34.2 ± 14.2	0.017
Male/Female	30/8[b]	20/20	0.010
BMI (kg/m^2)	24.8 ± 4.7	24.3 ± 4.9	0.691
Smoking *n* (%)	25 (65.8)[b]	3 (7.5)	< 0.001
Alcohol *n* (%)	6 (15.8)	1 (2.5)	0.054
History of iv drug use *n* (%)	9 (23.7)[b]	0 (0)	0.001

[a]$P < 0.05$, [b]$P < 0.01$ *vs* control group.

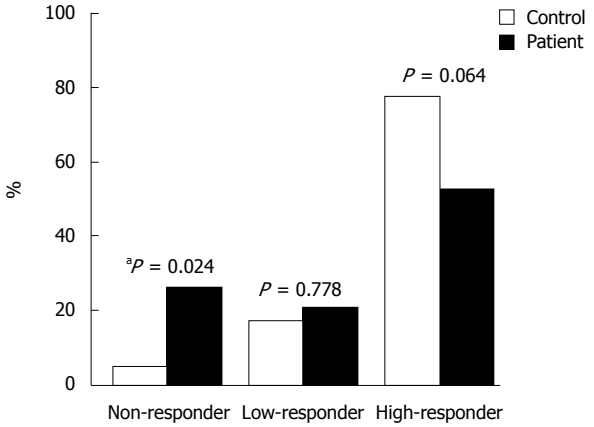

Figure 1 Response to HBV vaccination in patient and control groups. Non-responder (anti-HBs < 10 IU/L); Low-responder (10 IU/L < anti-HBs < 100 IU/L); High-responder (anti-HBs > 100 IU/L). [a]$P < 0.05$ *vs* control group.

RESULTS

Characteristics of patients and controls

Patients were significantly older than healthy subjects ($P = 0.017$). Also, patients were more frequently males ($P = 0.010$), smokers ($P < 0.001$) and previous intravenous drug users ($P = 0.001$) (Table 1).

Antibody response

A total of 28/38 (73.7%) chronic hepatitis C patients responded to the vaccination course (anti-HBs > 10 IU/L) compared with 38/40 (95.0%) controls ($P = 0.012$). In the patient group, there were 10/38 (26.3%) non-responders, 8/38 (21.1%) low-responders and 20/38 (52.6%) high-responders. The corresponding values in the control group were 2/40 (5.0%), 7/40 (17.5%) and 31/40 (77.5%), respectively (Figure 1). The response pattern was statistically different between the two groups ($P = 0.021$). The frequency of non-responders was significantly higher in the patient group ($P = 0.024$ after Bonferroni's correction). However, the frequency of low-responders ($P = 0.778$) and high-responders ($P = 0.064$) was not significantly different between the two groups. Since

Table 2 Characteristics of hepatitis C patients according to vaccine response (mean ± SD)

Characteristics	Non-responder (n = 10)	Responder (n =28)	P
Age (yr)	41.5 ± 11.3	41.0 ± 10.2	0.897
Male/Female	8/2	22/6	1.000
BMI (kg/m^2)	26.6 ± 6.0	24.2 ± 4.1	0.192
Smoking n (%)	9 (90.0)	16 (57.1)	0.118
Alcohol n (%)	2 (20.0)	4 (14.3)	0.644
Hx of iv drug use n (%)	2 (20.0)	7 (25.0)	1.000
ALT (IU/L)	177.1 ± 293.9	78.3 ± 165.3	0.199
Liver disease			
HAI grade (0-18)[1]	5.4 ± 2.1	5.6 ± 1.9	0.773
HAI stage (0-6)[1]	2.3 ± 1.1	2.6 ± 1.6	0.669
HCV genotype n (%)	8	26	
1a	6 (75.0)	14 (53.8)	0.422
Other than 1a	2 (25.0)	12 (46.2)	

[1]According to Knodell's histological activity index (HAI) as modified by Ishak *et al*[25].Non-responder (anti-HBs < 10 IU/L); Responder (anti-HBs > 10 IU/L). Hx:history.

Table 3 Characteristics of hepatitis C patients according to vaccine response

Characteristic	Non-responder (n = 10)	Low-responder (n = 8)	High-responder (n = 20)	P
Age (yr)	41.5 ± 11.3	46.1 ± 9.0	39.0 ± 10.1	0.394
Male/Female	8/2	5/3	17/3	0.417
BMI (kg/m^2)	26.6 ± 6.0	24.9 ± 3.0	23.8 ± 4.6	0.903
Smoking n (%)	9 (90.0)	4 (50.0)	12 (60.0)	0.150
Alcohol n (%)	2 (20.0)	0 (0)	4 (20.0)	0.387
Hx of iv drug use n (%)	2 (20.0)	2 (25.0)	5 (25.0)	0.950
ALT (IU/L)	177.1 ± 293.9	149.8 ± 304.6	49.8 ± 40.3	0.711
Liver disease				
HAI grade (0-18)	5.4 ± 2.1	5.4 ± 2.8	5.7 ± 1.3	0.607
HAI stage (0-6)	2.3 ± 1.1	2.4 ± 1.8	2.7 ± 1.5	0.986
HCV genotype n (%)	8	8	18	
1a	6 (75.0)[a]	7 (87.5)[a]	7 (38.9)[a]	0.038
Other than 1a	2 (25.0)	1 (12.5)	11 (61.1)	

Non-responder (anti-HBs < 10 IU/L); Low-responder (10 IU/L < anti-HBs < 100 IU/L); High-responder (anti-HBs > 100 IU/L). [a]P < 0.05 comparison between three groups.

the patient and control groups were not matched in age, sex, smoking and history of iv drug use, binary logistic regression was performed to adjust for these parameters. Response (anti-HBs > 10 IU/L) was considered as the dependent variable, while hepatitis C infection, age, sex, smoking and history of iv drug use were included as covariates. None of hepatitis C infection (P = 0.448), age (P = 0.078), sex (P = 0.480) and history of iv drug use (P = 0.127) were independently correlated with lower antibody response in the patient group. However, smoking was a significant confounder (P = 0.024; odds ratio: 25.64; 95% confidence interval: 1.54-500).

Characteristics of hepatitis C patients according to vaccine response

The comparison of characteristics of patients between responders and non-responders to HBV vaccine showed no significant difference regarding age, sex ratio, BMI, smoking, alcohol use, history of iv drug use, baseline ALT level, stage and grade of liver disease and genotype (1a *vs* others, Table 2). When patients were categorized into three groups of non-, low- and high-responders, none of the variables except genotype (P = 0.038) had a significant correlation with response category anymore (Table 3). Genotype 1a was more frequently observed in non-responders. However, when Bonferroni's correction was applied for subgroup analysis, this correlation was no longer significant. In summary, no correlation was found between the variables studied and response in either type of analysis.

Side effects

No severe side effects following vaccination were observed in chronic hepatitis C patients. Local adverse effects (erythema, pain at injection point, induration) following vaccination were observed in 4/38 (10.5%) patients. Systemic side effects such as flulike syndrome, headache, fever and fatigue occurred several days following vaccine injections in 1/38 (2.6%) patients.

DISCUSSION

In the present study, the antibody response to standard HBV vaccination with a dose of 20 μg at mo 0, 1 and 6 in individuals with non-cirrhotic chronic hepatitis C infection was evaluated and compared with healthy controls. The frequency of high-responders, low-responders and non-responders in the patient and control groups was 52.6%, 21.1%, 26.3% and 77.5%, 17.5%, 5.0%, respectively (P = 0.021). Non-responders were significantly more common in the patient group (P = 0.024). However, this correlation was not significant in multivariate analysis anymore when age, sex, smoking and history of iv drug use were controlled as potential confounders. In our patient group, there was no correlation between antibody response and variables such as age, sex, BMI, smoking, alcohol use, history of iv drug use, baseline ALT levels, stage and grade of liver disease and genotype.

Several studies have compared the immunogenicity of hepatitis B vaccination with different protocols between healthy individuals and hepatitis C patients. Some of them, like our study, have failed to demonstrate a significant correlation between chronic hepatitis C and antibody response[22,26-28]. However, some authors have shown that responses were weaker in patients than in controls[23,24,29,30]. Hence the results still remain controversial. Among the above mentioned studies, only three have used the same vaccination protocol as ours[22-24]. Lee *et al*[22] compared the immunogenicity of HBV vaccination between 26 hepatitis C patients and 35 controls. The groups were similar in age, but the control group was significantly younger than the patient group. One month after the last dose, 88.5% of patients and 91.4% of controls responded to vaccination with anti-HBs > 10 IU/L. The difference was not statistically significant[22].

In another study of 48 patients and 11 controls, Chlabicz *et al*[23] showed that 72.9% of patients and 90.9% of controls responded (anti-HBs > 10 IU/L) to HBV vaccination one month after the last dose. The groups

were similar in age, sex, BMI and smoking frequency but the difference in antibody response was not significant either. One year after the last dose, there was a significant reduction in antibody response among patients so that only 34.1% of them remained responders. The corresponding value in the control group was 90% at the same time ($P < 0.05$).

Finally, Mattos *et al*[24] reported in their study of 85 patients and 46 healthy adults that 55.3% of patients and 97.8% of controls responded (anti-HBs > 10 IU/L) to HBV vaccination one month after the third vaccine dose. Non-responders were significantly more common in the patient group ($P < 0.001$). The patient and control groups were matched in sex, BMI, alcohol use and smoking, but the patient group was significantly older than the control group. In multivariate regression to control for age as a potential confounder, HCV positivity remained significantly correlated with the lower antibody response ($P = 0.0013$). The patient group in this study included both cirrhotic and non-cirrhotic individuals. Considering that cirrhosis is associated with a lower antibody response[26,31], inhomogeneity of the patient group might have had a role in the significant correlation in this study[24].

We only considered non-cirrhotic patients in our study. The results of multivariate regression showed that hepatitis C infection did not play an independent role in decreasing antibody response. Rather, smoking was a significant confounder ($P = 0.024$; odds ratio: 25.64; 95% confidence interval: 1.54-500). This finding is in agreement with previous studies[32,33]. When patients were categorized into two (responder and non-responder) or three groups (non-, low- and high-responder), no variables studied had a significant correlation with antibody response. Previous studies, as well as ours, failed to show a significant correlation between antibody response and age, sex, BMI, smoking, alcohol use, iv drug use, baseline ALT level or liver histology (grade, stage)[24,29,30]. Mattos *et al*[24] showed that the percentage of non-responders was significantly higher in patients with genotype 1 ($P = 0.04$). Considering that they had three subgroups of patients according to their response, subgroup analysis with a Bonferroni's correction (which changes the P value to $P_c = 0.08$) seemed to be necessary to make a justifiable conclusion. We did not achieve a significant correlation, which was supported by Leroy *et al*[29].

No clinically significant adverse effect was seen in our patients. Local side effects following vaccination were observed in 10.5%, while systemic side effects such as flulike syndrome, headache, fever and fatigue occurred in 2.6% of patients. These rates are almost similar to those reported in other studies[22,26,30]. In conclusion, patients with chronic hepatitis C infection tend to respond weakly to HBV vaccination compared to healthy individuals, though this correlation is not independent according to multivariate analysis.

COMMENTS

Background

Several studies have compared the immunogenicity of hepatitis B vaccination between healthy individuals and hepatitis C patients. Some of them have failed to demonstrate a significant correlation between chronic hepatitis C and antibody response. However, some authors have shown that responses were weaker in patients than in controls.

Research frontiers

Coinfection with both hepatitis B and C viruses has synergistic effects with regard to histological lesions, progression to cirrhosis and cancer development. Therefore, it may be very beneficial to prevent HBV superinfection in hepatitis C patients.

Innovations and breakthroughs

Considering the various vaccination protocols used in HCV patients and also controversial results, we found it valuable to compare the response of standard HBV vaccination between patients with chronic HCV infection and healthy individuals in a prospective case-control study. The results showed that hepatitis C infection does not decrease the immune response to HBV vaccination.

Applications

Based on the results of this study, in the absence of factors known to weaken the immune response, hepatitis C patients do not seem to need additional doses of HBV vaccine or antibody titration after standard HBV vaccination. However, these considerations should be taken into account when vaccinating a hepatitis C patient in general, i.e. one with commonly coexisting immunity-related risk factors.

Terminology

Multivariate analysis: When compared groups are not similar in some possibly important features such as sex or age, performing a multivariate analysis using multiple logistic regression can adjust groups for such potential confounders.

Bonferroni's correction: A method to adjust the level of significance when multiple comparisons are made.

Peer review

If we accept that HBV vaccine may be useful in HCV patients, the basic steps of research should be: to evaluate the rate of response in HCV carriers and to verify whether this rate is acceptable in terms of cost benefit. The patients and controls were significantly different in age, sex, smoking frequency and intravenous drug use.

REFERENCES

1 **Alter MJ**. Epidemiology of hepatitis C. *Hepatology* 1997; **26**: 62S-65S

2 Recommendations for prevention and control of hepatitis C virus (HCV) infection and HCV-related chronic disease. Centers for Disease Control and Prevention. *MMWR Recomm Rep* 1998; **47**: 1-39

3 **Alter MJ**, Kruszon-Moran D, Nainan OV, McQuillan GM, Gao F, Moyer LA, Kaslow RA, Margolis HS. The prevalence of hepatitis C virus infection in the United States, 1988 through 1994. *N Engl J Med* 1999; **341**: 556-562

4 **Murphy EL**, Bryzman SM, Glynn SA, Ameti DI, Thomson RA, Williams AE, Nass CC, Ownby HE, Schreiber GB, Kong F, Neal KR, Nemo GJ. Risk factors for hepatitis C virus infection in United States blood donors. NHLBI Retrovirus Epidemiology Donor Study (REDS) *Hepatology* 2000; **31**: 756-762

5 **Balasekaran R**, Bulterys M, Jamal MM, Quinn PG, Johnston DE, Skipper B, Chaturvedi S, Arora S. A case-control study of risk factors for sporadic hepatitis C virus infection in the southwestern United States. *Am J Gastroenterol* 1999; **94**: 1341-1346

6 **Kiyosawa K**, Sodeyama T, Tanaka E, Nakano Y, Furuta S, Nishioka K, Purcell RH, Alter HJ. Hepatitis C in hospital employees with needlestick injuries. *Ann Intern Med* 1991; **115**: 367-369

7 **Cacciola I**, Pollicino T, Squadrito G, Cerenzia G, Orlando ME, Raimondo G. Occult hepatitis B virus infection in patients with chronic hepatitis C liver disease. *N Engl J Med* 1999; **341**: 22-26

8 **Villa E**, Grottola A, Buttafoco P, Trande P, Merighi A, Fratti N, Seium Y, Cioni G, Manenti F. Evidence for hepatitis B virus infection in patients with chronic hepatitis C with and without serological markers of hepatitis B. *Dig Dis Sci* 1995; **40**: 8-13
9 **Crespo J**, Lozano JL, Carte B, de las Heras B, de la Cruz F, Pons-Romero F. Viral replication in patients with concomitant hepatitis B and C virus infections. *Eur J Clin Microbiol Infect Dis* 1997; **16**: 445-451
10 **Ohkawa K**, Hayashi N, Yuki N, Masuzawa M, Kato M, Yamamoto K, Hosotsubo H, Deguchi M, Katayama K, Kasahara A. Long-term follow-up of hepatitis B virus and hepatitis C virus replicative levels in chronic hepatitis patients coinfected with both viruses. *J Med Virol* 1995; **46**: 258-264
11 **Zarski JP**, Bohn B, Bastie A, Pawlotsky JM, Baud M, Bost-Bezeaux F, Tran van Nhieu J, Seigneurin JM, Buffet C, Dhumeaux D. Characteristics of patients with dual infection by hepatitis B and C viruses. *J Hepatol* 1998; **28**: 27-33
12 **Liaw YF**, Yeh CT, Tsai SL. Impact of acute hepatitis B virus superinfection on chronic hepatitis C virus infection. *Am J Gastroenterol* 2000; **95**: 2978-2980
13 **Kaklamani E**, Trichopoulos D, Tzonou A, Zavitsanos X, Koumantaki Y, Hatzakis A, Hsieh CC, Hatziyannis S. Hepatitis B and C viruses and their interaction in the origin of hepatocellular carcinoma. *JAMA* 1991; **265**: 1974-1976
14 **NIH consensus development conference targets prevention and management of hepatitis C**. *Am Fam Physician* 1997; **56**: 959-961
15 **Dienstag JL**, Werner BG, Polk BF, Snydman DR, Craven DE, Platt R, Crumpacker CS, Ouellet-Hellstrom R, Grady GF. Hepatitis B vaccine in health care personnel: safety, immunogenicity, and indicators of efficacy. *Ann Intern Med* 1984; **101**: 34-40
16 **Rahman F**, Dahmen A, Herzog-Hauff S, Böcher WO, Galle PR, Löhr HF. Cellular and humoral immune responses induced by intradermal or intramuscular vaccination with the major hepatitis B surface antigen. *Hepatology* 2000; **31**: 521-527
17 **Keeffe EB**, Krause DS. Hepatitis B vaccination of patients with chronic liver disease. *Liver Transpl Surg* 1998; **4**: 437-439
18 **Stevens CE**, Szmuness W, Goodman AI, Weseley SA, Fotino M. Hepatitis B vaccine: immune responses in haemodialysis patients. *Lancet* 1980; **2**: 1211-1213
19 **Collier AC**, Corey L, Murphy VL, Handsfield HH. Antibody to human immunodeficiency virus (HIV) and suboptimal response to hepatitis B vaccination. *Ann Intern Med* 1988; **109**: 101-105
20 **Jacobson IM**, Jaffers G, Dienstag JL, Tolkoff-Rubin NE, Cosimi AB, Delmonico F, Watkins E, Hinkle C, O'Rourke S, Russell PS. Immunogenicity of hepatitis B vaccine in renal transplant recipients. *Transplantation* 1985; **39**: 393-395
21 **Van Thiel DH**, el-Ashmawy L, Love K, Gavaler JS, Starzl TE. Response to hepatitis B vaccination by liver transplant candidates. *Dig Dis Sci* 1992; **37**: 1245-1249
22 **Lee SD**, Chan CY, Yu MI, Lu RH, Chang FY, Lo KJ. Hepatitis B vaccination in patients with chronic hepatitis C. *J Med Virol* 1999; **59**: 463-468
23 **Chlabicz S**, Grzeszczuk A, Łapiński TW. Hepatitis B vaccine immunogenicity in patients with chronic HCV infection at one year follow-up: the effect of interferon-alpha therapy. *Med Sci Monit* 2002; **8**: CR379-CR383
24 **Mattos AA**, Gomes EB, Tovo CV, Alexandre CO, Remião JO. Hepatitis B vaccine efficacy in patients with chronic liver disease by hepatitis C virus. *Arq Gastroenterol* 2004; **41**: 180-184
25 **Ishak K**, Baptista A, Bianchi L, Callea F, De Groote J, Gudat F, Denk H, Desmet V, Korb G, MacSween RN. Histological grading and staging of chronic hepatitis. *J Hepatol* 1995; **22**: 696-699
26 **De Maria N**, Idilman R, Colantoni A, Van Thiel DH. Increased effective immunogenicity to high-dose and short-interval hepatitis B virus vaccination in individuals with chronic hepatitis without cirrhosis. *J Viral Hepat* 2001; **8**: 372-376
27 **De Maria N**, Idilman R, Colantoni A, Harig JM, Van Thiel DH. Antibody response to hepatitis B virus vaccination in individuals with hepatitis C virus infection. *Hepatology* 2000; **32**: 444-445
28 **Kamel M**, el Manialawi M, Miller FD. Recombinant hepatitis B vaccine immunogenicity in presence of hepatitis C virus seropositivity. *Lancet* 1994; **343**: 552
29 **Leroy V**, Bourliere M, Durand M, Abergel A, Tran A, Baud M, Botta-Fridlund D, Gerolami A, Ouzan D, Halfon P, Zarski JP. The antibody response to hepatitis B virus vaccination is negatively influenced by the hepatitis C virus viral load in patients with chronic hepatitis C: a case-control study. *Eur J Gastroenterol Hepatol* 2002; **14**: 485-489
30 **Wiedmann M**, Liebert UG, Oesen U, Porst H, Wiese M, Schroeder S, Halm U, Mössner J, Berr F. Decreased immunogenicity of recombinant hepatitis B vaccine in chronic hepatitis C. *Hepatology* 2000; **31**: 230-234
31 **Domínguez M**, Bárcena R, García M, López-Sanroman A, Nuño J. Vaccination against hepatitis B virus in cirrhotic patients on liver transplant waiting list. *Liver Transpl* 2000; **6**: 440-442
32 **Hollinger FB**. Factors influencing the immune response to hepatitis B vaccine, booster dose guidelines, and vaccine protocol recommendations. *Am J Med* 1989; **87**: 36S-40S
33 **Lemon SM**, Thomas DL. Vaccines to prevent viral hepatitis. *N Engl J Med* 1997; **336**: 196-204

S- Editor Wang GP **L- Editor** Zhu LH **E- Editor** Liu WF

PO Box 2345, Beijing 100023, China
www.wjgnet.com
wjg@wjgnet.com

World J Gastroenterol 2007 January 14; 13(2): 299-305
World Journal of Gastroenterology ISSN 1007-9327
© 2007 The WJG Press. All rights reserved.

RAPID COMMUNICATION

Ginkgo biloba extract (EGb 761) attenuates lung injury induced by intestinal ischemia/reperfusion in rats: Roles of oxidative stress and nitric oxide

Ke-Xuan Liu, Wei-Kang Wu, Wei He, Chui-Liang Liu

Ke-Xuan Liu, Department of Anesthesiology, The First Affiliated Hospital, Sun Yat-Sen University, Guangzhou 510080, Guangdong Province, China
Wei-Kang Wu, The Institute of Integrated Traditional Chinese Medicine and Western Medicine, Sun Yat-Sen University, Guangzhou 510080, Guangdong Province, China
Wei He, Department of Anesthesiology, Guangdong Provincial People's Hospital, Guangzhou 510080, Guangdong Province, China
Chui-Liang Liu, Department of Anesthesiology, Guangdong Provincial Hospital of Traditional Chinese Medicine, Guangzhou 510120, Guangdong Province, China
Supported by grants from the Administration of Traditional Chinese Medicine of Guangdong Province, China, No. 1040066; Natural Science Foundation of Guangdong Province, China, No. 05300758; National Natural Science Foundation of China, No. 30672021
Correspondence to: Dr. Ke-Xuan Liu, Department of Anesthesiology, the First Affiliated Hospital, Sun Yat-Sen University, Guangzhou 510080, Guangdong Province, China. liukexuan807@yahoo.com.cn
Telephone: +86-20-87755766-8273
Received: 2006-10-12 Accepted: 2006-11-23

Abstract

AIM: To investigate the effect of ginkgo biloba extract (EGb 761) on lung injury induced by intestinal ischemia/reperfusion (Ⅱ/R).

METHODS: The rat model of Ⅱ/R injury was produced by clamping the superior mesenteric artery for 60 min followed by reperfusion for 180 min. The rats were randomly allocated into sham, Ⅱ/R, and EGb + Ⅱ/R groups. In EGb + Ⅱ/R group, EGb 761 (100 mg/kg per day) was given *via* a gastric tube for 7 consecutive days prior to surgery. Rats in Ⅱ/R and sham groups were treated with equal volumes of the vehicle of EGb 761. Lung injury was assessed by light microscopy, wet-to-dry lung weight ratio (W/D) and pulmonary permeability index (PPI). The levels of malondialdehyde (MDA) and nitrite/nitrate (NO_2^-/NO_3^-), as well as the activities of superoxide dismutase (SOD) and myeloperoxidase (MPO) were examined. Western blot was used to determine the expression of inducible nitric oxide synthase (iNOS).

RESULTS: EGb 761 markedly improved mean arterial pressure and attenuated lung injury, manifested by the improvement of histological changes and significant decreases of pulmonary W/D and PPI ($P < 0.05$ or 0.01). Moreover, EGb 761 markedly increased SOD activity, reduced MDA levels and MPO activity, and suppressed NO generation accompanied by down-regulation of iNOS expression ($P < 0.05$ or 0.01).

CONCLUSION: The results indicate that EGb 761 has a protective effect on lung injury induced by Ⅱ/R, which may be related to its antioxidant property and suppressions of neutrophil accumulation and iNOS-induced NO generation. EGb 761 seems to be an effective therapeutic agent for critically ill patients with respiratory failure related to Ⅱ/R.

© 2007 The WJG Press. All rights reserved.

Key words: Ginkgo biloba Extract; Intestine; Reperfusion injury; Lung; Adult respiratory distress syndrome; Vascular permeability; Nitric oxide; Lipid peroxidation

Liu KX, Wu WK, He W, Liu CL. Ginkgo biloba extract (EGb 761) attenuates lung injury induced by intestinal ischemia/reperfusion in rats: Roles of oxidative stress and nitric oxide. *World J Gastroenterol* 2007; 13(2): 299-305

http://www.wjgnet.com/1007-9327/13/299.asp

INTRODUCTION

Intestinal ischemia/reperfusion (Ⅱ/R) injury is a grave condition resulting from acute mesenteric ischemia, hemorrhagic, traumatic or septic shock, or severe burns and some surgical procedures including small bowel transplantation and abdominal aortic surgery[1]. It is well-known that Ⅱ/R not only causes injury of the intestine itself, but also involves severe destruction of remote organs and even multiple organ dysfunction[2,3]. Of these remote organ injuries, lung injury has been well-characterized as an acute inflammation with sequestration of leukocytes and their enzymatic products in lung tissue, increased microvascular permeability, perivascular and interstitial edema, and pulmonary edema[4]. These pulmonary processes incited by remote Ⅱ/R injury frequently lead to the clinical picture of acute respiratory distress syndrome[5].

The mechanisms of lung injury induced by Ⅱ/R are very complex. It is well-established that lipid peroxidation is one of the major factors causing lung injury[6,7]. In

addition, evidence showed that overproduction of nitric oxide (NO) generated by inducible nitric oxide synthase (iNOS) not only aggravates oxidative damage[8,9], but leads to pulmonary microvascular dysfunction as well[10]. Thus, the therapeutical strategy by removing free radicals and reducing NO overproduction should be potential effective strategies for the protection against lung injury following Ⅱ/R.

Extracts from the leaves of ginkgo biloba have been widely used therapeutically in China and Western countries for years. Standard ginkgo biloba extract, EGb 761, contains 22%-27% flavonoids and 5%-7% terpenoids, which are the most important active substances in the extract[11]. Today, EGb 761 is widely prescribed for treatment of disorders such as Alzheimer's disease and neuronal hypoxia, both of which have etiologies associated with oxidative stress[11-13]. In the cardiovascular system, it can protect the heart against ischaemia/reperfusion damage[14] and alleviate vascular endothelial cell injury[15]. Thus, currently, EGb 761 is also widely used in treating cardiovascular diseases[16].

EGB 761 has a broad spectrum of pharmacological activities. However, most of the investigations were focused on cardio-cerebral vascular diseases. Recently, several studies showed that EGb 761 decreases malondialdehyde (MDA) and myeloperoxidase (MPO, an indicator of tissue neutrophil accumulation) levels[17] and protects against histological damage in intestinal mucosa after Ⅱ/R[18]. However, there is no report about the effect of EGb 761 on lung injury induced by Ⅱ/R.

Based on the above findings, we postulate that EGb 761 can exert a protective effect on Ⅱ/R-induced lung injury. Thus, the present study was undertaken to confirm the above hypothesis and elucidate the mechanisms related to pulmonary lipid peroxidation, neutrophil sequestration and nitric oxide (NO) production regulated by induced nitric oxide synthase (iNOS) expression.

MATERIALS AND METHODS

Animal preparation

The current study was approved by the Animal Care Committee of Sun Yat-sen University and performed in accordance with the guidelines for the use of experimental animals by the Ministry of Health. Twenty-four adult pathogen-free male Wistar rats weighing between 230-302 g were housed in individual cages in a cohorted temperature-controlled room with alternating 12 h light/dark cycles, and acclimated for a week before the study. Food was removed 8 h prior to the study, and all rats had free access to water.

Establishment of intestinal ischemia/reperfusion rat models

All rats were anesthetized with pentobarbital (30 mg/kg body weight, intraperitoneally). A polyethylene catheter (PE-10) was inserted into the left carotid artery. The catheter was connected to MacLab digital data acquisition system (PowerLab/4SP ADI Instruments, Ugo Basile Comerio, VA, Italy) *via* a pressure transducer (TSD104A Biopac Systems, 2 Biological Instruments, Besozzo, VA, Italy) for monitoring mean arterial pressure (MAP). Periodically, the cannula was flushed with normal saline (100 μL) to maintain recording fidelity. The rat model was established according to our previous method[19]. The small intestine was exteriorized by midline laparotomy and the superior mesenteric artery (SMA) was occluded by microvascular clip. After 60 min of ischemia, the SMA was reperfused for 180 min. Ischemia was determined by the existence of pulseless or pale color of the small intestine. The return of pulse and restoration of pink color were assumed to be due to the reperfusion of the intestine.

Experimental protocol

The rats were randomly allocated into one of 3 equal groups (n = 8): Sham, Ⅱ/R and EGb + Ⅱ/R. The surgical sham group underwent full surgical preparation including the isolation of SMA without the occlusion. In EGb + Ⅱ/R group, EGb 761 (100 mg/kg per day) was given *via* gastric tube for 7 consecutive days prior to surgery. EGb 761 was dissolved in normal saline at the concentration of 100 mg/mL. Rats in Ⅱ/R group and sham group were treated with equal volumes of the vehicle (normal saline solution) of EGb 761. EGb 761 was supplied by Zhejiang Kangenbei Pharmaceutical Company, China (No. 21003). It contains 24% ginkgo-flavonole glycosides and 6% terpenoids.

Sample collection of blood and lung tissues

After 3-h reperfusion, blood samples were taken from carotid artery. A median sternotomy was performed, and the left main bronchus and right lower lobe bronchus were clamped. The trachea was cannulated and the right upper and middle lobes were lavaged three times with 2 mL of saline containing 0.07 mmol/L EDTA. The collected blood and bronchoalveolar lavage (BAL) fluids were centrifuged at 3000 r/min for 15 min, and the supernatant was stored at -80℃ for subsequent measurement of protein content. The right lower lung lobe was divided into two parts for histology examination and the assessment of pulmonary edema. The left upper and lower lung lobes were used for biochemical and Western blotting analyses, respectively.

Lung histology examination

Part of the right lower lung lobe was harvested and fixed in 10% formalin. After embedded in paraffin, sections of 8 mm were stained with hematoxylin and eosin for light microscopy.

Assessment of pulmonary vascular permeability and pulmonary edema

Pulmonary permeability index (PPI) served as indicators of high pulmonary vascular permeability. PPI was assessed by the ratio of protein concentration in BAL fluid to that in plasma. The protein concentrations of blood and BAL fluid were detected by Coomassie brilliant blue method according to the manufacturer's instructions (Nanjing Jiancheng Corp., China). The severity of pulmonary edema was estimated by wet-to-dry lung weight ratio (W/D). After the wet weight of the lungs was measured, the lungs

were completely dried in a vacuum oven (DP22; Yamato Scientific, Tokyo, Japan) at 95℃ for 48 h to remove any gravimetrically detectable water.

Detection of myeloperoxidase activity in lung tissue

Myeloperoxidase (MPO) activity was detected according to the method described by Barry *et al*[20]. After weighing, the lung assay sample was homogenised in 5 mL of 0.5% hexadecyltrimethyl ammonium bromide (Sigma, U.K.) in 50 mmol potassium phosphate buffer (pH 6). The homogenate was freeze-thawed twice, and then centrifuged at 13000 *g* for 5 min. The resulting supernatant was assayed spectrophotometrically for MPO activity by incubating 0.1 mL of the supernatant with 2.9 mL of solution B. Solution B was prepared by dissolving 2.9 mL of O-dionisidine hydrochloride (Sigma, U.K.) in 90 mL of distilled water and addition of 10 mL of 50 mmol potassium phosphate buffer (pH 6) and hydrogen peroxide (final concentration 0.0005%). The change in absorbance with time at 460 nm was then recorded continuously (Philips PU/VIS specvasculature trophotometer). One unit of MPO was defined as that degrading 1 μmol peroxide per minute at 25℃. Results were expressed as units per gram of lung tissue.

Detection of oxidative stress in lung tissue

Lung tissues were homogenized on ice in normal saline. The homogenates were centrifuged at 4000 r/min at 4℃ for 10 min. MDA levels in the supernatants were determined by measurement of thiobarbituric acid-reactive substance levels using MDA assay kit (Nanjing Jiancheng Corp., China) according to the manufacturer's instructions. The results were calculated as nmol per 100 mg of protein (nmol/100 mg). SOD activity in the supernatants was evaluated by inhibition of nitroblue tetrazolium (NBT) reduction by O_2^- generated by the xanthine/xanthine oxidase system in accordance with the manufacturer's instructions (Nanjing Jiancheng Corp., China). The results were expressed as U/100 mg protein.

Detection of nitrite/nitrate in lung tissue

Lung tissues (100 mg) were weighed and made into 10% homogenates with 0.9 mL normal saline. After centrifugation for 10 min at 10000 r/min, the supernatant was placed in boiling water for 3 min and then centrifuged for 5 min at 10000 g. The supernatant (0.1 mL) was taken for the detection of nitrite/nitrate (NO_2^-/NO_3^-) production, an indicator of NO synthesis, with an NO assay kit (Nanjing Jiancheng Corp., China) following the manufacturer's instructions. Results were calculated as micromoles per 100 grams of protein (μmol/100 mg protein).

Western blotting analysis for inducible nitric oxide synthase in lung tissue

The left lower lung lobe was homogenized with PBS (pH 7.2) and centrifuged at 4℃, 18 000 r/min for 10 min. After precipitation, the unsolubilized fraction was discarded. The protein concentration in the supernatant was determined by Coomassie blue dyebinding assay (Nanjing Jiancheng Corp. China). Aliquots (30 mg) of proteins from each sample were electrophoresed on a 120 g/L SDS-polyacrylamide gel for 4 h at 100 V. The protein samples were transferred onto a nitrocellulose membrane (Amersham, USA). The membrane was then probed with polyclonal rabbit anti-rat inducible nitric oxide synthase (iNOS) antibody (1:50 dilution, Santa Cruz Co., USA) for 2 h at 37℃. After 3 washes with TPBS, blots were visualized with the use of an amplified HRP kit (Wuhan Boshide Corp, China). The presence of iNOS was indicated by the presence of brown color.

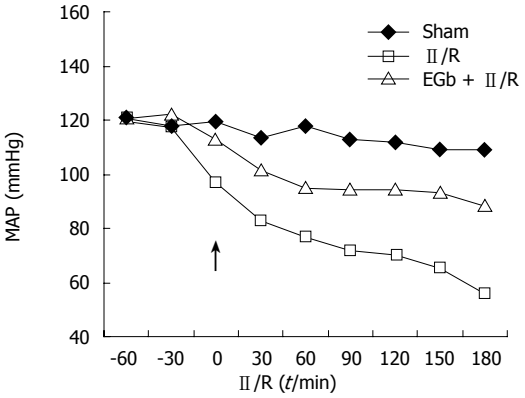

Figure 1 Effects of EGb 761 (arrow indicates the starting point of reperfusion) on mean arterial pressure (MAP) after Ⅱ/R in anaesthetized rats. A rapid drop in MAP was recorded immediately after the beginning of reperfusion of the ischemic bowel. Data are the means of 8 rats (SD not shown). EGb 761 markedly increased MAP. There were significant differences in MAP at all time points after reperfusion between Ⅱ/R and EGb + Ⅱ/R groups ($P < 0.01$).

Statistical analysis

Statistical analysis was performed using SPSS (version 10.1; SPSS for Windows, Chicago, IL) software. Data were expressed as mean ± SD. One-way analysis of variance was used for multiple comparisons and least significant difference test (LSD-t) was used for intra-group comparison. $P < 0.05$ was considered statistically significant.

RESULTS

Changes in MAP

There was no death of any rats during the experiment. There were no significant differences in the weight of the rats and the temperature in the laboratory among the groups. Figure 1 illustrates the time course of MAP in the three experimental groups. A rapid drop in MAP was recorded immediately after the release of the arterial occlusion and the beginning of reperfusion of the ischemic bowel. EGb 761 significantly improved MAP. There was a significant difference in MAP at all time points after reperfusion between Ⅱ/R and EGb + Ⅱ/R groups ($P < 0.01$).

Pathological changes of lung tissue

The histological structure of alveolar and mesenchymal cells was normal in the lungs of sham group (Figure 2A), while the lung tissues from Ⅱ/R group were significantly damaged with pulmonary edema, hemorrhage and

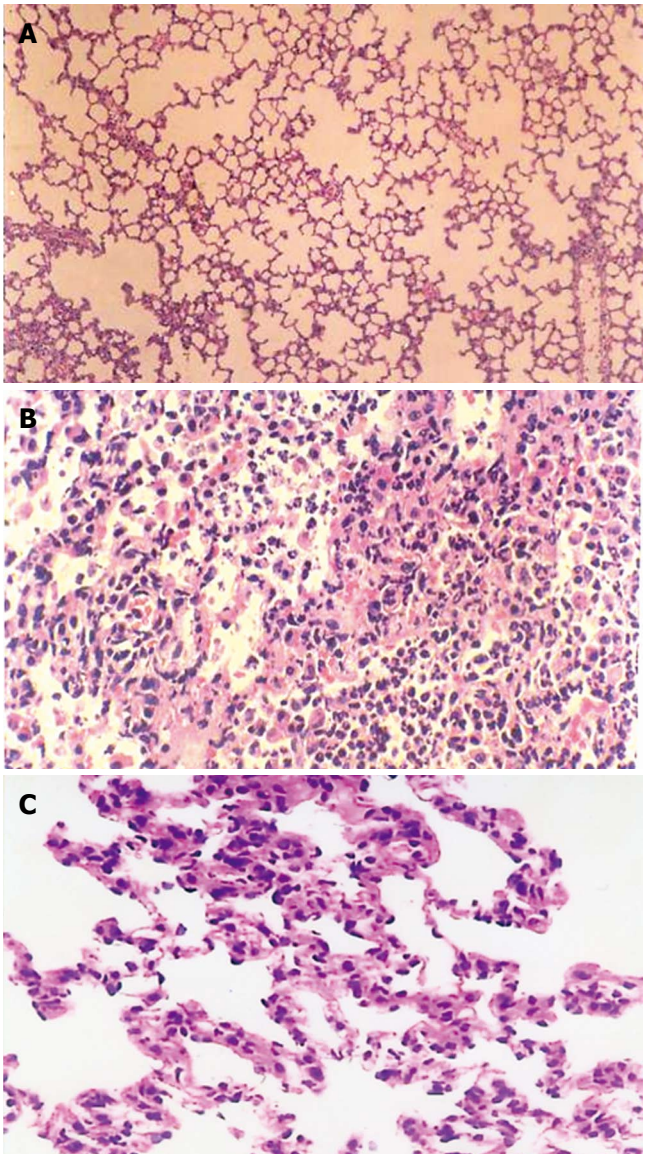

Figure 2 Light microscopic observation of the lung tissues after Ⅱ/R with pretreatment of EGb 761 in rats. **A**: The normal lung tissue structure was found in sham group (× 100); **B:** Lung edema, hemorrhage and inflammatory cell sequestration were found in Ⅱ/R group (× 200); **C**: Decreased morphological changes induced by Ⅱ/R were found in EGb + Ⅱ/R group (× 200).

inflammatory cell infiltration (Figure 2B). Pretreatment with EGb 761 could attenuate significantly the lung injury as shown by light microscopy (Figure 2C).

Changes in W/D and PPI in lung tissues

Compared with the sham group, the lung W/D and PPI in Ⅱ/R group were increased significantly ($P < 0.05$, $P < 0.01$). Compared with the Ⅱ/R group, the lung W/D and PPI in EGb + Ⅱ/R group were significantly decreased ($P < 0.05$ or 0.01) (Table 1).

Changes in MPO activity in lung tissues

MPO activity in Ⅱ/R group was significantly higher than that in the sham group ($P < 0.01$). Compared with Ⅱ/R group, MPO activity in EGb + Ⅱ/R group was markedly reduced ($P < 0.01$), but still higher than that in the sham group ($P < 0.05$) (Table 2).

Table 1 Changes in W/D and PPI in lung tissues (mean ± SD)

	n	Sham	Ⅱ/R	EGb + Ⅱ/R
PPI ($\times 10^{-3}$)	8	1.08 ± 0.42	4.02 ± 0.82[b]	2.23 ± 0.45[a,c]
W/D (%)	8	13.75 ± 5.18	29.62 ± 3.39[a]	16.34 ± 6.45[d]

[a]$P < 0.05$, [b]$P < 0.01$ *vs* sham group; [c]$P < 0.05$, [d]$P < 0.01$ *vs* Ⅱ/R group. W/D: Wet-to-dry lung weight ratio, PPI: pulmonary permeability index.

Table 2 Changes in the activities of SOD and MPO, the levels of MDA and NO_2^-/NO_3^- in lung tissues (mean ± SD)

	n	Sham	Ⅱ/R	EGb + Ⅱ/R
MDA (nmol/100 mg)	8	41.34 ± 6.45	68.52 ± 8.69[b]	44.56 ± 6.13[d]
SOD activity (U/100 mg)	8	101.8 ± 10.32	61.09 ± 6.52[b]	84.36 ± 8.25[a,c]
NO_2^-/NO_3^- (μmol/100 mg)	8	40.36 ± 9.68	78.54 ± 12.36[b]	44.13 ± 8.56[d]
MPO activity (U/g)	8	3.26 ± 0.78	6.93 ± 0.79[b]	4.14 ± 0.76[a,d]

[a]$P < 0.05$, [b]$P < 0.01$ *vs* sham group; [c]$P < 0.05$, [d]$P < 0.01$ *vs* Ⅱ/R group. MPO: Myeloperoxidase; NO_2^-/NO_3^-: nitrite/nitrate; MDA: malondialdehyde; SOD: superoxide dismutase.

Changes in lung MDA levels and SOD activity in lung tissues

MDA levels in Ⅱ/R group were significantly higher than that in the sham group ($P < 0.01$). Compared with Ⅱ/R group, MDA levels in EGb+ Ⅱ/R group were markedly decreased ($P < 0.01$). SOD activity in Ⅱ/R group was markedly lower than that of the sham group ($P < 0.01$). It was increased significantly in EGb + Ⅱ/R group ($P < 0.01$), but still lower than that of the sham group ($P < 0.05$) (Table 2).

Changes in lung NO_2^-/NO_3^- levels in lung tissues

Compared with the sham group, lung NO_2^-/NO_3^- levels in Ⅱ/R group were increased significantly ($P < 0.01$). Compared with the Ⅱ/R group, NO_2^-/NO_3^- levels in EGb + Ⅱ/R group were decreased significantly ($P < 0.01$) (Table 2).

Changes in iNOS expression in lung tissues

Western blotting showed that very weak positive signals were found in the lung tissues of the sham group. Significant increases of iNOS protein expression were seen in the Ⅱ/R group. There were still notable positive signals in EGb + Ⅱ/R group, but it was weaker for the Ⅱ/R group (Figure 3).

DISCUSSION

Currently, EGb 761 is commonly used in treating cardiovascular diseases and cerebral vascular diseases in many countries. As far as we know, the present study is the first to investigate its effects on Ⅱ/R-induced lung injury. The results showed that EGb 761 can markedly improve MAP and attenuate lung injury, manifested by the improvement of the histological damage and significant decreases of pulmonary W/D and PPI (variables related to lung injury). These findings suggest that the administration

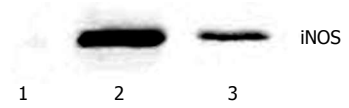

Figure 3 Western blotting analysis of iNOS in rat lung. 1. Sham group; 2. Ⅱ/R group; 3. EGb + Ⅱ/R group. The intensity of the bands was greater in Ⅱ/R group compared with EGb + Ⅱ/R group. A prominent band of iNOS protein was demonstrated at approximately 70 Kd.

of EGb 761 may be a potential effective therapeutical approach for the prevention from Ⅱ/R-induced lung injury.

The mechanisms of lung injury after Ⅱ/R are complex and poorly understood. It is thought that the damage of intestinal mucosal barrier following Ⅱ/R causes the dislocation of bacteria or endogenous endotoxins, leading to systemic inflammatory reactions[20-22]. The neutrophil and their enzymatic products are sequestrated in lung tissues, which causes increased microvascular permeability, perivascular and interstitial edema, and pulmonary edema[4,22,23].

MPO is a haem-containing enzyme located within the azurophil granules of neutrophils, and its activity is known as an indicator of tissue neutrophil accumulation[24]. The present study showed that EGb 761 markedly reduced MPO activity, suggesting that its protective effect on Ⅱ/R-induced lung injury might be related to the suppression of neutrophil accumulation. Our findings are well supported by previous studies, in which EGb 761 suppressed neutrophil sequestration in hepatic and renal tissues evidenced by decreased MPO activity[25,26]. Previous studies also demonstrated that EGb 761 increases peripheral and cerebral blood flow and improves microcirculation, and reduces capillary permeability[27,28], indicating the effect of EGb 761 on neutrophil accumulation. However, the related mechanisms need further investigation.

It is well documented that lipid peroxidation due to Ⅱ/R is one of the main causes for lung injury[6,7]. MDA is the direct product of lipid peroxidation. Therefore, the extent of lipid peroxidation can be assessed by measuring MDA levels in tissues[29]. SOD is the major enzyme for scavenging oxygen free radicals, and its activity can reflect its functional status[30]. Previous studies have shown that EGb 761 can interact as a free radical scavenger and an inhibitor of lipid peroxidation with all, or nearly all, reactive oxygen species[27]. In the present study, EGb 761 was demonstrated to inhibit MDA production and increase SOD activity, suggesting that the inhibition of lipid peroxidation may be one of the mechanisms attributable to the protective effects of EGb 761 on Ⅱ/R-induced lung injury.

Several recent observations implicate that NO may be an important participant in the pulmonary response to Ⅱ/R[31]. It has been suggested that NO, produced from endothelial constitutive nitric oxide synthase (ecNOS), may be an important protective molecule at the onset of Ⅱ/R. In this regard, inhibitors of endogenous NO production greatly exacerbate the increase in epithelial permeability and cardiovascular dysfunction in the reperfused post-ischemia intestine[31,32]. Excessive NO production has been attributed to the second NOS (inducible NOS, iNOS) that is not present under normal conditions but can be induced in response to systemic inflammatory states, including Ⅱ/R. The induction of iNOS has been implicated in the pathogenesis of Ⅱ/R and it was reported that the inhibitions of iNOS activity and NO production could attenuate Ⅱ/R injury[10,33]. In the present study, we further studied the contribution of iNOS to Ⅱ/R-induced lung injury. The results showed that 60 min of intestinal ischemia followed by 180 min of reperfusion significantly upregulated the lung iNOS expression, accompanied by marked elevation of pulmonary nitrate/nitrite (stable metabolites of NO) levels. This is consistent with the findings of Virlos *et al*[10], who demonstrated that pulmonary iNOS activity in rats subjected to Ⅱ/R was significantly increased and of Zhou *et al*[8], who showed that systemic inflammatory response and lung injury occur following Ⅱ/R with an overproduction of NO accompanied by the increases of iNOS expression and the formation of peroxynitrite in the lungs. The mechanisms of the cytotoxic actions of excessive NO production have not been fully understood. It has been suggested that the superoxide ions react with NO to produce peroxynitrite, which then causes accentuated lipid peroxidation, proteic and DNA modifications resulting in cellular damages[34]. Taken together, the iNOS-NO-peroxynitrite dependent pathway may be one of the mechanisms of Ⅱ/R-induced lung injury.

The effect of EGb 761 on NO generation in lung tissue following Ⅱ/R was studied for the first time in the present study. The results showed that EGb 761 significantly reduced the generation of NO accompanied by the down-regulation of iNOS expression. Varga *et al* showed that EGb 761 directly acts as an NO scavenger and concomitantly inhibits the expression of iNOS mRNA in myocardial tissues, thus improving the recovery of postischemic cardiac function after myocardial ischemia/reperfusion[35]. In addition, EGb 761 inhibits NO production in lipopolysaccharide/gamma interferon (LPS/IFN-γ)-activated macrophages by concomitantly scavenging NO and inhibiting iNOS mRNA and enzyme activity[36,37]. Although the experimental models employed in previous studies are different from the present study, these findings can, at least in part, support our current conclusion that the protective effect of EGb 761 on lung injury may be attributable to its suppression on the iNOS-NO dependent pathway.

There is little information on the mechanisms of the effect of EGb 761 on the iNOS-NO dependent pathway. A most recent study showed the preventive effect of EGb on the lipopolysaccharide-induced expressions of iNOS *via* the suppression of nuclear factor-kappaB (NF-κB) in RAW 264.7 cells. Thus, the suppression of NF-κB might be the potential mechanism underlying the findings that EGb 761 reduces NO production and concomitantly inhibits iNOS expression in lung tissues following Ⅱ/R[38].

There are some limitations in the present study. First, EGb 761 is a specific and complex product prepared from ginkgo leaves. EGb 761 used in this study contained 24% ginkgo-flavonole glycosides and 6% terpenoids. Which

components produce the protective effect or work more in protecting against Ⅱ/R-induced lung injury in the present study remains to be elucidated. Second, we did not employ selective inhibitor of iNOS to strengthen the present conclusion, because we focused on investigating the protective effect of EGb 761 on lung injury and thus only preliminarily studied the related mechanisms.

In conclusion, the present study indicates that EGb 761 has a protective effect on lung injury induced by Ⅱ/R, which may be related to its antioxidative property and the suppressions of neutrophil accumulation and iNOS-induced NO generation. EGb 761 appears to be an effective therapeutic agent for some critically ill patients with respiratory failure related to Ⅱ/R, although its mechanisms remain to be elucidated.

ACKNOWLEDGMENTS

We thank Dr. You-Kai Zhu and Dr. Ming-Qi Zhao for their help with experimental techniques.

COMMENTS

Background

EGb 761 is widely used in treating cardio-cerebral vascular diseases mainly due to its action of anti-oxidative damage; however, there is no report about its effect on lung injury induced by intestinal ischemia/reperfusion. The present study was undertaken to confirm the above hypothesis and elucidate the mechanisms related to pulmonary lipid peroxidation, neutrophil sequestration and nitric oxide (NO) production regulated by induced nitric oxide synthase (iNOS) expression.

Research frontiers

EGb 761 has been reported to be effective for the disorders such as Alzheimer's disease and neuronal hypoxia and to protect the heart against ischaemia/reperfusion damage and to alleviate vascular endothelial cell injury, which all have etiologies associated with oxidative stress.

Innovations and breakthroughs

Previous studies showed the protective effect of EGb 761 on cardio-cerebral ischemia/reperfusion injury and intestinal mucosa injury following intestinal ischemia/reperfusion (II/R). The present study indicates that EGb 761 has a protective effect on lung injury induced by II/R and the mechanism may be related to its antioxidative property and the suppressions of neutrophil accumulation and iNOS-induced NO generation.

Applications

Remote lung injury induced by intestinal ischemia reperfusion (II/R) due to acute mesenteric ischemia, hemorrhagic, traumatic or septic shock, or severe burns and some surgical procedures including small bowel transplantation and abdominal aortic surgery often leads to the clinical picture of acute respiratory distress syndrome. EGb 761 has been demonstrated to have the protective effect on lung injury and thus appears to be an effective therapeutic agent for some critically ill patients with respiratory failure related to II/R.

Terminology

Excessive production of nitric oxide (NO) is attributed to the upregulation of inducible nitric oxide synthase (iNOS) expression that is not present under normal conditions, but can be induced in response to systemic inflammatory states, including II/R. NO can react with superoxide ions to produce peroxynitrite, which then causes accentuated lipid peroxidation, proteic and DNA modifications, resulting in cellular damages. This is described as an iNOS-NO-peroxynitrite dependent pathway.

Peer review

This manuscript is very interesting. The title accurately reflects the major contents of the article. The results provide sufficient experimental evidences from which conclusions are drawn. The conclusions are scientifically reliable and valuable.

REFERENCES

1 **Homer-Vanniasinkam S**, Crinnion JN, Gough MJ. Post-ischaemic organ dysfunction: a review. *Eur J Vasc Endovasc Surg* 1997; **14**: 195-203
2 **Deitch EA**. Role of the gut lymphatic system in multiple organ failure. *Curr Opin Crit Care* 2001; **7**: 92-98
3 **Mitsuoka H**, Kistler EB, Schmid-Schönbein GW. Protease inhibition in the intestinal lumen: attenuation of systemic inflammation and early indicators of multiple organ failure in shock. *Shock* 2002; **17**: 205-209
4 **Turnage RH**, Guice KS, Oldham KT. Pulmonary microvascular injury following intestinal reperfusion. *New Horiz* 1994; **2**: 463-475
5 **Ware LB**, Matthay MA. The acute respiratory distress syndrome. *N Engl J Med* 2000; **342**: 1334-1349
6 **Rossman JE**, Caty MG, Zheng S, Karamanoukian HL, Thusu K, Azizkhan RG, Dandona P. Mucosal protection from intestinal ischemia-reperfusion reduces oxidant injury to the lung. *J Surg Res* 1997; **73**: 41-46
7 **Giakoustidis AE**, Giakoustidis DE, Iliadis S, Papageorgiou G, Koliakou K, Kontos N, Taitzoglou I, Botsoglou E, Papanikolaou V, Atmatzidis K, Takoudas D, Antoniadis A. Attenuation of intestinal ischemia/reperfusion induced liver and lung injury by intraperitoneal administration of (-)-epigallocatechin-3-gallate. *Free Radic Res* 2006; **40**: 103-110
8 **Zhou JL**, Jin GH, Yi YL, Zhang JL, Huang XL. Role of nitric oxide and peroxynitrite anion in lung injury induced by intestinal ischemia-reperfusion in rats. *World J Gastroenterol* 2003; **9**: 1318-1322
9 **Pararajasingam R**, Weight SC, Bell PR, Nicholson ML, Sayers RD. Pulmonary nitric oxide metabolism following infrarenal aortic cross-clamp-induced ischaemia-reperfusion injury. *Eur J Vasc Endovasc Surg* 2000; **19**: 47-51
10 **Turnage RH**, Wright JK, Iglesias J, LaNoue JL, Nguyen H, Kim L, Myers S. Intestinal reperfusion-induced pulmonary edema is related to increased pulmonary inducible nitric oxide synthase activity. *Surgery* 1998; **124**: 457-462; discussion 462-463
11 **Kleijnen J**, Knipschild P. Ginkgo biloba. *Lancet* 1992; **340**: 1136-1139
12 **Luo Y**. Alzheimer's disease, the nematode Caenorhabditis elegans, and ginkgo biloba leaf extract. *Life Sci* 2006; **78**: 2066-2072
13 **Chandrasekaran K**, Mehrabian Z, Spinnewyn B, Drieu K, Fiskum G. Neuroprotective effects of bilobalide, a component of the Ginkgo biloba extract (EGb 761), in gerbil global brain ischemia. *Brain Res* 2001; **922**: 282-292
14 **Yuan LP**, Chen ZW, Li F, Dong LY, Chen FH. Protective effect of total flavones of rhododendra on ischemic myocardial injury in rabbits. *Am J Chin Med* 2006; **34**: 483-492
15 **Cheung F**, Siow YL, Chen WZ, O K. Inhibitory effect of Ginkgo biloba extract on the expression of inducible nitric oxide synthase in endothelial cells. *Biochem Pharmacol* 1999; **58**: 1665-1673
16 **Diamond BJ**, Shiflett SC, Feiwel N, Matheis RJ, Noskin O, Richards JA, Schoenberger NE. Ginkgo biloba extract: mechanisms and clinical indications. *Arch Phys Med Rehabil* 2000; **81**: 668-678
17 **Pehlivan M**, Dalbeler Y, Hazinedaroglu S, Arikan Y, Erkek AB, Günal O, Türkçapar N, Türkçapar AG. An assessment of the effect of Ginkgo Biloba EGb 761 on ischemia reperfusion injury of intestine. *Hepatogastroenterology* 2002; **49**: 201-204
18 **Onen A**, Deveci E, Inalöz SS, Isik B, Kilinc M. Histopathological assessment of the prophylactic effect of gingko-biloba extract on intestinal ischemia-reperfusion injury. *Acta Gastroenterol Belg* 1999; **62**: 386-389
19 **Liu KX**, Wu WK, He W, Sun HL. Study on sini decoction in treatment of intestinal ischemia-reperfusion injury in rats: mechanism relating to oxygen radical and bcl-2 protein.

Zhongguo Zhongyao Zazhi 2006; **31**: 329-332, 348
20 **Turnage RH**, Guice KS, Oldham KT. Endotoxemia and remote organ injury following intestinal reperfusion. *J Surg Res* 1994; **56**: 571-578
21 **Yao Y**, Yu Y, Chen J. The effect of intestinal ischemia/reperfusion on increased sensitivity to endotoxin and its potential mechanism. *Zhonghua Zhengxing Shaoshang Waike Zazhi* 1999; **15**: 301-304
22 **Olanders K**, Sun Z, Börjesson A, Dib M, Andersson E, Lasson A, Ohlsson T, Andersson R. The effect of intestinal ischemia and reperfusion injury on ICAM-1 expression, endothelial barrier function, neutrophil tissue influx, and protease inhibitor levels in rats. *Shock* 2002; **18**: 86-92
23 **Ishii H**, Ishibashi M, Takayama M, Nishida T, Yoshida M. The role of cytokine-induced neutrophil chemoattractant-1 in neutrophil mediated remote lung injury after intestinal ischaemia/reperfusion in rats. *Respirology* 2000; **5**: 325-331
24 **Winterbourn CC**, Kettle AJ. Biomarkers of myeloperoxidase-derived hypochlorous acid. *Free Radic Biol Med* 2000; **29**: 403-409
25 **Sener G**, Kabasakal L, Yüksel M, Gedik N, Alican Y. Hepatic fibrosis in biliary-obstructed rats is prevented by Ginkgo biloba treatment. *World J Gastroenterol* 2005; **11**: 5444-5449
26 **Gulec M**, Iraz M, Yilmaz HR, Ozyurt H, Temel I. The effects of ginkgo biloba extract on tissue adenosine deaminase, xanthine oxidase, myeloperoxidase, malondialdehyde, and nitric oxide in cisplatin-induced nephrotoxicity. *Toxicol Ind Health* 2006; **22**: 125-130
27 **Clostre F**. Ginkgo biloba extract (EGb 761). State of knowledge in the dawn of the year 2000. *Ann Pharm Fr* 1999; **57** Suppl 1: S18-S88
28 **Lagrue G**, Behar A, Kazandjian M, Rahbar K. Idiopathic cyclic edema. The role of capillary hyperpermeability and its correction by Ginkgo biloba extract. *Presse Med* 1986; **15**: 1550-1553
29 **Requena JR**, Fu MX, Ahmed MU, Jenkins AJ, Lyons TJ, Thorpe SR. Lipoxidation products as biomarkers of oxidative damage to proteins during lipid peroxidation reactions. *Nephrol Dial Transplant* 1996; **11** Suppl 5: 48-53
30 **Cuzzocrea S**, Mazzon E, Dugo L, Caputi AP, Aston K, Riley DP, Salvemini D. Protective effects of a new stable, highly active SOD mimetic, M40401 in splanchnic artery occlusion and reperfusion. *Br J Pharmacol* 2001; **132**: 19-29
31 **Khanna A**, Rossman JE, Fung HL, Caty MG. Attenuated nitric oxide synthase activity and protein expression accompany intestinal ischemia/reperfusion injury in rats. *Biochem Biophys Res Commun* 2000; **269**: 160-164
32 **Virlos IT**, Inglott FS, Williamson RC, Mathie RT. Differential expression of pulmonary nitric oxide synthase isoforms after intestinal ischemia-reperfusion. *Hepatogastroenterology* 2003; **50**: 31-36
33 **Suzuki Y**, Deitch EA, Mishima S, Lu Q, Xu D. Inducible nitric oxide synthase gene knockout mice have increased resistance to gut injury and bacterial translocation after an intestinal ischemia-reperfusion injury. *Crit Care Med* 2000; **28**: 3692-3696
34 **Pryor WA**, Squadrito GL. The chemistry of peroxynitrite: a product from the reaction of nitric oxide with superoxide. *Am J Physiol* 1995; **268**: L699-L722
35 **Varga E**, Bodi A, Ferdinandy P, Droy-Lefaix MT, Blasig IE, Tosaki A. The protective effect of EGb 761 in isolated ischemic/reperfused rat hearts: a link between cardiac function and nitric oxide production. *J Cardiovasc Pharmacol* 1999; **34**: 711-717
36 **Kobuchi H**, Packer L. Bio-normalizer modulates interferon-gamma-induced nitric oxide production in the mouse macrophage cell line RAW 264.7. *Biochem Mol Biol Int* 1997; **43**: 141-152
37 **Marcocci L**, Maguire JJ, Droy-Lefaix MT, Packer L. The nitric oxide-scavenging properties of Ginkgo biloba extract EGb 761. *Biochem Biophys Res Commun* 1994; **201**: 748-755
38 **Park YM**, Won JH, Yun KJ, Ryu JH, Han YN, Choi SK, Lee KT. Preventive effect of Ginkgo biloba extract (GBB) on the lipopolysaccharide-induced expressions of inducible nitric oxide synthase and cyclooxygenase-2 via suppression of nuclear factor-kappaB in RAW 264.7 cells. *Biol Pharm Bull* 2006; **29**: 985-990

S- Editor Liu Y **L- Editor** Zhu LH **E- Editor** Liu WF

PO Box 2345, Beijing 100023, China
www.wjgnet.com
wjg@wjgnet.com

World J Gastroenterol 2007 January 14; 13(2): 306-309
World Journal of Gastroenterology ISSN 1007-9327
© 2007 The WJG Press. All rights reserved.

CASE REPORT

Are heat stroke and physical exhaustion underestimated causes of acute hepatic failure?

Kilian Weigand, Carina Riediger, Wolfgang Stremmel, Christa Flechtenmacher, Jens Encke

Kilian Weigand, Carina Riediger, Wolfgang Stremmel, Jens Encke, Department of Gastroenterology and Hepatology, Medicine Ⅳ, University of Heidelberg, 69120 Heidelberg, Germany
Christa Flechtenmacher, Department of Pathology, University of Heidelberg, 69120 Heidelberg, Germany
Correspondence to: Kilian Weigand, Universitaetsklinikum Heidelberg, Medizin Ⅳ, Abteilung fuer Gastroenterologie, Im Neuenheimer Feld 410, Heidelberg D-69120, Germany. kilian.weigand@med.uni-heidelberg.de
Telephone: +49-6221-5638747 Fax: +49-6221-565361
Received: 2006-04-28 Accepted: 2006-10-27

Abstract

While cardiopulmonary symptoms are common in patients undergoing classical or, due to physical exercise, exertional heat stroke, the failure of other organs is a rarely described phenomenon. Here we present two cases of acute hepatic failure, one due to classic heat shock, while the other occurred while the patient was doing a marathon-type running. Both cases presented with very high transaminases and significantly elevated international normalized ratio (INR). No other causes for liver failure could be identified but physical exhaustion and hyperthermia.

© 2007 The WJG Press. All rights reserved.

Key words: Heat stroke; Acute hepatic failure; Heat shock; Liver failure; Hyperthermia

Weigand K, Riediger C, Stremmel W, Flechtenmacher C, Encke J. Are heat stroke and physical exhaustion underestimated causes of acute hepatic failure? *World J Gastroenterol* 2007; 13(2): 306-309

http://www.wjgnet.com/1007-9327/13/306.asp

INTRODUCTION

Heat stroke is a life-threatening condition that can be fatal if proper assessment and treatment are not initiated rapidely[1,2]. A variable degree of organ involvement is present in heat stroke[3]. At the beginning, there is heat exhaustion, characterized by nonspecific symptoms such as malaise, headache and nausea. Untreated this illness results in heat stroke, a serious disease possibly involving central nervous system dysfunction, rhabdomyolysis, arrhythmias, disseminated intravascular coagulation and hepatic failure, not uncommon followed by death[4].

The current model of heat stroke favors hyperthermia as trigger, while endotoxaemia drives the disease. However, the pathology is not fully understood[2]. In athletes undergoing intense training a variety of immune and gastrointestinal disturbances can occur. We here describe two completely different causes of heat stroke resulting in acute and severe liver failure as leading symptom.

CASE REPORTS

Case one

A 23-year old male was delivered to our intensive care unit (ICU) after he collapsed running a half-marathon. He had no former medical history and was in good physical shape. He took no medication and was negative for an obtained drug screening. By admission he felt fatigue and complained about nausea and vomiting. The laboratory results showed elevated levels of 12427 U/L creatinine kinase (CK) (normal < 145 U/L), 5821 U/L lactate dehydrogenase (LDH) (normal < 248 U/L), 8378 U/L aspartate aminotransferase (AST) (normal < 31 U/L), 9765 U/L alanine aminotransferase (ALT) (normal < 34 U/L), 40 mg/dL bilirubin (normal < 1.0 mg/dL) and 2.8 international normalized ratio (INR) (normal < 1.2) (Figure 1). The other basic laboratory parameters were within normal range. The patient was monitored and treated with intravenous fluid (5 to 6 liters per 24 h).

To exclude other causes for acute hepatic failure, virus serologies were obtained. Besides positive IgG of hepatitis A and B due to immunization, there were no serological findings for acute or chronic hepatitis A, B, C or human immunodeficiency virus (HIV). Also acute infection with cytomegaly virus (CMV), herpes simplex virus (HSV) or epstein-barr virus (EBV) was ruled out. The autoimmune antibodies (ANA, ANCA, SMA, LKM, mitochondrial antibodies) were also negative. In addition, protein electrophoresis gave no pathologic findings. Serum levels for alpha-1-antitrypsin, iron and transferrin were within normal range. Ferritin was raised to 29490 μg/L (normal 30-300 μg/L), probably due to destruction of hepatocytes. Because of lowered caeruloplasmin (serum) and copper (serum and 24-h urine) levels, a liver biopsy was performed. The histology showed intact architecture of the lobules. Portal fields showed no signs of fibrosis or inflammatory infiltration. Accentuated centrolobular

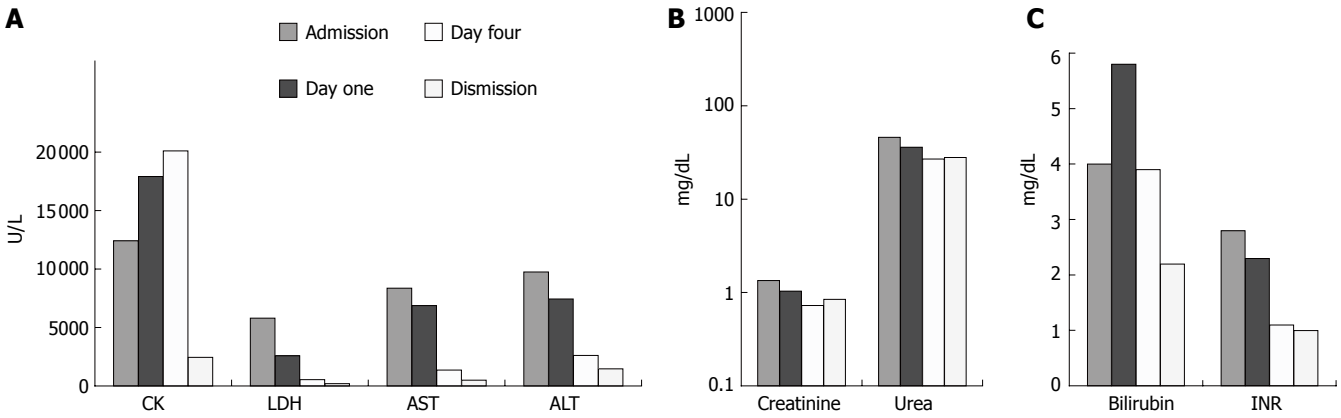

Figure 1 Basic laboratory parameters of a 23-yr-old male patient presenting with liver failure after exertional heat stroke. **A**: Creatinine kinase (CK), lactate dehydrogenase (LDH), aspartate aminotransferase (AST) and alanine amino-transferase (ALT) at admission and during progression in a linear scale; **B**: Creatinine and urea in a logarithmic scale; **C**: Bilirubin and international normalized ratio (INR) in a linear scale.

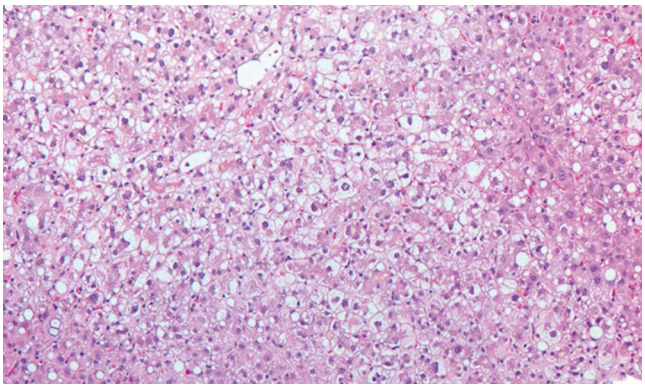

Figure 2 HE-staining of a liver biopsy derived from a 23-yr-old male presenting with liver failure after exertional heat stroke. Microscopy showed liver tissue with intact architecture of the lobules. Portal fields showed no signs of fibrosis or inflammatory infiltration. Accentuated centrolobular necrosis was accompanied with fatty degeneration of hepatocytes. Additionally, focal bile inclusions were found without Mallory bodies, iron debris and atypical cellular proliferation. Altogether, the morphological picture does not fit acute Wilson's disease, hemochromatosis or infection, but ischemic liver disease.

necrosis and fatty degeneration of hepatocytes were seen. Additionally, focal bile inclusions were found. Altogether, the morphological picture did not fit acute Wilson's disease, hemochromatosis or infection, but ischemic liver disease (Figure 2).

Abdominal ultrasound including duplex sonography, besides a slight hepatosplenomegaly, demonstrated no abnormal findings. To exclude a cardiac reason for the patient's collapse, both a 24-h electrocardiogram and an echocardiogram showed normal heart function and structure.

The patient stayed in the ICU for 5 d, while the laboratory results were declining (Figure 1) (208 U/L LDH, 676 U/L AST, 1438 U/L ALT, 2.2 mg/dL bilirubin, 1.1 INR). Initially, the CK did rise to levels higher than 30000 U/L, but on d 5 after admission it dropped to 4948 U/L. Renal function was normal at all times due to high fluid application and keeping the urine-pH above 7.5. On d 6, the patient was transferred from ICU to a regular ward in good health and mostly recompensated laboratory parameters for further monitoring. At follow-up one week later the patient was in good health and showed normal laboratory parameters.

Case two

A 46-year old male was delivered to our ICU after he had collapsed due to heat shock. His working place was below a roof window and it was a very hot day. In the after-noon, after working all day, he finally suffered from a seizure and was found cardiorespiratory stable but unconscious with his temperature of 42℃.

By admission laboratory findings demonstrated a clinical picture of acute hepatic failure with very high levels of transaminases (15929 U/L AST, 10050 U/L ALT), bilirubin (1.9 mg/dL) and malfunction in liver synthesis (1.9 INR) (Figure 3). Further laboratory parameters showed an elevated LDH (15831 U/L), CK (6452 U/L), Troponin T (1.18 μg/L, normal < 0.03 μg/L), creatinine (1.78 mg/dL, normal < 1.3 mg/dL) and urea (50 mg/dL, normal < 45 mg/dL). All other basic parameters were within normal range.

Besides a seizure in 1989 due to an intra-cerebral bleeding, the patient had no past medical history. We started to treat him with intravenous fluid (5 to 6 liters per 24 h). Because of acute renal dysfunction he was treated two times with hemodialysis.

To exclude other reasons for acute hepatic failure he received further examinations. An abdominal ultrasound including duplex sonography showed no alterations. No pathologic serum markers for alpha1-antitrypsin, caeruloplasmin, copper, iron, ferritin, AFP or autoimmune antibodies (ANA, ds-DNA, ANCA, LKM, SMA, mitochondrial antibodies) were observed. Virus serologies were positive for HSV-IgG, VZV-IgG, EBV-IgG, but negative for IgM, as a parameter for acute infection. Hepatitis A was IgG positive due to immunization. All other infectious causes tested, like CMV, influenza A and B, hanta virus, hepatitis B and C, HIV and leptospirosis, were negative. Additionally, an obtained drug screening was negative.

The patient was further monitored in our ICU and received treatment of cooling and intravenous fluid. The

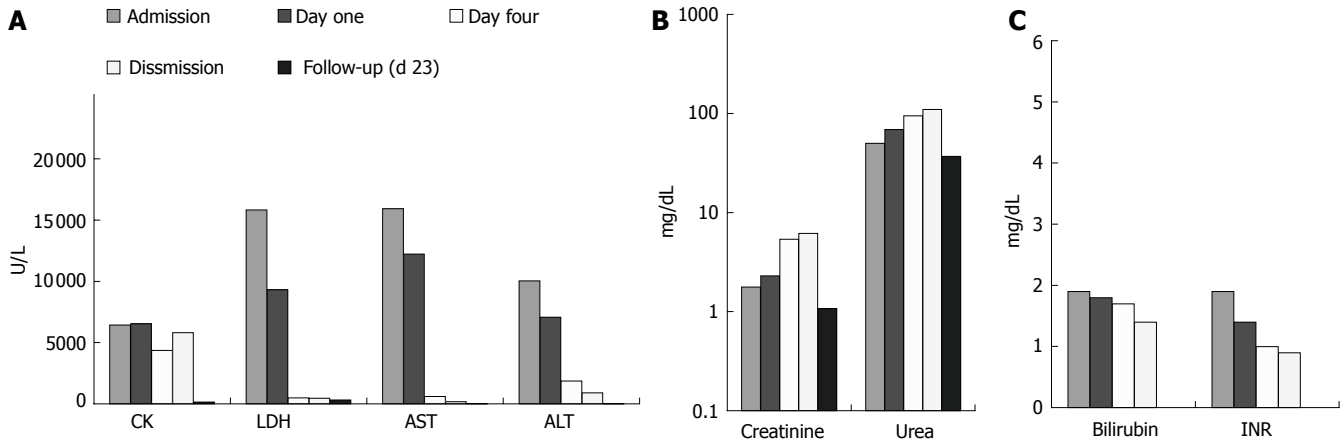

Figure 3 Basic laboratory parameters of a 46-year old male presenting with liver failure due to classic heat stroke. **A**: Creatinine kinase (CK), lactate dehydrogenase (LDH), aspartate aminotransferase (AST) and alanine amino-transferase (ALT) at admission and during progression in a linear scale; **B**: Creatinine and urea in a logarithmic scale; **C**: Bilirubin and international normalized ratio (INR) in a linear scale.

patient regained consciousness within 36 h after therapy was started and the abnormal laboratory parameters excluding creatinine and urea, returned slowly to normal within a few days. Because of the elevated myocardial enzymes at admission, an echocardiogram and an electro cardiogram (ECG) were obtained. While the ECG was normal, the echocardiogram showed a very mild hypertrophic obstructive cardiomyopathy (HOCM), unknown so far, but a good right and left ventricular function and no contraction disorders of the myocardium. Also, the patient did not suffer from chest pain or dyspnoea at all times.

Six days after admission the patient had lowered laboratory parameters (Figure 3) (512 U/L LDH, 620 U/L AST, 1889 U/L ALT, 1.7 mg/dL bilirubin, 4376 U/L CK, 0.35 μg/L TNT, 1.0 INR), but still high urea and creatinine levels. He was transferred to a nephrology ward where he continued to get hemodialysis, until the kidney function was resolved. Twenty-three days later he presented again at the outpatient clinic with almost normalized laboratory parameters (Figure 3).

DISCUSSION

Described in this paper are two cases of acute hepatic failure due to physical exhaustion/heat shock. While the first patient had no other organ disorders, the second suffered from multi-organ failure including heart, kidneys and brain, and mainly liver malfunction.

It has been rarely reported that physical exhaustion can lead to hyperthermia, coma, rhabdomyolysis and organ failure[5,6]. Classic heat stroke however, is a more common disease with the life-threatening core body temperature higher than 40.5℃. Its associated clinical manifestations are exsiccosis, fatigue, nausea, vomiting, disorientation and coma[7]. Possible complications are cardiopulmonary dysfunction, acid-base or electrolyte disorders, as well as failure of other organs. Recently, a study demonstrated that 21 of 28 patients with heat stroke developed organ dysfunctions. Acute respiratory distress syndrome is the frequently encountered complication[8], while liver malfunction has not been reported. Our two cases indicate that liver failure may be more often than expected. Liver failure due to heat stroke begins with the same common symptoms, like nausea and exhaustion. When collapse, hyperthermia and multi-organ failure occur, it may be diagnosed[9], indicating that a rise in liver enzymes is an important predictive factor[8]. In our cases, liver failure was the leading symptom, causing cerebral disorders and renal dysfunction. Liver transplantation is the only possible treatment for severe hepatic damage. Recently, the first long-term follow-up of liver transplantation for hepatic failure due to heat stroke has been reported[10].

The recommended treatment for such severe cases is fluid application and rebalancing acid-base and electrolyte disorders as well as close monitoring, except for liver transplantation. Other treatments, like application of human umbilical cord blood cells as described in rats, to lower intracerebral changes due to heat stroke, remain speculative and under experiment at present[11].

The mechanism underlying liver failure in heath shock patients is not totally understood. An earlier study showed that systemic or intrahepatic circulatory disturbance as seen in disseminated intravascular coagulation (DIC), may be the cause[12]. In one case, a portal vein thrombosis has been found[9], which could result in liver and other organ failure. However, in our cases, the duplex sonography showed no big vessel thrombosis, whereas DIC could not be excluded. Although DIC could explain the raised liver enzymes in our second case, the cardiac problems due to HOCM contributing to the liver failure could not be ruled out. Nevertheless, we think that a cardiac reason is unlikely, because the right and left ventricular function of the patients was excellent at all times.

It has been reported that the intracranial pressure rises and cerebral ischemia occurs due to lower arterial pressure during heat stroke, resulting in lower blood flow and intracranial pO_2[11]. It remains for further study if the same mechanism is responsible for liver damage. If so, this could result in a therapeutic application of vasoactive substances to increase intrahepatic blood flow in patients with severe liver damage after heat stroke.

Another review published in 2004 has discussed a possible function of immune response in organ failure

of patients suffering from hyperthermia during physical exercise[13]. Since a reduced splanchnic blood flow which can result in gastrointestinal barrier dysfunction and increased permeability can be measured, endotoxin causing immune reactions could enter internal organs and drive organ damage. This may lead to the assumption that application of immune suppressive medication could be tested.

Besides liver malfunction, renal problems were the leading cause of liver failure in our cases. This is most likely explained by exsiccosis. Nevertheless, it is also possible that the high CK is an additionally cause of renal disorder.

In conclusion, patients with hepatic failure due to physical exhaustion or heat stroke should be closely monitored and severe problems like bleeding, hepatic coma and acute renal malfunction should be recognized as early as possible.

REFERENCES

1 **Casa DJ**, Armstrong LE, Ganio MS, Yeargin SW. Exertional heat stroke in competitive athletes. *Curr Sports Med Rep* 2005; **4**: 309-317

2 **Lim CL**, Mackinnon LT. The roles of exercise-induced immune system disturbances in the pathology of heat stroke: the dual pathway model of heat stroke. *Sports Med* 2006; **36**: 39-64

3 **Sucholeiki R**. Heatstroke. *Semin Neurol* 2005; **25**: 307-314

4 **Glazer JL**. Management of heatstroke and heat exhaustion. *Am Fam Physician* 2005; **71**: 2133-2140

5 **Lepape A**, Sarron C, Grozel JM, Perdrix JP, Banssillon V. A severe form of heat stroke in a long-distance runner. *Ann Fr Anesth Reanim* 1986; **5**: 441-444

6 **Bruguera M**. Liver and sports. *Med Clin* (Barc) 2004; **122**: 111-114

7 **Yeo TP**. Heat stroke: a comprehensive review. *AACN Clin Issues* 2004; **15**: 280-293

8 **Varghese GM**, John G, Thomas K, Abraham OC, Mathai D. Predictors of multi-organ dysfunction in heatstroke. *Emerg Med J* 2005; **22**: 185-187

9 **Scobie BA**. Gastrointestinal emergencies with marathon-type running: omental infarction with pancreatitis and liver failure with portal vein thrombosis. *N Z Med J* 1998; **111**: 211-212

10 **Takahashi K**, Chin K, Ogawa K, Kasahara M, Sakaguchi T, Hasegawa S, Sumi K, Nakamura T, Tamaki A, Mishima M, Nakamura T, Tanaka K. Living donor liver transplantation with noninvasive ventilation for exertional heat stroke and severe rhabdomyolysis. *Liver Transpl* 2005; **11**: 570-572

11 **Chen SH**, Chang FM, Tsai YC, Huang KF, Lin MT. Resuscitation from experimental heatstroke by transplantation of human umbilical cord blood cells. *Crit Care Med* 2005; **33**: 1377-1383

12 **Irie H**, Mori W. Fatal hepatic necrosis after shock. *Acta Pathol Jpn* 1986; **36**: 363-374

13 **Lambert GP**. Role of gastrointestinal permeability in exertional heatstroke. *Exerc Sport Sci Rev* 2004; **32**: 185-190

S- Editor Wang GP **L- Editor** Wang XL **E- Editor** Ma WH

PO Box 2345, Beijing 100023, China
www.wjgnet.com
wjg@wjgnet.com

World J Gastroenterol 2007 January 14; 13(2): 310-312
World Journal of Gastroenterology ISSN 1007-9327
© 2007 The WJG Press. All rights reserved.

CASE REPORT

Jejuno-jejunal invagination due to intestinal melanoma

Giuseppe Resta, Gabriele Anania, Federico Messina, Damiano de Tullio, Gloria Ferrocci, Federico Zanzi, Davide Pellegrini, Rocco Stano, Giorgio Cavallesco, Gianfranco Azzena, Savino Occhionorelli

Giuseppe Resta, Gabriele Anania, Federico Messina, Damiano de Tullio, Gloria Ferrocci, Federico Zanzi, Davide Pellegrini, Rocco Stano, Giorgio Cavallesco, Gianfranco Azzena, Savino Occhionorelli, Università degli Studi di Ferrara, Dipartimento di Scienze Chirurgiche Anestesiologiche e Radiologiche, Istituto di Clinica Chirurgica, Arcispedale "S. Anna", Ferrara, Italy

Correspondence to: Dr. Federico Messina, Università degli Studi di Ferrara, Dipartimento di Scienze Chirurgiche Anestesiologiche e Radiologiche, Istituto di Clinica Chirurgica. Arcispedale "S. Anna", Corso Giovecca, Ferrara 203-44100, Italy. f.messina@email.it
Telephone: +39-532-236316 **Fax:** +39-532-209819
Received: 2006-10-22 **Accepted:** 2006-12-07

Abstract

Cutaneous melanoma is one of the most studied neoplastic lesions in biology and clinical oncology. It has been well documented that this type of neoplasm presents a high metastatic rate, and is able to involve nearly every tissue. Non-cutaneous melanoma represents an unusual pattern of melanoma, and the small intestine is an uncommon anatomic localization. Herein we report an extremely rare clinical case of a young woman affected by a bleeding jejunal melanoma, whose early clinical presentation was an intestinal invagination.

© 2007 The WJG Press. All rights reserved.

Key words: Cutaneous melanoma; Intestinal obstruction; Intestinal melanoma; Invagination

Resta G, Anania G, Messina F, de Tullio D, Ferrocci G, Zanzi F, Pellegrini D, Stano R, Cavallesco G, Azzena G, Occhionorelli S. Jejuno-jejunal invagination due to intestinal melanoma. *World J Gastroenterol* 2007; 13(2): 310-312

http://www.wjgnet.com/1007-9327/13/310.asp

INTRODUCTION

Cutaneous melanoma is a malignancy characterized by a high mortality rate. It can metastasize to all organs, although the gastrointestinal tract is an unusual metastatic localization. In 50% of cutaneous melanomas, in fact, metastases in the gastroenteric tract are diagnosed upon autopsy, and only in 5% of cases, they are diagnosed clinically[1,2]. Intestinal metastases of cutaneous melanomas are linked to a baleful prognosis, with a survival average of 6-10 mo after surgery[3,4].

Many studies have demonstrated that only surgery can lead to a control of chronic anemia related to intestinal melanoma bleeding and resolution of the episodes of intestinal sub-occlusion. Surgery on melanoma metastases moreover, can guarantee an increase of survival, in addition to an excellent improvement in quality of life[5-7]. Intestinal metastases represent the occurrence of an occult skin melanoma in only 3%-5% of cases, in which a spontaneous regression of the cutaneous lesion happens[8]. Intestinal metastasis bleeding is extremely rare[9,10].

In order to add more information about surgical presentation of intestinal occult melanoma herein we describe a case of a young woman affected by bloody jejunal metastasis of occult cutaneous melanoma, complicated by intestinal invagination-an extremely rare case in the adult population.

CASE REPORT

A 45-year old woman complained of continual nausea and biliary vomiting, associated with a weight loss of 5 kg. Due to localized abdominal pain, mainly in the right hypochondrium and episodes of hematemesis, the patient was admitted to our hospital. Blood tests revealed sideropenic anemia with 81 g/L haemoglobin, serum iron 100 pg/L, ferritin 23 μg/L, and fecal occult blood test (FOBT) positive in three fecal samples. A gastroscopy was performed, which showed the presence of grade I esophagitis, moderate hiatal hernia and chronic erosive gastritis. The colonoscopy was incomplete due to the presence of colic stools. Abdominal ultrasonography highlighted a distension of the intestinal loops without signs of parenchymatous organ pathology. The patient therefore received an abdominal CT, which suggested the presence of a gastric distension with duodenum-jejunal distension and the presence of a jejunal loop with thickened walls. A second hyperdense image inside the intestinal lumen, forming a target-shaped image was also present: typical feature of intestinal invagination (Figure 1). We therefore decided to proceed to urgent surgical operation after blood transfusion. During surgery, intra-peritoneal fluid was found and samples were removed for cytological testing. Invagination at the third jejunal loop (Figure 2) was evidenced. The presence of hypertrophic lymphatic tissue with intestinal mesenteric lymphoadenomegalia was also present. Manual resolution of the invagination was carried out. This procedure highlighted the presence of a hyperchromic ulcerated neo-

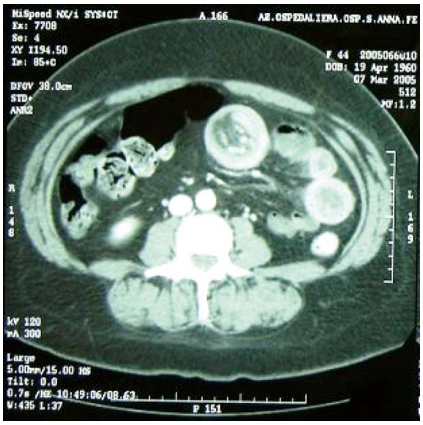

Figure 1 Duodenum-jejunal distension and the presence of a jejunal loop with thickened walls, with a second hyper-dense image inside the same lumen, forming a target-shaped aspect characteristic of intestinal invagination.

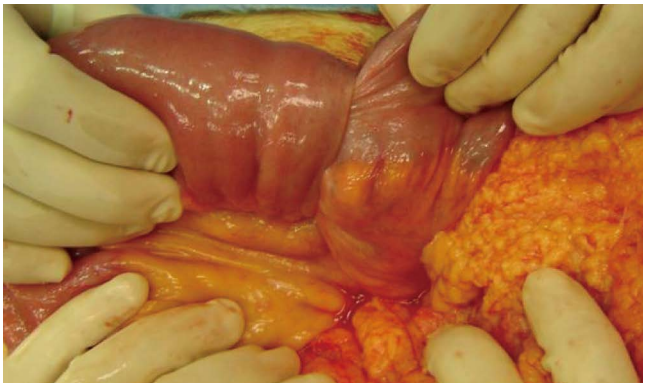

Figure 2 Invagination at the third jejunal loop.

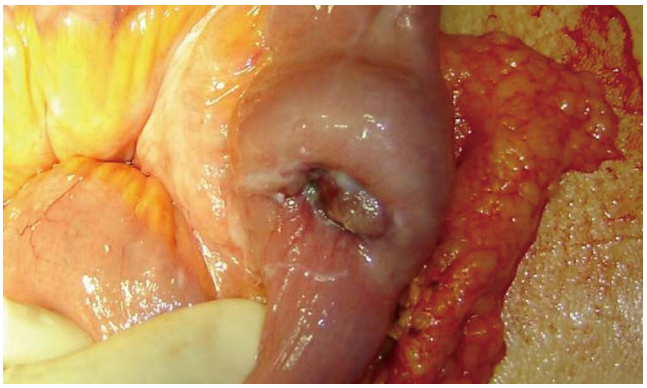

Figure 3 Presence of a hyperchromic ulcerated neoformation, with signs of recent bleeding of the serosa.

formation, with obvious signs of recent bleeding coming from the serosa (Figure 3).

Thorough exploration of the abdominal cavity did not detect further replicative lesions. Resection of the third jejunal loop containing the neoformations and the whole underlying mesentery with its lymph nodes, was performed. The intestinal continuity was restored through a latero-lateral jejuno-jejunal anastomosis.

The post-operative course was uneventful and the patient was discharged after 10 postoperative days. The definitive histological examination showed the presence of an intestinal metastasis of cutaneous melanoma of unknown origin (Figures 4 and 5). The patient was then referred to an oncologic centre for the search of the primary melanoma localization. At three, six months and a year follow-up, the patient is alive and no signs of skin melanoma have been detected.

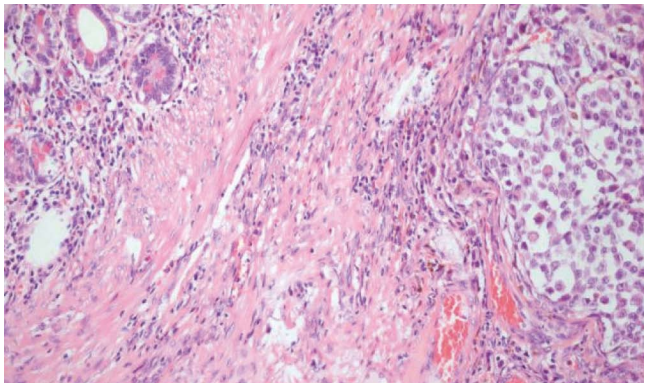

Figure 4 Ileal wall infiltrated with metastatic melanomatous cells with nuclear pseudoinclusions and nucleoli, in nest and trabecular arrangement (HE x 10).

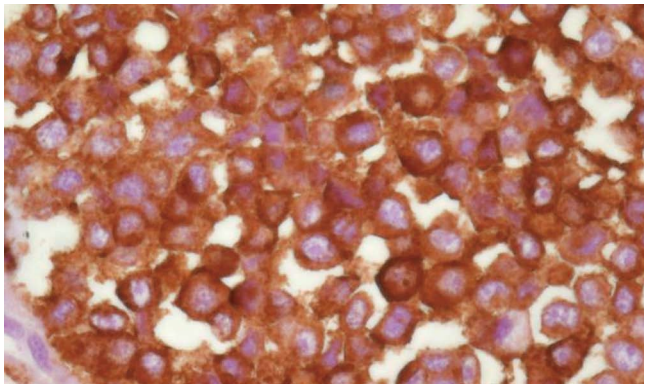

Figure 5 Strong positivity at immunohistochemical assay for HMB45.

DISCUSSION

The peculiar rarity of this clinical case represents the principal reason for our interest. In spite of the clinical manifestation and the diagnostic-therapeutic approach adopted, this case presents many conditions that have been previously poorly documented in international literature.

Our patient presented a chronic anemia and repeated biliary vomiting that were related to the erosive gastritis and esophagitis identified by the gastroscopy, even if this did not necessarily exclude chronic bleeding from neoplastic lesions. The pre-operative CT scan of parajejunal lymphoadenomegalia prompted us to suspect the presence of a neoplastic lesion causing the jejunal invagination. Jejunal invagination in an adult, in fact, can cause 1%-3% of surgically treated intestinal occlusion but is mainly due to peritoneal adhesion or to the presence of intestinal anastomosis[11] and less frequently to a neoplasm. Melanoma intestinal metastasis is clinically diagnosed only in 3%-5% of cases, and is usually found to affect the stomach or the colon. Jejunal location is much less frequent[12] and, if present, does not show clinical signs till diagnosed at autopsy. A diagnosis based on the finding of metastatic

lesions, without identification of the primary cutaneous source, as described in our report, is carried out in only 3% of melanomas. Even if the etiology of primary gastrointestinal melanomas remain undefined, some authors suggest that primary gastrointestinal melanomas are derived from melanoblastic cells of the neural crest which, migrating through the omphalomesenteric canal or APUD cells, reach the intestinal tract, undergoing neoplastic transformation[13]. Non-cutaneous melanomas represent a rare form of melanoma. In a review of 84 836 cases of melanoma, 91.2% were cutaneous, 5.2% ocular, 2.2% of unknown primary site and only 1.3% of gastrointestinal mucosa[14]. Melanomas that arise on mucosal surfaces appear to be more aggressive and are associated with worse prognosis than cutaneous melanomas. The poorer prognosis may be related to the delay in diagnosis, to their more aggressive behaviour, or to earlier dissemination because of the rich lymphatic and vascular supply of the gastrointestinal mucosa[15,16].

Our case shows that the presence of an early complication due to intestinal occlusion, through a sequential and appropriate instrumental diagnostic evaluation, gave us the opportunity to identify a rare melanotic lesion. Moreover, the right surgical approach has given us the opportunity to improve the length and quality of the life of this unlucky patient.

REFERENCES

1 **Reintgen DS**, Thompson W, Garbutt J, Seigler HF. Radiologic, endoscopic, and surgical considerations of melanoma metastatic to the gastrointestinal tract. *Surgery* 1984; **95**: 635-639

2 **de la Monte SM**, Moore GW, Hutchins GM. Patterned distribution of metastases from malignant melanoma in humans. *Cancer Res* 1983; **43**: 3427-3433

3 **Ihde JK**, Coit DG. Melanoma metastatic to stomach, small bowel, or colon. *Am J Surg* 1991; **162**: 208-211

4 **Caputy GG**, Donohue JH, Goellner JR, Weaver AL. Metastatic melanoma of the gastrointestinal tract. Results of surgical management. *Arch Surg* 1991; **126**: 1353-1358

5 **Khadra MH**, Thompson JF, Milton GW, McCarthy WH. The justification for surgical treatment of metastatic melanoma of the gastrointestinal tract. *Surg Gynecol Obstet* 1990; **171**: 413-416

6 **Agrawal S**, Yao TJ, Coit DG. Surgery for melanoma metastatic to the gastrointestinal tract. *Ann Surg Oncol* 1999; **6**: 336-344

7 **Ollila DW**, Essner R, Wanek LA, Morton DL. Surgical resection for melanoma metastatic to the gastrointestinal tract. *Arch Surg* 1996; **131**: 975-979; 979-980

8 **Reintgen DS**, McCarty KS, Woodard B, Cox E, Seigler HF. Metastatic malignant melanoma with an unknown primary. *Surg Gynecol Obstet* 1983; **156**: 335-340

9 **Loualidi A**, Spooren PF, Grubben MJ, Blomjous CE, Goey SH. Duodenal metastasis: an uncommon cause of occult small intestinal bleeding. *Neth J Med* 2004; **62**: 201-205

10 **Wulf V**, Schröder HJ. Metastasis to the small intestine of malignant melanoma as a rare cause of intestinal hemorrhage. *Zentralbl Chir* 1994; **119**: 515-516

11 **Begos DG**, Sandor A, Modlin IM. The diagnosis and management of adult intussusception. *Am J Surg* 1997; **173**: 88-94

12 **Pacovský Z**, Fait V. Distant metastasis of malignant melanoma in the small intestine. *Rozhl Chir* 1992; **71**: 424-428

13 **Elsayed AM**, Albahra M, Nzeako UC, Sobin LH. Malignant melanomas in the small intestine: a study of 103 patients. *Am J Gastroenterol* 1996; **91**: 1001-1006

14 **Chang AE**, Karnell LH, Menck HR. The National Cancer Data Base report on cutaneous and noncutaneous melanoma: a summary of 84,836 cases from the past decade. The American College of Surgeons Commission on Cancer and the American Cancer Society. *Cancer* 1998; **83**: 1664-1678

15 **Sachs DL**, Lowe L, Chang AE, Carson E, Johnson TM. Do primary small intestinal melanomas exist? Report of a case. *J Am Acad Dermatol* 1999; **41**: 1042-1044

16 **Lagoudianakis EE**, Genetzakis M, Tsekouras DK, Papadima A, Kafiri G, Toutouzas K, Katergiannakis V, Manouras A. Primary gastric melanoma: a case report. *World J Gastroenterol* 2006; **12**: 4425-4427

S- Editor Wang GP **L- Editor** Zhu LH **E- Editor** Liu WF

PO Box 2345, Beijing 100023, China
www.wjgnet.com
wjg@wjgnet.com

World J Gastroenterol 2007 January 14; 13(2): 313-315
World Journal of Gastroenterology ISSN 1007-9327
© 2007 The WJG Press. All rights reserved.

CASE REPORT

An unusual cause of cholecystitis: Heterotopic pancreatic tissue in the gallbladder

Gülsüm Özlem Elpek, Sevgi Bozova, Gökben Yıldırım Küpesiz, Mehmet Öğüş

Gülsüm Özlem Elpek, Sevgi Bozova, Gökben Yıldırım Küpesiz, Akdeniz University, Medical School, Department of Pathology, Yeni Tıp, Dekanlık, 07070, Antalya, Turkey
Mehmet Öğüş, Akdeniz University, Medical School, Department of General Surgery, Yeni Tıp, Dekanlık, 07070, Antalya, Turkey
Correspondence to: Gülsüm Özlem Elpek, Akdeniz University, Medical School, Yeni Tıp, Dekanlık, 07070, Antalya, Turkey. elpek@akdeniz.edu.tr
Telephone: +90-242-2274488 Fax: +90-242-2274488
Received: 2006-09-29 Accepted: 2006-12-05

Abstract

Gallbladder localization of heterotopic pancreas (HP) is uncommon and very rarely gives rise to symptoms. Herein we report a case of HP found in the gallbladder neck presented with signs and symptoms of cholecystitis. The patient was a 40-year old male, suffering from epigastric pain, abdominal fullness and fever. On physical examination, the right upper abdomen was tender with a positive Murphy's sign. Ultrasonographic examination showed a hydropic gallbladder without stones and he underwent a cholecystectomy. Pathological examination revealed an intramural nodule (9 mm) in the neck region which is consisted of acini, ducts and islet cells of an aberrant pancreatic tissue. Although HP is encountered rarely in the gallbladder and is found incidentally during pathological studies, this case emphasizes that HP might cause symptoms and present clinically as cholecystitis. For this reason, in patients presenting with symptomatic gallbladder diseases, including cholecystitis without any other pathology, HP should be taken into consideration before it is diagnosed as "idiopathic".

© 2007 The WJG Press. All rights reserved.

Key words: Heterotopic tissues; Pancreas; Acalculous cholecystitis; Gallbladder

Elpek GÖ, Bozova S, Küpesiz GY, Öğüş M. An unusual cause of cholecystitis: Heterotopic pancreatic tissue in the gallbladder. *World J Gastroenterol* 2007; 13(2): 313-315

http://www.wjgnet.com/1007-9327/13/313.asp

INTRODUCTION

Heterotopic pancreas (HP) is defined as the presence of pancreatic tissue lying outside its normal location and lacking anatomical or vascular continuity with the pancreas proper[1]. In 85% to 90% of reported cases, HP has been found in stomach, duodenum, upper jejunum, whereas its presence in the gallbladder is very rare[1-3]. Similar to HP of other organs, HP of the gallbladder itself has no clinical importance and is found incidentally in most cases. However, there have been some reports of symptomatic gallbladder disease[4-7]. Herein we report a case of HP in the neck of the gallbladder who presented with clinical findings of cholecystitis.

CASE REPORT

A 40-year old male presented to the hospital with epigastric pain, abdominal fullness and fever three days ago. On physical examination, the right upper abdomen was tender with a positive Murphy's sign. His laboratory data revealed total bilirubin = 1.5 mg/dL, direct bilirubin = 0.8 mg/dL, ALP = 398 U/dL, SGOT = 70 U/dL, SGPT = 60 U/dL, GGT = 90U/dL. Ultrasonographic (US) examination showed a hydropic gallbladder without stones. A cholecystectomy was performed. The macroscopic findings were as follows: gallbladder measuring 80 mm × 50 mm × 40 mm, wall thickness 3-12 mm. In the neck region, a yellowish-white intramural nodule measuring 9 mm × 8 mm × 8 mm was observed. Microscopic examination revealed aberrant pancreatic tissue consisting of acini, ducts and chromogranin A expressing islet cells. No direct connection with the gallbladder lumen was observed (Figure 1). The whole specimen was embedded stepwise for further microscopic evaluation, but any other pancreatic tissue was not detected. The diagnosis was thereby established as chronic cholecystitis with heterotopic pancreas. All symptoms disappeared following cholecystectomy and the patient recovered completely.

DISCUSSION

Although HP is the second most prevalent pancreatic anomaly, the incidence in gastrointestinal tract is estimated to be from 0.55% to 13.7% on autopsy, and 0.2% in laparatomy[6]. Despite the frequent occurrence of HP in the stomach, duodenum and upper jejunum, the gallbladder localization is extremely rare. Since the first publication by Poppi in 1916, only 29 more cases of HP worldwide in the gallbladder have been reported in a review of the literature up to the present[8]. In these cases there is a higher incidence of female patients between 40 and 50 years of age[9]. However, similar to our case, its

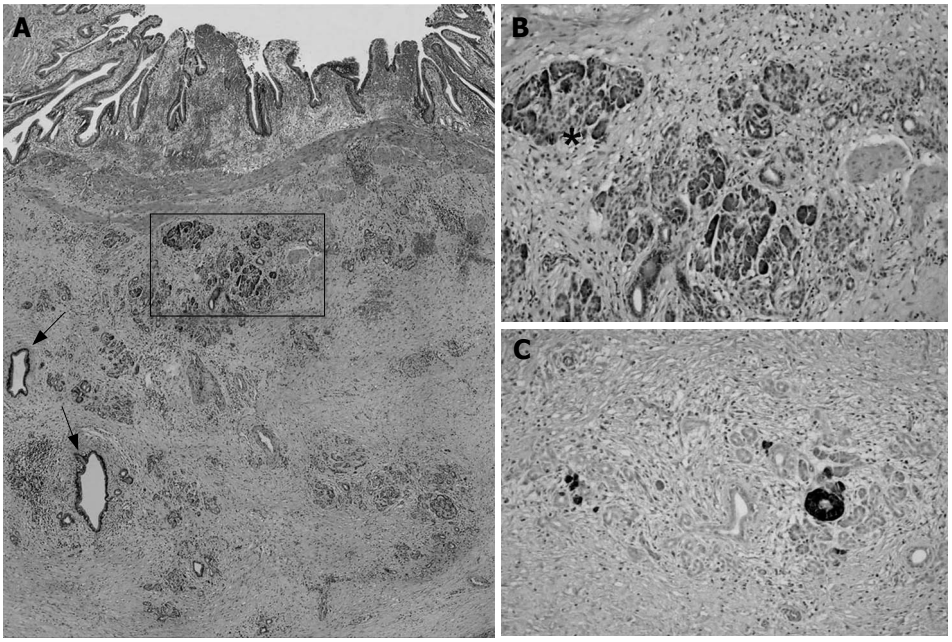

Figure 1 Histological sections of HP showing dilated ducts (arrows, H&E x 100) and acini (**A**), acinar and islet cells (asterisk, H&E x 250) (**B**), and chromogranin A expressing islet cells (Mayer's haematoxylin x 250) (**C**) in submucosa of gallbladder neck.

occurrences have been reported in men. In half of the reported cases, HP is preferentially localized close to the neck of the gallbladder[9]. Parallel to this observation, in our patient HP was located in the neck region.

HP in the gallbladder is very rarely symptomatic. In most reported cases, it is an incidental pathological findings and coexists with gallstones[9,10]. However, there have been some reported symptomatic gallbladder diseases due to HP[4-7]. In one case HP has been found to cause perforation of the gallbladder and lead to peritonitis[5]. Similar to our case, in two cases HP has been found to stimulate cholecystopathy with all symptoms disappearing following cholecystectomy[4,7]. Inceoglu *et al*[6] have reported a case of HP in the cystic duct with hydrops of the gallbladder and chronic pancreatitis of the ectopic tissue. In all cases including the case presented here, because of its rare occurrence as a symptomatic lesion, HP is not taken into consideration in the clinical differential diagnosis. Indeed, as in other organs, the preoperative diagnosis of HP in gallbladder is difficult[10,11]. Symptomatology and clinical findings in most cases suggest gallbladder disease, mainly lithiasis and cholecystitis[9]. It was pointed out that HP located especially in the neck region might prevent bile flow like a stone and cause hydrops of the gallbladder mimicking the clinical findings of these diseases[6]. From this point of view, in our case localization of HP in the neck region might explain the clinical findings of cholecystitis related to hydrops of the gallbladder without cholelithiasis. Recently it was indicated that, despite its high resolution, US is not specific for HP and impossible to distinguish HP from other lesions such as cholesterol polyps, adenoma and carcinoma[9,11]. Parallel to these observations, in our case while US examination revealed a hydropic gallbladder without stones, it failed to detect HP. For these reasons, we suggest that the rare occurrence of HP in the gallbladder and its presence as an incidental finding in cholecystectomy materials do not exclude its consideration in the differential diagnosis of symptomatic gallbladder diseases.

Our histopathological examination revealed a HP constituted of acini, ducts and islet cells, corresponding to the total heterotopia[8]. Although panreatitis may occur in HP, the present case had no histopathological findings of pancreatitis[6].

The origin of heterotopic pancreatic tissue is controversial but two theories have been proposed. One suggests that pancreatic tissue is separated from the main pancreas during embryonic rotation[5,6], the other is that during the growth of the ventral pancreatic bud a proportion is transported by the longitudinal growth of the intestines[5,6]. Therefore its presence in the gallbladder might indicate derivation from the ventral diverticulum. On the other hand, the site of organ/tissue formation is also determined by strictly coordinated developmental programs involving interplay between extracellular signaling and intracellular transcriptional factor networks. It has been demonstrated that in mammals the developmental decisions according to the state of the immediate neighbors are controlled through the Notch signaling system[12]. Several studies indicate that this system also plays an essential role in the precise orchestration of cell-fate decisions in the developing pancreas[13]. Hes-1 (Hairy enhancer of split), a main effector of Notch signaling is required for region-appropriate specification of the pancreas in the developing foregut endoderm[14]. In experimental studies, ectopic pancreas formation has been observed in Hes-1 knockout mice and the plasticity of endodermal progenitors of the gut, bile duct, and pancreas has been suggested[14,15]. In light of these observations, we consider that besides two proposed theories, abnormalities in the Notch signaling system, especially in Hes-1 expression during embryogenesis may also contribute to the formation of HP of the gallbladder.

In conclusion, HP of the gallbladder is a very rare condition which is diagnosed incidentally, but may cause clinical symptoms such as cholecystitis and should be taken into consideration in patients with symptomatic

gallbladder disease without any other specific clinical and laboratory findings before it is diagnosed as idiopathic.

REFERENCES

1 **Armstrong CP**, King PM, Dixon JM, Macleod IB. The clinical significance of heterotopic pancreas in the gastrointestinal tract. *Br J Surg* 1981; **68**: 384-387

2 **Dolan RV**, ReMine WH, Dockerty MB. The fate of heterotopic pancreatic tissue. A study of 212 cases. *Arch Surg* 1974; **109**: 762-765

3 **Rosai JR**. Pancreas and periampullary region: heterotopic pancreas In: Rosai JR, editor. Ackerman's Surgical Pathology. *St Louis: Mosby*, 2004: 10063.

4 **Brown HW**, Tabbah I. Aberrant pancreatic tissue in the wall of the gallbladder: report of a case simulating gallstone disease. *Int Surg* 1979; **64**: 43-44

5 **Ben-Baruch D**, Sandbank Y, Wolloch Y. Heterotopic pancreatic tissue in the gallbladder. *Acta Chir Scand* 1986; **152**: 557-558

6 **Inceoglu R**, Dosluoglu HH, Kullu S, Ahiskali R, Doslu FA. An unusual cause of hydropic gallbladder and biliary colic--heterotopic pancreatic tissue in the cystic duct: report of a case and review of the literature. *Surg Today* 1993; **23**: 532-534

7 **Bhana BD**, Chetty R. Heterotopic pancreas--an unusual cause of cholecystitis. *S Afr J Surg* 1999; **37**: 105-107

8 **Neupert G**, Appel P, Braun S, Tonus C. Heterotopic pancreas in the gallbladder. Diagnosis, therapy, and course of a rare developmental anomaly of the pancreas. *Chirurg* 2007; **78**: 261-264

9 **Kondi-Paphiti A**, Antoniou AG, Kotsis T, Polimeneas G. Aberrant pancreas in the gallbladder wall. *Eur Radiol* 1997; **7**: 1064-1066

10 **Mboti F**, Maassarani F, De Keuleneer R. Cholecystitis associated with heterotopic pancreas. *Acta Chir Belg* 2003; **103**: 110-112

11 **Mönig SP**, Selzner M, Raab M, Eidt S. Heterotopic pancreas. A difficult diagnosis. *Dig Dis Sci* 1996; **41**: 1238-1240

12 **Artavanis-Tsakonas S**, Rand MD, Lake RJ. Notch signaling: cell fate control and signal integration in development. *Science* 1999; **284**: 770-776

13 **Murtaugh LC**, Stanger BZ, Kwan KM, Melton DA. Notch signaling controls multiple steps of pancreatic differentiation. *Proc Natl Acad Sci USA* 2003; **100**: 14920-14925

14 **Sumazaki R**, Shiojiri N, Isoyama S, Masu M, Keino-Masu K, Osawa M, Nakauchi H, Kageyama R, Matsui A. Conversion of biliary system to pancreatic tissue in Hes1-deficient mice. *Nat Genet* 2004; **36**: 83-87

15 **Fukuda A**, Kawaguchi Y, Furuyama K, Kodama S, Horiguchi M, Kuhara T, Koizumi M, Boyer DF, Fujimoto K, Doi R, Kageyama R, Wright CV, Chiba T. Ectopic pancreas formation in Hes1 -knockout mice reveals plasticity of endodermal progenitors of the gut, bile duct, and pancreas. *J Clin Invest* 2006; **116**: 1484-1493

S- Editor Liu Y **L- Editor** Wang XL **E- Editor** Lu W

PO Box 2345, Beijing 100023, China
www.wjgnet.com
wjg@wjgnet.com

World J Gastroenterol 2007 January 14; 13(2): 316-319
World Journal of Gastroenterology ISSN 1007-9327
© 2007 The WJG Press. All rights reserved.

CASE REPORT

A case of interstitial pneumonitis in a patient with ulcerative colitis treated with azathioprine

Ferenc Nagy, Tamas Molnar, Eva Makula, Ildiko Kiss, Peter Milassin, Eva Zollei, Laszlo Tiszlavicz, Janos Lonovics

Ferenc Nagy, Tamas Molnar, Janos Lonovics, First Department of Medicine, University of Szeged, Faculty of Medicine, Szeged, Hungary
Eva Makula, Ildiko Kiss, Peter Milassin, Department of Radiology, University of Szeged, Faculty of Medicine, Szeged, Hungary
Eva Zollei, Medical Intensive Care Unit, University of Szeged, Faculty of Medicine, Szeged, Hungary
Laszlo Tiszlavicz, Institute of Pathology, University of Szeged, Faculty of Medicine, Szeged, Hungary
Correspondence to: Ferenc Nagy MD, PhD. First Department of Medicine, Faculty of Medicine, University of Szeged, Koranyi fasor 8, H-6701, Szeged, POB 427, Hungary. agyferi@in1st.szote.u-szeged.hu
Telephone: +36-62-545189 Fax: +36-62-545185
Received: 2006-09-20 Accepted: 2006-10-25

Abstract

The early hypersensitivity reaction and late bone marrow depression are well-known side-effects of azathioprine, whereas interstitial pneumonia is a rare complication. A 40-year old male patient had been treated with azathioprine in consequence of extensive ulcerative colitis for 10 years. He then complained of 7 d of fever, cough and catarrhal signs, without symptoms of active colitis. Opportunistic infections were ruled out. The chest X-ray, CT and lung biopsy demonstrated the presence of interstitial inflammation. Azathioprine therapy was discontinued as a potential source of the pulmonary infiltrate. In response to steroid therapy, and intensive care, the pulmonary infiltrate gradually decreased within 4 wk. Three months later, his ulcerative colitis relapsed, and ileo-anal pouch surgery was performed. In cases of atypical pneumonia, without a proven infection, azathioprine-associated interstitial pneumonitis may be present, which heals after withdrawal of the drug.

© 2007 The WJG Press. All rights reserved.

Key words: Inflammatory bowel disease; Ulcerative colitis; Azathioprine; Interstitial pneumonitis

Nagy F, Molnar T, Makula E, Kiss I, Milassin P, Zollei E, Tiszlavicz L, Lonovics J. A case of interstitial pneumonitis in a patient with ulcerative colitis treated with azathioprine. *World J Gastroenterol* 2007; 13(2): 316-319

http://www.wjgnet.com/1007-9327/13/316.asp

INTRODUCTION

Azathioprine (Imuran® Glaxo-SmithKline) (AZA), one of the most commonly prescribed immunosuppressive drugs, is mainly administered in the treatment of immune-mediated diseases. AZA has been used to combat inflammatory bowel diseases (IBD) such as ulcerative colitis and Crohn's disease since the 1960s[1]. It has been shown to reduce the number of lamina propria plasma cells, to alter the function of lymphocytes and natural killer cells and to exert an anti-inflammatory effect[2]. In IBD, azathioprine is used in both steroid-dependent and steroid-resistant cases. The clinical efficacy starts within 3-6 mo after the initiation of therapy. It is effective in more than half of the patients[3]. The early hypersensitivity reaction (nausea, fever, hepatitis and pancreatitis) and late bone marrow depression (leukopenia and macrocytosis) are relatively common side-effects[4], but interstitial pneumonitis is rare.

CASE REPORT

A 41-year old male patient with known ulcerative colitis since 1988 was referred to the Department of Medicine by his GP in June 2003 with symptoms and signs of relapse. His pancolitis had been treated with AZA (1.8 mg/kg per day) since 1993 because of frequent relapses. During the therapy only mild (1-2 blood-streaked stools) and rare (for 1-2 wk periods, once or twice yearly) relapses occurred. The patient was in good physical condition for his age and he was able to work. Six weeks before his admission, there was a severe relapse. He complained of anorexia, a weight loss (15 kg) and frequent bowel movements (10-12 times/d), accompanied with colicky pain and blood in the stools. Fever, dyspnoea and cardiac symptoms were not present. His treatment on admission was: 1 g olsalazine, 150 mg azathioprine, 12 mg methylprednisolone daily. Physical examination of the cardiorespiratory system was negative and diffuse abdominal tenderness was detected. His weight was 91 kg, his height was 182 cm, and his temperature was normal. The blood chemistry at the time of admission was as follows: ESR = 76 mm/h, serum sodium = 132 mmol/L, potassium = 3.7 mmol/L, haematocrit = 32%, hb = 111 g/L, TIBC = 55 μmol/L, white blood cell count = 4.400 G/L, and platelets = 368.000 G/L. Liver function tests were normal. Colonoscopy revealed severe active extensive ulcerative colitis involving the whole transversal colon. In response to parenteral corticosteroid treatment, his condition improved. He was discharged in good condition after

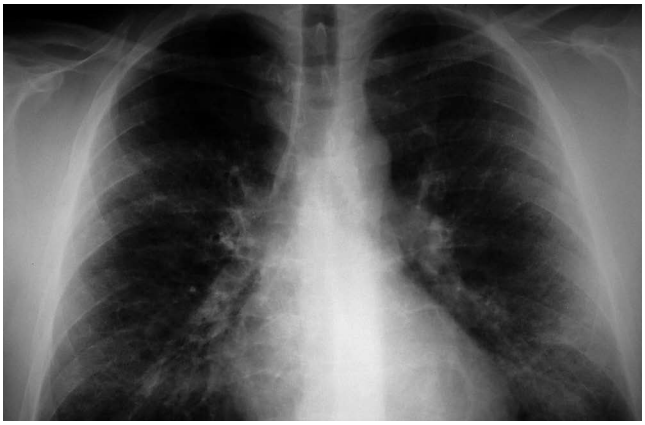

Figure 1 Chest X-ray (2003-09-09) showing moderate reticular enhancement with ring-like consolidation in both lungs (but predominantly the right), without cardiac or aortic abnormalities.

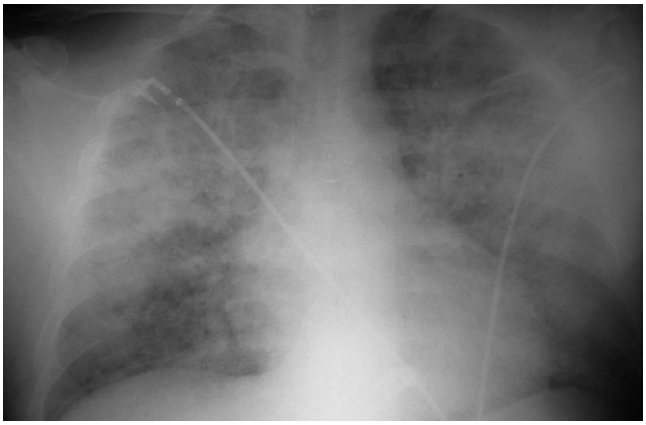

Figure 2 Chest X-ray (2003-09-14) showing significant progression and volume loss in both lungs. A palm-sized homogeneous consolidation developed in the central part of the lung, a marked interstitial enhancement was seen in other parts of the lung. The radiological image suggested ARDS. The heart was enlarged.

11 d on 48 mg/d oral methylprednisolone and 150 mg/d AZA.

After a remission period, which lasted throughout the summer, he presented to the Department of Medicine in September 2003 with complaints of weakness, weight loss, coughing and fever, the latter appearing every evening for a week. He did not cough up blood. He had 2-4 stools daily, without blood. He had no abdominal symptoms. His daily treatment on admission was 150 mg AZA, 16 mg methylprednisolone and doxycycline (prescribed by his GP). The results of physical examinations (cardiovascular and respiratory systems and abdomen) were normal. Septic fever was present. Blood chemistry values were as follows: ESR = 125 mm/h, haematocrit = 31%, hb = 10.7 g/L, white blood cell count = 4.100 G/L, platelets = 325.000 G/L, CRP = 351 mg/L, and uric acid = 471 μmol/L. The haemoculture was negative and procalcitonin was 0.07 ng/mL. The bacteriology (pharynx, sputum and urine) and virology (CMV, EBV, Coxackie and adenovirus) tests were negative.

The chest X-ray (2003-09-09) revealed moderately increased interstitial shadowing with a ring-like consolidation in both lungs (predominantly in the right), without cardiac or aortic abnormalities. The follow-up chest X-ray revealed progression (Figure 1). Despite the discontinuation of AZA, progressive interstitial inflammation was detected in both lungs. The patient was treated with 1 g/d clarithromycin intravenously and 12 mg methylprednisolone orally. He was transferred to the intensive care unit because of the possibility of a severe opportunistic infection or an autoimmune disease. AZA-associated pneumonitis was also suspected.

His respiratory failure was treated in the intensive care unit. Dyspnoea occurred on minor exertion, the patient had orthostatic hypotension, and he was weak. On physical examination, the liver was palpable 2 cm beyond the costal margin. Except for dyspnoea nothing abnormal was detected. Blood chemistry showed ESR = 120 mm/h, haematocrit = 26%, hb = 90 g/L, white blood cell count = 2.970-3.200 G/L, platelets = 426.000 G/L, SGOT = 246 U/L, SGPT = 91 U/L, gamma GT = 600 U/L, LDH = 1125 U/L, and procalcitonin = 0.07 ng/L. Nasal oxygen supplementation was initiated, and a bronchial lavage sample was collected from the lower respiratory tract under anaesthesia. Arterial blood gas analyses displayed pH = 7.455, pCO_2 = 33.0, pO_2 = 50.9 mmHg, and sO_2 = 86.2%. Two days later the corresponding values of pH, pCO_2, pO_2, and sO_2 were: 7.394%, 41.7%, 75.1% and 94.0%, respectively. Neither typical nor atypical pathogens were detected in bacteriology samples. CMV PCR and Legionella IgM-IgG were also negative.

The follow-up chest X-ray examination (Figure 2), revealed a significant progression of the interstitial shadowing in both lungs. A palm-sized homogeneous consolidation was seen in the hilar area and marked interstitial shadowing in the remaining parts of the lungs. The radiological appearance was suggestive of acute respiratory distress syndrome (ARDS). Cardiac enlargement was demonstrated.

The chest CT examination revealed a 2-cm wide pleural effusion with increased alveolar/air-space shadowing bilaterally. The X-ray and CT examinations suggested ARDS. A needle biopsy was performed from the apex of the right lung. The histology showed intraluminal myxoid polyps (Masson bodies) in the alveoli (Figures 3,4,5). Vasculitis and *Pneumocystis carinii* infection were excluded. The results of the histology and immuno-histochemistry suggested a diagnosis of bronchiolitis obliterans organizing pneumonia (BOOP), but hypersensitivity pneumonitis was also regarded as a possibility. After sulphametoxasol/trimetroprim and methylprednisolone therapy, his condition gradually improved (Figure 6), and his liver and renal functions became normal. At the time of discharge, he was treated with 3 g sulphasalazine, 1 g sulphamethoxazole/trimethroprim and 8 mg methylprednisolone daily.

Three months later (2004-09-01) only mild dyspnoea occurred on exertion, but he had 8-10 liquid stools daily, occasionally with some blood on the surface of faeces. He had neither fever nor extraintestinal symptoms. The results of chest and heart examination were normal, but the sigma was tender. Corticosteroid therapy was restarted with 64 mg/d methylprednisolone. Blood chemistry

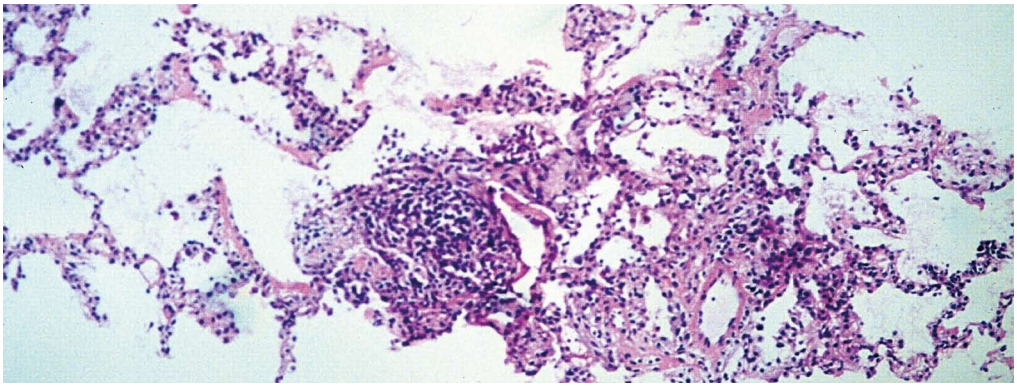

Figure 3 Histology of lung needle biopsy (HE, 112 ×).

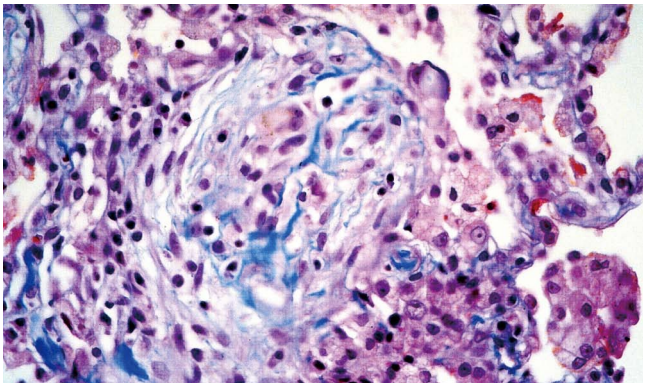

Figure 4 Histology showing the pathognomic Masson bodies for BOOP and polypous proliferation of new connective tissue in the alveolus (trichrome, 224 ×).

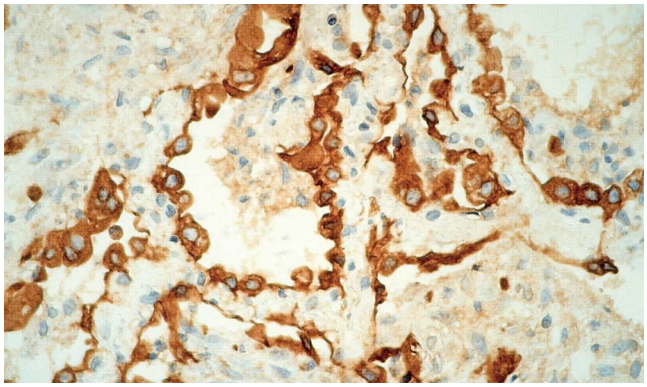

Figure 5 Immunohistochemistry for the expression of CK 7. Interstitial fibrosis and proliferation of type II pneumocytes are apparent (224 ×).

showed serum Fe = 21.3 μmol/L, uric acid = 461 μmol/L, gamma GT = 121 U/L, cholesterol = 7.75 mmol/L, triglyceride = 2.3 mmol/L, white blood cell count = 7. 870 G/L and platelets = 223. 000 G/L. Pulmonary functions were VC = 110%, RV = 109%, spirometry FVC = 104%, FEV_1 = 112%. The diffusion capacity values (DLCO = 74%, DLCO/VA = 60%) suggested a slightly decreased diffusion capacity. The chest X-ray revealed a further improvement of the lung volume. Interstitial shadowing was still present in the perihilar region of the lungs. Colonoscopy could only be carried out to 20 cm because of the pain and active colitis. The surface of mucosa was reddish, vulnerable and ulcerated, corresponding to active ulcerative colitis. In view of his previous history, proctocolectomy had to be considered. The first surgical intervention was carried out a month later and, after the ileal-pouch anal anastomosis (IPAA), the temporary anus prae was closed in August 2004. He had no complaints after the operation, produced 4-5 stools daily and was not on any medication.

DISCUSSION

In IBD patients, AZA treatment is worth starting if the patient is steroid-refractory (the effective dose does not lead to remission) or steroid dependent (discontinuation of the steroid causes a relapse)[5]. The first clinical results were inhomogeneous as concerns efficacy, because of the long time until the onset of action. Hawthorne *et al*[6] have proven the beneficial effect of the medication on the maintenance of remission in ulcerative colitis. In their study, seventy-nine patients who had been taking AZA for 6 mo were then divided into two groups. One of the groups continued to receive the therapy while placebo was administered to the patients in the other. The relapse rate was 36% in the AZA-treated group and 59% in the placebo group.

The mechanism of action of AZA is unknown. In IBD, the drug decreases the number of lamina propria plasma cells and alters the functions of lymphocytes and natural killer cells.

The therapeutic effect has been explained by the apoptosis-inducing behaviour of the drug. Tiede *et al*[7] considered that 6-thioGTP, a metabolite of AZA, could alter the apoptosis of T cells. The metabolite inhibits the activation of certain genes inside the cells, and induces apoptosis via a mitochondrial path.

Bedrossian *et al*[8] have noted bilateral lung infiltration with a reduced pO_2 in 7 kidney-transplanted patients treated with AZA, which was not cured by antibiotic therapy. In their study, lung biopsy revealed an abnormal histology, which varied from diffuse alveolar damage to interstitial pneumonia and pulmonary fibrosis. No immune deposition, eosinophilia, vasculitis or granuloma could be detected, and the bacteriologyical findings were negative. When AZA was withdrawn from the treatment, the infiltration was significantly diminished in 2 patients who exhibited diffuse alveolar damage, but 4 patients diagnosed as interstitial pneumonitis, died of ARDS. The biopsies revealed hyaline membranes, intraalveolar oedema and damage to

Figure 6 Chest X-ray (2003-10-15) showing improvement of lung volumes. Reticular enhancement of the middle part of the lungs is still present.

the alveolar epithelium in those who received low doses of AZA, and atypical epithelial hyperplasia, reorganization of the distal air spaces and fibrosis in the cases treated with high doses of AZA. Histologically the changes observed could not be distinguished from the characteristic changes caused by other pulmonary toxic drugs.

In our case, AZA treatment, initiated because of the common and serious relapses of extensive ulcerative colitis, ensured a good condition for almost 10 years. The patient was hospitalized because of a severe relapse in June 2003, but at that time no pulmonary abnormality was found. Remission was achieved with intravenous corticosteroid therapy. Three months later (2003-09-09), the patient presented with cough, catarrhal signs and pulmonary infiltration. We initially thought of concomitant infection, which may be expected during immunosuppressive treatment. In consequence of earlier therapy the pancolitis was in remission. After admission, the dose of AZA was reduced, and doxycycline was changed to chlarythromycin. However, despite his good general condition and the conventional treatment, the pulmonary infiltration rapidly deteriorated. Dyspnoea developed, which necessitated intensive care. Concomitant infection was not confirmed by the diagnostic examinations, and broad-spectrum antibiotics were proven ineffective. The lung biopsy results and the clinical features strongly suggested that he had AZA-associated interstitial pneumonia. Other causes of BOOP, such as eosinophilic pneumonia, vasculitis, irradiation, nitrofurantoin, gold, amiodarone and methotrexate, were excluded. In view of the results, AZA treatment was discontinued, oral corticosteroid medication was continued and the patient's condition gradually improved. Three months later (December 2003), ulcerative colitis relapsed. In view of the clinical course of ulcerative colitis (frequent recurrences and AZA-induced interstitial pneumonitis), proctocolectomy was recommended. After surgery, the patient's condition normalized without any further treatment.

In summary, in cases of atypical pneumonia without a proven opportunistic infection, AZA-associated interstitial pneumonitis may be present, which heals after withdrawal of the drug.

REFERENCES

1 **Dubinsky MC**. Azathioprine, 6-mercaptopurine in inflammatory bowel disease: pharmacology, efficacy, and safety. *Clin Gastroenterol Hepatol* 2004; **2**: 731-743

2 **Siegel CA**, Sands BE. Review article: practical management of inflammatory bowel disease patients taking immunomodulators. *Aliment Pharmacol Ther* 2005; **22**: 1-16

3 **Carter MJ**, Lobo AJ, Travis SP. Guidelines for the management of inflammatory bowel disease in adults. *Gut* 2004; **53** Suppl 5: V1-V16

4 **Domènech E**. Inflammatory bowel disease: current therapeutic options. *Digestion* 2006; **73** Suppl 1: 67-76

5 **Nagy F**. Conservative therapy of inflammatory bowel diseases. *Orv Hetil* 2002; **143**: 2763-2768

6 **Hawthorne AB**, Logan RF, Hawkey CJ, Foster PN, Axon AT, Swarbrick ET, Scott BB, Lennard-Jones JE. Randomised controlled trial of azathioprine withdrawal in ulcerative colitis. *BMJ* 1992; **305**: 20-22

7 **Tiede I**, Fritz G, Strand S, Poppe D, Dvorsky R, Strand D, Lehr HA, Wirtz S, Becker C, Atreya R, Mudter J, Hildner K, Bartsch B, Holtmann M, Blumberg R, Walczak H, Iven H, Galle PR, Ahmadian MR, Neurath MF. CD28-dependent Rac1 activation is the molecular target of azathioprine in primary human CD4+ T lymphocytes. *J Clin Invest* 2003; **111**: 1133-1145

8 **Bedrossian CW**, Sussman J, Conklin RH, Kahan B. Azathioprine-associated interstitial pneumonitis. *Am J Clin Pathol* 1984; **82**: 148-154

S- Editor Wang J **L- Editor** Wang XL **E- Editor** Liu WF

PO Box 2345, Beijing 100023, China
www.wjgnet.com
wjg@wjgnet.com

World J Gastroenterol 2007 January 14; 13(2): 320-323
World Journal of Gastroenterology ISSN 1007-9327
© 2007 The WJG Press. All rights reserved.

CASE REPORT

Gallbladder lymphangioma: A case report and review of the literature

Jwa-Kyung Kim, Kyo-Sang Yoo, Joon Ho Moon, Kwang Hyuk Park, Yong Woo Chung, Kyoung Oh Kim, Cheol Hee Park, Taeho Hahn, Sang Hoon Park, Jong Hyeok Kim, Jang Yeong Jeon, Min Jung Kim, Kwang Seon Min, Choong Kee Park

Jwa-Kyung Kim, Kyo-Sang Yoo, Joon Ho Moon, Kwang Hyuk Park, Yong Woo Chung, Kyoung Oh Kim, Cheol Hee Park, Taeho Hahn, Sang Hoon Park, Jong Hyeok Kim, Choong Kee Park, Department of Gastroenterology and Hepatology, Hallym University College of Medicine, Anyang, Korea
Jang Yeong Jeon, Department of Surgery, Hallym University College of Medicine, Anyang, Korea
Min Jung Kim, Department of Diagnostic Radiology, Hallym University College of Medicine, Anyang, Korea
Kwang Seon Min, Department of Pathology, Hallym University College of Medicine, Anyang, Korea
Correspondence to: Kyo-Sang Yoo, MD, PhD, Department of Gastroenterology and Hepatology, Hallym University Sacred Heart Hospital, 896 Pyeongchon-dong, Dongan-gu, Anyang, Gyeonggi 431-070, Korea. stanyoo@hallym.ac.kr
Telephone: +82-31-380-6065 Fax: +82-31-386-2269
Received: 2006-11-08 Accepted: 2006-12-06

Abstract

Lymphangiomas are rare, benign tumors of the lymphatic system, usually present in children aged 5 years and younger. Because they are asymptomatic until the mass enlarges to cause symptoms, most lymphangiomas are diagnosed at adulthood incidentally. We experienced a case of a 60-year-old man diagnosed with a cystic lymphangioma of the gallbladder, which was successfully resected without any complication. Magnetic resonance imaging and magnetic resonance cholangiopancreatography were very helpful for the diagnosis of the cystic lesion around the gallbladder as were ultrasonography and computed tomography scan. These showed a multi-lobulated cystic mass with intact cystic duct and bile duct in the gallbladder fossa. The patient underwent an open cholecystectomy and the histological findings were consistent with a cystic lymphangioma of the gallbladder. We here report the case of cystic lymphangioma of the gallbladder with a review of the literature.

© 2007 The WJG Press. All rights reserved.

Key words: Lymphangioma; Gallbladder; Cholecystectomy

Kim JK, Yoo KS, Moon JH, Park KH, Chung YW, Kim KO, Park CH, Hahn T, Park SH, Kim JH, Jeon JY, Kim MJ, Min KS, Park CK. Gallbladder lymphangioma: A case report and review of the literature. *World J Gastroenterol* 2007; 13(2): 320-323

http://www.wjgnet.com/1007-9327/13/320.asp

INTRODUCTION

Lymphangiomas are uncommon benign congenital malformations of the lymphatic system[1-3]. About 95% lymphangiomas occur in the skin and the subcutaneous tissues of the head, neck and axillary region and the remaining 5% appear in other parts of the body such as lungs, pleura, pericardium, esophagus, stomach, jejunum, colon, pancreas, liver, gallbladder, kidney, and the mesentery[3-5]. Because most lymphangiomas are multicystic, lobulated lesions, they may be confused with other lesions, such as intrahepatic simple cysts, ductal ectasia, liver hemangiomas, pericholecystic cystic tumors or angiosarcomas. Various imaging studies are often required for accurate diagnosis and to differentiate gallbladder lymphangiomas from other lesions[3,6,7]. Recently, magnetic resonance imaging (MRI) and magnetic resonance cholangiopancreatography (MRCP) have been shown to be helpful for the characterization of the lesions as well as an evaluation of the relation to the adjacent organs. Complete surgical resection is the treatment of choice for gallbladder lymphangioma, and recently successful laparoscopic resection also has been reported[8].

CASE REPORT

A 60-year-old man was admitted to Hallym University Sacred Heart Hospital for treatment of aspiration pneumonia. He presented a high fever, chills and coughing, and had no abdominal pain or discomfort. Chest computed tomography (CT) scan for evaluation of the pneumonia unexpectedly showed a large lobulating low density lesion in the liver near the gallbladder in addition to pneumonic infiltration of the lungs. The patient was referred to our department for evaluation of the large cystic lesion. Abdominal ultrasonography (US) showed a hypoechoic mass encircling the gallbladder lumen in the liver (Figure 1). Abdominal CT showed an approximately 5.2 cm-sized multi-lobulated cystic mass, insinuating gallbladder lymphangioma, between the liver and the gallbladder bed (Figure 2). Abdominal MRI was performed for the characterization and anatomical evaluation of the lesion. Axial T2-weighted image showed an intact lumen

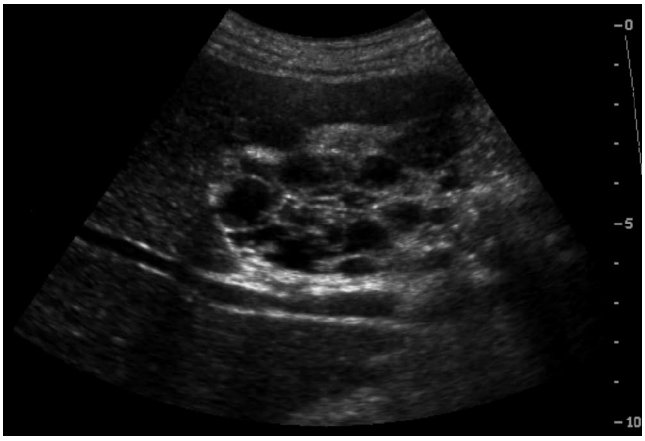

Figure 1 Abdominal ultrasonography showing multi-loculated cystic mass and intact gallbladder lumen.

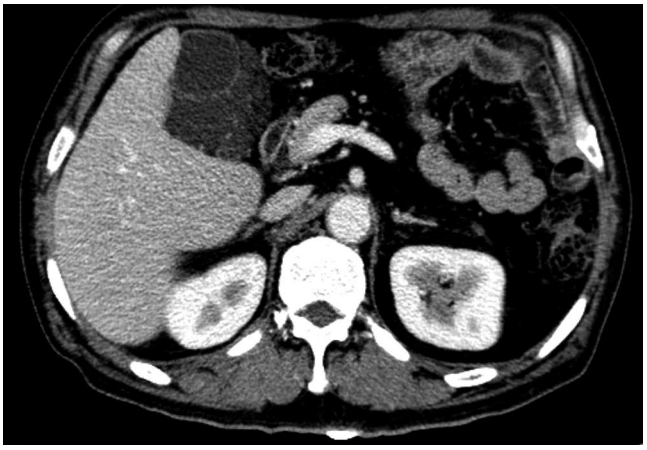

Figure 2 Abdominal computed tomography (CT) image showing a low-density multilocular cystic lesion with septation originated from the gallbladder fossa.

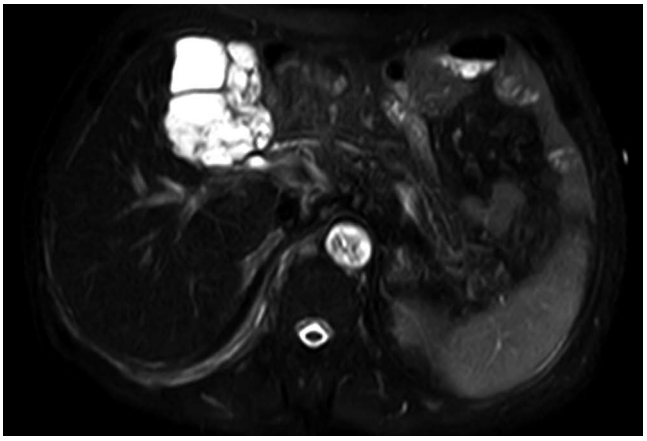

Figure 3 Axial T2-weighted magnetic resonance (MR) image showing a thin multi-septated cystic mass (high-signal intensity) with scalloping margin.

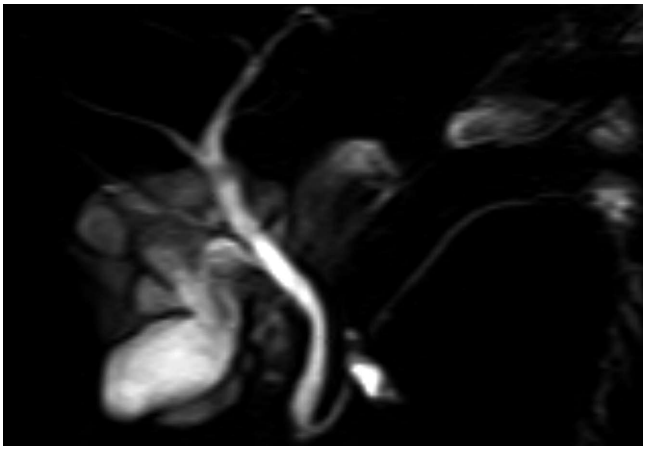

Figure 4 Magnetic resonance cholangiopancreatography (MRCP) image showing gallbladder encapsulated by variable sized multi-cystic lesions, which have no communication with biliary system.

of the gallbladder (low-signal intensity) surrounded by a thin multi-septated cystic mass (high-signal intensity) with scalloping margin (Figure 3). This finding strongly suggested a lymphangioma arising from the lymphatic tissue of the gallbladder wall. MRCP also clearly showed a large multi-cystic gallbladder lymphangioma in the gallbladder fossa (Figure 4). Characteristically, the cystic duct and bile duct were completely separated from the lymphangioma, and were well preserved. Additionally, the gallbladder was obviously visualized and its contraction was grossly normal (ejection fraction = 89%) on hepatobiliary DISIDA scan.

An open cholecystectomy was performed after resolution of the pneumonia. At surgical exploration, a well-defined multi-lobular cystic tumor encapsulating the gallbladder was observed. Grossly the tumor was measured 5.5 cm × 4.3 cm × 3.5 cm in size and was clearly separated from the liver. When the tumor was cut off from the surface, the gallbladder mucosa was intact and various-sized multiple cysts were shown. Each cyst was filled with serous or hemorrhagic lymphatic fluid. Histological evaluation revealed a flat endothelial lining encircling each cyst and multiple lymphocyte aggregations beside the cyst (Figure 5). This demonstrated that the cyst was a lymphatic space. The lesion was diagnosed as a cystic lymphangioma of the gallbladder because it had no connection with adjacent normal lymphatics. CT at 12 mo following the surgical resection showed no evidence of recurrence.

DISCUSSION

Lymphangiomas are benign tumors that may appear in any organ of the body except the brain. It more commonly involves the skin and soft tissue of the head and neck (95%), and lymphangioma occurring in the gastrointestinal tract is rare. A lymphangioma arising from the gallbladder is extremely rare, representing only 0.8%-1% of all intra-abdominal lymphangiomas[1-5], and only a few cases have been reported. Lymphangiomas are classified as simple, cavernous, and cystic types based on their histological findings[3,6,9-11]. The simple type is usually situated superficially in the skin and is composed of small thin-walled lymphatic vessels. The cavernous type is composed of dilated lymphatic vessels and lymphoid stroma, and has a connection with spaces of various normal adjacent lymphatics. The cystic type consists of lymphatic spaces

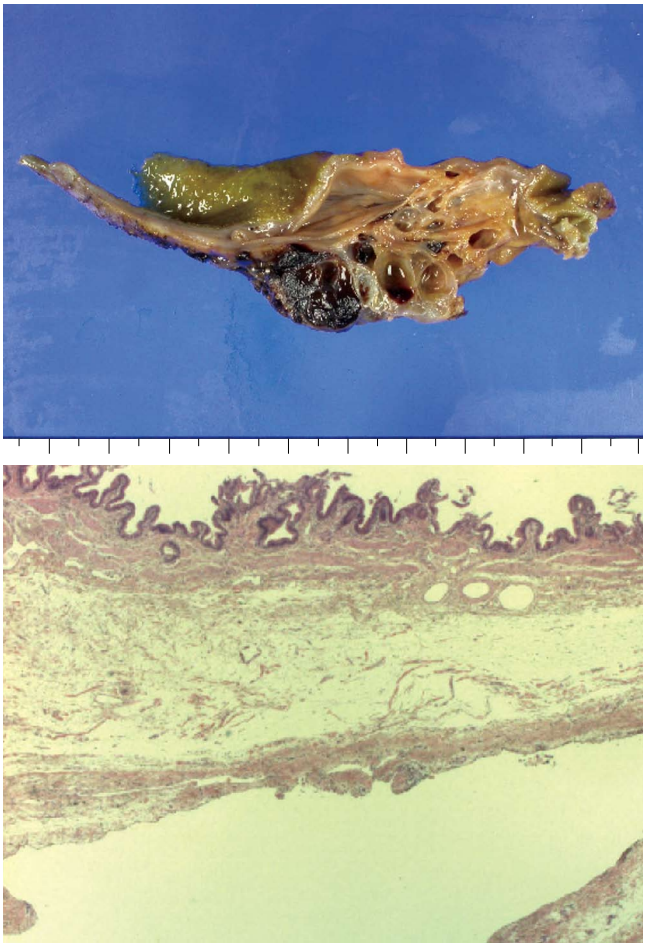

Figure 5 Gross appearance of resected specimen showing a well-marginated multi cystic lesion filled with yellowish fluid, and microphotograph from the cholecystectomy specimen showing a lymphatic space lined with flat endothelium (hematoxylin and eosin staining, × 12.5).

of various sizes that contain fascicles of smooth muscle and collagen bundles, but has no connection with adjacent normal lymphatics[11,12].

The etiology of lymphangiomas could be explained by several theories[1,6]. The most powerful one is that it is a congenital abnormality of the lymphatic system. Failure to establish connection with the normal drainage vessel causes sequestration of lymphatic tissue during embryogenesis. This theory would explain why lymphangioma occurs primarily in children. However, other views suggest that secondary causes such as abdominal trauma, lymphatic obstruction, inflammatory processes, surgery, or radiation therapy may lead to the formation of lymphangiomas[1,6].

Clinical presentations of these tumors are variable. Most cases are asymptomatic or have non-specific symptoms, such as nausea, vomiting, dyspepsia, abdominal discomfort or a palpable mass. In the past it was somewhat difficult to diagnose a lymphangioma before surgical or histological identification. Preoperative diagnosis of gallbladder lymphangioma remains difficult because it is very rare, and sometimes imaging studies such as US and CT cannot distinguish it from other lesions. The findings of US and CT show a large cystic lesion, but it is difficult to find where the lesion originates from and to understand its relation to surrounding organs.

However recently, various advanced imaging studies, especially MRI and MRCP, can support the diagnosis of lymphangiomas more easily before exploration[1,6,7]. US seems to be useful in defining the mass as a multilocular cystic lesion, but often does not distinguish between a hepatic lesion and a pericholecystic lesion. CT shows a simple or multilocular cystic lesion with the density of water. The septa of the cysts are of uniform thickness. Administering contrast agents intravenously can enhance the wall of the cysts[6]. However, the findings of CT of previous reports only showed cystic lesion in the gallbladder fossa or inferior to the liver, but could not show that the lesion was arising from the gallbladder. Moreover, the gallbladder was not visible due to cystic lesions in most of them, as was evident in the present case. Although hemorrhage within the lymphangioma was readily noted on follow-up CT, it might have been difficult to differentiate it from an intracystic solid lesion if the case was initially presented after hemorrhage[6].

In our study, MRI and MRCP are very helpful for making the correct diagnosis. One recent report described the MR findings of gallbladder lymphangiomas based on the findings of splenic cystic lymphangiomas[6]. This report suggested that characteristic MR findings would be very helpful for the differential diagnosis of gallbladder lymphangioma, and characterizing the mass even if the cystic lesion was complicated by intracystic hemorrhage. Axial T1- and T2-weighted and coronal MR images clearly depicted the lumen of the gallbladder and the multiseptated cystic mass originating in the gallbladder wall. MR imaging, including MRCP, clearly defined the mass and its relation to the gallbladder. The characteristic thin-walled multilocular cystic appearance was clearly depicted on MR imaging and was helpful for making the correct diagnosis[1,3,6,7]. MRCP characteristically showed that the cystic duct and bile duct were well preserved and were completely separated from the lymphangioma, as the finding of the present case. This was the typical feature of such lymphangiomas that had no communication between the mass and the biliary system. Therefore, if a gallbladder lymphangioma is suspected, MRI and MRCP should be recommended.

For the management of lymphangiomas, complete total surgical excision is known to be the standard treatment. If the mass grows large to compress surrounding structures and vessels, it can cause significant symptoms and morbidities. Furthermore, if it progresses to be complicated, intra-abdominal infection, rupture, torsion or hemorrhage can occur. A recent report suggested that two cases of gallbladder lymphangiomas were successfully treated by laparoscopic cholecystectomy, even though their size was more than 15 cm in diameter[8]. While we did not perform laparoscopic cholecystectomy, laparoscopic resection was possible because the lesion was relatively small compared to the previous report and was easily separated from the adjacent organs at surgical exploration. However, in a recent case, *en bloc* resection of the extrahepatic bile duct including the gallbladder was necessary because a huge cystic lesion adhered to the entire extrahepatic bile duct anteriorly and posteriorly, and part of the cyst also adhered to the right hepatic artery[1]. Therefore, laparoscopic resection was preferably

performed after evaluation of the extent of the cystic mass and its relation to adjacent organs. Recurrence has been reported with incomplete resection, but if the lesion is completely resected, long-term prognosis is excellent[12].

REFERENCES

1 **Noh KW**, Bouras EP, Bridges MD, Nakhleh RE, Nguyen JH. Gallbladder lymphangioma: a case report and review of the literature. *J Hepatobiliary Pancreat Surg* 2005; **12**: 405-408

2 **Ohba K**, Sugauchi F, Orito E, Suzuki K, Ohno T, Mizoguchi N, Koide T, Terashima H, Nakano T, Mizokami M. Cystic lymphangioma of the gall-bladder: a case report. *J Gastroenterol Hepatol* 1995; **10**: 693-696

3 **Lörken M**, Marnitz U, Manegold E, Schumpelick V. Intra-abdominal lymphangioma. *Chirurg* 2001; **72**: 72-77

4 **Bishop MD**, Steer M. Pancreatic cystic lymphangioma in an adult. *Pancreas* 2001; **22**: 101-102

5 **Takiff H**, Calabria R, Yin L, Stabile BE. Mesenteric cysts and intra-abdominal cystic lymphangiomas. *Arch Surg* 1985; **120**: 1266-1269

6 **Choi JY**, Kim MJ, Chung JJ, Park SI, Lee JT, Yoo HS, Kim L, Choi JS. Gallbladder lymphangioma: MR findings. *Abdom Imaging* 2002; **27**: 54-57

7 **Vargas-Serrano B**, Alegre-Bernal N, Cortina-Moreno B, Rodriguez-Romero R, Sanchez-Ortega F. Abdominal cystic lymphangiomas: US and CT findings. *Eur J Radiol* 1995; **19**: 183-187

8 **Yang HR**, Jan YY, Huang SF, Yeh TS, Tseng JH, Chen MF. Laparoscopic cholecystectomy for gallbladder lymphangiomas. *Surg Endosc* 2003; **17**: 1676

9 **Yoshida Y**, Okamura T, Ezaki T, Yano K, Kodate M, Murata I, Kaido M. Lymphangioma of the oesophagus: a case report an d review of the literature. *Thorax* 1994; **49**: 1267-1268

10 **Roisman I**, Manny J, Fields S, Shiloni E. Intra-abdominal lymphangioma. *Br J Surg* 1989; **76**: 485-489

11 **Chung JH**, Suh YL, Park IA, Jang JJ, Chi JG, Kim YI, Kim WH. A pathologic study of abdominal lymphangiomas. *J Korean Med Sci* 1999; **14**: 257-262

12 **Amadori G**, Micciolo R, Poletti A. A case of intra-abdominal multiple lymphangiomas in an adult in whom the immunological evaluation supported the diagnosis. *Eur J Gastroenterol Hepatol* 1999; **11**: 347-351

S- Editor Liu Y **L- Editor** Zhu LH **E- Editor** Liu WF

PO Box 2345, Beijing 100023, China
www.wjgnet.com
wjg@wjgnet.com

World J Gastroenterol 2007 January 14; 13(2): 324
World Journal of Gastroenterology ISSN 1007-9327
© 2007 The WJG Press. All rights reserved.

ACKNOWLEDGMENTS

Acknowledgments to Reviewers of *World Journal of Gastroenterology*

Many reviewers have contributed their expertise and time to the peer review, a critical process to ensure the quality of *World Journal of Gastroenterology*. The editors and authors of the articles submitted to the journal are grateful to the following reviewers for evaluating the articles (including those were published and those were rejected in this issue) during the last editing period of time.

Gary A Abrams, Associate Professor
Department of Medicine, University of Alabama at Birmingham, 1530 3rd Ave South, Birmingham 35294, United States

Agustin Albillos, Associate Professor
Departamento de Medicina, Facultad de Medicina-Campus Universitario, Universidad de Alcalá, Carretera Madrid-Barcelona km.33.600, Alcalá de Henares, Madrid 28871, Spain

Masahiro Arai, MD, PhD
Department of Gastroenterology, Toshiba General Hospital, 6-3-22 Higashi-ooi, Shinagawa-ku,Tokyo 140-8522, Japan

Olivier Barbier
CHUQ-CHUL Research Center, 2705 Laurier Boulevard, Québec G1V 4G2, Canada

Gabrio Bassotti, MD
Department of Clinical and Experimental Medicine, University of Perugia, Via Enrico dal Pozzo, Padiglione W, Perugia 06100, Italy

Edmund J Bini, Professor
VA New York Harbor Healthcare System, Division of Gastroenterology (111D), 423 East 23rd Street, New York, NY 10010, United States

Luigi Bonavina, Professor
Department of Surgery, Policlinico San Donato, University of Milano, via Morandi 30, Milano 20097, Italy

Josep M Bordas, MD
Department of Gastroenterology IMD, Hospital Clinic", Llusanes 11-13 at, Barcelona 08022, Spain

Joseph Daoud Boujaoude, Assistant Professor
Department of Gastroenterology, Hotel-Dieu de FranceHospital, aint-Joseph University, Beirut 961, Lebanon

Michele Cicala, Professor
Ipartimento di Malattie dell'Apparato Digerente, Università Campus Bio-Medico, Via Longoni, 83-00155 Rome, Italy

Andrew D Clouston, Associate Professor
Histopath Laboratories, Suite 4, Level 9, Strathfield Plaza, Strathfield, Sydney, 2135, Australia

Zong-Jie Cui, PhD, Professor
Institute of Cell Biology, Beijing Normal University, 19 XinJieKouWaiDaJie, Beijing 100875, China

Paolo Del Poggio, Dr.
Hepatology Unit, Department of Internal Medicine, Treviglio Hospital, Piazza Ospedale 1, Treviglio Bg 24047, Italy

Olivier Detry, Dr.
Department of Abdominal Surgery and Transplantation, University of Liège, CHU Sart Tilman B35, B-4000 Liège, Belgium

John Frank Di Mari, Assistant Professor
Internal Medicine, Gastroenterology ,9.138 MRB 301 University Blvd. Galveston, Texas 77555-1064, United States

Michael Anthony Fink
MBBS FRACS, Department of Surgery, The University of Melbourne, Austin Hospital, Melbourne, Victoria 3084, Australia

Kazuma Fujimoto, Professor
Department of Internal Medicine, Saga Medical School, Nabeshima, Saga, Saga 849-8501, Japan

Kazuma Fujimoto, Professor
Department of Internal Medicine, Saga Medical School, Nabeshima, Saga, Saga 849-8501, Japan

Mitsuhiro Fujishiro, Dr.
Department of Gastroenterology, Faculty of Medicine, University of Tokyo, 7-3-1 Hongo, Bunkyo-ku, Tokyo, Japan

Elizabeth Furrie, PhD
Department of Immunology, Ninewells hospital and Medical School, Dundee DD1 9SY, United Kingdom

Florian Graepler, Dr.
Department of Gastroenterology, Hepatology and Infectious Diseases, University Hospital Tuebingen, Otfried-Mueller-Str. 10, D-72076 Tuebingen, Germany

Khek-Yu Ho, Professor
Department of Medicine, National University Hospital, 119074, Singapore

Yik-Hong Ho, Professor
Department of Surgery, School of Medicine, James Cook University, Townsville 4811, Australia

Myung-Hwan Kim, Professor
Department of Internal Medicine, University of Ulsan College of Medicine, Asan Medical Center, 388-1 Pungnap-dong, Songpa-gu, Seoul 138-736, South Korea

Elias A Kouroumalis, Professor
Department of Gastroenterology, University of Crete, Medical School, Department of Gastroenterology, University Hospital, PO Box 1352, Heraklion, Crete 71110, Greece

Peter Laszlo Lakatos, MD, PhD, Assistant Professor
1st Department of Medicine, Semmelweis University, Koranyi S 2A, Budapest H1083, Hungary

Kurt Lenz, Professor
Department of Internal Medicine, Konventhospital Barmherzige Brueder, A-4020 Linz, Austria

María Isabel Torres López, Professor
Experimental Biology, University of Jaen, araje de las Lagunillas s/n, Jaén 23071, Spain

Giulio Marchesini, Professor
Department of Internal Medicine and Gastroenterology, "Alma Mater Studiorum" University of Bologna, Policlinico S. Orsola, Via Massarenti 9, Bologna 40138, Italy

Giulio Marchesini, Professor
Department of Internal Medicine and Gastroenterology, "Alma Mater Studiorum" University of Bologna, Policlinico S. Orsola, Via Massarenti 9, Bologna 40138, Italy

George Michalopoulos, MD, PhD
Department of Pathology, University of Pittsburgh, School of Medicine, S-410 Biomedical Science Tower, Pittsburgh, PA 15261, United States

Gerald Y Minuk, Dr.
Section of Hepatology, University of Manitoba, Room 803E-715 McDermot Avenue, Winnipeg, Manitoba R3E 3P4, Canada

Thierry Piche, MD, PhD
Department of Gastroenterology, Archet 2 Hospital, 151 RTE ST Antoine de Ginestiere 06202, Nice CEDEX 3, France

Eamonn M Quigley, Professor
Department of Medicine National University of Ireland, Cork, Cork University Hospital Clinical Sciences Building Wilton, Cork, Ireland

Luis Rodrigo, Professor
Gastroenterology Service, Hospital Central de Asturias, c/ Celestino Villamil, s.n., Oviedo 33.006, Spain

Yoshio Shirai, Associate Professor
Division of Digestive and General Surgery, Niigata University Graduate School of Medical and Dental Sciences, 1-757 Asahimachi-dori, Niigata City 951-8510, Japan

Qin Su, Professor
Department of Pathology, Cancer Hospital and Cancer Institute, Chinese Academy of Medical Sciences and Peking Medical College, PO Box 2258, Beijing 100021, China

Tadashi Takeda, MD
Department of Hepatology, Osaka City University, 1-4-3 Asahimachi, Abeno-ku, Osaka 545-8585, Japan

Kiichi Tamada, MD
Department of Gastroenterology, Jichi Medical Shool, 3311-1 Yakushiji,Minamikawa chi,Kawachigun, Tochigi 329-0498, Japan

Minoru Toyota, Dr.
First Department of Internal Medicine, Sapporo Medical University, South-1, West-16, Sapporo 060-8543, Japan

Yvan Vandenplas, Professor
Department of Pediatrics, AZ-VUB, Laarbeeklaan 101, Brussels 1090, Belgium

Takayuki Yamamoto, MD
Inflammatory Bowel Disease Center, Yokkaichi Social Insurance Hospital, 10-8 Hazuyamacho, Yokkaichi 510-0016, Japan

PO Box 2345, Beijing 100023, China
www.wjgnet.com
wjg@wjgnet.com

World J Gastroenterol 2007 January 14; 13(2): 325
World Journal of Gastroenterology ISSN 1007-9327
© 2007 The WJG Press. All rights reserved.

Meetings

MAJOR MEETINGS COMING UP

Meeting Falk Research Workshop: Morphogenesis and Cancerogenesis of the Liver
25-26 January 2007
Goettingen
symposia@falkfoundation.de

Meeting Canadian Digestive Diseases Week (CDDW)
16-20 February 2007
Banff-AB
cagoffice@cag-acg.org
www.cag-acg.org/cddw/cddw2007.htm

Meeting Falk Symposium 158: Intestinal Inflammation and Colorectal Cancer
23-24 March 2007
Sevilla
symposia@falkfoundation.de

Meeting BSG Annual Meeting
26-29 March 2007
Glasgow
www.bsg.org.uk/

NEXT 6 MONTHS

Meeting 42nd Annual Meeting of the European Association for the Study of the Liver
11-15 April 2007
Barcelona
easl2007@easl.ch
www.easl.ch/liver-meeting/

Meeting Falk Symposium 159: IBD 2007 - Achievements in Research and Clinical Practice
4-5 May 2007
Istanbul
symposia@falkfoundation.de

Meeting European Society for Paediatric Gastroenterology, Hepatology and Nutrition Congress 2007
9-12 May 2007
Barcelona
espghan2007@colloquium.fr

Digestive Disease Week
19-24 May 2007
Washington Convention Center, Washington DC

Meeting Gastrointestinal Endoscopy Best Practices: Today and Tomorrow, ASGE Annual Postgraduate Course at DDW
23-24 May 2007
Washington-DC
tkoral@asge.org

Meeting ESGAR 2007 18th Annual Meeting and Postgraduate Course
12-15 June 2007
Lisbon
fca@netvisao.pt

Meeting Falk Symposium 160: Pathogenesis and Clinical Practice in Gastroenterology
15-16 June 2007
Portoroz
symposia@falkfoundation.de

Meeting ILTS 13th Annual International Congress
20-23 June 2007
Rio De Janeiro
www.ilts.org

Meeting 9th World Congress on Gastrointestinal Cancer
27-30 June 2007
Barcelona
meetings@imedex.com

EVENTS AND MEETINGS IN 2007

Meeting Falk Research Workshop: Morphogenesis and Cancerogenesis of the Liver
25-26 January 2007
Goettingen
symposia@falkfoundation.de

Meeting Canadian Digestive Diseases Week (CDDW)
16-20 February 2007
Banff-AB
cagoffice@cag-acg.org
www.cag-acg.org/cddw/cddw2007.htm

Meeting Falk Symposium 158: Intestinal Inflammation and Colorectal Cancer
23-24 March 2007
Sevilla
symposia@falkfoundation.de

Meeting BSG Annual Meeting
26-29 March 2007
Glasgow
www.bsg.org.uk/

Meeting 42nd Annual Meeting of the European Association for the Study of the Liver
11-15 April 2007
Barcelona
easl2007@easl.ch
www.easl.ch/liver-meeting/

Meeting Falk Symposium 159: IBD 2007 - Achievements in Research and Clinical Practice
4-5 May 2007
Istanbul
symposia@falkfoundation.de

Meeting European Society for Paediatric Gastroenterology, Hepatology and Nutrition Congress 2007
9-12 May 2007
Barcelona
espghan2007@colloquium.fr

Meeting Gastrointestinal Endoscopy Best Practices: Today and Tomorrow, ASGE Annual Postgraduate Course at DDW
23-24 May 2007
Washington-DC
tkoral@asge.org

Meeting ESGAR 2007 18th Annual Meeting and Postgraduate Course
12-15 June 2007
Lisbon
fca@netvisao.pt

Meeting Falk Symposium 160: Pathogenesis and Clinical Practice in Gastroenterology
15-16 June 2007
Portoroz
symposia@falkfoundation.de

Meeting ILTS 13th Annual International Congress
20-23 June 2007
Rio De Janeiro
www.ilts.org

Meeting 9th World Congress on Gastrointestinal Cancer
27-30 June 2007
Barcelona
meetings@imedex.com

Meeting 15th International Congress of the European Association for Endoscopic Surgery
4-7 July 2007
Athens
info@eaes-eur.org
congresses.eaes-eur.org/

Meeting 39th Meeting of the European Pancreatic Club
4-7 July 2007
Newcastle
www.e-p-c2007.com

Meeting XXth International Workshop on Heliobacter and related bacteria in cronic degistive inflammation
20-22 September 2007
Istanbul
www.heliobacter.org

Meeting Falk Workshop: Mechanisms of Intestinal Inflammation
10 October 2007
Dresden
symposia@falkfoundation.de

Meeting Falk Symposium 161: Future Perspectives in Gastroenterology
11-12 October 2007
Dresden
symposia@falkfoundation.de

Meeting Falk Symposium 162: Liver Cirrhosis - From Pathophysiology to Disease Management
13-14 October 2007
Dresden
symposia@falkfoundation.de

American College of Gastroenterology Annual Scientific Meeting
12-17 October 2007
Pennsylvania Convention Center
Philadelphia, PA

Meeting APDW 2007 - Asian Pacific Digestive Disease Week 2007
15-18 October 2007
Kobe
apdw@convention.co.jp
www.apdw2007.org

15th United European Gastroenterology Week, UEGW
27-31 October 2007
Le Palais des Congrès de Paris, Paris, France

Meeting The Liver Meeting® 2007 - 57th Annual Meeting of the American Association for the Study of Liver Diseases
2-6 November 2007
Boston-MA
www.aasld.org

Gastro 2009, World Congress of Gastroenterology and Endoscopy London, United Kingdom 2009

PO Box 2345, Beijing 100023, China
www.wjgnet.com
wjg@wjgnet.com

World J Gastroenterol 2007 January 14; 13(2): 326-328
World Journal of Gastroenterology ISSN 1007-9327
© 2007 The WJG Press. All rights reserved.

Instructions to authors

GENERAL INFORMATION

World Journal of Gastroenterology (*WJG, World J Gastroenterol* ISSN 1007-9327 CN 14-1219/R) is a weekly journal of more than 48 000 circulation, published on the 7th, 14th, 21st and 28th of every month.

Original Research, Clinical Trials, Reviews, Comments, and Case Reports in esophageal cancer, gastric cancer, colon cancer, liver cancer, viral liver diseases, *etc.*, from all over the world are welcome on the condition that they have not been published previously and have not been submitted simultaneously elsewhere.

Indexed and abstracted in

Current Contents®/Clinical Medicine, Science Citation Index Expanded (also known as SciSearch®) and Journal Citation Reports/Science Edition, *Index Medicus*, MEDLINE and PubMed, Chemical Abstracts, EMBASE/Excerpta Medica, Abstracts Journals, *Nature Clinical Practice Gastroenterology and Hepatology*, CAB Abstracts and Global Health. ISI JCR 2003-2000 IF: 3.318, 2.532, 1.445 and 0.993.

Published by

The WJG Press

SUBMISSION OF MANUSCRIPTS

Manuscripts should be typed double-spaced on A4 (297 mm × 210 mm) white paper with outer margins of 2.5 cm. Number all pages consecutively, and start each of the following sections on a new page: Title Page , Abstract, Introduction, Materials and Methods, Results, Discussion, acknowledgements, References, Tables, Figures and Figure Legends. Neither the editors nor the Publisher is responsible for the opinions expressed by contributors. Manuscripts formally accepted for publication become the permanent property of The WJG Press, and may not be reproduced by any means, in whole or in part without the written permission of both the authors and the Publisher. We reserve the right to put onto our website and copy-edit accepted manuscripts. Authors should also follow the guidelines for the care and use of laboratory animals of their institution or national animal welfare committee.

Authors should retain one copy of the text, tables, photographs and illustrations, as rejected manuscripts will not be returned to the author(s) and the editors will not be responsible for the loss or damage to photographs and illustrations in mailing process.

Online submission

Online submission is strongly advised. Manuscripts should be submitted through the Online Submission System at: http://www.wjgnet.com/index.jsp. Authors are highly recommended to consult the ONLINE INSTRUCTIONS TO AUTHORS (http://www.wjgnet.com/wjg/help/instructions.jsp) before attempting to submit online. Authors encountering problems with the Online Submission System may send an email you describing the problem to wjg@wjgnet.com for assistance. If you submit your manuscript online, do not make a postal contribution. A repeated online submission for the same manuscript is strictly prohibited.

Postal submission

Send 3 duplicate hard copies of the full-text manuscript typed double-spaced on A4 (297 mm × 210 mm) white paper together with any original photographs or illustrations and a 3.5 inch computer diskette or CD-ROM containing an electronic copy of the manuscript including all the figures, graphs and tables in native Microsoft Word format or *.rtf format to:

Editorial Office

World Journal of Gastroenterology
Editorial Department: Apartment 1066, Yishou Garden,
58 North Langxinzhuang Road,
PO Box 2345, Beijing 100023, China
E-mail: wjg@wjgnet.com
http: //www.wjgnet.com
Telephone: +86-10-85381892
Fax: +86-10-85381893

MANUSCRIPT PREPARATION

All contributions should be written in English. All articles must be submitted using a word-processing software. All submissions must be typed in 1.5 line spacing and in word size 12 with ample margins. The letter font is Tahoma. For authors from China, one copy of the Chinese translation of the manuscript is also required (excluding references). Style should conform to our house format. Required information for each of the manuscript sections is as follows:

Title page

Full manuscript title, running title, all author(s) name(s), affiliations, institution(s) and/or department(s) where the work was accomplished, disclosure of any financial support for the research, and the name, full address, telephone and fax numbers and email address of the corresponding author should be included. Titles should be concise and informative (removing all unnecessary words), emphasize what is new, and avoid abbreviations. A short running title of less than 40 letters should be provided. List the author(s)' name(s) as follows: initial and/or first name, middle name or initial(s) and full family name.

Abstract

An informative, structured abstract of no more than 250 words should accompany each manuscript. Abstracts for original contributions should be structured into the following sections: AIM: Only the purpose should be included. METHODS: The materials, techniques, instruments and equipments, and the experimental procedures should be included. RESULTS: The observatory and experimental results, including data, effects, outcome, *etc.* should be included. Authors should present *P* value where necessary, and the significant data should accompany. CONCLUSION: Accurate view and the value of the results should be included.

The format of structured abstracts is at: http://www.wjgnet.com/wjg/help/11.doc

Key words

Please list 5-10 key words that could reflect content of the study mainly from *Index Medicus*.

Text

For most article types, the main text should be structured into the following sections: INTRODUCTION, MATERIALS AND METHODS, RESULTS and DISCUSSION, and should include in appropriate Figures and Tables. Data should be presented in the body text or in Figures and Tables, but not in both.

Illustrations

Figures should be numbered as 1, 2, 3 and so on, and mentioned clearly in the main text. Provide a brief title for each figure on a separate page. No detailed legend should be involved under the figures. This part should be added into the text where the figures are applicable. Digital images: black and white photographs should be scanned and saved in TIFF format at a resolution of 300 dpi; color images should be saved as CMYK (print files) but not as RGB (screen-viewing files). Place each photograph in a separate file. Print images: supply images of size no smaller than 126 mm × 85 mm printed on smooth surface paper; label the image by writing the Figure number and orientation using an arrow. Photomicrographs: indicate the original magnification and stain in the legend. Digital Drawings: supply files in EPS if created by freehand and illustrator, or TIFF from photoshops. EPS files must be accompanied by a version in native file format for editing purposes. Existing line drawings should be scanned at a resolution of 1200 dpi and as close as possible to the size where they will appear when printed. Please use uniform legends for the same subjects. For example: Figure 1 Pathological changes of atrophic gastritis after treatment. A: ...; B: ...; C: ...; D: ...; E: ...; F: ...; G: ...

Tables

Three-line tables should be numbered as 1, 2, 3 and so on, and mentioned clearly in the main text. Provide a brief title for each table. No detailed legend should be included under the tables. This part should be added into the text where the tables are applicable. The information should complement but not duplicate that contained in the text. Use one horizontal line under the title, a second under the column heads, and a third below the Table, above any footnotes. Vertical and italic lines should be omitted.

Notes in tables and illustrations

Data that are not statistically significant should not be noted. $^{a}P<0.05$, $^{b}P<0.01$ should be noted ($P>0.05$ should not be noted). If there are other series of *P* values, $^{c}P<0.05$ and $^{d}P<0.01$ are used. Third series of *P* values can be expressed as $^{e}P<0.05$ and $^{f}P<0.01$. Other notes in tables or under

illustrations should be expressed as ^{1}F, ^{2}F, ^{3}F; or some other symbols with a superscript (Arabic numerals) in the upper left corner. In a multi-curve illustration, each curve should be labeled with ●, ○, ■, □, ▲, △, *etc.* in a certain sequence.

Acknowledgments

Brief acknowledgments of persons who have made genuine contributions to the manuscripts and who endorse the data and conclusions are included. Authors are responsible for obtaining written permission to use any copyrighted text and/or illustrations.

REFERENCES

Coding system

The author should code the references according the citation order in text in Arabic numerals, put references codes in square brackets, superscript it at the end of citation content or the author name of the citation. For those citation content as the narrate part, the coding number and square brackets should be typeset normally. For example, Crohn's disease (CD) is associated with increased intestinal permeability[1,2]. If references are directly cited in the text, they would be put together with the text, for example, from references [19,22-24], we know that...

When the authors code the references, please ensure that the order in text is the same as in reference part and also insure the spelling accuracy of the first author's name. Do not code the same citation twice.

PMID requirement

PMID roots in the abstract serial number indexed by PubMed (http://www.ncbi.nlm.nih.gov/entrez/query.fcgi?db=PubMed). The author should supply the PMID for journal citation. For those references that have not been indexed by PubMed, a printed copy of the first page of the full reference should be submitted.

The accuracy of the information of the journal citations is very important. Through reference testing system, the authors and editor could check the authors name, title, journal title, publication date, volume number, start page, and end page. We will interlink all references with PubMed in ASP file so that the readers can read the abstract of the citations online immediately.

Style for journal references

Authors: the first author should be typed in bold-faced letter. The surname of all authors should be typed with the initial letter capitalized and followed by their name in abbreviation (For example, Lian-Sheng Ma is abbreviated as Ma LS, Bo-Rong Pan as Pan BR). Title of the cited article and italicized journal title (Journal title should be in its abbreviation form as shown in PubMed), publication date, volume number (in black), start page, and end page [PMID: 11819634]

Note: The author should test the references through reference testing system (http://www.wjgnet.com/cgi-bin/index.pl)

Style for book references

Authors: the first author should be typed in bold-faced letter. The surname of all authors should be typed with the initial letter capitalized and followed by their name in abbreviation (For example, Lian-Sheng Ma is abbreviated as Ma LS, Bo-Rong Pan as Pan BR) Book title. Publication number. Publication place: Publication press, Year: start page and end page.

Format

Journals

English journal article (list all authors and include the PMID where applicable)

1 **Grover VP**, Dresner MA, Forton DM, Counsell S, Larkman DJ, Patel N, Thomas HC, Taylor-Robinson SD. Current and future applications of magnetic resonance imaging and spectroscopy of the brain in hepatic encephalopathy. *World J Gastroenterol* 2006; **12**: 2969-2978 [PMID: 16718775]

Chinese journal article (list all authors and include the PMID where applicable)

2 **Lin GZ**, Wang XZ, Wang P, Lin J, Yang FD. Immunologic effect of Jianpi Yishen decoction in treatment of Pixu-diarrhoea. *Shijie Huaren Xiaohua Zazhi* 1999; **7**: 285-287

In press

3 **Tian D**, Araki H, Stahl E, Bergelson J, Kreitman M. Signature of balancing selection in Arabidopsis. *Proc Natl Acad Sci U S A* 2006; In press

Organization as author

4 **Diabetes Prevention Program Research Group**. Hypertension, insulin, and proinsulin in participants with impaired glucose tolerance. *Hypertension* 2002; **40**: 679-686 [PMID: 12411462]

Both personal authors and an organization as author

5 **Vallancien G**, Emberton M, Harving N, van Moorselaar RJ; Alf-One Study Group. Sexual dysfunction in 1, 274 European men suffering from lower urinary tract symptoms. *J Urol* 2003; **169**: 2257-2261 [PMID: 12771764]

No author given

6 21st century heart solution may have a sting in the tail. *BMJ* 2002; **325**: 184 [PMID: 12142303]

Volume with supplement

7 **Geraud G**, Spierings EL, Keywood C. Tolerability and safety of frovatriptan with short- and long-term use for treatment of migraine and in comparison with sumatriptan. *Headache* 2002; **42** Suppl 2: S93-99 [PMID: 12028325]

Issue with no volume

8 **Banit DM**, Kaufer H, Hartford JM. Intraoperative frozen section analysis in revision total joint arthroplasty. *Clin Orthop Relat Res* 2002; (**401**): 230-238 [PMID: 12151900]

No volume or issue

9 Outreach: bringing HIV-positive individuals into care. *HRSA Careaction* 2002; 1-6 [PMID: 12154804]

Books

Personal author(s)

10 **Sherlock S**, Dooley J. Diseases of the liver and billiary system. 9th ed. Oxford: Blackwell Sci Pub, 1993: 258-296

Chapter in a book (list all authors)

11 **Lam SK**. Academic investigator's perspectives of medical treatment for peptic ulcer. In: Swabb EA, Azabo S. Ulcer disease: investigation and basis for therapy. New York: Marcel Dekker, 1991: 431-450

Author(s) and editor(s)

12 **Breedlove GK**, Schorfheide AM. Adolescent pregnancy. 2nd ed. Wieczorek RR, editor. White Plains (NY): March of Dimes Education Services, 2001: 20-34

Conference proceedings

13 **Harnden P**, Joffe JK, Jones WG, editors. Germ cell tumours V. Proceedings of the 5th Germ Cell Tumour Conference; 2001 Sep 13-15; Leeds, UK. New York: Springer, 2002: 30-56

Conference paper

14 **Christensen S**, Oppacher F. An analysis of Koza's computational effort statistic for genetic programming. In: Foster JA, Lutton E, Miller J, Ryan C, Tettamanzi AG, editors. Genetic programming. EuroGP 2002: Proceedings of the 5th European Conference on Genetic Programming; 2002 Apr 3-5; Kinsdale, Ireland. Berlin: Springer, 2002: 182-191

Electronic journal (list all authors)

Morse SS. Factors in the emergence of infectious diseases. Emerg Infect Dis serial online, 1995-01-03, cited 1996-06-05; 1(1): 24 screens. Available from: URL: http//www.cdc.gov/ncidod/EID/eid.htm

Patent (list all authors)

16 **Pagedas AC**, inventor; Ancel Surgical R&D Inc., assignee. Flexible endoscopic grasping and cutting device and positioning tool assembly. United States patent US 20020103498. 2002 Aug 1

Inappropriate references

Authors should always cite references that are relevant to their article, and avoid any inappropriate references. Inappropriate references include those that are linked with a hyphen and the difference between the two numbers at two sides of the hyphen is more than 5. For example, [1-6], [2-14] and [1, 3, 4-10, 22] are all considered as inappropriate references. Authors should not cite their own unrelated published articles.

Statistical data

Present as mean ± SD or mean ± SE.

Statistical expression

Express t test as t (in italics), F test as F (in italics), chi square test as χ^2 (in Greek), related coefficient as r (in italics), degree of freedom as γ (in Greek), sample number as n (in italics), and probability as P (in italics).

Units

Use SI units. For example: body mass, m (B) = 78 kg; blood pressure, p(B) = 16.2/12.3 kPa; incubation time, t (incubation) = 96 h, blood glucose concentration, c (glucose) 6.4 ± 2.1 mmol/L; blood CEA mass concentration, p (CEA) = 8.6 24.5 μg/L; CO_2 volume fraction, 50 mL/L CO_2 not 5% CO_2; likewise for 40 g/L formaldehyde, not 10% formalin; and mass fraction, 8 ng/g, *etc.* Arabic numerals such as 23, 243, 641 should be read 23 243 641.

The format about how to accurately write common units and quantum is at: http://www.wjgnet.com/wjg/help/15.doc

Abbreviations
Standard abbreviations should be defined in the abstract and on first mention in the text. In general, terms should not be abbreviated unless they are used repeatedly and the abbreviation is helpful to the reader. Permissible abbreviations are listed in Units, Symbols and Abbreviations: A Guide for Biological and Medical Editors and Authors (Ed. Baron DN, 1988) published by The Royal Society of Medicine, London. Certain commonly used abbreviations, such as DNA, RNA, HIV, LD50, PCR, HBV, ECG, WBC, RBC, CT, ESR, CSF, IgG, ELISA, PBS, ATP, EDTA, mAb, can be used directly without further mention.

Italics
Quantities: *t* time or temperature, *c* concentration, *A* area, *l* length, *m* mass, *V* volume.
Genotypes: *gyr*A, *arg* 1, *c myc*, *c fos*, *etc.*
Restriction enzymes: *Eco*RI, *Hin*dI, *Bam*HI, *Kbo* I, *Kpn* I, *etc.*
Biology: *H pylori, E coli, etc.*

SUBMISSION OF THE REVISED MANUSCRIPTS AFTER ACCEPTED

Please revise your article according to the revision policies of *WJG*. The revised version including manuscript and high-resolution image figures (if any) should be copied on a floppy or compact disk. Author should send the revised manuscript, along with printed high-resolution color or black and white photos, copyright transfer letter, the final check list for authors, and responses to reviewers by a courier (such as EMS) (submission of revised manuscript by e-mail or on the *WJG* Editorial Office Online System is NOT available at present).

Language evaluation
The language of a manuscript will be graded before sending for revision. (1) Grade A: priority publishing; (2) Grade B: minor language polishing; (3) Grade C: a great deal of language polishing; (4) Grade D: rejected. The revised articles should be in grade B or grade A.

Copyright assignment form
Please downloaded CAF from http://www.wjgnet.com/wjg/help/9.doc.

We certify that the material contained in this manuscript:

Ms:

Title:

is original, except when appropriately referenced to other sources, and that written permission has been granted by any existing copyright holders. We agree to transfer to WJG all rights of our manuscript, including: (1) all copyright ownership in all print and electronic formats; (2) the right to grant permission to republish or reprint the stated material in whole or in part, with or without a fee; (3) the right to print copies for free distribution or sale; (4) the right to republish the stated material in a collection of articles or in any other format. We also agree that our article be put on the Internet.

Criteria for authorship: The WJG requests and publishes information about contributions of each author named to the submitted study. Authorship credit should be based on (1)direct participation in the study, including substantial contributions to conception and design of study, or acquisition of data, or analysis and interpretation of data; (2) manuscript writing, including drafting the article, or revising it critically for important intellectual content; (3)supportive work, including statistical analysis of data, or acquisition of funding, or administration, technology and materials support, or supervision, or supportive contributions. Authors should meet at least one of the three conditions. The WJG does not publish co-first authors and co-corresponding authors.

We hereby assign copyright transfer to WJG if this paper is accepted.

Author Name in full (Full names should be provided, with first name first, followed by middle names and family name at the last, eg, Eamonn MM Quigley). Handwritten names are not accepted.

Author Name in abbreviation (Family name is put first in full, followed by middle names and first name in abbreviation with first letter in capital, eg, Quigley EMM). Handwritten names are not accepted.

1 Full Name: _____
Abbreviation Name: _____
Signed: _____
Date: _____

2 Full Name: _____
Abbreviation Name: _____
Signed: _____
Date: _____

3 Full Name: _____
Abbreviation Name: _____
Signed: _____
Date: _____

4 Full Name: _____
Abbreviation Name: _____
Signed: _____
Date: _____

5 Full Name: _____
Abbreviation Name: _____
Signed: _____
Date: _____

6 Full Name: _____
Abbreviation Name: _____
Signed: _____
Date: _____

7 Full Name: _____
Abbreviation Name: _____
Signed: _____
Date: _____

8 Full Name: _____
Abbreviation Name: _____
Signed: _____
Date: _____

9 Full Name: _____
Abbreviation Name: _____
Signed: _____
Date: _____

10 Full Name: _____
Abbreviation Name: _____
Signed: _____
Date: _____

Final check list for authors
The format is at: http://www.wjgnet.com/wjg/help/13.doc

Responses to reviewers
Please revise your article according to the comments/suggestions of reviewers. The format for responses to the reviewers' comments is at: http://www.wjgnet.com/wjg/help/10.doc

Proof of financial support
For paper supported by a foundation, authors should provide a copy of the document and serial number of the foundation.

Publication fee
Authors of accepted articles must pay publication fee.
EDITORIAL and LETTERS TO THE EDITOR are free of change.